City Research Online

City St George's, University of London

Citation: Little, John Antony (1984). Engineering properties of glacial tills in the Vale of St. Albans. (Unpublished Doctoral thesis, City, University of London)

This is the submitted version of the paper.

This version of the publication may differ from the final published version. To cite this item please consult the publisher's version.

Permanent repository link: https://openaccess.city.ac.uk/id/eprint/21115/

Copyright and Reuse: Copyright and Moral Rights remain with the author(s) and/or copyright holders. Copies of full items can be used for personal research or study, educational, or not-for-profit purposes without prior permission or charge, unless otherwise indicated, provided that the authors, title and full bibliographic details are credited, a hyperlink and/or URL is given for the original metadata page and the content is not changed in any way. For full details of reuse please refer to City Research Online policy.

City Research Online: http://openaccess.city.ac.uk/ publications@citystgeorges.ac.uk

ENGINEERING PROPERTIES OF GLACIAL TILLS IN THE VALE OF ST. ALBANS.

by

John Anthony Little.

A THESIS
SUBMITTED TO THE CITY UNIVERSITY
FOR THE DEGREE OF DOCTOR OF PHILOSOPHY
IN CIVIL ENGINEERING.

OCTOBER 1984.

To

Gail and Matthew and Ceri and Emma.

Thank you for your patience and understanding.

CONTENTS.

	Page
TITLE PAGE	I
CONTENTS	II
LIST OF TABLES	VII
LIST OF FIGURES	X
ACKNOWLEDGEMENTS	XVIII
DECLARATION	XIX
ABSTRACT	XX
LIST OF SYMBOLS AND ABBREVIATIONS	XXI
CHAPTER 1. INTRODUCTION.	1
1.1 General.	1
1.2 The Study.	3
CHAPTER 2. THE GEOLOGICAL SETTING.	5
2.1 Introduction.	5
2.2 The Quaternary in the U.K.	6
2.2.1 The Quaternary : a definition.	6
2.2.2 Anglian Cold Stage.	7
2.2.3 Hoxnian Interglacial.	7
2.2.4 Wolstonian Cold Stage.	8
2.2.5 Ipswichian and Devensian.	8
2.3 The Vale of St. Albans.	9
2.3.1 Physical and geological setting.	9
2.3.2 The ancestral Thames in the Vale.	10
2.4 The sequence of Pleistocene sediments in the Vale.	12
2.4.1 Leavesden Green Gravel	12
2.4.2 Westmill Lower Gravel and Westmill Gravel.	12
2.4.3 Watton Road Laminated Silts.	13
2.4.4 Ware Till.	13
2.4.5 Westmill Upper Gravel.	14
2.4.6 Moor Mill Laminated Clays.	14
2.4.7 Eastend Green Till.	15
2.4.8 Smug Oak Gravel.	15
2.4.9 Hatfield Organic Deposits.	15
2.4.10 Post-Hoxnian sediments in the Vale.	16
2.5 Summary.	16

Page

CHAPTER 3. SOME ASPECTS OF THE MECHANICS OF ENGINEERING SOILS. 25

3.1 Introduction. 25

3.2 Stress invariants and a volumetric parameter. 25

3.3 One-dimensional and isotropic drained compression of a clay. 27

3.4 Behaviour during compression shear testing. 28

3.5 Normalising procedures : a general view of the state boundary surface. 31

3.6 Pore pressure response in undrained loading. 34

CHAPTER 4. THE CLASSIFICATION OF TILLS AND THEIR ENGINEERING PROPERTIES. 42

4.1 Introduction. 42

4.2 Glacial till : a definition. 42

4.3 Tills and their depositional environment : a landsystems approach. 43

4.3.1 Subglacial tills. 45
4.3.2 Supraglacial tills. 46

4.4 Till fabric. 47

4.4.1 The geological and the engineering meaning of fabric. 47
4.4.2 The presence, origins and significance of discontinuities in till. 49

4.5 Till as an engineering material. 52

4.5.1 Plasticity. 53
4.5.2 Particle size. 54
4.5.3 One-dimensional compression. 56
4.5.4 Permeability and rate of consolidation. 60
4.5.5 Undrained and drained shear strength. 62
4.5.6 Elastic modulus. 67

4.6 Summary. 69

CHAPTER 5. FIELD INVESTIGATIONS. 92

5.1 Introduction. 92

5.2 Site locations and descriptions of Pleistocene sediments. 93

5.2.1 Moor Mill Quarry, Bricket Wood. 93
5.2.2 Hatfield Quarry, St. Albans. 94
5.2.3 Holwell Hyde Quarry, Welwyn Garden City. 95
5.2.4 Foxholes Quarry, Hertford. 96
5.2.5 Westmill Quarry, Ware. 97

Page

5.3 In situ testing. 98

5.3.1 Clast orientation and dip. 99
5.3.2 Discontinuity survey, Holwell Hyde Quarry. 103
5.3.3 A new till fabric instrument. 105
5.3.4 Shear vane testing. 107

5.4 Sampling procedures. 109

5.4.1 Bulk disturbed samples. 109
5.4.2 Undisturbed samples for oedometer and direct shear testing. 109
5.4.3 Undisturbed 38mm diameter samples for triaxial compression testing. 111

CHAPTER 6. LABORATORY WORK. 129

6.1 Introduction. 129

6.2 Classification tests. 130

6.2.1 Atterberg limits. 130
6.2.2 Particle specific gravity. 131
6.2.3 Particle size. 131
6.2.4 Quantity and distribution of chalk. 132

6.3 Mineralogy. 133

6.3.1 X - ray diffraction analysis (XRD). 133
6.3.2 Energy dispersal analysis (EDAX). 134

6.4 Fossil assemblages. 134

6.5 Oedometer compression tests. 135

6.6 Motorised shear vane tests. 138

6.7 Drained direct shear box tests. 139

6.8 Consolidated undrained triaxial compression tests. 140

6.8.1 Testing schedule. 140
6.8.2 Laboratory services. 142
6.8.3 Instrumentation. 144
6.8.4 Transducer calibration procedures. 145
6.8.5 Preparation of samples. 148
6.8.6 Testing procedures. 149

CHAPTER 7. LABORATORY TEST RESULTS. 175

7.1 Classification tests. 175

7.1.1 Atterberg limits and particle specific gravity. 175
7.1.2 Particle size. 175
7.1.3 Quantity and distribution of chalk in the tills. 175

7.2 Mineralogical tests. 176

7.2.1 Clay mineral content. 176
7.2.2 Element composition. 176

Page

7.3 Oedometer compression test results. 177

7.4 Motorised shear vane test results. 178

7.5 Drained direct shear box test results. 178

7.6 Consolidated undrained triaxial compression test results. 179

CHAPTER 8. ANALYSIS AND DISCUSSION. 269

8.1 Engineering classification of the tills. 269

8.1.1 Plasticity. 269
8.1.2 Grading characteristics. 270
8.1.3 Activity of the tills. 271
8.1.4 The distribution and effect of chalk in the tills. 272

8.2 One-dimensional and isotropic compression. 275

8.3 Permeability and consolidation. 279

8.4 The strength of the tills. 282

8.4.1 Undrained shear strength from the vane tests. 282
8.4.2 Peak (Mohr - Coulomb) states from the triaxial tests. 285
8.4.3 Ultimate or critical states. 285

8.5 Normalised critical state parameters: the Hvorslev and Roscoe state boundary surfaces. 288

8.6 Aspects of behaviour inside and on the state boundary surface. 291

8.6.1 Pore pressure response. 291
8.6.2 Undrained elastic modulus. 294

8.7 Carbonate cementation. 296

8.7.1 The mineralogical evidence. 297
8.7.2 The evidence from the grading analyses. 298
8.7.3 The evidence from the oedometer tests. 299
8.7.4 The evidence from the strength tests. 300

CHAPTER 9. SUMMARY AND CONCLUSIONS. 377

9.1 The geological origin of the tills. 377

9.2 The post-depositional history of the tills. 378

9.3 An overview of the engineering properties of the tills. 380

9.4 An overview of the field and laboratory methods used in the sampling and testing of the tills. 384

Page

REFERENCES. 386

APPENDICES.

Appendix I - Till fabric instrument : engineering drawings. 406

LIST OF TABLES

Table		Page
2.1	British Quaternary stages.	18
2.2	The Anglian stratotype, Corton Cliff, Lowestoft.	19
2.3	Pleistocene stratigraphy in the Vale of St. Albans.	20
4.1	Classification of tills - associated landforms and sediments.	71
4.2	Summary of plasticity data : site locations and sources.	72
4.3	Gradational series of till textures.	74
5.1	Summary of till fabric data.	112
5.2	Results of in situ shear vane tests.	113
5.3	Summary of samples obtained at the five sites.	114
6.1	Microfauna from tills HH(a) , HH(b), Holwell Hyde.	155
6.2	Index of oedometer tests.	156
6.3	Index of drained shear box tests.	157
6.4	Index of CU triaxial compression tests.	158
6.5	Summary of transducer calibrations, panels 1 - 4.	159
7.1	Natural water content, plasticity and particle specific gravity results.	181
7.2	Activity of the tills.	182
7.3	The effect of the removal of acid solubles on various size fractions during sedimentation.	182
7.4	Chalk and acid soluble content, tills HH(a) , HH(b) , Holwell Hyde.	183
7.5	Mineralogical composition of the tills.	184
7.6	Element composition of the tills.	184
7.7	Oedometer test OR(1), reconstituted till HH(a).	185
7.8	Oedometer test OR(2), reconstituted till HH(b).	185
7.9	Oedometer test OR(3), reconstituted till F(b).	186
7.10	Oedometer test OR(4), reconstituted till W(b).	186
7.11	Oedometer test OR(5), reconstituted till W(d).	187
7.12	Oedometer test OU1(V), undisturbed till HH(a), vertical drainage.	188
7.13	Oedometer test OU2(V), undisturbed till HH(b), vertical drainage.	188

7.14	Oedometer test OU3(V), undisturbed till F(b), vertical drainage.	189
7.15	Oedometer test OU4(V), undisturbed till W(b), vertical drainage.	189
7.16	Oedometer test OU5(V), undisturbed till W(d), vertical drainage.	190
7.17	Oedometer test OU(1) H(p), undisturbed till HH(a), horizontal drainage, parallel to fabric.	191
7.18	Oedometer test OU(1) H(n), undisturbed till HH(a), horizontal drainage, normal to fabric.	191
7.19	Oedometer test OU(1) H(r), undisturbed till HH(a), horizontal drainage, random orientation.	192
7.20	Oedometer test OU(2) H(p), undisturbed till HH(b), horizontal drainage, parallel to fabric.	193
7.21	Oedometer test OU(2) H(n), undisturbed till HH(b), horizontal drainage, normal to fabric.	193
7.22	Oedometer test OU(2) H(r), undisturbed till HH(b), horizontal drainage, random orientation.	194
7.23	Oedometer test OU(3) H(p), undisturbed till F(b), horizontal drainage, parallel to fabric.	195
7.24	Oedometer test OU(3) H(n), undisturbed till F(b), horizontal drainage, normal to fabric.	195
7.25	Oedometer test OU(3) H(r), undisturbed till F(b), horizontal drainage, random orientation.	196
7.26	Oedometer test OU(4) H(p), undisturbed till W(b), horizontal drainage, parallel to fabric.	197
7.27	Oedometer test OU(4) H(n), undisturbed till W(b), horizontal drainage, normal to fabric.	197
7.28	Oedometer test OU(4) H(r), undisturbed till W(b), horizontal drainage, random orientation.	198
7.29	Oedometer test OU(5) H(p), undisturbed till W(d), horizontal drainage, parallel to fabric.	199
7.30	Oedometer test OU(5) H(n), undisturbed till W(d), horizontal drainage, normal to fabric.	199
7.31	Oedometer test OU(5) H(r), undisturbed till W(d), horizontal drainage, random orientation.	200
7.32	Water content : undrained shear strength relationship for tills HH(a) , HH(b) , F(b). (Motorised shear vane).	201
7.33	Isotropic consolidation test TR(1), reconstituted till HH(a).	202
7.34	Isotropic consolidation test TR(2), reconstituted till HH(b).	202
7.35	Isotropic consolidation test TU(1), undisturbed till HH(a).	203

Page

7.36 Isotropic consolidation test TU(2), undisturbed till HH(b). 203

8.1 Soil constants derived from the oedometer tests. 303

8.2 Soil constants for HH(a) , HH(b) , from the isotropic compression tests. 304

8.3 Critical state predictions , q'_u , reconstituted and undisturbed till HH(a), Ro = 1. 305

8.4 Critical state predictions , q'_u , q' , overconsolidated reconstituted till HH(a). 306

8.5 Critical state predictions , q'_u , q' , overconsolidated undisturbed till HH(a). 307

8.6 Undrained modulus, reconstituted till HH(a). 308

8.7 Undrained modulus, undisturbed till HH(a). 309

LIST OF FIGURES

Figure		Page
2.1	Probable limits of Pleistocene ice sheet advance in the U.K.	21
2.2	The Vale of St. Albans : location.	22
2.3	The Vale of St. Albans : solid and superficial geology.	23
2.4	Inferred generalised flow of the ancestral Thames in the Vale.	24
3.1	Idealised drained isotropic compression and swelling of the soil.	37
3.2	q , q' : p' : V relationship for soil in drained and undrained compression.	38
3.3	General state boundary surface for soil.	39
3.4	The state boundary surface in q'/p'_e : p'/p'_e space.	40
3.5	The reference section in q'/p' : V_λ space.	40
3.6	Isotropic overconsolidation of a soil.	41
4.1	Schematic diagram to illustrate the formation of the subglacial/proglacial sediment association and landsystem.	75
4.2	Plasticity data for various lodgement tills in the U.K.	76
4.3	Grading characteristics of lodgement tills in the U.K.	77
4.4	Oedometer compression : Milwaukee Till.	78
4.5	Oedometer compression characteristics, glacial till, N.Sea. (Depth 64·0m , boring D).	79
4.6	Oedometer compression characteristics, glacial till, N.Sea. (Depth 112·0m , boring A).	80
4.7	Oedometer compression characteristics, glacial till, N.Sea. (Depth 50·0m , boring K).	81
4.8	Permeability : specific volume relationship for tills and related soils.	82
4.9	Permeability : specific volume : coefficient of consolidation relationship for N.Sea tills, borings A , D , J , K .	83
4.10	Relationship between undrained shear strength and liquidity index for U.K. tills.	84
4.11	Undrained shear strength : water content relationship for lodgement tills.	85

Page

4.12 ϕ'_p : PI for various lodgement tills. 86

4.13 ϕ'_R : PI for various lodgement tills. 87

4.14 Residual shear mechanisms and particle packing. 88

4.15 Anisotropy and elastic modulus. 89

4.16 Soil modulus : undrained shear strength relationship for tills. 90

4.17 E_u : Ro relationship for two tills. 91

5.1 Lithostratigraphic units at the five study sites in the Vale. 115

5.2 Dark grey chalky lodgement till (HH(a)) at Holwell Hyde Quarry, Welwyn Garden City. 116

5.3 Till HH(a) in hand specimen. 116

5.4 Light grey chalky lodgement till (HH(b)) at Holwell Hyde Quarry, Welwyn Garden City. 117

5.5 Till HH(b) in hand specimen. 117

5.6 Till fabric study on a prepared face, Westmill Quarry, Ware. 118

5.7 Clast fabric, till HH(a) , Holwell Hyde. 119

5.8 Clast fabric, till HH(b) , Holwell Hyde. 120

5.9 Clast fabric, till F(b) , Foxholes. 121

5.10 Clast fabric, till W(b) , Westmill. 122

5.11 Clast fabric, till W(d) , Westmill. 123

5.12 Spherical projection of discontinuities (great circles) in till HH(a). 124

5.13 Spherical projection of discontinuities (great circles) in till HH(b). 125

5.14 The till fabric instrument. 126

5.15 The fabric instrument with trowel attachments. 126

5.16 Obtaining undisturbed fabric-oriented (horizontal drainage) oedometer sample, till W(b), Westmill. 127

5.17 Full penetration of the 38mm sampling tube. 128

5.18 The sampling tube exposed. 128

6.1 Jurassic fauna from tills HH(a) (top, centre) and HH(b) (bottom) , Holwell Hyde. 160

6.2 Middle Jurassic (?) microfauna from Holwell Hyde. 161

6.3 Measured elastic compressions in consolidation cells 1 - 5 . 162

6.4 Diagrammatic layout of equipment and instrumentation for one 38mm triaxial cell. 163

6.5 Minimum and maximum air temperatures recorded during 1982 in the laboratory space now occupied by the new laboratory housing the triaxial equipment, and recorded temperatures in this new laboratory 1983/1984. 164

Page

6.6	Calibration of the load cell calibrator.	165
6.7	Load cell calibration graphs, panels 1 - 4 .	166
6.8	Pore pressure transducer calibration graphs, panels 1 - 4 .	167
6.9	Volume change transducer (50cc) calibration graphs, panel 1 , using (A) 200 kPa , (B) 750 kPa back pressure.	168
6.10	Volume change transducer (100cc) calibration graphs, panel 2 , using (A) 200 kPa , (B) 750 kPa back pressure.	169
6.11	Volume change transducer (100cc) calibration graphs, panel 3 , using (A) 200 kPa , (B) 750 kPa back pressure.	170
6.12	Volume change transducer (100cc) calibration graphs, panel 4 , using (A) 200 kPa , (B) 750 kPa back pressure.	171
6.13	Displacement transducer calibration graphs, panels 1 - 4 .	172
6.14	Measured elastic compressions in the triaxial cells, panels 1 - 4 .	173
6.15	Dry unit weight : water content relationship for till HH(a).	174
7.1	Plasticity data for the Vale of St. Albans tills and related sediments.	204
7.2	Grading characteristics of tills HH(a) , HH(b) , F(b) , W(b) , W(d) .	205
7.3	Total and acid soluble grading characteristics of till HH(a)..	206
7.4	Total and acid soluble grading characteristics of till HH(b).	207
7.5	Till HH(a) : electronmicrograph and EDAX trace on chalk particle and matrix.	208
7.6	Till HH(b) : electronmicrograph and EDAX trace on chalk particle and matrix.	209
7.7	Oedometer compression characteristics, till HH(a).	210
7.8	Oedometer compression characteristics, till HH(b).	211
7.9	Oedometer compression characteristics, till F(b).	212
7.10	Oedometer compression characteristics, till W(b).	213
7.11	Oedometer compression characteristics, till W(d).	214
7.12	τ : ε_L : ε_V; drained shear box tests SR1(i) , (ii) , (iii).	215
7.13	τ : ε_L : ε_V; drained shear box tests SR1(iv), (v) , (vi).	216
7.14	τ : ε_L : ε_V; drained shear box tests SU1(i) , (ii) , (iii).	217

		Page
7.15	τ : ε_L : ε_v ; drained shear box tests SU3(i), (ii) , (iii).	218
7.16	Isotropic compression characteristics, reconstituted and undisturbed till HH(a).	219
7.17	Isotropic compression characteristics, reconstituted and undisturbed till HH(b).	220
7.18	CU triaxial test results : RA1(i).	221
7.19	CU triaxial test results : RA1(ii).	222
7.20	CU triaxial test results : RA1(iii).	223
7.21	CU triaxial test results : RA2(ii).	224
7.22	CU triaxial test results : RA2(iii).	225
7.23	CU triaxial test results : RB(ii).	226
7.24	CU triaxial test results : RB(iii).	227
7.25	CU triaxial test results : RB(v).	228
7.26	CU triaxial test results : R2 - 02.	229
7.27	CU triaxial test results : R2 - 03.	230
7.28	CU triaxial test results : UA1(i).	231
7.29	CU triaxial test results : UA1(ii).	232
7.30	CU triaxial test results : UA1(iii).	233
7.31	CU triaxial test results : UA1(v).	234
7.32	CU triaxial test results : UA2(i).	235
7.33	CU triaxial test results : UA2(ii).	236
7.34	CU triaxial test results : UA2(iii).	237
7.35	CU triaxial test results : UB(i).	238
7.36	CU triaxial test results : UB(ii)a.	239
7.37	CU triaxial test results : UB(ii)b.	240
7.38	CU triaxial test results : UB(iii).	241
7.39	CU triaxial test results : UB(v).	242
7.40	CU triaxial test results : UB(vi).	243
7.41	CU triaxial test results : UB(vii).	244
7.42	q , q' : p' and V : p' : RA1(i).	245
7.43	q , q' : p' and V : p' : RA1(ii).	246
7.44	q , q' : p' and V : p' : RA1(iii).	247
7.45	q , q' : p' and V : p' : RA2(ii).	248
7.46	q , q' : p' and V : p' : RA2(iii).	249
7.47	q , q' : p' and V : p' : RB(ii).	250
7.48	q , q' : p' and V : p' : RB(iii).	251
7.49	q , q' : p' and V : p' : RB(v).	252
7.50	q , q' : p' and V : p' : R2 - 02.	253

Page

7.51 q , q′ : p′ and V : p′ : R2 - 03. 254
7.52 q , q′ : p′ and V : p′ : UA1(i). 255
7.53 q , q′ : p′ and V : p′ : UA1(ii). 256
7.54 q , q′ : p′ and V : p′ : UA1(iii). 257
7.55 q , q′ : p′ and V : p′ : UA1(v). 258
7.56 q , q′ : p′ and V : p′ : UA2(i). 259
7.57 q , q′ : p′ and V : p′ : UA2(ii). 260
7.58 q , q′ : p′ and V : p′ : UA2(iii). 261
7.59 q , q′ : p′ and V : p′ : UB(i). 262
7.60 q , q′ : p′ and V : p′ : UB(ii)a. 263
7.61 q , q′ : p′ and V : p′ : UB(ii)b. 264
7.62 q , q′ : p′ and V : p′ : UB(iii). 265
7.63 q , q′ : p′ and V : p′ : UB(v). 266
7.64 q , q′ : p′ and V : p′ : UB(vi). 267
7.65 q , q′ : p′ and V : p′ : UB(vii). 268

8.1 K_o as a function of overconsolidation ratio and plasticity index. 310
8.2 Variation of K_o with overconsolidation ratio for one-dimensionally unloaded kaolin. 311
8.3 Compression characteristics, reconstituted till HH(a). 312
8.4 Compression characteristics, undisturbed till HH(a). 313
8.5 Compression characteristics, reconstituted till HH(b). 314
8.6 Compression characteristics, undisturbed till HH(b). 315
8.7 Compression characteristics, reconstituted till F(b). 316
8.8 Compression characteristics, undisturbed till F(b). 317
8.9 Compression characteristics, reconstituted till W(b). 318
8.10 Compression characteristics, undisturbed till W(b). 319
8.11 Compression characteristics, reconstituted till W(d). 320
8.12 Compression characteristics, undisturbed till W(d). 321
8.13 Isotropic and oedometer compression characteristics, reconstituted till HH(a). 322

Page

8.14 Isotropic and oedometer compression characteristics, undisturbed till HH(a). 323

8.15 Isotropic and oedometer compression characteristics, reconstituted till HH(b). 324

8.16 Isotropic and oedometer compression characteristics, undisturbed till HH(b). 325

8.17 λ/K : Ro , test TR(1) , till HH(a). 326

8.18 λ/K : Ro , test TU(1) , till HH(a). 327

8.19 λ/K : Ro , test TR(2) , till HH(b). 328

8.20 λ/K : Ro , test TU(2) , till HH(b). 329

8.21 λ/K : Ro , N.Sea till , boring D. 330

8.22 λ/K : Ro , N.Sea till , boring A. 331

8.23 λ/K : Ro for various soils. 332

8.24 (λ/K)max : Ro for Vale of St. Albans tills and other soils. 333

8.25 c_vR : c_vU : till HH(a) (Tests OR(1) , OU(1)V ; TR(1) , TU(1)). 334

8.26 c_vR : c_vU : till HH(b) (Tests OR(2) , OU(2)V ; TR(2) , TU(2)). 335

8.27 c_vR : c_vU : till F(b) (Tests OR(3) , OU(3)V). 336

8.28 c_vR : c_vU : till W(b) (Tests OR(4) , OU(4)V). 337

8.29 c_vR : c_vU : till W(d) (Tests OR(5) , OU(5)V). 338

8.30 Oedometer determined permeability, till HH(a). 339

8.31 Oedometer determined permeability, till HH(b). 340

8.32 Oedometer determined permeability, till F(b). 341

8.33 Oedometer determined permeability, till W(b). 342

8.34 Oedometer determined permeability, till W(d). 343

8.35 k : c_v : m_v relationship, till HH(a). (Reconstituted, undisturbed). 344

8.36 k : c_v : m_v relationship, till HH(b). (Reconstituted, undisturbed). 345

8.37 k : c_v : m_v relationship, till F(b). (Reconstituted, undisturbed). 346

8.38 k : c_v : m_v relationship, till W(b). (Reconstituted). 347

8.39 k : c_v : m_v relationship, till W(b). (Undisturbed). 348

8.40 k : c_v : m_v relationship, till W(d). (Reconstituted). 349

Page

8.41 k : c_v : m_v relationship, till W(d). (Undisturbed). 350

8.42 Relationship between shear strength and liquidity index. 351

8.43 Mohr - Coulomb peak effective stress circles, undisturbed and reconstituted till HH(a). 352

8.44 Peak drained shear strength, direct shear tests. 353

8.45 q , q' : p' and V : p' , reconstituted till HH(a). 354

8.46 q , q' : p' and V : p' , undisturbed till HH(a). 355

8.47 $\log_e p'$: V , reconstituted till HH(a). 356

8.48 $\log_e p'$: V , undisturbed till HH(a). 357

8.49 Normalised stress paths, reconstituted till HH(a). 358

8.50 Normalised stress paths, undisturbed till HH(a). 359

8.51 The reference section in q'/p' : $V\lambda$ space : reconstituted till HH(a). 360

8.52 The reference section in q'/p' : $V\lambda$ space : undisturbed till HH(a). 361

8.53 Reference sections in q'/p' : $V\lambda$ space for U , R , matched at $V\lambda = V_o$ for the reconstituted soil. 362

8.54 Rates of pore pressure change, reconstituted till HH(a). 363

8.55 Rates of pore pressure change, undisturbed till HH(a). 364

8.56 Pore pressure parameter A_f versus overconsolidation ratio. 365

8.57 Pore pressure parameters $A_{c.s.}$, A_f versus overconsolidation ratio, reconstituted till HH(a). 366

8.58 Pore pressure parameters $A_{c.s.}$, A_f versus overconsolidation ratio, undisturbed till HH(a). 367

8.59 E_u / σ'_r : Ro , reconstituted till HH(a). 368

8.60 E_u / σ'_r : Ro , undisturbed till HH(a). 369

8.61 σ'_a / σ'_r : ε_a (%) : normally consolidated, reconstituted. 370

8.62 σ'_a / σ'_r : ε_a (%) : normally consolidated, undisturbed. 371

8.63 σ'_a / σ'_r : ε_a (%) : lightly overconsolidated (reconstituted and undisturbed). 372

Page

8.64 σ'_a / σ'_r : ε_a (%) : Ro = 2 . 373

8.65 σ'_a / σ'_r : ε_a (%) : Ro = 4 . 374

8.66 σ'_a / σ'_r : ε_a (%) : Ro = 8 . 375

8.67 σ'_a / σ'_r : ε_a (%) : Ro = 16 - 32 . 376

ACKNOWLEDGEMENTS.

I should like to express my great debt of gratitude to Dr. J.H.Atkinson who, in 1980, unhesitatingly agreed to supervise my research for this thesis and who, since then, has continuously provided me with encouragement, support and advice. I would like to thank him particularly for giving me the benefit of his considerable experience and knowledge in all matters relating to soil and its testing.

My thanks also go to the academic and technical staff and postgraduate students in the Geotechnical Engineering Research Centre for the help they have given me and for the useful discussions we have had from time to time.

The work described in this thesis was carried out in the Division of Civil Engineering, Hatfield Polytechnic and I should like to thank the Polytechnic for making available the resources and facilities which made this possible. I particularly appreciate the award of a period of sabbatical leave, January - July 1984, which enabled me to complete this thesis. I wish to thank all the staff in the Division for their cooperation and support, especially during this time. The various contributions of technician staff are also acknowledged, especially those of Ted Waring, Len White and Linda Hamling. Others, outside the Division have also given valuable help, notably John Foster (who sorted and mounted the microfossils), Colin Johnson (who made the load cell calibrator), Ralph Taylor (who made the till fabric instrument) and Jim Rice (who took the photographs).

Dr. E. Robinson of University College, London identified the microfossils; Dr. H. Midgley gave help with XRD techniques; Mr. A. Prince supplied laboratory data for N.Sea tills; Mr. A.S. Little helped with the formulation of computer programs. I thank them all.

I extend especially warm thanks to my colleague in Natural Sciences, Allan Cheshire. His unselfish interest and enthusiasm for my research has been a source of considerable encouragement to me throughout.

Finally, I wish to thank my wife, Gail , who has painstakingly deciphered an illegible manuscript and who has spent many hours typing this thesis.

DECLARATION.

I grant powers of discretion to the University Librarian to allow this thesis to be copied in whole or in part without further reference to me. This permission covers only single copies made for study purposes , subject to normal conditions of acknowledgement.

ABSTRACT.

The Vale of St. Albans, whilst nowhere being precisely defined, generally occupies the ground below 150m O.D. between Watford and Ware, a total distance of approximately 30km.

The considerable thicknesses of Anglian sediments found here, and which have hitherto been largely neglected by the engineering fraternity, have been the focus of attention by those whose particular interests lie in the reconstruction of the Pleistocene environments in this area.

Detailed lithostratigraphic sequences of the tills and associated proglacial sediments have been established at five quarry sites selected for study in the Vale. At least two, possibly three, different tills are recognised and described which satisfy the various criteria for a lodgement method of emplacement within the basal traction zone of separate ice sheets.

A programme of fieldwork is described involving in situ testing and sampling of these tills. Clast fabric vectors have been established for these sediments, thus providing a framework within which undisturbed sampling of fabric oriented soils could take place. A new till fabric instrument has been developed for this purpose.

The considerable quantities of colloidally inactive chalk present in the tills is a particularly distinguishing characteristic and, despite their classification as matrix dominant tills, is shown to account for their relatively low activity.

The presence of disseminated carbonate in these soils is also shown to have an effect on other measured engineering properties. The results of tests carried out on samples of both undisturbed and reconstituted till clearly indicate the presence and effect of a cement, possibly calcite, in the matrix.

Based on the combined criteria of microfauna and measured fabric vectors, the probable geographical and geological provenance of the source material for these tills is speculated.

LIST OF SYMBOLS AND ABBREVIATIONS

A	sample cross sectional area (page179)
A , B ,	Skempton's pore pressure parameters
$A_{c.s.}$	critical state pore pressure parameter
A_f	pore pressure parameter A at failure
BP	before present
C	constant (page 58)
C_c	compression index
C_{cr}	recompression index
CD	consolidated - drained
CU	consoliadted - undrained
Cp	permeability index
CSL	critical state line
D_{60} , D_{10}	grain size diameter at 60% , 10% points on soil grading curve
E	modulus of elasticity
E_i	initial loading (tangent) modulus
$E_{i(an)}$	initial anisotropic modulus
$E_i(K_o)$	initial K_o modulus
E_r	reload modulus
E_s	secant modulus
E_u	undrained modulus
$E_u nc$	undrained modulus, normal consolidation
$E_u oc$	undrained modulus, overconsolidation
G_s	particle specific gravity
I_B	brittleness index
Im , Is	peak X - ray diffraction trace intensities for mineral, internal standard
K	X - ray diffraction calibration constant
K_o	coefficient of earth pressure at rest
K_o^{NC} , K_o^{RB}	coefficient of earth pressure along recompression, normal compression line
K_p	coefficient of passive earth pressure
L	magnitude of resultant (clast fabric) vector (eg. page 102) and sample height (eg. page 179)
LI	liquidity index
LL	liquid limit

Ms , Mm	mass of internal standard, mineral in X - ray diffraction
NCL	normal compression line
O.D.	Ordnance Datum
PI	plasticity index
PL	plastic limit
Qu	unconfined compressive strength (page 64)
R	reconstituted
RC	Radiocarbon
Ro	isotropic/one-dimensional overconsolidation ratio
S	degree of saturation
T	torque
U	undisturbed
V	specific volume (= 1 + e)
V_f	specific volume at failure (drained test, page 31), final specific volume (page 179)
V_i	initial specific volume
V_o , N_o	specific volume (isotropic, one-dimensional compression) at p = 1kPa on the normal compression line
V_κ	specific volume on a swelling or recompression line
$V_{\kappa o}$	specific volume (isotropic compression) at $p' = 1$kPa on a swelling or recompression line
$\underline{Vr}$	preferred (clast fabric) vector
V_λ	specific volume on the reference section ($= V + \lambda \ln p'$)
c'	effective cohesion
c'_D	drained peak cohesion
c'_R	drained residual cohesion
c_u	undrained cohesion, shear strength
$c_u r$	remoulded undrained shear strength
$c_u p$	peak undrained shear strength
$c_u PL$, $c_u LL$	undrained shear strength at plastic , liquid limit
c_v	coefficient of consolidation
d	differential operator
d , h	diameter or width , height (page 178)
e	voids ratio
e_g	granular voids ratio
e_o	initial voids ratio
f	percentage clay content (Bernell, 1957 , page 57)
g , h	soil constants defining the Hvorslev surface
$\bar{h}$	average drainage path length
k	coefficient of permeability

ka	thousand years
ko	permeability at specific volume Vo (Bernell, 1957 , page 60)
k_v , k_h	coefficient of permeability for vertical, horizontal drainage
$\log_e$, ln	natural logarithm
ma	million years
m_s	mass of solids
m_v	coefficient of volume decrease, compressibility
p	probability
p'	$= \frac{1}{3}(\sigma'_1 + \sigma'_2 + \sigma'_3)$
p'_c	past maximum effective pressure, preconsolidation pressure
p'_e	equivalent pressure : value of p' at the point on the normal compression line at the same specific volume
p'_o	initial effective isotropic stress
p_T	total stress at the critical state
p'_u	value for p' at the point on the critical state line at the same specific volume
q , q'	$= (\sigma_1 - \sigma_3)$, $(\sigma_a - \sigma_r)$
q'_u	value for q' at ultimate failure
r	a parameter related to the spacing of the normal compression and critical state lines (page 35) ; strength of resultant (fabric) vector.
t_1	time to first reading
t_{100}	time for 100% consolidation
u	pore water pressure
w	water content
Γ	value for V on the critical state line at $p' = 1$kPa
Δ	large increment of ....
Λ	$= (\lambda - \kappa/\lambda)$
M	slope of critical state line in q , q : p space
α	constant (page 59)
γ	unit weight
γ_{dry}	dry unit weight
γ_w	unit weight of water
δ	small increment of ....
ε	strain
ε_a	axial stain
ε_L	longitudinal strain

ε_s	shear strain
ε_v	vertical strain
$\bar{\theta}$	azimuth of resultant fabric vector
κ	slope of swelling or recompression line between adjacent average effective pressure points
$\bar{\kappa}$	average slope of swelling or recompression line (negative)
λ	slope of normal compression line (negative)
$\mu\varepsilon$	microstrain ($\varepsilon \times 10^{-6}$)
ρ	density
σ'_1, σ'_2, σ'_3	major , intermediate , minor principal effective stress
σ_a, σ_r	axial radial stress
σ'_n	normal effective stress
σ'_{oct}	octahedral normal effective stress
σ'_v, σ'_h	effective vertical , horizontal stress
σ_{oct}	octahedral shear stress
τ_p, τ_R	peak , residual shear stress
ϕ'	effective friction angle
ϕ'_D	drained peak friction angle
ϕ'_R	drained residual friction angle

CHAPTER 1. INTRODUCTION.

1.1 General.

The distribution of glacial sediments associated with the Pleistocene is widespread in both the northern and southern hemispheres. In particular, the literature contains extensive reporting of the effects of the Quaternary in the United States, in Canada (where it is estimated (Scott, 1980) that more than 95% of the land surface has been glaciated), in South America, in Northern Europe and in the British Isles. Indeed, even a cursory look at the Quaternary map of the United Kingdom (1st Edition, 1977) is sufficient to demonstrate the extent to which the land surface cover is of glacial origin.

The very large variety of different soil types represented by this relatively short geological period is a particular feature and includes coarse outwash gravels, glacilacustrine silts, fibrous organic peats and very stiff lodgement tills. The very diverse nature of these Pleistocene sediments primarily reflects the changing sedimentary environments resulting from climatic fluctuations, which may have numbered as many as 22 in the last 780,000 years (Shackelton and Opdyke, 1973) .

It is this rich diversity which provides the unifying thread for the study of the Quaternary : it spans many disciplines and brings together specialists with a variety of backgrounds, interests and work experience. These include biologists, botanists, physical geographers, climatologists, soil scientists, glacier physicists, Quaternary geologists and geotechnical engineers.

With such large tracts of land both covered and underlain by glacial sediments of the Pleistocene, it has inevitably meant that the geotechnical engineer's involvement is an important and necessary one. As the number of industrial, residential and recreational developments and projects which require construction on or in these materials grows, then so will, hopefully, the understanding and knowledge of their engineering behaviour.

The scope and nature of the ground investigations required prior to construction in the areas of glacial deposition can, and often do,

provide a considerable challenge to the soils engineer, faced as he is with sediments of roughly similar age but quite different properties. Examples include the metastable Devensian loessic soils of E. England (Fookes and Best, 1969); the fissured, heavily overconsolidated lodgement tills of the West of Scotland (McGown et al, 1975); the deep silt and peat in-filled buried channels of glaciated areas, such as the 38m deep Hoxnian buried channel found during the investigation for the M25 motorway at Higher Denham, Buckinghamshire (Gibbard, 1983). Alternatively, the soils engineer may be faced with the by-products of the glacial processes themselves, for example the extensive effects of Devensian periglacial degradation in the lowland areas of Britain (Jones and Derbyshire, 1983).

On a larger scale, the geotechnical engineer may be involved with the broader design aspects of a gravity structure sited on the floor of the North Sea. Although, almost certainly, the North Sea was a dry land bridge during the late Devensian (Godwin, 1978), today engineers are presented with the many difficulties associated with the investigation of these submarine sediments. Of particular interest are the tills laid down as basal deposits under very great thicknesses of ice, thought to be as much as 1700m in places (Boulton et al, 1978). These tills now carpet a very large part of the North Sea bed.

The nearest equivalent land surface deposits of this type occur on the Norfolk coast. Here, although early Anglian deposits have been recognised and reported on for some considerable time (for example Reid, 1882; Solomon, 1932), they have been investigated only recently from the engineering viewpoint, notably by Kazi and Knill (1969, 1973); El-Ghamrawy (1978) and Gens (1982). The Pleistocene history of these sediments is, both on land and under the sea, extremely complex and no doubt the exact reconstructions will never be fully achieved due, in large part, to uncertainties of correlation resulting from incomplete sedimentary sequences brought about by depositional lacunae or from post-depositional erosion.

Within the broad spectrum of the E. Anglian suite of early Pleistocene deposits may be included the chalky boulder clays of Buckinghamshire reported by Cratchley and Denness (1972) and Denness (1974). Between those parts of Norfolk where the relatively chalk-free Cromer Till occurs and these latter chalky tills lie the Anglian cold stage deposits of the Vale of St. Albans.

This area, due to its geographical location, is extremely important in the elucidation of the Quaternary history of E. England lying as it does between the well documented regions of E. Anglia to the north and east, and the Thames Basin to the south and west.

From the engineering viewpoint very little systematic work on the tills in this area has been carried out. Apart from the findings of Marsland (1977), who has reported the results of triaxial and plate bearing tests on a fissured chalky boulder clay at the site of the Building Research Station, Garston, the literature contains no mention of the engineering properties of these soils.

A detailed investigation of the engineering properties of the tills in the Vale of St. Albans was therefore commenced by the writer in 1981.

1.2 The Study.

At this time a programme of fieldwork and laboratory testing, carried out over the following 3 years, was planned. This work was designed to fulfil the following broad aims :

(i) To locate, identify, describe and record the observed characteristics of the tills exposed in situ at various sites in the Vale and to establish their relationship with the other glacial (and pro-glacial) sediments associated with them.

(ii) To formulate suitable and appropriate site procedures for the undisturbed sampling of these tills so that the laboratory tests described in Chapter 6 could be expedited.

(iii) To carry out both analytical and standard laboratory tests to identify and quantify the mineralogy of the tills and to establish an engineering classification for them, based on their grading and plasticity characteristics.

(iv) To determine the origin, quantity, distribution, effects and significance of chalk in the tills.

(v) To determine the fundamental mechanical properties of the tills in a series of laboratory compression and strength tests using reconstituted till material; to compare these properties with those of the undisturbed soils determined from a parallel series of tests.

(vi) To examine the nature of the engineering properties of the reconstituted and undisturbed tills in their normally consolidated and overconsolidated states and to construct a framework unifying their behaviour across a range of overconsolidation ratios.

(vii) To examine, describe and account for variations in observed behaviour; to compare the findings with those reported for other tills.

(viii) To indicate the likely geological and geographical sources of the till materials and to describe the nature of the post-depositional changes which have taken place in these soils.

In this way, it was anticipated that the results of the research work would not only provide specific engineering parameters characterising the chalky tills of Hertfordshire (where major on-going construction projects involving these soils include the A602 Watton-at-Stone By-Pass and the A1(M) Improvement Scheme at Hatfield), they would also augment the growing bank of engineering data currently available for tills in other areas.

It was also hoped that a careful and detailed examination of the laboratory compression, consolidation and strength characteristics of these tills in the manner proposed would result in a modest contribution being made to present knowledge and understanding of the engineering behaviour of these naturally overconsolidated sediments.

CHAPTER 2. THE GEOLOGICAL SETTING.

2.1 Introduction.

The glacial soils found within the Vale of St. Albans, whilst having been largely neglected by the engineering fraternity, nevertheless have been the focus of considerable geological attention by those whose particular interests lie in the understanding of the various sedimentary processes responsible for them and also in the reconstruction of their depositional environments.

Views and opinions regarding the order in which the inferred events took place during the Pleistocene are being continuously modified as new sections become exposed and are examined. Therefore, although there is general agreement regarding the evidence for an ancestral (pre-glacial) Thames in the Vale (and beyond here into E.Essex), there are still differing opinions concerning when and how its diversion from the Vale first occurred.

Nevertheless, generalisations have been made (Gibbard, 1977) regarding the Pleistocene history of the Vale and a stratigraphy based on an interpretation of the observed sedimentary sequences has been proposed by this author. It is this stratigraphic model which is presented in section 2.4.

However, the findings of a more recent examination of the glacigenic sediments both in the Vale of St. Albans and on the South Hertfordshire Plateau by Cheshire (1983) have implications which affect this stratigraphy and therefore these are also included in this section.

Section 2.2 deals briefly with the Quaternary and its subdivisions in the U.K. The generalised regional descriptions for the various Pleistocene stages which are included here preface the more detailed descriptions which follow for the cold stage sediments found in the Vale.

2.2 The Quaternary in the U.K.

2.2.1 The Quaternary : a definition.

The term 'Quaternary', originally due to Desnoyers (1829) who initially applied it to deposits overlying Tertiary strata in the Paris Basin, was subsequently defined by Reboul (1833) so as to include deposits with fauna or flora still living. Lyell (1839) introduced the term Pleistocene for deposits containing more than 70% of mollusca still living.

The Quaternary Era Sub-Committee of the International Geological Congress, London in 1948 made the recommendation that the base of the marine Calabrian of Italy (stratotype at Santa Maria di Catanzaro, Calabria) should be considered as marking the world-wide beginning of the Pleistocene.

The Red Crag deposits of Walton-on-the-Naze, whose fauna reflect a marked deterioration of climate, are of Calabrian age; hence the Waltonian is recognised as the first stage of the British Pleistocene.

During the Pleistocene there were two major changes or episodes in the magnetic polarity of the earth (the so-called Brunhes and Matuyama epochs) and associated with these a few events - opposite changes of short-lived duration. The beginning of the Olduvai normal event in the Matuyama epoch, dated by the K/Ar method at 1·8Ma (Grommé and Hay, 1971) is now being used by many as the start of the Quaternary (Shotton, 1975). Alternative evidence based on 'calcareous plankton datum events' and 'multiple overlapping criteria' also put the base of the Quaternary here (Haq, Berggren and van Couvering, 1977).

Subsequent subdivision of the Quaternary is based on biological, chemical and physical evidence for climate change from either a cold to a warm stage, or vice versa.

The glacial-interglacial[1] sequence in the British Isles is, therefore, assumed to commence at the top of the Cromer Forest Bed series in Norfolk. The classic succession of cold and warm stage Pleistocene

---

1. An interglacial period separates two cold stages.

deposits found in East Anglia and described by West (1963) is the most complete in this country. A stratigraphic refinement (Mitchell et al, 1973) of the previous nomenclature based on boundary stratotypes for the base of each stage is shown in Table 2.1. In this scheme three cold stages are recognised (Anglian, Wolstonian, Devensian), each being associated with its characteristic tills and fluvioglacial sediments. The probable limits of ice sheet cover in the U.K. inferred from the distribution of these glacial sediments are shown in Fig. 2.1. Early (preglacial) Pleistocene deposits show no evidence of ice sheet cover, but both cold (Beestonian) and temperate (Pastonian, Cromerian) stages have been identified, (West and Wilson, 1966). The first indications of extensive ice sheet cover during the Pleistocene occur at the top of the Cromerian, marking the onset of the Anglian stage.

2.2.2 Anglian Cold Stage.

This stage is known from the extensive deposits of till associated with it. The succession of the type site at Corton Cliff, near Lowestoft (TM 548965) is shown in Table 2.2. The two glacial units in the succession, the Cromer Till and the Lowestoft Till represent two separate incursions of ice into the area, the former from the North Sea and the latter from the west. They are separated by estuarine and backwater environment deposits indicating a cold periglacial environment (West and Wilson, 1966) with no marked amelioration of climate, the Corton Interstadial[1], (Mitchell et al, 1973). Beds 5 - 7 of the succession represent ice marginal conditions associated with deglaciation of the Lowestoft Advance (Bowen,1981). It is representatives of these tills which are in evidence in the Vale of St. Albans and their local distribution and significance will be discussed in later sections.

2.2.3 Hoxnian Interglacial.

Lowestoft Till can be traced inland from Corton to Hoxne in Suffolk (TM 175767) where interglacial lacustrine deposits are seen directly on top of the till. These lake deposits provide the type locality for

---

1. An interstadial signifies a short period within a glacial stage when the climate was (relatively) mild.

the Hoxnian Interglacial stage in Britain (West, 1956). Another section at Marks Tey in Essex (TL 912242) and where the full interglacial cycle is represented is estimated to have a duration of approximately 25ka (Turner, 1970, 1975). Representatives of these sediments are also present in the Vale of St. Albans and will be discussed further in section 2.4.9.

2.2.4 Wolstonian Cold Stage.

Originally designated the Gipping Stage (West, 1963), this has now been renamed Wolstonian and the type area transferred from the Gipping Valley in Suffolk to the type site at Wolston gravel pit in Warwickshire (SP 411750). The revised nomenclature for the divisions of the Wolstonian (Shotton, 1976) are shown below :

Dunsmore Gravel
Upper Oadby Till
Lower Oadby Till
Wolston Sand
Bosworth Clays and Silts
Thrussington Till
Baginton Sand
Baginton - Lillington Gravel

There are, nevertheless, considerable difficulties in clearly defining exact limits for Wolstonian glaciation sediments due mainly to the conflicting results which are obtained when using palaeontological, archaeological, lithological and geomorphological criteria in isolation for dating and long-distance correlation purposes. These difficulties and the various views held by researchers on this point are discussed, amongst others, by Bowen (1981), Catt (1980, 1981) and Cox (1981). A Wolstonian cold stage representative is recognised in the Pleistocene sequence of sediments in the Vale of St. Albans (Gibbard 1974, 1977). and is described in section 2.4.10.

2.2.5 Ipswichian and Devensian.

Following the Ipswichian Interglacial, early Devensian ice advanced almost certainly before 50ka (Catt, 1980) and probably reached its limit in eastern England by 18ka before finally disappearing about

14ka (Penny et al, 1969). Following a short temperate period (about 3ka duration), the final phase of the Devensian (the Loch Lomond Advance) was cold enough to cause reglaciation of the mountainous areas in N.Wales, the Lake District and parts of Scotland.

Within the study area there are indications of a temperate Ipswichian flora and fauna, whilst the cold Devensian stage is represented by aeolian silts derived from a periglacial fringe (see 2.4.10).

2.3 The Vale of St. Albans.

2.3.1 Physical and geological setting.

The Vale of St. Albans in Hertfordshire, whilst nowhere being precisely defined, generally occupies the relatively wide (in places up to 7·5km), gently undulating plain between the towns of Watford in the south-west and Ware to the north-east, a total length of approximately 30km, Fig. 2.2. On its northern flank lie the towns of St. Albans and Welwyn Garden City, whilst to the south lie Borehamwood, Potters Bar and Hoddesdon. Ordnance Survey Sheet 166 (Luton and Hertford) shows much of the Vale occupying ground between 65m and 85m O.D., although parts may occasionally be below 50m O.D., for example the 45m recorded 1km west of Bayfordbury College at TL 308105. The Vale is dissected by a number of river valleys; to the east by the River Lea and its tributaries - the Mimram, Rib, Beane and Rash, and in the west by the Colne and its main tributary, the Ver. The River Colne, rising in Colney Heath (TL 205065) drains the Vale in a south-westerly direction before joining the south-east flowing Ver 1km south-east of Bricket Wood (TL 143012). The Mimram, occupying a relatively broad, and in places steep-sided valley (for example at TL 245150, the site of the Welwyn Garden City viaduct) rises in high ground between Luton and Hitchin to the north-west of the Vale and follows an easterly course north of Welwyn Garden to Hertford, thus making the north-western boundary of the Vale. The River Lea drains in a similar direction but on a more southerly route , separating the towns of Welwyn Garden City and Hatfield. Its confluence with the Mimram is in the county town of Hertford (TL 330135) whence the river is joined by both the Beane and the Rib to drain southwards as the River Lea.

The Geological Survey revised 1 : 50,000 (Drift) sheet 239, Hertford (1978) shows that the Vale is underlain by extensive deposits of

glacial gravel and associated chalky till or 'boulder clay', Fig. 2.3. The Vale is bounded by higher ground to its north and south. In the north the ground rises as the glacial sediments infilling the Vale thin and eventually give way to the Chalk on which they rest unconformably. To the north the Chalk is first seen on the south facing hillsides north of the Mimram at TL 255155. Beyond this and also to the west the chalk hills of the Chilterns reach over 135m O.D. at Corner Farm 1km south of Westwick Hall (TL 098061) in the vicinity of St. Albans, and are covered by variable thicknesses of clay-with-flints.

South of the Vale a distinctive south-west to north-east trending ridge of relatively high ground is formed by Tertiary sediments comprising Reading Beds and overlying London Clay. This high ground reaches 128m O.D. approximately 1·5km east of Brookmans Park at TL 269037 and it is this ridge which forms the southern and eastern boundaries of the Vale.

The most recent geological deposits are those associated with the post glacial (Flandrian) accumulations of river bed alluvium and sand. These deposits are present to a lesser or greater extent in or adjacent to each of the aforementioned rivers.

2.3.2 The ancestral Thames in the Vale.

The glacial deposits in the Vale are diverse and complex and have been variously described by a number of workers. The earliest records of descriptions of the sediments in the Vale are those of Hughes (1868) and Whitaker (1889) whilst working for the Geological Survey. Salter (1905) first suggested that a proglacial Thames had been diverted from an earlier course through the Vale by the Chalky Till ice described previously by Woodward (1897), Prestwich (1890) and Gregory (1894). This idea was later extended by Sherlock and Noble (1912) who invoked two phases of diversion of the Thames in the Vale, an early (Chiltern ice) and a later (Eastern, Chalky Till) diversion. Much has since been written and discussed concerning the Quaternary reconstruction of the proglacial Thames in the Vale and adjacent areas and its subsequent diversion. Notable amongst these are Wooldridge (1938, 1960), Hare (1947) and Wooldridge and Henderson (1955). Wooldridge and Linton (1955) suggest that a Stage I Thames in the Vale was diverted by Chiltern ice southwards into a Stage II course northeastwards via the so-called Finchley depression to rejoin its old

course near Ware. They also suggest that, subsequent to this diversion, ice advancing from the northeast into the Finchley depression blocked the northwards flowing Stage II Thames, diverted it to its present course and, in so doing, deposited the Finchley moraine.

Green and McGregor (1978), examining gravel trains of the Thames, conclude however that diversion of the Thames from the Vale of St. Albans occurred before the end of the Chalky Till (Anglian) glaciation - a view opposite to the two-stage diversion hypothesis of Wooldridge. Indeed, they suggest that the Thames is unlikely to have ever occupied the Finchley depression as it was, in all probability, blocked by Anglian ice at this time.

Earlier, Clayton and Brown (1958) describing the bedded silts and glacial sediments in the Hertford area interpret the sequence as a tripartite glacial unit belonging to one ice advance (Eastern glaciation). They suggest that a large proglacial lake (Lake Hertford) grew as the Thames was dammed at this locality and that subsequent waxing and waning of the ice eventually led to its final advance (Springfield Till ice) at Finchley in the Middlesex loopway.

Gibbard (1974, 1977) describes a pre-Anglian Thames flowing eastwards through the Vale of St. Albans cutting a wide, gently curving valley on a floor of Chalk, Fig. 2.4, joined by a major tributary from the north west in the region of Ware and Hertford. Ice moving from this direction across the Vale dammed the river and a lake of local extent developed. On the basis of varve couplet counts in the laminated glacilacustrine silts, Gibbard has estimated the life of this lake as approximately 500 years. Because there is little evidence of ice overflow by the lake it is concluded by Gibbard that drainage continued eastwards, either partially over or through (via crevasses) or under the ice at this time. Eventually ice overrode the lake and it is possible that the ice lobe (Ware Till ice) moved as far south as Finchley. Following ice retreat the ancestral Thames, it is proposed, resumed its former course in the Vale and was later joined by an increasingly vigorous southwards flowing tributary at Ware. This river preceded the advancing Eastend Green Till ice sheet from the north-east which entered the Vale and again dammed the eastwards flowing river. In so doing, a proglacial lake was formed at London Colney (Moor Mill lake). Drainage of the Vale continued in part eastwards, possibly by means of an ice marginal lake.

Following ice stagnation, a westward flowing braided river fed by glacial meltwater deposited gravels but ceased to flow shortly afterwards.

Cheshire (1983) suggests, however, that diversion of the Thames southwards down the Lea Valley took place during the earlier Ware Till ice stage and that the upper till at Westmill (Eastend Green Till of Gibbard, 1977) had little permanent effect on the main drainage alignments in the area.

2.4 The sequence of Pleistocene sediments in the Vale.

A comprehensive account of the Pleistocene lithostratigraphic units in the Vale of St. Albans is given by Gibbard, 1977. This stratigraphy is adopted and described in this section, although more recent research indicates that a revision in the order of succession consequent upon a reassessment of till types may be required. (Cheshire, 1983 and 1984 , personal communication). Where there are currently difficulties in the interpretation, these are highlighted and alternative viewpoints are expressed. Table 2.3 contains the generalised Pleistocene stratigraphy for the Vale proposed by Gibbard. Included in this Table are notes regarding the later revisions proposed by Cheshire.

2.4.1 Leavesden Green Gravel.

The earliest recognised glacial gravel deposits in the Vale are those found underlying Leavesden Green north-east of Watford (TL 105004). Here a braided river deposit (ancestral Thames) up to 9m thick is seen resting on bedrock Chalk at between 80-84m O.D. It is suggested that these gravels may be correlated with the Westland Green Gravel (Hey, 1965) and are therefore pre-Anglian in age.

2.4.2 Westmill Lower Gravel and Westmill Gravel.

The type section of these deposits at Westmill Quarry (TL 344158) shows a sequence of two thick gravel horizons, the lower resting on Chalk at 58m O.D. and separated from the upper gravel by a layer of chalky till (Ware Till) of variable thickness. The lower deposit comprises a cross-bedded and stratified coarse flinty gravel with chalk, particularly in the Hertford/Ware area of the Vale. The Westmill Lower Gravel, it is suggested, is at least partially the

product of an immature glacial outwash tributary system flowing southwards and joining the proglacial Thames in this area, and is therefore contemporaneous with the Thames Westmill Gravels in the south-east parts of the Vale. (see Table 2.3). The presence of these gravels in the Vale has led to their commercial exploitation by at least two large gravel extraction companies.

2.4.3 Watton Road Laminated Silts.

At Watton Road Quarry (TL 341149), approximately 1·5km west of Ware, 2·5m of brown laminated clayey silts are reported by Gibbard resting on sand correlated with the Westmill Lower Gravel. He describes alternating varved couplets of buff silt (< 10mm thick) and dark brown silty clay (< 3mm thick) numbering 485 pairs. The upper part of the silts is overlain by unlaminated grey brown silty clay grading upwards into (Ware) till above. These laminated deposits have also been recognised by others in the nearby Ware Quarry where Sherlock and Pocock (1924) for example describe 5·6m of brown laminated silty clays. Gibbard concludes that the laminated beds are of local extent, but see the later discussion in 2.4.6 on this observation.

2.4.4 Ware Till.

The lower till at Westmill lies on the Westmill Lower Gravel at between 55m and 60m O.D. On freshly broken surfaces this till is typically dark grey and occasionally dark brown in colour weathering mid-brown in an oxidised and partially decalcified zone (about 300mm thick) at its top and bottom. The till contains chalk clasts and flint in abundance. Gibbard does not recognise this till anywhere west of the Hertford/Ware area of the Vale, although Cheshire (1983) notes that till from a borehole at the site of the British Aerospace factory in Hatfield (TL 216090), 15km south-west of Westmill Quarry, shows particle size and other characteristics typical of the Ware Till type. Associated with this till at Westmill is a pale brown, very chalky deposit lying upon a strongly erosional base cut in a channel partly in the Ware Till and partly on the Westmill Lower Gravel. It is thought that this till represents a later pulse of the same ice sheet associated with the Ware Till.

2.4.5 Westmill Upper Gravel.

At Westmill Quarry the base of this deposit lies between 58 and 62m O.D. either on the eroded surface of the Ware Till or directly on the Westmill Lower Gravel beneath.

This unit is a complex of large gravel lenses with associated current bedded sands and is up to 11m thick. Palaeocurrent directions in the lower 4m of the unit are towards the north-east whilst the upper cross-bedded sands indicate a depositional flow direction from the north-east. "This change in current direction .....at c. 68m O.D. is accompanied by a very marked increase in chalk and other exotic lithologies, and probably marks the appearance of further ice to the north of the area" (Cheshire, op cit).

An interesting feature towards the top of these gravels is the occurrence of calcrete lenses, occasionally over 5m in length. Locally referred to as 'motherstone' by the quarrymen, these very hard naturally cemented (calcrete) gravels result from carbonate deposition derived by solution from the very abundant quantities of chalk at these levels.

2.4.6 Moor Mill Laminated Clays.

Gibbard (1977) describes 2·60m of variegated and laminated silty clays resting on Westmill Gravel at approximately 65m O.D. at Moor Mill Quarry (TL 143025) which he correlates with identical laminated clays at nearby Harper Lane Quarry (TL 164019) 2km to the east. These clays, the product of a proglacial lake, grade upwards into a till designated Eastend Green. Cheshire however, using the combined diagnostic criteria of particle size, acid soluble content and quartz flint ratios has suggested that the till sheet above these clays at this locality is Ware Till type and, therefore, by implication places the Moor Mill Laminated Clays stratigraphically above the Westmill Lower Gravel but below the Ware Till. This proposal is not inconsistent with the presence of a similar thickness of laminated silts at approximately 60m O.D. below the Ware Till at Watton Road (2.4.3). Whilst not observed at Westmill Quarry, these (Watton Road) silts could, nevertheless be equivalent to those at Moor Mill if Cheshire's findings are adopted.

2.4.7 Eastend Green Till.

The type section at Waterhall Farm (TL 297106) described by Gibbard originally exposed 11m of very chalky light grey to blue grey/green till resting on the eroded surface of gravel correlated with Westmill Gravel. Since then this quarry locality has been infilled and an incomplete section of this till has a now well-exposed equivalent at Westmill Quarry. Here, an 'Upper Till' (see Table 2.3) lies on an eroded surface of the Westmill Upper Gravel at approximately 69m O.D. In places the till is stratified in the basal 100 - 150mm ; its upper surface at 73m forms the land surface. It is a light grey to buff very chalky deposit with many small and medium-sized flint clasts.

A till superficially similar in character to this upper till is seen within a quarry at Holwell Hyde (TL 265116) on the eastern outskirts of Welwyn Garden City, (see 5.2.3). At this locality the till is seen to lie both directly on a fine sand of presumed glacial outwash origin and, at a lower level, on another darker till, containing less chalk and with characteristics of the Ware Till.

2.4.8 Smug Oak Gravel.

Gravels associated with glacial outwash of the Eastend Green Till ice sheet have been recognised by Gibbard in several localities in the Vale from Panshanger Quarry (TL 296122) east of Welwyn Garden City as far west as Moor Mill (TL 144026) where over 5m of cross-stratified sand and gravel rest on an uneven channelled surface of Eastend Green Till at between 69 and 73m O.D. Lithologically this unit is predominantly of flint gravel with subsidiary vein quartz and quartzite. Occasional chalky till pebbles are present. Palaeocurrent directions indicate a north-east provenance for this material.

2.4.9 Hatfield Organic Deposits.

Hoxnian interglacial deposits are recognised near Hatfield (TL 212075) in a pit formerly operated by the St. Albans Sand and Gravel Company and have been described by Sparks et al (1969). Here, 400mm of organic deposits lie on 500mm of Smug Oak Gravel overlying a lower till and a slumped till (Rose, 1974). Formerly ascribed Lowestoftian, these tills have been locally correlated (Gibbard, 1977, 1983) with the Eastend Green Till, but again, it is possible that this is the Ware Till

(Cheshire, 1983).

The biogenic deposits, comprising a lower marl and silty clay and an upper organic peat (containing pollen flora) and detritus mud horizons, correspond to the Hoxnian interglacial stage (see 2.2.3)

2.4.10 Post-Hoxnian sediments in the Vale.

Following the period of climatic amelioration marking the deposition of the Hoxnian organics, a cold stage was re-established and, although no till deposits are present, periglacial freeze-thaw conditions returned leading to soliflucted gravel deposits like those represented by the Roe Green Gravel at Hatfield Polytechnic (TL 212075).

The initiation of the present river system in the Vale was probably established at this time and in places the rivers cut down through the entire thickness of glacial deposits.

Mammal and amphibian remains found by Jarvis and reported by Gibbard (1977) at Waterhall Farm (TL 299099) then indicate a temperate climate, of assumed Ipswichian age but of unknown duration, coincident with continuing but intermittent sand aggradation of the Lea Valley.

Following this interglacial stage, evidence from gravels indicating renewed aggradation of the River Lea taken together with the accumulation of substantial volumes of silt and loess in this area indicate, once again, the onset of cold climatic (Devensian) conditions.

After the cessation of gravel aggradation, Flandrian marls and organic silts and muds gradually accumulated adjacent to the rivers in the Vale on the floodplains.

At this time it is likely that the land supported a temperate mixed oak forest flora of the type described by Sparks and West (1972).

2.5 Summary.

Three cold stages of the Pleistocene are recognised in the UK; each stage is characterised by a (glacial) till deposit. Occasionally, in the absence of till, a cold stage is inferred by observing the proximal effects of a large ice mass within an adjacent periglacial fringe.

Interglacial stages are represented by sediments containing fauna and

flora indicative of a temperate, sometimes warm climate.

The Quaternary history of the Vale of St. Albans includes a pre-Anglian stage during which the ancestral River Thames drained the Vale towards the north-east in a valley cut into the underlying Chalk. An examination of subsurface bedrock profiles based primarily on borehole data clearly demonstrates the shape of this valley. Its presence in the Vale at this time is also inferred by a close examination of its associated gravel trains.

These gravels, together with others attributed to subsequent glacial outwash processes, are an important economic asset. There are differing opinions concerning where and how exactly the diversion of the proglacial Thames out of the Vale was achieved. The most recent evidence suggests that the first of two incursions of Anglian ice into the Vale (Ware Till ice) may have been responsible for this and caused its realignment initially down the north to south trending Lea Valley on the eastern boundary of the Vale.

At least one other, later, Anglian cold stage deposit (Eastend Green Till) is present in this area, although local ice pulsing may have produced others.

Evidence suggests that the post-Anglian Pleistocene history of the Vale comprised two further cold stages (Wolstonian, Devensian) but without till deposition, and that these were separated by the warmer interglacials of the Hoxnian and the Ipswichian.

Detailed descriptions and sections of the glacigenic and other Pleistocene sediments which have been identified in selected study sites within the Vale are reported in Chapter 5.

	STAGE	TYPE LOCALITY	ASSUMED CLIMATE	APPROX. AGE (BP) AT BASE
Holocene	Flandrian	(Recent sediments)	Temperate	10ka } RC
PLEISTOCENE	Devensian	Four Ashes Pit, Wolverhampton.	Cold	10-26ka Late 26-50ka Middle } RC 50ka Early
	Ipswichian	Bobbitshole, Ipswich.	Temperate	125ka
	Wolstonian	Wolstan, Warwickshire.	Cold	200ka
	Hoxnian	Hoxne, Suffolk.	Temperate	300ka
	Anglian	Corton, Lowestoft.	Cold	500ka
	Cromerian	West Runton, Norfolk.	Temperate	
	Beestonian	Beeston cliffs, Norfolk.	Cold	
	Pastonian	Paston foreshore, Norfolk.	Temperate	
	Baventian	Easton Bavents cliff, Suffolk.	Cold	
	Antian		Temperate	
	Thurnian	Ludham, Norfolk.	Cool	
	Ludhamian	(borehole)	Temperate	
	Preludhamian	Stradbroke, Suffolk. (borehole)	Cool	2ma
	Pliocene	(TERTIARY)		

Note: RC Radiocarbon dating.
ka, ma, thousand, million years respectively.

Table 2.1 British Quaternary stages.

(Based on Mitchell et al 1973; Bowen,1981; Catt, 1980, 1981.)

Bed	Environment	Nomenclature	
7. Plateau Gravels	glacial outwash		ANGLIAN
6. Pleaure Gardens Till	flow till	Lowestoft Stadial	
5. Oulton Beds	lacustrine		
4. Lowestoft Till	ice		
3. Corton Sands	estuarine	Corton Interstadial	
2. Cromer Till	ice	Gunton Stadial	
1. Silt clay and mud	estuarine and fresh water	Cromerian Interglacial	

Table 2.2 The Anglian stratotype, Corton Cliff, Lowestoft.
(Based on Banham, 1971)

VALE OF ST. ALBANS		
West	East	Stage
Smug Oak Gravel		Anglian
Eastend Green Till (1)		
Moor Mill Laminated Clays (2)		
Westmill Gravel	Westmill Upper Gravel	
	Ware Till	
	Watton Road Laminated Silts	
	Westmill Lower Gravel	
Leavesden Green Gravel		Pre-Anglian

NOTES:

1. The term 'Eastend Green Till' originally proposed by Gibbard (1974) is referred to as 'Upper Till' by Cheshire (1983) who does not recognise this till or its correlative west or south of Hatfield. The till designated Eastend Green type by Gibbard at Moor Mill is correlated with the type Ware Till at Westmill by Cheshire.
2. Therefore, the Moor Mill Laminated Clays which appear below Eastend Green Till in the west in the Gibbard scheme appear below the Ware Till in that of Cheshire.

Table 2.3 Pleistocene stratigraphy in the Vale of St. Albans.

(Based on Gibbard, 1977).

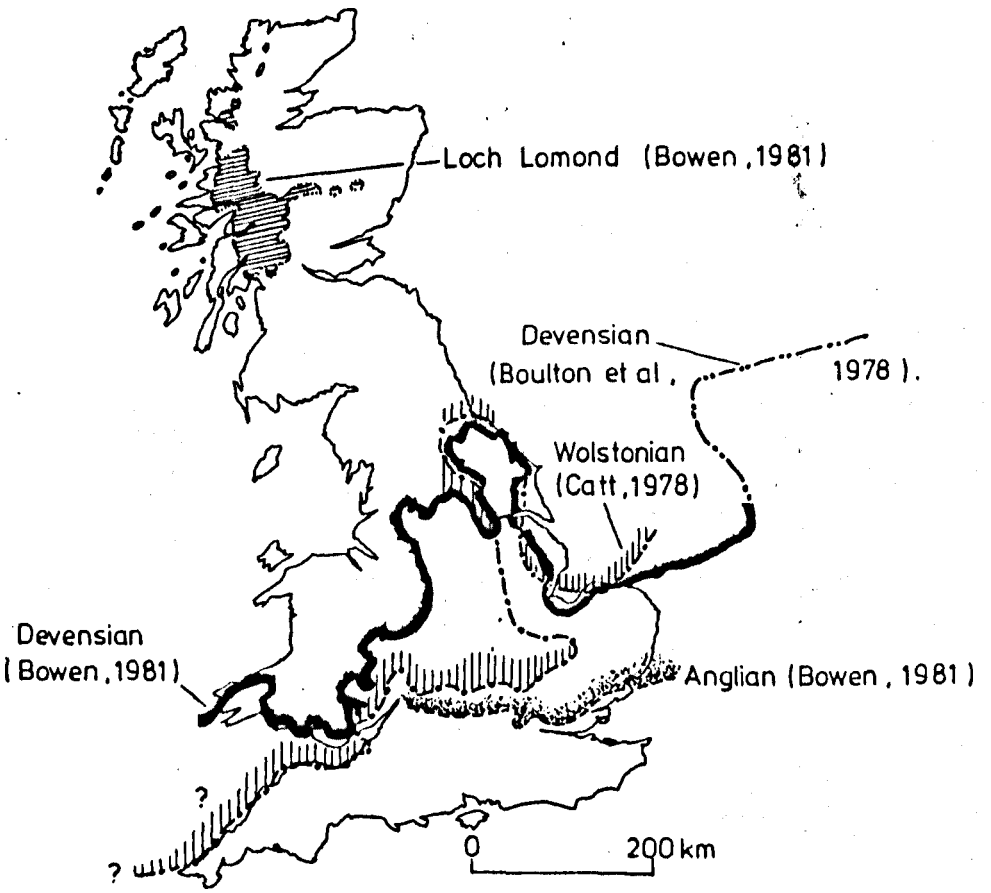

Figure 2.1 Probable limits of Pleistocene ice sheet advance in the U.K.

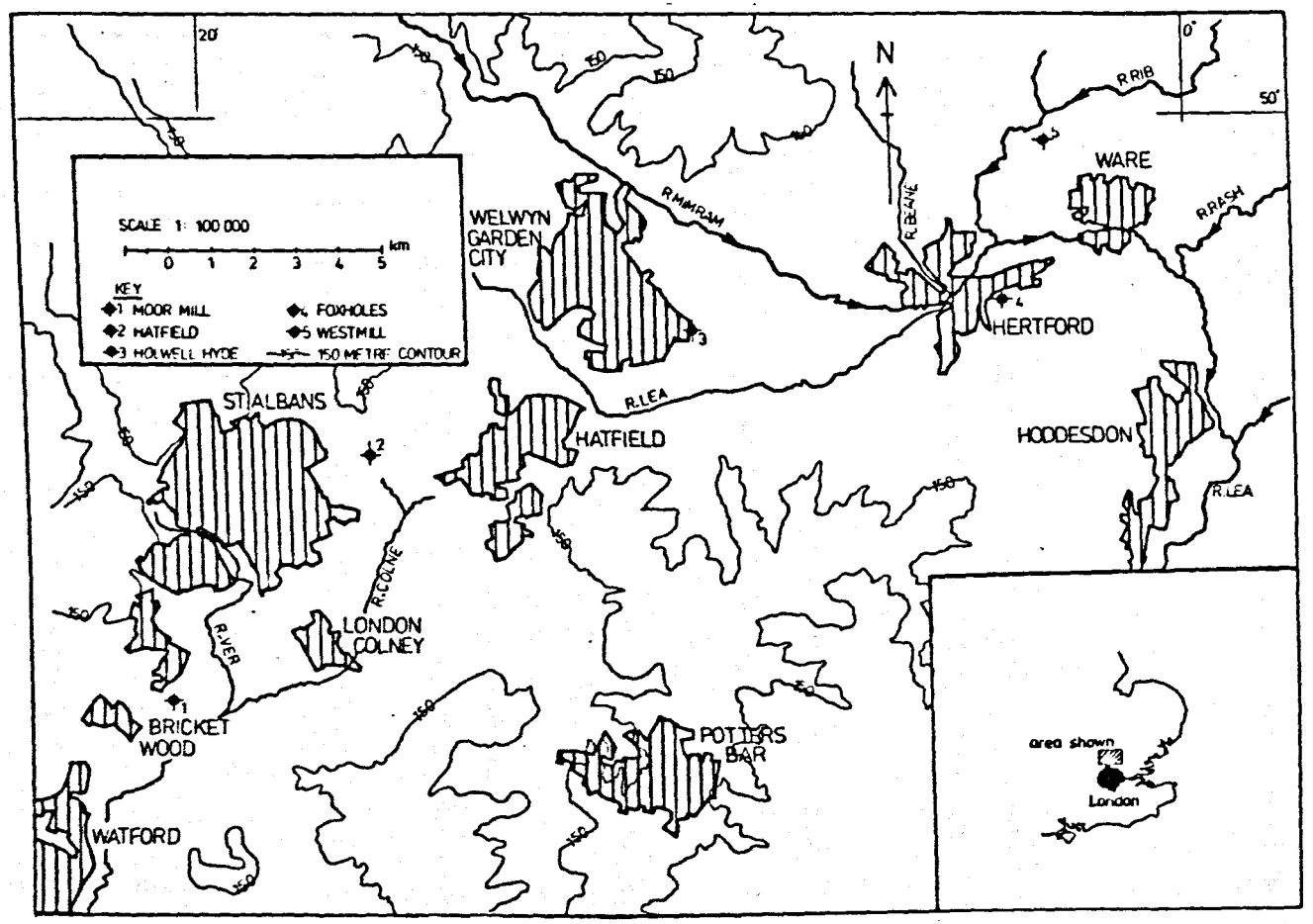

Figure 2.2 The Vale of St. Albans : location.

Figure 2.3 The Vale of St. Albans : solid and superficial geology.
(Sites 1 - 5 as for Fig. 2.2)

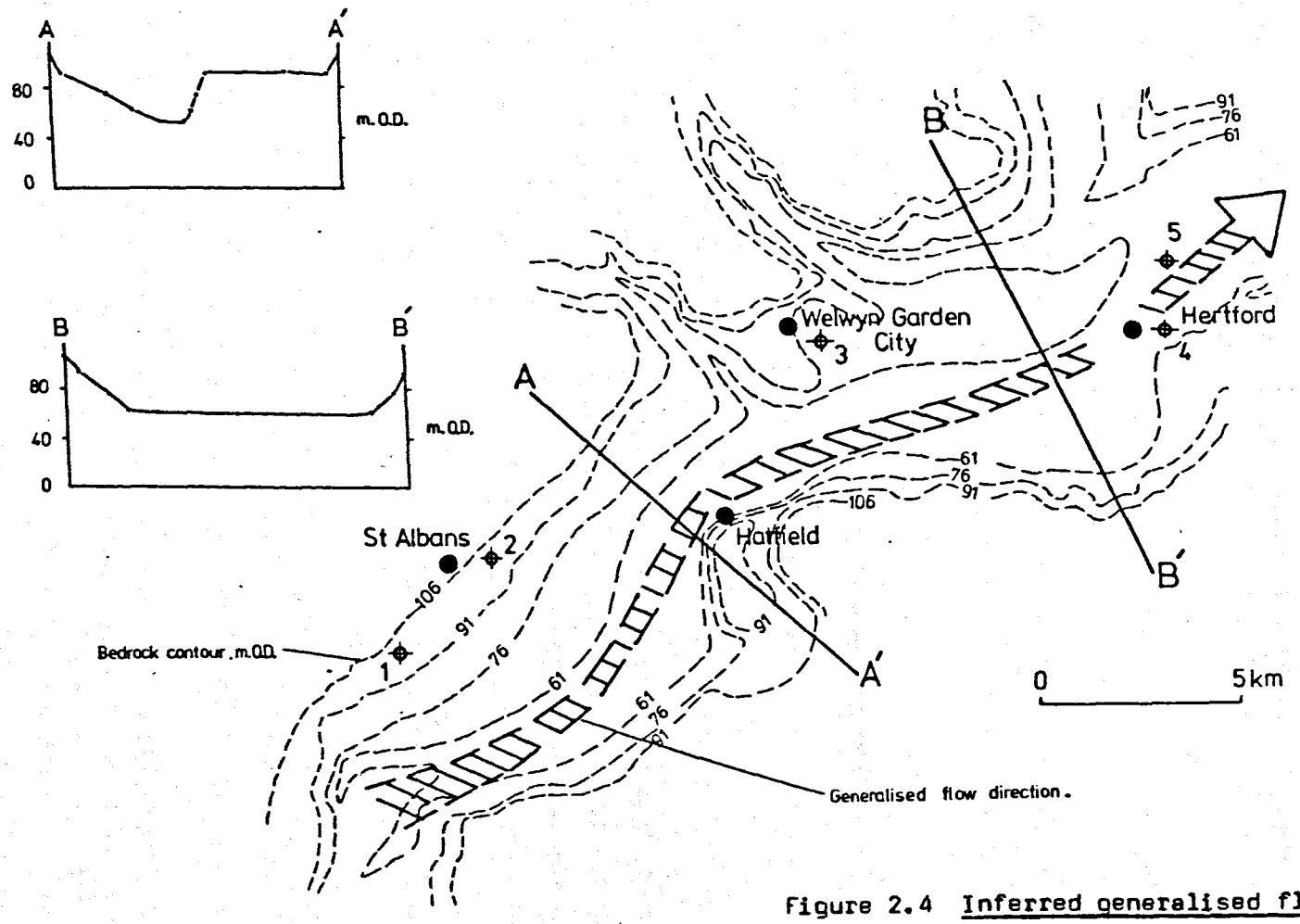

Figure 2.4 Inferred generalised flow of the ancestral Thames in the Vale.

CHAPTER 3. SOME ASPECTS OF THE MECHANICS OF ENGINEERING SOILS.

3.1 Introduction.

This short chapter covers those aspects of the basic framework of soil mechanics within which the test data reported in Chapter 7 are analysed. The statements and assumptions which are made here are not those of the writer but are attributable to others whose various contributions to the development of critical state soil mechanics are widely recognised. Notable amongst these are Roscoe et al (1958); Schofield and Wroth (1968); Atkinson and Bransby (1978) and Atkinson (1981).

The usual assumptions regarding the applicability of Darcy's law, the fundamental theory of one dimensional consolidation and the principle of effective stress are implied throughout.

3.2 Stress invariants and a volumetric parameter.

The choice of stress invariants whose magnitudes do not change as the stress reference axes are varied is an appropriate convention and one which has been adopted by others in their plotting and analysis of soil test data.

Although a coverage of invariant theory is outside the scope of this thesis, it may be noted that the octahedral normal effective stress σ'_{oct} and the octahedral shear stress τ_{oct} are such invariants and, in terms of principal effective stresses σ'_1, σ'_2, σ'_3, are defined :

$$\sigma'_{oct} = \frac{1}{3}(\sigma'_1 + \sigma'_2 + \sigma'_3), \qquad \ldots 3.1$$

$$\tau_{oct} = \frac{1}{3}\left[(\sigma'_1 - \sigma'_2)^2 + (\sigma'_2 - \sigma'_3)^2 + (\sigma'_3 - \sigma'_1)^2\right]^{\frac{1}{2}} \qquad \ldots 3.2$$

In the conventional triaxial test $\sigma'_2 = \sigma'_3$,

$$\therefore \sigma'_{oct} = \frac{1}{3}(\sigma'_1 + 2\sigma'_3) , \qquad ...3.3$$

$$\text{and } \tau_{oct} = \frac{1}{3}\left[(\sigma'_1 - \sigma'_3)^2 + (0)^2 + (\sigma'_3 - \sigma'_1)^2\right]^{\frac{1}{2}}$$

$$= \frac{1}{3}\left[(\sigma'^2_1 - 2\sigma'_3\sigma'_1 + \sigma'^2_3) + (\sigma'^2_3 - 2\sigma'_3\sigma'_1 + \sigma'^2_1)\right]$$

$$= \frac{1}{3}\left[2\sigma'^2_1 - 4\sigma'_3\sigma'_1 + 2\sigma'^2_3\right]$$

$$= \frac{\sqrt{2}}{3}(\sigma'_1 - \sigma'_3) . \qquad ...3.4$$

Redefining terms,

$$p' = \frac{1}{3}(\sigma'_1 + 2\sigma'_3), \quad \text{... mean principal effective stress} \qquad ...3.5$$

$$\text{and } q = q' = (\sigma'_1 - \sigma'_3). \quad \text{... deviator stress} \qquad ...3.6$$

Unlike other engineering materials such as steel and concrete, the volume changes which occur during the drained loading of a soil are not insignificant. The choice therefore of a third variable, the specific volumetric parameter V , is also convenient for it enables volume changes which take place in different sized soil samples to be compared directly. The specific volume is defined as the volume of an element of soil containing unit volume of solids , viz.

$$V = 1 + e , \qquad ...3.7$$

where e is the voids ratio. For a fully saturated soil,

$$e = wG_s , \qquad ...3.8$$

where w, G_s are respectively the measured water content and particle specific gravity of the soil. Hence,

$$V = 1 + wG_s . \qquad ...3.9$$

3.3 One-dimensional and isotropic drained compression of a clay.

An idealised representation of the relationship between V , $\ln p'$ for a soil undergoing drained isotropic compression and swelling is shown in Fig. 3.1 . In this Figure, a soil with no previous stress history and initial state A will, with increasing p' , move along a normal compression line of unique slope $-\lambda$. Defining V_o as the specific volume for the soil at $p' = 1$kPa the equation of isotropic normal compression is

$$V = V_o - \lambda \ln p' , \qquad ...3.10$$

where λ , V_o are soil constants.

If, with state B, the soil is now allowed to swell under isotropic stress reduction, it will move along the unloading line BC with slope $-\kappa$. Defining $V_{\kappa o}$ in a similar manner to V_o , then the equation of a κ - line for isotropic swelling is

$$V = V_{\kappa o} - \kappa \ln p' . \qquad ...3.11$$

Assuming all swelling lines to be parallel κ , too, is a soil constant; unlike V_o however, $V_{\kappa o}$ is not a constant but will depend on the value p'_c where the stress reversal which initiated swelling occurred. Subsequent reloading will cause the state of the soil to move back along BC until the soil reattains a condition of normal compression.

Data from soils subjected to one-dimensional (e.g. oedometer) drained compression can also be expressed in the form $V : \ln p'$ if the values for σ'_v , σ'_h (the effective vertical and horizontal stresses acting on the soil boundaries), are known or can be inferred throughout.

The compression index C_c for a normally consolidated soil in one-dimensional compression in $e : \log_{10} \sigma'_v$ space is defined :

$$- C_c = \frac{de}{d\,(\log_{10} \sigma'_v)} \qquad ...3.12$$

Converting to natural logarithms and writing $\frac{1}{3}\sigma_v'(1 + 2K_o)$ for p', leads to

$$-C_c = \frac{d(V-1)}{0{\cdot}434\, d\left[\ln(3p'/1 + 2K_o)\right]} \quad , \qquad \ldots 3.13$$

where $K_o = \sigma_h'/\sigma_v'$.

During one-dimensional normal compression, the coefficient K_o is assumed to be constant hence, as only differences apply,

$$-C_c = \frac{dV}{0{\cdot}434\, d(\ln p')} \quad ; \qquad \ldots 3.14$$

utilising equation 3.10 , in conjunction with 3.14 ,

$$-C_c = (-0{\cdot}434\,\lambda)^{-1} \quad . \qquad \ldots 3.15$$

Alternatively,

$$\lambda = C_c / 2{\cdot}303 \quad . \qquad \ldots 3.16$$

By a similar argument,

$$-m_v = \delta V / V / \delta\sigma_v' \qquad \ldots 3.17$$

where $\delta V / V$ is the infinitesmal increment in (specific) volumetric strain resulting from an infinitesmal increment in the vertical effective stress $\delta\sigma_v'$; m_v is a parameter variously called the coefficient of volume compressibility or the coefficient of volume decrease.

With a little further manipulation, it can be shown that

$$m_v = \lambda / V\sigma_v' \qquad \ldots 3.18$$

3.4 Behaviour during compression shear testing.

A soil sample is brought to a state of isotropic equilibrium (position B on the normal compression line , lower diagram, Fig. 3.2) in a conventional triaxial apparatus. The drainage valve is then closed and

shearing takes place with no further volume changes permitted. The positive excess pore pressure so generated will cause a reduction in the average effective pressure p' within the sample until, with increasing axial strain, no further changes in effective stress occur. The effective stress path for this sample, when mapped in $q' : p'$ space, (upper diagram, Fig. 3.2) has a starting point B ($q' = 0$; $p' = \sigma'_r$) and an end state, denoting ultimate failure, at B' . In the lower diagram ($V : p'$) point B is shown moving from the normal compression line at constant specific volume to B' . If, on the other hand, drainage from the sample is permitted and the rate of application of axial load is sufficiently slow to prevent excess pore pressures building up, then the total stress and effective stresses are equal and the two stress paths are coincident ($B - B''$, upper diagram). It can readily be shown that the slope of all total stress and drained effective stress paths is $3(q') : 1(p')$. The volumetric strains which can take place in a normally consolidated soil during this type of test are such that the overall volume of the sample reduces, ($B - B''$, lower diagram).

A sample initially normally consolidated to B and then permitted to swell back to A such that an overconsolidated soil is produced will, in undrained compression, initially generate small positive and, subsequently, negative pore pressures. The size of this negative pressure will depend on the initial degree of overconsolidation: thus a heavily overconsolidated sample, for example, will have produced a relatively large negative pore pressure at ultimate failure. With a reducing pore pressure the effective stress will increase, hence the effective stress path for such a sample will be like $A - A'$ shown in Fig. 3.2 . Heavily overconsolidated samples in drained compression are strongly dilatant and, as volume changes are permitted to take place, these samples demonstrate volumetric expansion at ultimate failure, ($A - A''$, lower diagram, Fig. 3.2).

It is a characteristic of this model of soil behaviour that the locus of end states for all normally consolidated and overconsolidated samples tested in undrained and drained compression is a line of critical states in $V : p'$ space, (line of 'critical voids ratio' of Roscoe et al, 1958). Hence, a lightly overconsolidated sample brought to a state C (lower diagram, Fig. 3.2) on the critical state line in $V : p'$ space will, in undrained compression, experience no change in either volume or average effective pressure and will possess an effective stress path which rises vertically from C in $q' : p'$ space.

The projection of the critical state line (of constant gradient M) in the upper diagram, Fig. 3.2 is also shown. Assuming that a soil fails on this line, then the relationship between the frictional constant M and the effective friction angle ϕ' for the soil can be obtained in terms of the corresponding Mohr-Coulomb general stress state. The major and minor principal effective stresses and the shear strength parameters ϕ' , c' at peak failure are related by :

$$\sigma'_1 = \sigma'_3 \left(\frac{1 + \sin \phi'}{1 - \sin \phi'} \right) + 2c' \left(\frac{1 + \sin \phi'}{1 - \sin \phi'} \right)^{\frac{1}{2}} \qquad ...3.19$$

Assuming $c' = 0$,

$$\text{then} \quad \frac{\sigma'_1}{\sigma'_3} = \left(\frac{1 + \sin \phi'}{1 - \sin \phi'} \right) . \qquad ...3.20$$

The corresponding octahedral effective shear stresses from equations 3.5 , 3.6 ,(assuming $\sigma'_2 = \sigma'_3$) are :

$$q' = (\sigma_1 - \sigma_3) \quad \text{and} \quad p' = \frac{1}{3} (\sigma'_1 + 2\sigma'_3) .$$

Therefore,

$$\frac{q'}{p'} = M = \frac{3 (\sigma_1 - \sigma_3)}{\sigma'_1 + 2\sigma'_3} \quad ; \qquad ...3.21$$

By substitution,

$$M = \frac{3 (1 + \sin\phi' - (1 - \sin \phi'))}{1 + \sin\phi' + 2 (1 - \sin \phi')} \quad ; \qquad ...3.22$$

expanding and simplifying,

$$M = \frac{6 \sin \phi'}{3 - \sin\phi'} \quad . \qquad ...3.23$$

In V : ln p' space the critical state line is both linear and assumed parallel to the normal compression line. Defining Γ as the specific volume of the soil at the critical state corresponding to $p' = 1$kPa , then the equation of the critical state line is :

$$V = \Gamma - \lambda \ln p'_u \quad . \qquad ...3.24$$

Therefore, a sample isotropically compressed to a mean normal effective stress p_o' and specific volume V will, during undrained compression, reach ultimate failure on the critical state line when

$$p_u' = \exp\left[(\Gamma - V)/\lambda\right] , \qquad ...3.25$$

and

$$q_u' = M \exp\left[(\Gamma - V)/\lambda\right] ; \qquad ...3.26$$

Therefore,

$$c_u = \frac{1}{2} M \exp\left[(\Gamma - V)/\lambda\right] . \qquad ...3.27$$

Remembering that the gradient of a drained stress path is $3(q')$: $1(p')$ then, for a drained test,

$$q_u' = 3(p_u' - p_o') . \qquad ...3.28$$

Also,

$$q_u' = M p_u' , \qquad ...3.29$$

therefore,

$$q_u' = 3M p_u' (3 - M) , \qquad ...3.30$$

and

$$p_u' = 3 p_o' / (3 - M) . \qquad ...3.31$$

Hence, the specific volume V_f at failure in a drained test may be found :

$$V_f = \Gamma - \lambda \ln p'\left[3 p_o' / (3 - M)\right] . \qquad ...3.32$$

3.5 Normalising procedures : a general view of the state boundary surface.

Samples of the same soil isotropically normally consolidated to different effective pressures will have undrained test paths of different size but similar shape. Furthermore, the path followed by a sample during a drained compression test will reflect its continuously changing specific volume - it will therefore move through an infinity of constant V sections, each of different size. One such constant V section is shown in Fig. 3.3 a). A method whereby differences in the size of undrained and drained test paths for both normally consolidated and overconsolidated samples are taken into

account by scaling stresses according to the equivalent pressure p_e' for the soil is described by Atkinson and Bransby (op cit, pg.201). For a sample in undrained compression the equivalent pressure is the initial isotropic consolidation pressure; for a sample in drained compression it is the mean normal effective stress on the normal compression line at that specific volume.

Therefore, from equation 3.10 ,

$$p_e' = \exp\left[(V_o - V)/\lambda\right] . \qquad ...3.33$$

By scaling both invariants of stress with the divisor p_e' the behaviour of normally consolidated and overconsolidated samples can be unified in the manner of Fig. 3.4 . Here, the test paths for all normally consolidated samples originate at $p'/p_e' = 1$, $q'/p_e' = 0$ and move towards the critical state line along a state boundary surface (Roscoe) which limits their behaviour, (path AD). Overconsolidated samples have normalised test paths originating at $p'/p_e' < 1$ (this ratio reducing with increasing overconsolidation ratio), $q'/p_e' = 0$ and, for perfectly elastic behaviour, rise vertically until reaching either the Roscoe surface (for lightly overconsolidated samples, B) or the Hvorslev state boundary surface (for the heavily overconsolidated samples, C). The behaviour of the most heavily overconsolidated samples is limited by a no tension cut-off of gradient 3 corresponding to tensile failure.

Idealising the Hvorslev surface as a straight line, its equation is

$$q'/p_e' = g + h\,(p'/p_e') , \qquad ...3.34$$

where g , h are the soil constants obtained from Fig. 3.4 .

Substituting for p_e' from equation 3.33 and rearranging gives

$$q' = g \exp\left[(V_o - V)/\lambda\right] + hp' . \qquad ...3.35$$

Using this result with equation 3.24 it can be shown that, on the Hvorslev surface,

$$q' = (M - h)\exp\left(\frac{\Gamma - V}{\lambda}\right) + hp' . \qquad ...3.36$$

An equation (e.g. for Cam clay) of the form

$$\frac{q'}{Mp'} + \left(\frac{\lambda}{\lambda - \kappa}\right) \ln p' - \left(\frac{\Gamma - V}{\lambda - \kappa}\right) = 1 \quad \text{(Atkinson, 1981 page 70)} \qquad \ldots 3.37$$

can be used to make predictions of drained and undrained behaviour for normally consolidated samples on the Roscoe surface.

Atkinson and Bransby (op cit, page 245) also describe an alternative procedure for presenting normalised triaxial compression data based on the size of the constant p' section of the state boundary surface. One such constant p' section is shown in Fig. 3.3 b) . These authors reason that V_o may be difficult to establish accurately, particularly for granular materials, and in addition λ will have a small value in these soil types. The term $\left[(V_o - V) / \lambda\right]$ in equation 3.33 will therefore be large, maybe of uncertain value, but will also have an exponential effect on the value for p_e'.

In this alternative method , the reference section of the state boundary surface is chosen at $p' = 1$kPa , then on this reference section $V = V_o$ on the normal compression line and $V = \Gamma$ on the critical state line. Values for V on the reference section, termed V_λ, are obtained by the projection of points on test paths along lines parallel to both NCL , CSL to intersect the vertical at $p' = 1$kPa. Hence,

$$V_\lambda = V + \lambda \ln p' , \qquad \ldots 3.38$$

where V , p' are the specific volume and mean normal effective pressure respectively.

These authors suggest plotting the deviator stress scaled in the ratio $1 / p'$ against the corresponding V_λ so as to demonstrate the nature of the two sections of the state boundary surface, as shown in Fig. 3.5 .

Here, all points on CSL have $q'/ p' = M$ and all points on the isotropic NCL have $q'/ p' = 0$. Hence, normally consolidated samples (A) will have normalised test paths originating at $V_\lambda = V_o$, $q'/ p' = 0$ and will move along the Roscoe surface to the critical state line when $V_\lambda = \Gamma$, $q'/ p' = M$. The more heavily overconsolidated samples (with initial states 'dry' of critical, e.g. B , C) will have $V_\lambda < \Gamma$ and

will be capable of sustaining $q'/p' > M$ (shaded portion in Fig. 3.5) before reaching the Hvorslev surface and then moving down it towards the critical state line. Predictions of soil behaviour for normally consolidated samples on the Roscoe surface and overconsolidated samples on the Hvorslev surface may be obtained by using equations of the types in 3.36 , 3.37 .

3.6 Pore pressure response in undrained loading.

The response of pore water pressure to undrained compression can be expressed in terms of the two empirical parameters A , B (Skempton 1954, Bishop 1954) according to the equation :

$$\Delta u = B\left[\Delta\sigma_1 + A\,(\Delta\sigma_1 - \Delta\sigma_3)\right] \qquad \ldots 3.39$$

For a fully saturated soil the pore pressure parameter B can be shown to be very nearly unity for a large range of soils. In the conventional undrained triaxial test $\Delta\sigma_3 = 0$, hence the pore pressure response due to an increment in deviator stress may be found from the expression :

$$\Delta u = A\left[\Delta(\sigma_1 - \sigma_3)\right] \qquad \ldots 3.40$$

For the special conditions of isotropy and elasticity, and assuming axial symmetry, the parameter $A = 1/3$. However, soils are not elastic and therefore the value for A has to be determined at a given stress level. Usually, the value for the pore pressure parameter at failure A_f is quoted, and a special interest has been shown in the variation of A_f with overconsolidation ratio , (see for example Bishop and Henkel, 1976, page 118).

An alternative pore pressure parameter has been suggested by Wroth (1981) based on the assumption that a soil reaches ultimate failure on the critical state line.

Fig. 3.6 shows a sample initially isotropically consolidated to A on the normal compression line at $p'A$ and then overconsolidated to O at p'_o to produce a sample with an isotropic overconsolidation ratio $R_o = p'A / p'_o$. It is then subjected to a conventional undrained triaxial compression test and reaches ultimate failure on the critical state line at $p' = p'_u$.

From the geometry of this Figure it can be shown that

$$p_u' / p_o' = \left(\frac{R_o}{r}\right)^{\Lambda} , \qquad ...3.41$$

where $\Lambda = \frac{\lambda - \kappa}{\lambda}$, and r (a parameter related to the the spacing of the NCL , CSL) = $p'A / p'B$.

Therefore, the effective stresses at critical state may be expressed

$$p_u' = p_o' \left(\frac{R_o}{r}\right)^{\Lambda} , \qquad ...3.42$$

and, from equation 3.29 ,

$$q_u' = M p_u' .$$

The total stress at the critical state is

$$p_T = p_o' + \frac{1}{3} q_u , \qquad ...3.43$$

therefore the excess pore pressure is given by :

$$\Delta u = p_T - p_u' , \qquad ...3.44$$

or $$\Delta u = p_o' + \frac{1}{3} q_u - p_u' . \qquad ...3.45$$

From equation 3.40 , and writing q_u for $\Delta(\sigma_1 - \sigma_3)$ max ,

$$A_f = \frac{\Delta u}{q_u} , \qquad ...3.46$$

hence, $$A_{c.s} = \frac{p_o' + \frac{1}{3} q_u - p_u'}{M p_u'} \qquad ...3.47$$

$$= \frac{1}{M}\left(\frac{R_o}{r}\right)^{-\Lambda} + \frac{\frac{1}{3} q_u}{M p_u'} - \frac{p_u'}{M p_u'} ,$$

or , $$A_{c.s} = \frac{1}{M}\left[\left(\frac{R_o}{r}\right)^{-\Lambda} + \frac{M}{3} - 1\right] . \qquad ...3.48$$

At very large overconsolidation ratios , the value of the term $\left(\frac{R_o}{r}\right)^{-\Lambda}$ becomes very small , and approximately,

$$A_{c.s} \longrightarrow \left[\frac{1}{3} - \frac{1}{M}\right] .$$

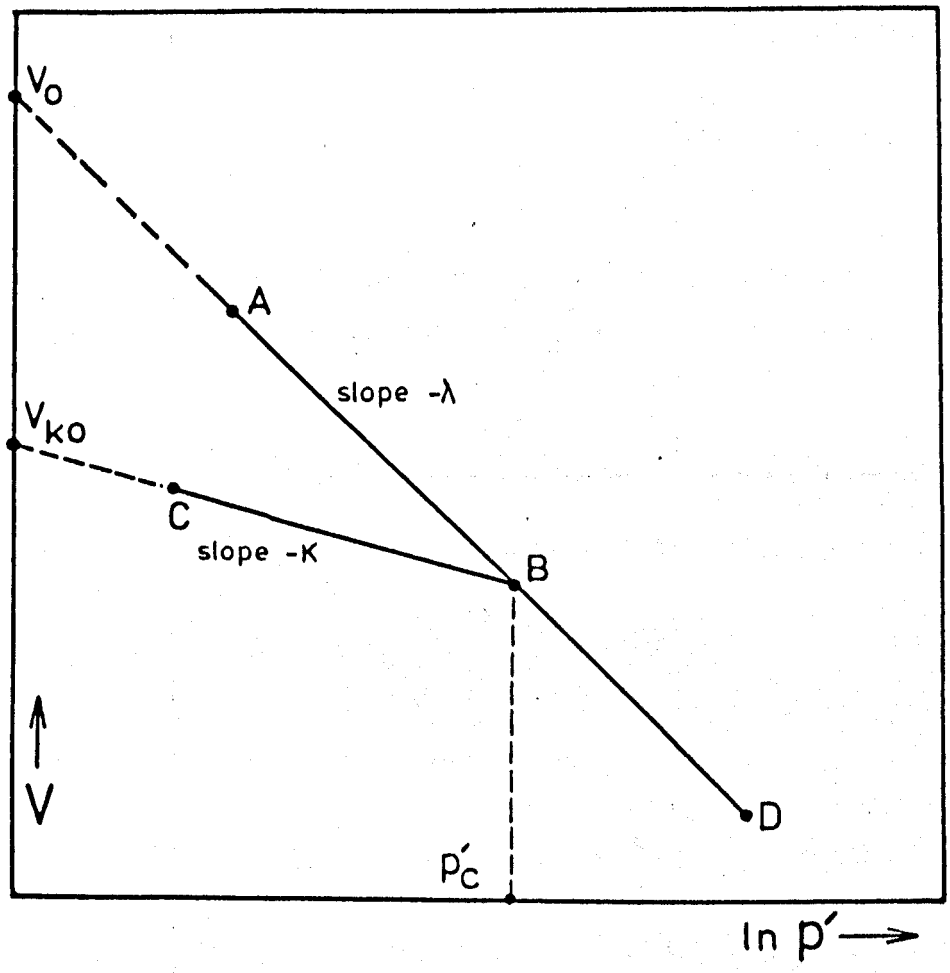

Figure 3.1 Idealised drained isotropic compression and swelling of a soil.

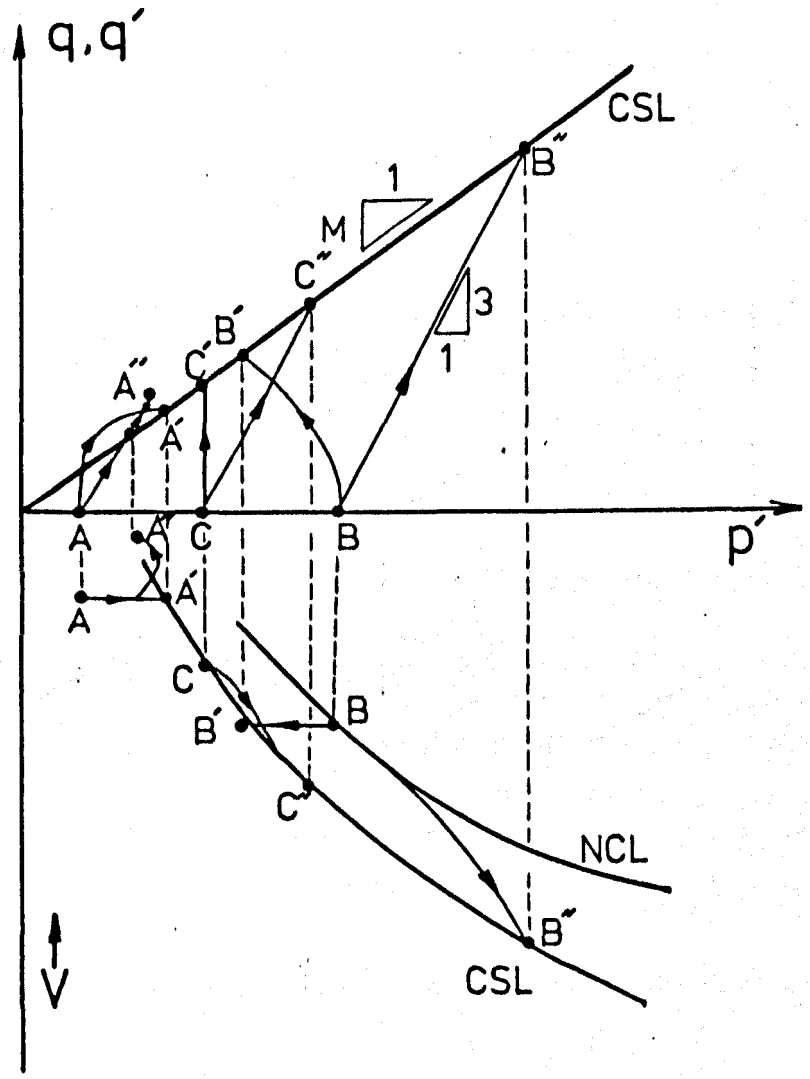

Figure 3.2 q , q´ : p´ : V relationship for soil in drained and undrained compression.

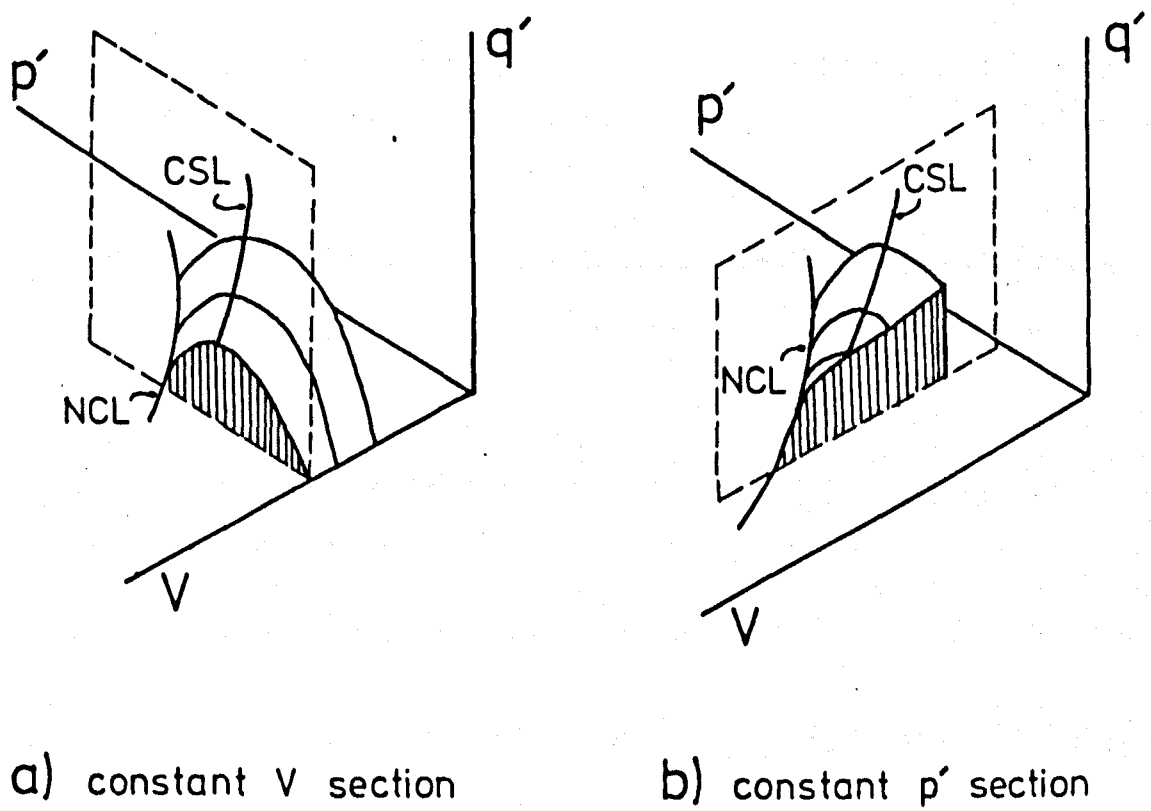

Figure 3.3 General state boundary surface for soil.
(After Atkinson, 1984).

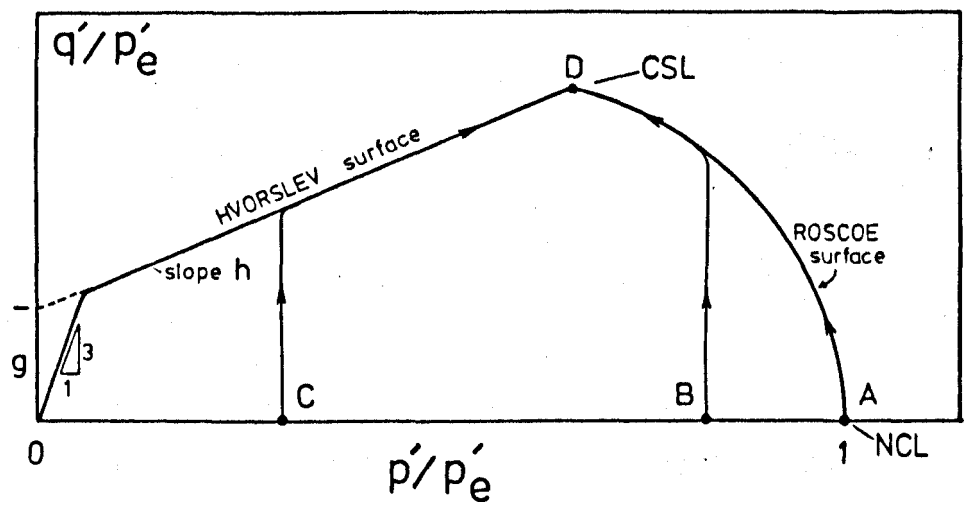

Figure 3.4 The state boundary surface in $q'/p'_e : p'/p'_e$ space.

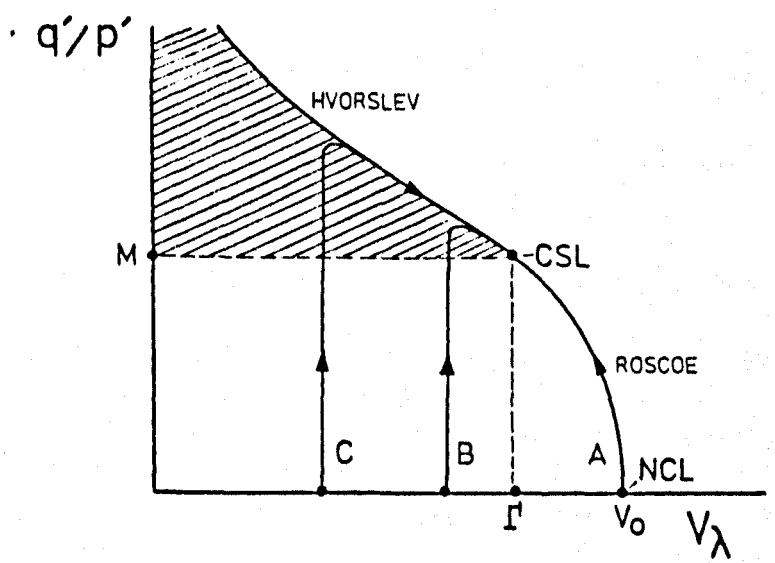

Figure 3.5 The reference section in q'/p' : $V\lambda$ space.

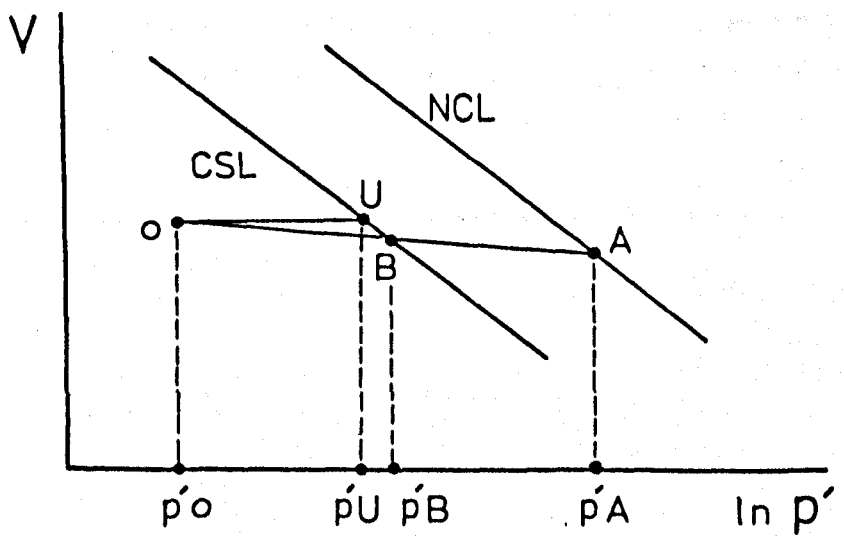

Figure 3.6 Isotropic overconsolidation of a soil.
(see 3.6 in text).

CHAPTER 4. THE CLASSIFICATION OF TILLS AND THEIR ENGINEERING PROPERTIES.

4.1 Introduction.

This chapter is intended to provide a framework within which the geological and engineering materials referred to collectively as 'till' may be viewed, examined and compared.

The variety of differing types of till which have been deposited during the Pleistocene can be related to contemporary processes operating at and beneath the margins of modern glaciers and therefore may be described and classified in terms of the landforms associated with these glacial environments (4.3). Furthermore, an engineering classification of tills, based primarily on grading, can be readily incorporated into a landsystems scheme of this type (4.5.2).

A short section in 4.4 discusses the geological and engineering meanings of 'till fabric' and looks at the presence, origin and significance of discontinuities in these soils.

Other aspects which are significant in the engineering description and classification of (lodgement) tills and which also give an insight into their engineering behaviour (compression, consolidation, strength and elasticity) are reviewed in section 4.5. Whilst it is recognised that not all aspects of engineering behaviour have been covered here, (for example the compaction characteristics of tills and their use as fill materials for earthworks), nevertheless it is hoped that the survey of currently available data contained herein will facilitate a comparison with those for the Vale of St. Albans contained in Chapters 5, 6 and 8.

4.2 Glacial till : a definition.

Although probably having been used for some time before the middle of the last century to describe non-specifically any stiff or hard, impervious and unstratified clay sub-soil (Dreimanis, 1980) , it was Geikie (1863) who defined till as "a stiff clay full of stones varying in size up to boulders produced by abrasion carried on by the ice

sheet as it moved over the land."

Terzaghi and Peck (1967) have defined till as "...an unstratified glacial deposit of clay, silt, sand, gravel and boulders." Sparks and West (1972) state that till "... consists of an unbedded mixture of clay and stones." Linnell and Shea (1960) quoting Goldthwaite (1948) describe till as "ground up rock débris which was carried by the glacier and deposited into a compact, unstratified mass of angular fragments of all sizes : clay, silt, sand, stones and boulders."

The English term 'boulder clay' is occasionally, though less frequently, used as a synonym for till. The term is no longer considered entirely appropriate because neither clay nor boulders are the main constituents of most tills. The French term 'moraine' is also used as a synonym for till, although in N. America the term is usually restricted to landforms only.

'Drift' is a broad generic term encompassing a variety of different clastic sediments during and after deposition by ice in a multitude of depositional environments, both continental and marine.

Eyles (1983) argues that the term 'till' has a specific genetic definition and, quoting Boulton (1972), refers to an aggregate "... whose particles have been brought into contact by the direct agency of glacier ice and which, though it may have undergone glacially-induced flow, has not been significantly disaggregated."

Despite the many diverse till types represented and the various names used to describe them, the glacigenic sediment termed till (or glacial till) must :

(i) have been ice transported,
(ii) be a clastic sediment,
(iii) show well graded particle size characteristics,
(iv) be unstratified (but see 4.3.2).

In addition, most till types will be petrographically and mineralogically heterogenous (McGown and Derbyshire, 1977) and some till types will be very compact and overconsolidated, depending on their mode of formation.

4.3 Tills and their depositional environment : a landsystems approach.

It is now generally recognised that textural and mineralogical criteria alone are inadequate as a basis for the identification of

different till types, due mainly to the considerable overlap evident in this respect. As a basis for discriminating between various till types there is, therefore, an increasing emphasis being placed on the interpretation of overall glacial stratigraphy within the particular geomorphological context of the till.

Fookes, Gordon and Higginbottom (1975) applied this technique of terrain analysis to glacial landscapes and have proposed a scheme of till classification based on the existence of discrete landsystems in glaciated environments. In their scheme, they recognise three landsystems :

(i) Lodgement Till Plain,
(ii) Glaciated Valley,
(iii) Fluvioglacial and Ice Contact.

Within each of the proposed landsystems are to be found tills which are a product of their particular glacial environment. Therefore, the Lodgement Till Plain is characterised by a relatively flat plain on which, classically, is imposed a drumlin topography. Examples of this type of landsystem are to be found in the West of Scotland (McGown et al, 1975) and would also include the 'drowned' drumlins of Clew Bay, Co. Mayo (Sparks and West, 1972).

The Glaciated Valley landsystem comprises glacial materials which include all those that have been deposited directly from melting ice, but without any modification by meltwater. According to these authors the materials belonging to this landsystem are deposited at the edges of the ice mass (which may be advancing, retreating or stagnating) and will give rise to terminal, medial and lateral moraines.

The third category of landsystem, which contains fluvioglacial and ice contact deposits, comprises all glacial sediments that have been laid down by meltwater streams. As a result these deposits are sorted, graded and stratified, are cohesionless, but often include till bodies. The most commonly recurring landforms in this landsystem are eskers, kames and ice stagnation features, for example kettle holes.

However, Boulton and Paul (1976) quoting Christian and Stewart (1957, 1968) believe that a landsystem should comprise "... an area with a recurring pattern of topography, soils and vegetation..." and suggest that Fookes et al "... offend this principle by placing in different landsystems elements which are normally intimately associated." They instance cases whereby lodgement tills often have push moraines and

fluted moraines on their surface and may also be very closely associated with proglacial outwash and eskers.

They have therefore proposed an alternative tripartite (glaciated valley; supraglacial; subglacial/proglacial) landsystems approach embodying two principal sediment associations. This original scheme is shown in Table 4.1. Eyles (1983, page 14) recognises the same three landsystems but shows an extended version of this scheme in his classification. Boulton and Paul basically distinguish two modes of till deposition in their scheme which depend on the position of transport of the glacial débris. In the following descriptions of these reference should also be made to Fig. 4.1.

4.3.1 Subglacial tills.

Glacial débris transported near to the glacier bed will be deposited subglacially as lodgement till. According to Boulton and Paul (op cit page 171) lodgement till deposition occurs "... when the force imposed by the moving ice on particles or débris-rich ice in traction over the glacier bed is inadequate to overcome the frictional drag between these and the bed." Ice flowing over an irregular bedrock surface will tend to form lee-side tills within the cavities on the lee of hummocks in the manner described by Boulton (1970) and Peterson (1970).

Lodgement tills show a wide range of particle size (4.5.2), may be fissured or jointed (4.4.2) and, according to McGown and Derbyshire (op cit page 398), "... are usually stiff, dense, relatively incompressible soils which behave in many respects like soft rocks." In addition, they invariably possess a fabric, (4.4.1).

McGown and Derbyshire also recognise a comminution till which is formed in the basal traction zone (within 500mm of the base of the ice) by mutual abrading and attrition of bedrock fragments, as well as a deformation till caused by glacial drag on the underlying bedrock.

The principal landforms on lodgement till surfaces comprise large ellipsoidal drumlins (cf Fookes et al. Lodgement Till Plain landsystem) elongated in the direction of ice movement, fluted moraine ridges lying parallel to ice sheet flow direction and push moraines formed parallel to the glacier margin.

Lodgement tills, therfore, would be grouped together into a combined

subglacial/proglacial landsystem possessing, as they do, geomorphic elements initiated in both of these glacial domains.

4.3.2 Supraglacial tills.

The supraglacial tills comprise one group which is derived principally from material falling onto the surface of glaciers from flanking valley sides and nunataks to form supraglacial morainic till. This type of till is angular, coarse grained, permeable and usually possesses a high angle of friction. Whalley (1975) reports stable slopes of between 35°- 70° in this type of material at the Fee Glacier near Saas Fee, Kanton Wallis. The medial and lateral moraines and kame terrace landforms characterising this till type are the dominant features of the glaciated valley landsystem.

Another supraglacial group of tills is derived directly from subglacially eroded débris. This latter group can be divided into two classes :

(i) Flow tills.

The entrainment of débris in thick layers near to the base of the ice mass (within englacial débris bands) can, during ablation near to the ice front, release débris from dykes within the containing ice onto the glacier surface. This débris assemblage is often fluid and, therefore, mobile. (Boulton reports débris at Aavatsmarkbreen, Spitsbergen with a water content of 25% equivalent to a liquidity index of 1·8). This can lead to a continuous mantle (perhaps 2 - 3m thick) of accumulated flow till fed both subaerially by sporadic high moisture content (allochthonous) flows and also by basal accretion of newly released (parautochthonous) débris, particularly in downglacier positions. According to McGown and Derbyshire (op cit) flow tills consist essentially of superglacial (sic) comminution débris, but can also occur by flow of subglacial melt-out tills (see (ii) below) in subglacial cavities. The allocthonous upper element of flow tills possesses a greater variation in both particle size and plasticity index than the parautochthonous lower element or in lodgement tills or in the englacial débris from which all these tills are derived.

(ii) Melt-out tills.

Flow till capping will inhibit ablation of underlying ice hence preserving extensive areas of stagnant ice both on and beyond the actively retreating margin of the ice sheet. During summer melting

free-standing frozen débris bands collapse to produce flow tills which grade down into melt-out tills which melt out of the underlying ice. These tills therefore retain some of the original englacial (banded) features. Boulton reports glaciers in Spitsbergen with débris bands containing 40-50% débris (by volume); loss of ice matrix during melting therefore produces melt-out tills with very open structures and with relatively low bulk unit weights.

The flow and melt-out tills belonging to the supraglacial landsystem described are therefore characterised by a supraglacial sediment association comprising supraglacial kamiform outwash and proglacial outwash, both of which may be superimposed on lodgement till. Thus there is frequently a complex till-outwash-till sequence in this glacial domain, Fig. 4.1 .

4.4 Till fabric.

4.4.1 The geological and the engineering meanings of fabric.

The term 'fabric' applied to till, and when used by Quaternary scientists, is usually assumed to mean the spatial arrangement and lineation of till pebbles or clasts in the matrix of the till (see for example Holmes, 1941; Andrews and Shimizu, 1966; Andrews and Smithson, 1966; Andrews and King, 1968; Cowan, 1968; Hill, 1968; Harris, 1969; Kirby, 1969 and Andrews, 1971.).

It has long been recognised (for example, Hind, 1859; Miller, 1884; Bell, 1888; Upham, 1891) that clasts assume a collective preferred orientation within a till body, and work by Richter (1932, 1933, 1936) first demonstrated the relationship between preferred till axis orientation and direction of ice movement. The classic treatise by Holmes (1941) describing till fabrics from New York State has been followed by many other published works since that date describing the applications of till fabric studies primarily in the reconstruction of glacial environments. West and Donner (1956), for example, used the technique to infer regional directions of ice movement in E. Anglia and their paper includes data from five sites in the Vale of St. Albans.(1)

---

1. Hertford, TL 337128; Stapleford, TL 308152; Cole Green, TL 274108, Smallford, TL 195070; Colney Street, TL 148023.

Subsequently, Gibbard (1974, 1977) and Cheshire (1981, 1983) have demonstrated the existence of pronounced till fabrics within the glacigenic sediments of the Vale and have used these data to infer directions of ice advance into the area.

The mechanisms by which till stones become oriented within the dynamic environment of the basal traction zone have been examined by Glen, Donner and West (1957) and will not be considered further here. Boulton (1976a),however, notes within recent lodgement tills that there is a "... tendency for the development of strong parallel fabric peaks with an up-glacier dip, except for those tills where post-depositional deformation has occurred."

The meaning of till fabric as described above is somewhat different from the broader meaning of the term 'fabric' applied to soils in the engineering sense. Mitchell (1956) who investigated the effect of remoulding soil on engineering properties, particularly permeability, defined soil fabric as "... the appearance of pattern produced by the shapes or arrangement of the soil grains, independently of the external boundaries of the material." Quigley and Thompson (1966), investigating the anisotropic consolidation characteristics of the sensitive and highly flocculated Leda clay from Ottawa, refer in their paper to "... measurements of the clay particle parallelism (fabric).."; while Fookes and Denness (1969) describe a "fissure fabric" in relation to contoured stereograms of fissure data from the Cretaceous sediments of S.E. England.

Rowe (1971, 1972) used the term 'fabric' to encompass the large, medium-sized and small syn- and post-depositional structures within a soil, including primary sedimentary structures (laminations, layers, varves) and also secondary structures, such as fissures, all of which could markedly affect the engineering behaviour of the soil. In the 1971 paper Rowe describes, amongst others, the'visual' fabric of a London clay and a silt-intruded weathered boulder clay.

McGown, Sali and Radwan (1974) again used the term 'fissure fabric' in relation to tills at Hurlford, Ayrshire, and later papers by McGown , Anderson and Radwan (1975), and McKinlay et al (1975) also refer to the 'soil fissure fabric' in relation to west central Scotland lodgement tills.

In their 1974 paper, McGown et al give an indication of fissure size appropriate to their geographical area by stating "... the features which are of particular interest in this study are the fine

cracks and joints which on very close examination are apparent in the boulder clays." Interestingly, Kazi and Knill (1973), describing the engineering characteristics of stiff, overconsolidated fissured glacial lake clays in Norfolk do not introduce the term 'fabric' in this context. (In fact nowhere does the term appear in their paper.) Derbyshire, McGown and Radwan (1976) describe the 'total' fabric of landforms and extend the term to include "... a wide range of features of both primary and secondary origin including folds, thrusts, fissures (the macrofabric), disposition of the clasts (the mesofabric) and organisation of the matrix (the microfabric)." (1)

A later, more general definition (McGown et al, 1980) of soil fabric is reported as meaning "... the nature, form and arrangement of units of soil materials and voids." Marsland, Prince and Love (1982) in a paper dealing with offshore glacial clays and tills state "... The summation of all directional properties and groupings of features at all scales is referred to as the total fabric." These authors also offer guidelines for the identification of a macro- , meso- and microfabric in a soil.

From the foregoing it would appear, therefore, that similar terms can, and will convey different meanings to workers in related but different disciplines. To the Quaternary geologist the term 'till fabric' has a quite restricted and precise usage which is conveyed more or less exactly by the engineer's term 'mesofabric'. To the engineer, however, 'till fabric' has a much broader meaning and encompasses three discrete elements (macro, meso, micro) which, taken together, describe the total geometrical organisation of soil structure, clast content and small particle (essentially clay and silt)(2) assemblage.

4.4.2 The presence, origins and significance of discontinuities in till.

The presence of fissures and discontinuities in clay soils has been reported by various workers and several schemes of classification,

---

1. The term 'macrofabric' had been used earlier than this by Ostry and Deane in a 1963 paper, but in a different context. Here the authors wrote "... Till-fabric analyses that involve the field measurements of stones in the till is (sic) herein defined as macrofabric analyses."

2. Korina and Faustova (1964) and Benedict (1968) include sand-sized particles in their definition of microfabric.

based on assumed origins, have been proposed for these. Fookes (1965) presents a tripartite scheme of fissure classification based on his field observations of the overconsolidated clay of the Siwalik system, Mangla, and in a later paper Fookes and Denness (1969) considerably extended this scheme and included the effects of depositional environment, lithology, bedding, stress release, tectonism, diagenesis, weathering and age of exposure on fissure patterns. Skempton et al (1969) established a scheme of classification for the discontinuities they observed in the London clay at Wrasbury and Edgware. Chandler (1973) presented an interesting scheme of classification (applicable to uniform clays) based on the four environmental controls of deposition, tectonism, erosion and weathering, together with their associated processes.

Although not related specifically to the origin of fissures in tills, these schemes are useful nevertheless as indicators of the likely fissure forming processes involved.

In their study of the fissuring in the glacial lake clays at Happisburgh and Cromer, Kazi and Knill (1973) conclude that "... the well defined fissure sets... are almost certainly a conjugate shear pattern associated with an east-west direction of ice movement overriding the clays." They also state that a subsidiary set of horizontal fissures are probably due to a release of the overburden.

An unusual occurrence of sub-vertical fissures (also described variously as 'fractures' and 'joints' in the paper) is reported by Derbyshire and Jones (1980) in tills of assumed Wolstonian age from Church Wilne, near Derby. These authors describe fissures possessing a marked concavity in both horizontal and vertical planes and they propose an unusual mechanism of point loading by englacial basal boulders on a frozen till surface for this feature, although they suggest that curved fissure sets in tills may be quite widely distributed. This paper also contains a useful summary of the types and causes of discontinuities in till. Significantly, it is pointed out that, with few exceptions, the reported occurrences of discontinuities in till indicate their large ($>$ 60mm) spacing. The authors conclude that the only features occurring on a 'micro' ($<$ 1mm spacing) scale[1] are those low angle shear planes due to stress

1. It is unfortunate that the authors introduce the terms micro, meso, macro to describe fissure spacing here which could lead to confusion, see earlier discussion, 4.4.1 .

relief, and also a variety of fissures produced by unloading of subaerial slopes, hydration, desiccation, freezing and a range of pedogenic processes. All other fissures are meso (1 - 60mm spacing) and macro (> 60mm spacing) features, almost exclusively sub-vertical, produced by overriding ice (Kupsch, 1955), vertical stress relief (de Sitter, 1964), ice pushing, or propagation (mimicking) of adjacent bedrock joints following glacial unloading, (Grisak et al, 1976).

Boulton and Dent (1974) and Boulton, Dent and Morris (1974) have reported the occurrence of numerous sub-horizontal joint planes in lodgement tills at both Nordenskioldbreen in Spitsbergen and Breidamerkurjokul, Iceland. Here these authors have consistently observed upper, remoulded and sheared (but not jointed) horizons in these till bodies lying above deeper, sub-horizontally jointed layers which, from the field evidence, suggests could "... be the result of elastic rebound in the till due to pressure release on deglaciation." (Boulton, 1976b, page 298). At Nordenskioldbreen the sub-horizontal joint surfaces also carried heavy slickensides in the direction of ice movement; associated with these were 'dilation joints' along which shear failure is presumed to have occurred during unloading. Other joint types observed by these authors in tills include close networks of sub-vertical joints with polygonal surface patterns which are due to rapid drying out after exposure in both lodgement and supraglacial tills, and jointing associated with the formation of segregation ice lenses in the surface horizons of till bodies resulting from freezing.

It was Terzaghi (1936) who first suggested that joints in clayey sediments could reduce soil strength by as much as one fifth to one tenth of that measured on unjointed samples in the laboratory. The effects of discontinuities on the engineering properties of different undisturbed soils have subsequently been investigated amongst others by Ward et al (1965), Fookes and Wilson (1966), Marsland and Butler (1967), Lo (1970) and Marsland (1971).

McGown et al (1974) have investigated the relationship between slope failure patterns and fissure fabric in till drumlins at Hurlford, Ayrshire. On the basis of 815 fissure[1] measurements within the till, the authors were able to demonstrate the existence of two sets of vertical and near-vertical planar fissure surfaces (with estimated

1. Fookes (1965) defined fissures as "small scale fractures existing in clay and siltstone beds but not crossing the boundary of the bed."

surface areas of between $0{\cdot}001m^2$ and $1m^2$) conjugate about the landform long axes, together with a subsidiary set of sub-horizontal fissures. They also identified a correlation between preferred fissure orientation in the till and a marked directional dependence of in situ shear strength, which in turn was demonstrably controlling slope failure patterns on cuttings made for the Hurlford By-Pass.

McKinlay et al (1975) produced guidelines for the representative sampling and testing of fissured lodgement till having examined the effects of sample size and orientation on the measured properties of strength, compressibility and consolidation in these materials. They have concluded that the presence of fissures (rather than the presence of stones) is the dominating factor in the selection of a representative sample size for laboratory testing purposes. They recommend that sample diameters for triaxial shear and one-dimensional consolidation tests should be 20 times the minimum fissure spacing and with a height to diameter ratio of unity.

A comprehensive treatment of the recording and analysis of soil macrofabric (discontinuity) data for engineering purposes is given by McGown et al (1980). Here, the authors endorse the recommendations previously given by McKinlay et al (op cit) regarding sample sizes based on fissure spacing coefficients. However, in a subsequent discussion to this paper, Koo (1981), reporting on the widely spaced relict joints in the residual soils of Hong Kong, makes the point that testing a sufficiently large sample containing representative joint sets would be impossible here due to their extensiveness.

4.5 Till as an engineering material.

The complex glacial processes based on the ice transport modes outlined in 4.3 produce a variety of different till end products with contrasting characteristics. Therefore, the density and porosity, for example, of a basal lodgement till will contrast with that of a till produced by a melt-out mechanism.

Lithological and mineralogical variations will also reflect the nature of the source bedrock character, and the distance over which the material is then transported will subsequently modify its textural composition. The distribution of glacial soils in Britain has been shown by Derbyshire (1975) to generally reflect source bedrock lithology. For example, the Precambrian gneisses, granites and

quartzites of N.E. Scotland support granular tills, whereas the younger Permo-Trias, Jurassic and Cretaceous strata of central and eastern England have given rise to the tills containing a higher percentage of fines found in E. Anglia. Source bedrocks of intermediate hardness, for example Carboniferous Limestone and Keuper Marl have given rise to the well-graded tills of Cumbria and Yorkshire. A similar correlation, based on predominant lithological characteristics of source bedrock and till type, has been established by Prest (1961) to account for the large variety of tills found in Canada.

The effects of post-depositional history on till character is also important. Interglacial and post-glacial processes are varied and complex and their effects are compounded. Therefore, one lodgement till subsequently overlain by another will have been ice loaded (and unloaded) twice; the effects of periglaciation (permafrost, freeze-thaw) together with the changing hydrological conditions of fluctuating ground water levels (Grisak et al, 1980), post-glacial weathering (Eyles and Sladen, 1981) and the cementing by minerals taken into solution (Milligan, 1976) will affect and modify, often radically, earlier genetic characteristics. Nevertheless, the rich variety of end products may be examined and assessed both in the field and in the laboratory from the engineering viewpoint so as to identify and categorize their salient geotechnical characteristics.

4.5.1 Plasticity.[1]

The index properties of lodgement tills reported from 33 sites (mainly in the British Isles) have been obtained from a survey of the literature and are shown on the plasticity chart, Fig. 4.2 . The data contained in this Figure have been compiled from various sources and these sources, together with site locations, are summarised in Table 4.2 . The plasticity data presented in Fig. 4.2 include representatives of well-graded, clast dominant and matrix dominant tills, (4.5.2) although the majority may be classified within the two Casagrande groups CL, CI , clays of low to medium plasticity.

The data points on this chart lie above the Casagrande A line and cluster along the T line (see 8.1.1) identified by Boulton and Paul (1976) who have investigated the index properties of a large number

---

1. Activity (see Table 7.2) is discussed in 8.1.3 .

of lodgement and other tills at the margins of modern glaciers in Spitsbergen and Iceland. Plasticity data for lodgement tills can produce consistent and revealing results. A brief examination of Fig. 4.2 shows that, despite occasionally there being large differences in the liquid limit for the same lodgement till (for example, note the difference between the two values for till 22, Cow Green boulder clay) there are, nevertheless, many consistencies. Notable amongst these are the remarkably similar values quoted by Fookes et al (1975) for the 'Upper' and 'Lower' tills at Hartlepool 'A' Power Station (2, 3) and the tills in weathering zones III - IV and I (4, 5) quoted by Eyles and Sladen (1981) for various other sites in Northumberland. Again, the Upper boulder clay at Redcar reported by Marsland (1975) compares very well with the 'Upper' till at Hartlepool and the weathered tills reported for Northumberland. Whilst the sites at Hartlepool and Redcar are not identified specifically by Eyles and Sladen in their paper, they do suggest that the previously recognised two (red, grey) tills of the Northumberland Lodgement Plain (4.3) may in fact be only one; the top (red) till is now believed to be the product of the post-glacial (Holocene) weathering of a single Devensian ice sheet. A careful examination of the index properties of these soils does tend to confirm this.

4.5.2 Particle size.

There is a considerable amount of published data relating to particle size characteristics of tills and it is not the intention here to attempt a definitive summary of these. Much of this work is reported in sedimentological and geological journals and is concerned with textural and lithological descriptions of these soils, the statistical treatment of the grading data and their method of presentation for classification purposes. Examples of these include the use of ternary or triangular textural composition diagrams (Krumbein, 1933; Elson, 1961; Singh et al, 1983; Eyles and Sladen, 1981; Sladen and Wrigley, 1983) , size factor graphs (Shepps, 1958) , Rosin and Rammlers "Law of Crushing" paper (Geer and Yancey, 1938) , frequency distribution plots (Dreimanis and Vagners, 1971) and the modified Wentworth Scale and 'phi' [1] classes (Doeglas, 1968) .

---

1. Particle size, $mm = 2^{-phi}$.

Traditionally, grading data for engineering purposes are presented as cumulative frequency graphs on semi-logarithmic paper (e.g. BS 1377 : 1975, page 121) . Whilst this method does have certain disadvantages (see discussion in 8.1.2), it does nevertheless permit a quick assessment to be made of the grading over a large range of particle sizes,

McGown (1971) used the semi-logarithmic plot as a basis for identifying the fractional composition of tills and, in a later paper, (McGown and Derbyshire, 1977) extended this 'composite soil' concept into a gradational series of till textures, Table 4.3 . In this scheme, tills are classed 'matrix dominated' if they consist of fines (silt and clay) in which the coarse fraction acts as an assemblage of discrete particles. On the basis of the experimentally derived relationship between the percentage of fines, the compacted dry unit weight, and the theoretical maximum dry unit weight for a variety of tills, McGown and Derbyshire proposed limits of between 30 to 45% fines for this type of material. Matrix dominated tills are subdivided into those exhibiting cohesive properties and those exhibiting granular properties. A till possessing less than 15% fines was found by these authors to behave as a soil with fine particles within a dominant coarse fraction and this is therefore described as a granular till. Between these limits the coarse and fine fractions interact and interfere with the structural arrangement of each other (such as may be found in a well-graded material) and such mixtures are thus described as well-graded tills.

Fig. 4.3 shows the grading characteristics (semi-logarithmic plot) of several lodgement tills in the U.K. which have been obtained from various literature sources. It will be seen from this Figure that, despite sharing a broadly similar formative mechanism (4.3.1), there are present here representatives of many different engineering materials. Whilst some of these tills possess a grading similar to that shown for London clay, others have characteristics more akin to those of a river gravel. On the basis of the McGown and Derbyshire scheme, only till 6 (Bradan Dam, Fookes et al, 1975) is classed granular or clastic. The groupings of the other tills with respect to the aforementioned fines criteria are also indicated on this Figure. It is interesting to note that tills 2, 4, 21, 33 representing those from the Northumberland and Durham Lodgement Plain (Fookes et al, 1975; Marsland, 1977; Eyles and Sladen, 1981) and the site of the Building Research Station (Marsland, 1977) are contained within a group possessing more than (approximately) 40% clay sized particles. The

west of Scotland tills 1, (McGown et al, 1975); till 32 (Lower Cromer Till, Gens, 1982) and possibly till 7 (Taff Vale Trunk Road, Fookes et al, 1975) contain between 10 - 25% clay fraction. A third group, which includes tills 6 (Bradan Dam) and 29 (Keswick Northern By-Pass), contains less than 10% clay. It is suggested , therefore, that an alternative and, possibly, a rather more sensitive indicator of till class or group may be obtained on the basis of the percentage clay fraction determined from a fine sediment analysis.

Some further aspects of particle size are dealt with in Chapter 8 when the results of the grading of the Vale of St. Albans tills are discussed.

4.5.3 One-dimensional compression.

One-dimensional compression (3.3) can be modelled in the laboratory by using either the small diameter (75mm) oedometer or the larger Rowe cell. The testing condition of zero lateral strain imposed by these apparatuses is approximated when the loaded area is large relative to the thickness of the sediment body, as it would be for example beneath an ice sheet of considerable extent.

The results of one-dimensional compression tests (via the modulus m_v , see 3.3) are used extensively to predict likely consolidation settlements occurring in clay soils under loaded areas, (Anderson, 1983) . Estimates of swelling under load reduction can similarly be made.

The stony nature of most tills can cause considerable difficulties in their sampling and the degree of disturbance caused to the soil can be severe (Somerville, 1983) . However, it is practical to satisfactorily test samples of cohesive till in the conventional oedometer, provided that the quality of the sample is good (see for example Idel et al, 1969) .

Kazi and Knill(1969) report oedometer compression data on glacial (not till) sediments associated with the Cromer Till at Cromer and Happisburgh and have used the results to estimate ice preconsolidation loads for these soils.

Aario (1971) investigated the effects of overconsolidation on ice loaded sediments in Finland and has pointed to the difficulties arising from estimates of this sort, particularly in ice marginal

areas where ice flotation may occur.

Bernell (1957) has reported a correlation between the compression index C_c for various remoulded Swedish 'moraines' and their percentage clay content,[1] f, in the form :

$$C_c = 0{\cdot}0044\ f + 0{\cdot}003$$

For moraines with very low clay content (less than 1 - 2%) the results indicated a constant value for $C_c = 0{\cdot}01$.

Fookes et al (1975) show a range of values for m_v for the two tills at the site of the Hartlepool 'A' Power Station. They quote values of 0·09 to 0·12 m^2MN^{-1} and 0·03 to 0·06 m^2MN^{-1} for the Upper and Lower Till respectively. McKinlay et al (1975) similarly present data for the west of Scotland tills. Here, these authors have demonstrated, by using specimen sizes varying from 76mm to 254mm over a range of pressures 107 - 604kPa, that sample size is not a significant factor in the measurement of vertical coefficients of volume compressibility.

Singh et al (1983) report the results of oedometer (63·5mm diameter) tests on undisturbed samples of a cohesive till from Milwaukee. (The testing of this soil formed part of a larger schedule undertaken for the Milwaukee Water Pollution Abatement Program). They quote average values for the compression index C_c and recompression index C_{cr} of 0·13, 0·014 respectively , and have reproduced compression curves for four tests possessing different initial voids ratios (e_o) on this till, graphs A - D, Fig. 4.4 . If it is assumed that the ratio of the undrained shear strength at a soils plastic limit ($c_{u\ PL}$) to the undrained shear strength at the liquid limit ($c_{u\ LL}$) is approximately 100 , as proposed by Wroth and Wood (1978) , then (for an insensitive soil) it can readily be shown that the compression index, the plasticity index (PI) and the soils particle specific gravity (G_s) are related in the form :

$$C_c = \frac{2{\cdot}303\ PI.\ G_s}{100\ \ln 100} \quad .$$

---

1. In his paper the 'clay' fraction is defined as soil particles $< 6\mu m$.

Inserting a typical value $G_s = 2{\cdot}70$ gives , approximately ,

$$C_c \simeq 0{\cdot}013\ PI\ .$$

Fig. 4.4 shows the graph of this equation drawn tangential to the compression curve A in the region where $\sigma'_v \gtrsim 10\ tft^{-2}$ ($\simeq$ 958kPa) and passing through the points $0{\cdot}42\ e_o$ A, D as proposed by Schmertmann (1953). Whilst not shown explicitly by Singh et al , it is suggested here that this line represents a reasonable reconstruction of the in situ normal compression line for this till and therefore permits a tentative extrapolation of the laboratory compression curves B, C, D onto it.

A similar approach is proposed by Sladen and Wrigley (1983) who, based on the work of Wroth (1979), also suggest an expression defining the infinite number of possible reload curves for an overconsolidated soil of the form :

$$LI \simeq 1{\cdot}4 - 0{\cdot}5 \log_{10} (\Delta\sigma'_v + C) \quad ,$$

where LI = liquidity index; $\Delta\sigma'_v$ = increase in effective pressure; C is a constant in the same units as σ'_v which depends on the values e_o (in situ voids ratio) and p'_o (effective overburden pressure) prior to reloading.

Lutenegger et al (1983) report the results of 36 oedometer tests on 'till-like' deposits in central Iowa and quote an average value for the ratio $C_c/C_{cr} \simeq 8{\cdot}3$ for these soils (compare $C_c/C_{cr} \simeq 9{\cdot}3$, Singh et al) . They have also consistently observed increasing values for C_c with increasing e_o and propose a linear relationship to model this of the type :

$$C_c \simeq 0{\cdot}258\ e_o + 0{\cdot}015\ .$$

(Although not stated by these authors, it is assumed that these tests were carried out on similar but different soils; if not, the uniqueness of the normal compression line for a given soil, see 3.3 and Fig. 4.4 , does not apply to their data).

Apart from providing valuable data on which to base estimates of consolidation settlement, oedometer compression testing of (matrix dominant) tills can also provide additional valuable information on

both the compression and unloading characteristics of these soils. Unfortunately, very few of the oedometer compression data reported in the literature provide information other than quoted values for m_v. Often the pressure range over which this coefficient has been calculated is not stated. Occasionally, compression curves are reproduced; unloading curves hardly ever.

However, high quality and complete compression data for tills are sometimes available. Figs. 4.5a , 4.6a , 4.7a , for example, show the relationship between equilibrium specific volume and $\log_{10}$ effective vertical pressure for three samples of glacial till from the North Sea.[1] The unusual features which distinguish these (commercial) test results are i) the large range of pressures over which the samples were compressed (6400 kPa samples A, K ; 12800 kPa sample D), and ii) a complete loading/unloading sequence. Often the normal compression characteristics of a heavily overconsolidated soil remain unknown because the normal compression line has not been adequately defined. In addition, unloading will usually take place as one decrement, and without the recording of data. Valuable information concerning the behaviour of the soil over a range of increasing overconsolidation ratios is therefore lost.

Having identified the normal compression line, estimates of the preconsolidation pressure can confidently be made in the usual way (Casagrande, 1936; Schmertmann,1953). Estimates of one-dimensional K_o^{RB} along reloading and swelling lines may also be made by either relating overconsolidation ratios to the plasticity index of the soil (Brooker and Ireland, 1965, and see 8.2) or, alternatively by estimation from :

$$K_o^{RB} = K_o^{NC} (Ro)^{\alpha} \quad \text{, (e.g. Schmidt, 1966; Alpan, 1967)}$$

Here, $K_o^{NC} = \dfrac{\sigma'_h}{\sigma'_v}$ for a normally consolidated soil,

Ro = overconsolidation ratio,

and α = a constant.

---

1. These samples, obtained from rotary cored boreholes by the Institute of Geological Sciences (now British Geological Survey), are located approximately 56° N, 1° E. The writer acknowledges A. Prince and M. Love for supplying these test results.

Meyerhof (1976) has suggested $\alpha = 0{\cdot}5$; K_o^{NC} may be calculated from the Jaky (1944) semi-empirical expression :

$$K_o = K_o^{NC} = 1 - \sin \phi' .$$

(A useful summary of K_o - Ro relationships in clays, silts and sands is given by Mayne and Kulhawy, 1982).

The compression data may thus be replotted in the form equilbrium specific volume : $\log_e$ average effective pressure, and the soil constants λ , $\bar{\kappa}$ derived , Figs. 4.5b , 4.6b , 4.7b . This method of presenting one-dimensional compression data will be discussed further in Chapter 8.

4.5.4 Permeability and rate of consolidation.

The early literature, particularly from the U.S.A. and Canada, reports results of laboratory permeability tests on compacted tills and moraines used as dam core fill material. Hence, Legget (1942) comments on the relatively impermeable nature of compacted (to optimum water content) glacial drift on an earth dam at Fergus, Ontario.(1)

Bernell (1957) reports the results of over 2000 laboratory permeability tests on a very large range of sediments, including many carried out on compacted moraine. Samples of glacial moraine were tested by this author over a range of water contents from Proctor optimum to full saturation and a relationship was established of the form :

$$V = Vo + Cp \log_{10} \frac{k}{ko} \quad ;$$

(ko is the permeability, cms^{-1} at specific volume Vo ; Cp is a permeability index, the slope of the permeability line on a semi-logarithmic plot of permeability to specific volume.). The author relates the index Cp to the grading uniformity coefficient D_{60}/D_{10} ; typically for moraines this was found to have a value 0·05. Olmstead (1969) quotes values for the permeability coefficient of compacted till in the Puget Lowland, Washington, and Fookes et al (1975) have reported the results of permeability testing of the 'Mountain Till' at Bradan Dam, Ayrshire.

---

1. Percolation rate ($ft^3/ft^2/yr$) at unit gradient as low as 0·0089 ($= 8{\cdot}47 \times 10^{-11}$ ms^{-1}) .

Lloyd (1983) presents laboratory and field data for typical permeabilities of various types of till and demonstrates the large variation of permeability evident for these sediments, (from 10^{-6} ms^{-1} for variable lithology till and solifluction débris to 10^{-11} ms^{-1} for matrix dominant tills).

Loiselle and Hurtubise (1980), investigating the compaction characteristics of well-graded and clast-dominant tills in the Outardes region of Northern Quebec, report permeability values for these materials and represent the data in the form k : V (permeability to specific volume). They also have attempted to correct specific volume on the basis of percentage fines in the tills less than 74mm. A compilation of these results and the findings of others are shown in this (k : V) form in Fig. 4.8 .

Similar 'permeability paths' have been constructed for the North Sea Tills (samples A,D,J,K) from the oedometer test data (4.5.3) and these are shown in Fig. 4.9 . (The envelope containing these permeability values is also shown in Fig. 4.8). It is often instructive to view reducing permeability over a range of increasing consolidation pressure. In this way, for example, the effects of soil structure on the calculated permeability may be examined. Comparative permeability from reconstituted and undisturbed tills in the Vale of St. Albans have been obtained in this way and will be presented and discussed in Chapter 8.

Also shown in Fig. 4.9 are the calculated initial and final values for the coefficient of consolidation, c_v for the North Sea Tills. Kazi and Knill (1969) investigated the variation of c_v over a range of oedometer consolidation pressures on oriented samples of fissured laminated glacial clays at Cromer. They concluded that the less fissured samples had lower calculated c_v values and this was particularly noticeable where drainage through the sample was normal to bedding. McKinlay et al (1975) have investigated the effects of sample size on consolidation rates for fissured west of Scotland tills and have demonstrated increased c_v values (up to a maximum x3) for pressures up to 100 kPa in larger (254mm) diameter undisturbed samples. (This difference, though, is very much less marked at larger pressures).

Rowe (1971, 1972) has shown data from large (250mm) undisturbed samples of till from Grimwith with c_v values between 10 and 70 times larger than those obtained on smaller (76mm) remoulded samples of the same till.

Vaughan and Walbancke (1975) have provided a useful summary of field determined c_v values for various 'sandy' and 'plastic' clay tills reported by others. They have highlighted the dependence of c_v on soil structure and heterogeneity, hence they stress the need for field measurements of c_v based either on the results of in situ permeability tests or the analysis of field records of changing rates of excess pore pressures. The data they report for the 'sandy' tills have also been included in Fig. 4.9 for comparative purposes.

4.5.5 Undrained and drained shear strength.

(i) Undrained shear strength.

The more usual approach to the estimation of safe bearing pressures for foundations on matrix-rich tills is via a total stress analysis using the appropriate shear strength parameters obtained from undrained triaxial tests on undisturbed samples, (see for example Anderson, 1983). Undrained shear strengths are also extensively used in pile design in till. (Weltman and Healy, 1978).

The factual data reported in the literature concerning undrained shear strength of tills includes, amongst others, the results of unconfined compression, 38mm and larger diameter triaxial tests (McKinlay et al, 1974), multistage triaxial (Anderson, 1974), plate loading and pressuremeter tests (Marsland, 1976; 1977; Powell et al, 1983), shear vane tests (Marsland, 1980) and in situ 300mm shear box tests (Radhakrishna and Klym, 1974).

Variations in undrained shear strength will reflect differences in water content and therefore it is advantageous to examine variations in shear strength as a function of changing water content. Fig. 4.10 shows the relationship between undrained shear strengths (log scale) and calculated (from values of natural water content, LL , PL) liquidity indices for various undisturbed lodgement tills reported in the literature. Frequently, a scattered number of shear strength values are obtained for one till at a locality and the range of values recorded are indicated on the Figure. The large range of undrained shear strengths (650 kPa) for all the tills covering a relatively small difference in liquidity index (0·3) is noteworthy, as are the inter-site variations in shear strength (same liquidity index) for some of the tills.

On this Figure the relationship log c_u : LI for various other (remoulded) soils obtained by Skempton and Northey (1952) is also shown. Whilst heavily overconsolidated soils will frequently have natural water contents below the plastic limit it is also expected that (undisturbed) matrix dominant lodgement tills would have correspondingly higher undrained shear strengths at these lower water contents and, therefore, for any given value of LI to plot to the right of the Skempton and Northey envelope. Clearly there are occasions when this is not the case.

The data may alternatively be plotted in the form suggested by Sladen and Wrigley (1983) and shown in Fig. 4.11 . Here, an expected relationship between undrained shear strength and water content for different PI has been derived on the basis that a simple relationship between c_u at LL , PL exists (Wroth and Wood, 1978; see also 6.6) of the form :

$$c_u = 170 \exp (- 4{\cdot}6 \text{ LI}) \text{ kPa.}$$

(It has also been assumed that all lodgement tills have plastcity data plotting on the 'T' line, whence :

$$\text{PI} = 0{\cdot}73 (\text{LL} - 11) \qquad) .$$

From these graphs it can clearly be seen that small variations in water content will exercise a significant control on the measured undrained shear strengths, particularly below water contents of about 16% .

Results from published data on this Figure confirm this expectation; at the lower water contents undrained shear strengths are high and, significantly, demonstrate considerable scatter. With increasing water content the expectation is for lower values of c_u and, because a smaller range of PI is supported by a large variation in water content, less scatter in the values of c_u might also be expected. This, too, appears to be reflected by the nature of the plotted data.

There is a noticeable exception to this trend. The data from site 1 (West Scotland lodgement tills), despite having low water contents (10%), do not possess the expected higher shear strengths. McKinlay et al (1974) who reported these results have demonstrated in their paper a high degree of consistency in the test values obtained from

both the field and laboratory. These tills are, however, not of the matrix dominant type and have a significant clast content (although they are designated well-graded). The same control of water content over undrained strength might therefore not be expected. The lower shear strengths may also result from the highly fissured nature of these tills , see 4.4.2 . On the other hand, Radhakrishna and Klym (1974) have published results from field and laboratory tests on a very dense clast dominant lodgement till in Wesleyville, Ontario. These tills have very low water contents, occasionally only 6% , and very high undrained shear strengths (occasionally 2000 kPa). Unfortunately, they do not report plasticity data for these soils and therefore it has not been possible to relate the results (included in the Figure) to the PI contours shown.

Lutenegger et al (1983) have correlated bulk density ρ with unconfined compressive strength Qu for undisturbed samples of two basal tills belonging to the Wolf Creek Formation (Hickory Hills Till, Aurora Till) in eastern Iowa. They have obtained the relationship :

$$Qu = 0{\cdot}14 \exp 0{\cdot}09\rho (\text{lb ft}^{-3}) \qquad \text{lb ft}^{-2} .$$

Jacobsen (1970) has proposed an alternative relationship between undrained shear strength and voids ratio based on field and laboratory testing of Swedish 'preconsolidated moraine clay' :

$$c_u = \exp (0{\cdot}77\, e^{-1{\cdot}2}) \quad \text{tm}^{-2} .$$

(ii) Drained shear strength.

The long term stability of clay slopes is controlled by their drained strength, and both peak and residual strengths must be considered, (Skempton, 1964) . The drained residual strength and drained brittleness (see below) of cohesive soils is important in the assessment of the stability of old landslips , or in slopes with pre-existing shear surfaces.

Drained strength is determined either by using the triaxial or direct shear apparatus in which the rate of loading is sufficiently slow not to induce excess pore pressures within the sample. In terms of Mohr-Coulomb, a peak drained strength ϕ'_p , c' may usually be

identified for a soil which , at larger strains, reaches a lower limiting or residual value denoted by ϕ'_R , c'_R . The drained residual cohesion c'_R is usually very small. The drained peak (τ_p) to residual (τ_R) reduction in shear strength may be expressed in terms of 'brittleness index' , I_B ; (Bishop, 1967) :

$$I_B = (\tau_p - \tau_R / \tau_p) .$$

Terzaghi and Peck (1967) have shown reducing ϕ'_p with increasing plasticity index for clays of low to medium plasticity in drained triaxial tests (Fig. 4.12) , although, quoting the exceptionally high value $\phi'_p = 47^\circ$ obtained by Lo (1962) for a clay with a liquid limit of 426% from Mexico City, they do advise caution in the general application of this trend. However, a similar trend has been observed by others for a variety of other soils , including lodgement tills. These include Skempton and Brown (1961), Jacobsen (1970) [1] , Tarbet (1973), Eyles and Sladen (1981) and Sladen and Wrigley (1983) ; the findings of these authors are also shown in Fig. 4.12 . Vaughan and Walbancke (1975) investigated the peak drained strength of Cow Green boulder clay using 38mm diameter samples in triaxial compression and were able to demonstrate reducing ϕ'_p with increasing PI for this soil. Their results indicated $\phi'_p \simeq 30^\circ$ for PI $\simeq$ 18 reducing to $\phi'_p \simeq 19^\circ$ at PI $\simeq$ 55. In addition, by investigating the variation of the stress ratio τ_p / σ'_n (termed 'peak frictional coefficient' in a later, 1981, paper) with isotropic consolidation pressures of 100 kPa , 500 kPa , they have suggested a drained failure envelope for Cow Green till with $c' \simeq 10$ kPa , "... which is typical for boulder clays of this type." , (op cit page 187). Sladen and Wrigley (1983) note that c' for lodgement tills generally falls within the range 0 - 25 kPa , whilst Thorburn and Reid (1973) have observed a tendency for c' to decrease with increasing ϕ'_p for lodgement tills from the Glasgow area.

The residual shear strength of an homogeneous soil will depend on grading and mineralogy (Kenney, 1967) and should therefore be independent of the method of deposition, (Vaughan and Walbancke, op cit) and of structure and density prior to shearing, (Bishop et al,

---

1. Jacobsen proposes $\phi'_p = 35{\cdot}3^\circ - 9^\circ e$ .... $(0{\cdot}25 < e < 0{\cdot}50)$ for low plasticity Swedish moraines.

1971). Grading and mineralogy are reflected in the plasticity index, and therefore a correlation of PI with ϕ'_R can be expected. The relationship ϕ'_R : PI for various lodgement tills is shown in Fig. 4.13 . A noticeable feature here is a marked increase in drained brittleness at PI $\simeq 20^\circ - 25^\circ$. Ingold (1975) has shown a similar phenomenon for other (non-till) soils with different geological origins; the trend indicated by his data is also shown in this Figure. Lupini et al (1981) have investigated this effect by testing reconstituted soils possessing differing grading characteristics in the ring shear apparatus. On the basis of these (and other) results they have proposed three different modes of residual shear :

(i) a turbulent mode in soils with a high proportion of 'rotund' particles , or with platy particles of high interparticle friction. Low plasticity soils are included here; drained residual shear strengths are high , brittleness low.

(ii) a sliding mode in which a low shear strength surface of strongly oriented low friction platy particles forms resulting in a marked drained brittleness. Soils with high plasticity are included here.

(iii) a transitional mode involving both turbulent and sliding shear in which the drained residual friction angle is extremely sensitive to small changes in grading.

Lupini et al propose mode (i) passing into mode (ii) with increasing 'granular voids ratio' (ratio of the volume of platy particles and water to the volume of rotund particles), see Fig. 4.14 . These authors observe in their paper that Cowden Till demonstrated a turbulent behaviour during testing (but with the development of a shear zone with slight orientation of clay particles within it) ; Penwortham Till and Trevor Bay Till (locations unspecified) also showed shear zones in thin section. Bingley and Cow Green tills should, on the basis of granular voids ratio, fall within the range of transitional behaviour. These tills are shown located with respect to the proposed residual shear mechanisms in Fig. 4.14 .

Cocksedge (1983) has utilised the concept of drained brittleness to advocate limiting stable slopes in tills of contrasting plasticity. His observations have been incorporated in Fig. 4.14 .

4.5.6 Elastic modulus.

Soderman et al (1968), in a paper describing their field and laboratory studies of the modulus of elasticity of a clay till, have remarked , "In the prediction of both immediate and time dependent deformations resulting from the application of loads to a soil mass, general use is made of the theory of elasticity, incorporating soil properties ... arrived at from ... tests made on the 'best samples' that can be obtained from the particular soil deposit. In addition to sample disturbance , the inelastic and non-linear load deformation characteristic of soil necessitates an arbitrary definition of modulus of elasticity ...." The stress-strain modulus used most commonly is that obtained from undrained tests (either laboratory or in situ), although as noted by Sladen and Wrigley (1983), it is becoming more usual to use a quasi-elastic approach together with an equivalent vertical 'drained' elastic modulus when estimating total settlements of foundations on lodgement till, (see Stroud and Butler, 1975). The most frequently defined moduli from undrained compression tests are (i) the initial tangent modulus E_i obtained from the gradient of the stress : strain curve at zero load, and (ii) the secant modulus E_s , defined as the ratio of stress to strain at a particular stress level. Commonly, the secant modulus in tills is determined over the stress range 0 - 0·5 ($\sigma_1 - \sigma_3$) max. , (for example, Marsland, 1975).

Lo (1961) has stated that the initial tangent modulus defined by the 'virgin loading curve' is not a true elastic modulus (due in part to bedding errors) and has suggested that cyclic or repetitive loading will produce a more linear compression curve. This in turn produces a more consistent and representative 'reload modulus', E_r . Ward et al (1965) and Crawford and Burn (1962) have investigated the undrained moduli of a range of soils in cyclic (laboratory) compression tests and have found that the ratio of reloading modulus to initial loading modulus E_r / E_i varied from 3 to 10 . Klohn(1965), however, found no appreciable difference in these two moduli for a dense glacial till obtained from unconfined compression and cyclic triaxial tests. Anderson and McKinlay (1975), on the other hand, found that the ratio of the first reload modulus to initial modulus for 100mm diameter samples of lodgement till varied from 1·65 to 6·15 (with a mean E_r / E_i = 3·30). In their paper, these authors report using a standardised five cycle régime commencing at approximately 1·5% axial strain (equivalent to about 25% of the failure stress).

Somewhat lower values for E_r / E_i (1·13 to 1·15) have been obtained by Marsland (1975) for the Upper boulder clay at Redcar. (These were obtained in situ from plate bearing tests). Radhakrishna and Klym (1974), also using the results of cyclic plate loading tests, report values for this ratio from 1·8 to 8·1 on a very dense sandy till at the site of Wesleyville Generating Station, Lake Ontario.

Generally, it is found that the moduli of elasticity determined from either in situ plate loading or from pressuremeter tests on a soil will underestimate the operational modulus , thus leading to overestimates of settlement. Marsland, (1980) has reviewed this aspect and Anderson and McKinlay (op cit) have provided much comparative data for West of Scotland tills tested both in the laboratory and in situ by plate tests, pressuremeter and 'Geoprobe'. (The large differences which can be obtained are demonstrated by the mean value E = 4720 kPa recorded from standard 100mm x 100mm undrained triaxial tests compared with 79000 kPa obtained from in situ testing the same till).

Hight and Gens (1979) have suggested that differences in the stress conditions between laboratory and field tests of tills could account for part of this discrepancy. They suggest that by anisotropically consolidating a till to re-establish the in situ stresses $\sigma'_{v\,c}$, $\sigma'_{h\,c}$ in the soil prior to sampling (Fig. 4.15, upper diagram) will subsequently produce a stress : strain curve of the type DEF (lower diagram), giving an initial loading modulus E_i(an) . By isotropically consolidating the sample at a chamber pressure equivalent to $\sigma'_v c$, however, will only produce that portion of the stress : strain curve above point E , thus giving a reduced modulus $E_i(K_o)$. These authors have conducted undrained compression tests on reconstituted samples of Cowden Till anisotropically overconsolidated to K_o = 1·6 . Using the elastic parameters so obtained they have shown that (i) a laboratory test procedure in which the initial in situ stress conditions are neglected will underestimate the in situ moduli , and (ii) a linear elastic model for back-analysis of a field loading (plate) test will overestimate the secant moduli of soils exhibiting non-linear behaviour , (see for example De Jong and Harris, 1971).

Frequently, values for loading moduli in tills are related to the undrained cohesion, Fig. 4.16 . Despite the large variations in the values for E_u shown at any one locality, an increase in undrained shear strength (and a reduction in liquidity index) is accompanied by an increase in soil modulus. For any given undrained shear strength

this expectation is somewhat less than that proposed by Weltman and Healy (1978) :

$$E_s = 1700\ (1{\cdot}0344)^{c_u} ,$$

and rather more than that predicted by Butler (1974) :

$$E_u \simeq 220\ c_u .$$

Alternative ways of presenting moduli data for tills are shown in Fig. 4.17 . The upper diagram of this Figure shows the relationship between the normalised modulus E_u/σ'_3 and overconsolidation ratio Ro for Milwaukee Till reported by Singh et al (op cit). An interpretation of the data presented by these authors in this form clearly demonstrates the dependence of the loading modulus on overconsolidation ratio.(1) A similar effect has been observed by El-Ghamrawy (1978) for Cromer Till (lower diagram)(2). An inspection of normalised undrained moduli relative to overconsolidation ratios (where known or can be estimated) can be particularly useful and this method has been adopted for the Vale of St. Albans tills, Chapter 8.

4.6 Summary.

Although the tripartite scheme of landsystems identified and discussed in 4.3 offers a systematic and unified approach to the interpretation of glacial environments, strictly a landsystem will "... portray (only) the soils and landforms of a single ice advance/retreat cycle, i.e. the latest." , Eyles (1983, page 7). Nevertheless, the landsystem approach can be applied to the very thick and complex Pleistocene sequences (often representing more than one ice advance/retreat cycle) which are observed in many mid-latitude areas.

Therefore, the model of the supraglacial landsystem, for example, has been applied (Boulton and Paul, 1976) to parts of N.W. England, particularly the Shropshire-Cheshire Plain, the Lancashire Plain, and the Carlisle Lowland. Here, the typical sediment association comprises flow tills, and a varied suite of outwash sediments and melt-out tills;

---

1. Estimates of Ro based on $p'_c = 6\ \mathrm{tft}^{-2}$ ($\simeq$ 575 kPa), page 297.

2. This author presents the modulus as the ratio of the overconsolidated to normally consolidated undrained values.

the surface expression is one typically of an undulating kame and kettle topography.

Similarly, Eyles, Dearman and Douglas (1983) , referring to their glacial landsystem distribution map of Britain, remark "The extensive dissected till sheets in the East Midlands and East Anglia ('chalky boulder clays') suggest that these may be the remnants of lodgement till plains, ... and they have thus been included in the subglacial terrain group." The nature of the subsurface (Anglian) glacial sequences in the Vale of St. Albans described in 2.4 would also suggest their inclusion in the subglacial/proglacial sediment association, 4.3.1 .

The complex processes operating on such (former) proglacial outwash surfaces in combination with the very complex mechanisms of transportation and emplacement of supraglacial, englacial and subglacial débris have produced till deposits with very contrasting engineering properties. A survey of the literature to date clearly shows that even within one such group (lodgement) many different engineering materials are represented.

Whilst this survey has revealed the existence of much basic, but useful, geotechnical data (e.g. plasticity, grading) covering the major till groups and although a number of workers have demonstrated correlations between the various geotechnical parameters investigated (e.g. E_u , c_u , e_o , γ) , it is noticeable that there is very little published work concerning the fundamental mechanical behaviour of these overconsolidated soils. This is a surprising result, especially in view of the earlier observation regarding the global distribution of tills and related sediments.

Landsystem	Sediment association	Source of glacial debris	Position of deposition	Principal till types
A Glaciated valley landsystem (medial, lateral moraines, kame terraces.)	Supraglacial sediment associated	Supraglacial (nunataks, valley sides.) →	Supraglacial	Supraglacial morainic till
B Supraglacial landsystem (kame moraines)			RARE	Flow till (Allochthonous, Parautochthonous) Melt-out till
C Subglacial/proglacial landsystem (drumlins, fluted moraines, pushed-moraines, outwash plains and terraces.)	Subglacial/proglacial sediment associated	Subglacial →	Subglacial	Melt-out till Lodgement till Lee-side till

Table 4.1 Classification of tills - associated landforms and sediments.

(After Boulton and Paul, 1976.)

Number	Location	Till type	Source
1.	W. Scotland	weathered/unweathered lodgement	McGown et al, 1975.
2.	Hartlepool 'A' Power Station	Upper till (red - brown)	Fookes et al, 1975.
3.	" "	Lower till (brown - grey)	" "
4.	Northumberland	weathering zone III - IV (red)	Eyles and Sladen, 1981.
5.	"	" " I (grey)	" "
6.	Bradan Dam, Ayrshire	Mountain till lodgement	Fookes et al, 1975.
7.	A470 Taff Vale Trunk Road	ablation + lodgement	Fookes et al, 1975.
8.	Chester	boulder clay	Stroud and Butler, 1975.
9.	Haltwhistle	"	" "
10.	Moffat	"	" "
11.	Bathgate	"	" "
12.	Macclesfield	"	" "
13.	Queensferry	"	" "
14.	Chelmsford	"	" "
15.	Northampton	"	" "
16.	Carlisle	"	" "
17, 18.	South Shields	"	" "
19.	Manchester	"	" "
20.	Chicago Circle, Illinois, USA.	till	Faillace and Silver, 1975.

/contd.

Number	Location	Till type	Source
21.	Redcar	Upper boulder clay	Marsland, 1975.
22.	Cow Green	boulder clay	Vaughan and Walbancke, 1975.
23.	Diddington	"	Hammond and Winder, 1967 in " .
24.	Seagahan	"	Lucks, 1966 in " .
25.	Usk	"	Sheppard and Aylen, 1957 in " .
26.	Black Esk	"	Lucks, 1966 in " .
27.	Selset	"	Bishop and Vaughan, 1962 in " .
28.	Teeside Parkway	glacial till	Cocksedge and Hight, 1975.
29.	Keswick Northern By - Pass	"	" "
30.	Milton Keynes	chalky boulder clay	Denness, 1974.
31.	Breidamerkurjokull, Iceland	lodgement till	Boulton and Paul, 1976.
32.	Cromer	Lower Cromer Till	Gens, 1982.
33.	site of BRS, Garston	chalky boulder clay	Marsland, 1977.

Table 4.2 Summary of plasticity data : site locations and sources.

Dominant soil fraction	Nature of dominant fraction	Textural description
Clasts	Granular	Granular or Clastic till
No dominant fraction	—	Well-graded till
Matrix	Granular	Granular matrix till
	Cohesive	Cohesive matrix till

Table 4.3 Gradational series of till textures.
(after McGown and Derbyshire, 1977.)

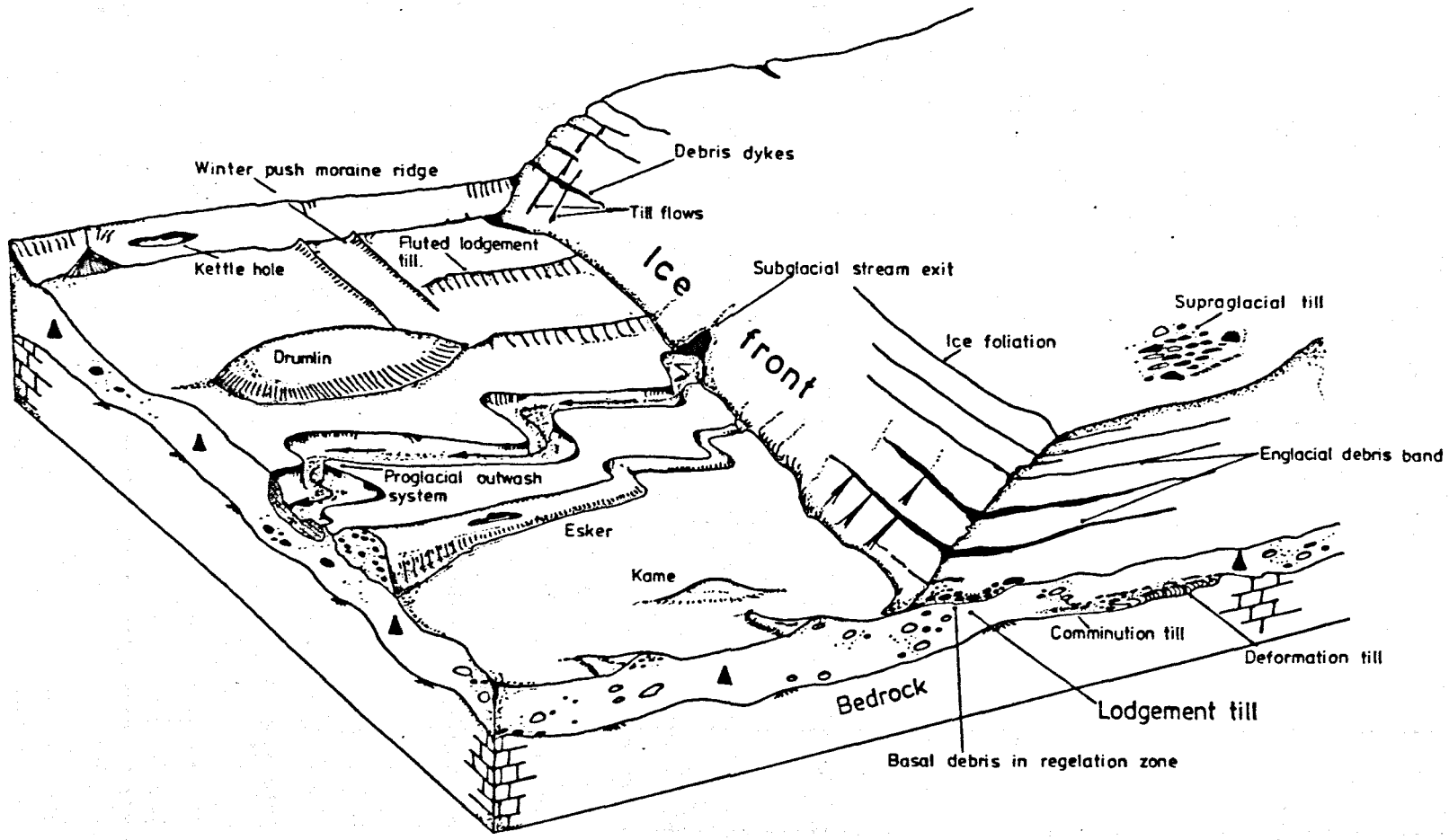

Figure 4.1 Schematic diagram to illustrate the formation of the subglacial/proglacial sediment association and landsystem. (Compiled from various sources).

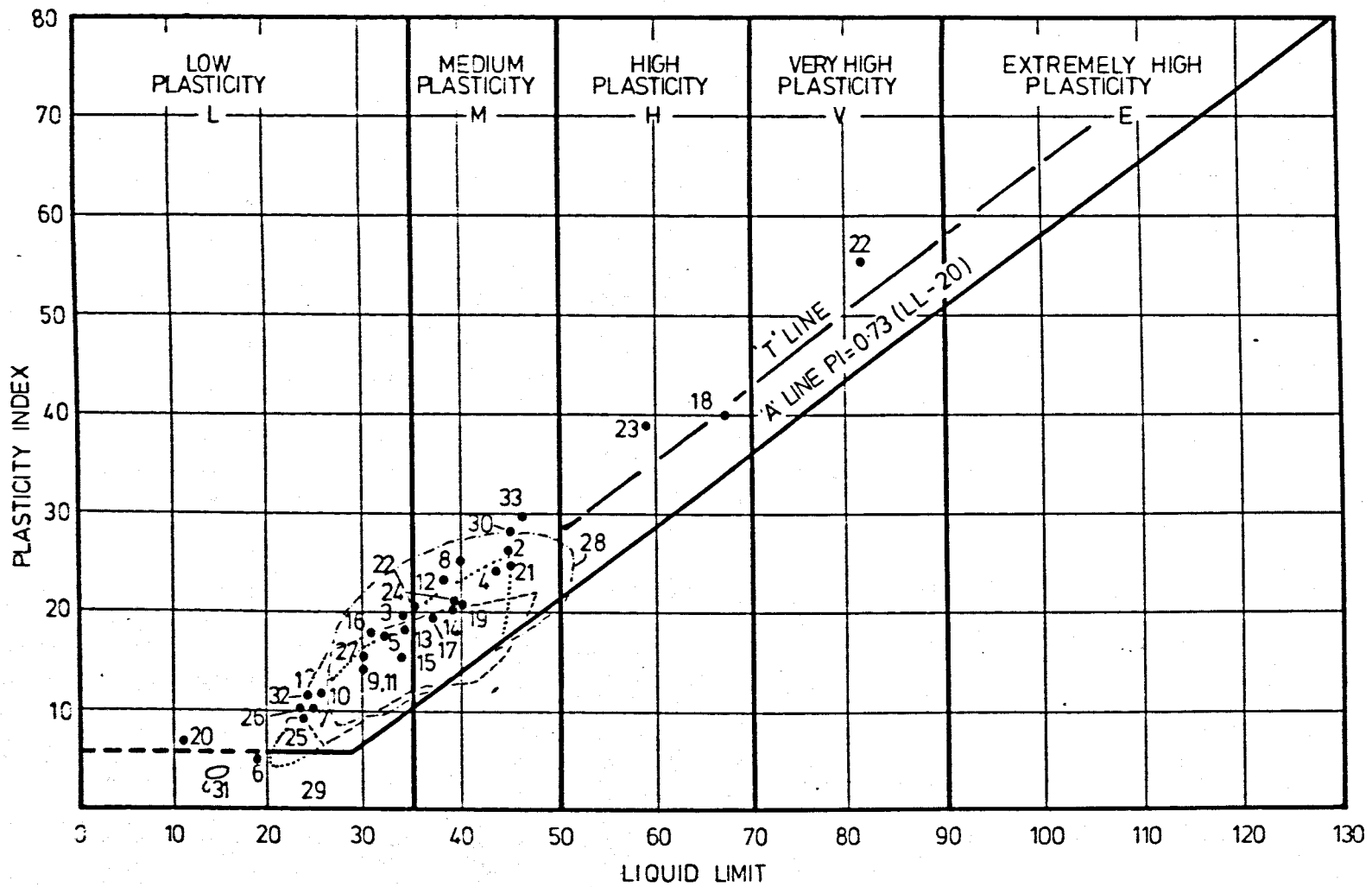

Figure 4.2 Plasticity data for various lodgement tills in the U.K. (Key as in Table 4.2).

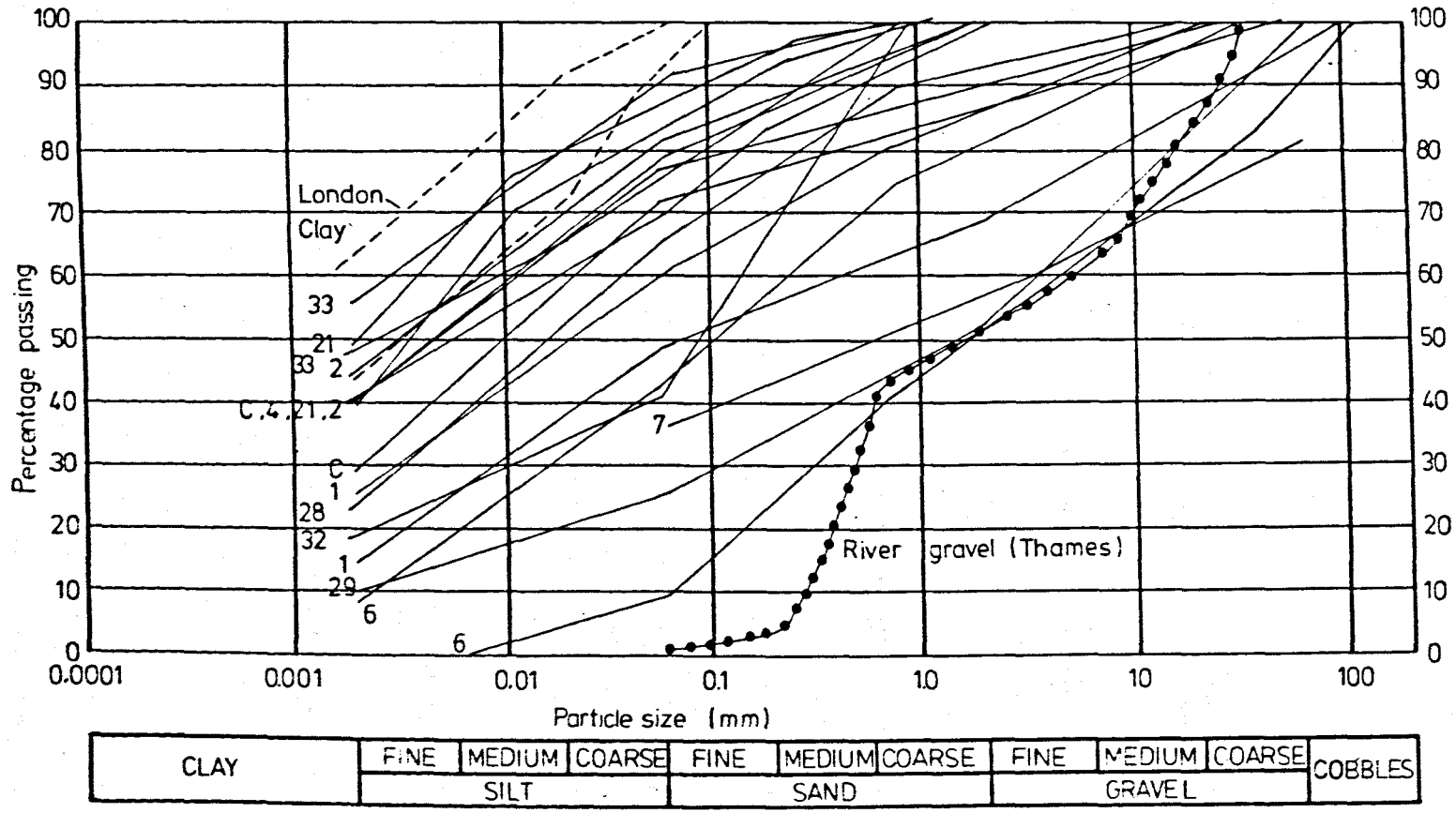

Figure 4.3 Grading characteristics of lodgement tills in the U.K.
(Key as in Table 4.2 : C = Cowden Till, Powell et al, 1983).

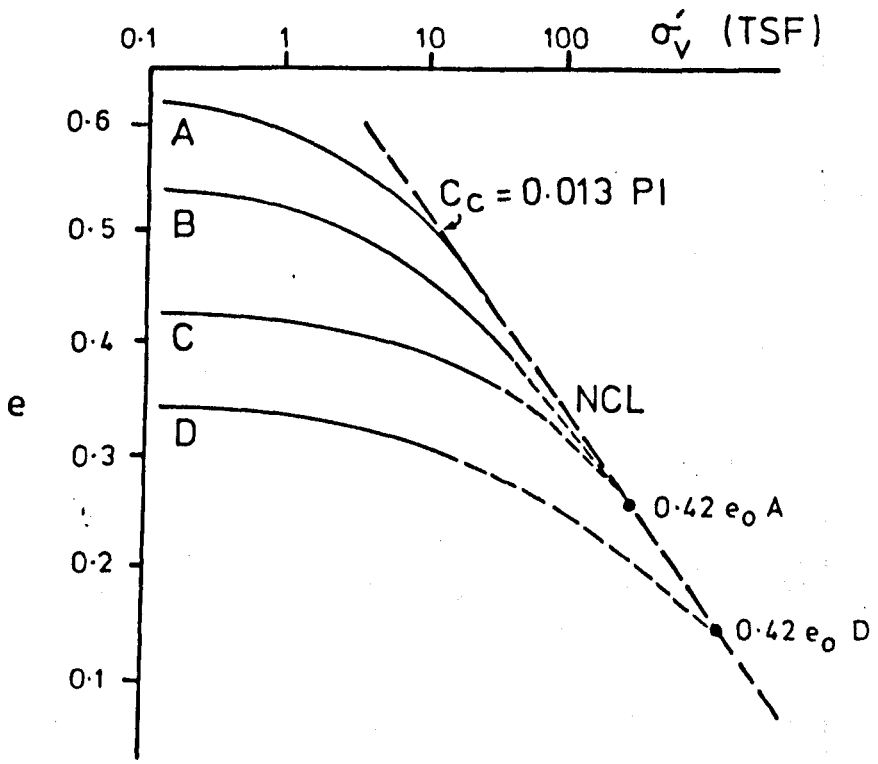

Figure 4.4 <u>Oedometer compression : Milwaukee Till.</u>
(After Singh et al, 1983).

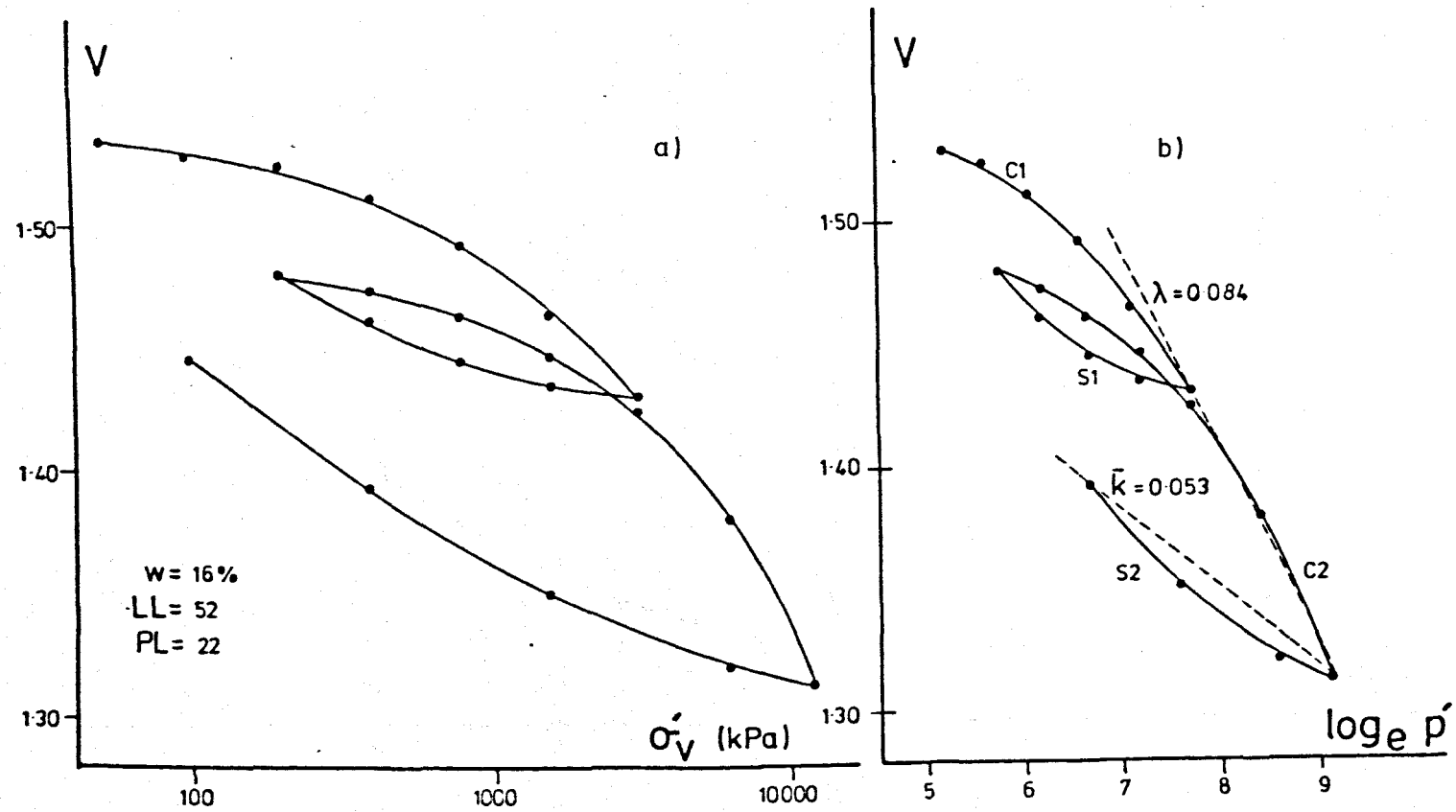

Figure 4.5 Oedometer compression characteristics, glacial till, N.Sea. (Depth 64·0m , boring D).

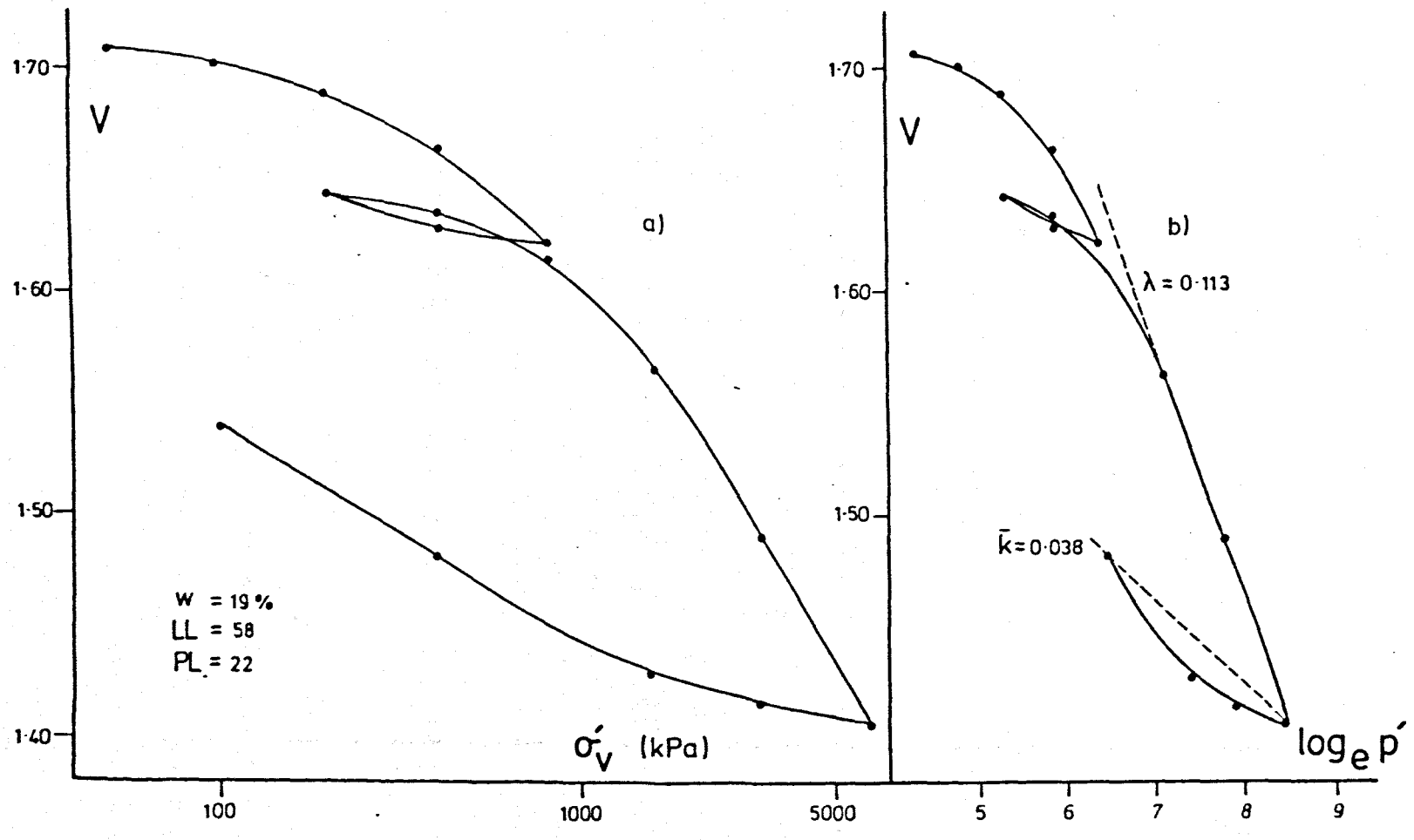

Figure 4.6 Oedometer compression characteristics, glacial till, N.Sea. (Depth 112·0m , boring A).

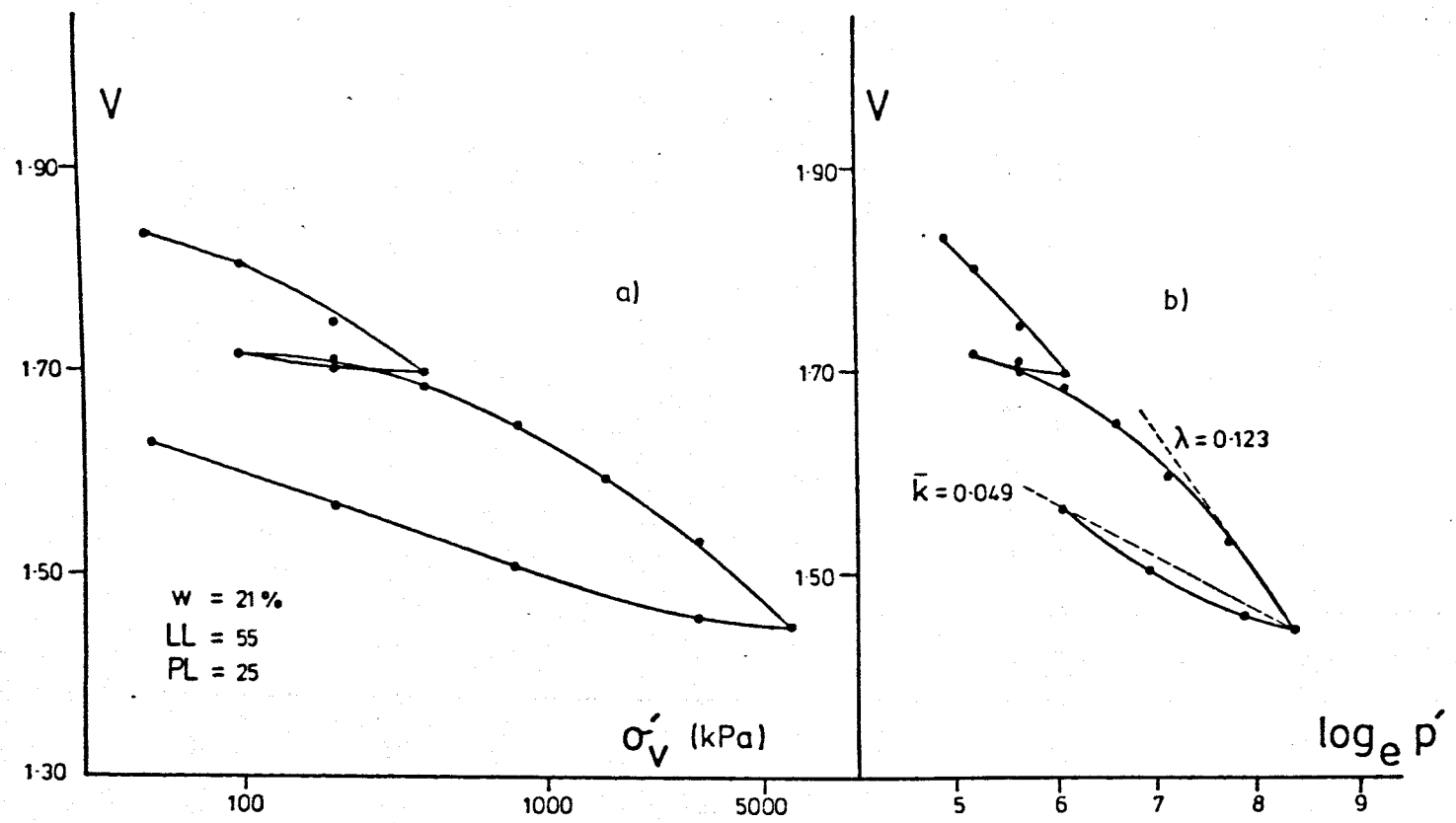

Figure 4.7 Oedometer compression characteristics, glacial till, N.Sea. (Depth 50·0m , boring K).

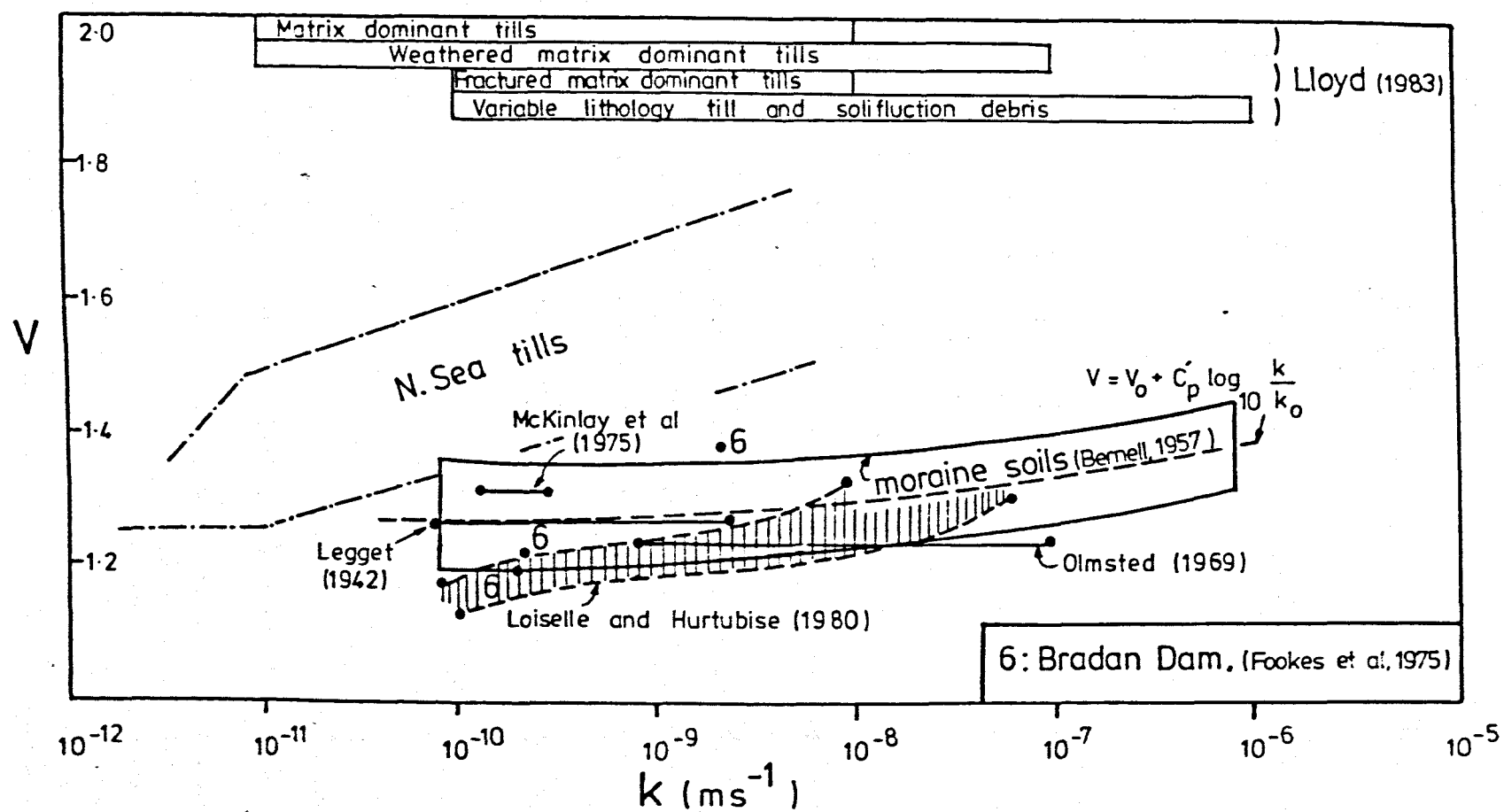

Figure 4.8 Permeability : specific volume relationship for tills and related soils.

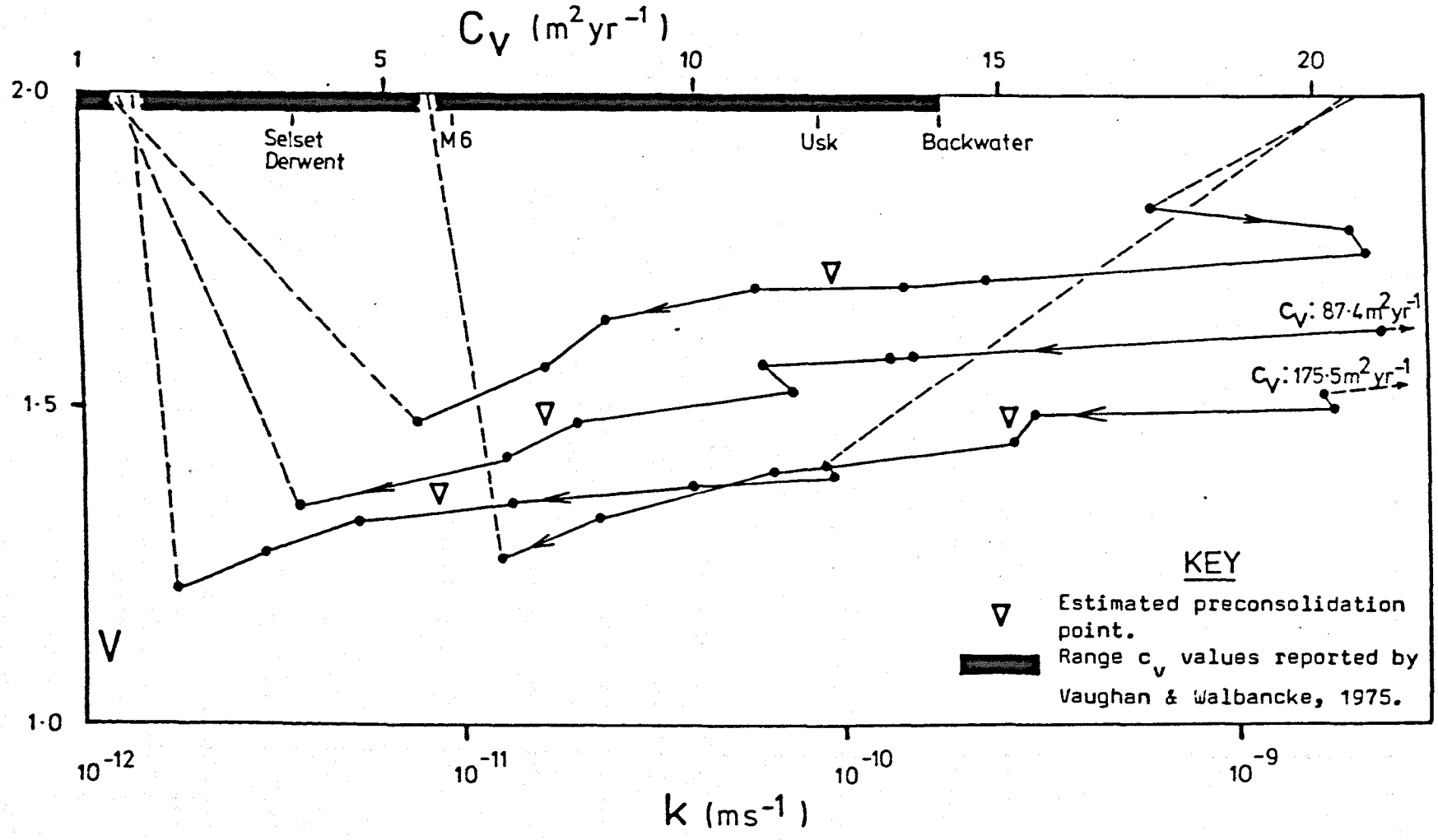

Figure 4.9 Permeability : specific volume : coefficient of consolidation relationship for N.Sea tills, borings A , D , J , K .

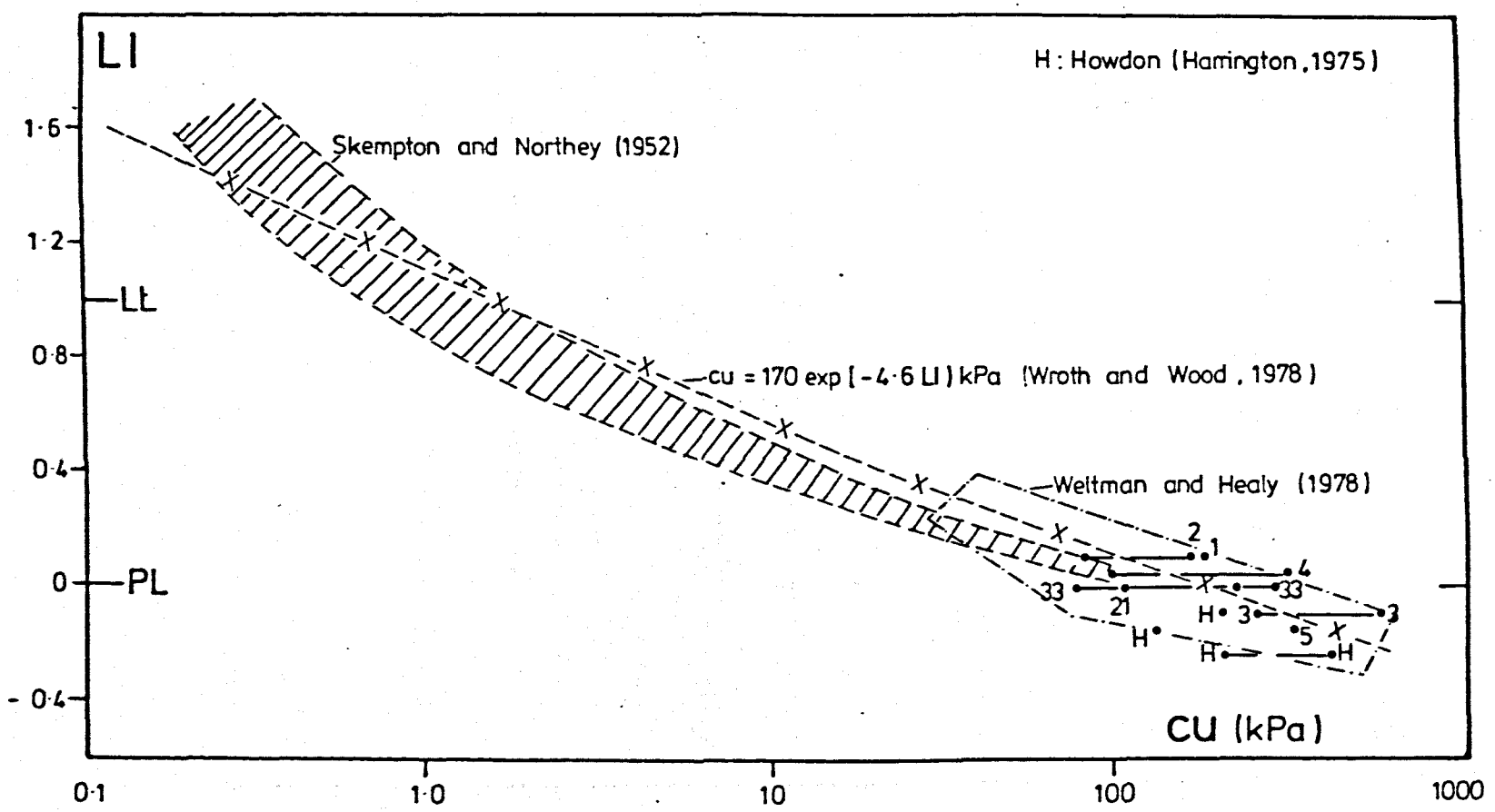

Figure 4.10 Relationship between undrained shear strength and liquidity index for U.K. tills.

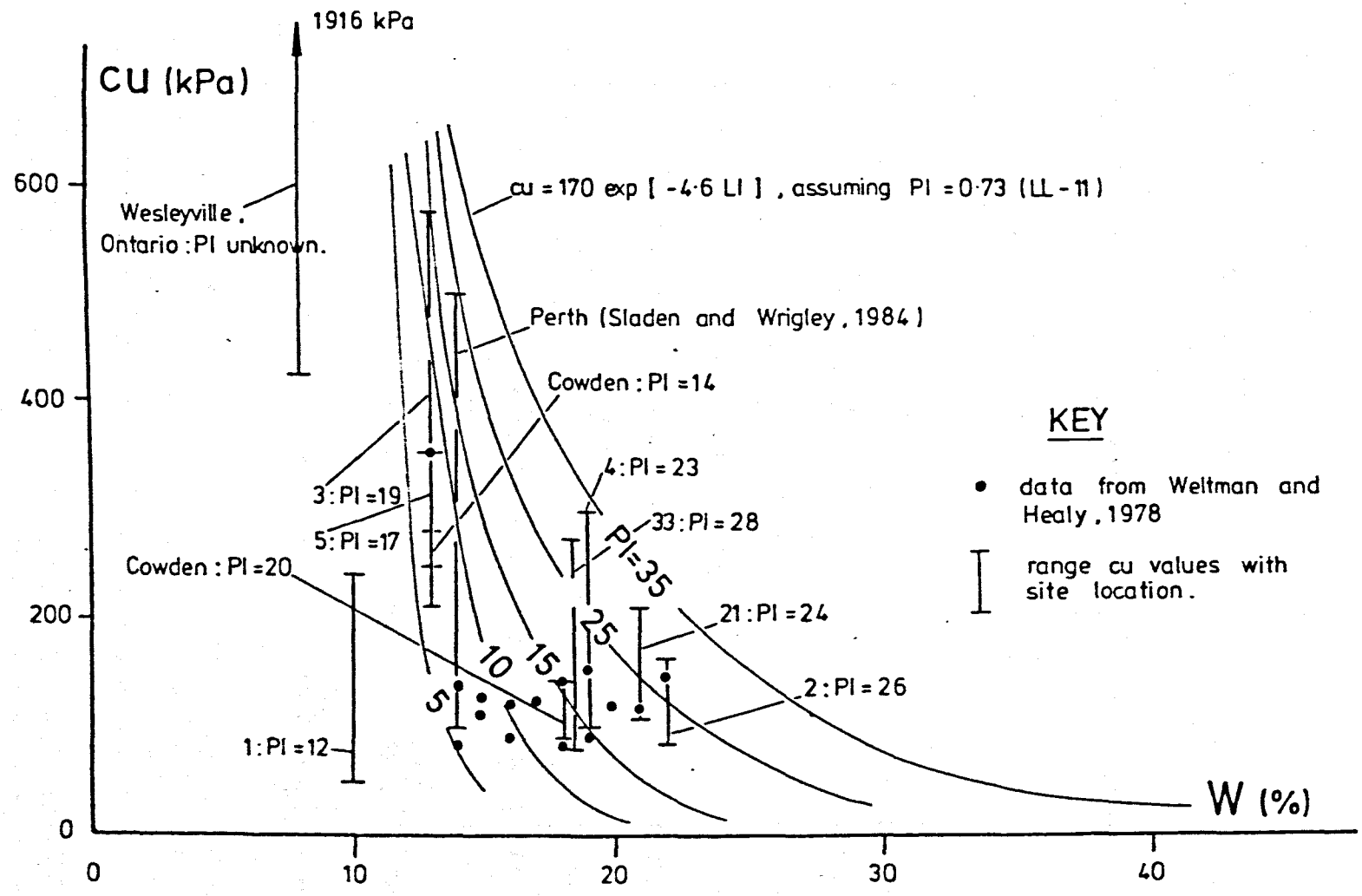

Figure 4.11 Undrained shear strength : water content relationship for lodgement tills.

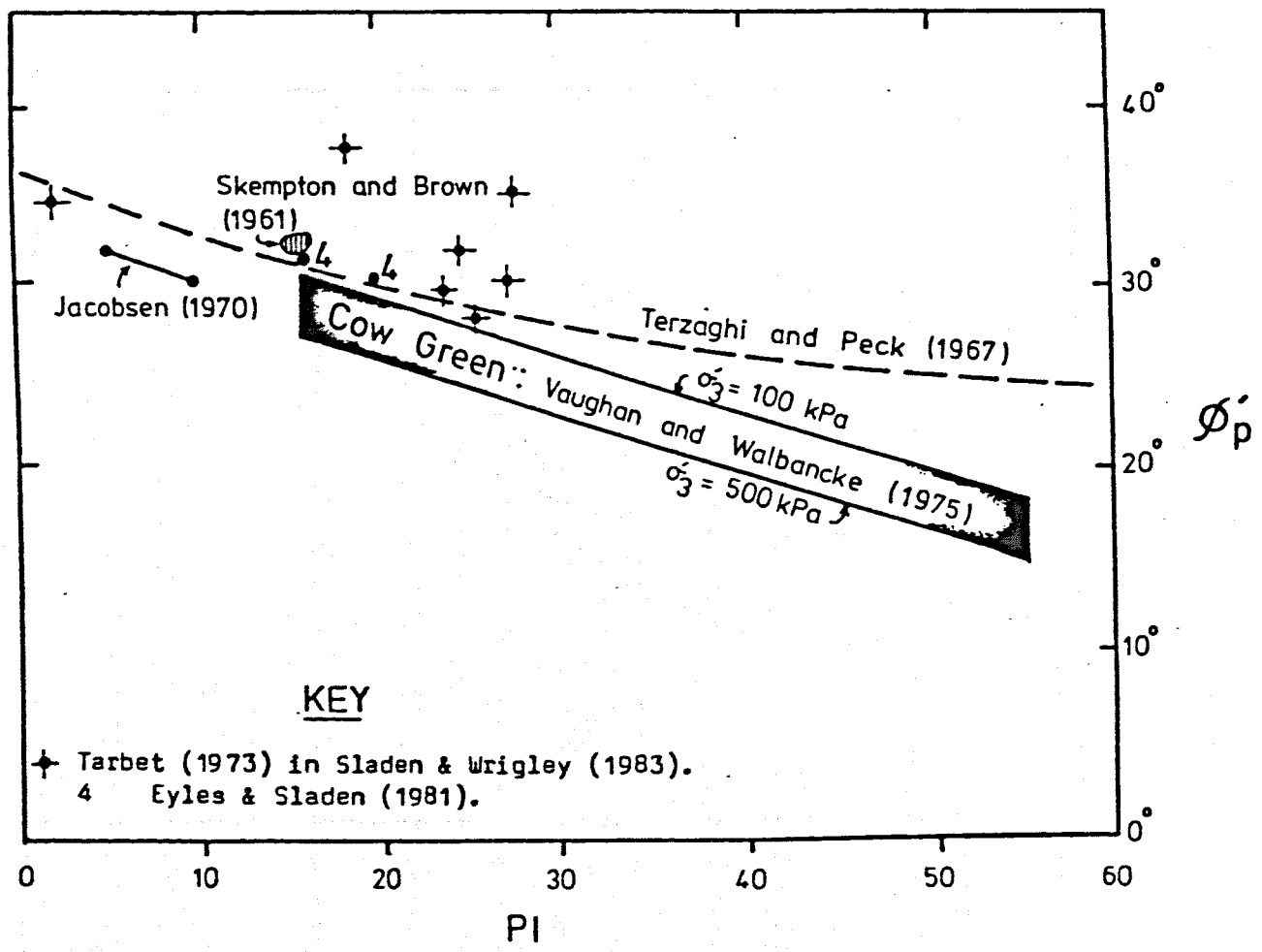

Figure 4.12 ϕ'_p : PI for various lodgement tills.
(Based on Sladen and Wrigley, 1983).

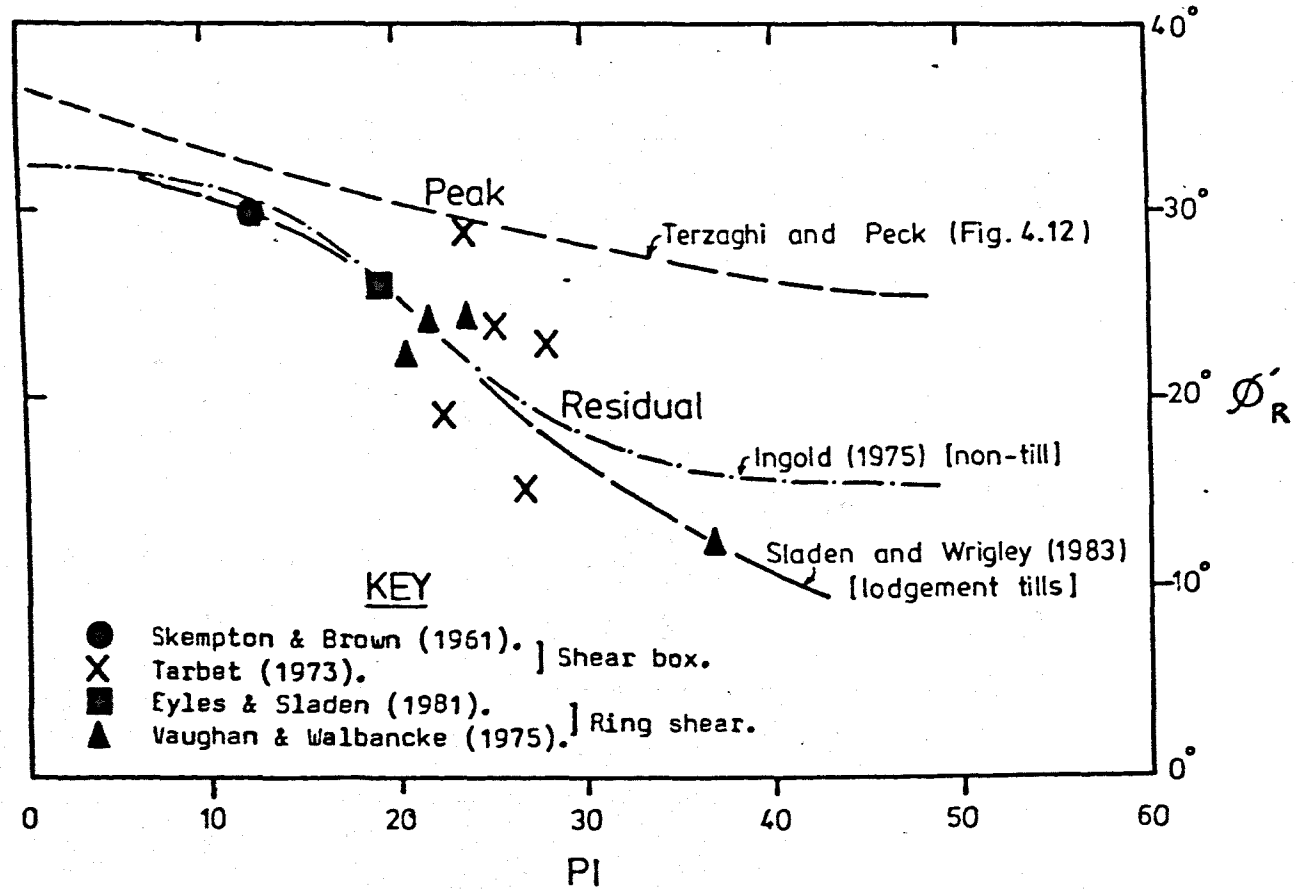

Figure 4.13 ϕ'_R : PI for various lodgement tills. (Based on Sladen and Wrigley, 1983).

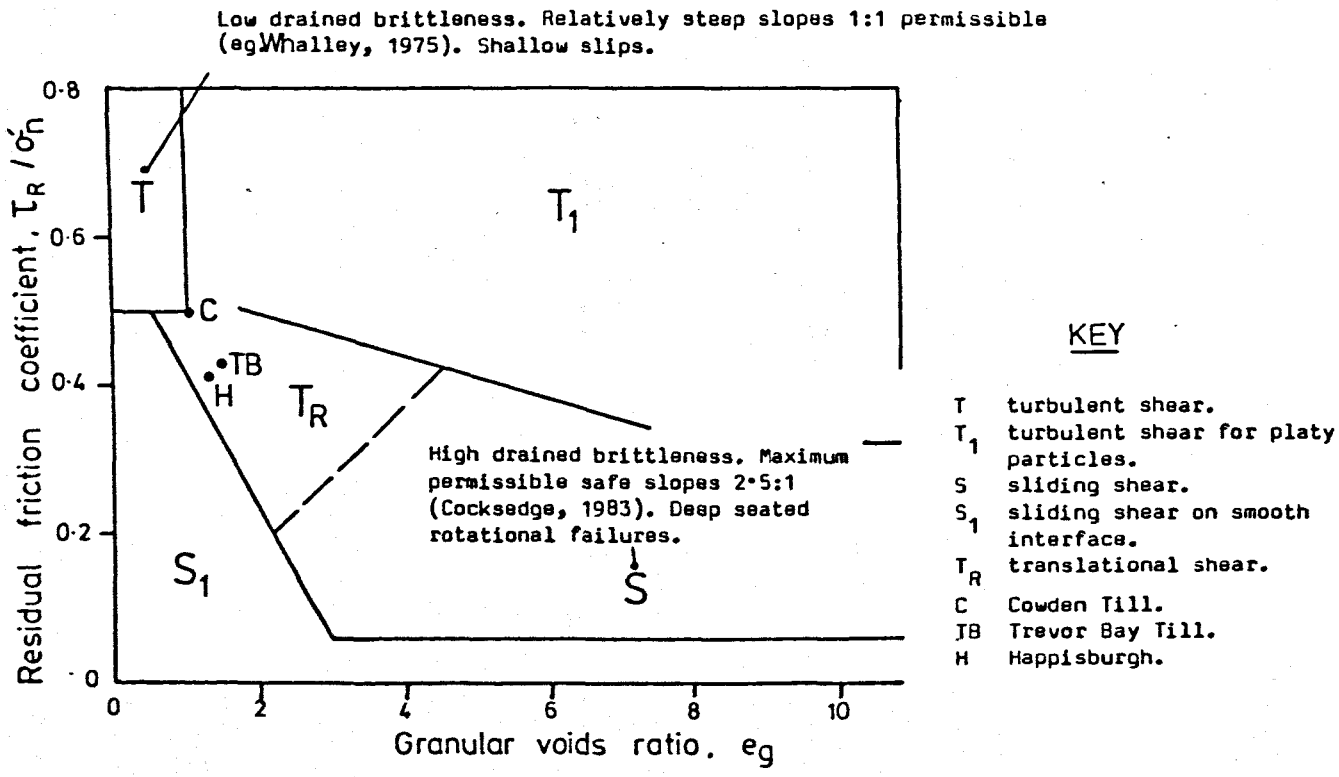

Figure 4.14 Residual shear mechanisms and particle packing. (Based on Lupini et al, 1981).

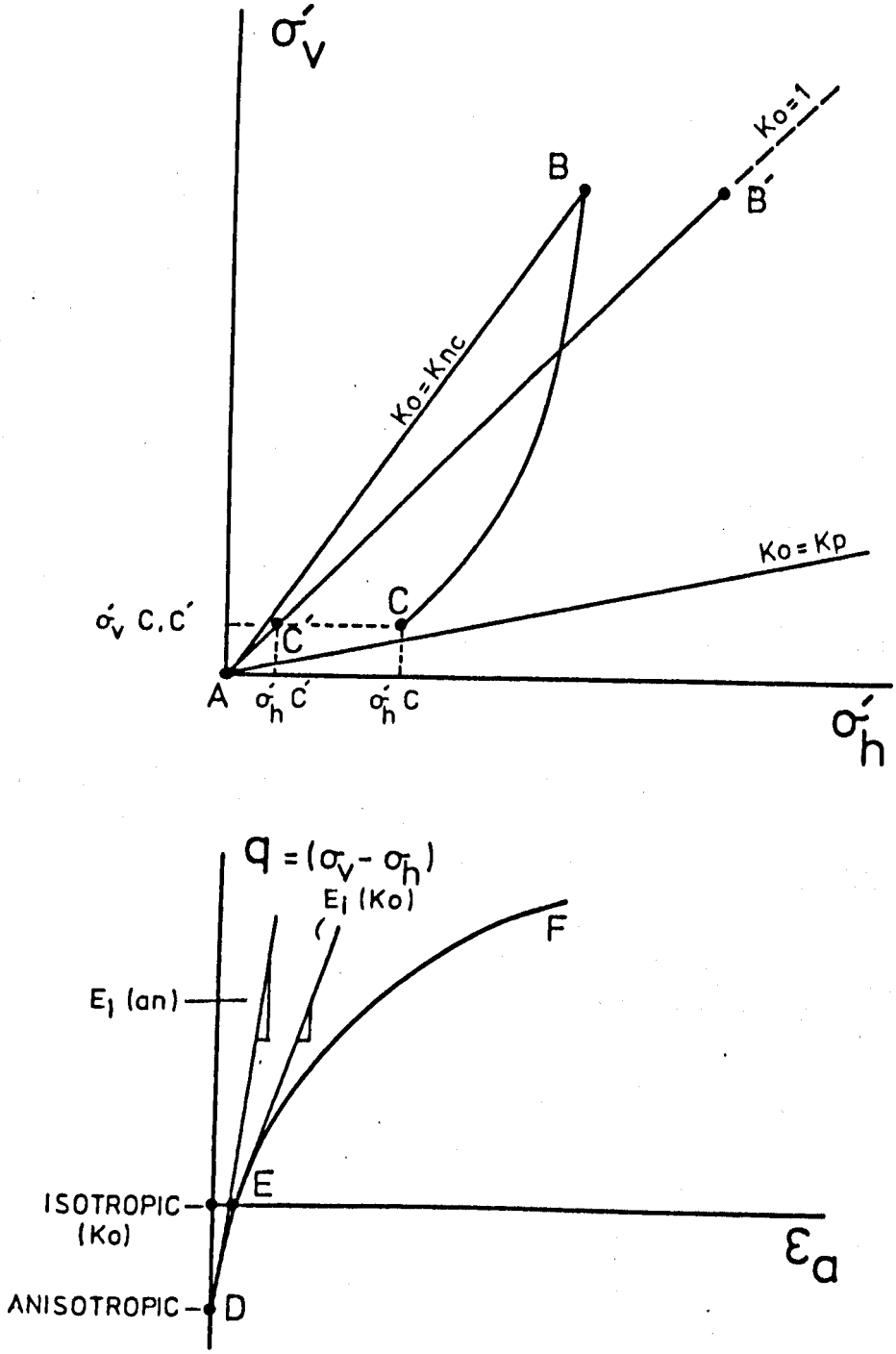

Figure 4.15 Anisotropy and elastic modulus.

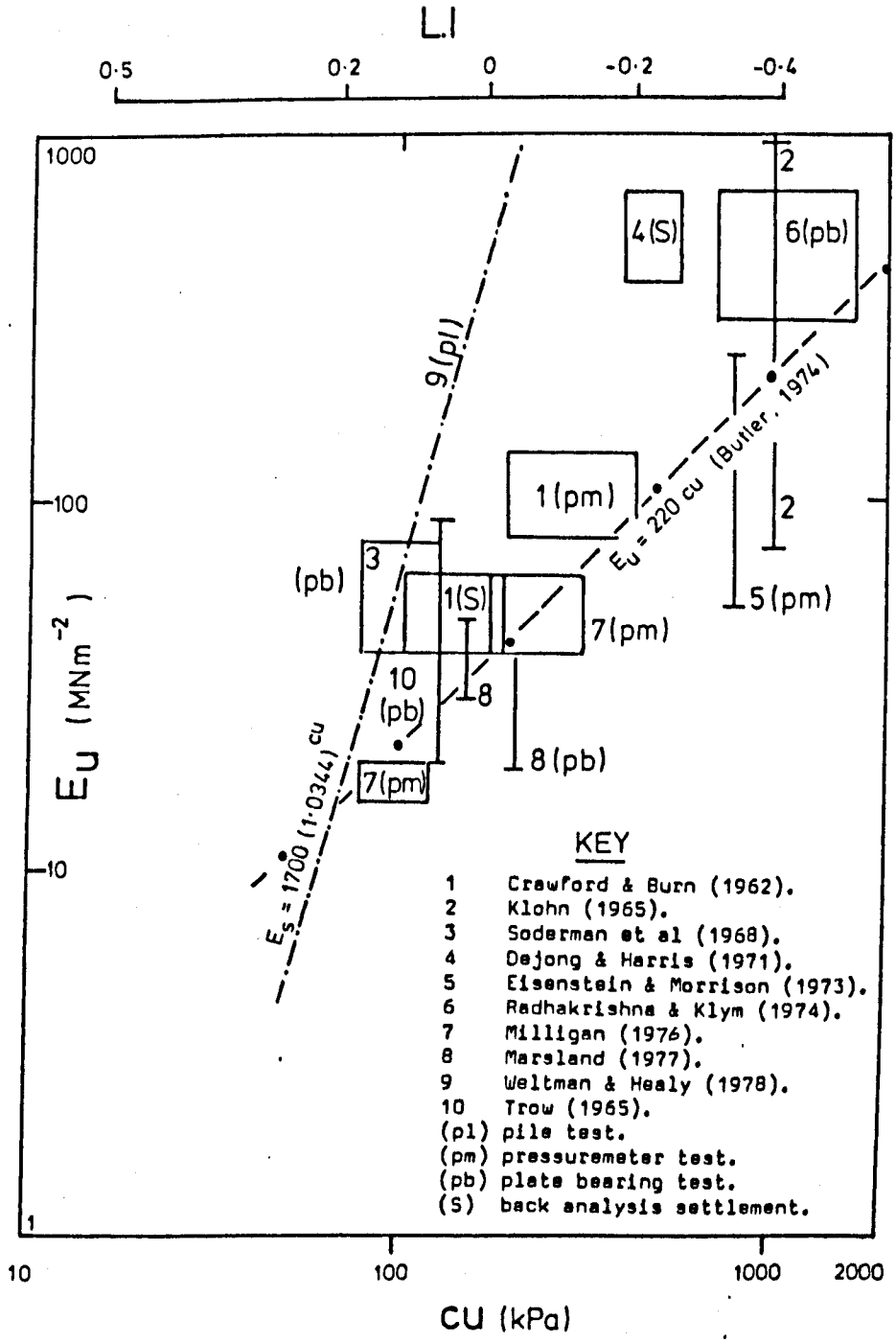

Figure 4.16 Soil modulus : undrained shear strength relationship for tills. (Based on various sources).

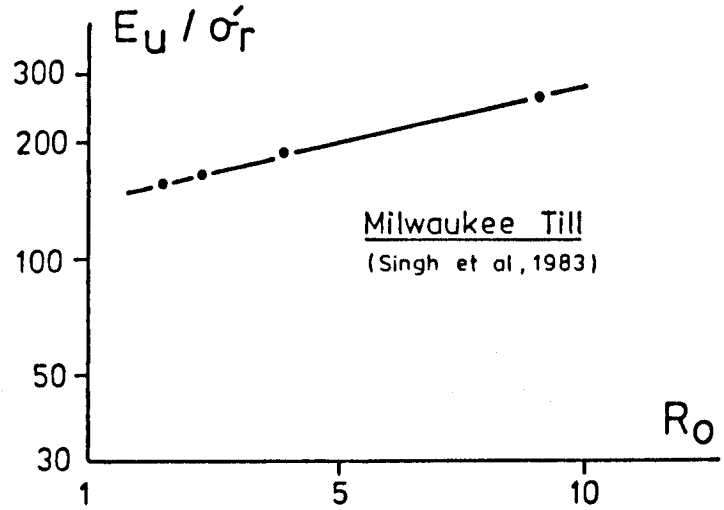

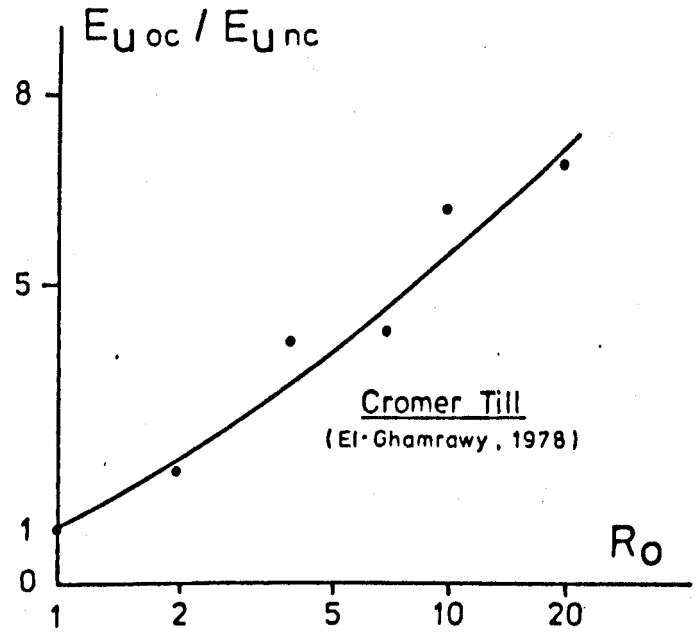

Figure 4.17 E_u : Ro relationship for two tills.

CHAPTER 5. FIELD INVESTIGATIONS.

5.1 Introduction.

A programme of field work was initiated during the summer of 1981, within the study area, which was designed to identify suitable and accessible sites in the Vale of St. Albans where the Pleistocene sediments detailed in Chapter 2 could be carefully examined and described.

The tills closely associated with the fluvial and glacial outwash gravels in the area are periodically exposed, either during quarrying operations or during the initial phases of construction work. Opportunities to inspect these fresh sections of interest must therefore be taken when the occasions arise and before they become degraded, removed or infilled.

Access to these working sites, particularly the quarries, is restricted by the owners and visits to them are arranged in advance, with their permission. Usually a period of two weeks prior notice is required before a visit takes place.(1)

Visits have been made to a number of quarry and other localities over the period 1981-83 where the tills have been exposed and also where their field relationships are reasonably well demonstrated. From these, 5 sites(2) have been selected for more detailed study. These sites, extending across the entire length of the Vale, demonstrate the rich variety of sediment types to be found in the area. The lithostratigraphic sequences established at these sites are described in detail in section 5.2 .

---

1. Messrs. Redland Aggregates Ltd. and St. Albans Sand and Gravel Co. Ltd. have been particularly generous and co-operative in granting permission for the many site visits made to their quarries.
2. Moor Mill , Hatfield , Holwell Hyde, Foxholes and Westmill Quarries.

The manner of description of the glacigenic sediments and their stratigraphic relationship with the other sediments are generally in accordance with those outlined by Scott and St. Onge (1969). Variations in till colour, occasionally an important diagnostic parameter, have been assessed in each case with reference to the hues in Munsell Soil Color Charts (1975 edition). Bed thicknesses are calculated on the basis of spot heights established by levelling to the nearest located Ordnance Survey bench mark.The vertical positioning of the junctions between the various sedimentary units described in 5.2 are therefore all relative to Ordnance Datum.

The series of in situ tests on the tills described in 5.3 and the various sampling procedures in 5.4 necessary to expedite the laboratory testing programme described in Chapter 6 have also been carried out during this period and are reported in this chapter.

5.2 Site locations and descriptions of Pleistocene sediments.

5.2.1 Moor Mill Quarry, Bricket Wood.

This quarry site (TL 143027) lies approximately 1km northeast of Bricket Wood (see site 1, Fig 2.2). At this locality a 2·1m unit of coarse fluviatile gravel and sand (Westmill Lower Gravel, Gibbard, 1977) lies on an uneven surface of Chalk at 63·13m O.D.(section 1, Fig 5.1). At 65·20m O.D. the gravels are overlain by 2·57m thickness of laminated silty clays. The lowest unit is a strong brown (7·5YR 4/4 to 4/6) stiff silty clay with dark brown (7·5YR 3/2) laminae or varve-like couplets of approximately 2mm thickness. The unit is strongly fissured and fissure surfaces exhibit black mottling and staining. Occasional fine, olive-yellow (2·5Y 5/4) firm to stiff laminated and blocky clayey silt with strongly developed undulose, sub-horizontal fissuring showing iron-stained yellow-brown (10YR 5/6) surfaces. Occasional inclusions of olive-brown (2·5Y 4/4) fissured clay are present.

At the top of the unit is 200mm of greyish brown (2·5Y 5/2) to dark greyish brown (2·5Y 4/2) firm to stiff, very silty clay with some evidence of fissuring.

At 66·77m O.D. the silts are overlain by 2·57m of dark chalky lodgement-type till. In hand specimen the till is a very dark greyish brown (10YR 3/2) to very dark grey (10YR 3/1), stiff to very stiff,

silty clay with medium (100mm) rounded and sub-rounded clasts of flint with small (5mm) angular fragments of flint. Small (2mm) pebbles of quartz occur throughout , together with finely dispersed (<3mm) particles of unweathered chalk. A narrow (100mm) discontinuous greyish brown (10YR 5/2) to brown (10YR 5/3) firm, friable fine silty sand pocket was present at 67·00mm O.D.

The top 300mm of the till is oxidised dark to mid-brown and is partially to completely decalcified. At 69·24m O.D. the till is overlain by 5·18m of current-bedded gravel and sand (Smug Oak Gravel). Ground surface is at 74·42m O.D.

5.2.2 Hatfield Quarry, St. Albans.

This quarry site (TL 186086) is situated 0·5km south of Beech Farm (TL 190090) and 1·5km west of Hatfield aerodrome (TL 205085), see site 2, Fig 2.2. At this locality the eroded surface of the Chalk lies between 68·50m and 69·50m O.D., see section 2, Fig 5.1. A 6·64m thick unit of fluviatile gravel and sand overlies the Chalk and is associated with a 1m thick interbedded silt unit at 74·14m O.D.

At 75·14m O.D. the silts and gravels are overlain by 4·67m of dark chalky till.

In hand specimen the till is a dark yellowish brown (10YR 4/4) stiff to very stiff, in places friable sandy clay showing occasional grey (5Y 6/1) streaking and mottling. Medium-sized (up to 50mm) angular flint fragments occur, with smaller (< 15mm) rounded to sub-rounded, slightly iron-stained fragments of chalk. The top 400mm of till is oxidised dark to mid-brown. In hand specimen this horizon comprises a dark yellowish-brown, very firm to stiff friable sandy clay with occasional grey silty streaking.

Medium-sized (up to 50mm) angular flint fragments abound with smaller (<15mm) rounded to sub-rounded, slightly iron-stained but relatively unweathered fragments of white (10YR 8/1) chalk.

At 79·24m O.D. the till is overlain by 1·52m of silty sand, sandy silt and clay with stones.

At 81·33m O.D. this granular layer is overlain by a light coloured chalky lodgement-type till. In hand specimen this till is dark yellowish brown (10YR 4/4) to yellow-brown (10YR 5/4) and light brownish grey (2·5Y 6/2) to light grey (2·5Y 7/2) stiff though friable,

sandy clay with medium-sized (up to 50mm) angular fragments of flint and smaller (30mm) rounded, black, brown and dark grey (Tertiary?) flint pebbles. Medium to small (< 30mm) clasts of sub-rounded unweathered chalk are abundant.

Ground surface is at 83·21m O.D.

5.2.3 Holwell Hyde Quarry, Welwyn Garden City.

This quarry site (TL 265116) is situated on the eastern outskirts of Welwyn Garden City, 1·5km south of Panshanger aerodrome (TL 265127), see site 3, Fig 2.2. Information supplied to the writer by Messrs. Redland Aggregates Ltd. indicates that Chalk lies at approximately 51·72m O.D. at this locality,(section 3, Fig 5.1). Above the Chalk is an 8·10m thick band of coarse, medium and fine chalky sand and gravel. At 59·82m O.D. these gravels are overlain by a 4m thick unit of hard dark grey calcareous lodgement-type till with flints; the basal 200mm of this unit is oxidised brown-grey.

At approximately 64m O.D. the till is overlain by a 2·30m thick unit of cross-bedded, uniformly graded (ice distal?) fluvioglacial sand. At 69·01m O.D. the top surface of the sand is seen below the oxidised basal unit of another dark grey calcareous till. Approximately 300mm above this junction the till becomes darker in colour (Fig 5.2) and in hand specimen (Fig 5.3) is a very dark grey (5Y 3/1) clay with fine, medium and coarse (up to 100mm) rounded to sub-rounded fresh white chalk clasts showing clearly marked glacial striae on their surfaces. Occasional angular fragments of medium to large flints are present. A Jurassic fauna (see Chapter 6) is present.[1]
This till is not exposed in a cutting 250m to the north east (TL 267106) of the lowest part of the quarry and the sand unit is here seen lying directly underneath a light calcareous lodgement till at 78·41m O.D. This till is shown in Fig 5.4. At TL 265116 however, the dark till is overlain directly by the light calcareous till at 73·50m O.D. The contact zone between the two tills is marked by sub-horizontal shearing planes and therefore could indicate a glaci-tectonically controlled junction. (D.A.Cheshire, personal communication).

---

1. This is till HH(a) in Table 5.3.

In hand specimen (Fig 5.5) the till is a light grey (5Y 7/1) and light yellowish brown (2•5Y 6/4) to brownish yellow (10YR 6/6) clay with angular fragments (up to 40mm) of flint and rounded to sub-rounded fragments (up to 60mm) of fresh white chalk. Occasional flecks of soft pink powdery silty clay are present (Red Chalk?). Jurassic bivalves are abundant.[1]

Ground surface is at 79•31m O.D.

5.2.4 Foxholes Quarry, Hertford.

This quarry site (TL 337125) lies 1•5km east of Hertford town centre on either side of the A414 dual carriageway between Balls Park at TL 335120 and its intersection with the A10(T) at TL350130, (site 4, Fig 2.2).The uneven, eroded surface of the Chalk and Reading Beds in this locality is approximately 56•50m O.D. Above this is seen a variable thickness of dark calcareous lodgement till, (see section 4, Fig 5.1).

In hand specimen this is a very dark grey (5Y 3/1), very stiff to hard clay with small to medium-sized, rounded to sub-rounded chalk clasts (up to 25mm) and angular fragments of small to medium-sized flint (up to 60mm). The top 300mm of this unit comprises an oxidised and partly decalcified yellowish brown (10YR 5/6) becoming dark greyish brown (10YR 4/2), stiff becoming very stiff sandy clay with small to medium-sized (up to 30mm) fragments of angular and rounded to sub-rounded flint and with small flecks (1-2mm) of light grey (10YR 7/1) to white (10YR 8/1) soft chalk.[2]

Excavation of a small pit by hand in nearby Foxholes North (TL 337124) quarry revealed a localised pocket of light grey, soft to very soft, occasionally firm, very chalky diamicton at the top of this till. Other occurrences of this type in this locality have been reported (for example, Cheshire, 1981). Above approximately 59m O.D. there occurs a succession of current bedded sands and gravels (Westmill Upper Gravel). In places, these gravels are extremely coarse and very large quartzitic boulders (1-2m) are not uncommon.

---

1. This is till HH(b) in Table 5.3

2. Till F(b), Table 5.3.

At the nearby Foxholes East (TL 344126) quarry a 1·30m thick lens of light till (Foxholes Till) is seen resting on a calcareous sand at 64·63m O.D. within a channel in the gravel. In hand specimen this till is a dark yellowish brown (10YR 4/4) and light grey (5Y 7/2) sandy clay with shattered, angular flint fragments (up to 30mm) and rounded to sub-rounded chalk pebbles (up to 35mm). The basal 100mm and top 250mm of this unit are decalcified.

Ground surface lies between 68·25m and 70·50m O.D.

5.2.5 Westmill Quarry, Ware.

This quarry site (TL 344153) is located approximately 1·5km north west of Ware between the B1001 and the A10(T), see site 5, Fig 2.2. The irregularly-eroded Chalk bedrock surface here occurs at a mean elevation of 51·20m O.D., section 5, Fig 5.1. Above this is 9m thickness of stratified fluviatile gravel and sand forming the Westmill Lower Gravel. At 60·00m O.D. the gravels are seen passing into a narrow band (150mm) of laminated silty clay. In hand specimen this soil is a firm, friable yellowish brown (10YR 5/6) very silty sand clay with distinct and regularly spaced (5mm) laminae. At 60·18m O.D. this unit (and a narrow, very coarse gravel band above it) is overlain by 2·32m of dark, calcareous lodgement till (Ware Till).[1] In hand specimen this soil is a dark greyish brown (2·5Y 4/2) very stiff, occasionally hard sandy clay with small (< 7·5mm) rounded and sub-rounded clasts of fresh white (10YR 8/1) chalk with small, medium and large (occasionally 100mm) angular, shattered fragments of flint. A variety of other stones are present in this deposit.

At TL 345159 a 4m deep channel extending from above the Ware Till down to 58·42m O.D. is infilled with gravel, silty sand and a light calcareous till (Westmill Middle Till).

In hand specimen this soil is a firm to stiff light olive brown (2·5Y 5/4) and light yellowish brown (2·5Y 6/4) to yellowish brown (10YR 5/4) sandy clay with medium (25mm) sub-rounded and angular, shattered clasts of relatively unweathered chalk.

At 62·48m O.D. the eroded, weathered and partly decalcified surface

---

1. This is till W(b) in Table 5.3.

of the Ware Till is overlain by a complex deposit of large gravel lenses with associated sand beds (Westmill Upper Gravel) of approximately 6·30m thickness.

At 68·88m O.D. these gravels are overlain by 4·06m thickness of light calcareous lodgement till (Eastend Green Till).[1]

In hand specimen this till is a light olive-grey (5Y 6/2) to brown (10YR 5/3) very stiff, occasionally hard clay with strong brown (7·5YR 4/6) mottling and streaking and small (2-3mm) patches of pink (5YR 7/4) silty clay (Red Chalk). There are many small, medium and large (occasionally 150mm) rounded clasts of relatively fresh chalk showing distinct surface striations. Medium to large, irregularly shaped, occasionally shattered flints abound. Bivalves are present.

Ground surface is at 72·94m O.D.

5.3 In situ testing.

Whilst the majority of the experimental work undertaken on the tills has been laboratory based, there are nevertheless aspects of this work which have necessitated recording features within the various till bodies and the carrying out of certain testing in situ.

In view of the importance of till stone fabric (clast orientation and dip) in the reconstruction of glacial environments (Chapter 4), the determination of such a fabric for five tills at three sampling sites has been undertaken. In this way, it was hoped that the results would confirm the findings of others who have worked with these sediments and their correlatives at these and other sites in the Vale. Of more immediate importance to this study however, was the necessity of establishing a clast fabric vector (see 5.3.1) for those tills from which would be obtained oriented undisturbed samples for oedometer compression and direct shear testing.

With the exception of the low level, possibly glacitectonic shear planes observed in the tills at both Holwell Hyde quarry (5.2.3) and Westmill quarry (Cheshire, 1983), there was no further evidence during the period 1981-83 for either the small scale fine cracking

---

1. This is till W(d) in Table 5.3.

and jointing (for example McGown et al , 1974) or the larger scale linear and convex discontinuities (Derbyshire and Jones, 1980) observed by others in lodgement tills elsewhere.

Fissuring was, however, occasionally observed in the sediments closely associated with these tills , for example in the Laminated Clays at Moor Mill quarry , 5.2.1. However, during the winter months of 1983, the reopening and reworking of Holwell Hyde quarry in Welwyn Garden City temporarily exposed sections of the two upper tills and in these was revealed a series of well-developed joints. The opportunity was therefore taken to measure and record details of these structures before infilling operations began.

Finally, to supplement the laboratory shear vane testing of selected reconstituted tills described in Chapter 6, in situ shear vane testing of four tills at two sites was carried out early in the schedule of work.

5.3.1 Clast orientation and dip.

The particulate nature of the tills described in section 5.2 is of some significance to this study in two respects:

(i) On the basis of measurements made of the a-axis orientation of stones within the tills in the Vale of St. Albans it has been possible to distinguish at least two ice advances into the area, each with its associated lodgement till (West and Donner, 1956; Gibbard, 1974, 1977; Cheshire, 1981). The measurement and analysis of clast axis orientation can therefore be of considerable assistance in the interpretation of the age relationships of these tills and can act as indicators of ice sheet provenance, hence pointing to the source(s) of the till materials.

(ii) The obtaining of undisturbed oedometer samples for the horizontal drainage condition (see section 5.4.2) necessitated, it was felt, a frame of reference within which sampling could be made. Orientation of the cutting ring became important in this respect in view of the very large number of possible ways of orientating the sampler by vertical rotation. Sampling at these locations was therefore carried out very precisely with respect to the till stone fabric which was determined beforehand by field measurements. The adoption of this convention carried with it other benefits: it would also enable, for example, a subsequent investigation to be made of the directional dependence of oedometer determined permeability with respect to the

established fabric vector for each soil.

Guidelines have been introduced which have helped in the standardisation of the techniques of till fabric analysis and the sampling and measuring procedures adopted for the present study are generally those which have been outlined by Andrews (1971). Because of the large number of till fabric analyses undertaken by Cheshire (1981,1983) in the Vale of St. Albans, his various parameter limits have been adopted for this study so that consistency and continuity in the sampling and measuring procedures is ensured. Cheshire's limits are reproduced below:

1. Sample size: Each sample consisted of 50 stones. One such sample was taken at each site.
2. Griffith's and Ondrick's (1968) a, b, c-axis convention was adopted. The b-axis is defined as the minimum dimension across the maximum projection plane, with the a- (long) axis and c- (short) axis normal to it.
3. Due to difficulties of size, a lower a-axis limit of 20mm was used. Anything smaller than this was rejected. No upper limit was employed.
4. An arbitrary axial (a : b) ratio upper limit was set at 3 : 1. Any stone with an axial ratio greater than this was assumed too elongate.
5. An axial ratio lower limit was established so as to reject stones with a tendency towards random orientation. This limit was set at 1·2 : 1.
6. The interference effect due to the proximity of any stone to a heavier clast was allowed for by rejecting any found within 20mm of such a clast.

A sampling site was prepared by exposing a 1m long by 300mm deep band of fresh till either in a pit on the quarry floor or on a vertical surface of the quarry face, Fig 5.6.
Sampling was non-selective and the orientation of every tillstone complying with the stated parameter limits was measured and recorded. After having carefully removed the till stone from the matrix its a-axis was determined and its position marked before replacing it into its cavity. The orientation and dip of the inscribed axis was then measured. Alternatively, a non-magnetic pin or needle may be used to

indicate the direction and dip of the stone axis when pushed into the till within the cavity formed by removing the stone. Readings (to the nearest degree) were made using a Silva liquid-filled combined compass and clinometer. The orientation of the down-dip direction of the a-axis (azimuthal reading, with grid magnetic angle correction) together with the inclination of the a-axis from the horizontal were recorded for each of the fifty samples.

This set of procedures was carried out on five tills at three sites:

(i) Dark grey calcareous till, HH(a), Holwell Hyde Quarry.
(ii) Light grey calcareous till, HH(b), Holwell Hyde Quarry.
(iii) Oxidised Ware Till, F(b), Foxholes Quarry.
(iv) Ware Till, W(b), Westmill Quarry.
(v) Eastend Green Till, W(d), Westmill Quarry.

Prior to obtaining an undisturbed (fabric) oriented till sample, (a procedure described in section 5.4.2 of this chapter), data from the fabric study at the sampling site required analysing in order to establish sampling direction. In view of this order in the sequence of events, the results of the fabric studies from the five sites, together with the method of their analysis, are presented in this section so as to precede descriptions of the sampling procedures themselves.

The results of this survey are shown in Figs 5.7 to 5.11. In these diagrams the a-axis dip direction and magnitude are plotted as single points on polar equidistant graph paper. The dip direction is measured clockwise from true north relative to the 10° rays; the dip magnitude is recorded relative to the 10° interval lines of radius, dip angles increasing from the outer radius (0°) to the innermost (90°). Any clustering of the data points is indicative of a preferred orientation of a-axis directions, the degree of clustering is a measure of the strength of the fabric so produced.

The direction and strength of a fabric may be quantified in a variety of different ways, depending on how the data are processed. In this study, each a-axis data point is considered to be a vector of known direction θ and of unit magnitude (Reiche, 1938; Krumbein, 1939; Curray, 1956). The north-south and east-west components of each observation vector are computed by multiplying its (unit) magnitude by the cosine and sine of the azimuth respectively. Algebraic summation of these components over the entire sample of 50 will yield

the north-south and east-west components of the resultant vector $\bar{\theta}$, whence

$$\tan \bar{\theta} = \frac{\Sigma n \sin \theta}{\Sigma n \cos \theta}$$

The magnitude (or strength) r of the resultant vector is therefore given by :

$$r = \left[(\Sigma n \sin \theta)^2 + (\Sigma n \cos \theta)^2\right]^{\frac{1}{2}}$$

or, reducing to a scale 0 - 100% :

$$L = \frac{100r}{\Sigma n}$$

where θ = azimuth from 0° to 360° of each observation.

$\bar{\theta}$ = azimuth of resultant vector.

n = number of observations. (= 50)

r = magnitude of resultant vector.

L = magnitude of resultant vector in terms of % [1]

Statistical tests may be employed to determine the likelihood of the plotted distribution occurring by chance alone. For example, the Rayleigh (1894) distribution can be used to test for the probability p of obtaining a greater magnitude percentage L for the resultant vector by pure change combination of n random data points in the form:

$$p = e^{(-L^2 n)(10^{-4})}$$

(Usually, no distribution is accepted as being significantly different from randomness unless there are less than 5 chances in 100 of its being due to chance.)

A summary of these results, including Rayleigh probability testing against randomness, is shown in Table 5.1.

A number of points emerge from a study of these data:

(i) The fabric resultant vector Vr is contained within the NE, SW quadrants for all the tills. Assuming parallelism of clast a-axes with direction of ice advance, this inferred direction is therefore generally from the north east.

---

1. Vector magnitude varies from 0 to 100% . A random distribution of clast orientations yields L = 0% , and a sample in which all the clasts are pointing in the same direction gives L = 100% .

(ii) The "preferred vector" (the dip direction of the resultant vector) is SW for tills HH(a) and W(d) and NE for W(b), F(b) and HH(b).

(iii) Vector magnitudes for tills HH(a), HH(b), W(d), (35·9, 59·1, 36·7%) are considerably higher than for W(b) (17·1%) and F(b) (16·8%). The reduced strength of the vector for these two tills is most probably due to the existence of well developed clusters at Vr $\pm$ 90° indicating a secondary, transverse lineation of clasts within these tills. (This is not an uncommon feature of lodgement tills and the mechanics of this phenomenon are discussed by Glen et al (1957).

5.3.2 Discontinuity survey, Holwell Hyde Quarry.

During the Autumn of 1983, Messrs. Redland Aggregates re-opened the quarry at Holwell Hyde, Welwyn Garden City, in order to complete the extraction of the sand above the lowermost till at this locality.

During this process, considerable vertical sections of the two uppermost tills HH(a), HH(b) were exposed for the first time along the quarry's western boundary. Although all field work had been completed by this time, a visit to this site was made nevertheless so as to examine the most recently exposed sections of these tills. This subsequently led to the discovery of at least one well-developed set of vertical joints common to both tills. The existence of these discontinuities in these sediments is important, particularly in the light of the discussions on this subject in Chapter 4. In addition, the rarity of this particular type of structure in the tills of the Vale of St. Albans sets them apart as a distinguishing feature of the tills at this locality.

Despite the unsuitable weather conditions for field work at this time of the year, it was felt that a survey of these discontinuities (even if only of limited extent) should be made, particularly in view of the impending quarry infilling operations scheduled to start before December. A later visit was therefore made to the site and a survey of the jointing was undertaken.

Due to the shortage of time, a comprehensive survey involving detailed measurements of joint spacing and vertical and horizontal continuity was not possible. In the time available for the work however, the dip and dip direction of every identifiable (and accessible) discontinuity

surface was measured and recorded for both tills. A Silva combined compass/clinometer (with magnetic correction) was used for this operation.

A total of 45 discontinuities was recorded; 17 in the light till, HH(b); 28 in the dark till , HH(a). Rather more recordings were made in the dark till due to access and to the light till being nearer the ground surface resulting in the combined effects of weathering and pedogenesis having either masked or destroyed these structures. The joints were all vertical or very nearly so. They were not closely spaced (no less than 200mm) and they were vertically continuous over 4 to 5 metres (the height of the face), apparently passing across both tills without interruption. Despite occasional oxidation and carbonate deposition on the surfaces of these joints (particularly in the dark till, see Fig 5.2), they were tight and not open. There was no evidence of movement having taken place across these surfaces (i.e. no slickensiding or shear marks) and they exhibited a roughened, granular texture.

The joint data for both tills are shown in Figs 5.12 and 5.13. In these Figures the family of great circles so formed by the two dimensional (joint) planes intersecting the outer surface of a hemisphere and viewed as vertical (upward) projections on the sphere's lower equatorial plane are shown. In this way, the orientation of these essentially vertical structures is most clearly demonstrated. Also shown in each case is the great circle for the quarry face (assumed vertical) and a great circle representing the resultant fabric vector for the respective tills. (In each case the one-dimensional linear axis representing the vector is assumed to be a two dimensional vertical plane.)

Despite the relatively small number of joints recorded in this survey, it is nevertheless clearly evident from these diagrams that a conjugate set of vertical discontinuities exists within the lower till HH(a). This set, trending approximately north to south, has associated with it another, orthogonally disposed, set trending west to east. A similar pattern emerges within the upper till, HH(b), although the fewer number of joints recorded here has not produced such strong evidence for a west to east set.

The predominant NS set of joints in both tills is also probably exerting some control on both the direction and dip of the quarry face

as can be seen by the coincident orientation of their respective great circles. The relationship between the joint sets and the fabric vector in each till is not entirely clear however, although there is a suggestion of parallelism between the vector and the west to east set within till HH(a).

5.3.3 A new till fabric instrument.

The procedures adopted for the measurement of clast a-axes in the till fabric studies undertaken for this work have been described in section 5.3.1.

Although guidelines are available which are designed to promote "good practice" and to introduce a degree of standardisation to the measuring procedures themselves (for example, see Andrews, 1971), the equipment used in these studies will vary from person to person. More usually, a good quality liquid-filled compass is used to record magnetic bearing and this may include an integral clinometer for measuring dip angles. A selection of stainless steel needles can also be usefully employed during this process along and down which, once oriented, bearing and dip angles are measured. With this type of equipment it is quite possible to complete a field-based fabric study (50 stones) in one day. Whilst having this advantage however, the accuracy with which the bearing and dip readings can be taken will depend on the type of instrumentation used.

Various alternative methods and equipment for use in till fabric studies have been employed by others and are reported in the literature. For example, till stones may be marked and referenced in situ by means of a template, transported to the laboratory, re-oriented and analysed using specially designed instrumentation. (see for example the "orientation goniometer" reported by Karlstrom, 1952) Again, McGown and Derbyshire (1974) have successfully employed a laboratory (and field) technique based on oriented blocks of till using a "contact goniometer". Although there are certain advantages in carrying out fabric studies on reoriented samples in the laboratory, the various methods do nevertheless carry with them some disadvantages: the transportation of heavy, bulky samples and, more important, the possibility of unnoticed error in sample reorientation, for example. Whenever practical therefore, it is more appropriate, and certainly more convenient to carry out the fabric study with the till in situ.

The bearing and dip of the till stone axis is most easily recorded by replacing the stone with a needle aligned along the clast a-axis. This particular principle has been adopted and incorporated into a new till fabric instrument designed and developed specifically for this purpose, Appendix I . The instrument was designed by the writer and the prototype was constructed in the workshop of the School of Engineering, Hatfield Polytechnic. It is now in commercial production by Wykeham Farrance Engineering Ltd.

The instrument is made up in three parts: A,C,D, Fig 5.14. Part A comprises a series of interchangeable hollow stainless steel needles of various sizes connected via the needle holder bracket B onto a central circular aluminium stage C. Rotating on a machined brass stud through this stage, a perspex platform carries a removeable precision clinometer in a slotted diametral housing, E. Once assembled, ABC has a fixed alignment but can rotate 360° about its axis by loosening the knurled brass nut connecting C to D. Stage D carries a 360° rotating aluminium plate (axis of rotation normal to ABC) housing a precision liquid-filled compass, F[1], and two orthogonal spirit bubbles.

The method of operation is as follows:

1. Selecting a pin to suit the size of the clast, align it along the a-axis scribed on the stone and, applying hand pressure, push into the till matrix beyond it.

2. Place one of the brass shrouds supplied over the end of the pin and tap gently with a small hammer until the pin is firmly embedded in the clay (preserving both axis and dip).

3. Sheath the pin with its hollow needle (internal stud guides will engage during this process) and, using the larger brass shroud, tap this into the clay (its direction of penetration will be that of its contained needle).

4. Connect the needle via the needle holder bracket B to central stage C and compass housing D.

5. Place the clinometer into its slot and rotate this stage until the clinometer axis is parallel to the needle (i.e. pointing down the dip of the clast axis).

---

1. Suunto Instruments liquid compass with optically sighted card pivoted on a sapphire needle. (0·5° calibration).

6. Place the compass into its housing and, rotating its stage in planes both normal and perpendicular to the needle, ensure that it is horizontal by referring to the spirit bubbles. Secure by tightening all locking nuts.

7. Take readings of dip and bearing on the clinometer and compass.

By replacing the pins with the stainless trowel attachments shown in Fig 5.15 the instrument can also be used for measuring the dip and bearing of any planar feature in soil (for example a fissure, crack, joint or bedding plane). In this case, depending on the attitude of the face (either horizontal or vertical) containing the discontinuity, the compass in stage D will either occupy the position shown or another machined at 90° to it.

The lengthy development and manufacturing period required to produce this instrument (and its prototype) has meant that it has not been available for use during the field work described in 5.3.1 and 5.3.2. However, it is hoped to formulate a programme of fieldwork based on its use at a number of quarry localities designed to evaluate its performance on a comparative basis.

5.3.4 Shear vane testing.

Whilst obtaining bulk disturbed and undisturbed samples at Westmill and Holwell Hyde quarries (see 5.4), the opportunity was taken to carry out in situ shear vane testing of tills HH(a), HH(b) at Holwell Hyde and tills W(b), W(d) at Westmill. The purpose of these tests was twofold: firstly, an estimate of the undrained in situ shear strength of the tills was desired; secondly, this limited series of tests was designed as a supplement to the motorised (laboratory) shear vane tests on the same reconstituted tills described in Chapter 6.

The instrument used was the Geonor A/S Inspection Vane Borer. This hand held instrument is approximately 300mm long with a handle width of 105mm. As supplied, it has 3 interchangeable cruciform blades of different sizes. By using the smallest vane supplied (16mm x 32mm), the maximum torque generated at the head is 2·93Nm. With this vane size fitted, it is possible to record shear strengths up to a maximum of 192kPa. For the very stiff tills, however, a smaller vane capable of recording shear strengths up to a maximum of 500kPa was manufactured.

A site was prepared so as to expose a sufficient area of fresh unweathered till either on a vertical face or on the floor of the

quarry. The vane was pushed into the soil by hand as far as was possible, usually between 50mm and 100mm. Having obtained an initial peak reading of undrained shear strength on the graduated scale of the instrument, a remoulded value was then obtained by quickly rotating the vane a number of times and then repeating the test. The rate of testing, although difficult to both judge precisely and control, corresponded approximately to 1 revolution of the vane per second. The vane was extracted from the soil and the sheared portion of soil within the area of the cruciform was scraped off and placed into an airtight polythene bag for subsequent water content determination. Three horizontal and three vertical tests were performed on each of the soil types.

From a vane test undrained shear strength is related to the measured torque. It is usually assumed that when maximum torque is achieved a peak isotropic undrained shearing resistance is mobilised uniformly over a swept vertical surface at the four outer edges and along the two horizontal surfaces at either end of the vane. The effects of anisotropy in the soil and the rate of testing, amongst other things, are therefore ignored.

Assumptions regarding the development, shape and size of the zone of shear together with the distribution of shear stresses in the soil and on the vane blades have been examined experimentally and reported by Menzies and Merrifield (1980). On the basis of tests carried out using an instrumented vane in both Leighton Buzzard sand and undisturbed London Clay, they have shown that at maximum torque shear distortion is concentrated in a narrow band of shear at the blade edges. Further, they have demonstrated that very little soil distortion will occur in the sectors between adjacent blades.

Nevertheless, it is recognised that there are limitations to this type of in situ test and that, in particular, there may be difficulties involved with the interpretation of the results of tests on small volumes of very stiff soil. In this context, Marsland (1977) states "While in some clays these (shear vane tests) may give values close to those obtained in triaxial tests, there is considerable evidence to show that such tests seriously overestimate the strength of the stiffer clays which contain discontinuities."

Notwithstanding these observations, and in defence of this type of test, it could be stated that a thin gauge cruciform vane will cause only a small amount of disturbance to the soil during its penetration and this will probably be considerably less than that resulting from driving a

conventional U100 sampling tube.

The results of the in situ vane testing and associated water content determinations are shown in Table 5.2. A discussion of the results contained therein is given in Chapter 8.

5.4 Sampling procedures.

At each of the five localities described, bulk disturbed (15 - 20kg) samples of the tills and silts were excavated by hand tools, transported to the laboratory and stored in airtight containers.

In addition, at three of the sites (Holwell Hyde, Foxholes, Westmill) undisturbed till samples were obtained for oedometer compression testing. At Foxholes and Holwell Hyde, undisturbed till samples were obtained for direct shear testing.

Details of all samples at the five sites and the heights of these sampling points relative to Ordnance Datum are given in Table 5.3.

5.4.1 Bulk disturbed samples.

The very stiff lodgement tills which have been described are difficult to work and require excavation by hand tools. All scree and superficial material and weathered soil is first removed to expose fresh, unweathered soil, usually 200 - 300mm beneath the surface or face of the exposure. Enough material was excavated at each site (approximately 15 - 20kg) to be sufficient for the laboratory testing described in Chapter 6.

Samples were placed into heavy duty polythene bags, tied and placed in plastic airtight containers. Samples were stored in this condition in the laboratory until required. Where silty clays occurred in conjunction with the tills, for example at Moor Mill and Westmill, then these too were sampled and stored in a like manner.
A total of 19 soil types were sampled at the 5 sites.

5.4.2 Undisturbed samples for oedometer and direct shear testing.

Five undisturbed samples of selected tills were taken for oedometer compression testing at three sites: Holwell Hyde (tills HH(a), HH(b)), Foxholes (till F(b)) and Westmill (tills W(b), W(d)). These samples were obtained in situ directly in the stainless steel cutting rings which were used subsequently in the oedometer cells. Beforehand, each

ring was given an identifier, weighed using a top pan balance accurate to 0·01g and the height and internal diameter (nominally 19mm and 75mm respectively) determined using vernier calipers. Finally, a thin smearing of silicone grease was applied to the inside surface of each ring before placing it into a small, labelled polythene bag.

On site each cutting ring was precisely positioned on a prepared horizontal surface of soil. With the cutting edge facing the soil, a wooden dolly was placed over the flat-edged surface of the ring and the ring was gently tapped into the soil using a small lump hammer. Once full penetration of the ring was achieved, the tapping was stopped and the ring (with its soil) was very carefully excavated using a small trowel and palette. The sample was then trimmed immediately and, if any stone inclusions larger than about 2mm (approximately 10% of the sample thickness) were seen on or near the surface of the sample, then it was rejected and an alternative sample was obtained on a freshly prepared surface. In this case, the same ring was used but after extruding the rejected sample and cleaning and regreasing the ring in the manner described. The samples so prepared were then double wrapped in cling film, each placed in a labelled polythene bag, sealed and transported to the laboratory in an airtight container. Once there, the samples were immediately taken from their polythene bags and placed in a humidifier until required for testing.

In addition to these samples, a further 15 fabric-oriented undisturbed samples (horizontal drainage) were also taken on the same till types. Reasons for obtaining oedometer samples in this manner have been previously described in section 5.3.1 . The angular orientation of the samplers was achieved in situ by preparing two orthogonal, smooth, vertical faces in the till immediately adjacent to the fabric study area, Fig 5.16. The strike direction of one of these faces corresponded exactly to the orientation of the calculated resultant vector at that locality. In this way samplers, when laid flush against these faces, produced soil samples both parallel and normal to the fabric vector. An additional undisturbed sample, but with random orientation, was also taken at this time on each of the five tills. Reorientation of the samplers for compression testing in the oedometer therefore ensured the desired mode of (horizontal) drainage through the sample.

A small number of undisturbed till samples were also obtained early in the research programme for testing in the direct shear apparatus. Sampling was carried out in such a way that the effects of clast fabric

during testing became relative. Samples were obtained using a 60mm x 60mm x 20mm stainless steel former with its cutting edge on a prepared, even, horizontal surface with one (referenced) side parallel to a line precisely 45° in plan to the established fabric vector for that locality. Samples were obtained, trimmed, stored and prepared in the same way as were the consolidation samples.[1]

5.4.3 Undisturbed 38mm diameter samples for triaxial compression testing.

Undisturbed samples of till HH(a) from Holwell Hyde quarry for use in the triaxial testing programme described in Chapter 6 were obtained in the following way:

Two types of sampling tube (nominal internal diameter 38mm) were prepared: one of standard wall thickness and another thinner-walled version. The thin-walled (0·75mm) tube was used to minimise disturbance to the soil during the sampling process. On site, an horizontal bench approximately 600mm x 600mm was formed in fresh, unweathered till by excavation of a suitable face or part of the quarry floor. The greased tube was aligned vertically on the bench with its leading cutting edge face downwards. A hardwood dolly was placed on top of the reinforced shoulder of the tube and carefully but firmly struck with a lump hammer, thus causing the tube to penetrate the soil. Once a penetration of approximately 125mm had been achieved (Fig 5.17) without undue resistance, the soil around the tube was carefully excavated by hand trowel and edging spade to fully expose it (Fig 5.18). The sample was immediately extruded from its tube using a portable extrusion device and examined for flaws and signs of disturbance. Any sample showing obvious signs of sampling disturbance (cracking, clast 'scarring'), or containing visible pieces of flint or chalk (> 4mm, approximately 10% of sample diameter), was rejected and another sample obtained. All samples were wrapped in cling film, placed in labelled polythene bags and, once in the laboratory, stored in a humidifier until required.

Considering the very stiff and stoney nature of the tills, this method of obtaining intact samples proved reasonably successful (the rejection rate was about 1 in 3).

---

1. Samples sheared along planes parallel and normal to fabric might, arguably, give minimum and maximum values respectively for shear strength. No account has been taken of a possible 3rd dimensional effect of fabric on strength.

SITE	TILL TYPE	Vr (degrees)	L (%)	Rayleigh probability against randomness.
Holwell Hyde quarry	Dark grey calcareous, HH(a)	75·1/255·1	35·9	0·998
Holwell Hyde quarry	Light grey calcareous, HH(b)	65·9/245·9	59·1	> 0·999
Westmill quarry	Ware, W(b)	28·7/208·7	17·1	0·768
Westmill quarry	Eastend Green, W(d)	45·3/225·3	36·7	0·999
Foxholes quarry	Oxidised Ware, F(b)	5·7/185·7	16·8	0·756

Underlining of Vr denotes azimuth of 'preferred vector', i.e. dip direction of the resultant vector.

Table 5.1 Summary of till fabric data.

SITE	TILL TYPE	HORIZONTAL/ VERTICAL	cu_p* (kPa)	cu_r* (kPa)	$\frac{cu_p}{cu_r}$	w*	LI
Holwell Hyde	HH(a)	H	484	113	4·28	0·141	-0·177
Holwell Hyde	HH(a)	V	459	102	4·50	0·142	-0·172
Holwell Hyde	HH(b)	H	387	67	5·78	0·161	-0·076
Holwell Hyde	HH(b)	V	437	111	3·94	0·158	-0·090
Westmill	W(b)	H	493	105	4·70	0·175	-0·050
Westmill	W(b)	V	402	81	4·96	0·186	-0·014
Westmill	W(d)	H	413	110	3·72	0·169	0·031
Westmill	W(d)	V	416	110	3·78	0·168	0·028

* Average of three determinations.

Table 5.2 Results of in situ shear vane tests.

Site 1: Moor Mill (TL 143027)

Brown silty clay M(a) (65·30m) :B
Yellow clayey silt M(b) (65·70m) :B
Grey silty clay M(c) (66·67m) :B
Dark grey calcareous till M(d) (66·80m) :B
Dark grey calcareous till M(e) (68·09m) :B
Dark grey calcareous till M(f) (68·94m) :B
Grey brown silty sand M(g) (67·00m) :B

Site 2: Hatfield (TL 186086)

Dark grey calcareous till H(a) (77·14m) :B
Oxidised dark grey calcareous till H(b) (78·84m) :B
Light grey calcareous till H(c) (81·83m) :B

Site 3: Holwell Hyde (TL 265116)

Dark grey calcareous till HH(a) (69·55m) :B; O(1V, 3H); S(3H)
Light grey calcareous till HH(b) (76·64m) :B; O(1V, 3H)

Site 4: Foxholes (TL 337125)

Dark grey calcareous till F(a) (60·00m approx) :B
Oxidised Ware Till F(b) (60·00m approx) :B; O(1V, 3H); S(3H)
Foxholes Till F(c) (64·95m) :B

Site 5: Westmill (TL 344158)

Laminated silty clay W(a) (59·90m) :B; O(1V)
Ware Till W(b) (61·18m) :B; O(1V, 3H)
Westmill Middle Till W(c) (62·00m approx) :B
Eastend Green Till W(d) (70·50m) :B; O(1V, 3H)

M = Moor Mill quarry
H = Hatfield quarry
HH = Holwell Hyde quarry
F = Foxholes quarry
W = Westmill quarry

B = bulk disturbed sample
O = oedometer undisturbed sample
V = vertical
H = horizontal
S = direct shear undisturbed sample.
(70·05m) denotes elevation m.O.D.

Table 5.3 Summary of samples obtained at the five sites.

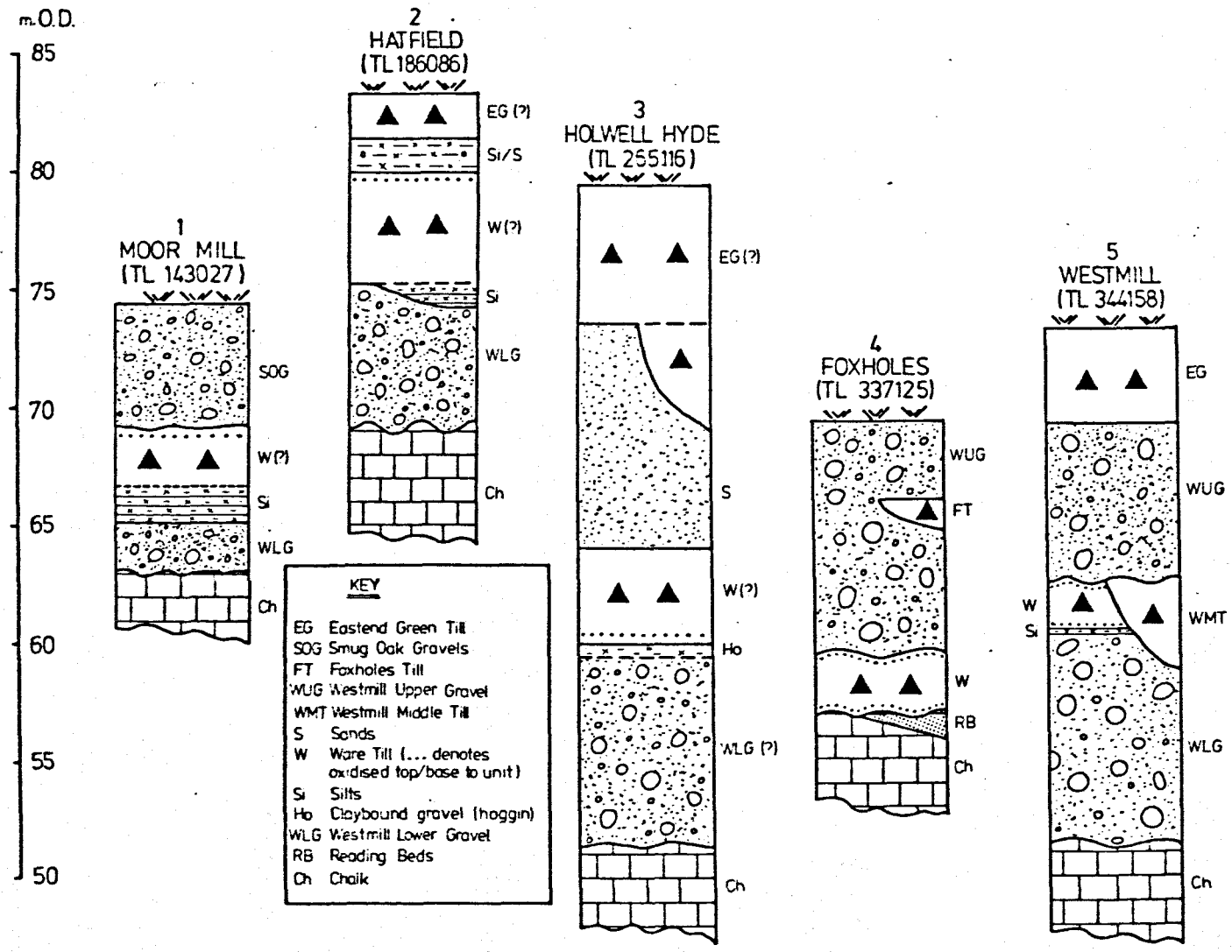

Figure 5.1 Lithostratigraphic units at the five study sites in the Vale.

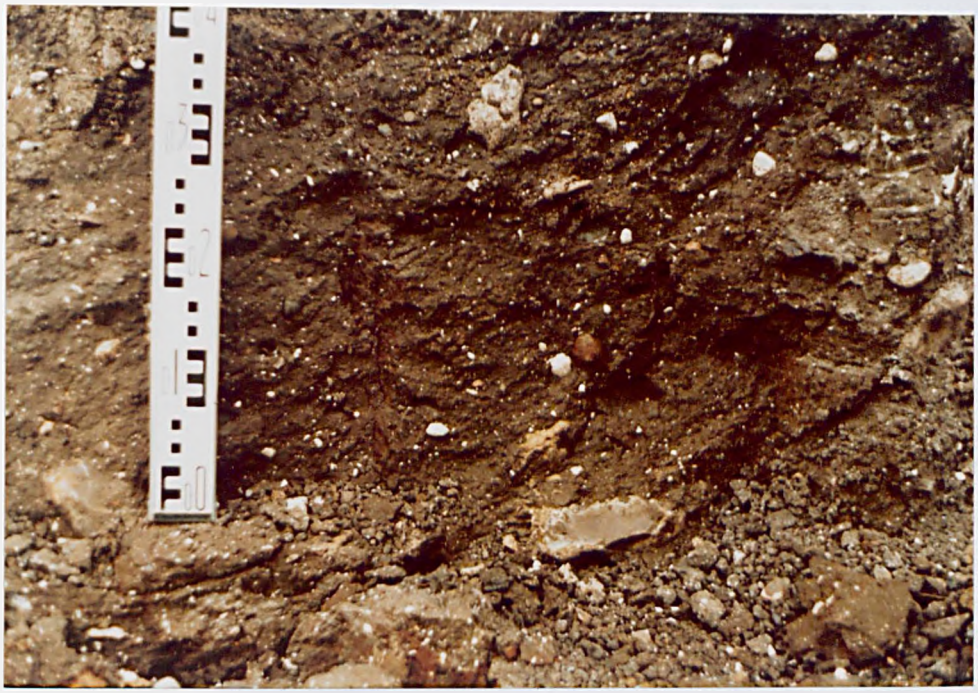

Figure 5.2 Dark grey chalky lodgement till (HH(a)) at Holwell Hyde Quarry, Welwyn Garden City.

Figure 5.3 Till HH(a) in hand specimen.

Figure 5.4 Light grey chalky lodgement till (HH(b)) at Holwell Hyde Quarry, Welwyn Garden City.

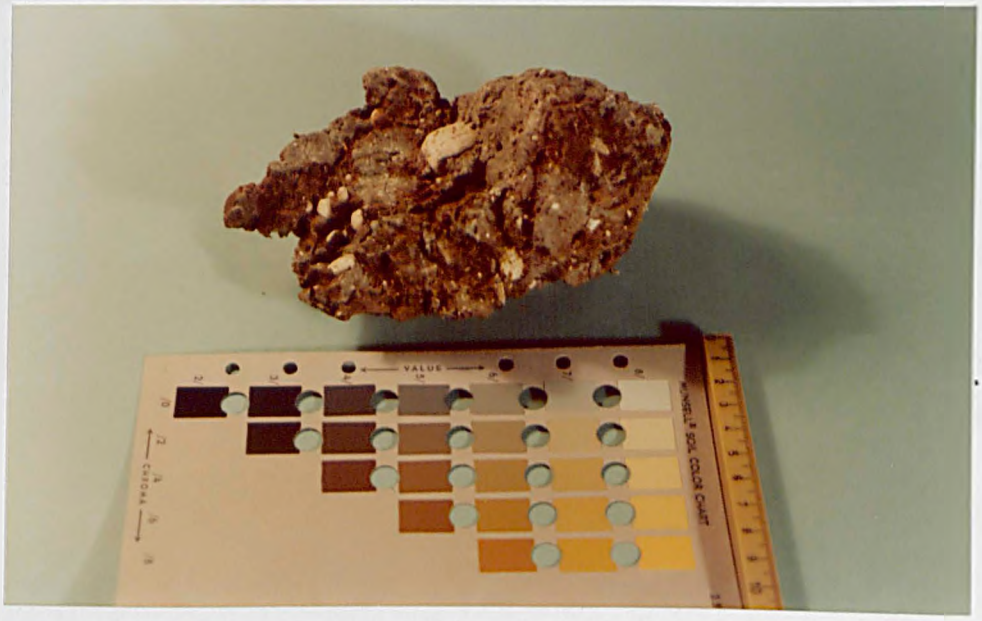

Figure 5.5 Till HH(b) in hand specimen.

Figure 5.6 Till fabric study on a prepared face, Westmill Quarry, Ware.

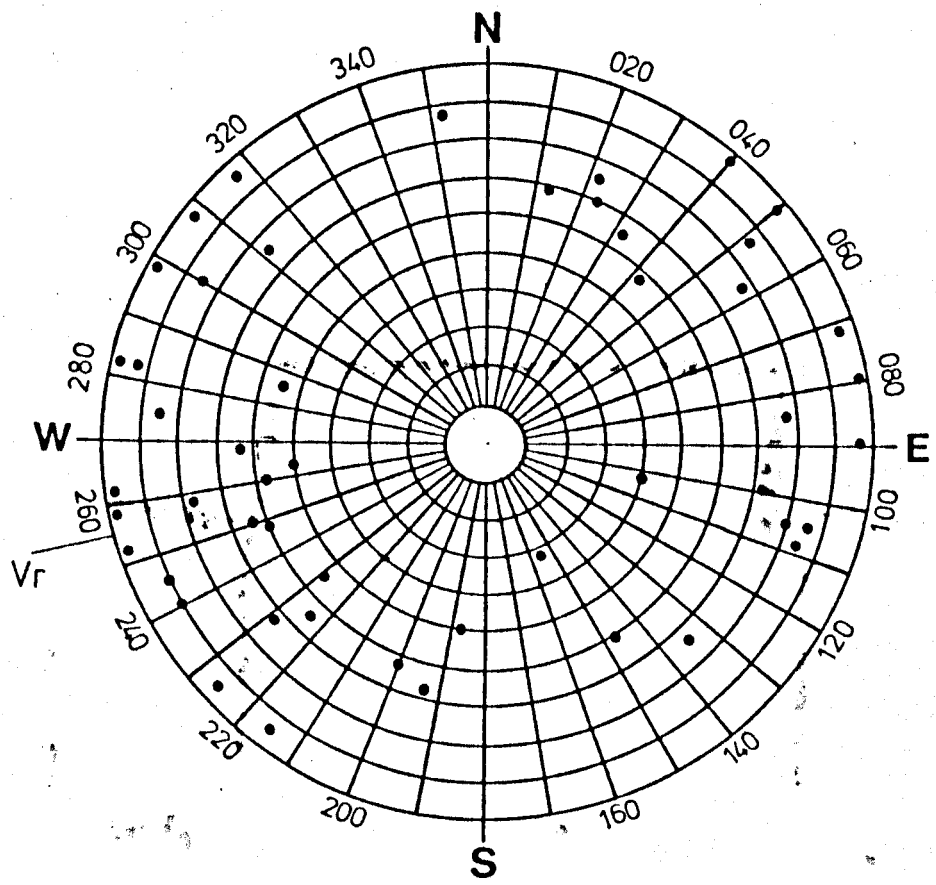

Figure 5.7 Clast fabric, till HH(a) , Holwell Hyde.

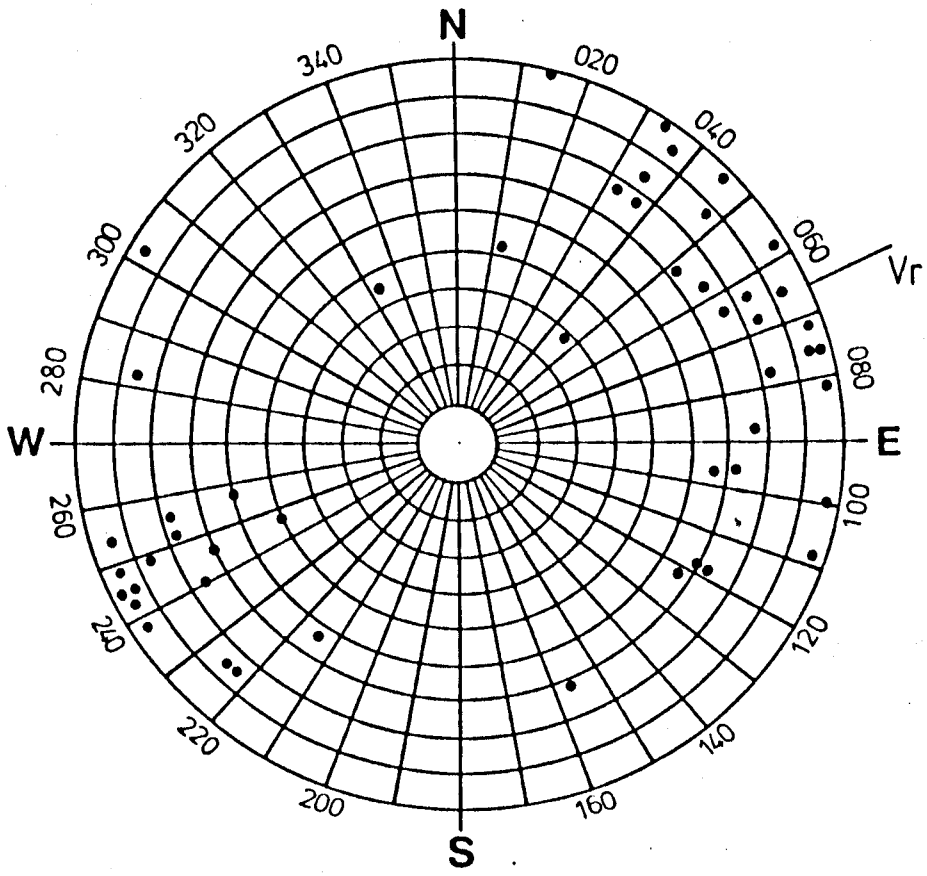

Figure 5.8 Clast fabric, till HH(b) , Holwell Hyde.

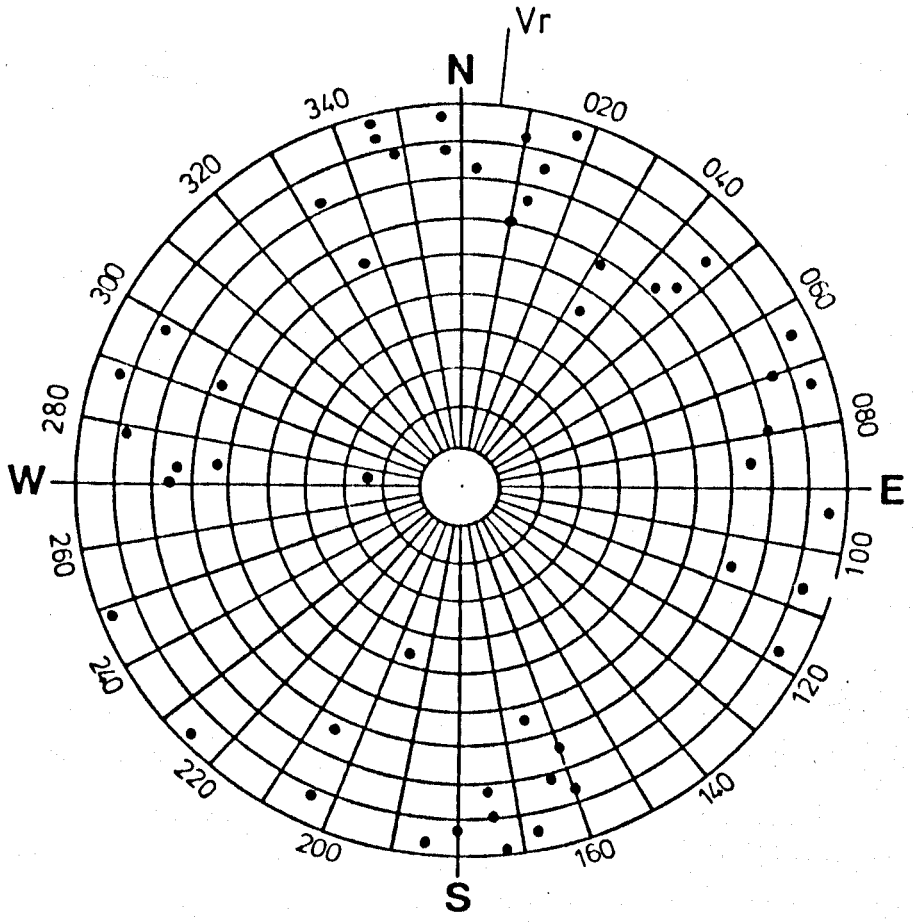

Figure 5.9 Clast fabric, till F(b) , Foxholes.

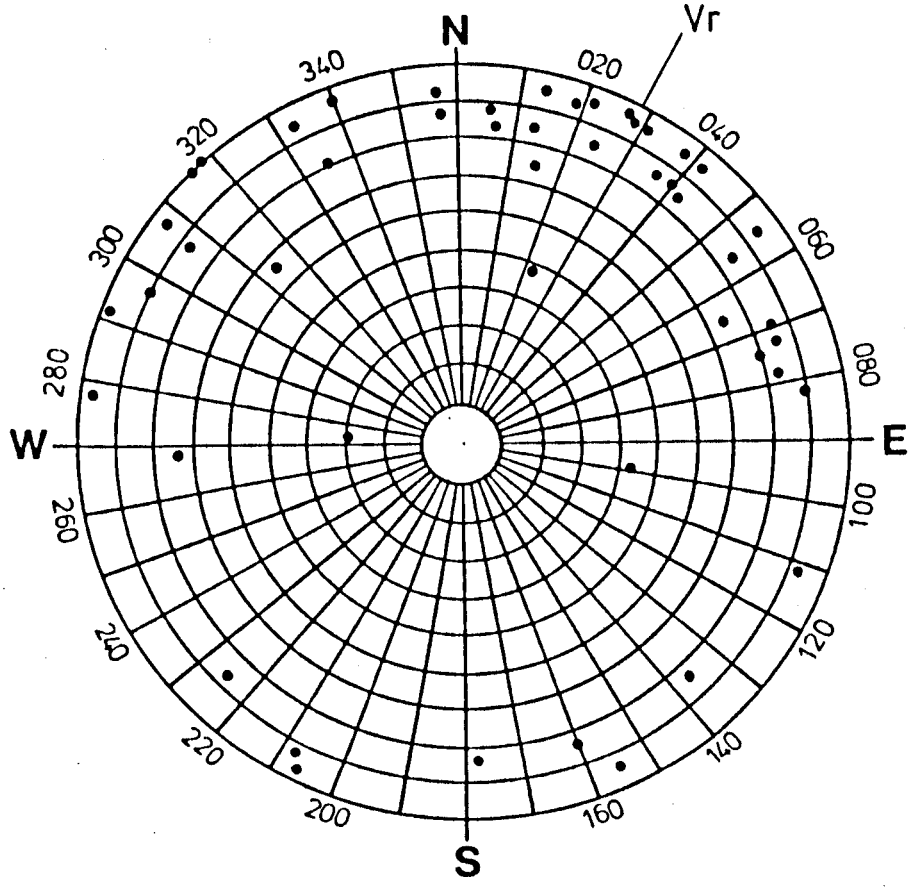

Figure 5.10 Clast fabric, till W(b) , Westmill.

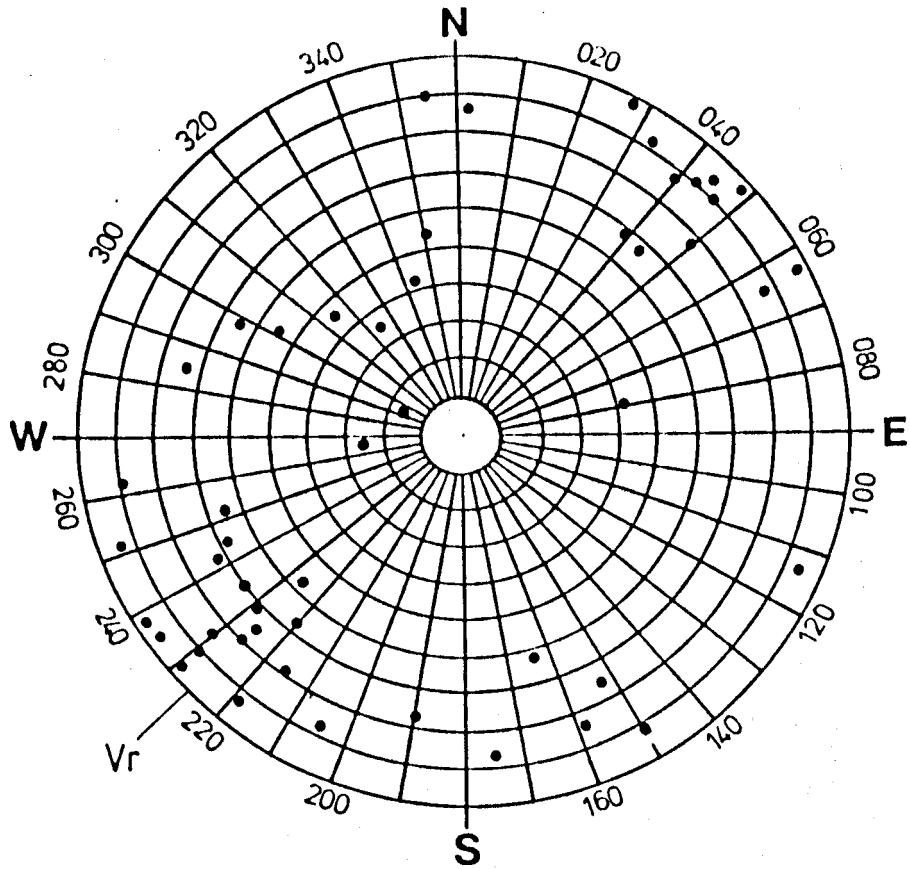

Figure 5.11 Clast fabric, till W(d) , Westmill.

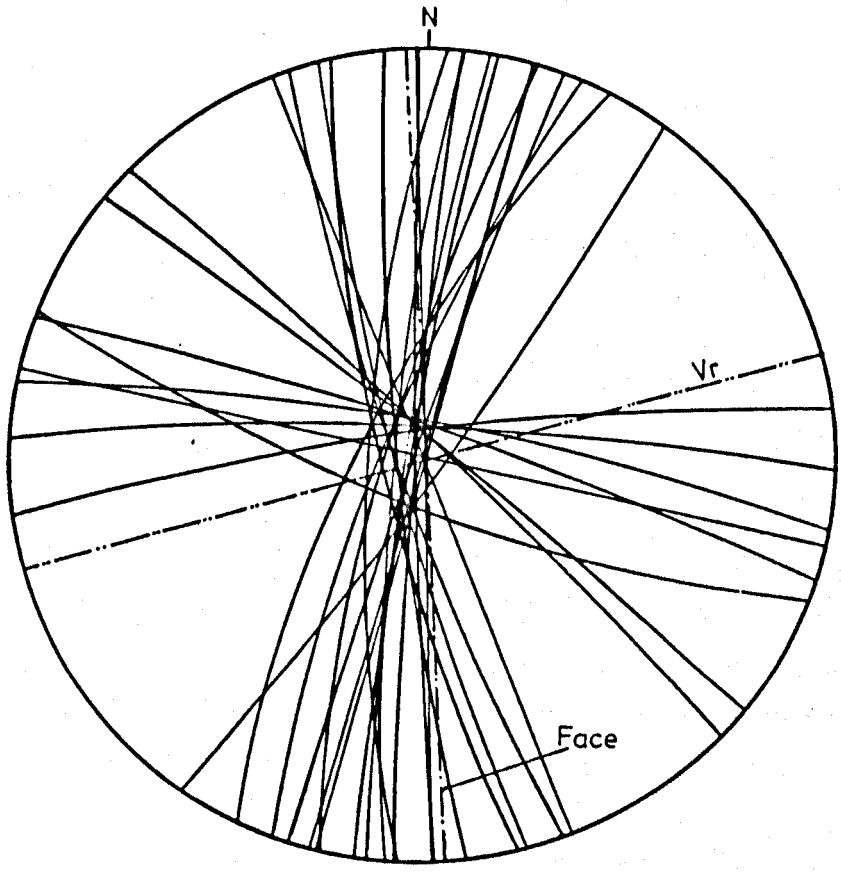

Figure 5.12 Spherical projection of discontinuities (great circles) in till HH(a).

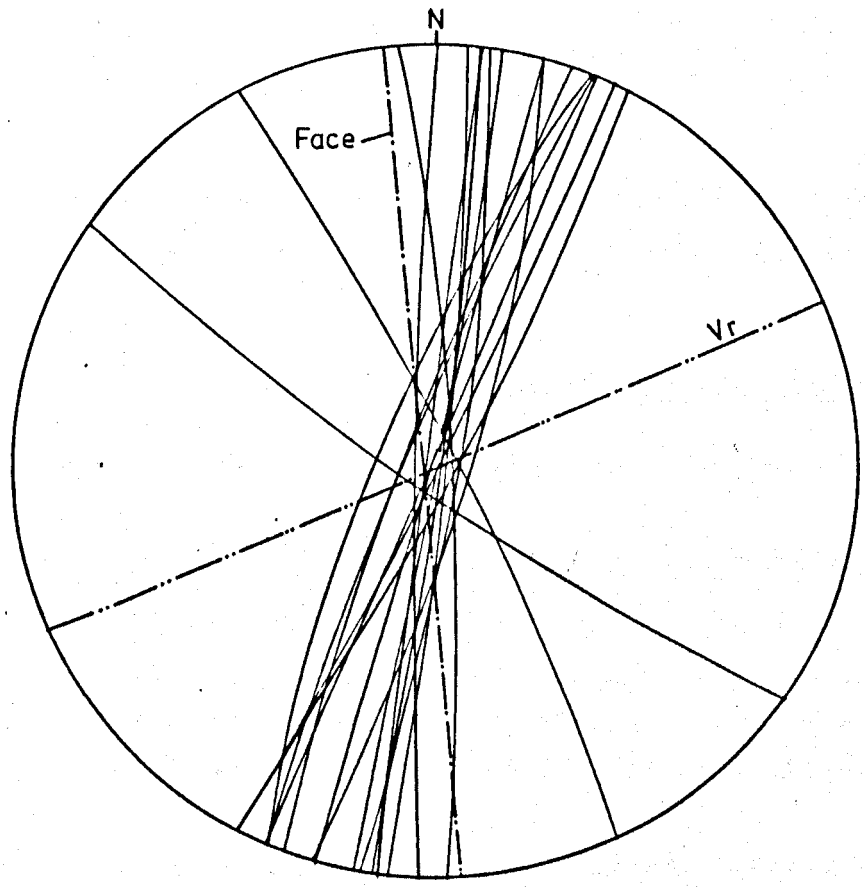

Figure 5.13 Spherical projection of discontinuities (great circles) in till HH(b).

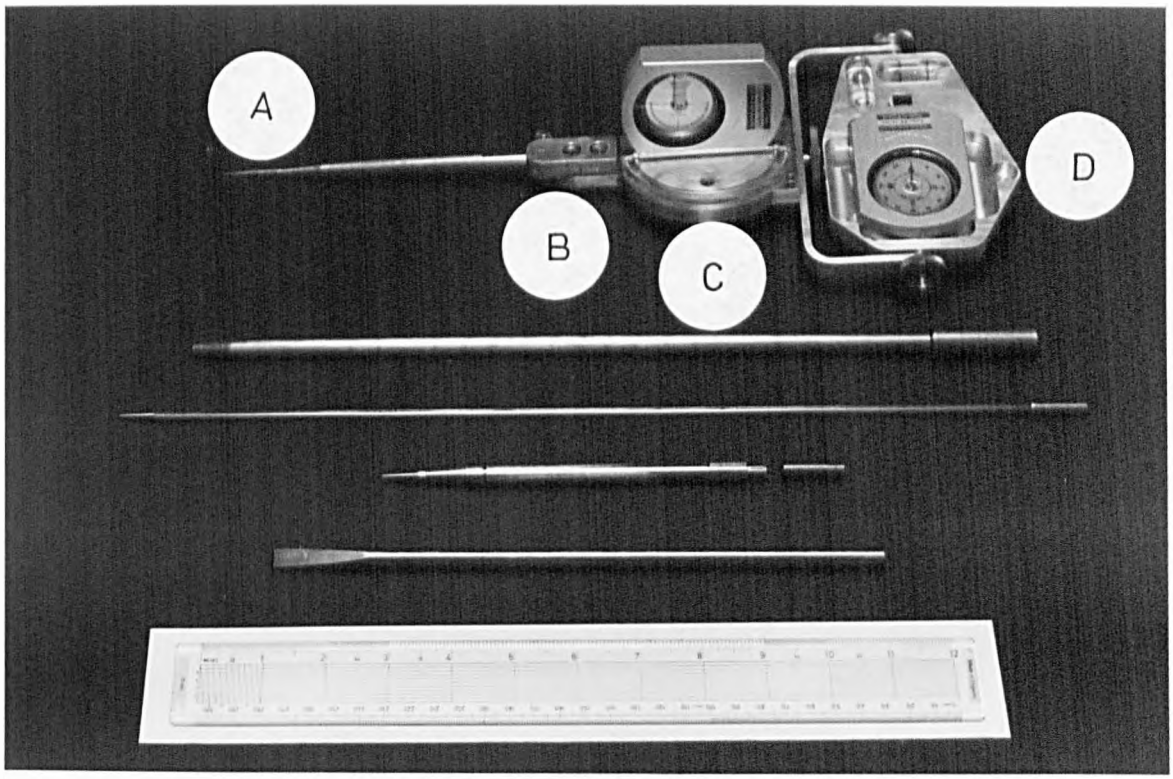

Figure 5.14 The till fabric instrument.

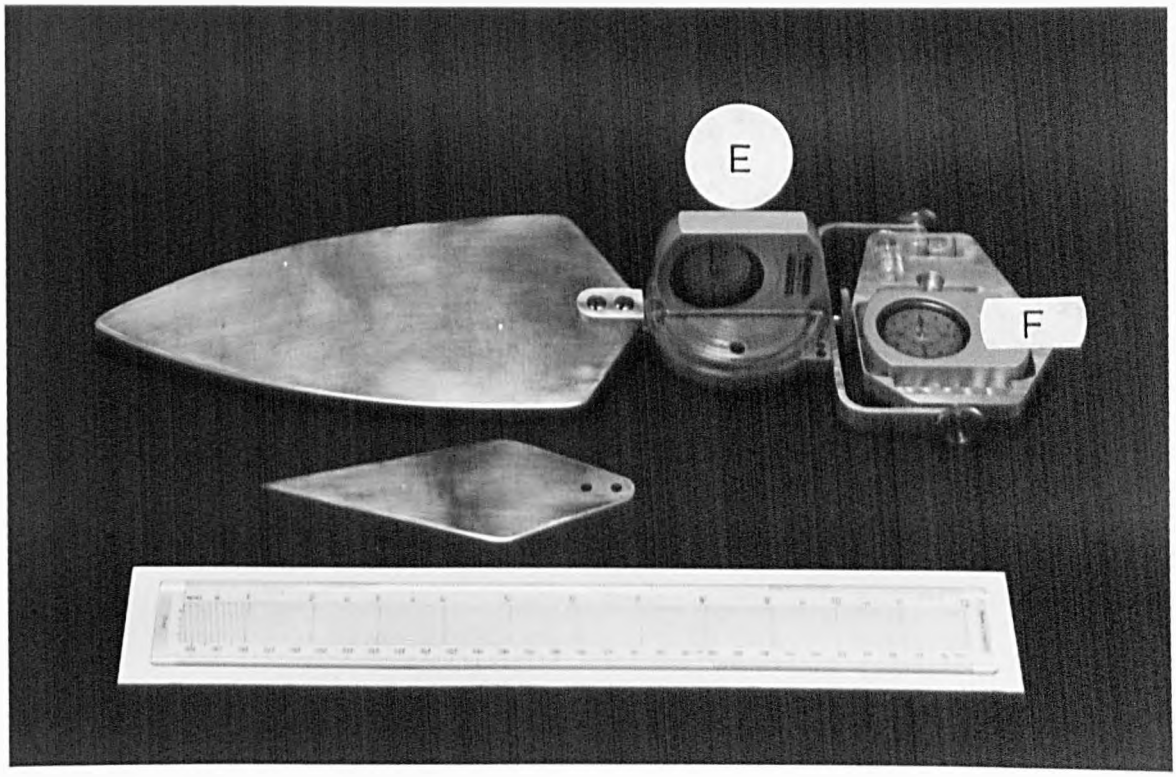

Figure 5.15 The fabric instrument with trowel attachments.

Figure 5.16 Obtaining undisturbed fabric-oriented (horizontal drainage) oedometer sample, till W(b) , Westmill.

Figure 5.17 Full penetration of the 38mm sampling tube.

Figure 5.18 The sampling tube exposed.

CHAPTER 6. LABORATORY WORK.

6.1 Introduction.

This chapter details the programme of laboratory-based research carried out during the period 1981 - 84 on samples of the various tills collected earlier on site and described in Chapter 5.

Although a limited amount of published engineering data are available for the (presumed Anglian) tills in the extreme south-west part of the Vale of St. Albans, at the site of the Building Research Station (Marsland, 1977), the soils described in this thesis had not been investigated from an engineering viewpoint prior to the commencement of this work. Therefore, in addition to the specific objectives associated with the particular tests detailed in later sections of this chapter, the laboratory testing has been designed to fulfil the broader aims of the work identified in 1.2.

Firstly, ((iii), (iv) in 1.2) , there had been a requirement to identify the basic geotechnical characteristics of the various tills in the study area with a view to their engineering classification. This series of tests is reported in section 6.2 . An investigation of soil mineralogy and an examination of the quantity and distribution of chalk in the tills supplements these tests and is contained in sections 6.2.4 and 6.3 .

Secondly, ((v) - (viii) in 1.2) , a series of tests has been carried out so as to examine in some detail aspects of the engineering behaviour of the tills.

The mineralogical and lithological heterogeneity of these soils, together with their uncertain post-depositional history would, it was reasoned, make extremely difficult an examination and interpretation of data from tests designed to evaluate fundamental soil behaviour. The legacy imposed by the transportation process on both grading and fabric, and the subsequent effects of ice loading and unloading (possibly twice for some of the tills) on measured compressions and strengths for example, might be examined and understood more easily by first investigating the behaviour of reconstituted samples of till prepared in a standardised manner. The compression and strength tests described

in sections 6.5 , 6.7 , 6.8 represent, therefore, parallel series on both undisturbed samples of till and other samples formed from the same soils by reconstituting their air-dried and screened fractions with distilled water.

The general method which has been adopted is not new. Henkel (1956), for example, reported the results of drained and undrained triaxial compression tests on isotropically normally and overconsolidated samples of remoulded London clay and Weald clay. In his paper Henkel describes a procedure for mixing the bulk of the soil with distilled water to a consistency corresponding to a shear strength of approximately 4 kPa (the lowest shear strength at which a satisfactory triaxial sample could be made). Parry (1960) reported a similar procedure for preparing remoulded samples of London clay and Weald clay for triaxial compression and extension testing purposes.

Furthermore, El Ghamrawy (1978) and Hight and Gens (1979) have described various methods of sample preparation for Cromer Till and Cowden Till respectively, including remoulding directly from intact material, static compaction after remoulding, and anisotropic consolidation from a slurried sediment.

The type of laboratory testing carried out has been based essentially on standard engineering tests which are commonly used for evaluating soil compression (oedometer) and strength (consolidated undrained triaxial; direct shear) characteristics. Emphasis has, however, been placed on close attention to detail in the testing procedures and care in the carrying out of the tests. With few exceptions, all testing has been undertaken personally by the writer.

The oedometer (6.5) , motorised shear vane (6.6) and 60mm shear box (6.7) testing utilised existing equipment housed in the Civil Engineering department's soils (teaching) laboratories at Hatfield Polytechnic. The strain-controlled triaxial series of tests, however, necessitated the design, construction and equipping of a new laboratory before this work could begin. This is also reported in section 6.8 .

6.2 Classification tests.

6.2.1 Atterberg limits.

The determination of the natural water contents and Atterberg limits for each of those samples listed in Table 5.3 have been carried out in

accordance with BS 1377 : 1975 , tests 1(A) , 2(A) and 3. Liquid limits were determined using the 80g , 4 point cone penetration method.

Samples of soil were prepared firstly by air drying, grinding using a rubber pestle, and then screening on a 0·425mm sieve. However, due to the very chalky nature of these tills (see 6.2.4), prior to air drying the soil, those particles of chalk larger than about 0·5mm were removed by hand from the sample. Chalk is a colloidally inactive material which dries out very rapidly and therefore its incorporation into the matrix during the grinding process would, it was felt, affect the results of the test in an unrealistic way. Despite being a very time consuming process, this step was nevertheless considered an important and necessary one.

In order to examine the effect of the presence of chalk and other acid solubles in the minus 425 microns fraction on the index properties of the soil, a parallel series of tests was carried out on samples of tills HH(a) , HH(b) from which all of the chalk had previously been removed. The method of removing the carbonate from the soil prior to testing is described in section 6.2.4 .

6.2.2 Particle specific gravity.

The particle specific gravities of five tills (HH(a), HH(b), F(b), W(b), W(d)) were also determined in accordance with test 6(B) of BS 1377 : 1975 . Testing was restricted to those soils for which fine sediment data were required (see section 6.2.3) and on which subsequent oedometer testing would also be carried out.

6.2.3 Particle size.

The procedures laid down in BS 1377 : 1975 , test 7(A) for the determination of soil particle size are not entirely satisfactory for cohesive glacial tills, due mainly to the fact that pretreatment with dispersant is required for both the sieving and the sedimentation processes. A far more appropriate set of procedures for pretreating and grading this type of soil is described by Head (Vol. 1, 1980) , and it was these methods which were adopted and used throughout.

The grading of five selected till samples (HH(a), HH(b), F(b), W(b), W(d)) was carried out in two separate stages : sieving down to 0·063mm, and sedimentation down to 0·002mm .

The precise details of the sieving procedure are not reproduced here, (there are 21 consecutive steps in this process), and the reader is referred to pages 177 - 182 of 'Manual of Soil Laboratory Testing', (Head, op cit) for further details.

6.2.4 Quantity and distribution of chalk.

Two samples of till (HH(a) , HH(b)) were also selected for a study to determine the amount and distribution of chalk within them. This involved the additional step of removing and weighing all chalk particles retained on each separate sieve down to 0·50mm , a tedious process which, for the smaller fractions required the use of a pair of tweezers and a binocular microscope. The chalk fraction smaller than 500 microns and larger than 63 microns was removed from the sample by treatment with dilute (1 Molar) hydrochloric acid. Filtration of the carbonate-free residue was then carried out using a Büchner funnel fitted with a Whatman No. 50 filter paper on a vacuum filtration flask. The sample was washed thoroughly with distilled water until all traces of acid had been removed. The sample was then oven-dried and cooled in a desiccator.

The sedimentation of pre-treated[1] soil particles between 0·063mm and 0·002mm was carried out in a 500ml sedimentation tube placed in a constant temperature bath maintained at 25°C to ± 0·5°C .[2] A calibrated Andreasen pipette was used to sample the suspension at specified times. Precise sampling times were determined based on the previously measured particle specific gravity of each soil. All weighings were accurate to 1 in 10,000 grams .

A parallel series of sedimentation tests was also carried out on samples of the carbonate-free soil in order to determine the percentage of true clay within the soil. Very finely dispersed carbonate will act as a cementing agent and will therefore inhibit the complete disaggregation of the clay colloids. The percentage of clay-sized

---

1. The soil was pre-treated with hydrogen peroxide, Analar (20 volumes) to remove organic matter and then dispersed with a solution (8g litre $^{-1}$) of sodium hexametaphosphate. Agitation of the sample was in an end-over-end shaker until completely broken down.

2. Head, (page 193) specifies a constant temperature bath to ± 0·1°C . With the majority of commercially available baths this tolerance is not achievable.

particles determined by this method will therefore be an underestimate of the true clay content of the soil. For a given plasticity index, therefore, the colloidal activity (Skempton, 1953) of the soil is overestimated. Samples of the soil for this series of tests were pre-treated in the usual way and the carbonate removed by the method previously described. Subsequent sedimentation procedures followed those outlined above.

6.3 Mineralogy.

6.3.1 X - ray diffraction analysis (XRD).

The mineralogical compositions of till samples HH(a), HH(b), F(b), W(b), W(d), have been determined by the X-ray diffraction method. (1)

Soil samples were prepared by using the air-dried fraction passing the 425 microns sieve and grinding this to a very fine powder with a stone pestle.

Quantative assessments of calcium montmorillonite, illite, kaolinite, calcite and quartz present in each sample were made by incorporating a very precise quantity (2) of calcium fluoride as an internal standard to various proportions of these minerals present in calibration samples beforehand. By varying the mass percentages of these minerals, whilst maintaining a given (here 10%) concentration of internal standard, it can be demonstrated that :

$$\frac{Im}{Is} \cdot \frac{Ms}{Mm} = K$$

where Im , Is are peak XRD trace intensities for the mineral and standard respectively;

Ms , Mm are the measured masses for the internal standard and the mineral in the sample;

K is a calibration constant.

---

1. Philips PW 1730 X-ray generator with 1050 vertical diffractometer using Cu. Kα radiation and Ni. filter.

2. Weighings accurate to 1 in 10,000 grams.

The determination of the constant K for each mineral in this way will, on examination of the X-ray diffraction traces, enable an assessment to be made of its percentage concentration in a given mass of soil containing a constant percentage of internal standard. The method outlined is essentially that described by Midgley (1976) and Hara and Midgley (1980).[1]

6.3.2 Energy dispersal analysis (EDAX).

These same samples of till were also analysed by the energy dispersal analysis of X-rays (EDAX) technique[2] for the determination of element types present in them. Whilst the traces so produced do not provide a direct measure of quantity in the manner of the XRD traces, they can nevertheless be examined in combination with each other and so provide a measure of the relative proportions of each element type identified.

6.4 Fossil assemblages.

Fossil (non-Pleistocene) forms are occasionally found within the matrix of these tills, having survived transportation and comminution during the soils' formation. Unfortunately, complete fossils in a good state of preservation are very rarely found although, usually, sufficient of the calcareous or siliceous exoskeleton remains to enable a broad identification to be made. In this way they can act as indicators of source material for the tills.

Fig. 6.1 shows a fossil assemblage obtained by the writer from tills HH(a), HH(b) at Holwell Hyde Quarry on several visits to this locality. Here may be identified several forms typical of the Jurassic , notably Amoebocerous serratam possibly Oxfordian, (top) and Gryphaea, Lias, (bottom). In the middle section of this Figure can be seen incomplete belemnite guards, coral, and convoluted calcareous worm casts.

The washed and sieved fractions obtained from the particle size analyses of the tills described in 6.2.3 were retained and stored in sealed, labelled containers.

---

1. The writer acknowledges the assistance given to him by Dr. H. Midgley in this series of tests.

2. Cambridge Instruments Stereoscan 2A combined with a Link Systems 290 Analyser.

A subsequent microscopic examination of these sorted fractions revealed an abundant (non-Pleistocene) foraminifera and ostracod microfauna contained within them.

A total of 108 fossil forms from tills HH(a), HH(b) were hand picked and mounted on slides for identification, Table 6.1 . Scanning electron microscopy of a selection of these has also made available a photographic record, Fig. 6.2 .

6.5 Oedometer compression tests.

A series of one-dimensional oedometer compression tests was carried out on both undisturbed and reconstituted samples of tills HH(a), HH(b), F(b), W(b), W(d). Details of the testing schedule are shown in Table 6.2. The following method of soil preparation for reconstituted samples has been tried and used with success.

Sealed polythene bags containing the bulk disturbed soil sample were opened and the soil removed and placed on a length of paper towelling, or other absorbant material, within a large shallow tray. All large cohesive lumps of soil were gently broken down into small crumbs with the fingers. Friable or crushable material, including chalk clasts, were removed and kept to one side. Air drying of the soil proceeded, usually for four to five days, until the sample was completely dry. The dried soil was then transferred to a large mortar and slowly ground using a rubber pestle and finally transferred onto a 2mm sieve. The air-dried lumps of chalk, etc. were then added to the sieve at this stage. Disaggregation of particles was considered to be complete when only individual particles were retained on the mesh. Reconstituted samples were prepared from this 2mm down fraction by mixing thoroughly with distilled water to a water content of 20% .

Although being considerably easier to reconstitute such a sample at higher water contents, it was felt that an attempt should be made to manufacture samples for testing as near as was possible to the soils' natural water content. In fact, this proved extremely difficult in view of the very low water contents involved (in samples HH(b), F(b), W(b) natural water content, although variable, was usually below the soils' plastic limit). By a method of trial and error, it was found that a satisfactory, homogeneous mix could be achieved, without extensive kneading, if the water content was not less than 20% . This water content was therefore used for all subsequent mixing. Immediately

following the moulding process, the soil was placed into a sealed polythene bag and placed into a humidifier for 24 hours to allow moisture equilibration.

When required for testing, the soil was carefully but firmly moulded into a lubricated stainless steel circular cutting ring, ensuring that no air pockets were trapped. After trimming and finishing top and bottom soil surfaces to be exactly flush with the top and bottom edges of the ring, sample and ring were weighed to ± 0·01 g . (The internal dimensions of the ring had previously been determined using vernier calipers). A piece of Whatman filter paper, cut to size, was placed top and bottom of the sample which was then placed onto the saturated porous stone in the oedometer apparatus.(1) The filter paper would prevent clogging of the pores of the stones with clay, thus ensuring an even distribution of drainage out of the top and bottom surfaces of the sample.

Having securely fixed the ring and sample into place with the locking nuts, the circular loading piston with its attached (saturated) porous stone was carefully placed onto the top of the sample and the yoke arrangement positioned centrally over the sample. The balanced cantilever carrying the platforms for the weights was adjusted to the horizontal position and held using the screwstop bearing on its underside.

A dial gauge (1 division = 0·002mm) was positioned on the smooth ball of the yoke directly above the centre of the sample to record vertical movement. The perspex pot housing the sample was filled with distilled water and was maintained full for the duration of the test.

Initially, weights were added to the cantilevered platform so as to produce a vertical stress on the sample equal to 100 kPa (± 1 kPa) (2), once the screw top was cranked to lower the beam. Thereafter weights were added (or removed) in stages to ensure that the ratio of stress increase (or decrease) to current stress was unity. The maximum vertical pressure achieved was 3200 kPa.(3)

---

1. Wykeham Farrance front loading presses, series 24250 (cells 1, 2) and 24251 (cells 3,4,5).

2. Allowance was made for the self weight of the piston bearing directly on top of the sample; the estimate ± 1 kPa is based on the smallest weight which was available (0·2 lb).

3. The loading/unloading sequence used for all reconstituted samples was 100, 200, 400, 800, 400, 200, 100, 200, 400, 800, 1600, 3200, 1600, 800, 400, 200, 100 kPa.

Readings of vertical deformation were made at the intervals of time suggested in BS 1377 : 1975 (page 94) after first application of pressure, and were continued until no further deformation occurred, usually not until 24 hours from the start of the test.

Following completion of the loading/unloading sequence, the sample was removed from the oedometer, the filter papers were removed and the soil and ring weighed. Having oven dried to constant mass, the final water content of the sample was determined.

Another series of oedometer tests was carried out on undisturbed samples of these same till types. The samples were obtained in situ in the manner described in 5.4.2 , sealed and then stored in a humidifier until required. Twenty undisturbed samples were collected and prepared : five horizontal for vertical drainage and fifteen vertical samples for horizontal drainage (five normal and five parallel to fabric vector ; five randomly oriented).

The testing procedures for these undisturbed samples were identical to those described above for the reconstituted samples, with the exception of the loading sequences.(1)

One additional undisturbed sample (vertical drainage) was obtained for the dark calcareous till HH(a) at Holwell Hyde Quarry within a smaller diameter cutting ring (63·35mm). Using a modified pot and porous stone/ piston arrangement, it was possible to achieve a vertical pressure of 6400 kPa with this sample.

The elastic compression under load of each of the five oedometer presses used during this study was determined by loading an incompressible (2) cylinder of 75mm diameter within the cutting ring of each apparatus, in place of the soil. Readings on the dial gauges (recording recoverable compressions of porous stones, pots, etc.) were thus made up to 3200 kPa (up to 6400 kPa for the smaller diameter, modified press), recorded and were subsequently used in the determination of net vertical deformations of soil under load. In this

---

1. The loading/unloading sequence used for undisturbed samples was (100), (200), 400, 800, 1600, 3200, 1600, 800, 400, 200, 100. (100) denotes only if swelling does not occur at this (100 kPa) pressure.

2. At the highest vertical pressure applied (6400 kPa), this tablet of mild steel will only experience an elastic compression of $5{\cdot}87 \times 10^{-4}$mm ($3{\cdot}09 \times 10^{-5} \mu\varepsilon$) assuming $E = 207$ GN m^{-2} .

way soil compressions become relative despite having been determined in presses of differing elastic characteristics. The results of these calibrations are shown in Fig. 6.3 .

6.6 Motorised shear vane tests.

Various authors have provided evidence associating particular values of mean normal effective stresses with the state of the soil at the liquid and plastic limits, or have suggested a fixed ratio between these stresses (e.g. Casagrande, 1958; Youssef et al, 1965; Schofield and Wroth, 1968). These ideas have been extended so as to relate the compression index of the reconstituted soil to its plasticity index and to suggest a unique relationship between reconstituted strength and liquidity index, irrespective of actual values of liquid and plastic limits (Wroth and Wood, 1978).

A series of tests has therefore been carried out on three of the tills (HH(a), HH(b), F(b)) to determine the variation of undrained shear strength over a range of water contents using a small motorised shear vane apparatus .[1]

The samples were prepared from the air-dried fraction passing the 425 microns sieve, see section 6.2.1 . The soils were thoroughly mixed with distilled water and then placed into a cylindrical container clamped securely on a horizontal surface directly beneath the vane. Having slowly lowered the vane completely into the soil by cranking the handle on the overhead carriage, shearing then took place at a fixed rate of approximately 10° min^{-1} angular rotation. Readings of both spring and vane deflection were made every 15s until shearing of the soil occurred around the swept area of the vane blades at their outer edges.[2] A portion of the soil was removed for water content determination. The test was repeated with a fresh sample of soil (at the same water content) in a clean and dried container.

Testing commenced at the lowest water content at which it was possible to mould the soil by hand (in all cases this was a little above plastic limit). A small (12·7mm x 12·7mm) vane was used here. At the higher

---

1. Wykeham Farrance Engineering Ltd. laboratory (V1) vane apparatus.

2. Time to failure in all cases was within 15min ; in some cases, less than 10min .

water contents (somewhat above the liquid limit) a larger vane (30·48mm x 59·26mm) was required in a larger cylindrical container. Tests were carried out at each of nine different water contents; the total number of tests was therefore 54.

6.7 Drained direct shear box tests.

A limited number of direct (60 x 60mm) shear tests were carried out on samples of the dark calcareous till HH(a) at Holwell Hyde, and the oxidised Ware Till F(b) at Foxholes. This series of tests was initiated and completed approximately 14 months before the main programme of strength testing to be described in section 6.8 was started. Although somewhat restricted in scope these tests do, nevertheless, provide additional data which supplement the later and substantially larger body of work based on the series of triaxial compression testing. The testing schedule is shown in Table 6.3 .

Both reconstituted and undisturbed samples were prepared for testing in the manner described in 5.4.2 and 6.5 . The reconstituted samples were prepared from the air-dried fraction passing the 2mm sieve, and thoroughly mixed with distilled water to a water content of 20% . The soil was then moulded with the fingers into a lubricated 60 x 60mm stainless steel former and extruded directly into the split shear box and onto a grooved and perforated grip plate over a saturated porous stone. An identical arrangement on top of the sample ensured drainage from both the top and bottom soil surfaces. Samples were kept fully saturated throughout the test.

Vertical load was transferred to the sample via a stainless ball bearing positioned centrally on the top piston, in turn supporting a weighted hanger suspended underneath the apparatus. A cantilever arrangement allowed a nominal 5:1 magnification of load to achieve the higher vertical pressures.[1]

Three of the reconstituted samples were consolidated to 100, 200, 400 kPa vertical pressure. The remaining three samples were

---

1. It can readily be shown that the 5:1 ratio will not operate until a load in excess of approximately 25kg is placed on the cantilevered hanger platform. Below this value of load, the mass of the entire hanger arrangement relative to the hanger load is significant enough to shift the mass centre of the system towards the central axis of the sample. At these lower loads, therefore, operating vertical pressures assuming the 5:1 ratio will always be lower than those calculated.

consolidated to 1600 kPa and then allowed to swell back under reduced load to achieve overconsolidation ratios of 4, 8, 16.

Six further samples were obtained in situ for undisturbed testing at Holwell Hyde Quarry and Foxholes Quarry. Sampling was carried out in such a way that the effects of soil (clast) fabric during testing were relative. Samples were obtained using the stainless steel former described above by placing the cutting edge on a prepared, even, horizontal surface with one (referenced) side parallel to a line 45° in plan to the established fabric vector for that locality. The sample was then obtained, trimmed, stored and prepared in the same way as the consolidation samples described earlier.

Samples were extruded directly from their formers into the shear box ensuring that the referenced side now paralleled the direction of horizontal travel in the apparatus. Hence, all undisturbed samples would subsequently be sheared on horizontal planes oriented 45° with respect to fabric.

The undisturbed samples from Holwell Hyde Quarry were consolidated and sheared with effective vertical pressures of 50, 200, 400 kPa and those from Foxholes Quarry at 50, 200, 800 kPa. Shearing took place at a rate which would ensure a fully drained condition. The slowest speed of travel permitted by the apparatus was therefore selected and this was equivalent to approximately 1·17% longitudinal strain every 24 hours ($4{\cdot}878 \times 10^{-4}$ mm min^{-1}). Each test therefore took about ten days, after consolidation, to complete.

Simultaneous readings of shearing force (via a proving ring) and horizontal and vertical displacement (via dial gauges accurate to 0·002mm) were recorded manually at convenient intervals up to approximately 10% longitudinal strain, at which point a microswitch operated an automatic cut-off on the machine motor.

6.8 Consolidated undrained triaxial compression tests.

6.8.1 Testing schedule.

A programme of laboratory work was formulated during 1982 which was

designed to examine, in some detail, the stress : strain characteristics of one of the tills determined using, at least initially, 38mm diameter samples in the strain controlled triaxial compression apparatus. The fundamental compression characteristics of the soil were investigated using samples of reconstituted till material. A parallel series of tests was subsequently carried out on the same till but using undisturbed soil samples thus allowing meaningful comparisons of behaviour to be made between the two types of material.

The middle till, HH(a) which, at that time, was well exposed in the quarry at Holwell Hyde was selected for this purpose due partly to this quarry's proximity to Hatfield and partly to this soil's suitability for obtaining undisturbed samples (see 5.4.2 , 5.4.3).

Both isotropically normally consolidated and overconsolidated samples were prepared which were then sheared slowly (with axial strain rate and cell pressure constant) in an undrained mode whilst monitoring the magnitude and sign of the excess pore pressures produced.

The programme of testing which was carried out is described below and is also summarised in Table 6.4.

A. A series of consolidated undrained triaxial tests was devised to identify the critical state line for this soil :
   (i) samples were isotropically normally consolidated with effective radial stresses of 400, 800, 1600 kPa.
   (ii) samples were initially isotropically consolidated with effective radial stresses of 400, 800, 1600 kPa and then allowed to swell at reduced radial stress to produce samples with an isotropic overconsolidation ratio = 4 .

B. A series of consolidated undrained triaxial tests was devised to explore the overconsolidated region of soil behaviour. Here, samples were prepared with the following isotropic overconsolidation ratios : 1, 1·5, 2, 4, 8, 16, 20, 32.

In addition, isotropic consolidation tests(without undrained compression) were carried out on samples of reconstituted and undisturbed tills HH(a), HH(b). These additional tests were included so that a) the position of the normal compression line for each of these tills (and particularly the naturally overconsolidated undisturbed samples) could be clearly identified and b) the isotropic

compression and permeability data so produced could be compared directly with those from the oedometer tests described in 6.5 .

The sequence of testing was σ'_3 = (100),[1] (200), 400, 800, 400, 200, 100, 200, 400, 800, 1600, 2000(U),[2] 1600(U), 800, 400, 200, 100 kPa . This sequence is comparable with that previously described for the oedometer tests in 6.5 with the exception that a value for σ'_3 = 3200 kPa could not be attained here due to limits imposed by the available equipment.

6.8.2 Laboratory services.

To expedite the part of the research work described in 6.8.1, it became clear that modifications to the existing triaxial equipment were required, in addition to the purchasing of several new items of equipment. A soil testing facility was planned which was based on the use of a microcomputer for data capture, storage, retrieval and processing purposes. A small laboratory was therefore designed and constructed to house the equipment and its associated instrumentation.

Started early in 1982, the laboratory was fully equipped and operational by February,1983. Details of the services and basic equipment purchased for and installed in this laboratory, specifically for the research work, are contained in an earlier report submitted by the writer to the City University in January, 1984. On completion, four fully instrumented 38mm triaxial cells were available, three of which were used with 10kN (25 speed) bench-mounted compression test machines, and another was contained within a 100kN floor-mounted stepless compression test machine. A diagrammatic layout of the equipment and instrumentation (6.8.3), together with compressed air/ water routes required to service one cell, is shown in Fig. 6.4.

With the new equipment, a facility now existed for applying a back pressure through the pore fluid of the sample to ensure a condition of full saturation. In fact, this improvement brought with it other considerations. To achieve the highest effective isotropic stresses (2000 kPa) required by the programme (for undisturbed samples) meant

1. (100) denotes only if swelling does not occur in undisturbed samples at this (100 kPa) pressure.

2. (U) denotes undisturbed sample.

also ensuring that a capacity of not less than 3000 kPa was available on the compressed air line. The existing on-line supply of compressed air rated at 800 kPa and which serviced the civil engineering laboratories had, therefore, to be enhanced to meet this requirement. This was achieved by commissioning a customised air amplification unit which, through a system of reducing pistons, enabled a nominal 4 : 1 amplification of compressed air.[1] Compressed air was cooled and dried before entry into this unit by a refrigerant air dryer handling 5·20 litres s^{-1} of air at 800 kPa to a dew point of 2°C.[2]

Conventional air pressure regulating valves of the type commonly used in soils laboratories (for example, the Manostat 0 - 800 kPa or the GEC - Elliot 0 - 1550 kPa) are not capable of regulating air supply at these higher pressures and therefore high pressure regulators[3] were installed to service the triaxial chambers and their air/water interfaces. Compressed air servicing back pressure lines was regulated using the conventional air pressure regulators.

Modifications were also made to all perspex chambers[4] containing pressurised fluid so as to ensure their integrity during the higher pressure testing.

A record of air temperatures in the area now occupied by the new laboratory, taken over the nine months period March - December 1982, indicated that daily temperature fluctuations of 5°C were not uncommon and indeed seasonal variations in excess of 10°C were recorded.[5] It was felt, therefore, that an attempt should be made to stabilise the air temperature in the new laboratory so as to minimise the effects of a fluctuating thermal regime on the proposed instrumentation. The relatively high cost of purchasing and installing an air conditioning unit to cool and stabilise air temperatures below 20°C here dictated

---

1. Floor-mounted Haskel Energy Systems AAD - 5 air amplifier.

2. Wall-mounted Broom Wade KA10 refrigerant air dryer.

3. Hale Hamilton GLD15 Mk.1 (0 - 5250 kPa).

4. Wykeham Farrance (reinforced) 38mm triaxial chambers and air/water cylinders have a maximum working stress of 1700 kPa.

5. Minimum (night) temperature 15·25°C on 12th February, compared with maximum (day) temperature 26·50°C on 1st June, 1982.

the alternative use of a wall-mounted air temperature thermostat in conjunction with a warm air convector fan unit so as to elevate the laboratory temperature above the ambient temperature outside. Two strategically positioned variable speed swivel fans circulated the warm air in the room. A continuous weekly (drum) chart recording of temperature and humidity[1] was made in the laboratory and records over the eight months period May, 1983 - January, 1984 showed that, although temperature fluctuations still existed, the situation had been improved, Fig. 6.5 .

6.8.3 Instrumentation.

All triaxial cells were instrumented for the measurement of axial force, pore pressure, volume change and axial deflection.

Axial force was measured directly on top of the sample by an internal 450 kgf (Imperial College type) load cell.

Pore pressures were measured external to the cell along the drainage line from a duct in the pedestal under the sample using either Sensimetric (0 - 800 kPa) or Drück (0 - 3500 kPa) pore pressure transducers.

Volume changes in the sample were measured using the Imperial College volume change device (50cc and 100cc versions) fitted with MPE [2] (25mm) displacement transducers. This volume change device was positioned along the drainage line carrying the pore pressure transducer. Back pressure in the sample pore fluid was applied via the lower chamber of this instrument.

Sample axial deflections were measured external to the cell by a displacement transducer in contact with the top of the chamber and clamped to a supporting bracket cantilevered from and fixed to the load cell piston slightly above its emergence from the cell's bushing collar.

Analogue output from the four transducers on each triaxial cell was via a junction box into a 16-channel 12 bit analogue/digital convertor unit[3] in series with a PET Commodore 32K (3008 series) microcomputer.

---

1. Casella 3083/TT thermohydrograph.

2. Minster Precision Instruments Ltd.

3. 3D Digital Design and Development Ltd.

Data storage was on Verbatim floppy minidisks and a CBM (3040 series) dual drive floppy disk unit. A Commodore 3022 tractor printer provided paper copy of the stored data.

6.8.4 Transducer calibration procedures.

Prior to the commencement of soil testing, all transducers were set up in place, ranged, tested for non-linearity and drift and then calibrated according to the following set of procedures. These procedures were repeated for each transducer following completion of the testing programme. A summary of all transducer calibration data is contained in Table 6.5 .

(i) Internal load cells :

A strain-gauged load cell calibrator was made and calibrated for use here. This comprised a hollow cylindrical mild steel tube 22·30mm O.D. , of wall thickness 1·50mm and length 45·00mm. Four active gauges[1] were used - two aligned along the direction of maximum principal strain, and two 'Poisson' gauges . This four gauge full bridge configuration permitted an output of approximately 600 $\mu\varepsilon$ at 4kN axial force. Two haunched aluminium caps, one bottom, one top (here with a seating for a ball bearing), were fitted to the calibrator for stability in compression and to eliminate any moment effects.

This calibrator was subsequently calibrated in two ways :

a) using a compression testing machine[2], and

b) using a dead weight rig.

Readings of strain output were taken using a conventional strain recording instrument.

It was felt that calibration according to procedure a) was a little coarse' (strain readings could be made only at 0·50kN intervals up to 6kN) and therefore procedure b) was also adopted , thus enabling more detail in the range 0 - 0·70kN , Fig. 6.6 . The kink shown in this graph at approximately 0·375kN is not an isolated feature but was evident on the two separate loading/unloading cycles performed during its calibration. Although precise reasons for this effect are not known,

---

1. Sangamo PL9 foil gauges.

2. Avery-Denison T420 0 - 67kN (grade A1).

with hindsight it would probably have proved more satisfactory had the calibrator not been fitted with a top cap of such contrasting stiffness. However, the bilinear nature of this graph has been taken into account by adopting the separate calibration 'constants' shown either side of the point $\simeq$ (0·375kN, 82 $\mu\varepsilon$) in subsequent calculations.

The calibrator itself having been calibrated, it was then placed on the pedestal of the triaxial chamber and this, togther with its load cell, was carefully positioned over the calibrator taking care not to nip the calibrator cables which were passed under the chamber and connected to the strain recorder on the bench, (the chamber was raised slightly off its base by placing washers underneath its bottom rim). The load cell piston was then seated on the ball bearing on top of the calibrator and the chamber was secured down in the usual way. Manual cranking of the triaxial stage upwards using an appropriately fine gearing now put the calibrator and the load cell into compression (assuming that the top end of the load cell piston made contact with the fixed crosshead of the triaxial frame).

Simultaneous readings of load cell output (continuous digital display on the PET screen) and calibrator compression (strain reading on the recorder) were made for every one revolution of the crank handwheel over the full working range of the load cell. In this way, through the previous calibration carried out for the calibrator, the axial compressive force applied to it through the load cell could be obtained. Finally, therefore, the force in the load cell could be related to its digital output displayed on the screen of the computer. The results of this exercise for each of the four load cells used (designated panels 1 - 4) are shown in Fig. 6.7 . Here, the slope of each graph (expressed: digits kN^{-1}) represents the constant subsequently used for the determination of axial compressive force through the load cell directly onto the top of the soil sample. The differences shown between the calibration values for the four load cells reflects the two different types of load cell used.[1]

(ii) Pore pressure transducers :

All pore pressure transducers were calibrated against previously calibrated Budenberg pressure gauges. Prior to calibration, each pore

---

1. Load cells for panels 1 , 2 were Wykeham Farrance series 1700; those for panels 3 , 4 were earlier versions supplied by Shape Instruments.

pressure transducer was secured tightly into the threaded hole at the base of its deairing block on the drainage side of the triaxial cell using a Dowty seal washer. With the deairing screw closed, deaired water was flushed through the drainage line from the volume change transducer by using either a small (fluid) back pressure acting in the bottom chamber of the volume change device via its air/water cylinder or, alternatively, by using a fluid pressure produced by the Bishop ram attached to the top chamber of this device (see Fig. 6.4). When air bubbles were no longer seen coming from the drainage duct of the base pedestal in the cell, the Klinger valve between the cell and the pore pressure block was closed.

The deairing screw on the pore pressure block was opened, bled and then closed tightly. The valve on the top of the volume change device was then closed, and the transducer was now calibrated directly against the Budenberg pressure gauge on the panel behind its cell using fluid pressure along the back pressure line through the volume change device. The results of this exercise are shown in Fig. 6.8.

(iii) Volume change transducers :

Before the calibration procedure described below was carried out, each transducer was deaired in its bottom chamber by first inverting and then allowing deaired water from the ceiling tank via the back pressure air/water distribution block to bleed from around the threaded coupling connector positioned on its underside.[1]

The inlet (drainage) coupling on the top of the instrument was then exchanged for one from a portable Bishop ram fully charged with deaired water. The top chamber of the volume change device was now deaired by cranking the perspex handwheel clockwise on the ram and allowing water to bleed from around the inlet coupling which was then tightened. Alternatively, deaired water was drawn directly from the ceiling tank into an empty ram via the top chamber of the device by first opening the Klinger valve here and then turning the handwheel on the ram slowly in an anticlockwise direction. When the ram was fully charged, the Klinger valve was closed.

With the Klinger valve this side of the pore pressure deairing block closed, the required (back) pressure in the bottom chamber was now

---

1. Medium gauge flexible Wadelon (4·69mm) nylon tubing with a nominal wall thickness of 2·97 (± 0·13mm) and burst pressure 6895 kPa was used in conjunction with Wade 'N' couplings on all drainage lines.

applied through the Manostat regulating valve and the air/water interface on the back pressure side of the panel. This pressure was read directly off the Budenberg gauge.

A one revolution clockwise rotation of the handwheel on the Bishop ram will move the internal piston forwards by 0·977mm in its machined cylindrical housing (internal bore 38·10mm) thus sweeping out a volume of 1·114cm^3. This volume of water should, therefore, enter (or leave) the top chamber of the volume change transducer with every 360° clockwise (or anticlockwise) rotation of the handwheel. This principle was used to calibrate each transducer and the results are shown in Figs. 6.9 to 6.12.

(iv) Displacement transducers :

Each displacement transducer was calibrated using a micrometer rig. This calibration rig comprised an inverted clamped micrometer at one end and a yoke separated from it by 2 x 8mm diameter INVAR cylinders spaced so as to accomodate the clamped transducer at the other. The shaft of the micrometer was adjusted to make contact with the transducer spindle and calibration proceeded in selected increments of measured travel of the micrometer shaft upwards. The results of these calibrations are shown in Fig. 6.13.

Displacement readings made with the transducer in its position on the triaxial cell and fixed to the load cell piston will include a component of machine compliance (elastic shortening of piston, compression in bottom stone and perspex top cap for example) which must be taken into account in subsequent calculations of sample axial shortening. This was achieved by placing a solid incompressible cylinder of mild steel (38mm x 76mm) on top of a porous stone and axially loading it via the internal load cell acting through a perspex top cap whilst recording simultaneous deflections on the displacement transducer. These results are shown in Fig. 6.14.

6.8.5 Preparation of samples.

(i) Reconstituted samples :

The procedure outlined in 6.5 for the preparation of reconstituted samples for oedometer testing were those followed for the series of tests carried out here. The air dried fraction passing the 425 microns aperture sieve size was reconstituted with distilled water to give a

homogeneous soil with a water content of approximately 20%. At this stage, samples were wrapped in clingfilm and bagged in polythene, placed in a humidifier and allowed to 'mature' for about 48 hours.

Cylinders of this soil were subsequently produced by placing a silicone-greased 38mm diameter sampling tube over an inverted piston of slightly smaller diameter which was fixed vertically in a vice. Small lumps (approximately 2·5g) of soil were carefully but firmly moulded onto the piston using the index finger of one hand. The sample was then built up gradually by holding the soil down whilst very slowly sliding the tube upwards in stages until eventually a sample of the correct length was produced. This was extruded, checked for flaws and, if found to be satisfactory, wrapped in clingfilm and then labelled and stored on end in a humidifier until required.

Of the 16 samples prepared in this manner, measured water content and unit weight variations (expressed as standard deviations) were 0·82% (mean 22·1%) and 0·24 kNm^{-3} (mean 20·55 kNm^{-3}) respectively.

(ii) Undisturbed samples :

Samples prepared for the parallel series of tests on undisturbed soil were in accordance with the procedures detailed in 5.4.3. Of the 15 samples obtained, measured water content and unit weight variations were 0·91% (mean 15·63%) and 0·13 kNm^{-3} (mean 21·19 kNm^{-3}) respectively.

6.8.6 Testing procedures.

A description of the general methods and procedures adopted in consolidated-undrained (CU) soil tests is contained in Bishop and Henkel (1976, pages 106-122). The testing procedures for the type of CU test used in the testing programme detailed in this section were broadly those which have been described by these authors.

The testing of both reconstituted and undisturbed samples of till HH(a) was carried out using cylinders with a length (L) to diameter (D) ratio of 2. This convention, based largely on the results of experimental work reported by Taylor (1941), is now generally accepted as standard laboratory practice.

Samples were tested between ordinary platens. Barden and McDermott (1965), who tested remoulded normally and overconsolidated clays, concluded that, although barrelling is minimised, the use of

lubricated platens will not change the effective strength parameters of specimens with L/D = 2 tested between ordinary platens. Bishop and Green (1965) reached the same conclusion for sand samples. Duncan and Dunlop (1968), testing undisturbed clay, report that (unless it is necessary to measure volumetric strains in drained tests on sand) the advantages gained from the use of lubrication are probably not worth the additional bother.

During isotropic consolidation of the till samples a back pressure acting through the pore fluid was used to ensure a condition of saturation. Back pressure saturation techniques, which are now widely used in both CU and consolidated-drained (CD) tests have been described by several workers, and these have been summarised by Saada and Townsend (1981). The size of the pore pressure response during an undrained loading increment prior to isotropic consolidation is usually used to determine the degree of saturation of the sample. This in turn can be used (see for example Lowe and Johnson, 1960) to estimate the level of back pressure required to attain a desired degree of saturation. Whilst the reconstituted soils examined in this way could be satisfactorily fully saturated with a back pressure of 200kPa, the undisturbed soils required much larger pressures(this despite a degree of saturation = 0·94 calculated using measured (average) values for the soils' natural water content, particle specific gravity and bulk unit weight). In fact, with some of the undisturbed samples satisfactory levels of saturation were achieved only after a back pressure of 750 kPa was in operation.[1]

Alternative evidence regarding levels of saturation for these samples may also be available by examining the dry unit weight : water content relationship established for till HH(a) in a standard compaction test, (Test 12 BS 1377: 1975, 2·5kg Standard Proctor). Here, soil was compacted in the Proctor mould at various water contents and the variation of unit weight of the compacted soil with increasing water content was established; the results are shown in the conventional form dry unit weight : percentage water content, Fig. 6.15. This Figure also shows the corresponding data calculated for the reconstituted and undisturbed samples of the same till prepared for triaxial testing purposes. Whilst possessing lower dry unit weights,

1. Similarly high back pressures (690 kPa) to ensure > 95% saturation have been reported by Soliman (1983) for Sterling Till, Wisconsin.

it is interesting to note that the reconstituted samples demonstrate a tendency towards higher levels of saturation than do the undisturbed samples.

Bishop and Henkel (1976) comprehensively discuss the various factors considered significant in the estimation of rates of testing in undrained tests with pore pressure measurements, and their observations have led to guidelines regarding loading rates designed to achieve required degrees of pore pressure equalisation in this type of test. They have concluded that, unless pore pressure equalisation is required only at failure, then an undrained test of several days duration is necessary in order to define the complete stress path for the soil. In fact, it can readily be shown that tests of a much longer duration would be required if the time to the first reading t_1 is that given by Bishop and Henkel (page 126) as :

$$t_1 = \frac{\pi h^2}{100 c_v}$$

where h is the half height of the sample
and c_v is the coefficient of consolidation.

(This expression assumes drainage from both ends and the radial boundary of the sample.)

It has been suggested (Atkinson, 1984a)that the errors implied by these very slow rates of loading are often less than the sensitivities of the instruments used to measure stress and strain.

A preliminary series of tests carried out on normally consolidated samples of reconstituted till HH(a) at rates of loading (0·052% axial strain min^{-1}) designed to contain tests within a working day[1], permitted only poor definition of the effective stress paths at small axial strain where rates of change in axial stress are large. A slower rate of loading, equivalent to approximately 1·5% sample axial strain per day (0·00104% min^{-1}), was therefore chosen and subsequently used for all tests.[2] Whilst this loading rate is somewhat slower than is more usual in both commercial and research laboratories for this type of test, it is nevertheless considered worthwhile in view of the additional information made available, particularly in the early

1. Insertion of measured values for c_v (till HH(a)) in the Bishop and Henkel equation gives a range of t_1 times up to 8 hours.

2. This gave an average measured loading rate of 12·32 kPa per hour for the reconstituted samples.

stages of compression. The effect of this, however, was to considerably extend the length of the testing period. Each CU test (including the consolidation stage) now took about two weeks to complete; the programme of work involved therefore extended to seven months.

A detailed set of procedural points which has been followed when setting samples up prior to testing has been reported by the writer in an earlier report[1], therefore these will not be reproduced here. The usual steps were taken beforehand to ensure that all drainage lines, extending from the volume change device to the pedestal under the sample, including the pore pressure block and the 'dead' drainage duct leading from the pedestal to the Klinger valve on the other side of the cell, were completely charged with deaired water. A saturated bauxilite porous stone (boiled in deaired water immediately prior to use to fully deair it) was used in conjunction with Whatman filter papers (top, bottom, radial) for drainage purposes. Reconstituted samples were sheathed with one good quality impermeable latex membrane. Undisturbed samples were sheathed with two membranes. Two tensioned rubber 'O' rings top and bottom secured the membrane(s) to the perspex top cap and base pedestal.

Chamber pressures (in excess of back pressures used) were always applied before the back pressure against a closed Klinger valve on the volume change transducer side of the pore pressure block. In this way neither swelling nor premature consolidation of the sample was able to take place. Isotropic consolidation could only take place once this drainage valve was opened. Volume change readings, either read manually from the screen of the PET or logged automatically and stored on disk, were made at the intervals of time recommended in BS 1377: 1975 for consolidation testing (see section 6.5). Readings continued until consolidation was complete, usually 24hrs. On completion of consolidation, the drainage valve was closed. If an isotropically overconsolidated sample was required, the chamber pressure was now reduced to give the desired overconsolidation ratio, the drainage valve was opened and the sample was allowed to swell back to equilibrium. Readings of volume change were made at the same intervals of time as for the consolidation stage. On completion, the drainage valve was closed.

---

1. See 6.8.2 .

Either at this stage, or before consolidation, the pore pressure response to an increment in total stress was obtained so as to evaluate the pore pressure parameter B. This was carried out by raising the chamber pressure by 100 kPa and recording the resulting change in pore pressure. Readings on the pore pressure transducer were taken at $\frac{1}{4}$, $\frac{1}{2}$, 1 , 2 , 4 , 8 , 15 , 30 min. etc... after the increment was first applied, thus allowing sufficient time for equalisation of the excess pore pressure produced in the sample. This was achieved when a stable reading was obtained on the pore pressure transducer. If the maximum value of the ratio $\Delta u/\Delta\sigma_3$ was less than 0·95 (see Barden, 1965) then the following procedure (once the chamber pressure was again reduced by 100 kPa), designed to flush the drainage lines, was followed :

a) A Bishop ram was coupled to the Klinger valve on the 'dead' drainage line of the cell via its attached deairing block. The line from the ram to the Klinger valve was deaired by slowly cranking the perspex handwheel clockwise on the ram and allowing water to bleed through the screw at the top of the block.

b) This screw was tightened down and, ensuring that the Klinger valve between this block and the cell was still closed, pressure was slowly generated by the ram equivalent to the back pressure operating along the active drainage line on the other side of the cell.

c) The Klinger valve in b) above was now opened. Fluid pressure in all drainage lines was now compatible with the pore fluid pressure in the sample.

d) Deaired water was drawn from the top chamber of the volume change device by slowly turning the perspex handwheel, now anticlockwise.

The pore pressure response to an increment in isotropic stress was then again determined.
By following this routine, satisfactory levels of saturation were achieved in all samples.

Undrained compression of the sample took place having ensured that the piston on the load cell was seated correctly on the ball bearing of the perspex top cap and that datum readings on all transducers were recorded. The machine motor was switched on manually and readings were taken automatically on all transducers at the intervals of time preselected in the logging programme.

When the displacement, load cell and pore pressure transducer readings taken together indicated that an end state had been achieved in the sample (with respect to the rate of change of additional axial stress carried by the sample and the size and sign of the excess pore pressure generated within it), then the motor on the machine was manually switched off. All Klinger valves around the chamber were closed to seal in the cell pressure. The load cell piston was kept in position. The Klinger valve which drains the chamber was opened and the chamber was emptied rapidly. The loading stage was now cranked down very quickly, the chamber was dismantled, the sample was taken off its pedestal and the 'O' rings, perspex top cap, bottom stone, latex membrane, top, bottom and radial filters removed.

The entire sample was weighed to the nearest 0·01g and its water content determined.

The processing and printing of the triaxial data (stored on disk) in terms of axial and volumetric strain, total axial stress, pore water pressure, additional (effective) axial stress and average effective pressure was achieved by a program written in-house for the PET.

The usual (manual calculation) checks were performed beforehand to ensure that this program produced the correct output in response to a range of digital input from the various transducers. Manual checking of data was also carried out periodically during testing.

Till type	Mount number	Fossil type and species	Stratigraphic designation
HH(a)	1 - 20	Various Cretaceous forams, Species indeterminate.	
	21 - 48	Various Jurassic forams.	(Oxford Clay)
	50	Ostracod, Lophocythera	M. Jurassic (Bathonian)
	51	Ostracod, Bairdia	M. Jurassic (Bathonian)
	52 - 54	Ostracod, Hungarella	Lias
	55 - 57	Ostracod, Galliacytheridea	Kimmeridge
HH(b)	1 - 23	Various Cretaceous forams, e.g. Globorotalites and Garalinella.	U. Chalk
	24 - 32	Various U. Jurassic forams	(Oxford Clay)
	35, 39, 42	Ostracod, Hungarella	Lias
	36, 41	Ostracod, Progonocythera	M. Jurassic
	37	Ostracod, Cytherilloidea	Cretaceous
	43	Fishtooth	(Unknown)
	50, 51	Forams, Lenticula	M. Jurassic

Table 6.1 Microfauna from tills HH(a), HH(b), Holwell Hyde.

TEST CONDITION	TILL TYPES				
	HH(a)	HH(b)	F(b)	W(b)	W(d)
RECONSTITUTED	OR(1)	OR(2)	OR(3)	OR(4)	OR(5)
UNDISTURBED					
vertical drainage	OU(1)V	OU(2)V	OU(3)V	OU(4)V	OU(5)V
horizontal drainage					
(parallel to fabric)	OU(1)H(p)	OU(2)H(p)	OU(3)H(p)	OU(4)H(p)	OU(5)H(p)
(normal to fabric)	OU(1)H(n)	OU(2)H(n)	OU(3)H(n)	OU(4)H(n)	OU(5)H(n)
(random orientation)	OU(1)H(r)	OU(2)H(r)	OU(3)H(r)	OU(4)H(r)	OU(5)H(r)

Table 6.2 Index of oedometer tests.

Till type	Initial vertical consolidation pressure (kPa)	Swelling pressure (kPa)	Ro	Test number
HH(a) (reconstituted)	100	-	1•0	SR(1)(i)
	200	-	1•0	SR(1)(ii)
	400	-	1•0	SR(1)(iii)
	1600	100	16•0	SR(1)(iv)
	1600	200	8•0	SR(1)(v)
	1600	400	4•0	SR(1)(vi)
HH(a) (undisturbed)	50	-	16•0(?)	SU(1)(i)
	200	-	4•0(?)	SU(1)(ii)
	400	-	2•0(?)	SU(1)(iii)
F(b) (undisturbed)	50	-	16•0(?)	SU(3)(i)
	200	-	4•0(?)	SU(3)(ii)
	800	-	1•0(?)	SU(3)(iii)

Table 6.3 Index of drained shear box tests.

	Initial isotropic consolidation pressure (kPa)	Swelling pressure (kPa)	Ro	Initial pore pressure (kPa)	Test number
RECONSTITUTED	400	-	1•0	200	RA1(i)
	800	-	1•0	200	RA1(ii)
	1600	-	1•0	200	RA1(iii)
	800	200	4•0	200	RA2(ii)
	1600	400	4•0	200	RA2(iii)
	400	267	1•5	200	RB (ii)
	400	200	2•0	200	RB (iii)
	1600	200	8•0	200	RB (v)
	1600	100	16•0	200	R2 - 02
	1600	50	32•0	200	R2 - 03
UNDISTURBED	400	-	2•0(?)	400	UA1(i)
	800	-	1•0(?)	200	UA1(ii)
	1000	-	1•0	750	UA1(iii)
	1600	-	1•0	400	UA1(v)
	400	100	8•0(?)	750	UA2(i)
	800	200	4•0(?)	750	UA2(ii)
	1600	400	4•0	200	UA2(iii)
	1000	800	1•25	750	UB (i)
	1000	667	1•50	750	UB (ii)a
	500	333	2•40(?)	750	UB (ii)b
	1000	500	2•0	750	UB (iii)
	1000	125	8•0	750	UB (v)
	1000	62•5	16•0	750	UB (vi)
	1000	50	20•0	750	UB (vii)

Table 6.4 Index of CU triaxial compression tests.

Load cell (digits kN^{-1})	Pore pressure transducer (digits kPa^{-1})		Volume change transducer (digits cc^{-1})		Displacement transducer (digits mm^{-1})	
838•89 (1•05kPa)	A	4•786 (0•21kPa)	A	105•07 (0•0095cc)	172•29 (0•0058mm)	PANEL 1
	B	1•039 (0•96kPa)	B	105•53 (0•0095cc)		
938•46 (0•94kPa)	A	3•961 (0•25kPa)	A	31•299 (0•032cc)	183•465 (0•0055mm)	PANEL 2
	B	1•181 (0•85kPa)	B	31•718 (0•032cc)		
510•40 (1•73kPa)	A	4•052 (0•25kPa)	A	39•767 (0•025cc)	181•405 (0•0055mm)	PANEL 3
	B	1•006 (0•99kPa)	B	39•258 (0•025cc)		
513•57 (1•72kPa)	A	4•343 (0•23kPa)	A	44•704 (0•022cc)	184•670 (0•0054mm)	PANEL 4
	B	1•309 (0•76kPa)	B	44•883 (0•022cc)		

A, B : pore pressure transducer denotes 0 – 1034kPa and 0 – 3448kPa transducers respectively.
A, B : volume change transducer denotes 200kPa, 750kPa back pressure respectively.
(Quantities in brackets denote maximum sensitivities.)

Table 6.5 Summary of transducer calibrations, panels 1 – 4.

Figure 6.1 Jurassic fauna from tills HH(a) (top, centre) and HH(b) (bottom), Holwell Hyde.
(Field of view, centre, approximately 300mm.)

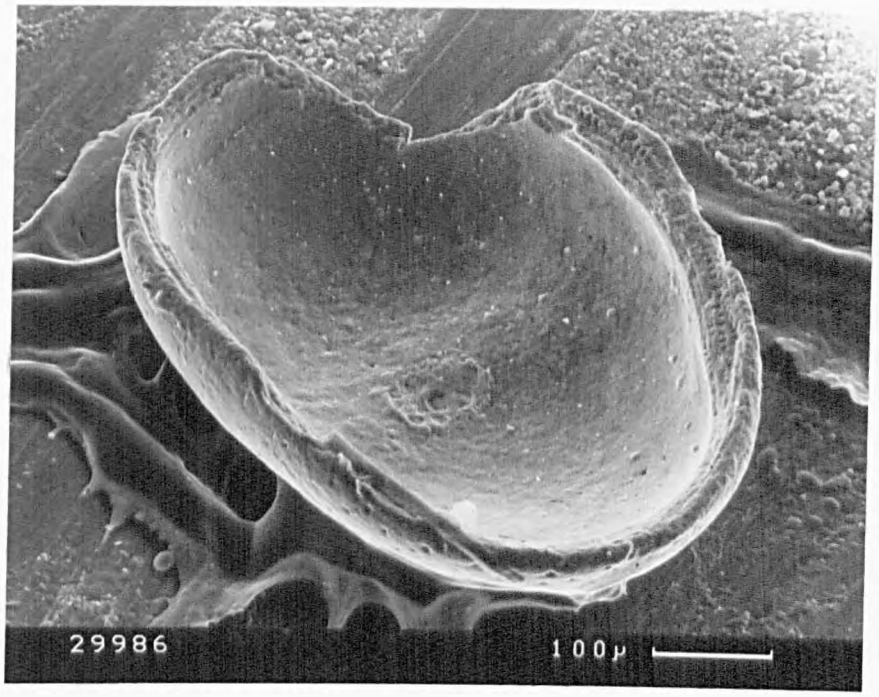

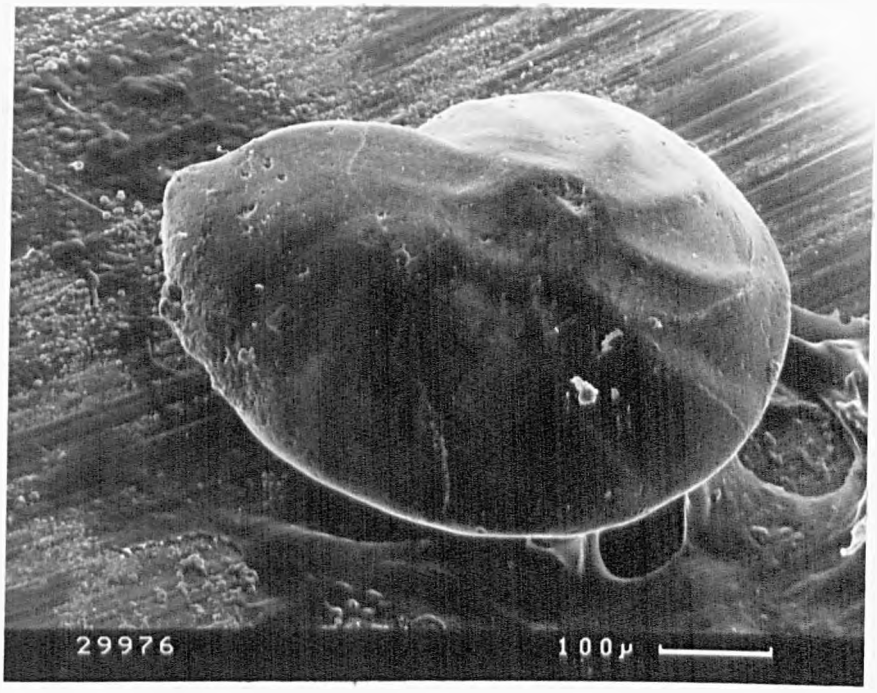

Figure 6.2 Middle Jurassic (?) microfauna from Holwell Hyde:
Top: ostracod carapace with dorsal hinge, till HH(a).
Bottom: lenticulinid foram, till HH(b).

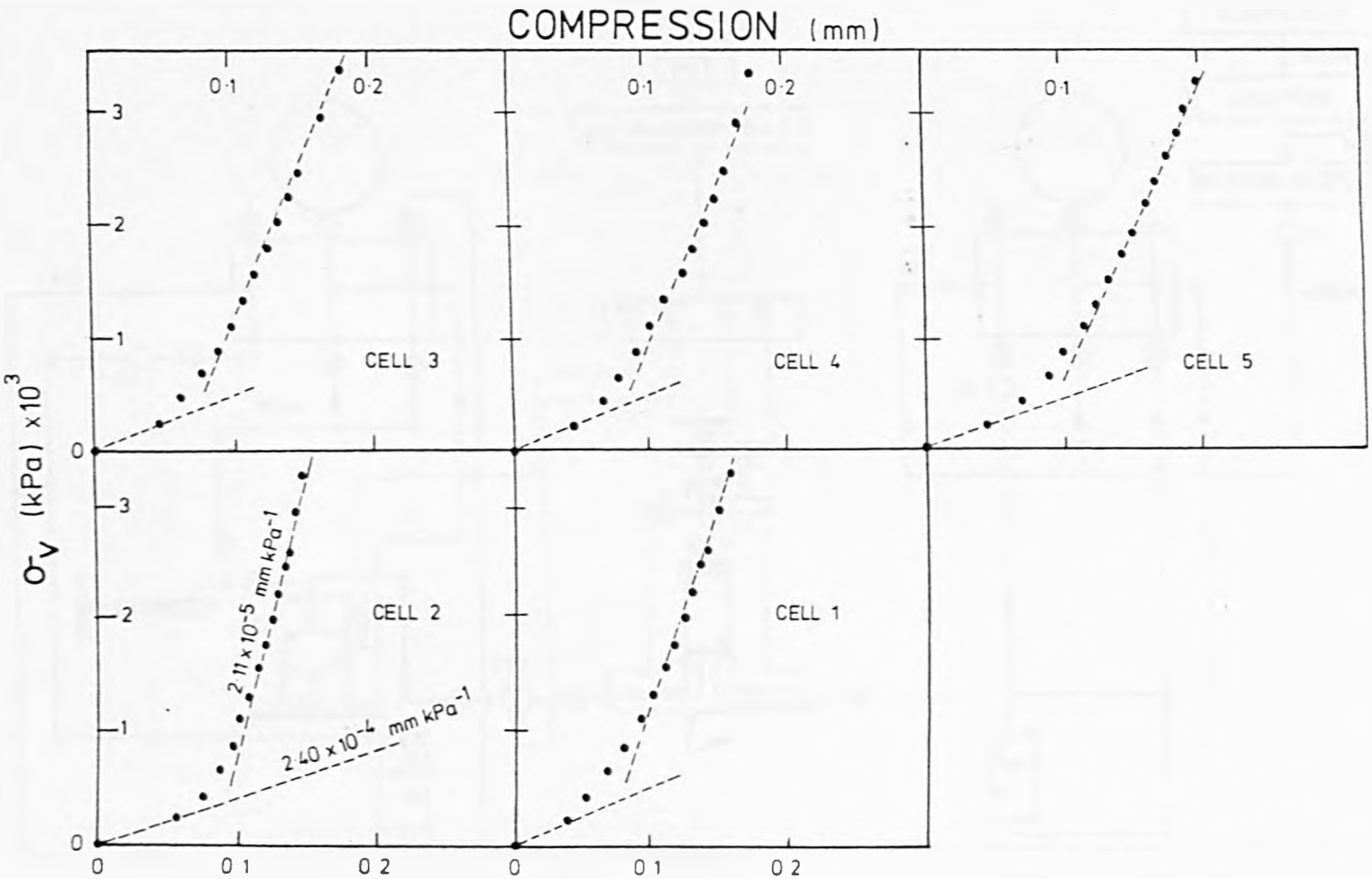

Figure 6.3 Measured elastic compressions in consolidation cells 1 - 5 .

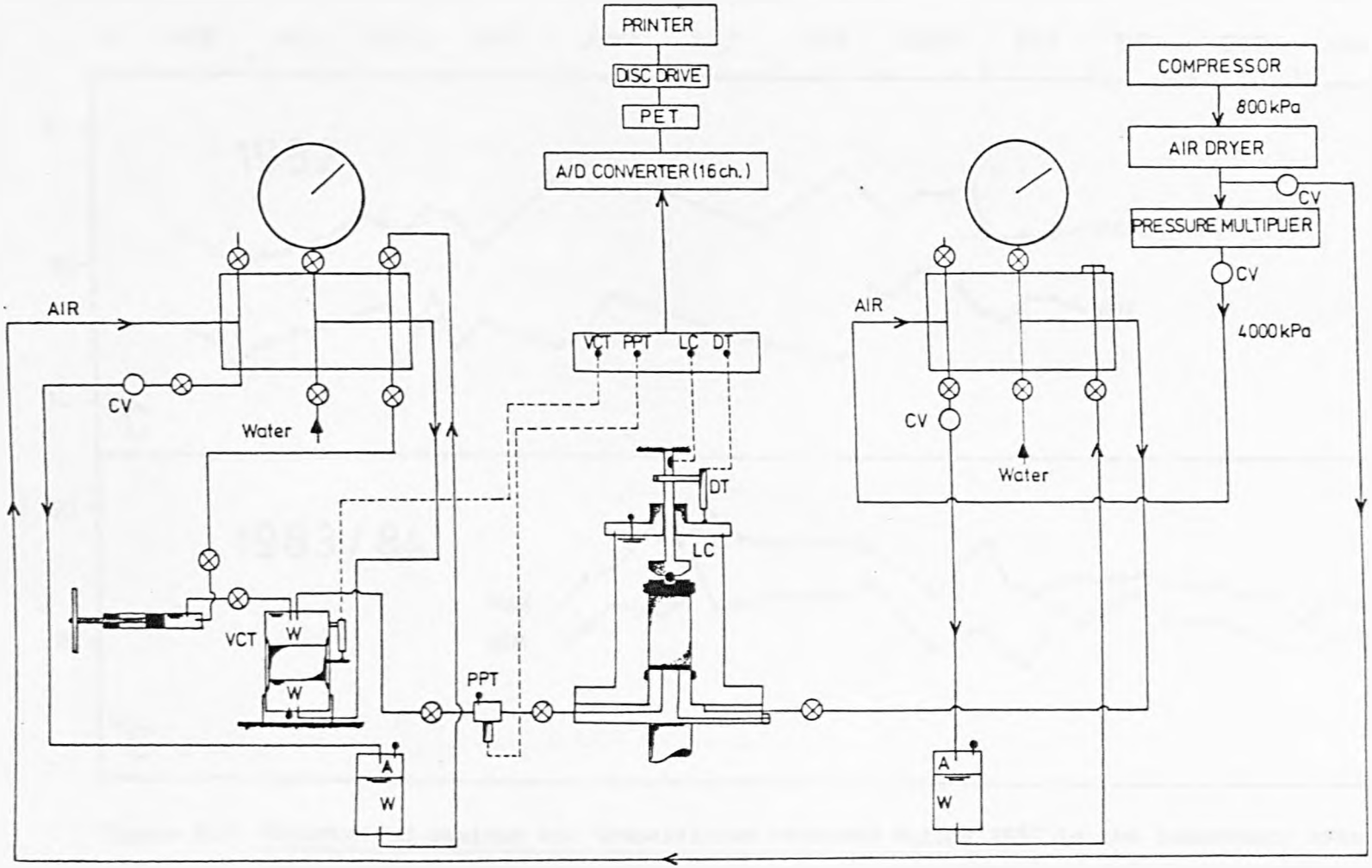

Figure 6.4 Diagrammatic layout of equipment and instrumentation for one 38mm triaxial cell.

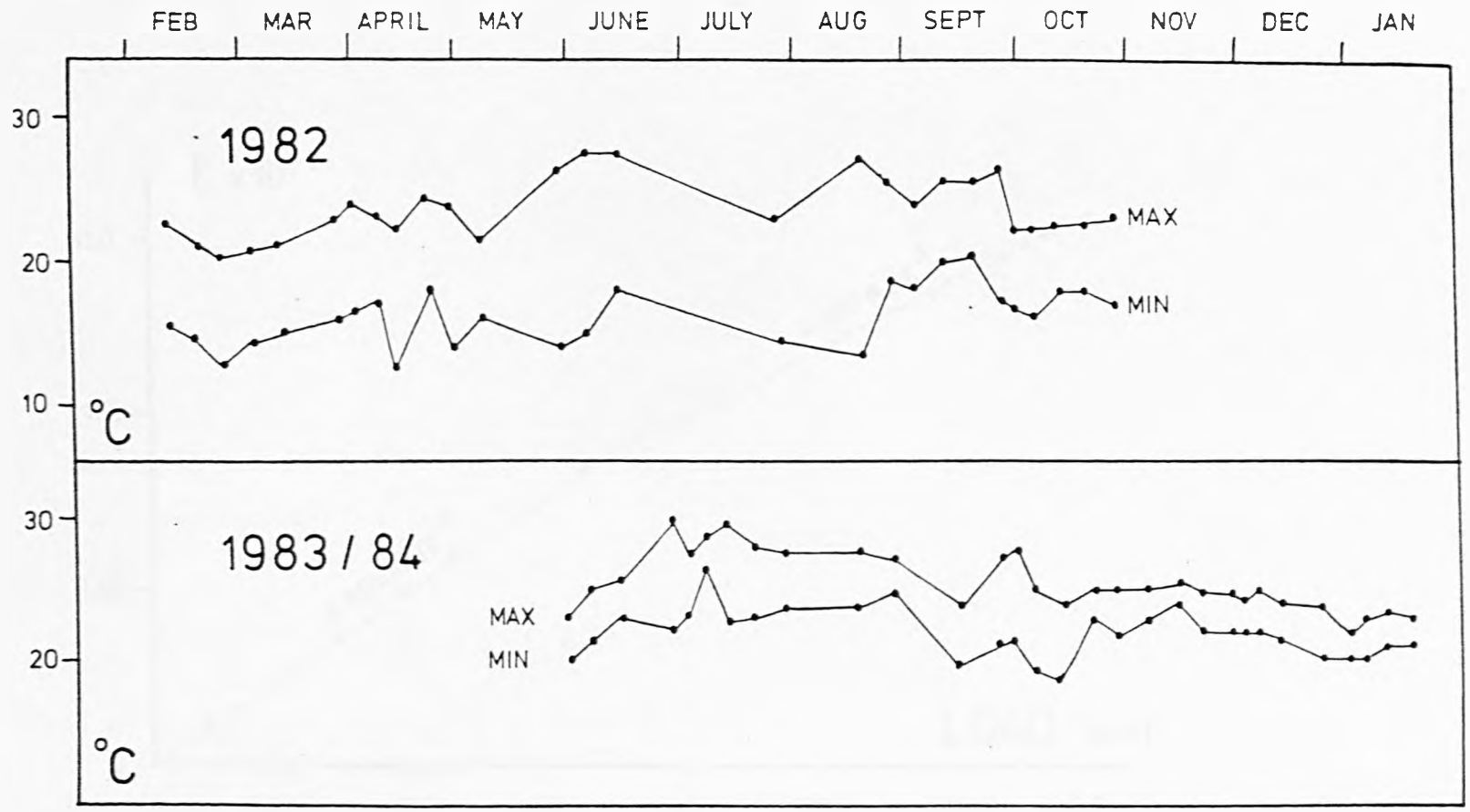

Figure 6.5 Minimum and maximum air temperatures recorded during 1982 in the laboratory space now occupied by the new laboratory housing the triaxial equipment, and recorded air temperatures in this new laboratory, 1983/1984.

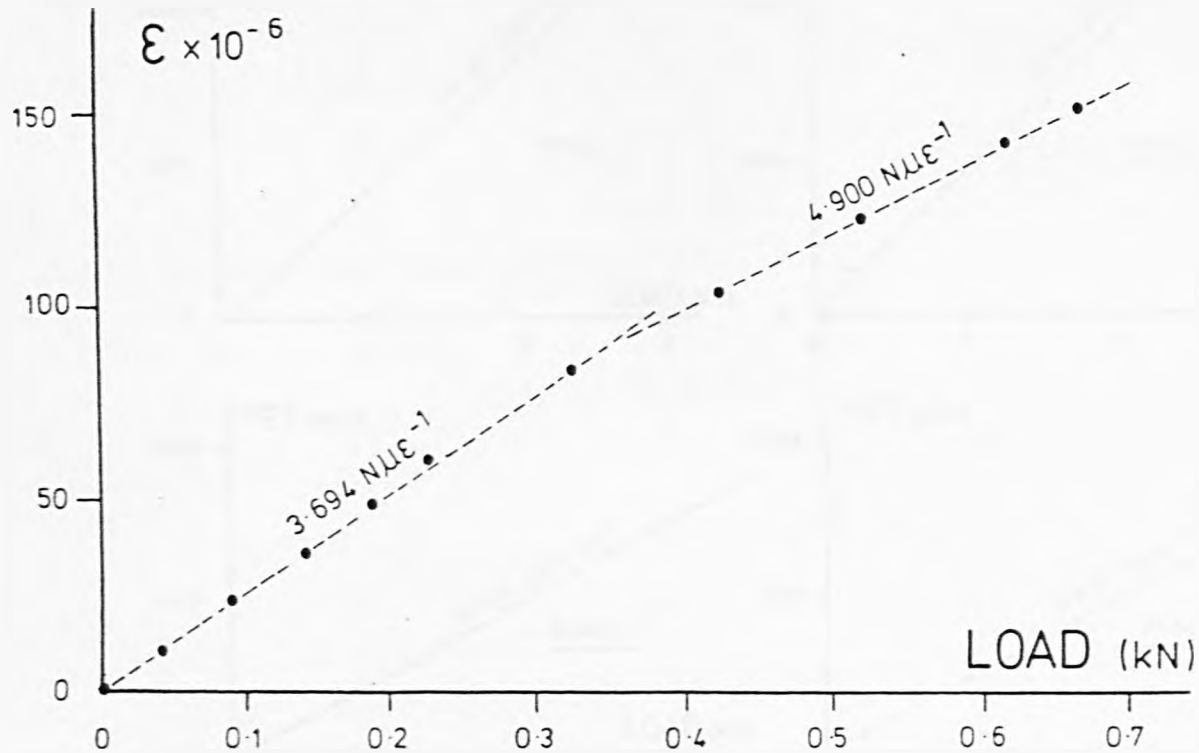

Figure 6.6 Calibration of the load cell calibrator.

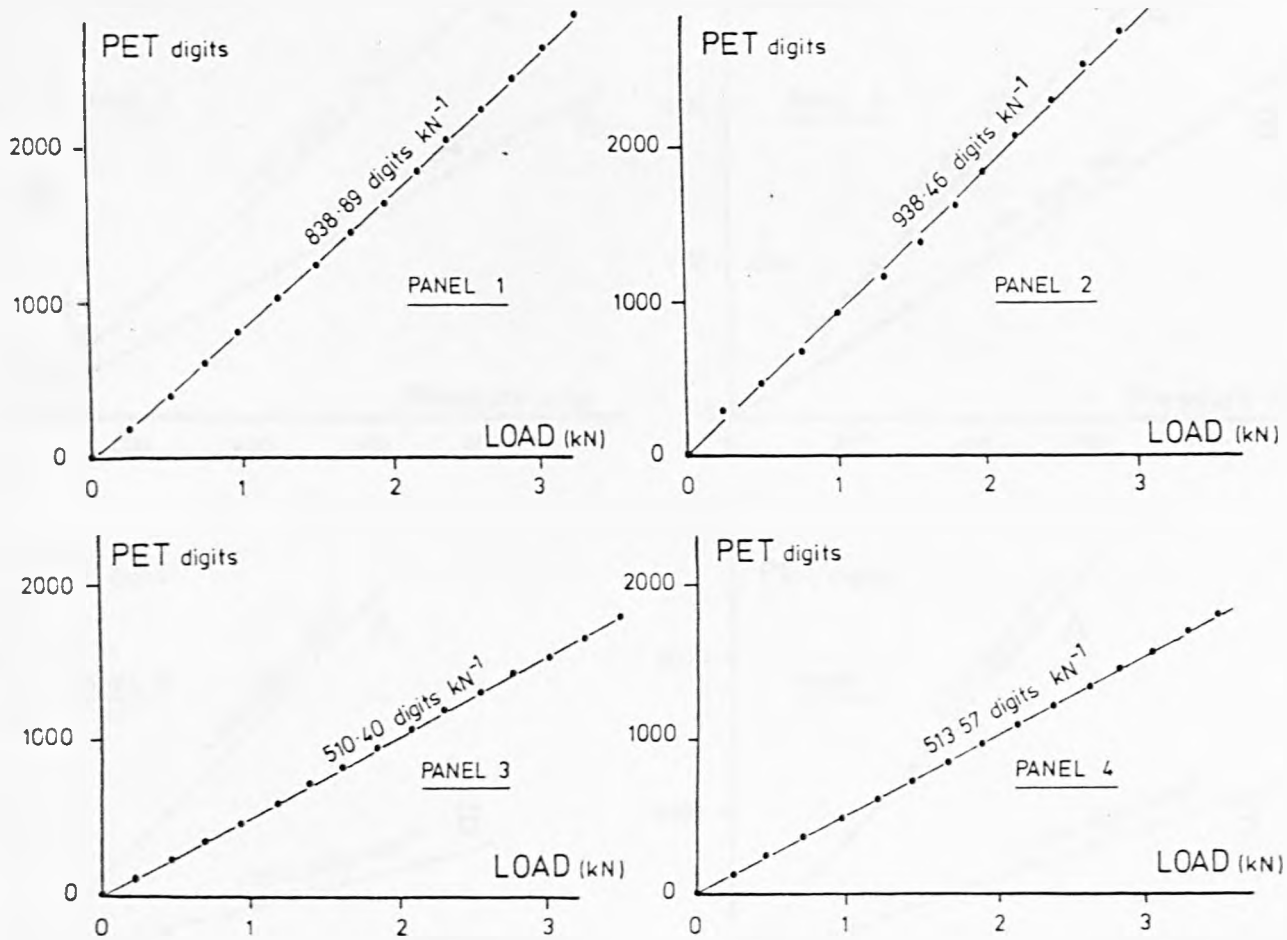

Figure 6.7 Load cell calibration graphs , panels 1 - 4 .

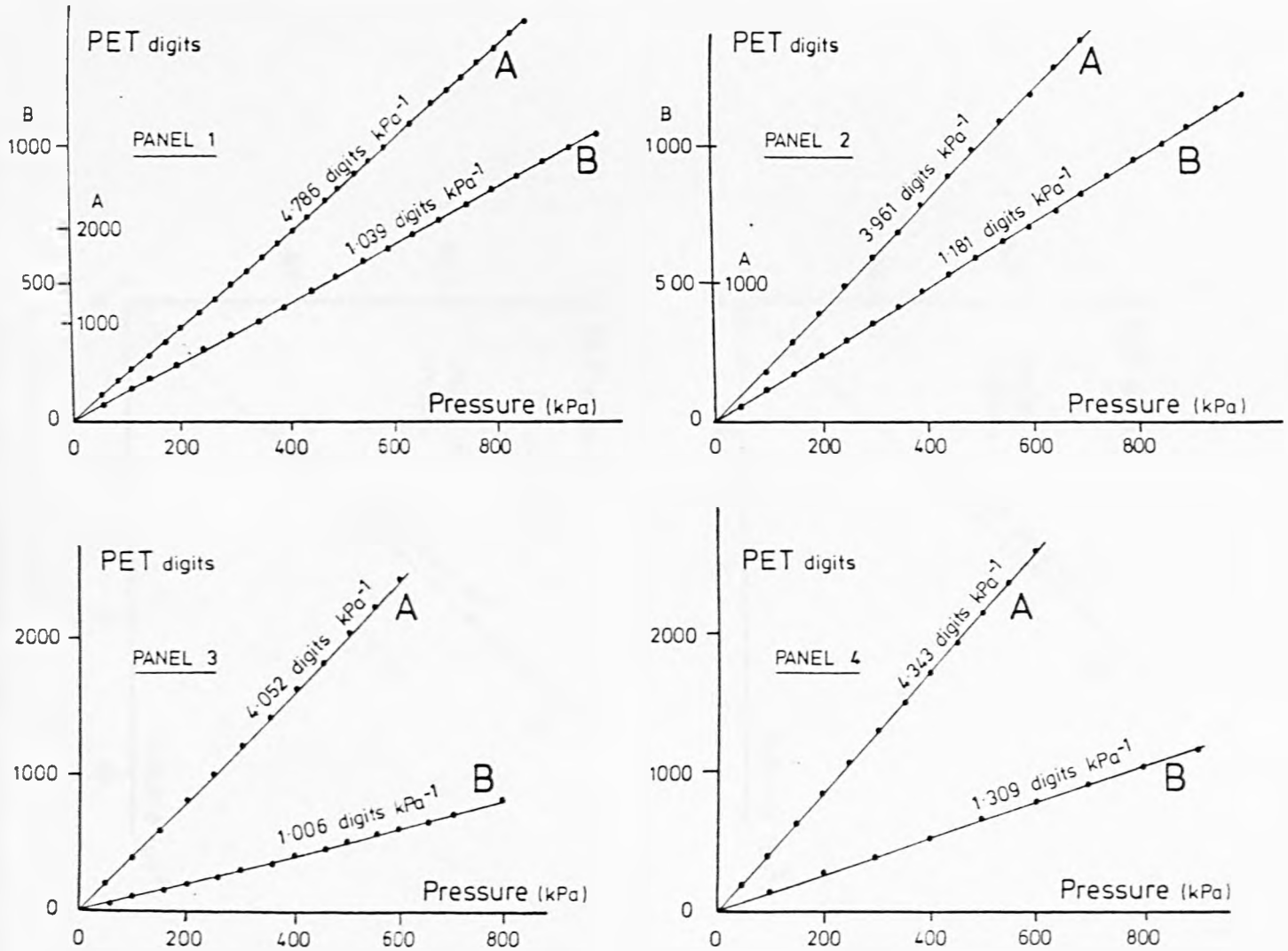

Figure 6.8 Pore pressure transducer calibration graphs , panels 1 - 4 .

(A , B denotes 0 - 1034 kPa and 0 - 3448 kPa transducers respectively).

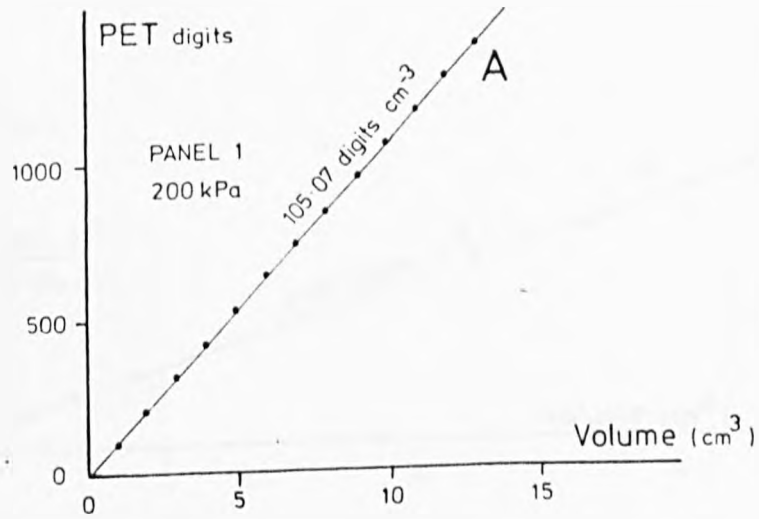

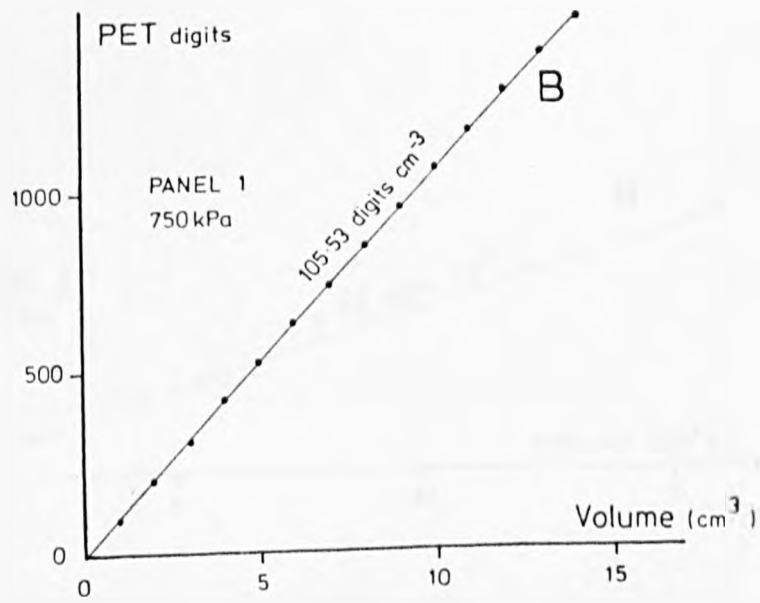

Figure 6.9 Volume change transducer (50cc) calibration graphs, panel 1, using (A) 200 kPa, (B) 750 kPa, back pressure.

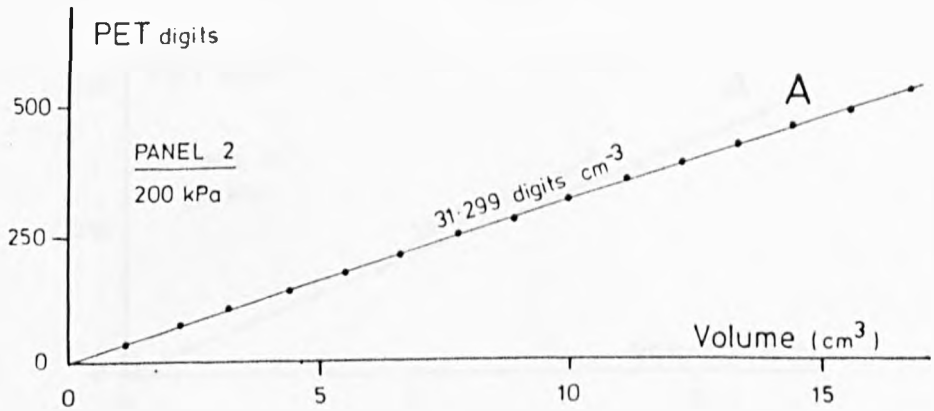

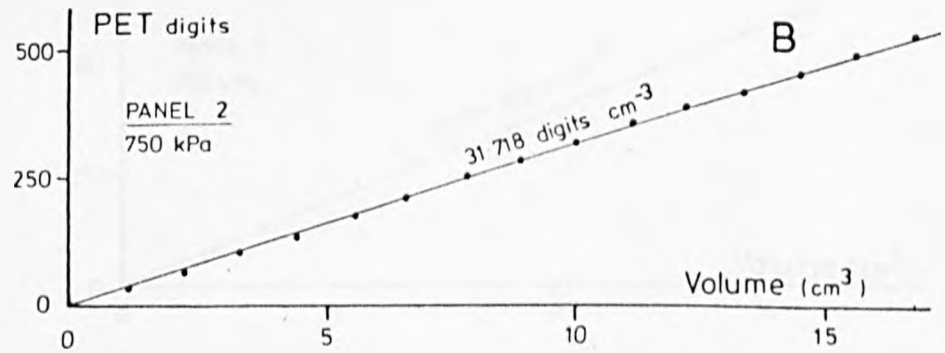

Figure 6.10 Volume change transducer (100cc) calibration graphs, panel 2, using (A) 200 kPa , (B) 750 kPa, back pressure.

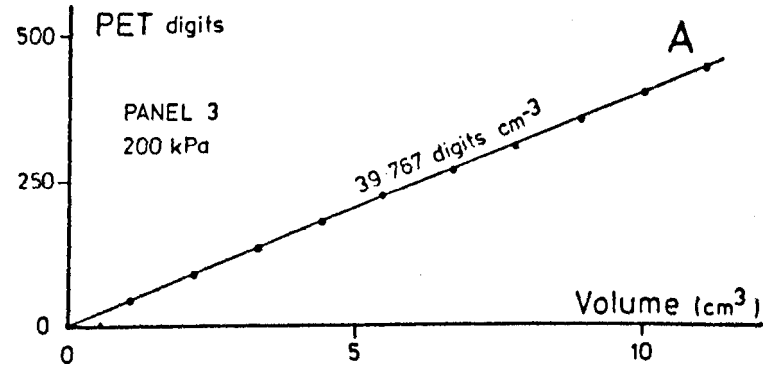

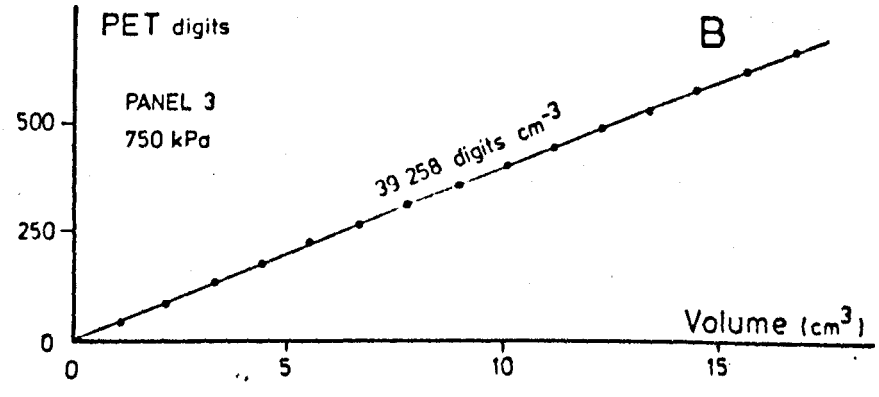

Figure 6.11 Volume change transducer (100cc) calibration graphs, panel 3, using (A) 200 kPa , (B) 750 kPa, back pressure.

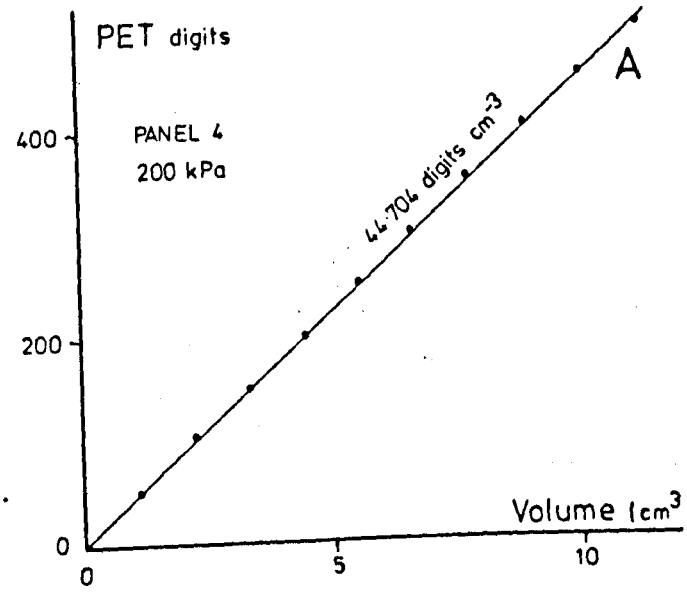

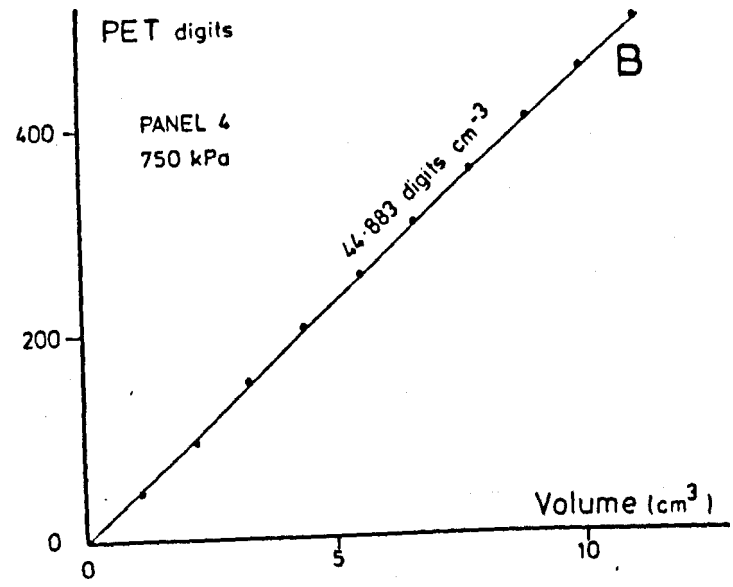

Figure 6.12 Volume change transducer (100cc) calibration graphs, panel 4, using (A) 200 kPa , (B) 750 kPa , back pressure.

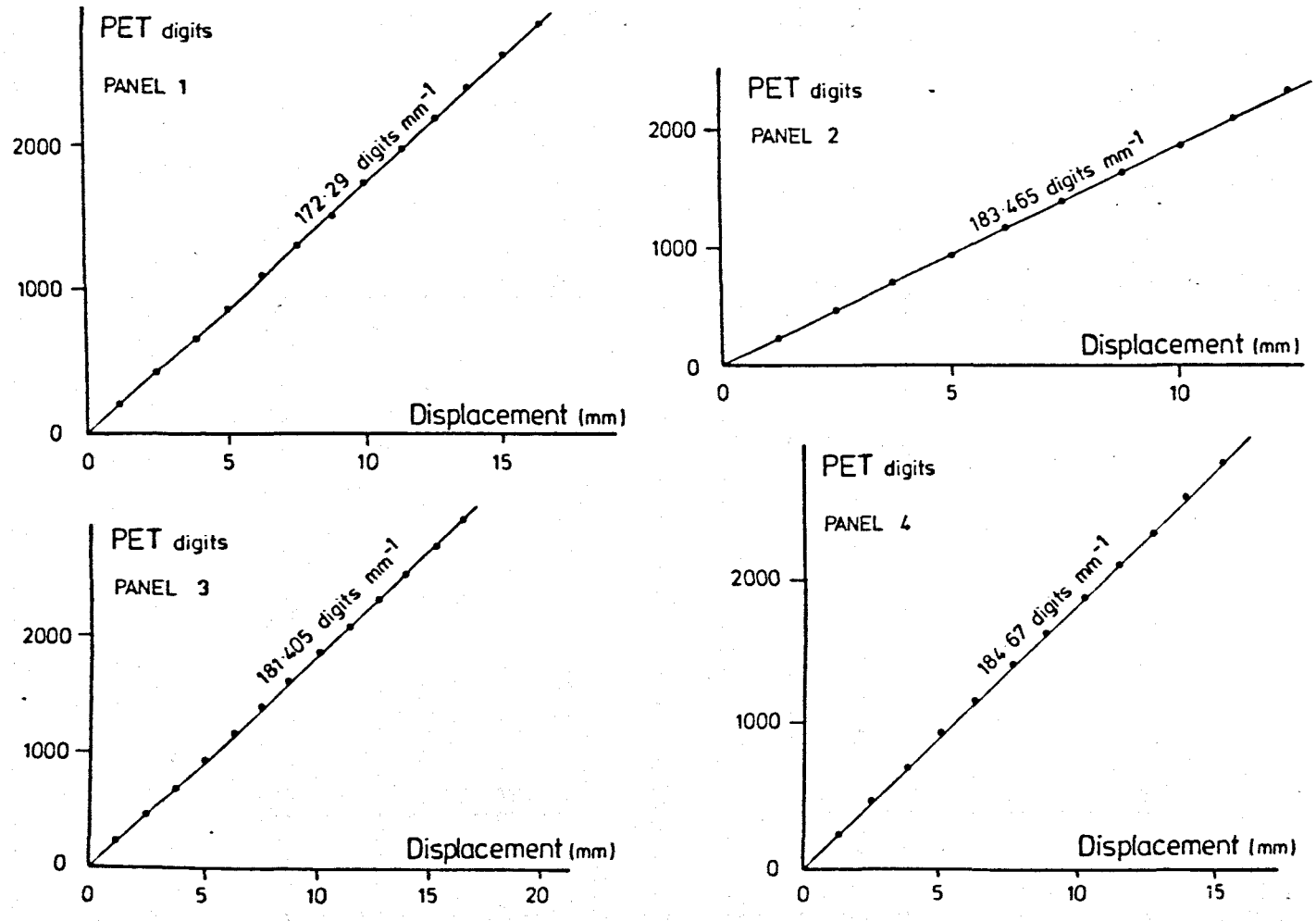

Figure 6.13 Displacement transducer calibration graphs , panels 1 - 4 .

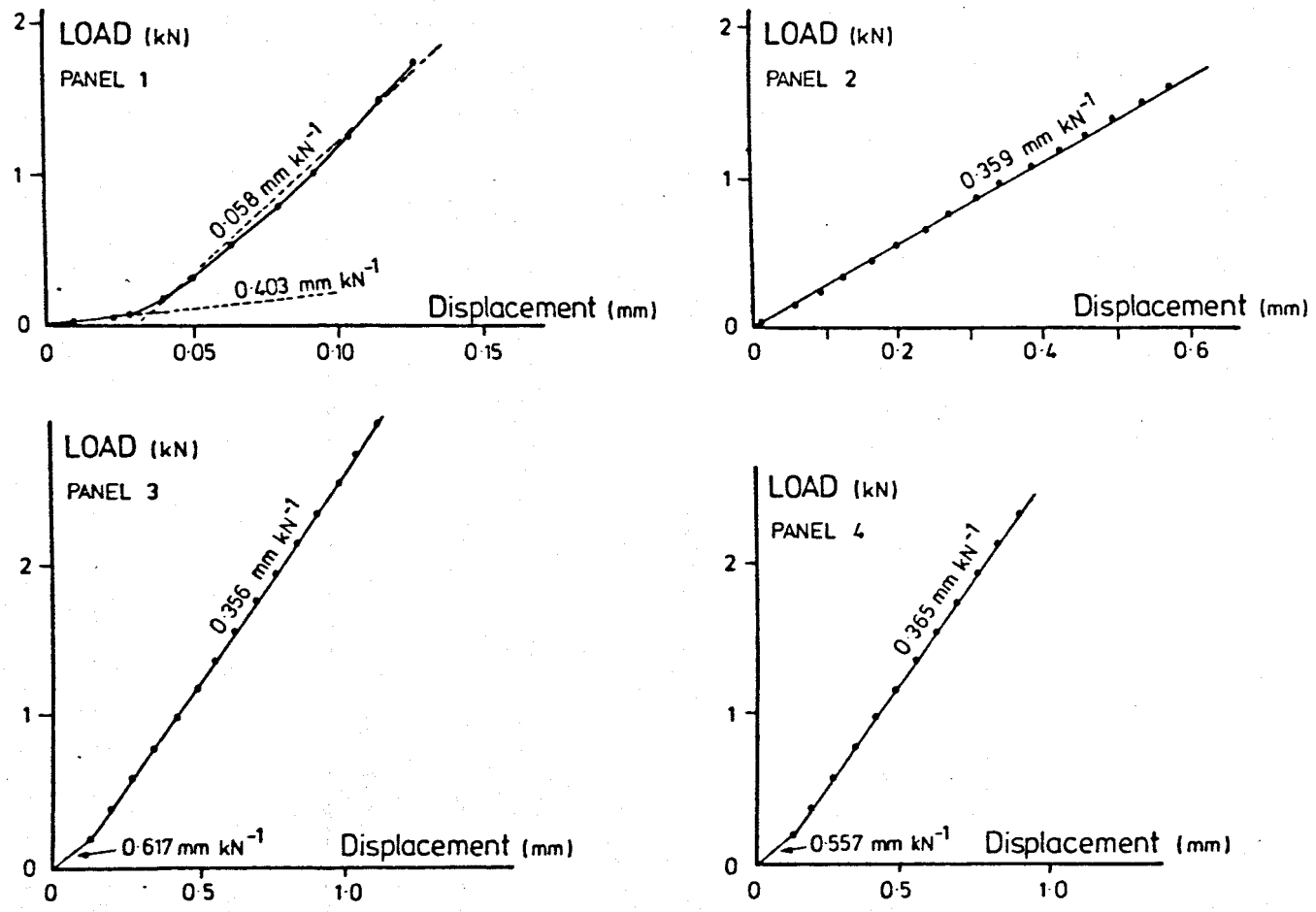

Figure 6.14 Measured elastic compressions in the triaxial cells , panels 1 - 4 .

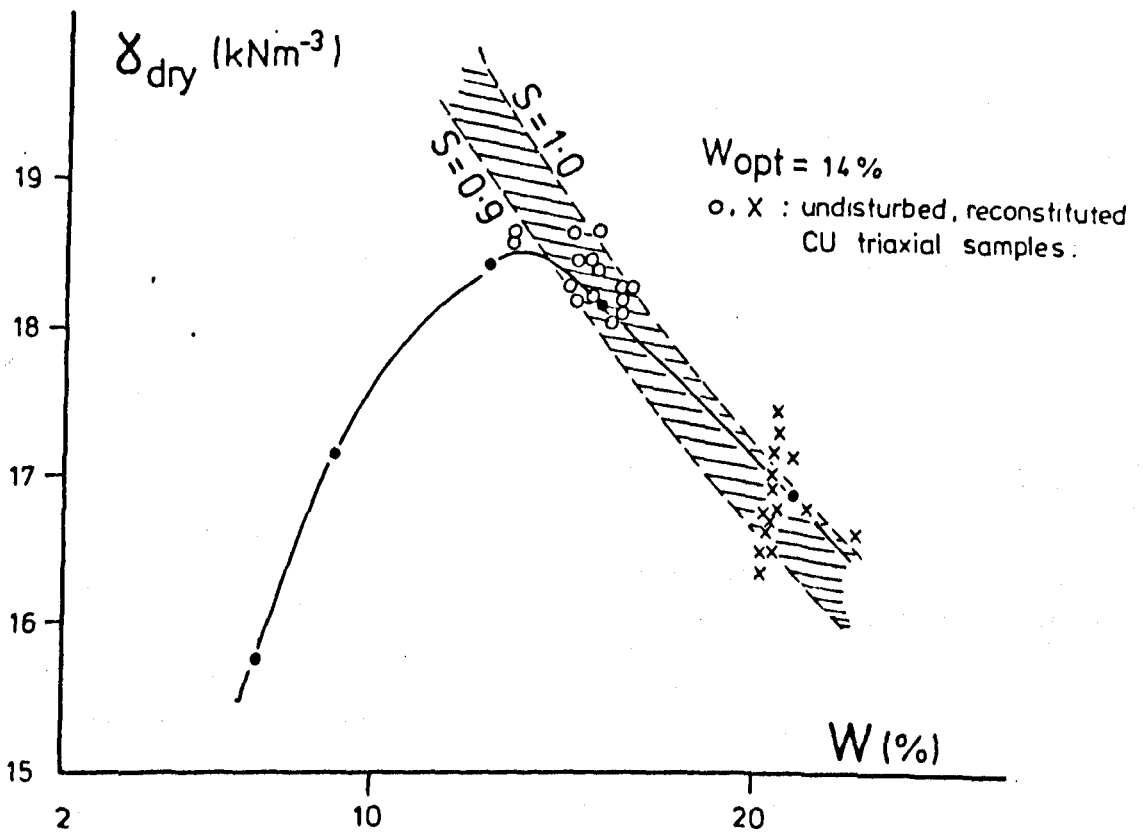

Figure 6.15 Dry unit weight : water content relationship for till HH(a).

CHAPTER 7. LABORATORY TEST RESULTS.

7.1 Classification tests.

7.1.1 Atterberg limits and particle specific gravity.

The results of testing to determine the natural water contents, liquid limits and plastic limits for those soils listed in Table 5.3 are shown in Table 7.1. The particle specific gravities of tills HH(a), HH(b), F(b), W(b) and W(d) are also included in this Table. The plasticity data for these tills and the other related soils are shown on the plasticity chart, Fig 7.1.

7.1.2 Particle size.

The results of the sieving and sedimentation tests on till samples HH(a), HH(b), F(b), W(b) and W(d) are shown in Fig 7.2. The effect of removing the acid soluble content from each of these soils on the percentage of material finer than 2 microns is also indicated in this Figure. Table 7.2 compares the activity of these soils with and without having removed the carbonate contained within them. The activity values for tills HH(a), HH(b) determined using carbonate-free soil to ascertain both PI and the 'true' clay fraction percentage are also shown (in parentheses) in this Table.

7.1.3 Quantity and distribution of chalk in the tills.

The results of the sedimentation tests on tills HH(a), HH(b), F(b), W(b), W(d) from which all carbonate had been removed beforehand are summarised in Table 7.3. Here, the effects of the removal of these acid solubles on the various size fractions during sedimentation are shown.

Table 7.4 summarises the results of sieving tests on tills HH(a), HH(b) designed to determine the distribution of chalk and other acid solubles in these tills in the range 16mm down to 0·063mm. Figs 7.3, 7.4 are suggested alternatives for plotting the grading data shown in Table 7.4 employing the 'phi' notation (see 4.5.2).

7.2 Mineralogical tests.

7.2.1 Clay mineral content.

The results of X-ray diffraction testing to determine the type and quantity of clay minerals present in tills HH(a), HH(b), F(b), W(b), W(d) are shown in Table 7.5. Here, the clay minerals content is expressed as a percentage proportion of the finer than 0·002mm fraction (with acid solubles removed) determined from the sedimentation tests described in 6.2.3. The amount of quartz and calcite present in these soils has also been determined and these results are included in this Table. The quantity of these two minerals is here expressed as a percentage of total solids in the soil. For purposes of comparison the percentage of acid soluble material at 2 microns determined from the sedimentation tests for each of these tills is also shown. These percentages should be compared, it is suggested, with those determined by XRD for calcite in this Table.[1]

7.2.2 Element composition.

The results of the EDAX testing on tills HH(a), HH(b), F(b), W(b), W(d) to determine the various element types present in these tills are shown in Table 7.6. This type of test does not enable quantification of elements in the way of XRD analysis, but an examination of the traces so produced will provide an assessment of the relative proportions of the various elements present in each of the tills.

A separate series of EDAX tests has also been carried out on prepared, undisturbed samples of tills HH(a), HH(b) which contained fresh unweathered chalk set in a clay matrix. For each of the tills an electron micrograph was produced of a localised area of contact between matrix and chalk and the image analyser of the instrument was subsequently used to produce EDAX signatures for both the clay in the

---

1. Where the percentage acid solubles at 2 microns is not positive (see for example -0·17% for the decalcified Ware Till F(b) in Table 7.3) then this is assumed zero in Table 7.5.

matrix of the soil and the chalk particle. The results of these tests are shown in Figs 7.5 and 7.6. In these Figures the separate EDAX (element) traces produced for the matrix and the chalk have been superimposed so as to enable direct compositional comparisons to be made. The compositional variabilty of the matrix is an expected feature shown very clearly on these graphs. The very small differences in calcium composition shown between the clay matrix and the chalk for both tills is, however, an unexpected result and the significance of this is discussed in Chapter 8.

7.3 Oedometer compression test results.

The results of the oedometer tests are shown in Tables 7.7 to 7.31. Here, compression and consolidation characteristics are reported for the tests carried out on reconstituted and undisturbed samples of till indexed in Table 6.2.

Values for equilibrium specific volume (V) have been obtained by the method of voids ratio difference. In this method, voids ratios are determined at the end of the final unloading stage and are based on measured values for the water content of the entire sample and the particle specific gravity of the soil at the end of the test. A condition of full saturation is assumed. These data have been used to show the relationship between equilibrium specific volume and effective vertical pressure in Figs 7.7 to 7.11. On each of these figures are plotted the graphs for both the reconstituted till (tests OR(1) to OR(5)) and the undisturbed till, vertical drainage condition, (tests OU(1)V to OU(5)V).

Values for the undisturbed stiffness modulii (m_v) have been determined for all loading/unloading stages; those for the reconstituted soils have been determined for the second loading/unloading cycles. In this way, soil behaviour can be compared across a range of similar overconsolidation ratios.

Estimates of the preconsolidation pressures for the undisturbed soil in these tests (and those reported in 7.6 (i)) have been made using the method described by Casagrande (1936). It has been assumed that a condition of normal compression is achieved in these samples when $\sigma'v > 1600$kPa.

Values for the soil permeability (k) have been derived from the stiffness modulii and the coefficient of consolidation (c_v) calculated using measured t_{50} times from $\log_{10} t$: sample deflection graphs for each load increment/decrement shown, according to the following :

$$c_v = (0{\cdot}196 \ \bar{h}^2 / t_{50})$$

where $\bar{h}$ = average drainage path length during the loading/unloading increment.

7.4 Motorised shear vane test results.

The results of the shear vane tests on reconstituted samples of tills HH(a), HH(b), F(b) are shown in Table 7.32. In these Tables the measured water contents and undrained shear strengths shown represent the averages obtained from two separate determinations. Water contents were obtained for the soil recovered from between the vane blades and near to the cylindrical surface of shearing. Undrained shear strengths were calculated from measured values of peak torque (see 5.3.4) via the vane spring constant according to the following :

$$T = \frac{cu \pi d^2 h}{2} \left(1 + \frac{d}{3h} \right)$$

where T = peak torque

d,h = measured width, height of vane

cu = undrained shear strength

7.5 Drained direct shear box test results.

The results of the drained shear box tests on reconstituted and undisturbed samples of till HH(a) and undisturbed samples of till F(b) indexed in Table 6.3 are shown in Figs 7.12 to 7.15. In these Figures are plotted graphs of shearing stress (τ) : longitudinal strain (ε_L) : vertical strain (ε_v) .

Shearing stress has been determined from the measured applied force (via the proving ring) and the current area calculated from the measured horizontal displacements.

Longitudinal (and vertical) strain is here defined as the ratio of the current horizontal (vertical) displacement to the original sample length (height). Compressive vertical strains are considered positive.

Also recorded on these Figures for each test are the initial (V_i) and final (V_f) specific volumes, these being those values after initial consolidation and at the end of the shearing stage respectively. These values were obtained from measured water contents of entire soil samples at the end of testing together with the particle specific gravities determined beforehand. (Table 7.1)

7.6 Consolidated undrained triaxial compression test results.

(i) Isotropic consolidation.

The results of the isotropic consolidation tests on reconstituted and undisturbed tills HH(a), HH(b), (Tests TR(1), TR(2), TU(1), TU(2)) are shown in Tables 7.33 to 7.36. In these Tables the effective radial stress (σ'_r) at any stage is the difference between the chamber pressure applied and the (constant) back pressure in the pore fluid of the sample. Corresponding values for equilibrium specific volume (V) have been calculated according to :

$$V = 1 + \frac{A(L - m_s / G_s \gamma_w A)}{m_s / G_s \gamma_w}$$

where A = sample cross sectional area

L = sample height

m_s = mass of solids in sample

G_s = particle specific gravity

Sample height is obtained from the measured volume changes during consolidation on the basis of a preserved aspect ratio (length to diameter) equal to 2.

These data have been used to show the relationship between equilibrium specific volume and isotropic consolidation pressure in Figs 7.16, 7.17.

The values for c_v shown in these Tables are those obtained from calculated t_{100} times obtained from $\log_{10} t$: sample volume change graphs according to the expression :

$$t_{100} = \pi h^2 / 100\, c_v$$ (Bishop and Henkel, 1976 pg 126.)

(here, $h = \bar{L} / 2$)

Values for the stiffness modulii and permeability also shown in these Tables have been obtained according to the procedures outlined in 7.3.

(ii) Undrained compression.

Graphs of total axial stress (σa), radial stress (σr) and porewater pressure (u) against percent axial strain for the series of undrained compression tests on samples of reconstituted and undisturbed till HH(a) indexed in Table 6.4 are shown in Figs 7.18 to 7.41.

Computations of axial stress and strain and porewater pressure have been performed using a short program written for the PET in conjunction with the transducer constants reported in Table 6.5.

Also shown in these Figures are the graphs of the principle effective stress ratio $\sigma a' / \sigma r'$ versus axial strain (percent).

Figs 7.42 to 7.65 contain graphs showing the relationship between deviator stress (q'), average effective pressure (p') and specific volume (V) for these tests. The positions on the effective stress paths ($q' : p'$) corresponding to the point ($\sigma a' / \sigma r'$) max. in each test are also shown.

The graphs of $p' : V$ contained in these Figures also include the appropriate isotropic consolidation data for either the reconstituted or the undisturbed till, reported in 7.6(i). The approximate position of the normal compression line for the undisturbed till in Figs 7.52 to 7.65 has been inferred from the critical state constants Γ, λ (Chapter 3) obtained for this soil and will be discussed further in Chapter 8.

Soil Type			w	LL %	PL %	LI	G_s
1	M(a)		0·28	49	21	0·25	
2	M(b)		0·28	53	20	0·24	
3	M(c)		0·27	55	22	0·15	
4	M(d)	t	0·19	51	19	0	
5	M(e)	t	0·19	48	19	0	
6	M(f)	t	0·19	45	19	0	
7	M(g)		0·17	38	17	0	
8	H(a)	t	0·15	40	15	0	
9	H(b)	t	0·19	52	19	0	
10	H(c)	t	0·15	42	15	0	
11	HH(a)	t	0·18	40 (54)	18 (23)	0	2·71 (2·68)
12	HH(b)	t	0·16	43 (54)	18 (21)	-0·008	2·73 (2·62)
13	F(a)	t	0·15	47	19	-0·143	
14	F(b)	t	0·20	58	22	-0·056	2·74 (2·73)
15	F(c)	t	0·18	46	19	-0·037	
16	W(a)		0·28	31	21	0·7	
17	W(b)	t	0·17	49	19	-0·067	2·74 (2·74)
18	W(c)	t	0·20	47	18	0·069	
19	W(d)	t	0·16	45	16	0	2·73 (2·71)

Numbers in parentheses denote test results for samples without acid solubles.
Soil identifiers M(a), M(b), etc. are those used in Table 5.3 ; for convenience they are replaced by 1, 2, etc. in Figs 7.1,7.2
(t = till)

Table 7.1 Natural water content, plasticity and particle specific gravity results.

Till type	with acid solubles	without acid solubles
HH(a)	0·571	0·464 (0·654)
HH(b)	0·671	0·522 (0·689)
F(b)	0·726	0·729
W(b)	0·653	0·573
W(d)	0·723	0·550
Activity = PI / clay fraction.		

Table 7.2 Activity of the tills.

Particle size (mm) / Till type	HH(a)	HH(b)	W(b)	W(d)	F(b)
0·063 (coarse silt)	-0·38	-1·05	-1·75	-2·18	-1·9
0·020 (medium silt)	-2·38	-2·17	-1·63	-1·11	+0·74
0·006 (fine silt)	-6·29	-7·39	-3·08	-9·28	+1·27
0·002 (clay)	+8·86	+10·60	+6·46	+12·57	-0·17
(+ , - , denotes percentage increase , decrease .)					

Table 7.3 The effect of the removal of acid solubles on various size fractions during sedimentation.

TILL HH(a)				
Particle size (mm) (phi)	Chalk retained (%)	Σ Chalk (%)	Acid soluble (%)	Σ Acid soluble (%)
16·0 (-4)	1·3	1·3	1·3	1·3
11·2	3·6	4·9	3·6	4·9
8·0 (-3)	4·1	9·0	4·1	9·0
5·6	2·5	11·5	2·5	11·5
4·0 (-2)	2·4	13·9	2·4	13·9
2·8	1·4	15·3	1·4	15·3
2·0 (-1)	1·3	16·6	1·4	16·7
1·4	0·99	17·59	1·1	17·8
1·0 (0)	0·41	18·0	0·7	18·5
0·71	0·53	18·53	0·6	19·1
0·50 (+1)	0·45	18·98	0·5	19·6
0·30			0·32	19·92
0·18			0·52	20·44
0·15			0·18	20·62
0·063(+4)			1·66	22·28

TILL HH(b)				
Particle size (mm) (phi)	Chalk retained (%)	Σ Chalk (%)	Acid soluble (%)	Σ Acid soluble (%)
16·0 (-4)	10·4	10·4	11·2	11·2
11·2	0·9	11·3	0·9	12·1
8·0 (-3)	4·2	15·5	5·3	17·4
5·6	2·8	18·3	4·5	21·9
4·0 (-2)	1·3	19·6	2·4	24·3
2·8	0·9	20·5	1·3	25·6
2·0 (-1)	0·5	21·0	0·7	26·3
1·4	0·9	21·9	2·0	28·3
1·0 (0)	0·5	22·4	0·9	29·2
0·71	0·4	22·8	0·7	29·9
0·50 (+1)	0·3	23·1	0·6	30·5
0·30			0·77	31·27
0·18			1·19	32·46
0·15			0·55	33·01
0·063(+4)			1·53	34·54

Table 7.4 Chalk and acid soluble content, tills HH(a), HH(b), Holwell Hyde.

	Mineral type	HH(a)	HH(b)	F(b)	W(b)	W(d)
Clay mineral / Clay content %	Illite	19	26	17	20	17
	Ca-Montmorillonite	9	15	12	15	14
	Kaolinite	8	9	8	7	7
	Amorphous iron and alumina hydrates	62	50	63	58	62
% Content	Quartz	18•2	26•3	27•2	23•1	18•0
	Calcite	10	14•9	0	4•3	12•6
	Acid soluble at 2μm	8•86	10•6	0	6•46	12•57

Table 7.5 Mineralogical composition of the tills.

	Element type	HH(a)	HH(b)	F(b)	W(b)	W(d)
Relative proportions (%)	Mg	1•7	1•5	2•3	1•7	1•6
	Al	10•8	11•1	19•4	14•6	10•2
	Si	30•4	31•7	48•7	42•9	29•3
	S	2•0	0	0	0	0
	K	5•7	5•2	7•6	7•0	4•7
	Ca	42•0	42•5	6•5	21•3	46•2
	Ti	1•4	1•5	2•3	2•0	1•4
	Fe	6•1	6•6	13•3	10•5	6•6

Table 7.6 Element composition of the tills.

σ'_v (kPa)	V	t_{50} (min)	m_v (kPa^{-1})	c_v ($mm^2\ min^{-1}$)	k (ms^{-1})	Ro
200	1•472	9	$4•84 \times 10^{-5}$	1•63	$1•29 \times 10^{-11}$	4
400	1•460	10	$4•25 \times 10^{-5}$	1•45	$1•01 \times 10^{-11}$	2
800	1•439	8	$3•53 \times 10^{-5}$	1•78	$1•03 \times 10^{-11}$	1
1600	1•394	11•25	$3•97 \times 10^{-5}$	1•22	$7•92 \times 10^{-12}$	1
3200	1•343	15	$2•33 \times 10^{-5}$	0•86	$3•26 \times 10^{-12}$	1
1600	1•355	4	$5•59 \times 10^{-6}$	3•12	$2•85 \times 10^{-12}$	2
800	1•370	14•5	$1•46 \times 10^{-5}$	0•87	$2•08 \times 10^{-12}$	4
400	1•389	29	$3•47 \times 10^{-5}$	0•45	$2•53 \times 10^{-12}$	8
200	1•410	60	$7•34 \times 10^{-5}$	0•22	$2•65 \times 10^{-12}$	16
100	1•432	120	$1•58 \times 10^{-4}$	0•11	$2•93 \times 10^{-12}$	32

Table 7.7 Oedometer test OR(1), reconstituted till HH(a).

σ'_v (kPa)	V	t_{50} (min)	m_v (kPa^{-1})	c_v ($mm^2\ min^{-1}$)	k (ms^{-1})	Ro
200	1•472	6	$3•22 \times 10^{-5}$	2•45	$1•29 \times 10^{-11}$	4
400	1•460	8	$4•05 \times 10^{-5}$	1•81	$1•20 \times 10^{-11}$	2
800	1•444	7	$2•41 \times 10^{-5}$	2•03	$8•01 \times 10^{-12}$	1
1600	1•403	12•5	$3•50 \times 10^{-5}$	1•09	$6•26 \times 10^{-12}$	1
3200	1•357	9	$2•07 \times 10^{-5}$	1•43	$4•84 \times 10^{-12}$	1
1600	1•362	4	$2•23 \times 10^{-6}$	3•12	$1•14 \times 10^{-12}$	2
800	1•374	12	$1•08 \times 10^{-5}$	1•05	$1•85 \times 10^{-12}$	4
400	1•387	20	$2•44 \times 10^{-5}$	0•64	$2•57 \times 10^{-12}$	8
200	1•405	37	$6•55 \times 10^{-5}$	0•36	$3•81 \times 10^{-12}$	16
100	1•425	85	$1•39 \times 10^{-4}$	0•16	$3•62 \times 10^{-12}$	32

Table 7.8 Oedometer test OR(2), reconstituted till HH(b).

σ'_v (kPa)	V	t_{50} (min)	m_v (kPa^{-1})	c_v ($mm^2\ min^{-1}$)	k (ms^{-1})	Ro
200	1·692	20	$4·60 \times 10^{-5}$	0·63	$4·73 \times 10^{-12}$	4
400	1·671	26	$6·21 \times 10^{-5}$	0·48	$4·83 \times 10^{-12}$	2
800	1·638	22	$5·05 \times 10^{-5}$	0·54	$4·49 \times 10^{-12}$	1
1600	1·564	35	$5·59 \times 10^{-5}$	0·32	$2·93 \times 10^{-12}$	1
3200	1·489	28	$2·99 \times 10^{-5}$	0·36	$1·78 \times 10^{-12}$	1
1600	1·505	14	$6·37 \times 10^{-6}$	0·70	$7·29 \times 10^{-13}$	2
800	1·527	30	$1·84 \times 10^{-5}$	0·34	$1·01 \times 10^{-12}$	4
400	1·559	59	$5·15 \times 10^{-5}$	0·18	$1·49 \times 10^{-12}$	8
200	1·589	115	$9·40 \times 10^{-5}$	0·09	$1·45 \times 10^{-12}$	16
100	1·619	160	$1·84 \times 10^{-4}$	0·07	$2·13 \times 10^{-12}$	32

Table 7·9 Oedometer test OR(3), reconstituted till F(b).

σ'_v (kPa)	V	t_{50} (min)	m_v (kPa^{-1})	c_v ($mm^2\ min^{-1}$)	k (ms^{-1})	Ro
200	1·623	20	$5·84 \times 10^{-5}$	0·76	$7·28 \times 10^{-12}$	4
400	1·604	25	$5·91 \times 10^{-5}$	0·60	$5·79 \times 10^{-12}$	2
800	1·576	27	$4·29 \times 10^{-5}$	0·54	$3·78 \times 10^{-12}$	1
1600	1·523	42	$4·27 \times 10^{-5}$	0·33	$2·30 \times 10^{-12}$	1
3200	1·463	22	$2·43 \times 10^{-5}$	0·58	$2·32 \times 10^{-12}$	1
1600	1·475	10	$4·86 \times 10^{-6}$	1·24	$9·87 \times 10^{-13}$	2
800	1·497	30	$1·81 \times 10^{-5}$	0·42	$1·23 \times 10^{-12}$	4
400	1·522	60	$4·18 \times 10^{-5}$	0·22	$1·49 \times 10^{-12}$	8
200	1·548	85	$8·46 \times 10^{-5}$	0·16	$2·21 \times 10^{-12}$	16
100	1·576	160	$1·78 \times 10^{-4}$	0·09	$2·56 \times 10^{-12}$	32

Table 7.10 Oedometer test OR(4), reconstituted till W(b).

σ'_v (kPa)	V	t_{50} (min)	m_v (kPa^{-1})	c_v ($mm^2\ min^{-1}$)	k (ms^{-1})	Ro
200	1•545	7•5	$3•27 \times 10^{-5}$	1•93	$1•03 \times 10^{-11}$	4
400	1•532	9•5	$4•16 \times 10^{-5}$	1•51	$1•02 \times 10^{-11}$	2
800	1•513	7•5	$3•07 \times 10^{-5}$	1•87	$9•38 \times 10^{-12}$	1
1600	1•468	9	$3•71 \times 10^{-5}$	1•42	$9•05 \times 10^{-12}$	1
3200	1•415	10	$2•25 \times 10^{-5}$	1•26	$4•62 \times 10^{-12}$	1
1600	1•423	8	$3•38 \times 10^{-6}$	1•52	$8•41 \times 10^{-13}$	2
800	1•436	7•5	$1•10 \times 10^{-5}$	1•65	$2•96 \times 10^{-12}$	4
400	1•453	20	$2•98 \times 10^{-5}$	0•63	$3•07 \times 10^{-12}$	8
200	1•471	41	$5•92 \times 10^{-5}$	0•32	$3•05 \times 10^{-12}$	16
100	1•492	80	$1•41 \times 10^{-4}$	0•17	$3•83 \times 10^{-12}$	32

Table 7.11 Oedometer test OR(5), reconstituted till W(d).

σ'_v (kPa)	V	t_{50} (min)	m_v (kPa^{-1})	c_v ($mm^2\ min^{-1}$)	k (ms^{-1})	Ro
400	1•383	13	$6•43 \times 10^{-5}$	1•27	$1•34 \times 10^{-11}$	1•9
800	1•361	12•5	$4•06 \times 10^{-5}$	1•28	$8•52 \times 10^{-12}$	1
1600	1•334	10	$2•52 \times 10^{-5}$	1•55	$6•38 \times 10^{-12}$	1
3200	1•302	8•75	$1•47 \times 10^{-5}$	1•66	$3•99 \times 10^{-12}$	1
1600	1•307	3•1	$2•17 \times 10^{-6}$	4•68	$1•66 \times 10^{-12}$	2
800	1•318	14	$1•01 \times 10^{-5}$	1•05	$1•73 \times 10^{-12}$	4
400	1•331	25	$2•48 \times 10^{-5}$	0•60	$2•42 \times 10^{-12}$	8
200	1•346	55	$5•80 \times 10^{-5}$	0•28	$2•63 \times 10^{-12}$	16

(1) Based on preconsolidation pressure = 760 kPa.

Table 7.12 Oedometer test OU(1)V, undisturbed till HH(a), vertical drainage.

σ'_v (kPa)	V	t_{50} (min)	m_v (kPa^{-1})	c_v ($mm^2\ min^{-1}$)	k (ms^{-1})	Ro
400	1•462	4	$6•37 \times 10^{-5}$	4•08	$4•24 \times 10^{-11}$	1•9
800	1•443	8	$4•40 \times 10^{-5}$	1•98	$1•42 \times 10^{-11}$	1
1600	1•418	9•5	$2•79 \times 10^{-5}$	1•60	$7•30 \times 10^{-12}$	1
3200	1•386	7	$1•58 \times 10^{-5}$	2•07	$5•32 \times 10^{-12}$	1
1600	1•351	3	$1•86 \times 10^{-6}$	4•72	$1•44 \times 10^{-12}$	2
800	1•355	8•5	$9•61 \times 10^{-6}$	1•68	$2•65 \times 10^{-12}$	4
400	1•366	14	$2•32 \times 10^{-5}$	1•04	$3•94 \times 10^{-12}$	8
200	1•378	38	$5•07 \times 10^{-5}$	0•39	$3•24 \times 10^{-12}$	16

(1) Based on preconsolidation pressure = 760 kPa.

Table 7.13 Oedometer test OU(2)V, undisturbed till HH(b), vertical drainage.

σ'_v (kPa)	V	t_{50} (min)	m_v (kPa^{-1})	c_v ($mm^2\ min^{-1}$)	k (ms^{-1})	Ro
200	1·756	3·31	$1·33 \times 10^{-4}$	5·00	$1·09 \times 10^{-10}$	3·9
400	1·728	11	$7·97 \times 10^{-5}$	1·44	$1·87 \times 10^{-11}$	1·95
800	1·669	11·5	$8·54 \times 10^{-5}$	1·31	$1·83 \times 10^{-11}$	1
1600	1·593	10·5	$5·69 \times 10^{-5}$	1·32	$1·23 \times 10^{-11}$	1
3200	1·509	8	$3·30 \times 10^{-5}$	1·57	$8·46 \times 10^{-12}$	1
1600	1·521	5	$4·93 \times 10^{-6}$	2·39	$1·93 \times 10^{-12}$	2
800	1·539	11·5	$1·46 \times 10^{-5}$	1·06	$2·53 \times 10^{-12}$	4
400	1·564	23	$4·00 \times 10^{-5}$	0·55	$3·56 \times 10^{-12}$	8
200	1·587	45	$7·25 \times 10^{-5}$	0·29	$3·40 \times 10^{-12}$	16
100	1·614	65	$1·67 \times 10^{-4}$	0·21	$5·62 \times 10^{-12}$	32

(1) Based on preconsolidation pressure = 780 kPa.

Table 7.14 Oedometer test OU(3)V, undisturbed till F(b), vertical drainage.

σ'_v (kPa)	V	t_{50} (min)	m_v (kPa^{-1})	c_v ($mm^2\ min^{-1}$)	k (ms^{-1})	Ro
400	1·541	17	$6·58 \times 10^{-5}$	1·03	$1·11 \times 10^{-11}$	2·33
800	1·512	22	$4·72 \times 10^{-5}$	0·77	$5·93 \times 10^{-12}$	1·16
1600	1·476	26	$2·96 \times 10^{-5}$	0·62	$3·02 \times 10^{-12}$	1
3200	1·435	20	$1·75 \times 10^{-5}$	0·77	$2·20 \times 10^{-12}$	1
1600	1·445	11·5	$4·42 \times 10^{-6}$	1·31	$9·46 \times 10^{-13}$	2
800	1·463	29	$1·50 \times 10^{-5}$	0·53	$1·30 \times 10^{-12}$	4
400	1·482	55	$3·21 \times 10^{-5}$	0·29	$1·50 \times 10^{-12}$	8
200	1·502	100	$6·78 \times 10^{-5}$	0·16	$1·79 \times 10^{-12}$	16

(1) Based on preconsolidation pressure = 930 kPa.

Table 7.15 Oedometer test OU(4)V, undisturbed till W(b), vertical drainage.

σ'_v (kPa)	V	t_{50} (min)	m_v (kPa^{-1})	c_v ($mm^2\ min^{-1}$)	k (ms^{-1})	Ro
200	1•503	2•8	$1•11 \times 10^{-4}$	6•18	$1•12 \times 10^{-10}$	3•45
400	1•484	10	$6•45 \times 10^{-5}$	1•67	$1•76 \times 10^{-11}$	1•73
800	1•457	8•5	$4•55 \times 10^{-5}$	1•90	$1•42 \times 10^{-11}$	1
1600	1•430	12	$2•35 \times 10^{-5}$	1•30	$4•99 \times 10^{-12}$	1
3200	1•394	15	$1•55 \times 10^{-5}$	0•99	$2•52 \times 10^{-12}$	1
1600	1•399	4•5	$2•48 \times 10^{-6}$	3•25	$1•32 \times 10^{-12}$	2
800	1•410	15	$9•14 \times 10^{-6}$	0•99	$1•47 \times 10^{-12}$	4
400	1•425	28	$2•59 \times 10^{-5}$	0•54	$2•27 \times 10^{-12}$	8
200	1•442	50	$5•92 \times 10^{-5}$	0•31	$2•98 \times 10^{-12}$	16
100	1•461	120	$1•29 \times 10^{-4}$	0•13	$2•78 \times 10^{-12}$	32

(1) Based on preconsolidation pressure = 690 kPa.

Table 7.16 Oedometer test OU(5)V, undisturbed till W(d), vertical drainage.

σ'_v (kPa)	V	t_{50} (min)	m_v (kPa^{-1})	c_v ($mm^2\ min^{-1}$)	k (ms^{-1})
100	1•526	8	$7•03 \times 10^{-5}$	2•23	$2•56 \times 10^{-11}$
200	1•506	23	$1•30 \times 10^{-4}$	0•76	$1•61 \times 10^{-11}$
400	1•485	12•5	$6•87 \times 10^{-5}$	1•36	$1•53 \times 10^{-11}$
800	1•459	12•5	$4•48 \times 10^{-5}$	1•32	$9•66 \times 10^{-12}$
1600	1•427	11•5	$2•75 \times 10^{-5}$	1•38	$6•19 \times 10^{-12}$
3200	1•390	12	$1•59 \times 10^{-5}$	1•26	$3•28 \times 10^{-12}$
1600	1•397	4	$3•09 \times 10^{-6}$	3•70	$1•87 \times 10^{-12}$
800	1•411	15	$1•24 \times 10^{-5}$	1•00	$2•04 \times 10^{-12}$
400	1•428	29•5	$2•94 \times 10^{-5}$	0•52	$2•50 \times 10^{-12}$
200	1•445	58	$5•95 \times 10^{-5}$	0•27	$2•63 \times 10^{-12}$
100	1•465	90	$1•35 \times 10^{-4}$	0•18	$3•96 \times 10^{-12}$

Table 7.17 Oedometer test OU(1) H(p), undisturbed till HH(a), horizontal drainage, parallel to fabric.

σ'_v (kPa)	V	t_{50} (min)	m_v (kPa^{-1})	c_v ($mm^2\ min^{-1}$)	k (ms^{-1})
100	1•532	5•5	$1•18 \times 10^{-4}$	3•16	$6•10 \times 10^{-11}$
200	1•516	12	$1•05 \times 10^{-4}$	1•42	$2•43 \times 10^{-11}$
400	1•497	11	$6•30 \times 10^{-5}$	1•51	$1•56 \times 10^{-11}$
800	1•475	10	$3•64 \times 10^{-5}$	1•62	$9•62 \times 10^{-12}$
1600	1•444	10	$2•64 \times 10^{-5}$	1•56	$6•72 \times 10^{-12}$
3200	1•408	10	$1•56 \times 10^{-5}$	1•49	$3•80 \times 10^{-12}$
1600	1•414	6	$2•70 \times 10^{-6}$	2•43	$1•07 \times 10^{-12}$
800	1•426	13	$1•03 \times 10^{-5}$	1•14	$1•92 \times 10^{-12}$
400	1•442	23	$2•88 \times 10^{-5}$	0•65	$3•08 \times 10^{-12}$
200	1•460	40	$6•27 \times 10^{-5}$	0•39	$0•39 \times 10^{-12}$
100	1•479	70	$1•26 \times 10^{-4}$	0•23	$4•67 \times 10^{-12}$

Table 7.18 Oedometer test OU(1) H(n), undisturbed till HH(a), horizontal drainage, normal to fabric.

σ'_v (kPa)	V	t_{50} (min)	m_v (kPa^{-1})	c_v ($mm^2\ min^{-1}$)	k (ms^{-1})
200	1•422	1•25	$9•42 \times 10^{-5}$	13•96	$2•15 \times 10^{-10}$
400	1•408	12	$5•10 \times 10^{-5}$	1•41	$1•18 \times 10^{-11}$
800	1•385	9•5	$4•00 \times 10^{-5}$	1•74	$1•14 \times 10^{-11}$
1600	1•359	8	$2•36 \times 10^{-5}$	1•99	$7•69 \times 10^{-12}$
3200	1•329	7	$1•39 \times 10^{-5}$	2•18	$4•96 \times 10^{-12}$
1600	1•334	4	$2•16 \times 10^{-6}$	3•75	$1•32 \times 10^{-12}$
800	1•343	11	$8•56 \times 10^{-6}$	1•38	$1•93 \times 10^{-12}$
400	1•356	19•5	$2•36 \times 10^{-5}$	0•79	$3•05 \times 10^{-12}$
200	1•370	43	$5•11 \times 10^{-5}$	0•37	$3•05 \times 10^{-12}$

Table 7.19 Oedometer test OU(1) H(r), undisturbed till HH(a), horizontal drainage, random orientation.

σ'_v (kPa)	V	t_{50} (min)	m_v (kPa^{-1})	c_v ($mm^2\ min^{-1}$)	k (ms^{-1})
100	1·527	0·5	$9·28 \times 10^{-5}$	35·05	$5·32 \times 10^{-11}$
200	1·515	2·4	$8·32 \times 10^{-5}$	7·17	$9·75 \times 10^{-11}$
400	1·492	4	$7·36 \times 10^{-5}$	4·21	$5·06 \times 10^{-11}$
800	1·460	8	$5·46 \times 10^{-5}$	2·03	$1·81 \times 10^{-11}$
1600	1·424	6·75	$3·04 \times 10^{-5}$	2·29	$1·14 \times 10^{-11}$
3200	1·382	6·25	$1·87 \times 10^{-5}$	2·34	$7·16 \times 10^{-12}$
1600	1·387	3·1	$2·30 \times 10^{-6}$	4·60	$1·73 \times 10^{-12}$
800	1·396	6·75	$8·24 \times 10^{-6}$	2·13	$2·88 \times 10^{-12}$
400	1·408	15	$2·13 \times 10^{-5}$	0·98	$3·40 \times 10^{-12}$
200	1·423	33	$5·38 \times 10^{-5}$	0·45	$3·97 \times 10^{-12}$
100	1·439	60	$1·08 \times 10^{-4}$	0·25	$4·47 \times 10^{-12}$

Table 7·20 Oedometer test OU(2) H(p), undisturbed till HH(b), horizontal drainage, parallel to fabric.

σ'_v (kPa)	V	t_{50} (min)	m_v (kPa^{-1})	c_v ($mm^2\ min^{-1}$)	k (ms^{-1})
100	1·513	1·5	$3·10 \times 10^{-5}$	11·15	$5·64 \times 10^{-11}$
200	1·499	2·9	$9·58 \times 10^{-5}$	5·69	$8·92 \times 10^{-11}$
400	1·479	4	$6·61 \times 10^{-5}$	4·03	$4·36 \times 10^{-11}$
800	1·455	6·5	$4·07 \times 10^{-5}$	2·41	$1·60 \times 10^{-11}$
1600	1·423	12	$2·78 \times 10^{-5}$	1·26	$5·70 \times 10^{-12}$
3200	1·385	8·5	$1·65 \times 10^{-5}$	1·69	$4·56 \times 10^{-12}$
1600	1·390	4	$2·38 \times 10^{-6}$	3·50	$1·36 \times 10^{-12}$
800	1·399	6·75	$8·04 \times 10^{-6}$	2·10	$2·76 \times 10^{-12}$
400	1·412	14	$2·25 \times 10^{-5}$	1·03	$3·78 \times 10^{-12}$
200	1·426	29	$4·87 \times 10^{-5}$	0·51	$4·03 \times 10^{-12}$
100	1·440	60	$9·52 \times 10^{-5}$	0·25	$3·87 \times 10^{-12}$

Table 7.21 Oedometer test OU(2) H(n), undisturbed till HH(b), horizontal drainage, normal to fabric.

σ'_v (kPa)	V	t_{50} (min)	m_v (kPa^{-1})	c_v ($mm^2\ min^{-1}$)	k (ms^{-1})
400	1•459	15	$5•89 \times 10^{-5}$	1•11	$1•07 \times 10^{-11}$
800	1•434	7•5	$4•32 \times 10^{-5}$	2•15	$1•52 \times 10^{-11}$
1600	1•401	5•9	$2•90 \times 10^{-5}$	2•63	$1•25 \times 10^{-11}$
3200	1•365	7	$1•62 \times 10^{-5}$	2•11	$5•58 \times 10^{-12}$
1600	1•369	2•5	$1•96 \times 10^{-6}$	5•76	$1•85 \times 10^{-12}$
800	1•378	6•2	$8•43 \times 10^{-6}$	2•35	$3•23 \times 10^{-12}$
400	1•391	13	$2•28 \times 10^{-5}$	1•14	$4•25 \times 10^{-12}$
200	1•406	32	$5•37 \times 10^{-5}$	0•47	$4•14 \times 10^{-12}$

Table 7.22 Oedometer test OU(2) H(r), undisturbed till HH(b), horizontal drainage, random orientation.

σ'_v (kPa)	V	t_{50} (min)	m_v (kPa^{-1})	c_v ($mm^2\ min^{-1}$)	k (ms^{-1})
100	1•640	7•5	$3•04 \times 10^{-4}$	2•27	$1•13 \times 10^{-10}$
200	1•615	8	$1•50 \times 10^{-4}$	2•04	$4•99 \times 10^{-11}$
400	1•588	7	$8•36 \times 10^{-5}$	2•25	$3•08 \times 10^{-11}$
800	1•554	7•5	$4•71 \times 10^{-5}$	2•02	$1•56 \times 10^{-11}$
1600	1•512	10	$3•32 \times 10^{-5}$	1•45	$7•85 \times 10^{-12}$
3200	1•466	8•25	$1•92 \times 10^{-5}$	1•65	$5•19 \times 10^{-12}$
1600	1•475	9	$3•77 \times 10^{-6}$	1•48	$9•11 \times 10^{-13}$
800	1•490	12	$1•23 \times 10^{-5}$	1•13	$2•26 \times 10^{-12}$
400	1•508	27	$3•05 \times 10^{-5}$	0•51	$2•55 \times 10^{-12}$
200	1•526	33	$5•77 \times 10^{-5}$	0•47	$4•43 \times 10^{-12}$
100	1•541	70	$9•80 \times 10^{-5}$	0•21	$3•31 \times 10^{-12}$

Table 7.23 Oedometer test OU(3) H(p), undisturbed till F(b), horizontal drainage, parallel to fabric.

σ'_v (kPa)	V	t_{50} (min)	m_v (kPa^{-1})	c_v ($mm^2\ min^{-1}$)	k (ms^{-1})
100	1•625	3	$1•23 \times 10^{-5}$	5•89	$1•18 \times 10^{-11}$
200	1•600	4•1	$1•53 \times 10^{-4}$	4•24	$1•06 \times 10^{-10}$
400	1•573	6•5	$8•59 \times 10^{-5}$	2•59	$3•63 \times 10^{-11}$
800	1•543	7•5	$4•78 \times 10^{-5}$	2•16	$1•69 \times 10^{-11}$
1600	1•503	13	$3•20 \times 10^{-5}$	1•19	$6•24 \times 10^{-12}$
3200	1•457	9•5	$1•90 \times 10^{-5}$	1•54	$4•79 \times 10^{-12}$
1600	1•466	2•9	$3•58 \times 10^{-6}$	4•92	$2•88 \times 10^{-12}$
800	1•480	7•5	$1•17 \times 10^{-5}$	1•93	$3•70 \times 10^{-12}$
400	1•498	19	$3•04 \times 10^{-5}$	0•78	$3•87 \times 10^{-12}$
200	1•519	40	$6•91 \times 10^{-5}$	0•38	$4•30 \times 10^{-12}$
100	1•540	86	$1•40 \times 10^{-4}$	0•18	$4•15 \times 10^{-12}$

Table 7.24 Oedometer test OU(3) H(n), undisturbed till F(b), horizontal drainage, normal to fabric.

σ'_v (kPa)	V	t_{50} (min)	m_v (kPa^{-1})	c_v ($mm^2\ min^{-1}$)	k (ms^{-1})
100	1·658	6	$1·72 \times 10^{-4}$	2·87	$4·11 \times 10^{-10}$
200	1·635	14	$1·37 \times 10^{-4}$	1·19	$2·67 \times 10^{-11}$
400	1·607	8	$8·71 \times 10^{-5}$	2·02	$2·88 \times 10^{-11}$
800	1·570	12	$5·79 \times 10^{-5}$	1·29	$1·22 \times 10^{-11}$
1600	1·520	10	$3·94 \times 10^{-5}$	1·47	$9·46 \times 10^{-12}$
3200	1·470	11	$2·08 \times 10^{-5}$	1·25	$4·26 \times 10^{-12}$
1600	1·479	2·5	$4·01 \times 10^{-6}$	5·35	$3·51 \times 10^{-12}$
800	1·495	10	$1·35 \times 10^{-5}$	1·36	$2·99 \times 10^{-12}$
400	1·513	22	$3·01 \times 10^{-5}$	0·63	$3·11 \times 10^{-12}$
200	1·535	40	$7·00 \times 10^{-5}$	0·36	$4·09 \times 10^{-12}$
100	1·554	60	$1·20 \times 10^{-4}$	0·24	$4·81 \times 10^{-12}$

Table 7.25 Oedometer test OU(3) H(r), undisturbed till F(b), horizontal drainage, random orientation.

σ'_v (kPa)	V	t_{50} (min)	m_v (kPa^{-1})	c_v ($mm^2\ min^{-1}$)	k (ms^{-1})
100	1·565	6·5	$1·14 \times 10^{-4}$	2·73	$5·11 \times 10^{-11}$
200	1·548	18	$1·05 \times 10^{-4}$	0·97	$1·66 \times 10^{-11}$
400	1·527	20	$6·85 \times 10^{-5}$	0·85	$9·49 \times 10^{-12}$
800	1·502	21	$4·13 \times 10^{-5}$	0·78	$5·28 \times 10^{-12}$
1600	1·471	20	$2·54 \times 10^{-5}$	0·79	$3·29 \times 10^{-12}$
3200	1·436	20	$1·49 \times 10^{-5}$	0·76	$1·85 \times 10^{-12}$
1600	1·444	7	$3·59 \times 10^{-6}$	2·13	$1·25 \times 10^{-12}$
800	1·458	20	$1·14 \times 10^{-5}$	0·76	$1·41 \times 10^{-12}$
400	1·476	35	$3·08 \times 10^{-5}$	0·44	$2·22 \times 10^{-12}$
200	1·495	60	$6·45 \times 10^{-5}$	0·26	$2·78 \times 10^{-12}$
100	1·512	125	$1·14 \times 10^{-4}$	0·13	$2·41 \times 10^{-12}$

Table 7.26 Oedometer test OU(4) H(p), undisturbed till W(b), horizontal drainage, parallel to fabric.

σ'_v (kPa)	V	t_{50} (min)	m_v (kPa^{-1})	c_v ($mm^2\ min^{-1}$)	k (ms^{-1})
100	1·567	4	$5·33 \times 10^{-5}$	4·47	$3·90 \times 10^{-11}$
200	1·533	15	$8·68 \times 10^{-5}$	1·17	$1·67 \times 10^{-11}$
400	1·532	15	$6·73 \times 10^{-5}$	1·15	$1·26 \times 10^{-11}$
800	1·506	24	$4·39 \times 10^{-5}$	0·70	$4·99 \times 10^{-12}$
1600	1·474	20	$2·64 \times 10^{-5}$	0·80	$3·47 \times 10^{-12}$
3200	1·436	20	$1·60 \times 10^{-5}$	0·77	$2·00 \times 10^{-12}$
1600	1·444	9	$3·63 \times 10^{-6}$	1·67	$9·92 \times 10^{-13}$
800	1·460	22	$1·37 \times 10^{-5}$	0·69	$1·55 \times 10^{-12}$
400	1·478	55	$2·96 \times 10^{-5}$	0·28	$1·38 \times 10^{-12}$
200	1·497	85	$6·25 \times 10^{-5}$	0·19	$1·92 \times 10^{-12}$
100	1·515	110	$1·19 \times 10^{-4}$	0·15	$2·90 \times 10^{-12}$

Table 7.27 Oedometer test OU(4) H(n), undisturbed till W(b), horizontal drainage, normal to fabric.

σ'_v (kPa)	.V	t_{50} (min)	m_v (kPa^{-1})	c_v ($mm^2\ min^{-1}$)	k (ms^{-1})
300	1•534	2•25	$7•52 \times 10^{-5}$	7•69	$9•45 \times 10^{-11}$
400	1•526	18	$5•28 \times 10^{-5}$	0•93	$8•06 \times 10^{-11}$
800	1•494	19	$5•31 \times 10^{-5}$	0•86	$7•48 \times 10^{-11}$
1600	1•457	22	$3•06 \times 10^{-5}$	0•71	$3•55 \times 10^{-12}$
3200	1•414	26	$1•87 \times 10^{-5}$	0•57	$1•74 \times 10^{-12}$
1600	1•424	12•5	$4•43 \times 10^{-6}$	1•16	$8•38 \times 10^{-13}$
800	1•440	27•5	$1•40 \times 10^{-5}$	0•54	$1•22 \times 10^{-12}$
400	1•458	50	$3•17 \times 10^{-5}$	0•30	$1•56 \times 10^{-12}$
300	1•467	100	$5•52 \times 10^{-5}$	0•154	$1•39 \times 10^{-12}$
200	1•479	150	$8•72 \times 10^{-5}$	0•104	$1•48 \times 10^{-12}$

Table 7.28 Oedometer test OU(4) H(r), undisturbed till W(b), horizontal drainage, random orientation.

σ'_v (kPa)	V	t_{50} (min)	m_v (kPa^{-1})	c_v ($mm^2\ min^{-1}$)	k (ms^{-1})
100	1·532				
200	1·515	2·4	$1·08 \times 10^{-4}$	7·17	$1·27 \times 10^{-10}$
400	1·495	3	$6·80 \times 10^{-5}$	5·60	$6·22 \times 10^{-11}$
800	1·462	3·2	$5·39 \times 10^{-5}$	5·06	$4·46 \times 10^{-11}$
1600	1·429	5·5	$2·88 \times 10^{-5}$	2·82	$1·33 \times 10^{-11}$
3200	1·391	6	$1·64 \times 10^{-5}$	2·46	$6·60 \times 10^{-12}$
1600	1·395	1·5	$1·84 \times 10^{-6}$	9·59	$2·88 \times 10^{-12}$
800	1·403	8	$7·39 \times 10^{-6}$	1·81	$2·19 \times 10^{-12}$
400	1·415	11	$2·05 \times 10^{-5}$	1·34	$4·49 \times 10^{-12}$
200	1·430	27	$5·38 \times 10^{-5}$	0·56	$4·89 \times 10^{-12}$
100	1·446	50	$1·07 \times 10^{-4}$	0·31	$5·34 \times 10^{-12}$

Table 7.29 Oedometer test OU(5) H(p), undisturbed till W(d), horizontal drainage, parallel to fabric.

σ'_v (kPa)	V	t_{50} (min)	m_v (kPa^{-1})	c_v ($mm^2\ min^{-1}$)	k (ms^{-1})
100	1·518	0·6	$2·24 \times 10^{-4}$	28·98	$1·06 \times 10^{-9}$
200	1·505	3·5	$8·89 \times 10^{-5}$	4·81	$7·00 \times 10^{-11}$
400	1·485	5	$6·55 \times 10^{-5}$	3·29	$3·53 \times 10^{-11}$
800	1·459	8	$4·29 \times 10^{-5}$	2·00	$1·40 \times 10^{-11}$
1600	1·427	9	$2·75 \times 10^{-5}$	1·71	$7·67 \times 10^{-12}$
3200	1·388	12	$1·70 \times 10^{-5}$	1·22	$3·39 \times 10^{-12}$
1600	1·393	3·5	$2·06 \times 10^{-6}$	4·07	$1·38 \times 10^{-12}$
800	1·403	10	$9·18 \times 10^{-6}$	1·44	$2·16 \times 10^{-12}$
400	1·418	21	$2·59 \times 10^{-5}$	0·70	$2·96 \times 10^{-12}$
200	1·436	40	$6·30 \times 10^{-5}$	0·38	$3·87 \times 10^{-12}$
100	1·452	80	$1·07 \times 10^{-4}$	0·19	$3·35 \times 10^{-12}$

Table 7.30 Oedometer test OU(5) H(n), undisturbed till W(d), horizontal drainage, normal to fabric.

σ'_v (kPa)	V	t_{50} (min)	m_v (kPa^{-1})	c_v ($mm^2\ min^{-1}$)	k (ms^{-1})
400	1·465	8	$6·03 \times 10^{-5}$	2·08	$2·05 \times 10^{-11}$
800	1·440	8	$4·35 \times 10^{-5}$	2·02	$1·43 \times 10^{-11}$
1600	1·410	10	$2·58 \times 10^{-5}$	1·55	$6·54 \times 10^{-12}$
3200	1·375	8	$1·56 \times 10^{-5}$	1·85	$4·72 \times 10^{-12}$
1600	1·379	15	$1·72 \times 10^{-6}$	0·97	$2·72 \times 10^{-13}$
800	1·388	7·5	$8·91 \times 10^{-6}$	1·95	$2·84 \times 10^{-12}$
400	1·402	20	$2·39 \times 10^{-5}$	0·74	$2·91 \times 10^{-12}$
200	1·417	38	$5·40 \times 10^{-5}$	0·40	$3·53 \times 10^{-12}$
100	1·432	90	$1·05 \times 10^{-4}$	0·17	$2·95 \times 10^{-12}$

Table 7.31 Oedometer test OU(5) H(r), undisturbed till W(d), horizontal drainage, random orientation.

HH(a)		HH(b)		F(b)	
w	cu (kPa)	w	cu (kPa)	w	cu (kPa)
0•184	48•59	0•210	55•70	0•262	52•70
0•195	36•90	0•234	31•70	0•338	14•50
0•216	22•40	0•261	19•80	0•474	3•90
0•246	11•80	0•373	3•50	0•527	2•70
0•320	3•95	0•424	1•90	0•582	1•70
0•379	0•74	0•478	1•40	0•629	1•30
0•427	0•45	0•509	0•89	0•719	0•64
0•487	0•25	0•543	0•64	0•786	0•50
0•523	0•20	0•599	0•42	0•847	0•31

Table 7.32 Water content : undrained shear strength relationship for tills HH(a), HH(b), F(b). (Motorised shear vane).

σ'_r (kPa)	V	t_{100} (min)	m_v (kPa^{-1})	c_v ($mm^2\ min^{-1}$)	k (ms^{-1})	Ro
200	1•472	205	$7•15 \times 10^{-5}$	0•21	$2•50 \times 10^{-12}$	4
400	1•452	275	$6•86 \times 10^{-5}$	0•16	$1•78 \times 10^{-12}$	2
800	1•431	260	$3•70 \times 10^{-5}$	0•17	$1•00 \times 10^{-12}$	1
1600	1•382	420	$4•26 \times 10^{-5}$	0•10	$7•05 \times 10^{-13}$	1
800	1•394	100	$1•14 \times 10^{-5}$	0•42	$7•84 \times 10^{-13}$	2
400	1•416	290	$3•91 \times 10^{-5}$	0•15	$9•35 \times 10^{-13}$	4
200	1•437	600	$7•49 \times 10^{-5}$	0•07	$8•74 \times 10^{-13}$	8
100	1•458	800	$1•43 \times 10^{-4}$	0•05	$1•27 \times 10^{-12}$	16
50	1•482	1050	$3•24 \times 10^{-4}$	0•04	$2•20 \times 10^{-12}$	32

Table 7.33 Isotropic consolidation test TR(1), reconstituted till HH(a).

σ'_r (kPa)	V	t_{100} (min)	m_v (kPa^{-1})	c_v ($mm^2\ min^{-1}$)	k (ms^{-1})	Ro
200	1•476	70	$6•06 \times 10^{-5}$	0•62	$6•14 \times 10^{-12}$	4
400	1•458	165	$5•86 \times 10^{-5}$	0•26	$2•51 \times 10^{-12}$	2
800	1•438	160	$3•51 \times 10^{-5}$	0•27	$1•54 \times 10^{-12}$	1
1600	1•391	280	$4•03 \times 10^{-5}$	0•15	$9•92 \times 10^{-13}$	1
800	1•402	85	$9•34 \times 10^{-6}$	0•49	$7•50 \times 10^{-13}$	2
400	1•419	230	$3•09 \times 10^{-5}$	0•18	$9•22 \times 10^{-13}$	4
200	1•438	275	$6•59 \times 10^{-5}$	0•15	$1•66 \times 10^{-12}$	8
100	1•461	500	$1•62 \times 10^{-4}$	0•09	$2•27 \times 10^{-12}$	16
50	1•479	1000	$2•40 \times 10^{-4}$	0•04	$1•69 \times 10^{-12}$	32

Table 7.34 Isotropic consolidation test TR(2), reconstituted till HH(b).

σ'_r (kPa)	V	t_{100} (min)	m_v (kPa^{-1})	c_v ($mm^2\ min^{-1}$)	k (ms^{-1})	Ro
200	1·464	100	$4·29 \times 10^{-5}$	0·46	$3·20 \times 10^{-12}$	4
400	1·456	34	$2·60 \times 10^{-5}$	1·34	$5·67 \times 10^{-12}$	2
800	1·445	40	$1·94 \times 10^{-5}$	1·13	$3·59 \times 10^{-12}$	1
1600	1·421	130	$2·03 \times 10^{-5}$	0·35	$1·15 \times 10^{-12}$	1
2000	1·413	480	$1·39 \times 10^{-5}$	0·09	$2·11 \times 10^{-13}$	1
1600	1·415	25	$1·95 \times 10^{-6}$	1·78	$5·66 \times 10^{-13}$	1·25
800	1·424	60	$8·13 \times 10^{-6}$	0·74	$9·88 \times 10^{-13}$	2·5
400	1·436	140	$2·19 \times 10^{-5}$	0·32	$1·15 \times 10^{-12}$	5
200	1·448	200	$4·18 \times 10^{-5}$	0·23	$1·54 \times 10^{-12}$	10
100	1·467	110	$1·27 \times 10^{-4}$	0·41	$8·57 \times 10^{-12}$	20

(1) Assumes p'_c = 760 kPa.

Table 7.35 Isotropic consolidation test TU(1), undisturbed till HH(a).

σ'_r (kPa)	V	t_{100} (min)	m_v (kPa^{-1})	c_v ($mm^2\ min^{-1}$)	k (ms^{-1})	Ro
200	1·442	100	$5·11 \times 10^{-5}$	0·45	$3·78 \times 10^{-12}$	4
400	1·434	90	$2·81 \times 10^{-5}$	0·50	$2·30 \times 10^{-12}$	2
800	1·420	60	$2·46 \times 10^{-5}$	0·75	$3·01 \times 10^{-12}$	1
1600	1·393	150	$2·37 \times 10^{-5}$	0·30	$1·15 \times 10^{-12}$	1
2000	1·385	500	$1·51 \times 10^{-5}$	0·09	$2·17 \times 10^{-13}$	1

(1) Assumes p'_c = 730 kPa.

Table 7.36 Isotropic consolidation test TU(2), undisturbed till HH(b).

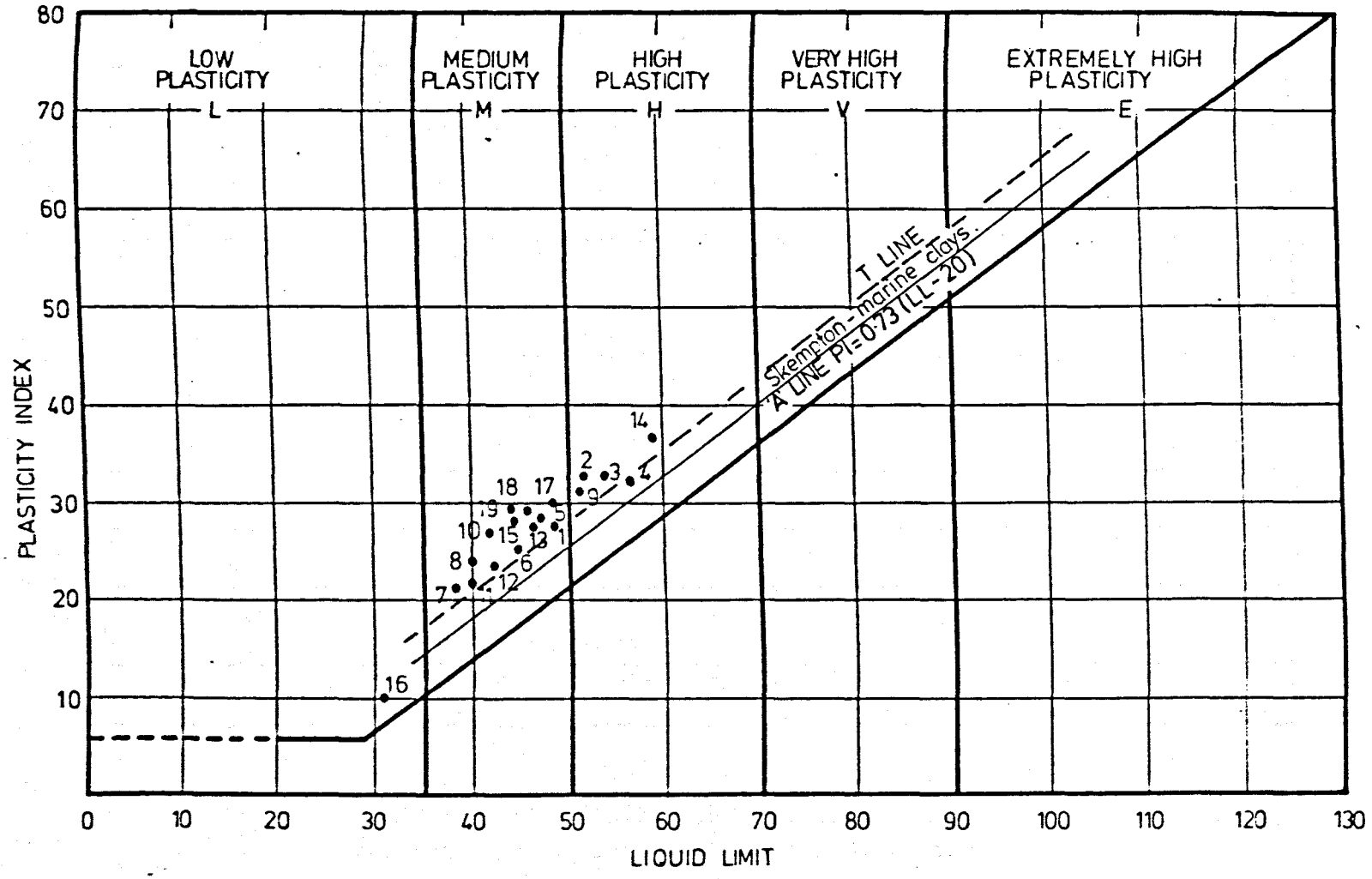

Figure 7.1 Plasticity data for the Vale of St. Albans tills and related sediments.

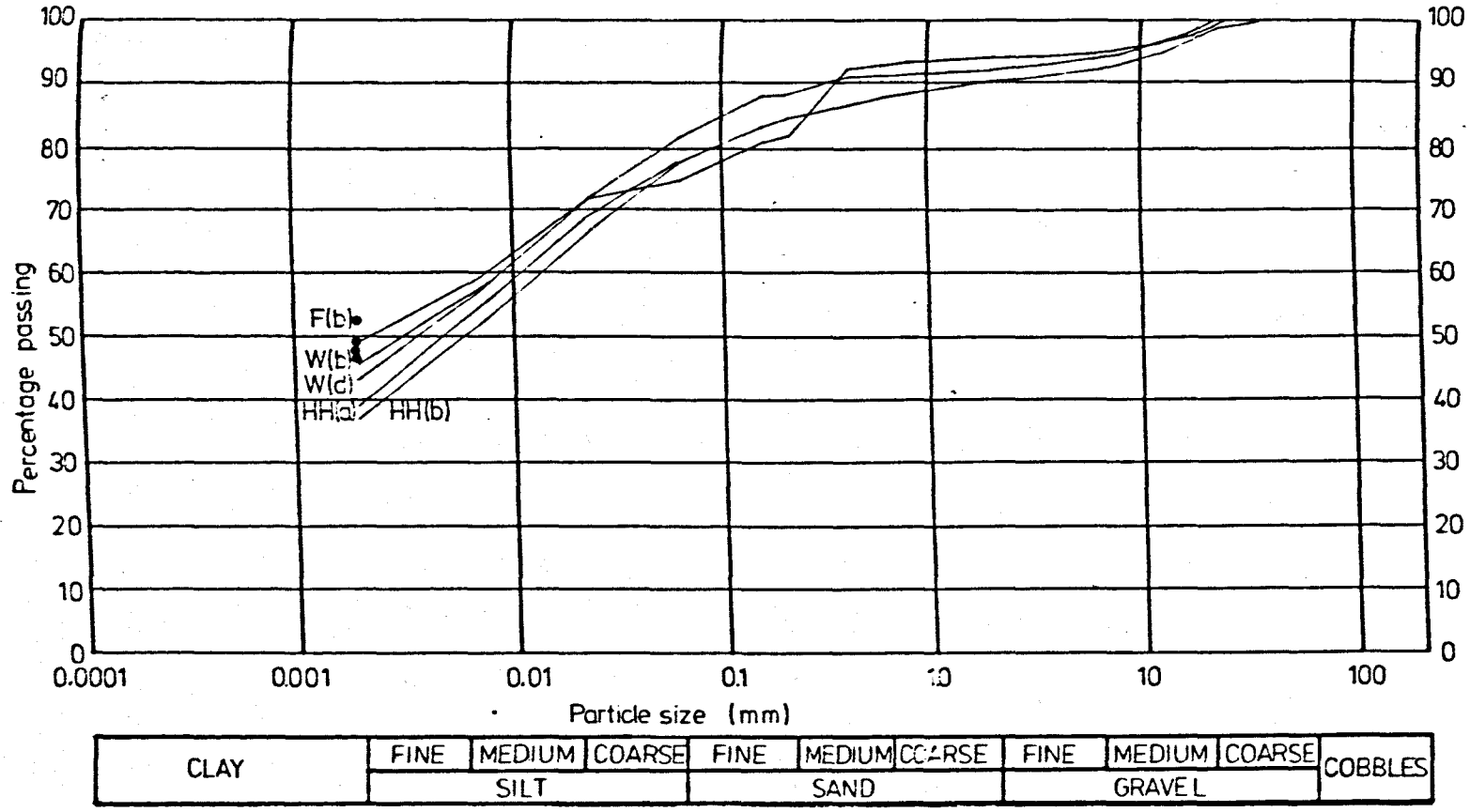

Figure 7.2 Grading characteristics of tills HH(a), HH(b), F(b), W(b), W(d).
(• denotes percentage < 0·002mm without acid solubles).

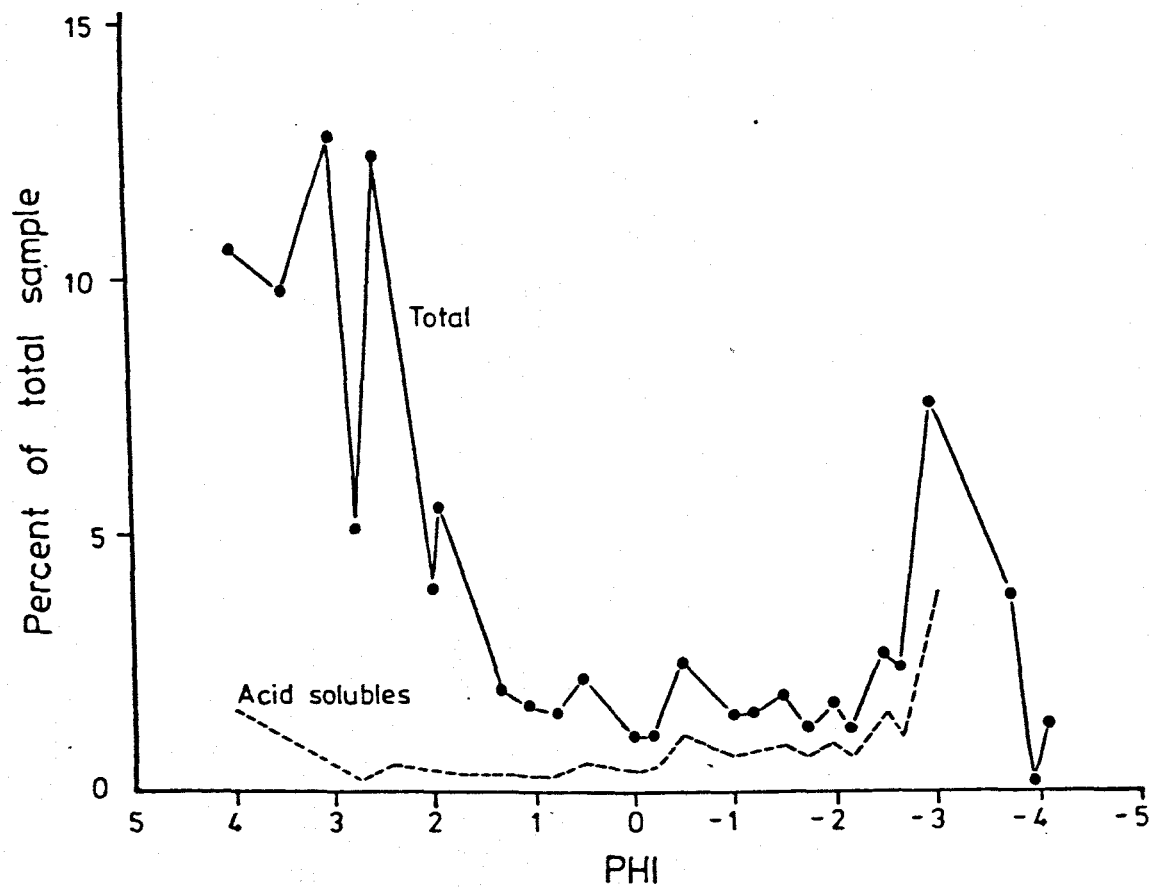

Figure 7.3 Total and acid soluble grading characteristics of till HH(a).

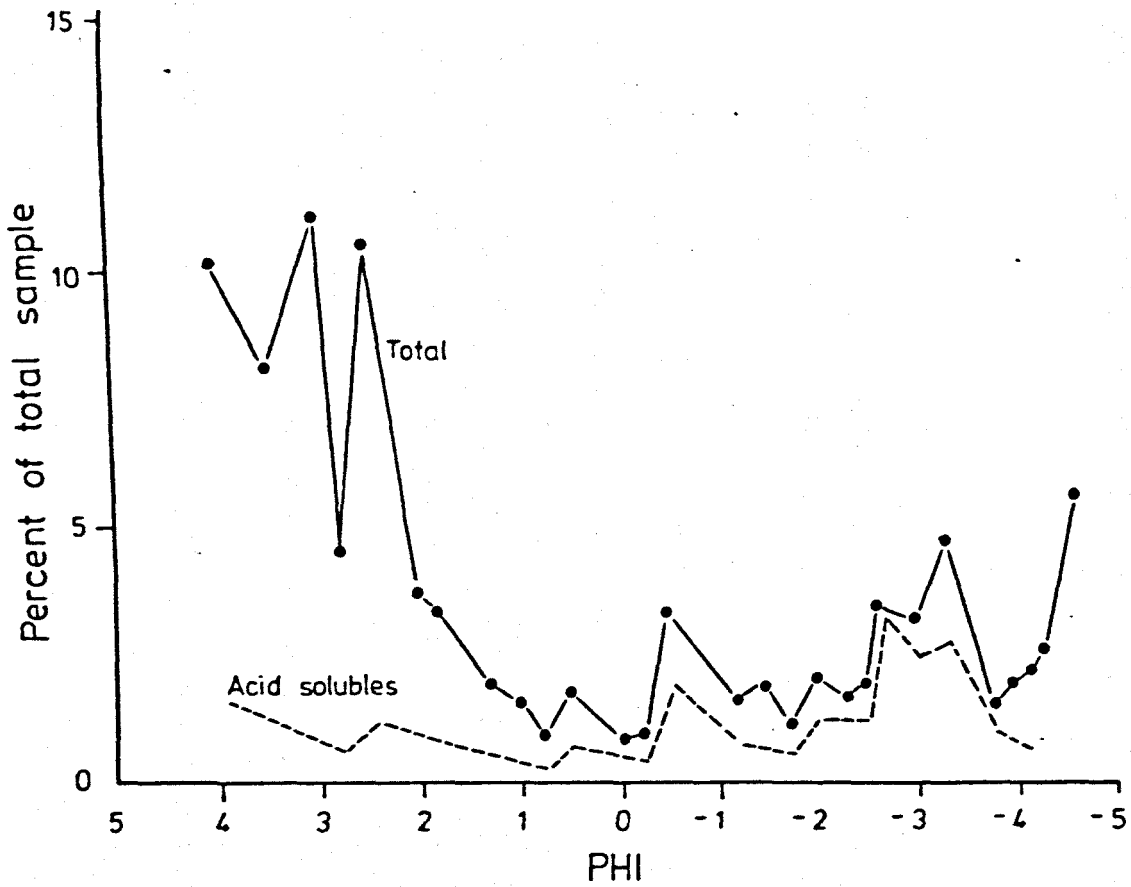

Figure 7.4 Total and acid soluble grading characteristics of till HH(b).

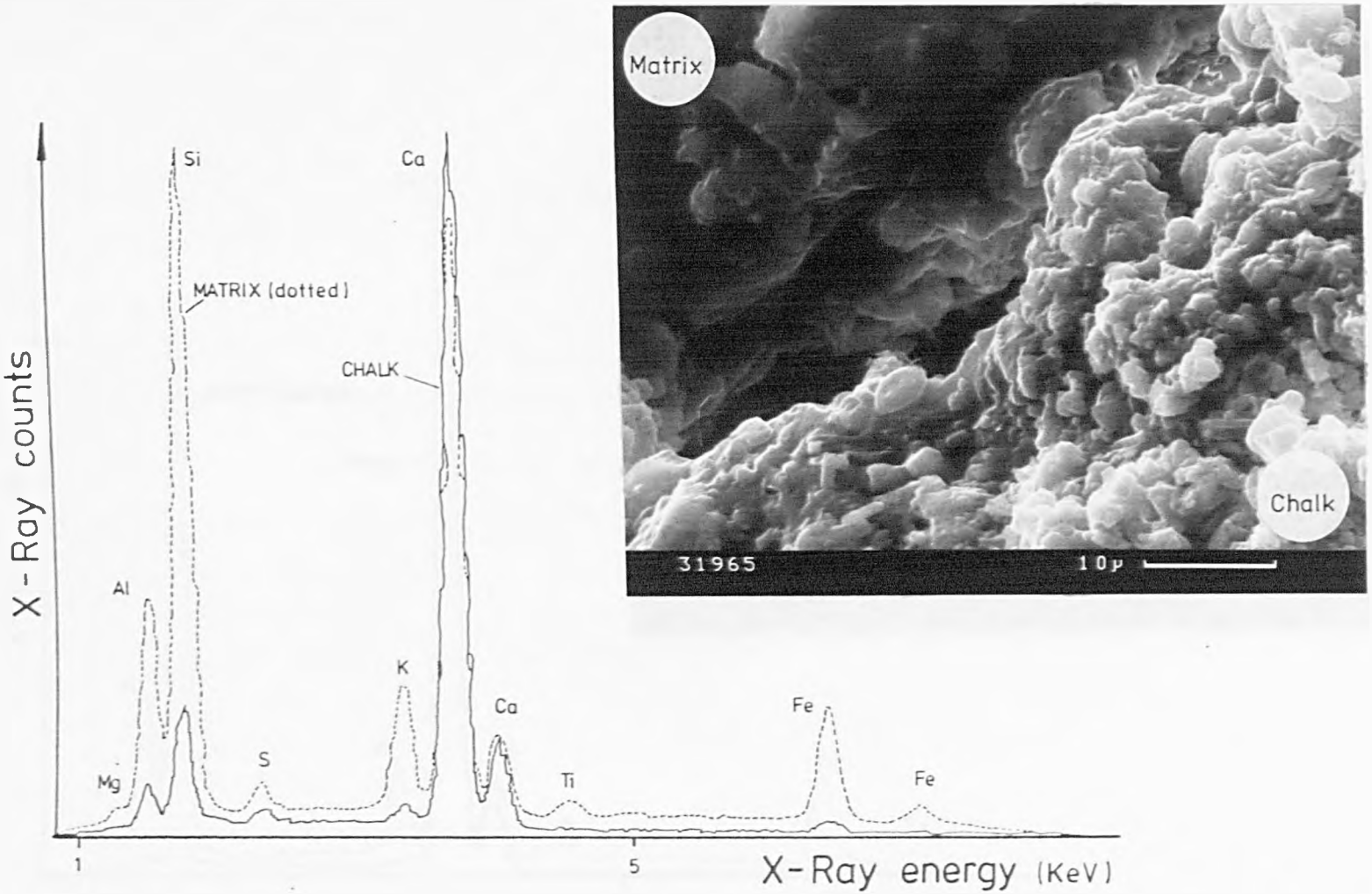

Figure 7.5 Till HH(a) : electronmicrograph and EDAX trace on chalk particle and matrix.

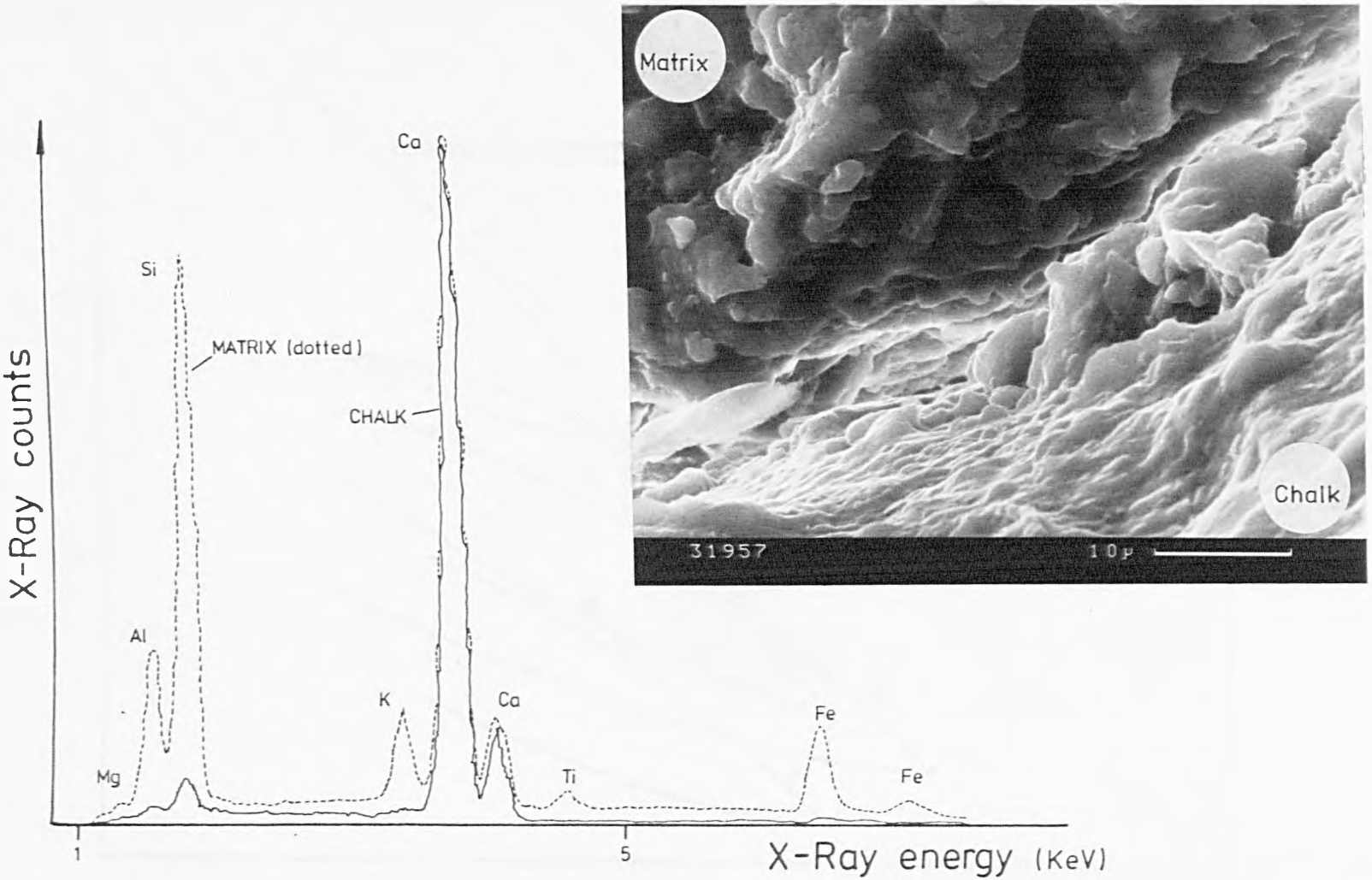

Figure 7.6 Till HH(b) : electronmicrograph and EDAX trace on chalk particle and matrix.

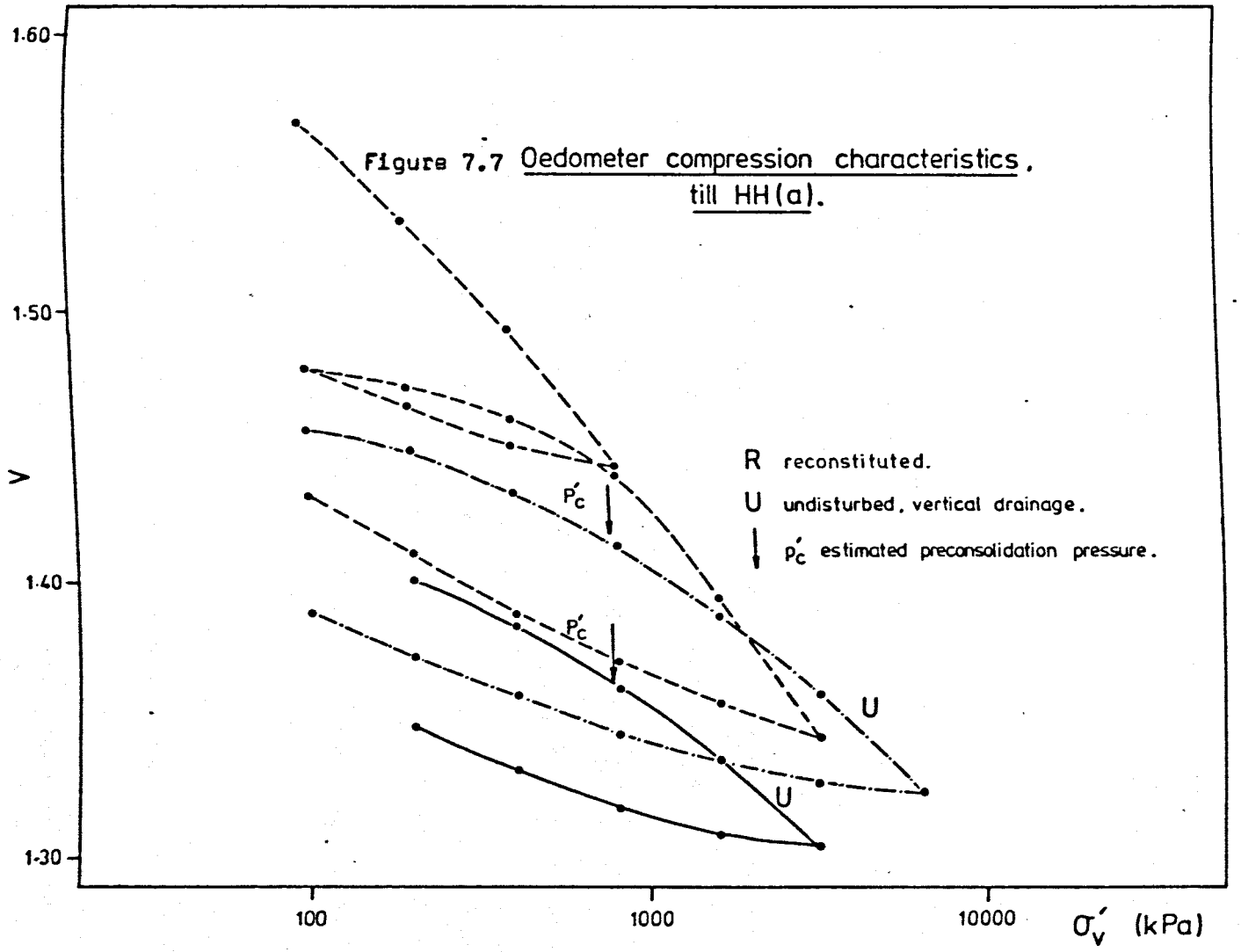

Figure 7.7 Oedometer compression characteristics, till HH(a).

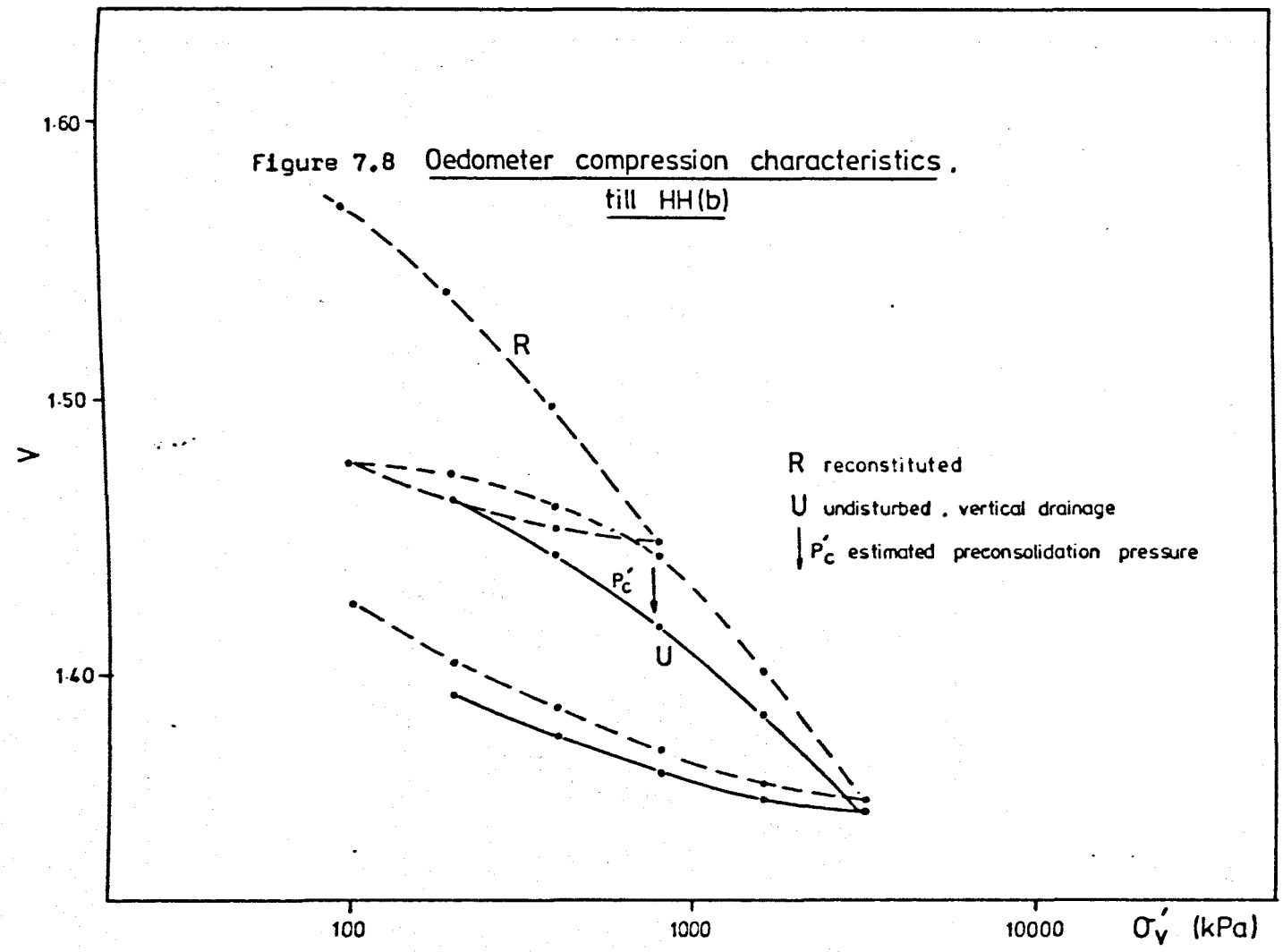

Figure 7.8 Oedometer compression characteristics, till HH(b)

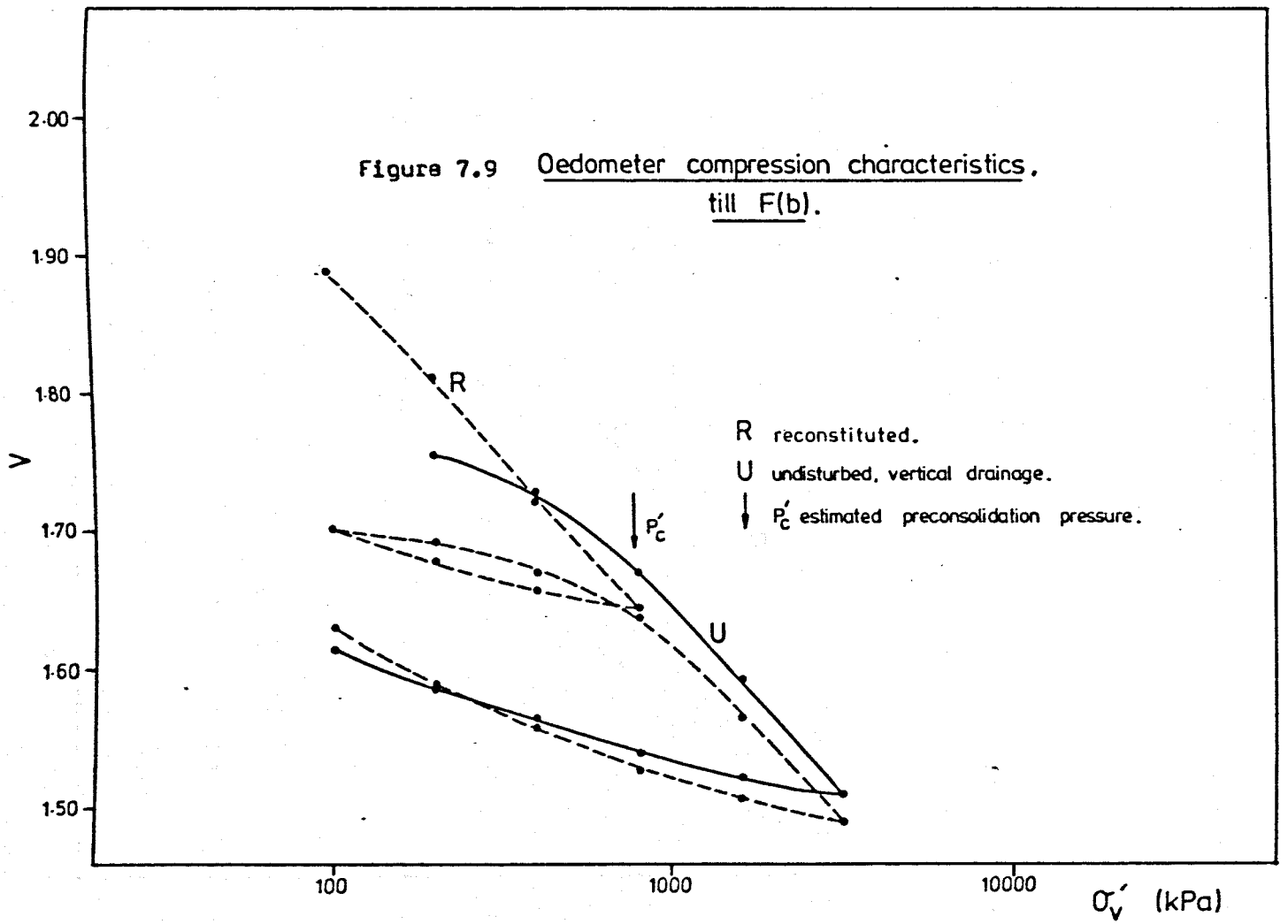

Figure 7.9 Oedometer compression characteristics, till F(b).

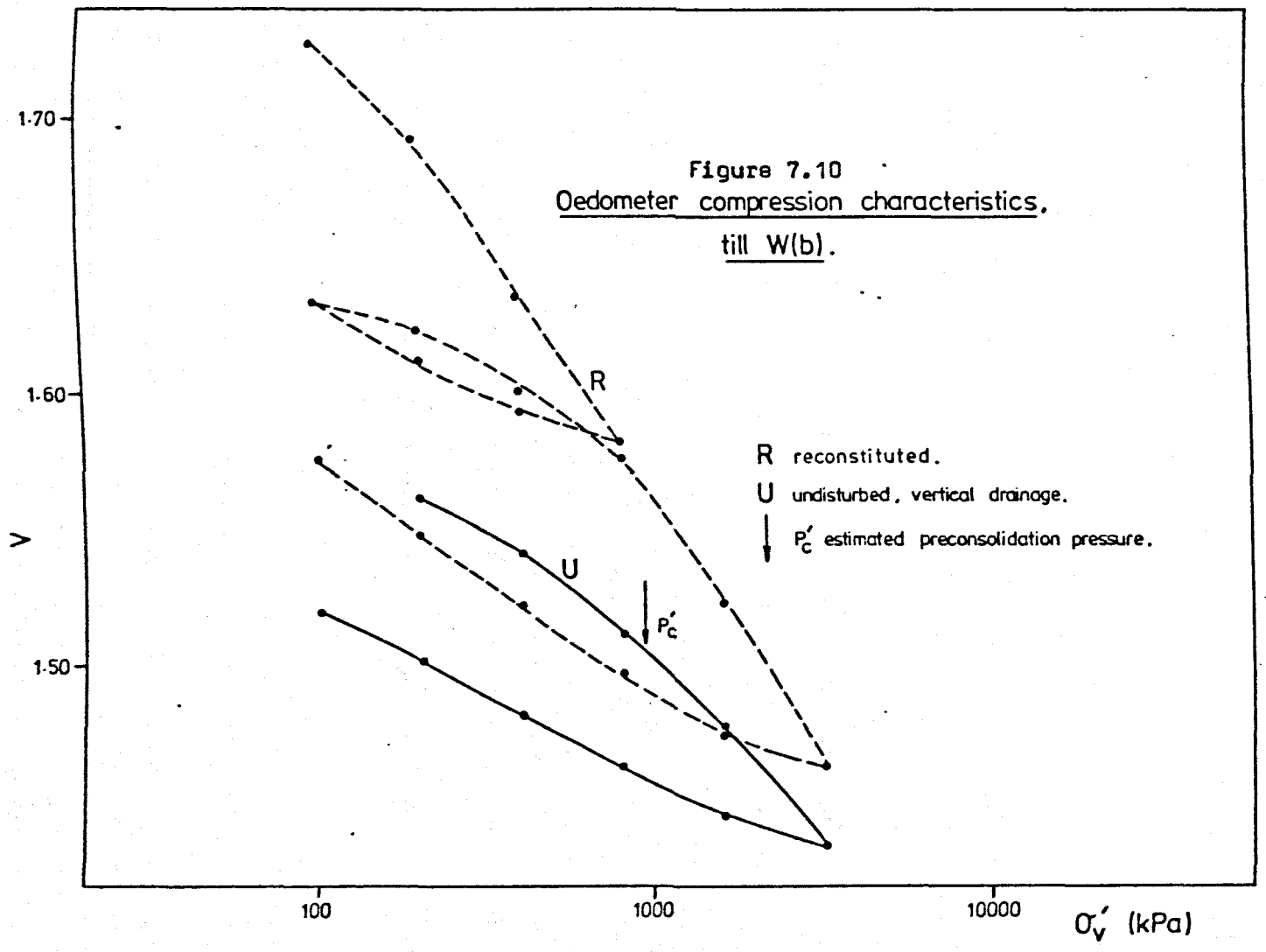

Figure 7.10
Oedometer compression characteristics, till W(b).

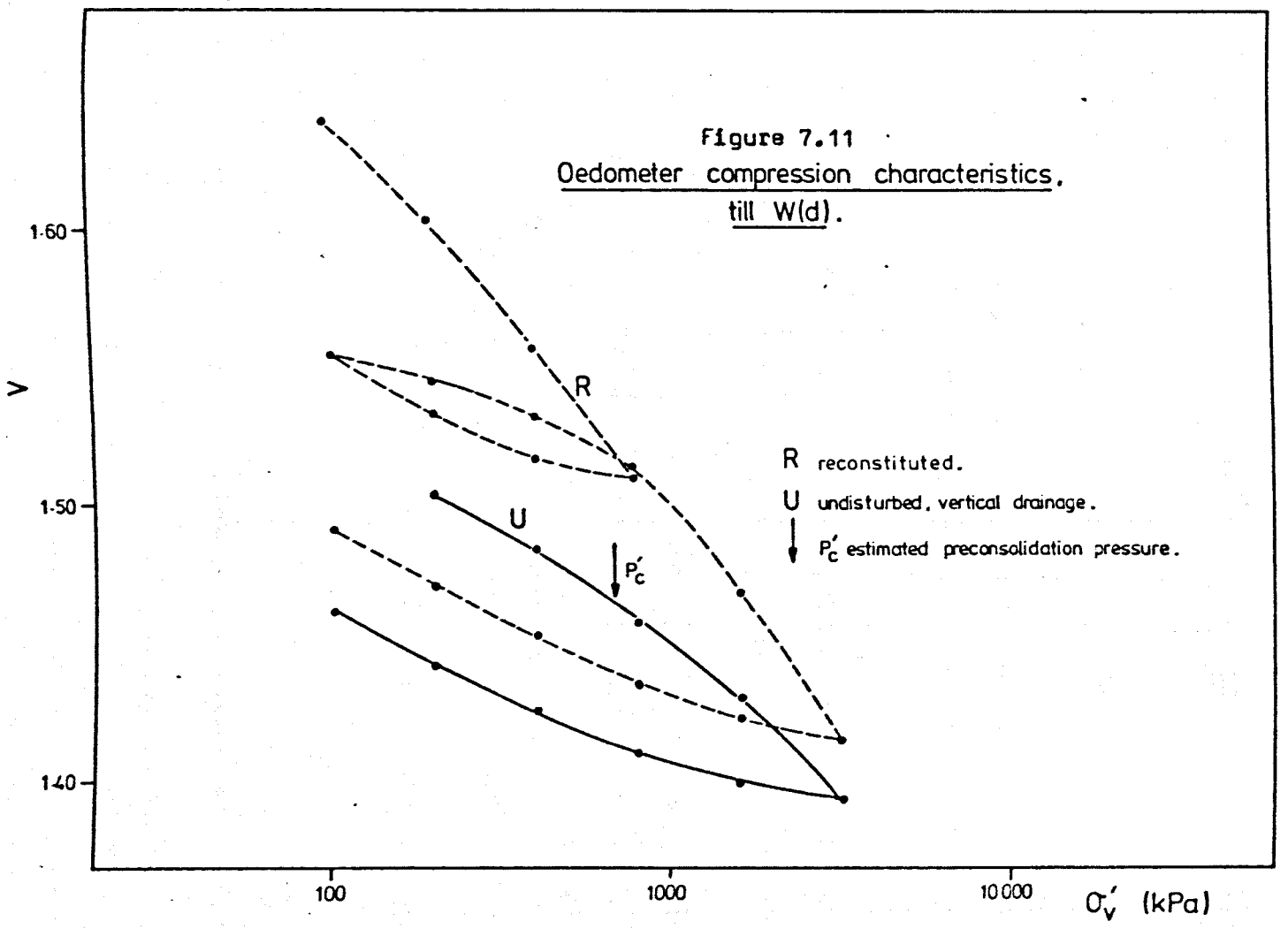

Figure 7.11
Oedometer compression characteristics, till W(d).

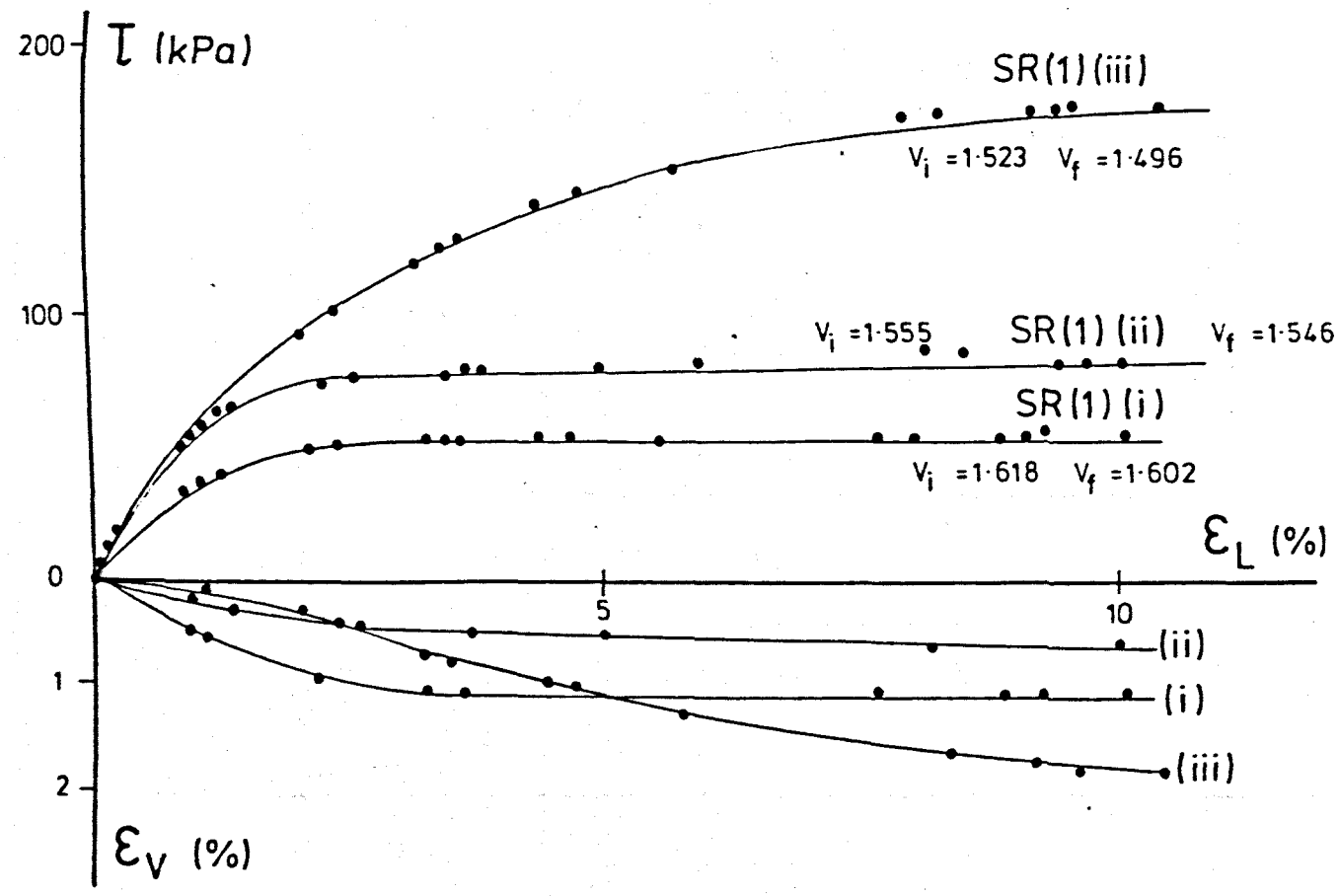

Figure 7.12 τ : ε_L : ε_v; drained shear box tests SR1(i), (ii), (iii).

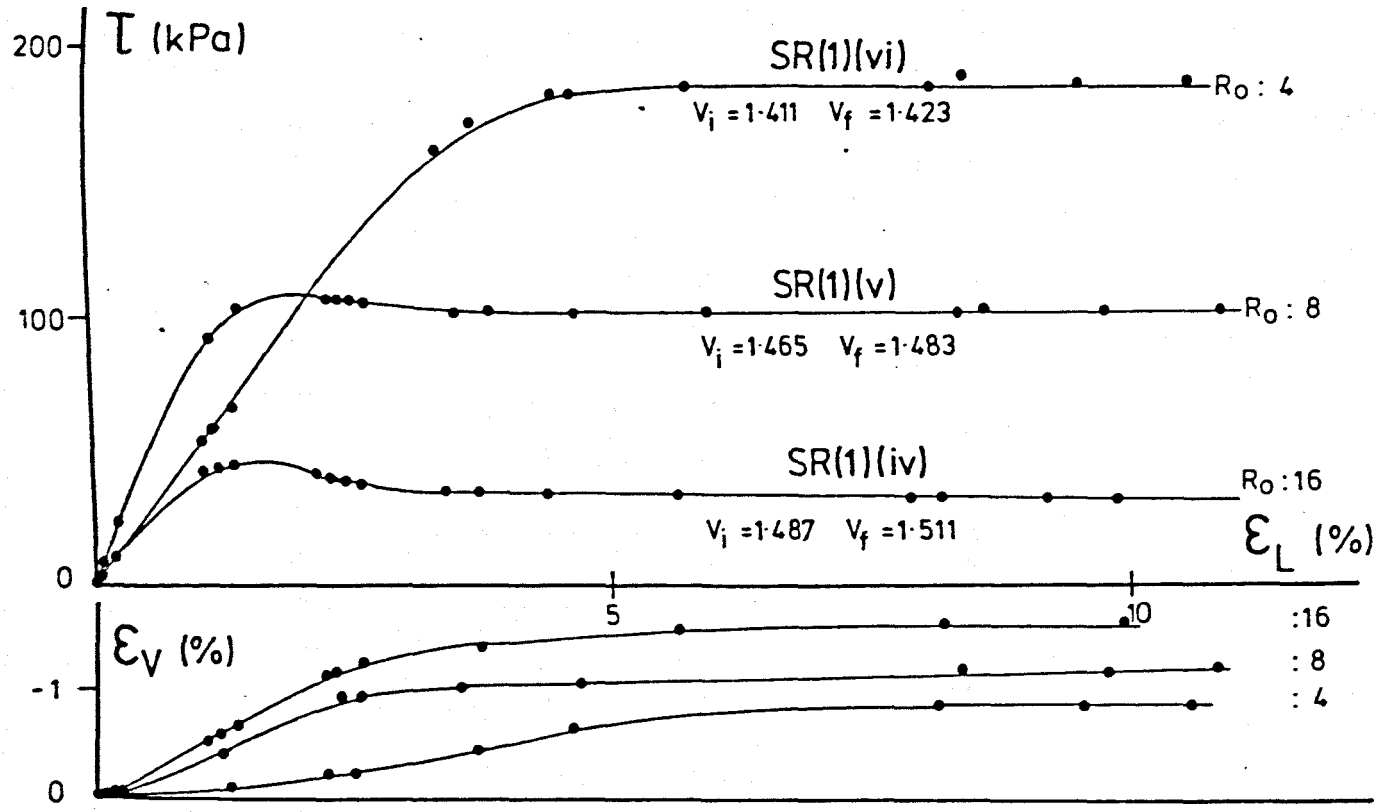

Figure 7.13 τ : ε_L : ε_v; drained shear box tests SR1 (iv) , (v) , (vi).

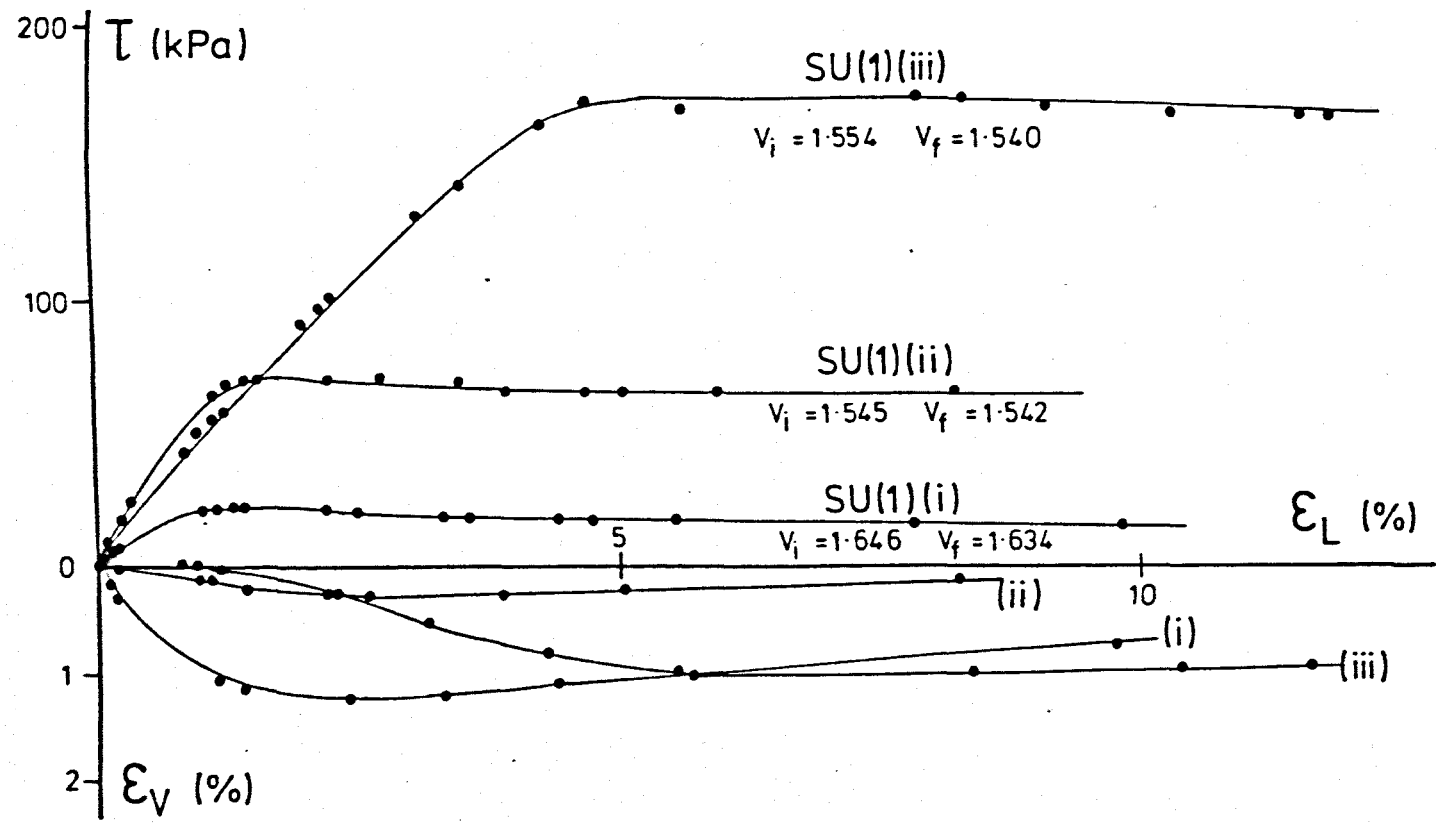

Figure 7.14 $\tau : \varepsilon_L : \varepsilon_V$; drained shear box tests SU1 (i), (ii), (iii).

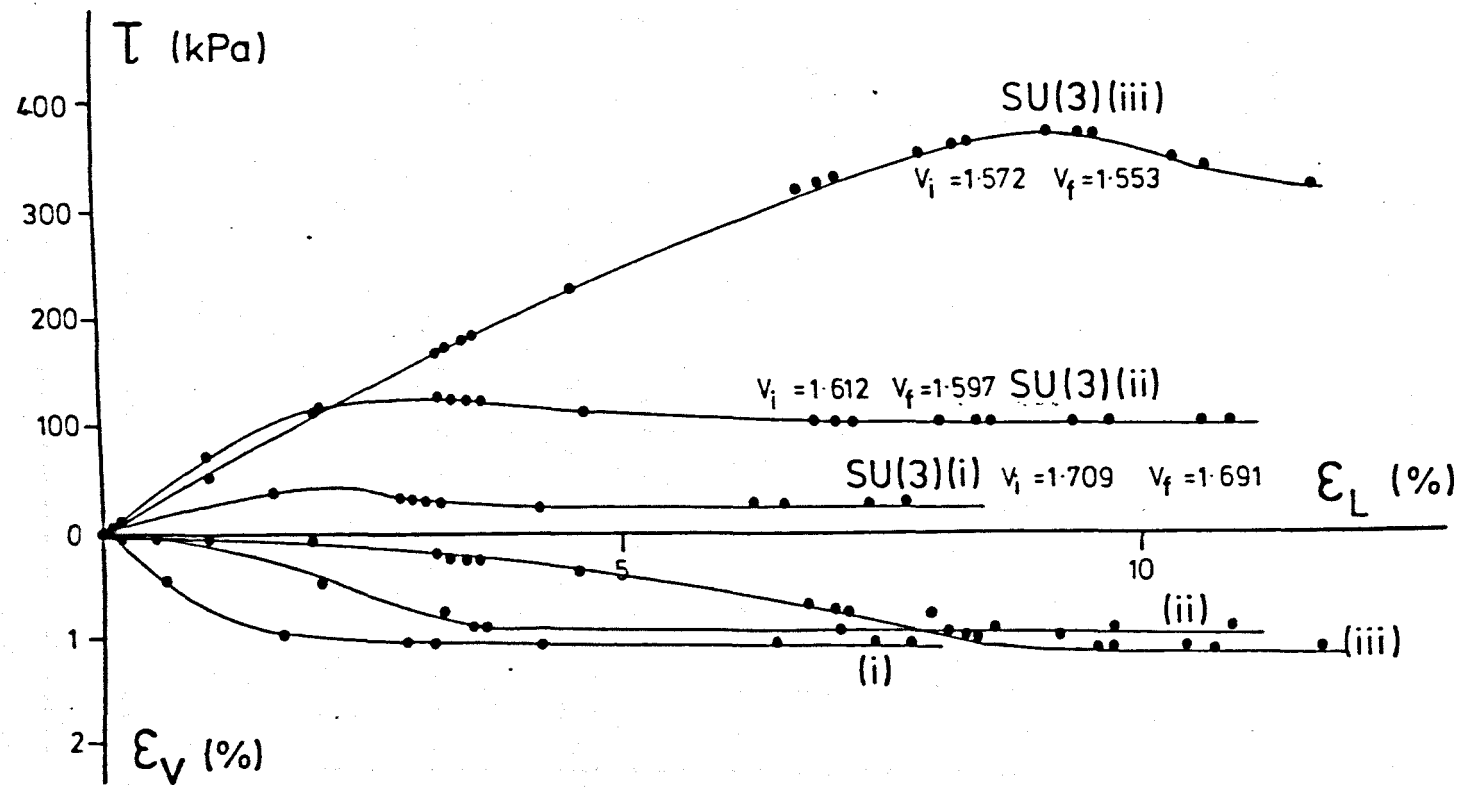

Figure 7.15 τ : ε_L : ε_V; drained shear box tests SU3 (i) , (ii) , (iii).

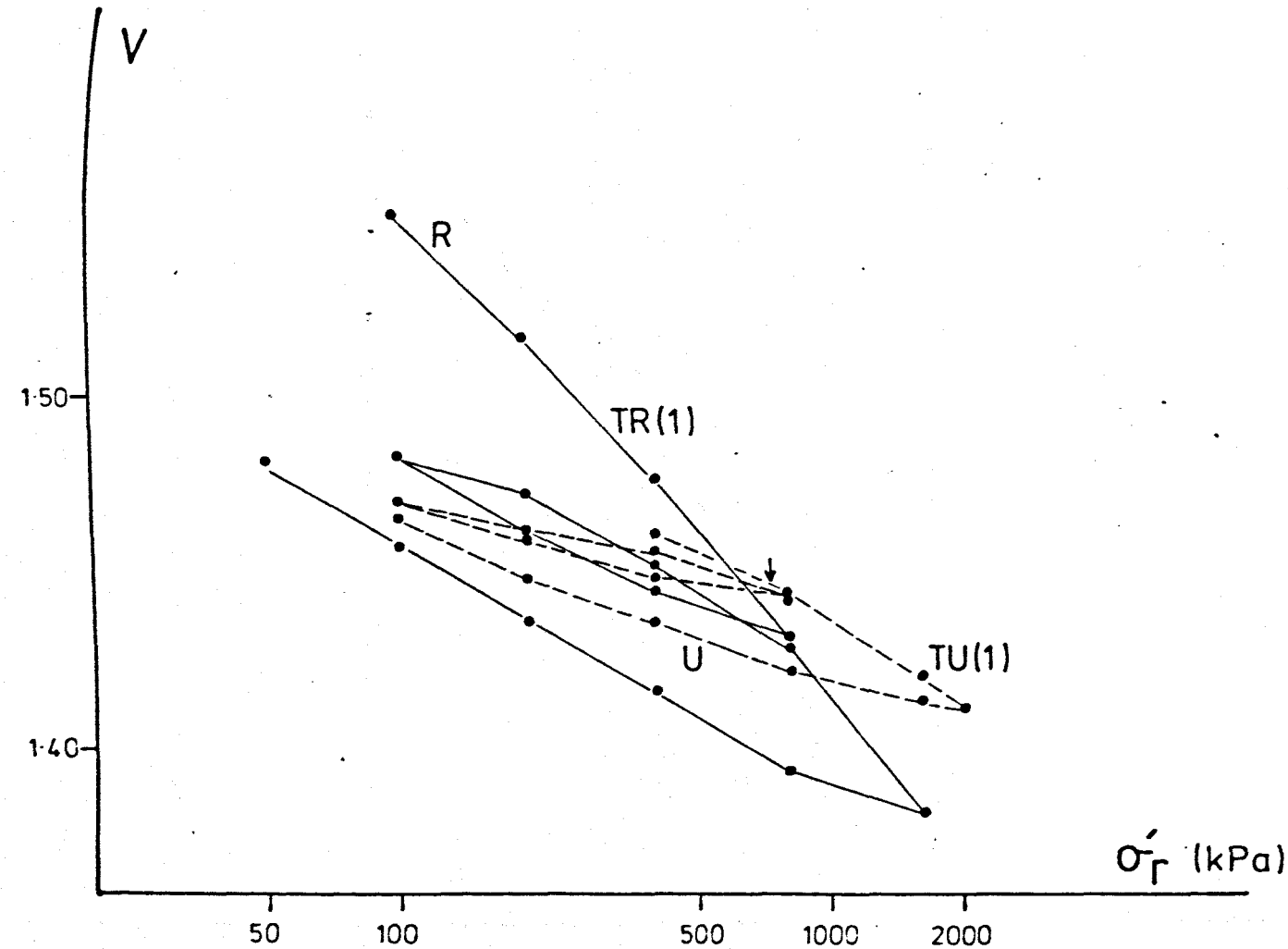

Figure 7.16 Isotropic compression characteristics, reconstituted and undisturbed till HH(a).

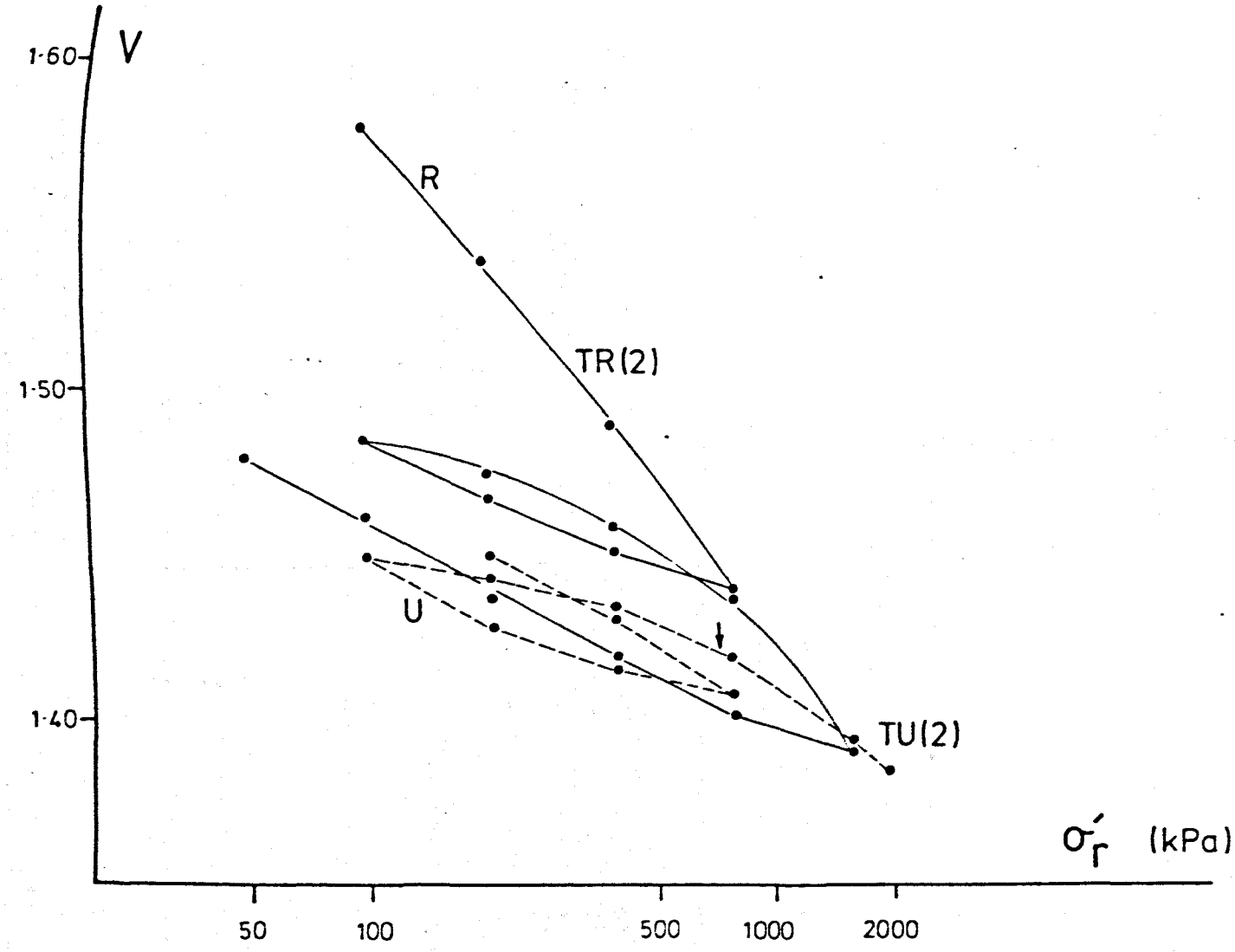

Figure 7.17 Isotropic compression characteristics, reconstituted and undisturbed till HH(b).

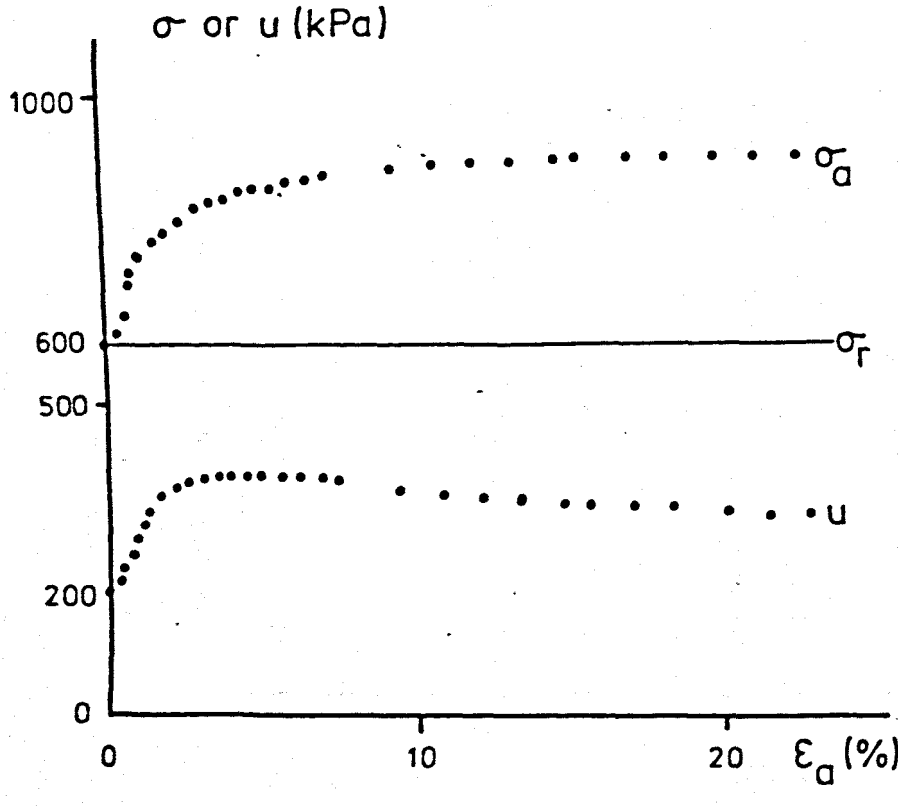
σ or u (kPa)
1000
600
500
200
0
0
10
20
ε_a (%)
σ_a
σ_r
u

Figure 7.18 CU triaxial test results : RA1(i).

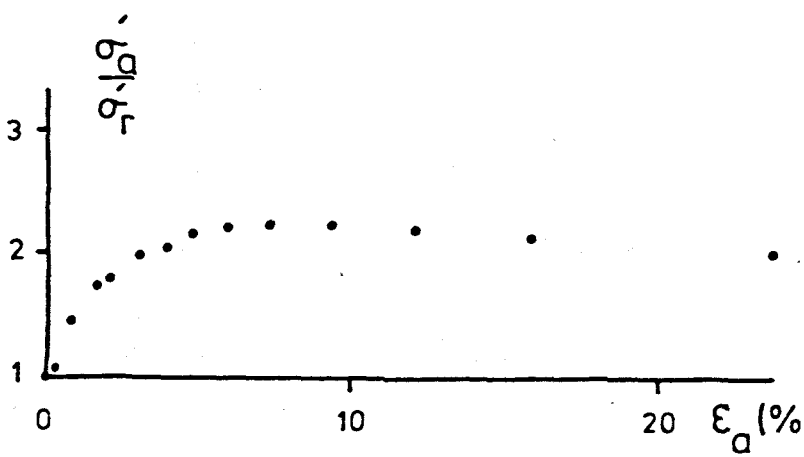

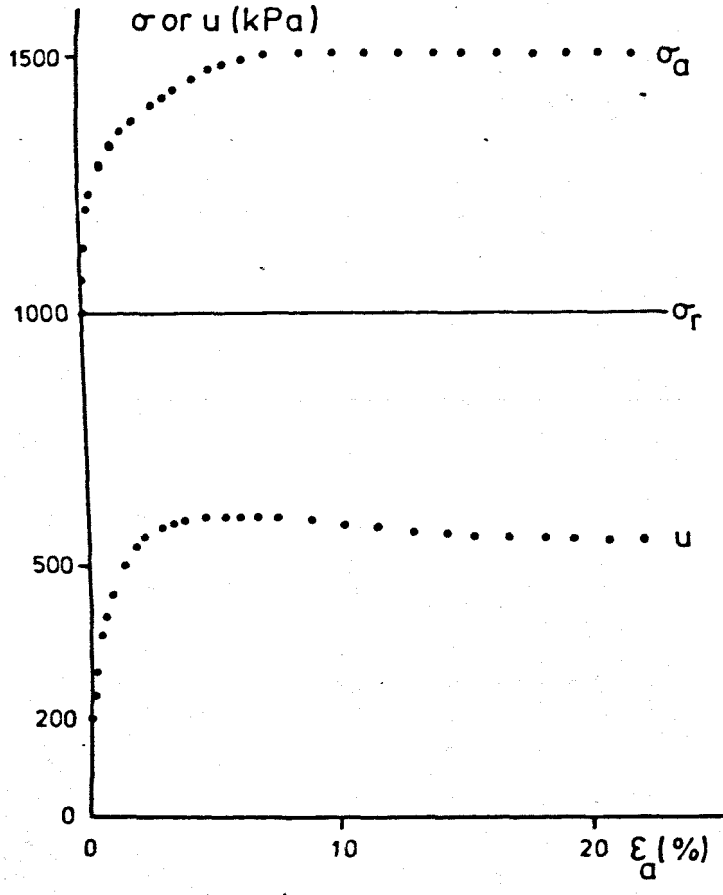
σ or u (kPa)
1500
1000
500
200
0
0
10
20
ε_a (%)
σ_a
σ_r
u

Figure 7.19 CU triaxial test results : RA1(ii).

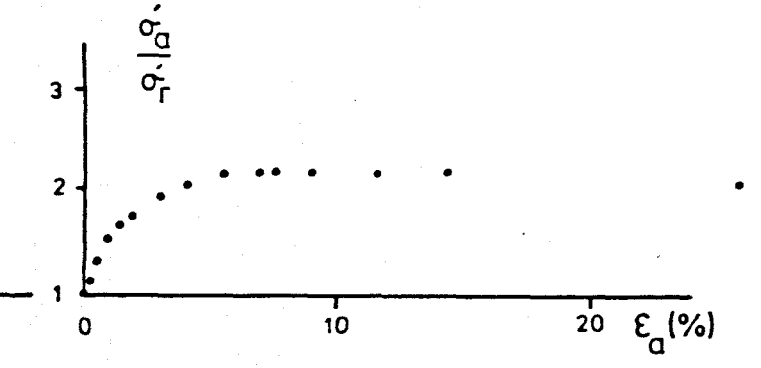

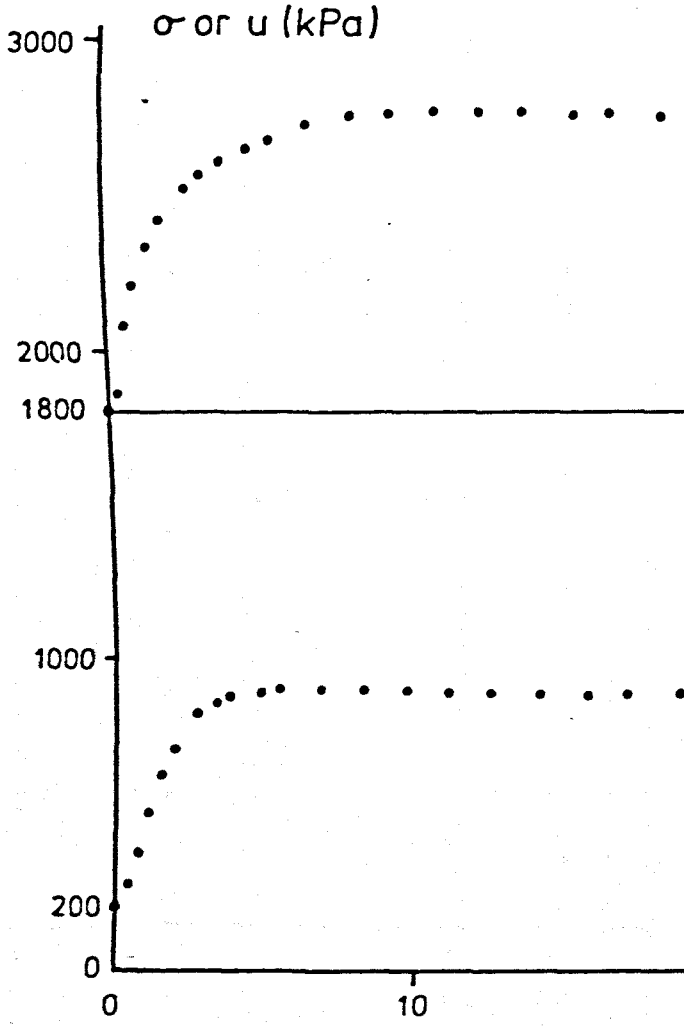
σ or u (kPa)
3000
2000
1800
1000
200
0
0
10

σ_a

σ_r

Figure 7.20 CU triaxial test results : RA1(iii).

u

20 ε_a (%)

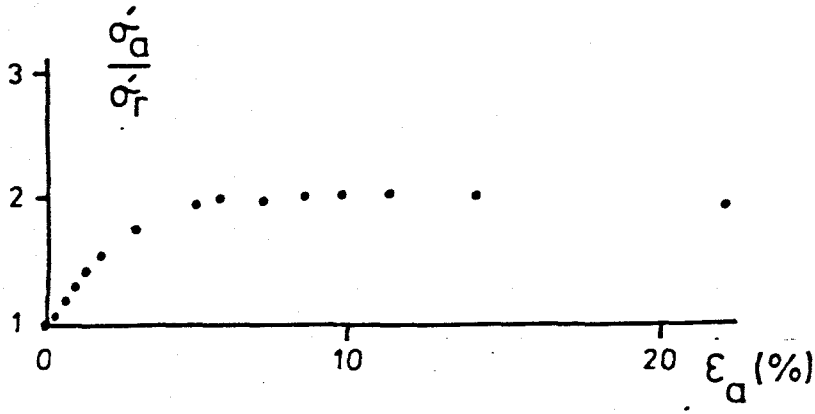

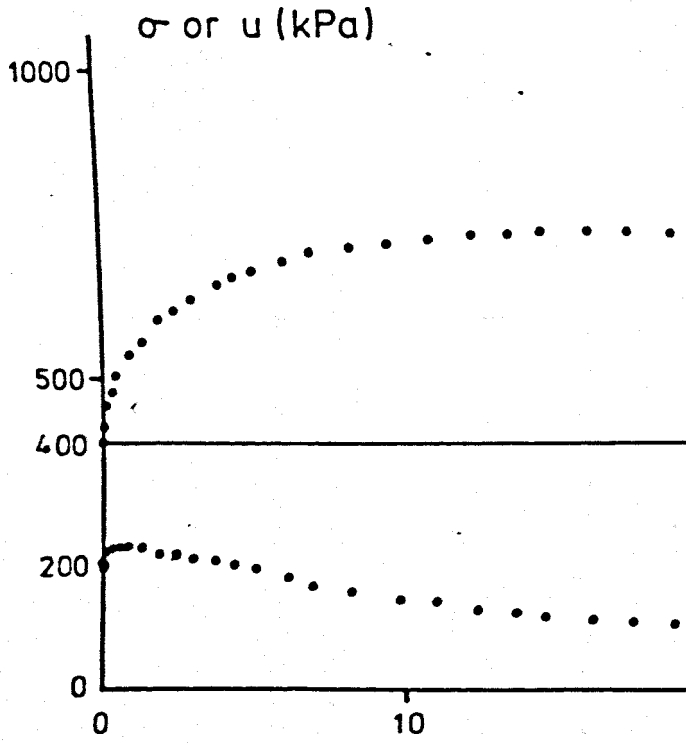
σ or u (kPa)
1000
500
400
200
0
0
10

Figure 7.21 CU triaxial test results : RA2(ii).

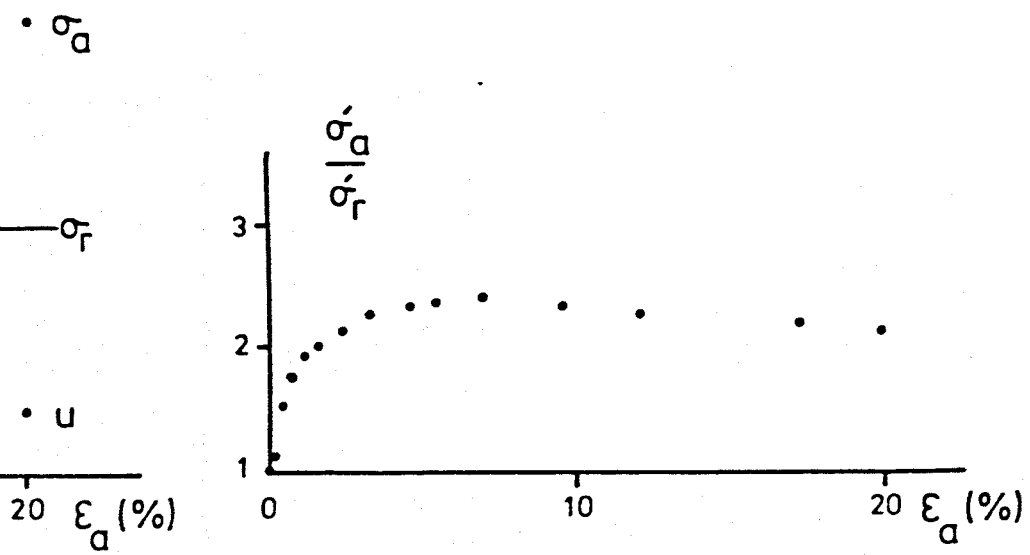

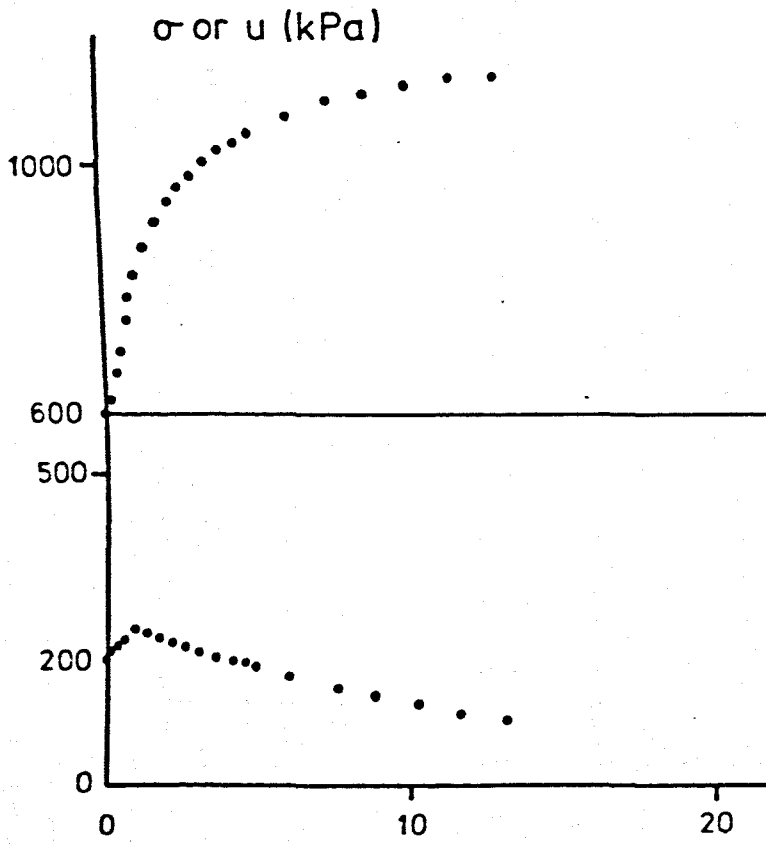
σ or u (kPa)
1000
600
500
200
0
0
10
20

• σ_a

Figure 7.22 CU triaxial test results : RA2(iii).

σ_r

• u

ε_a (%)

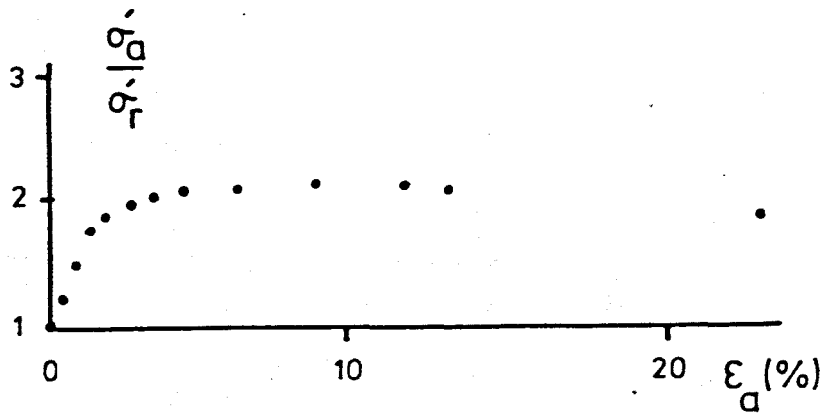

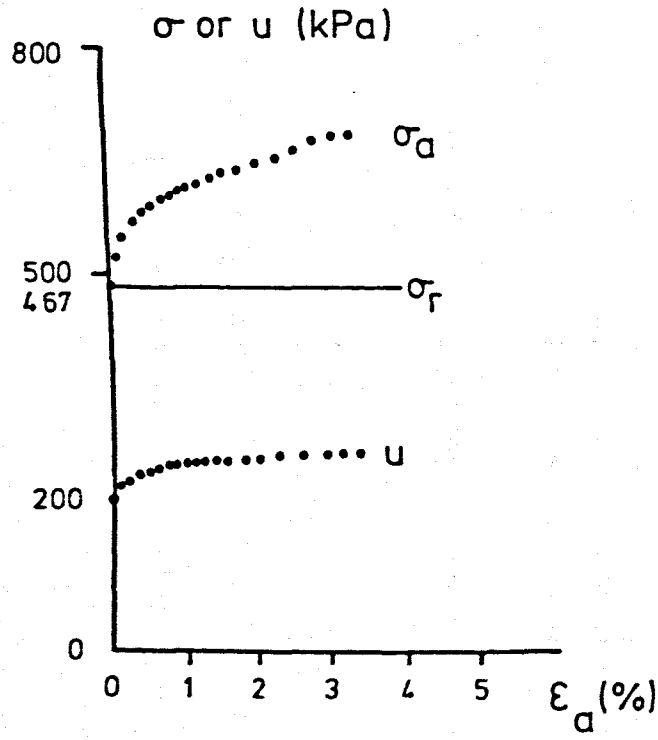
σ or u (kPa)
800
500
467
200
0
σa
σr
u
0
1
2
3
4
5
εa (%)

Figure 7.23 CU triaxial test results : RB(ii).

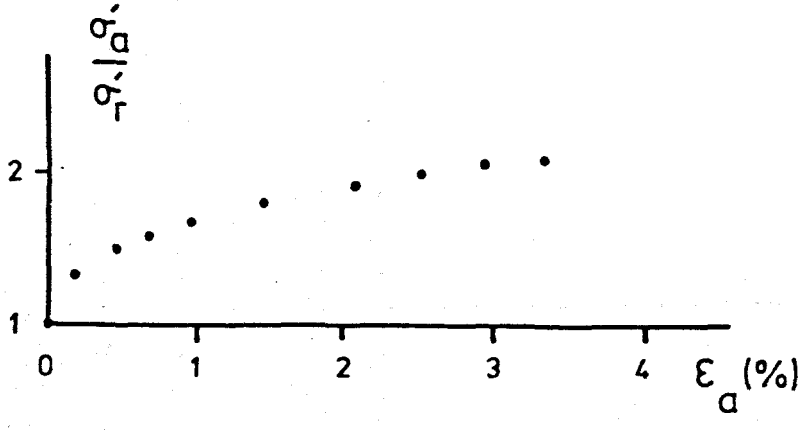

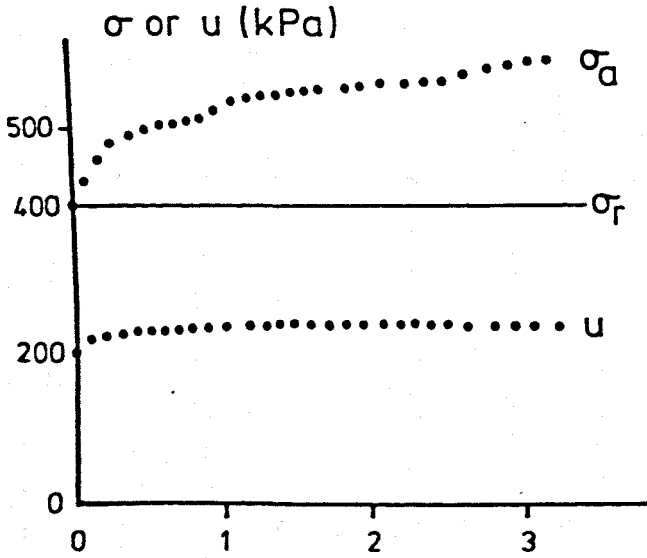
σ or u (kPa)
500
400
200
0
0
1
2
3
σa
σr
u

Figure 7.24 CU triaxial test results : RB(iii).

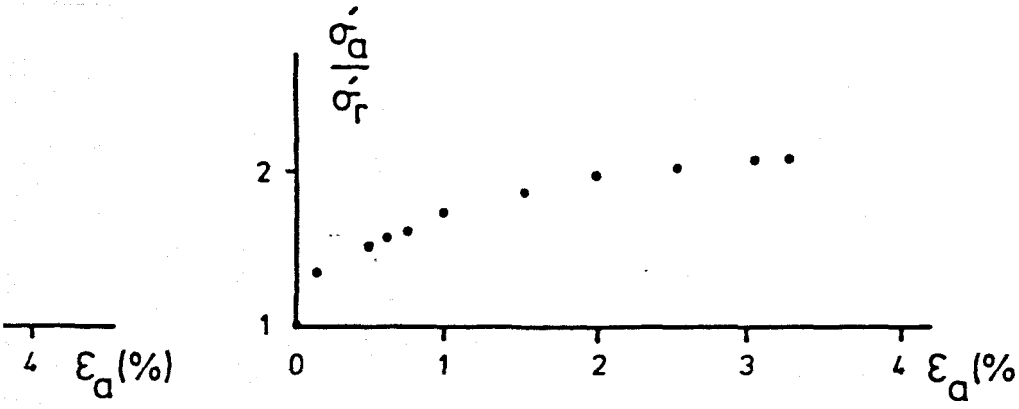

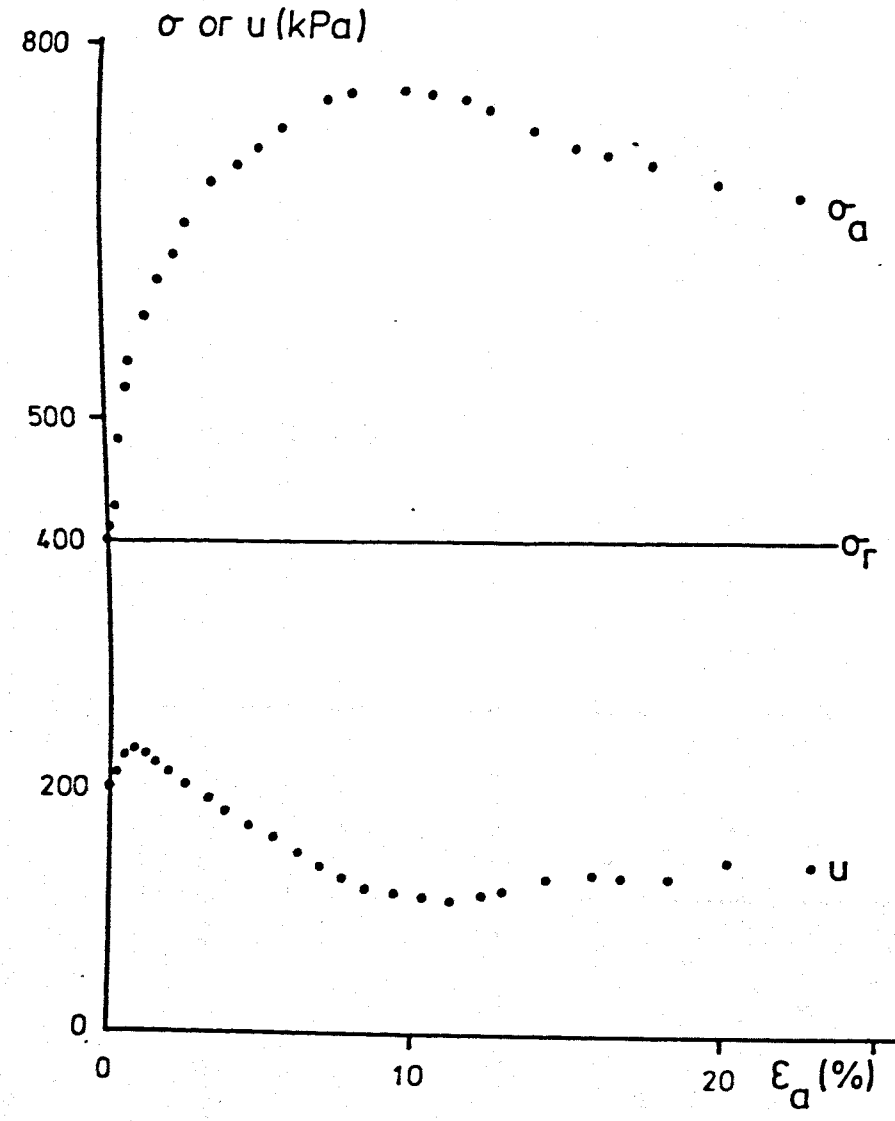
σ or u (kPa)
800
500
400
200
0
0
10
20
ε_a (%)
σ_a
σ_r
u

Figure 7.25 CU triaxial test results : RB(v).

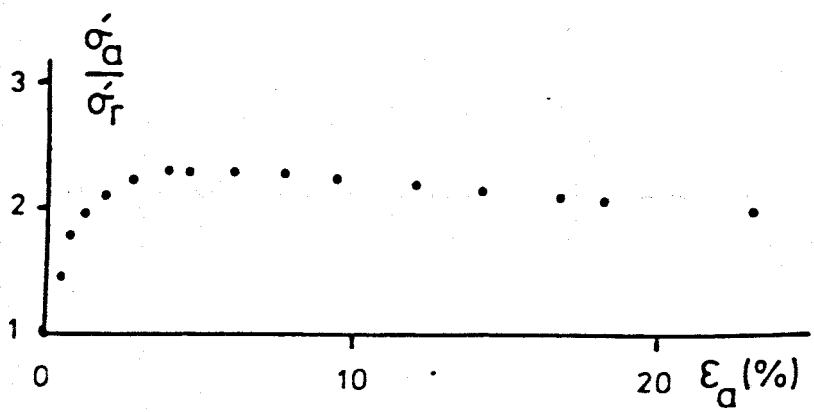

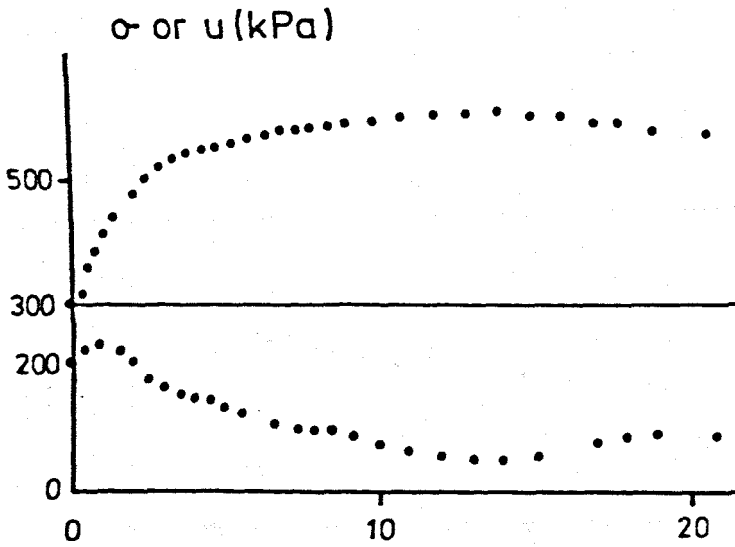
σ or u (kPa)
500
300
200
0
0
10
20

Figure 7.26 CU triaxial test results : R2 - 02.

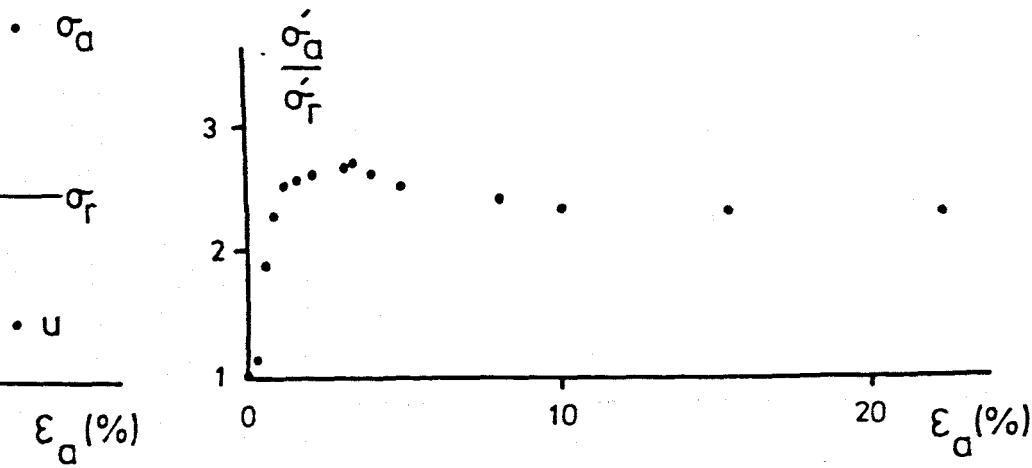

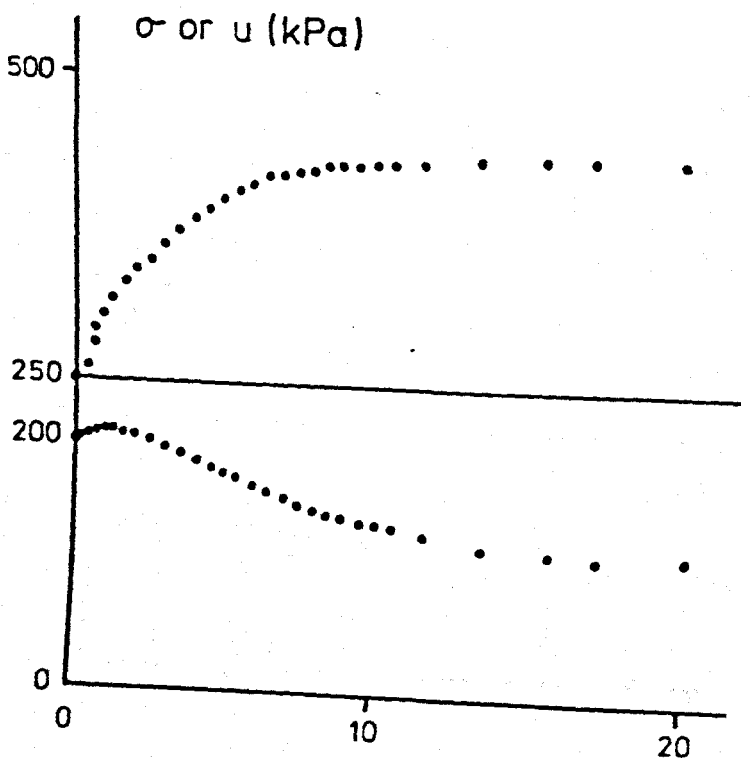
σ or u (kPa)
500
250
200
0
0
10
20

Figure 7.27 CU triaxial test results : R2 - 03.

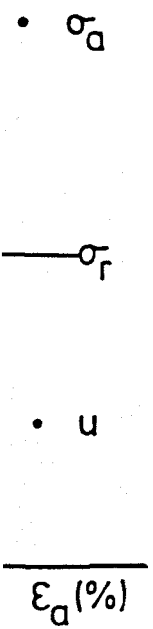

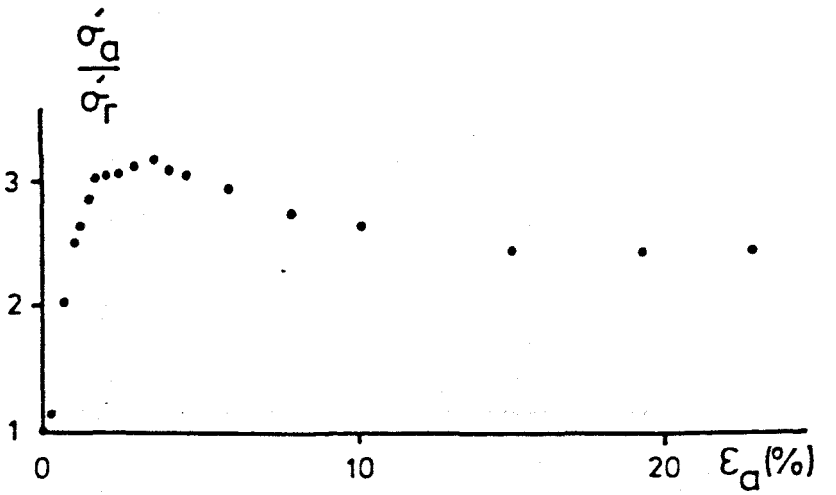

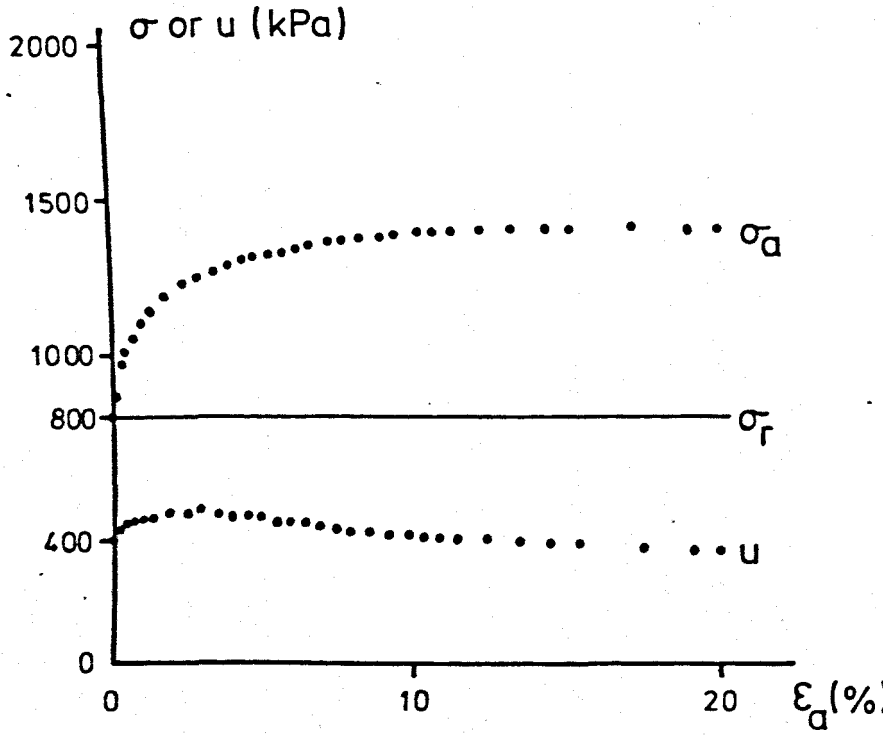
σ or u (kPa)
2000
1500
1000
800
400
0
0
10
20
ε_a(%)
σ_a
σ_r
u

Figure 7.28 CU triaxial test results : UA1(i).

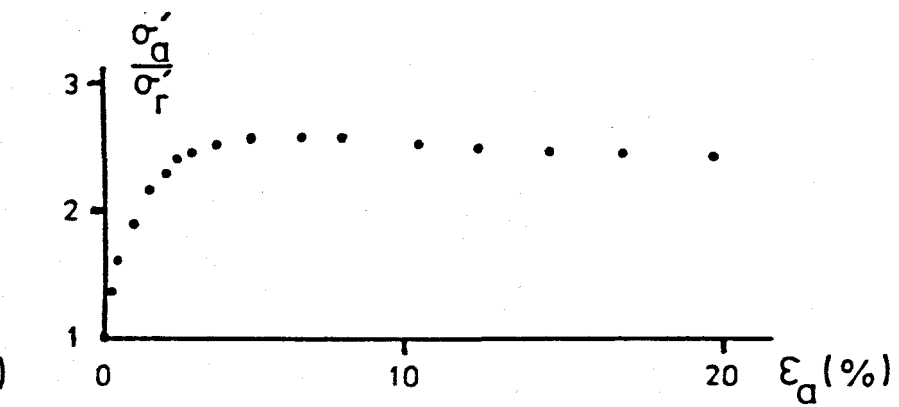

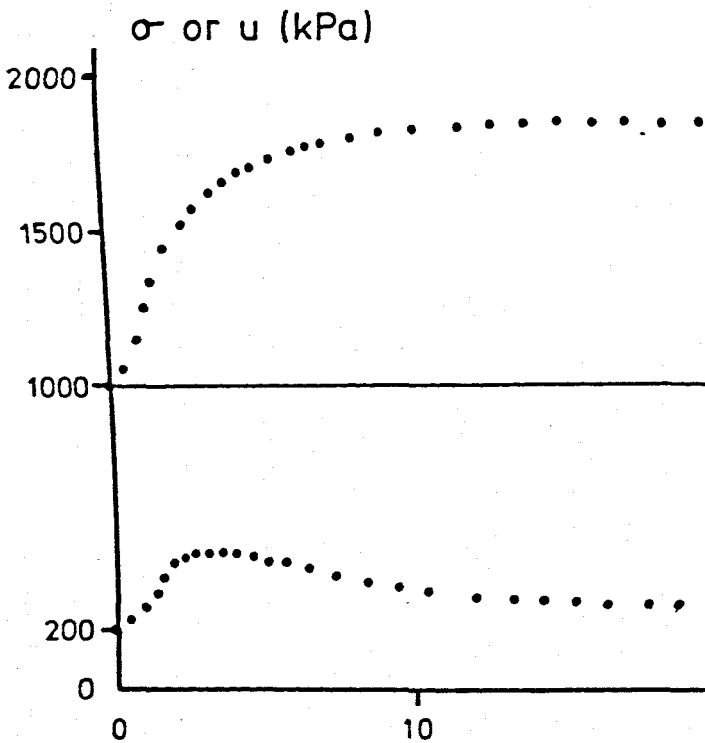
σ or u (kPa)
2000
1500
1000
200
0
0
10

Figure 7.29 CU triaxial test results : UA1(ii).

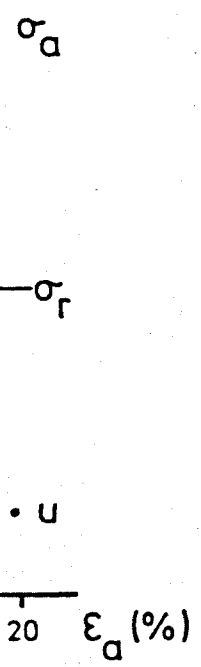

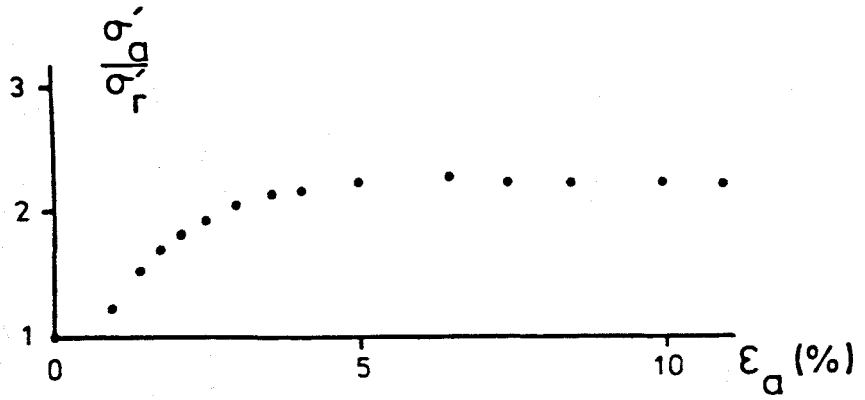

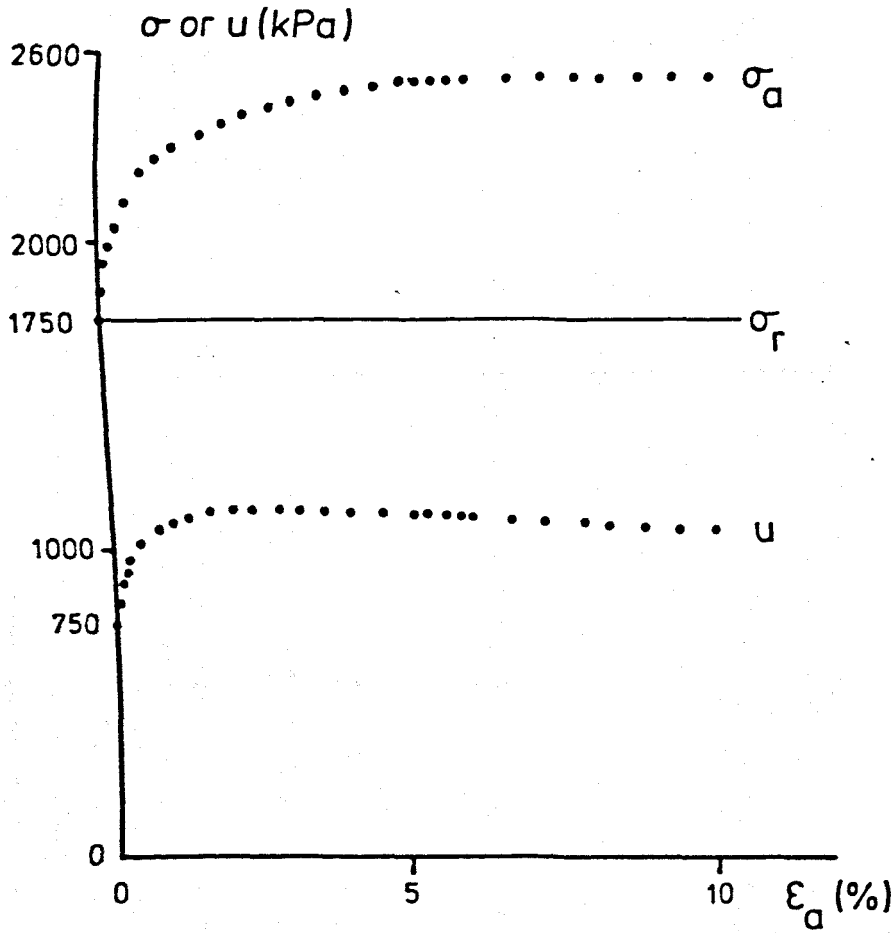
σ or u (kPa)
2600
2000
1750
1000
750
0
σa
σr
u
0
5
10
εa (%)

Figure 7.30 CU triaxial test results : UA1(iii).

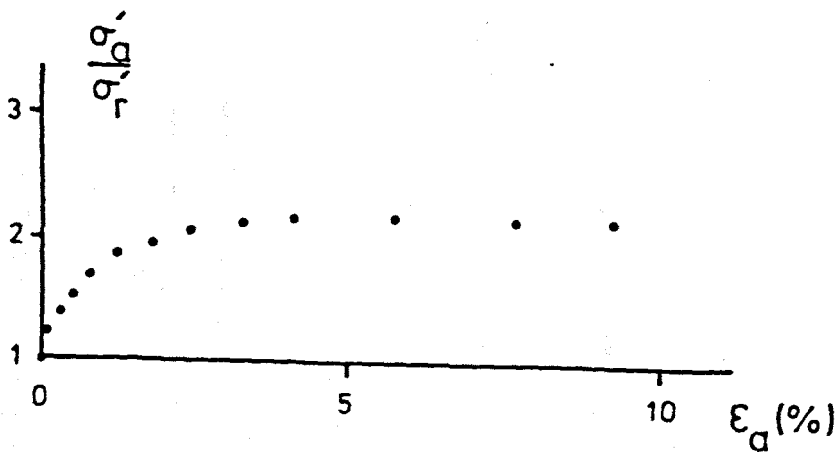

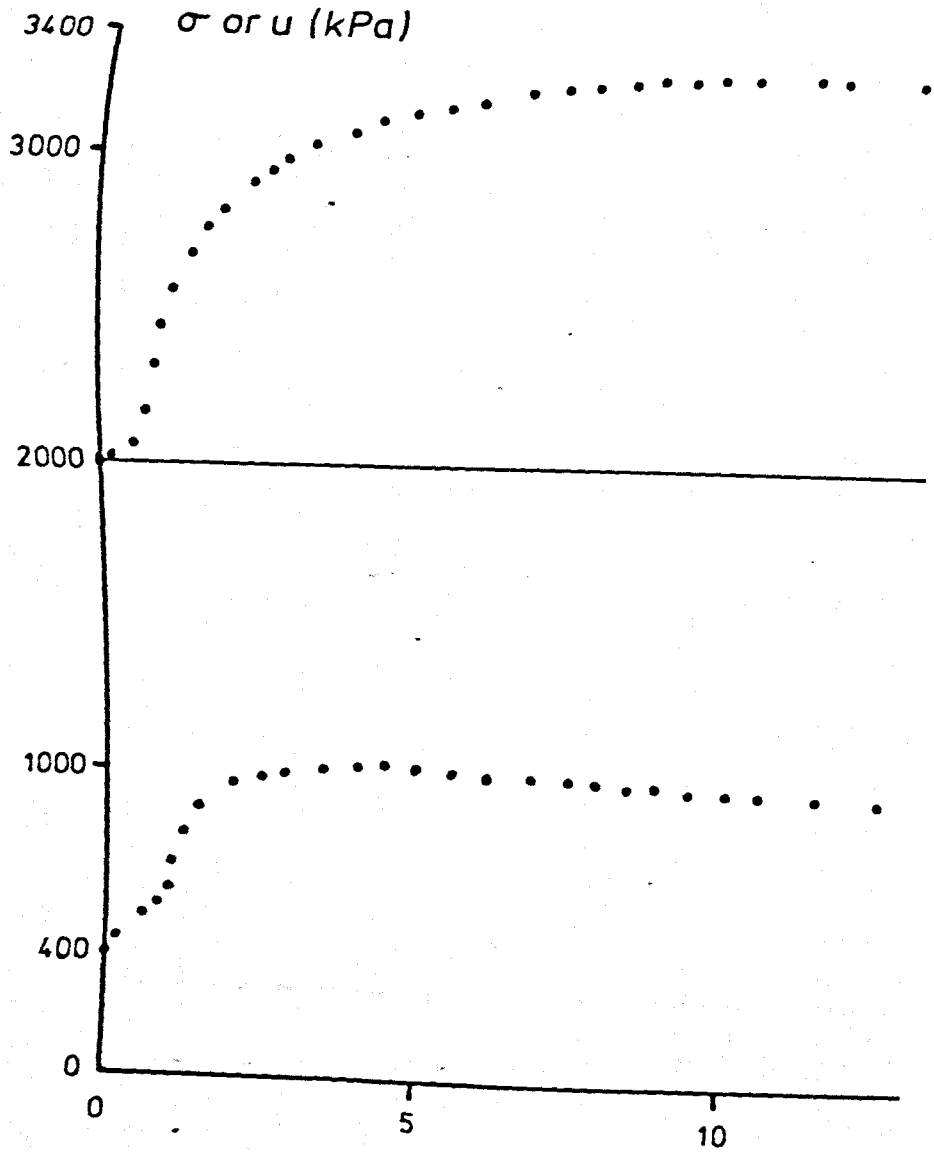
σ or u (kPa)
3400
3000
2000
1000
400
0
0
5
10

Figure 7.31 CU triaxial test results : UA1(v).

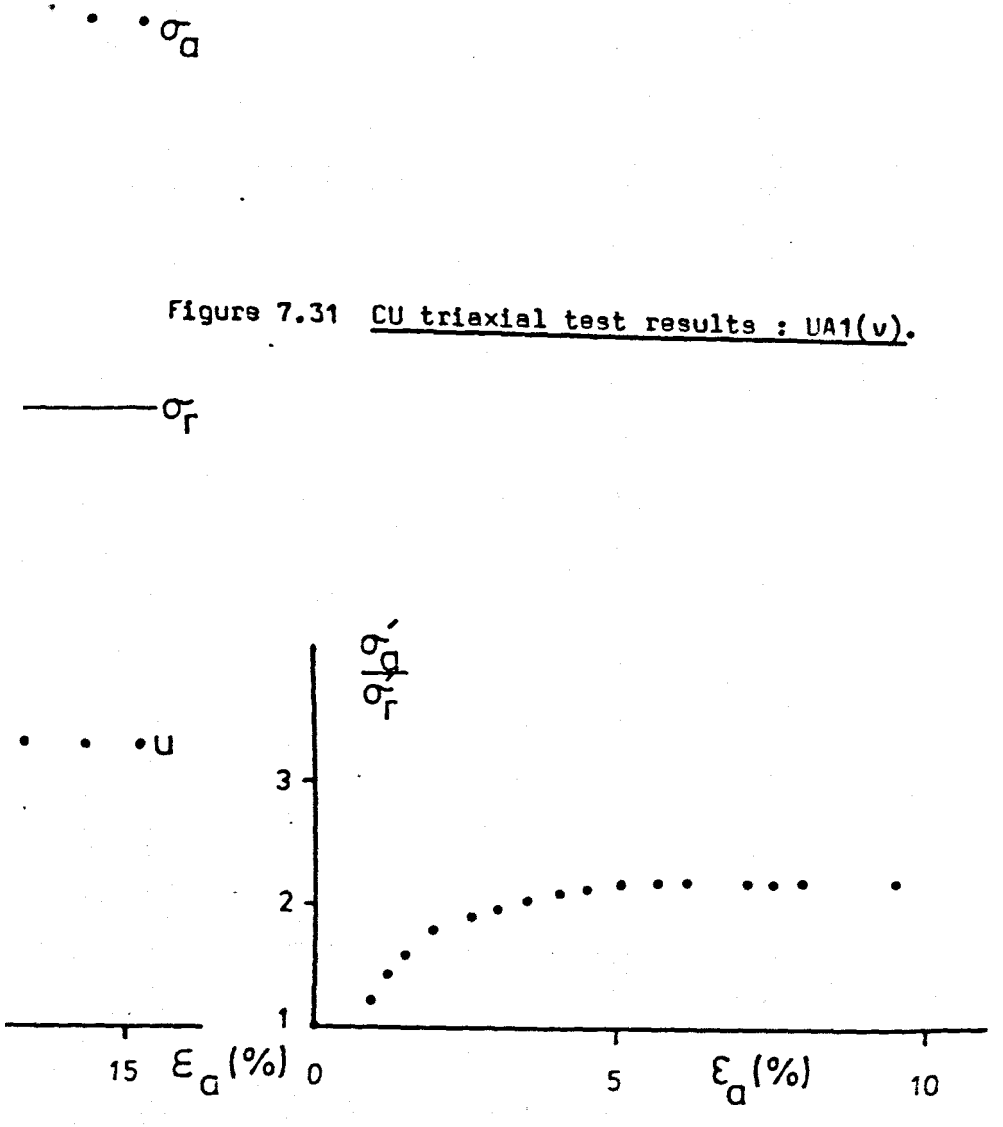

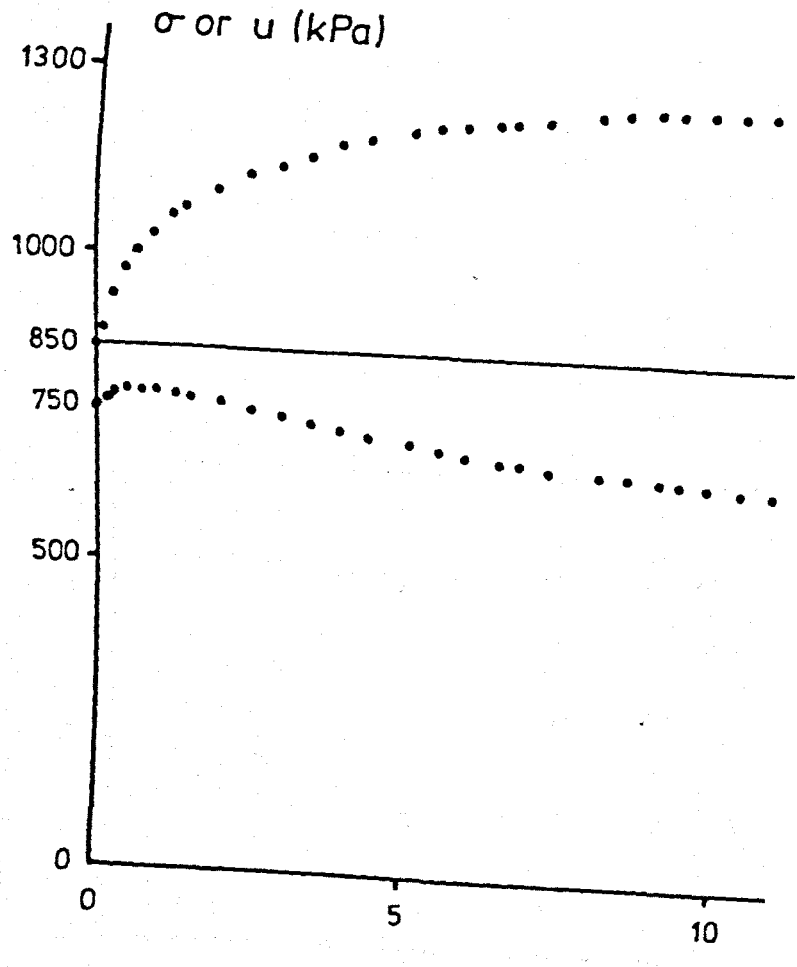
σ or u (kPa)
1300
1000
850
750
500
0
0
5
10

Figure 7.32 CU triaxial test results : UA2(i).

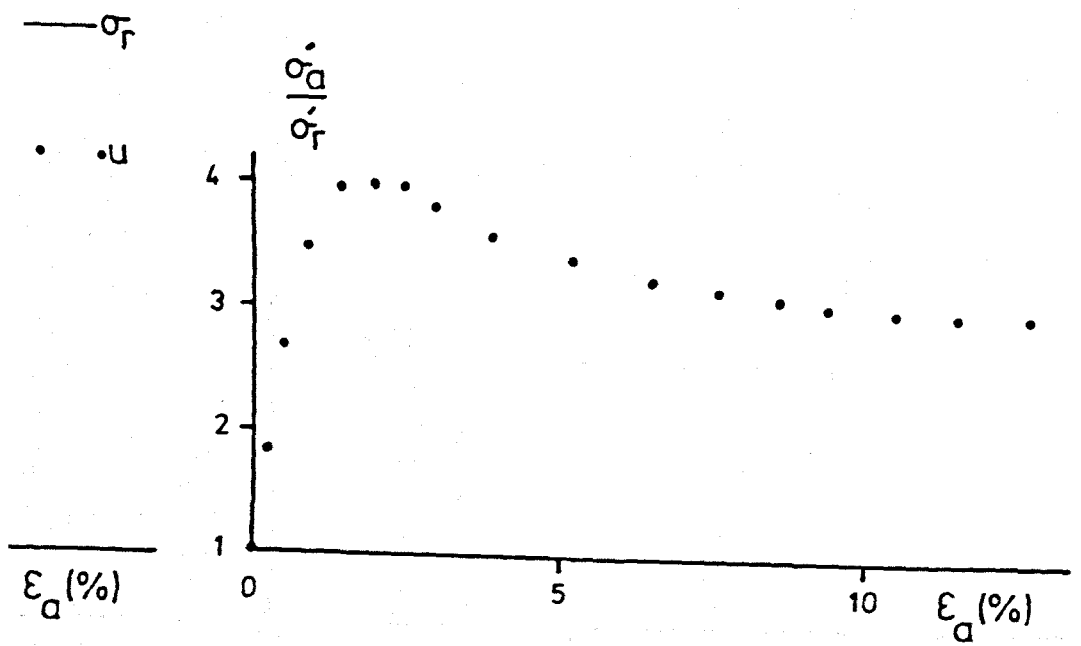

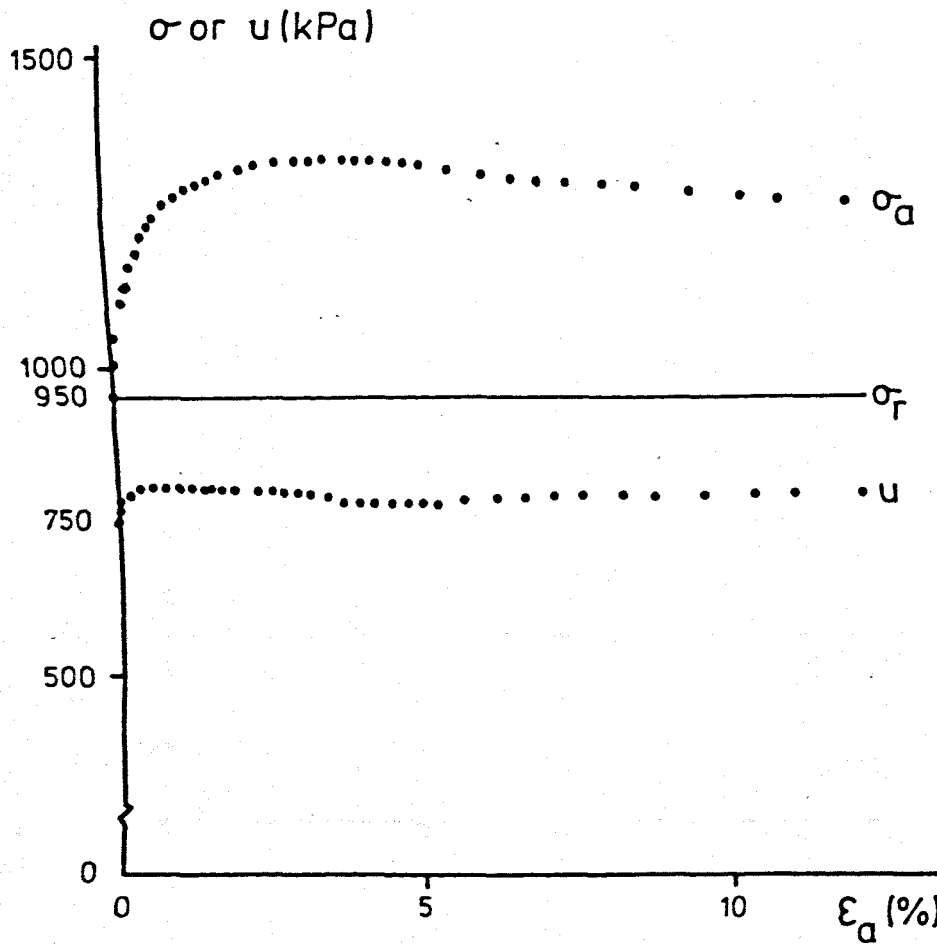
σ or u (kPa)
1500
1000
950
750
500
0
0
5
10
ε_a (%)
σ_a
σ_r
u

Figure 7.33 CU triaxial test results : UA2(ii).

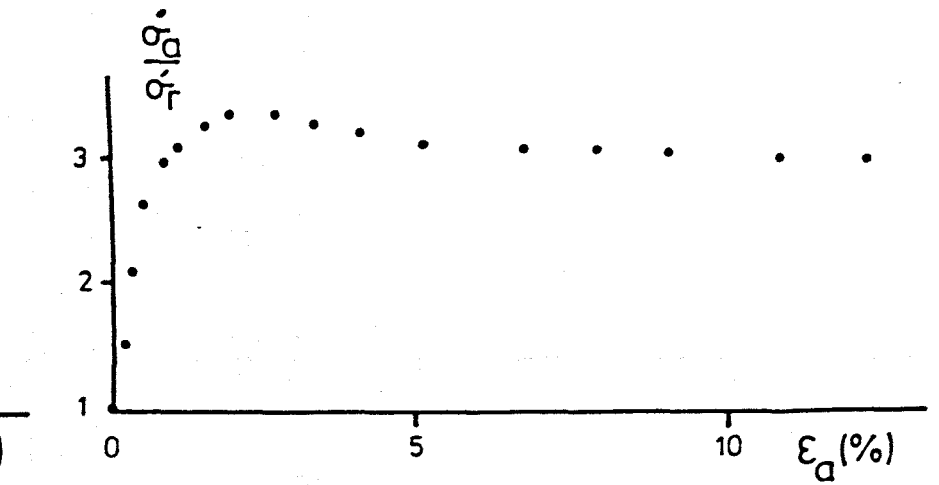

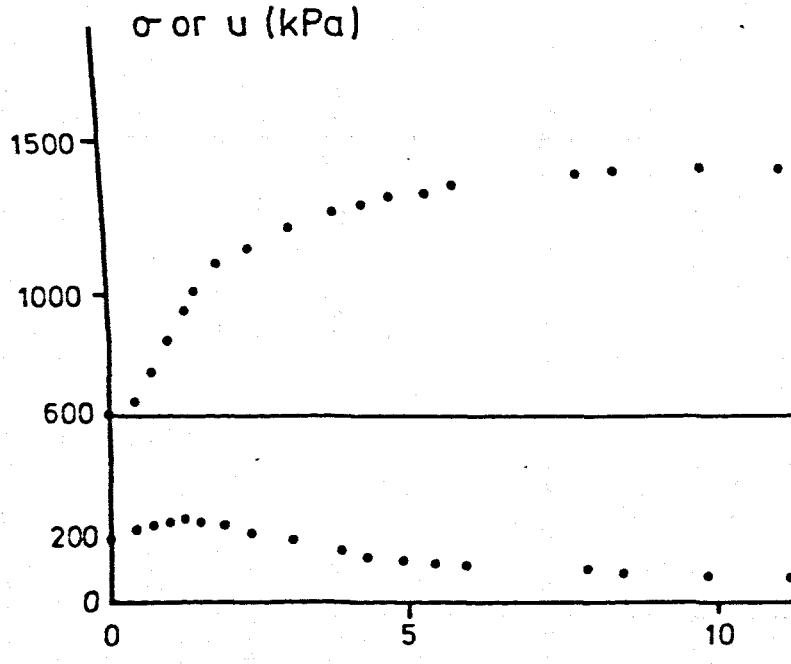
σ or u (kPa)
1500
1000
600
200
0
0
5
10

Figure 7.34 CU triaxial test results : UA2(iii).

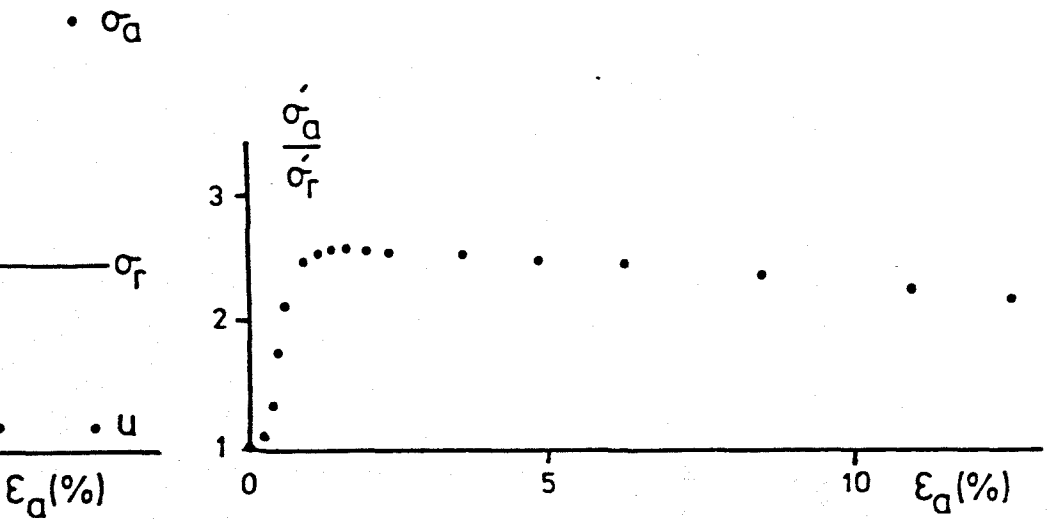

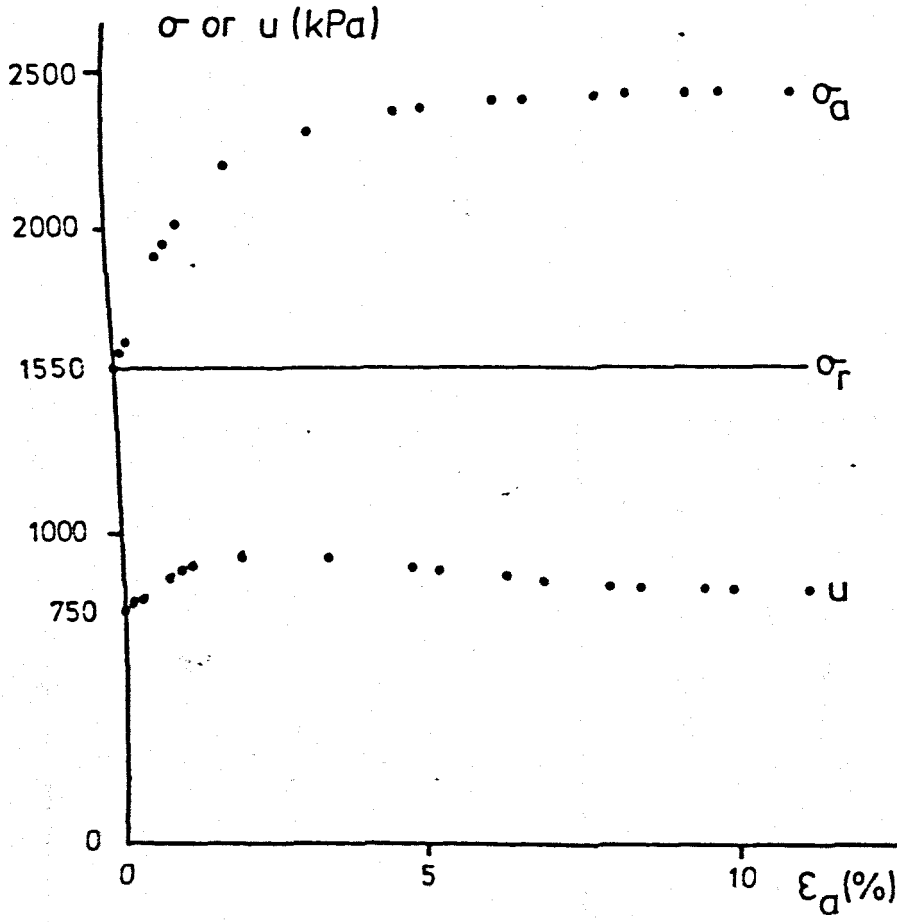
σ or u (kPa)
2500
2000
1550
1000
750
0
0
5
10
ε_a(%)
σ_a
σ_r
u

Figure 7.35 CU triaxial test results : U8(i).

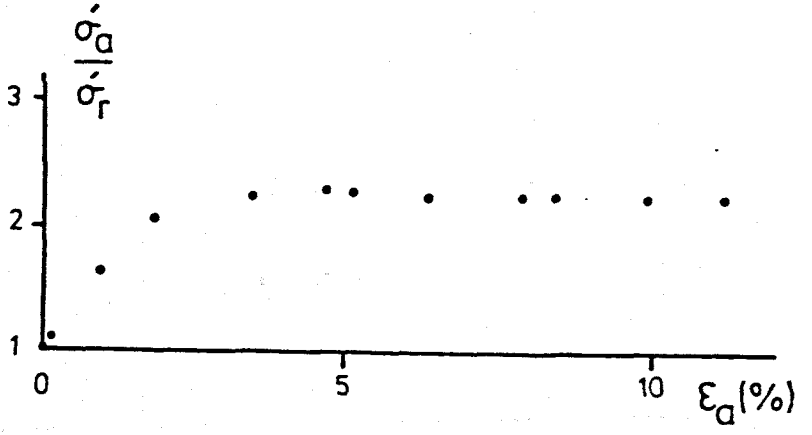

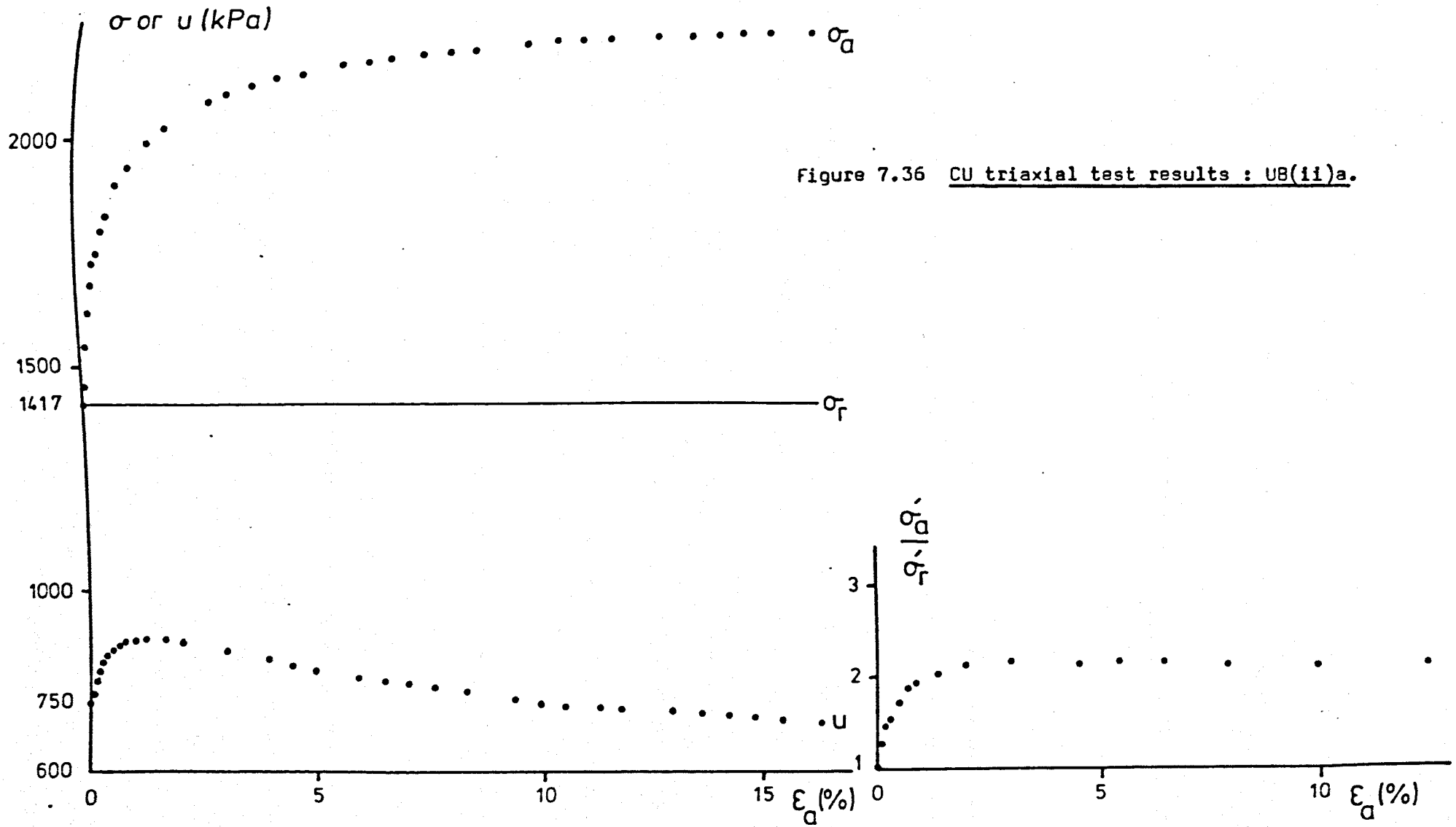

Figure 7.36 CU triaxial test results : UB(ii)a.

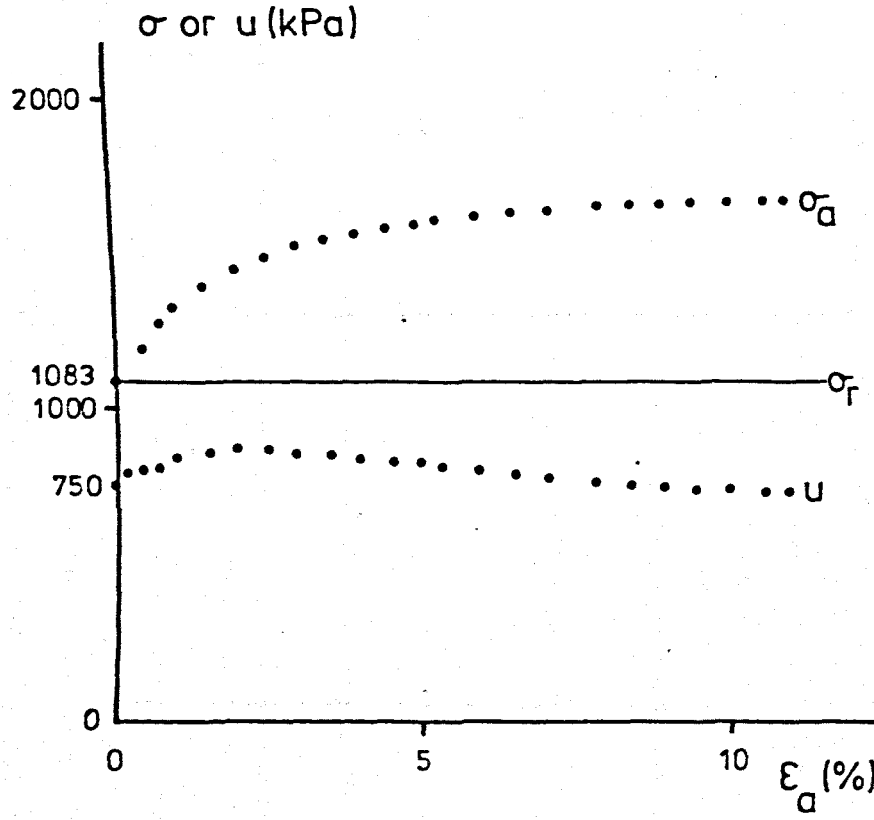
σ or u (kPa)
2000
1083
1000
750
0
0
5
10
ε_a (%)
σ_a
σ_r
u

Figure 7.37 CU triaxial test results : UB(ii)b.

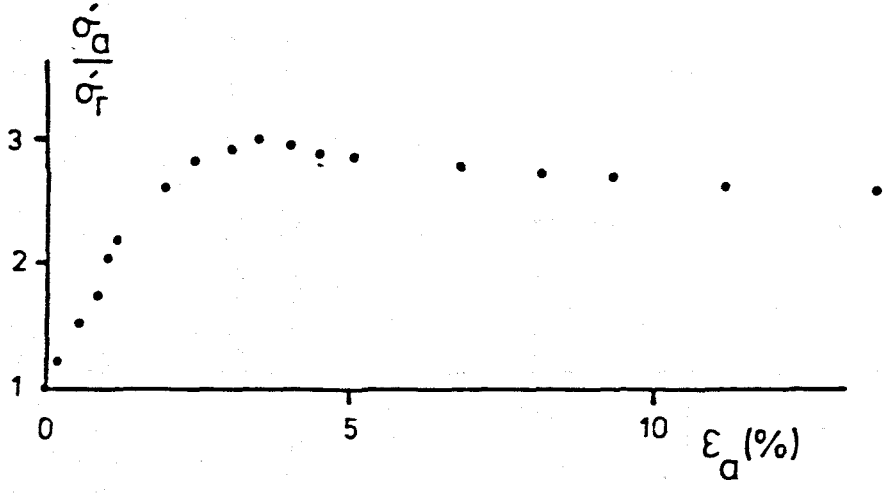

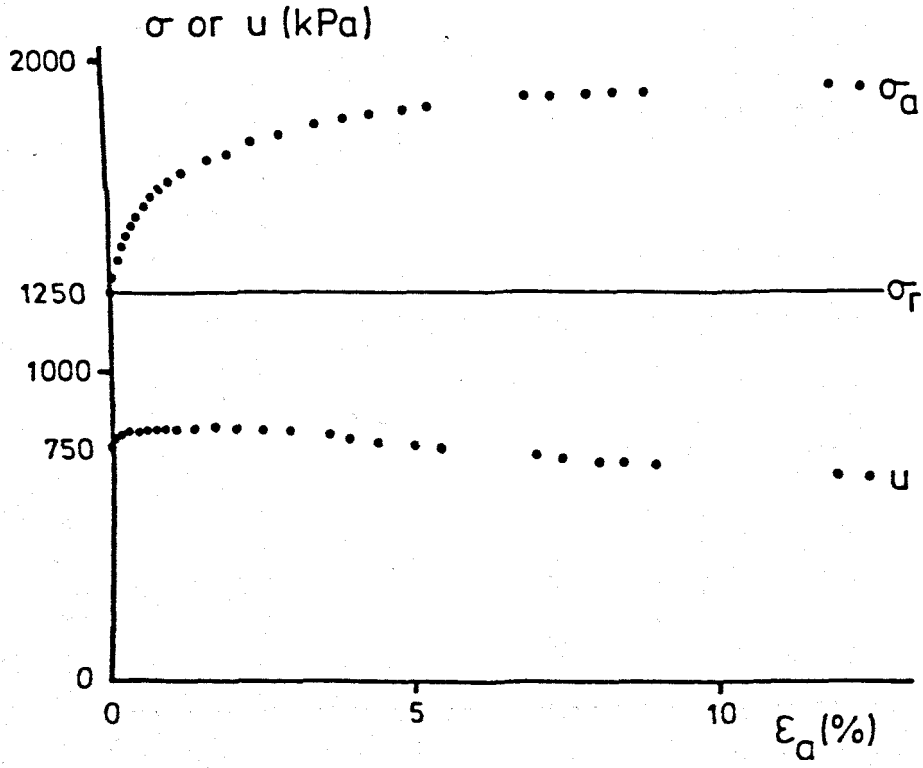
σ or u (kPa)
2000
1250
1000
750
0
0
5
10
ε_a(%)
σ_a
σ_r
u

Figure 7.38 CU triaxial test results : UB(iii).

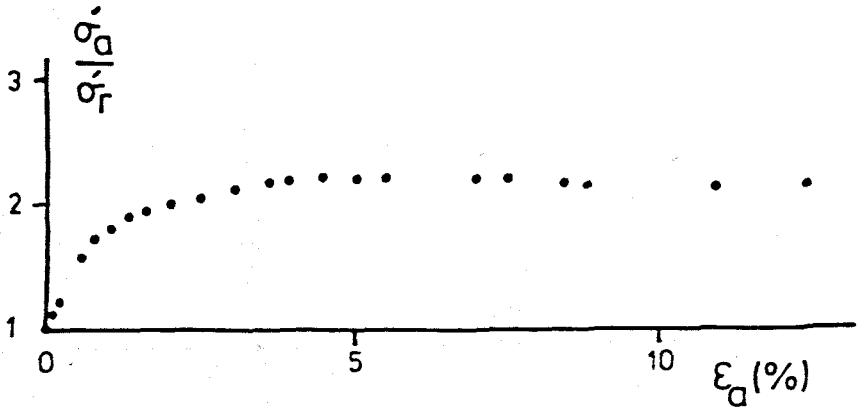

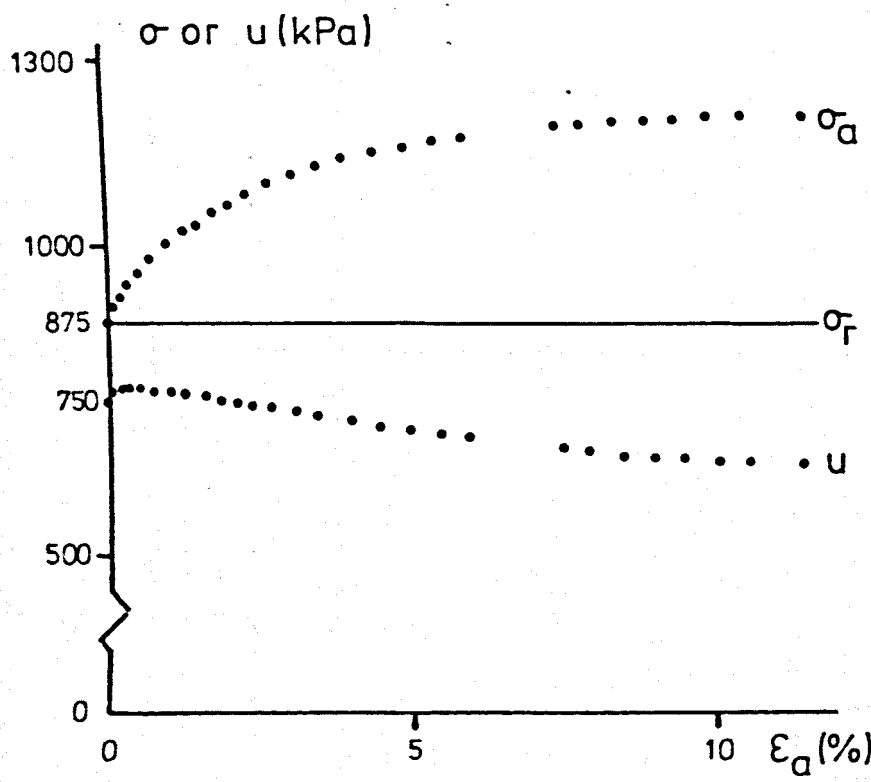
σ or u (kPa)
1300
1000
875
750
500
0
0
5
10
ε_a (%)
σ_a
σ_r
u

Figure 7.39 CU triaxial test results : UB(v).

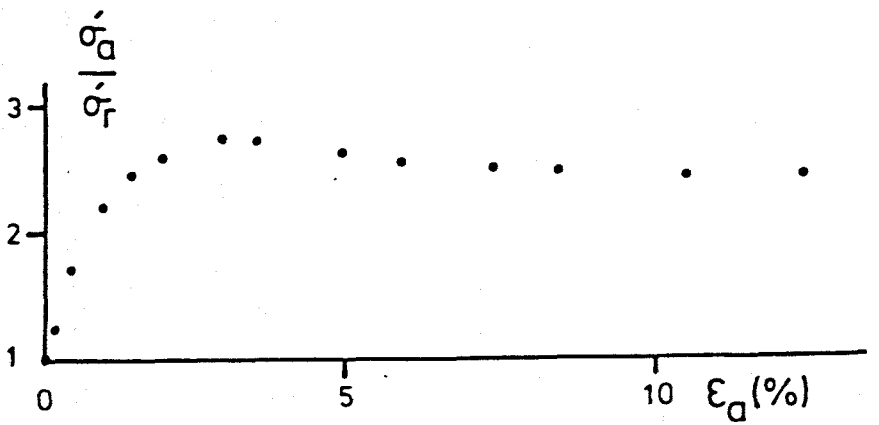

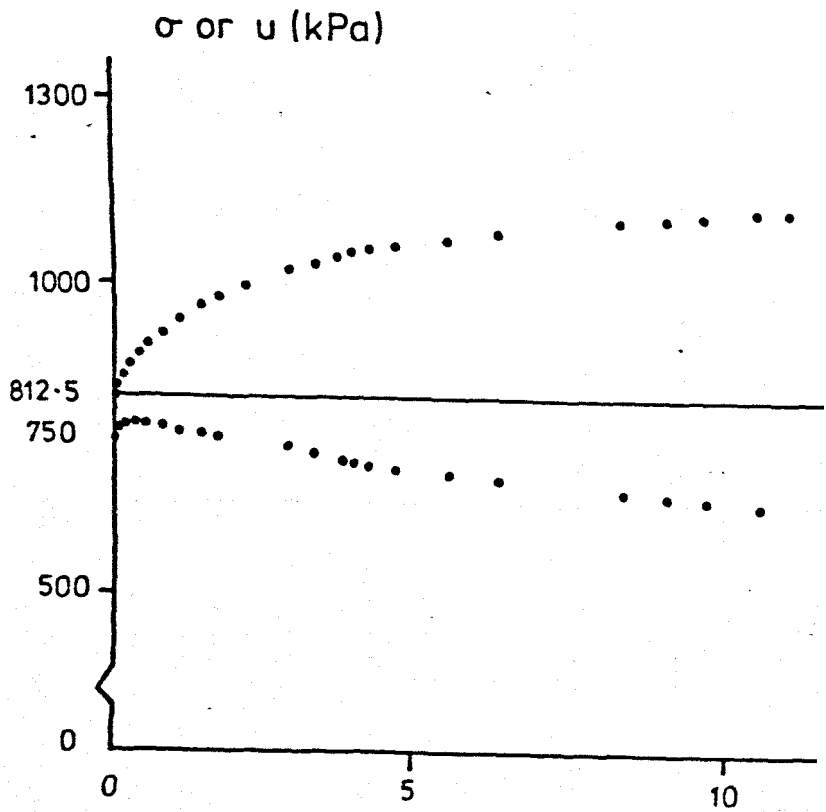
σ or u (kPa)
1300
1000
812·5
750
500
0
0
5
10

Figure 7.40 CU triaxial test results : UB(vi).

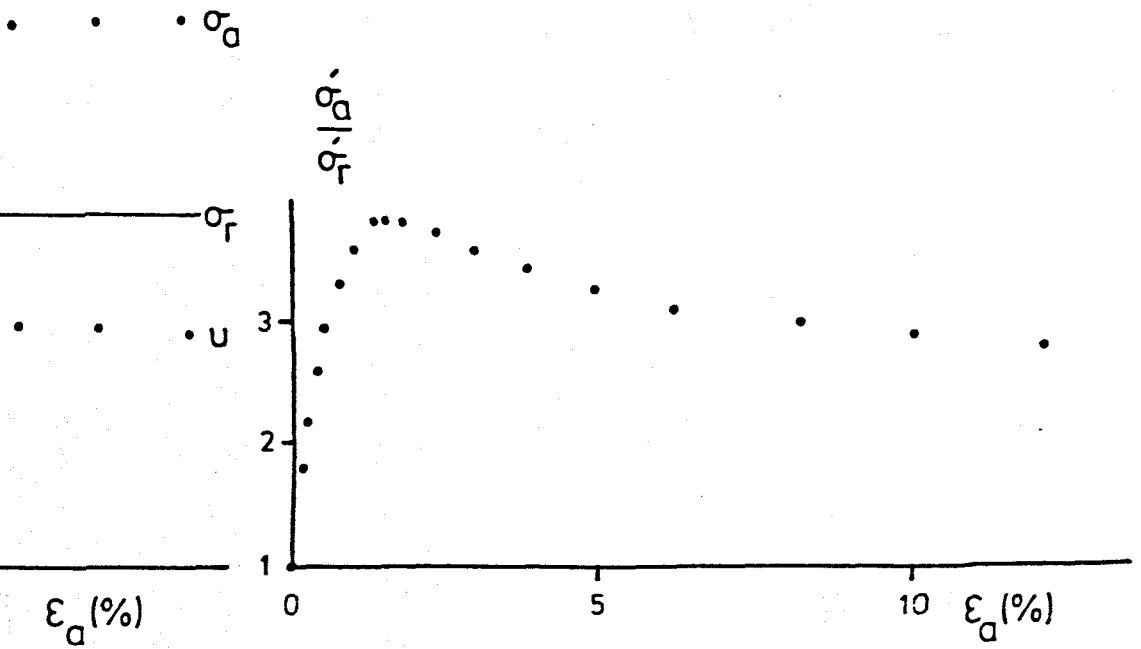

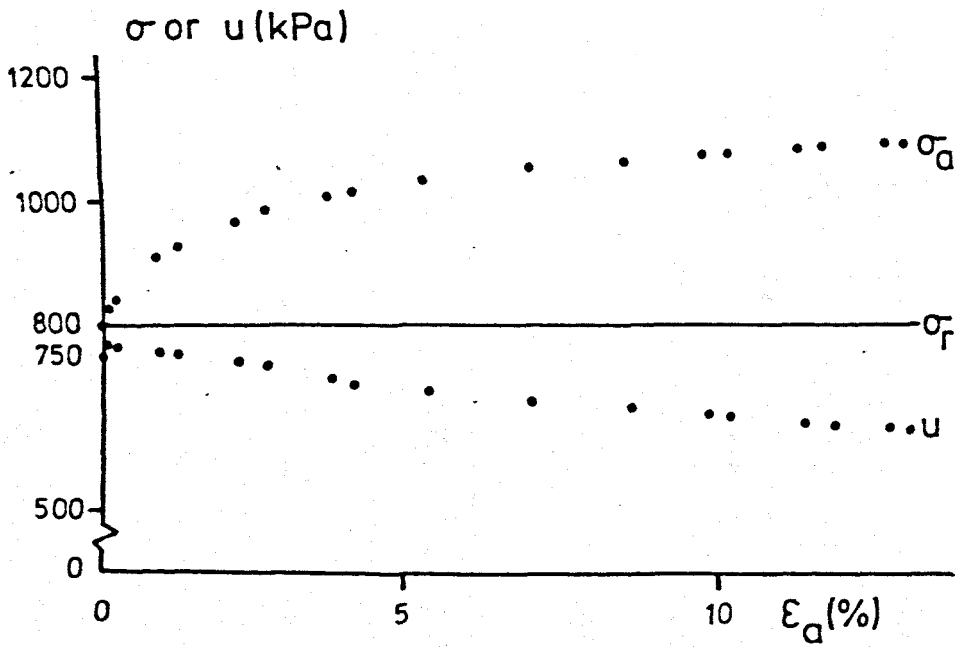
σ or u (kPa)
1200
1000
800
750
500
0
0
5
10
ε_a(%)
σ_a
σ_r
u

Figure 7.41 CU triaxial test results : UB(vii).

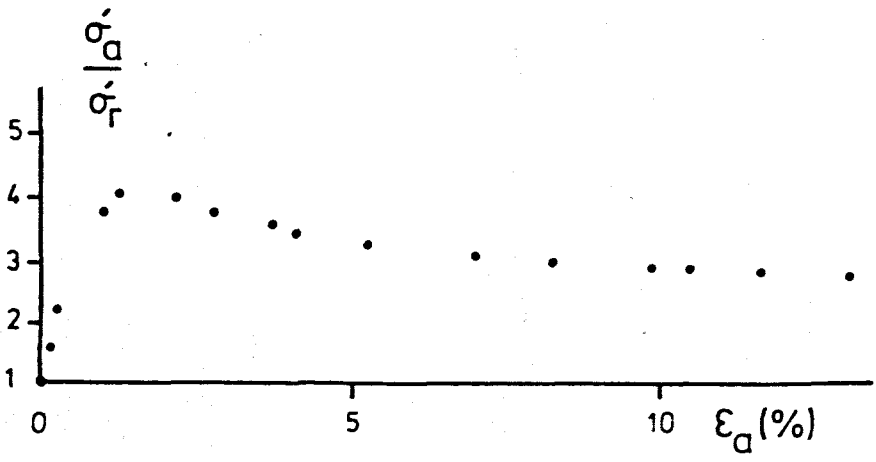

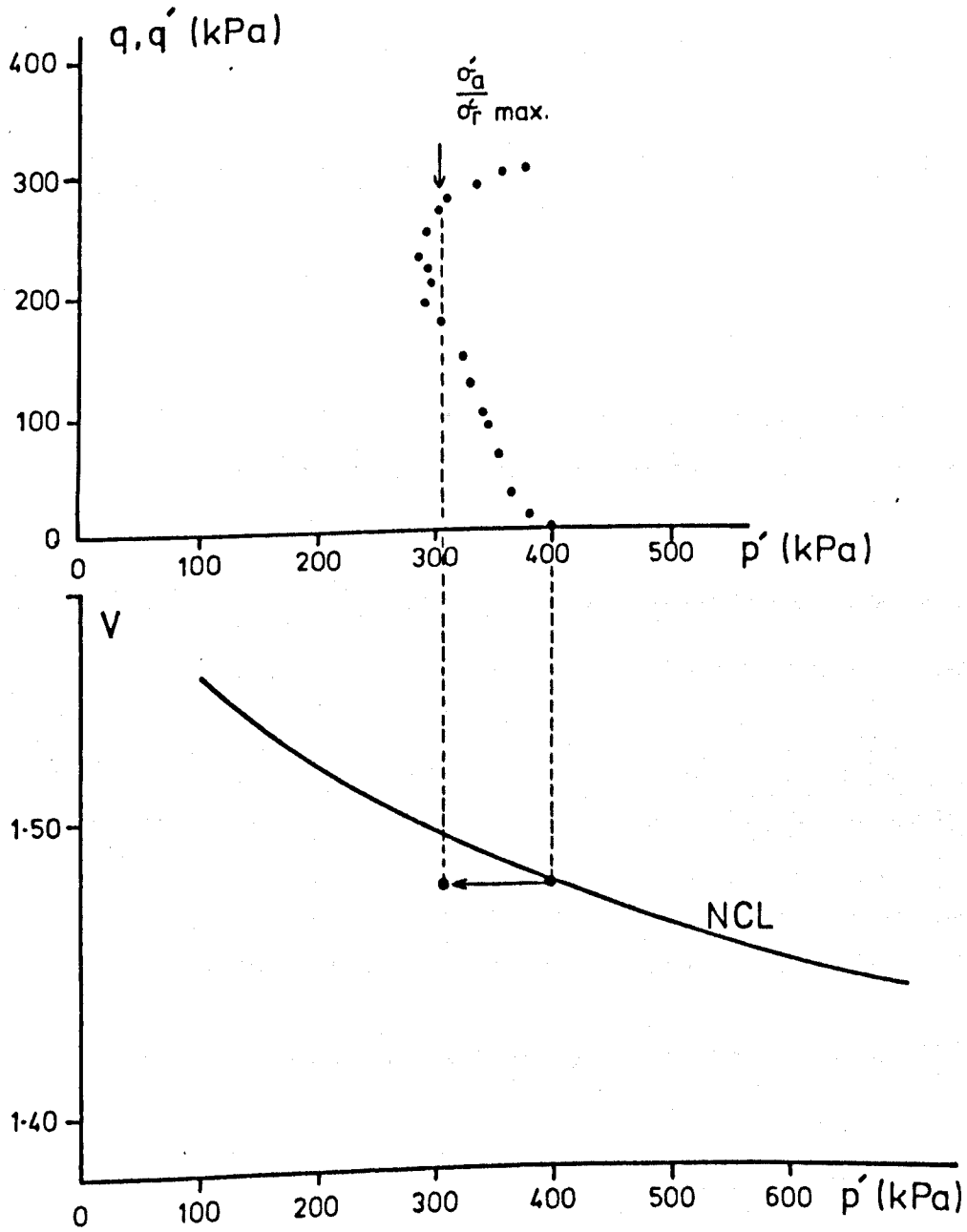

Figure 7.42 q , q′ : p′ and V : p′ : RA1(i).

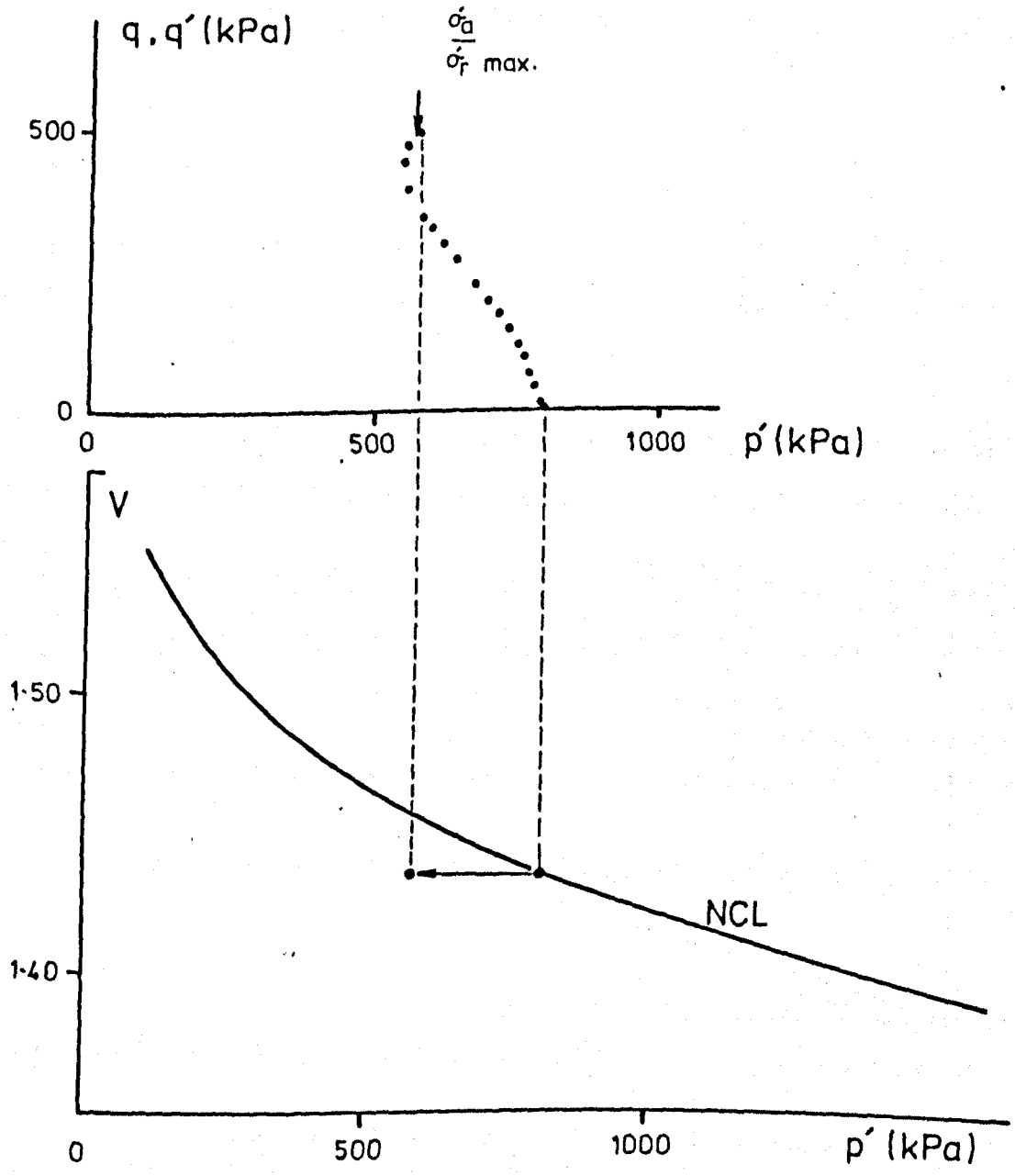

Figure 7.43 q , q′ : p′ and V : p′ : RA1(ii).

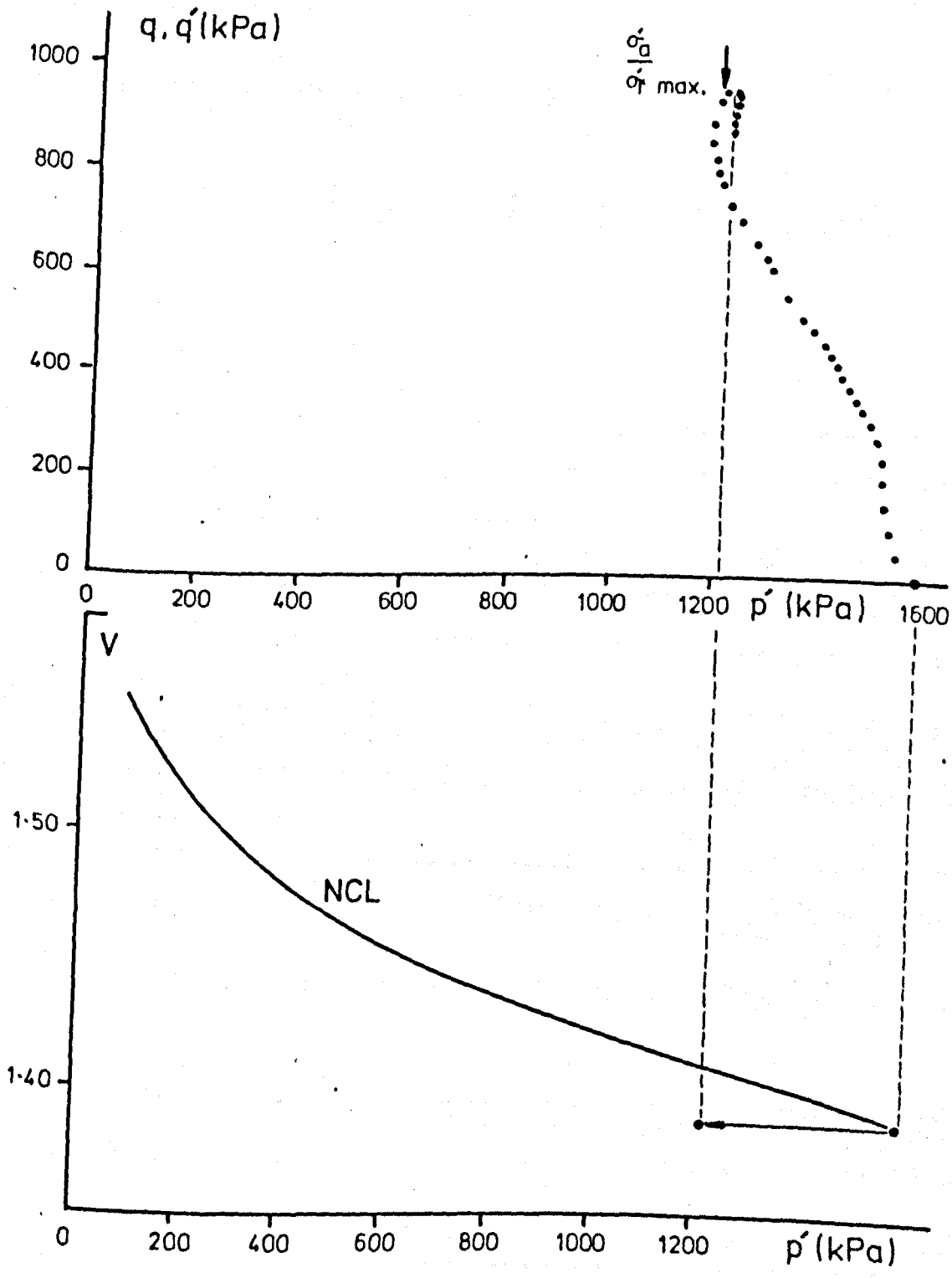

Figure 7.44 q , q′ : p′ and V : p′ : RA1(iii).

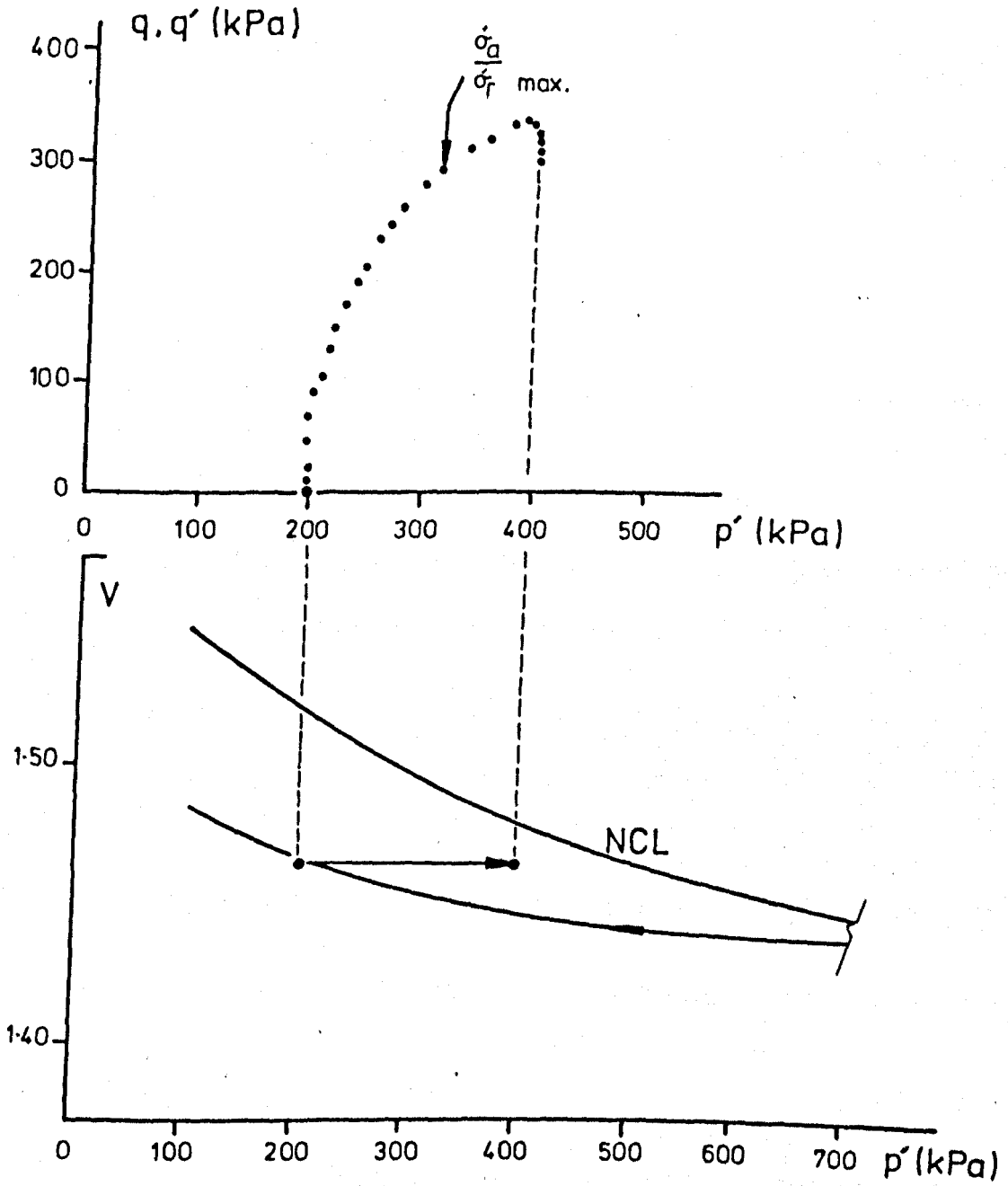

Figure 7.45 q , q′ : p′ and V : p′ : RA2(ii).

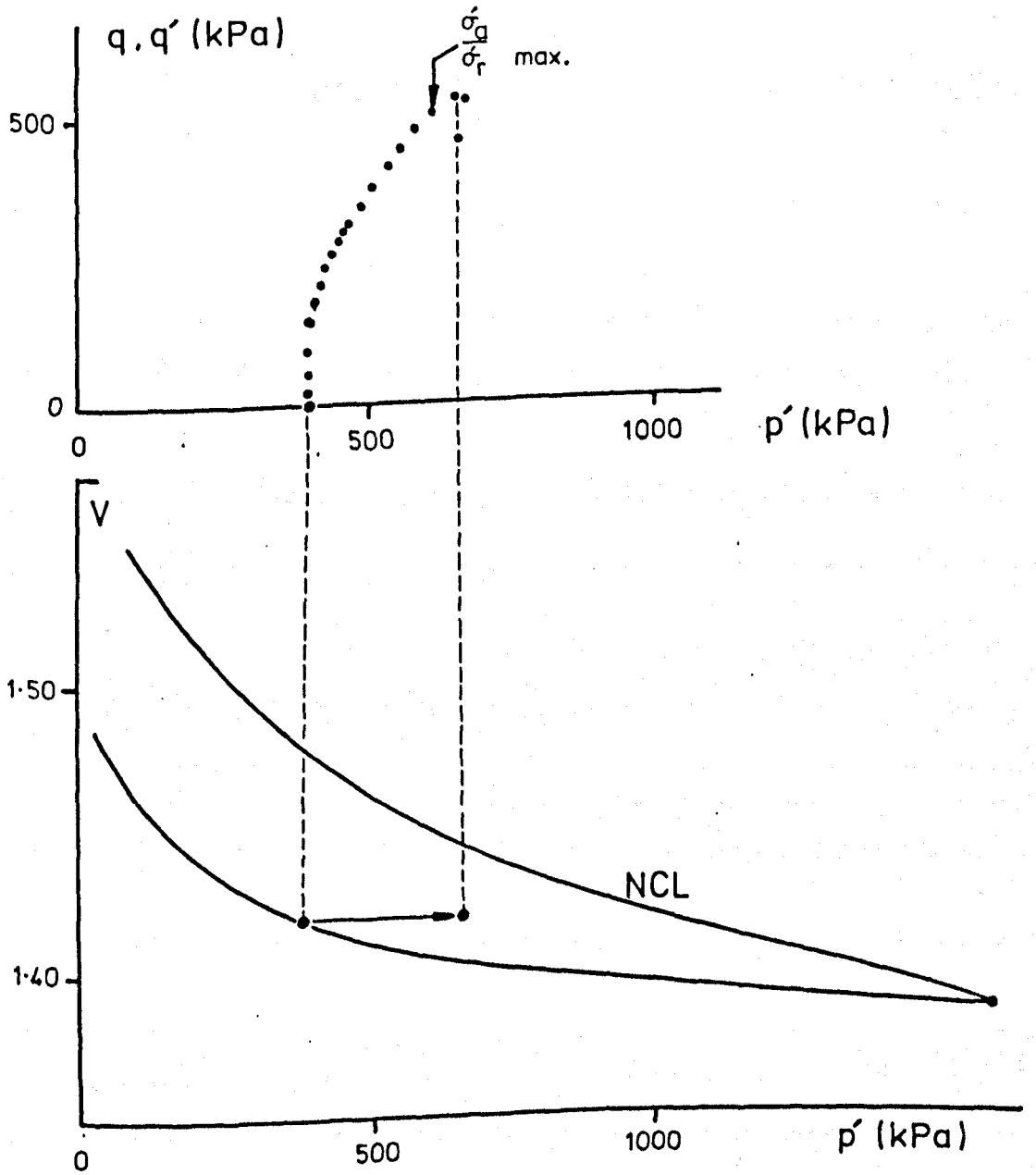

Figure 7.46 q , q′ : p′ and V : p′ : RA2(iii).

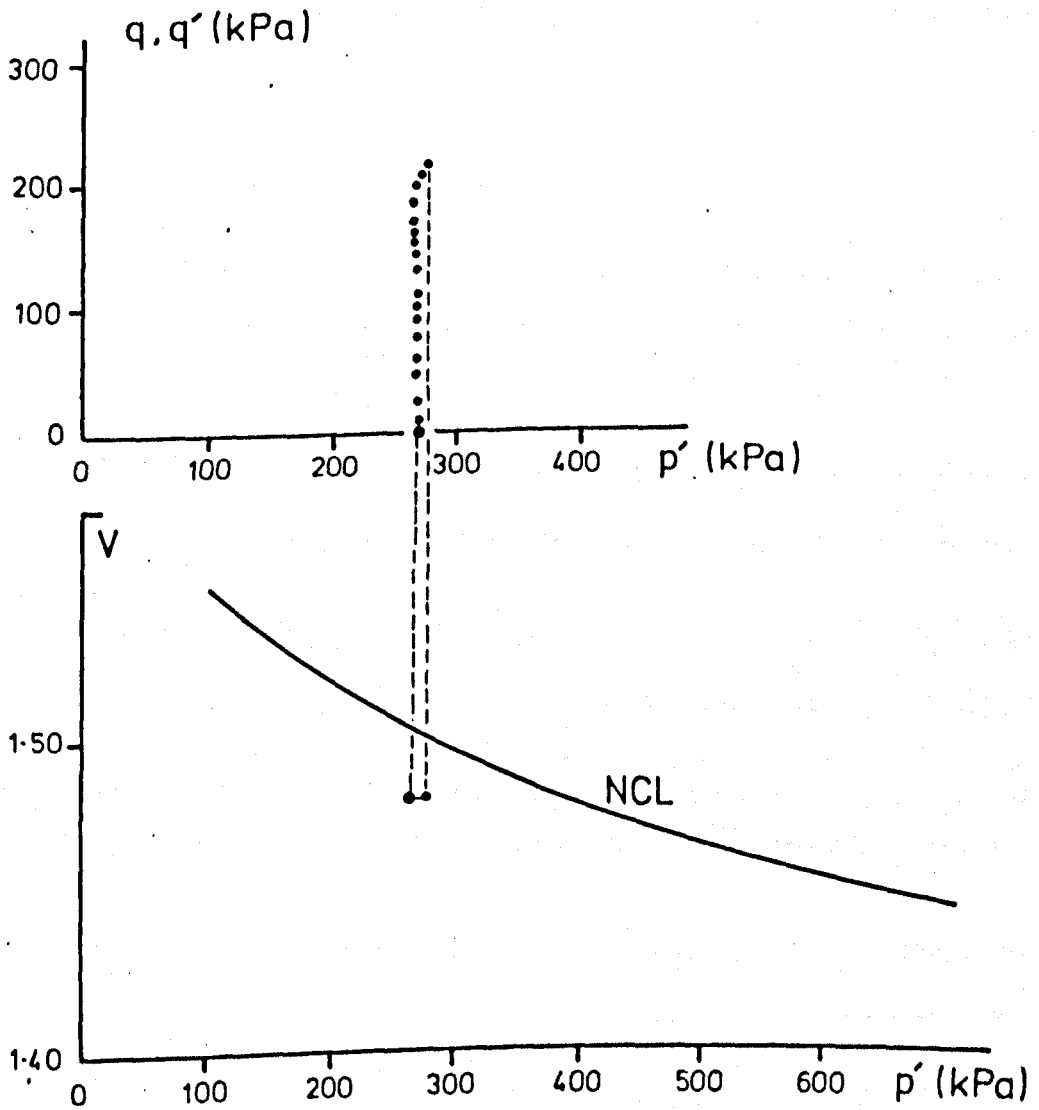

Figure 7.47 q , q′ : p′ and V : p′ : RB(ii).

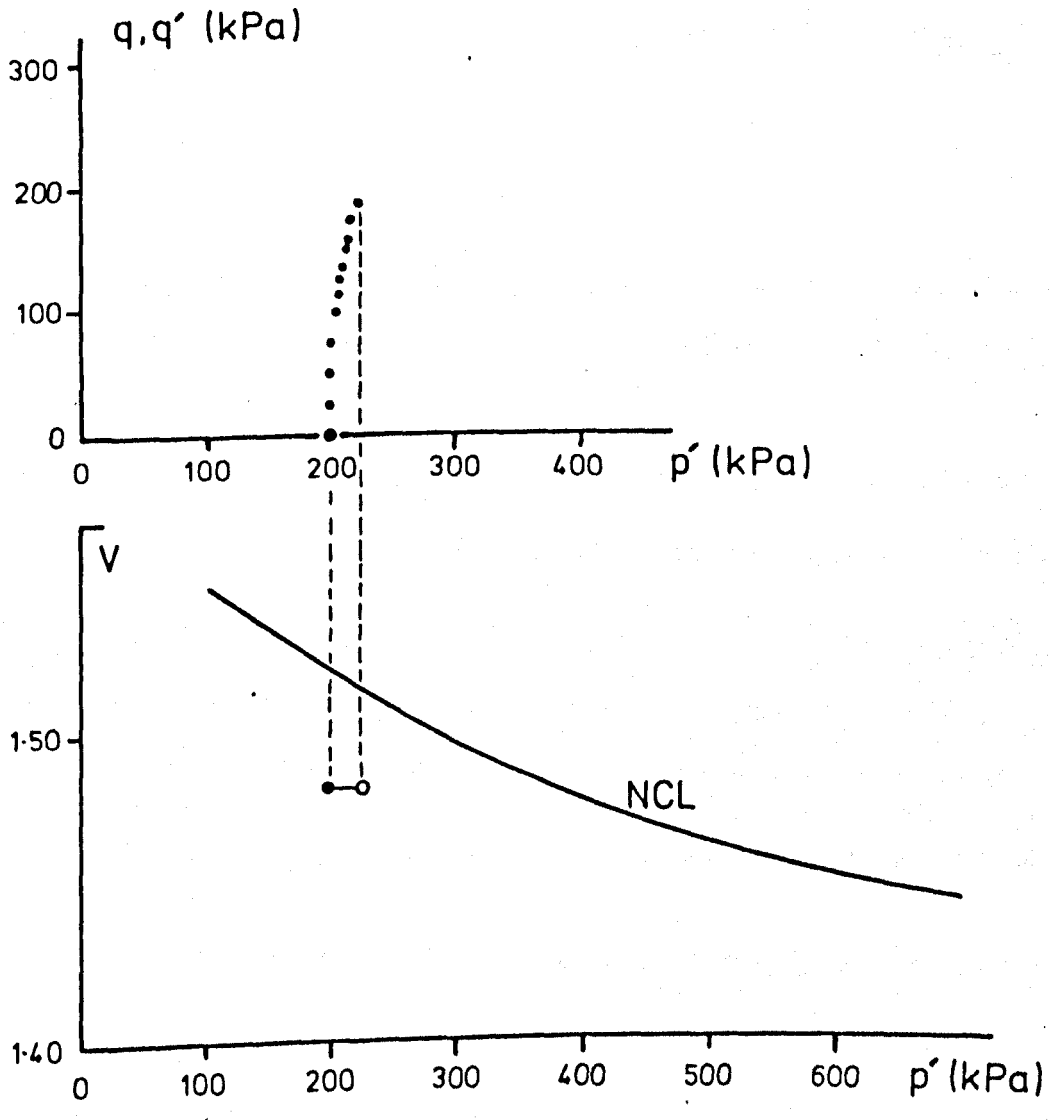

Figure 7.48 q , q′: p′ and V : p′: RB(iii).

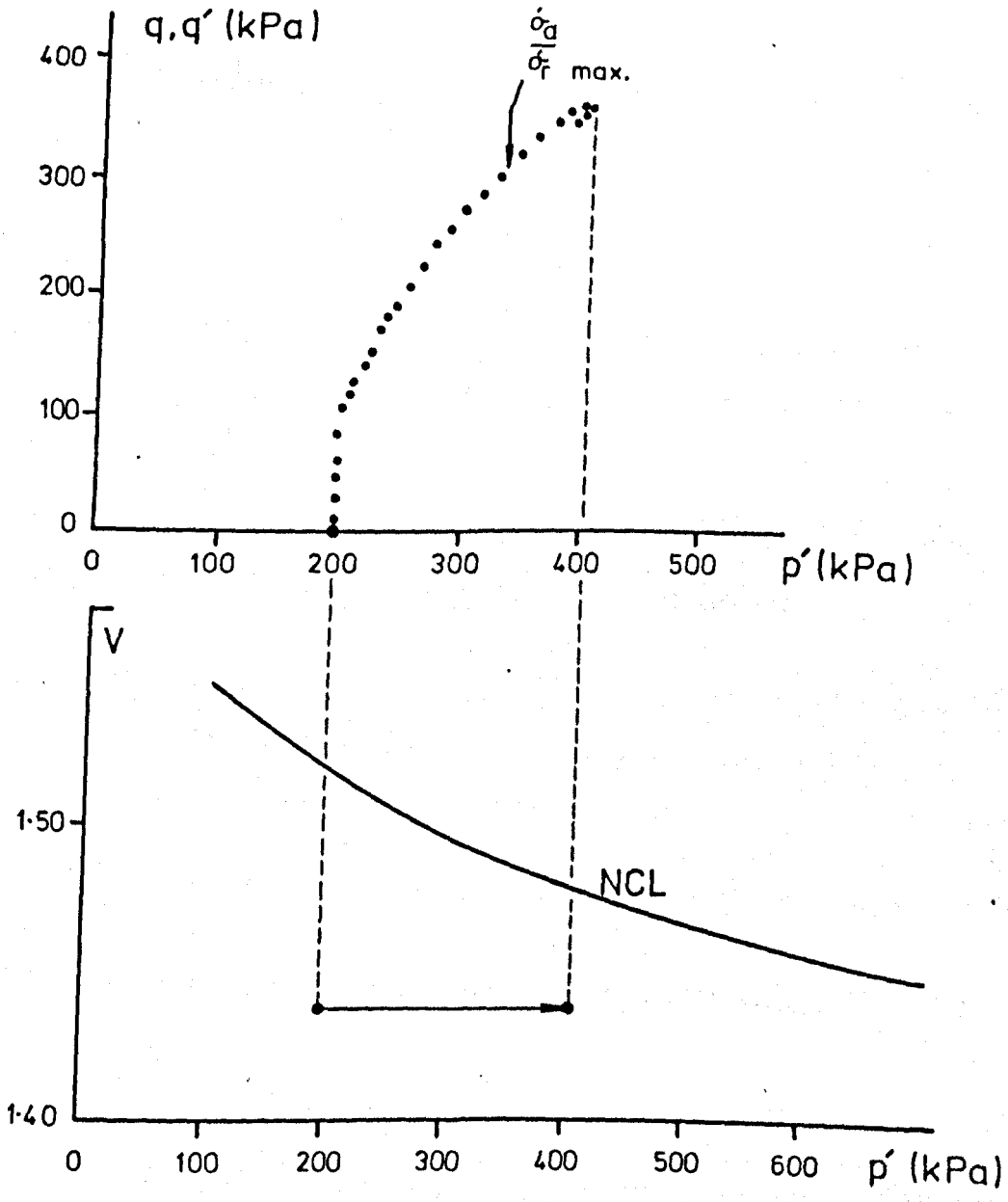

Figure 7.49 q , q′ : p′ and V : p′ : RB(v).

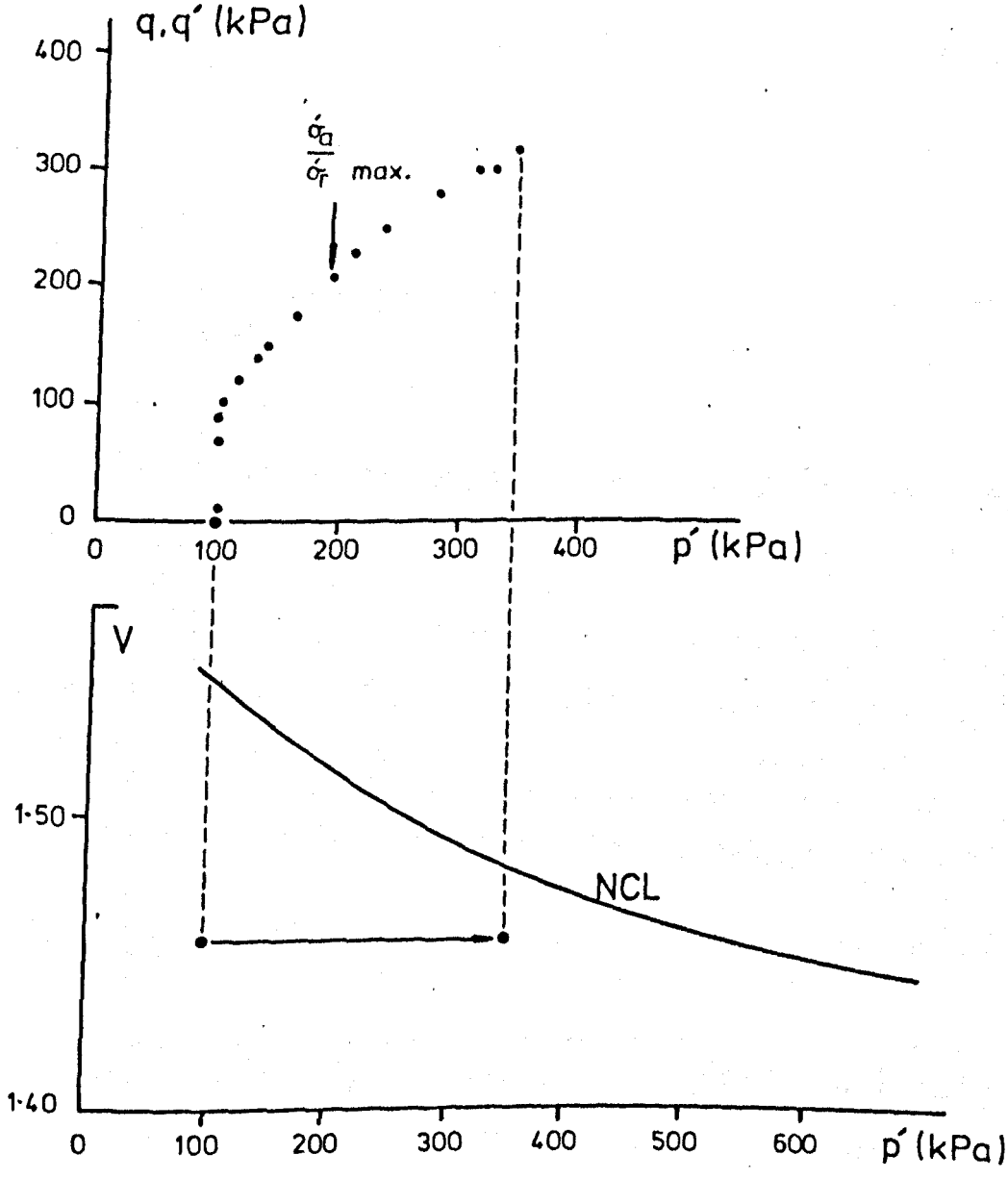

Figure 7.50 q , q′ : p′ and V : p′ : R2 - 02.

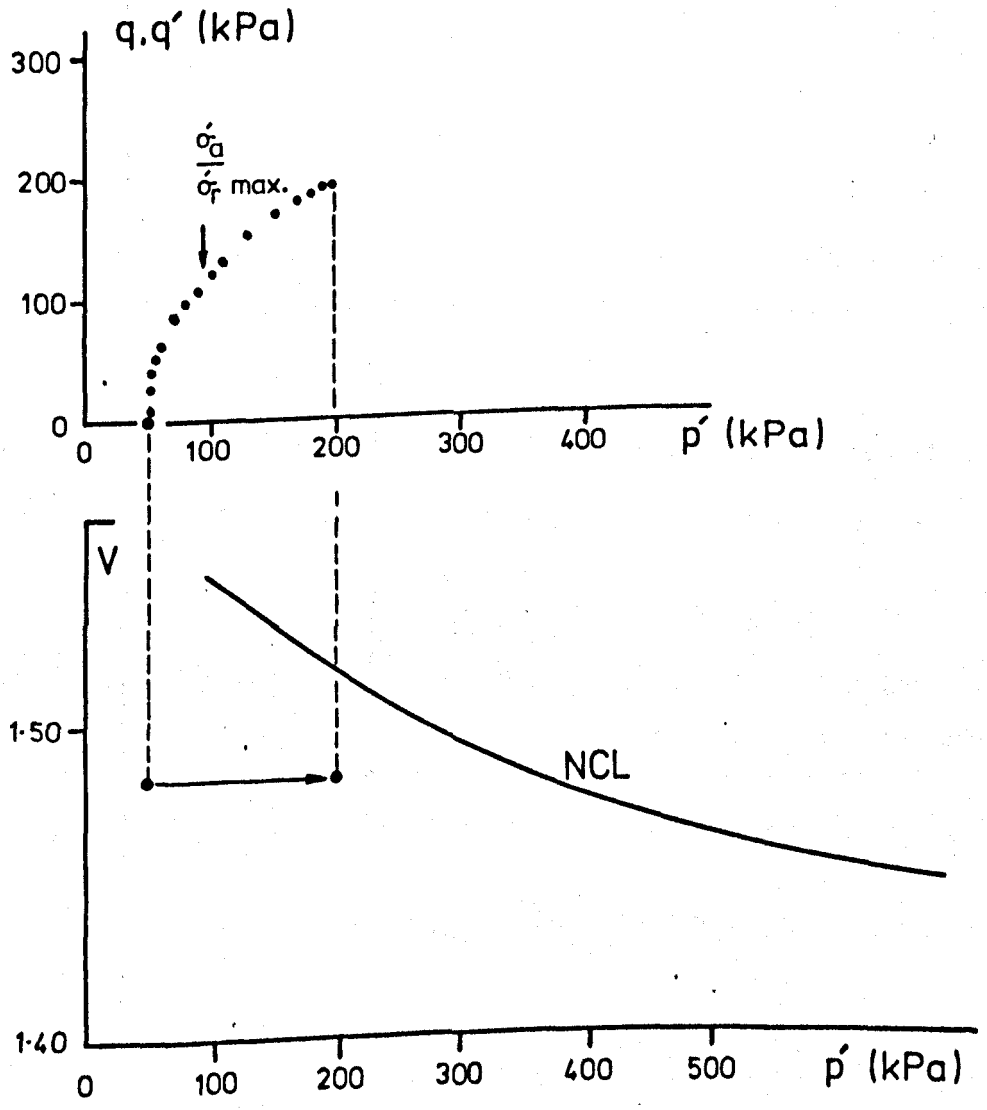

Figure 7.51 q , q′ : p′ and V : p′ : R2 - 03.

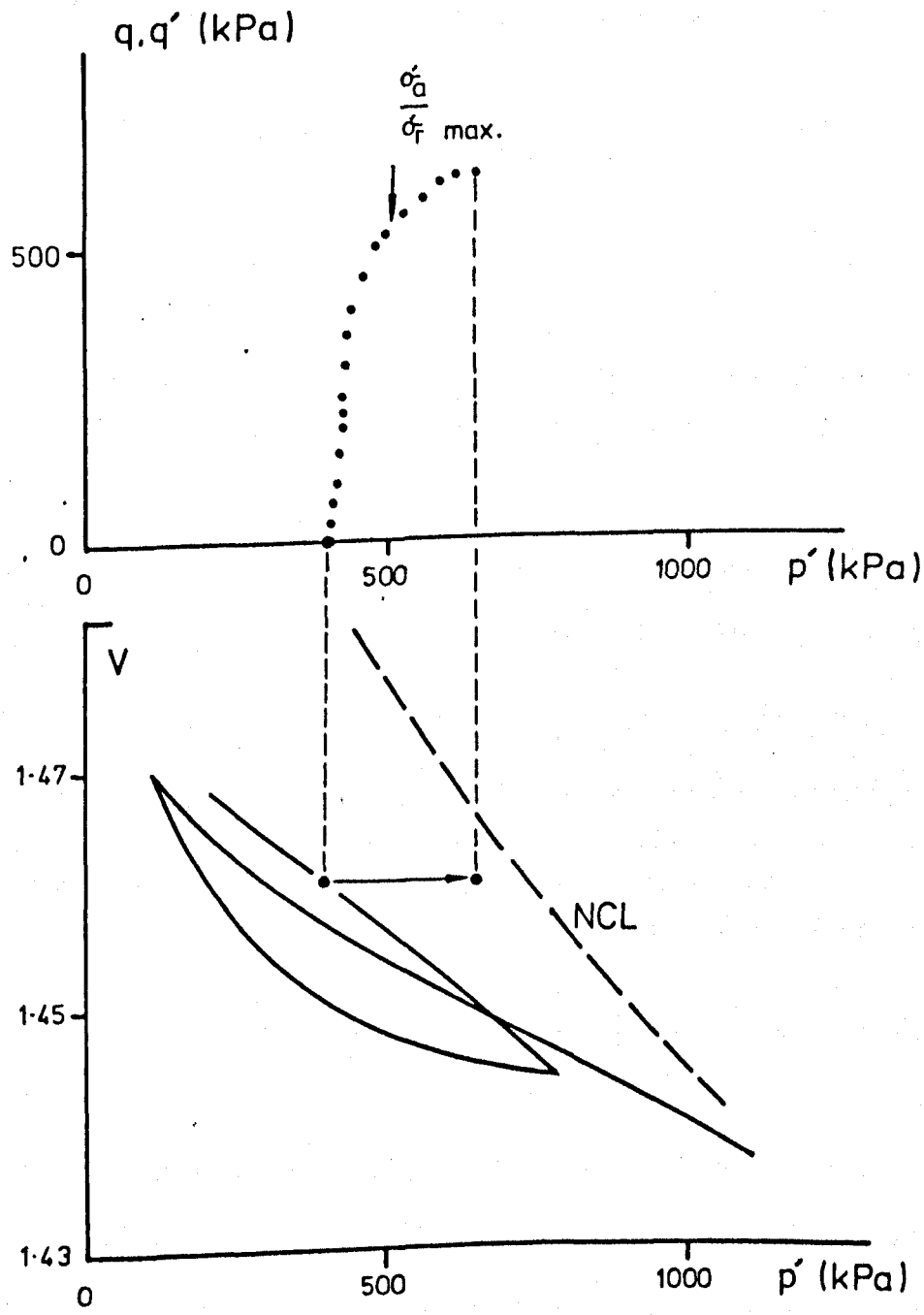

Figure 7.52 q , q′ : p′ and V : p′ : UA1(i).

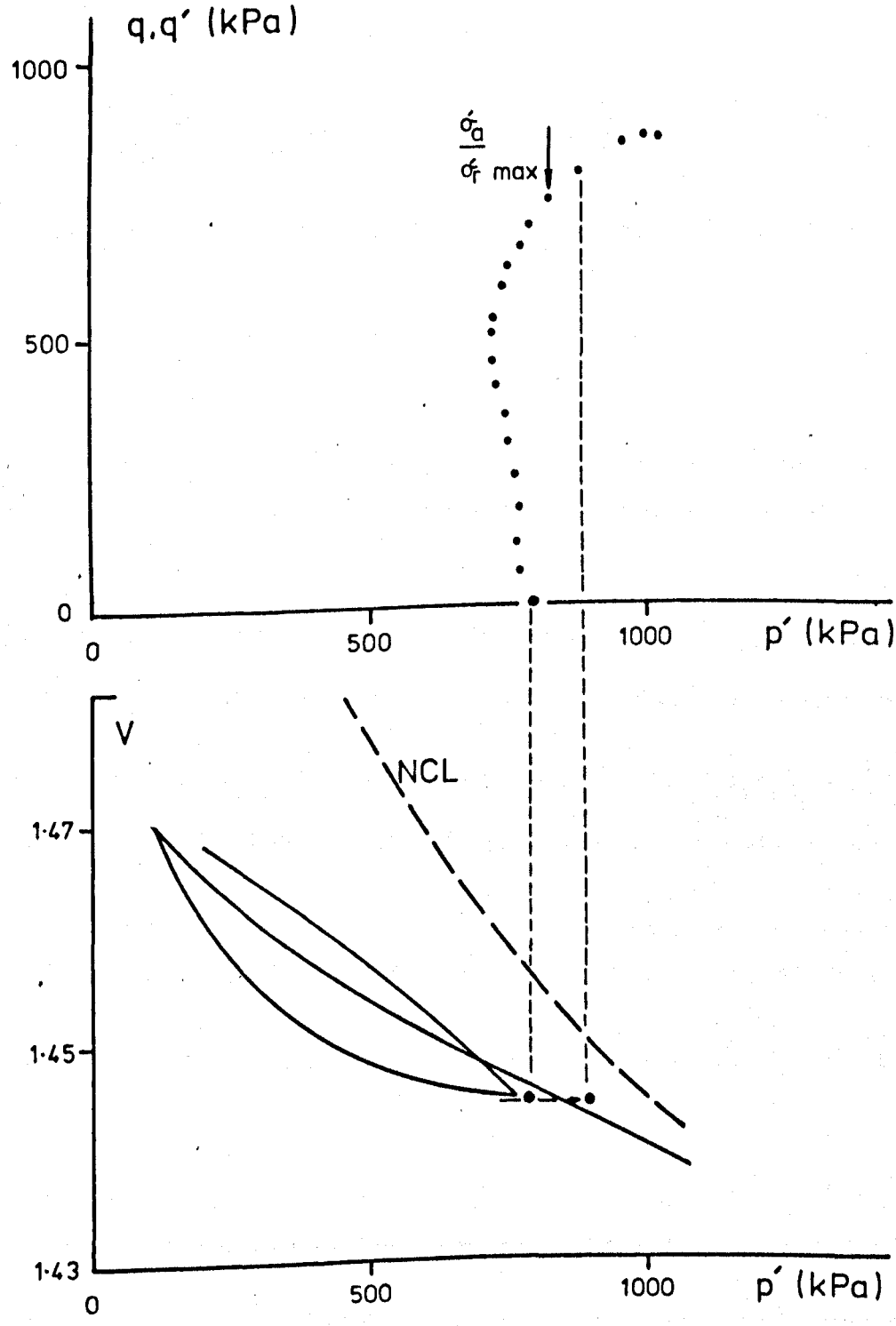

Figure 7.53 q , q′ : p′ and V : p′ : UA1(ii).

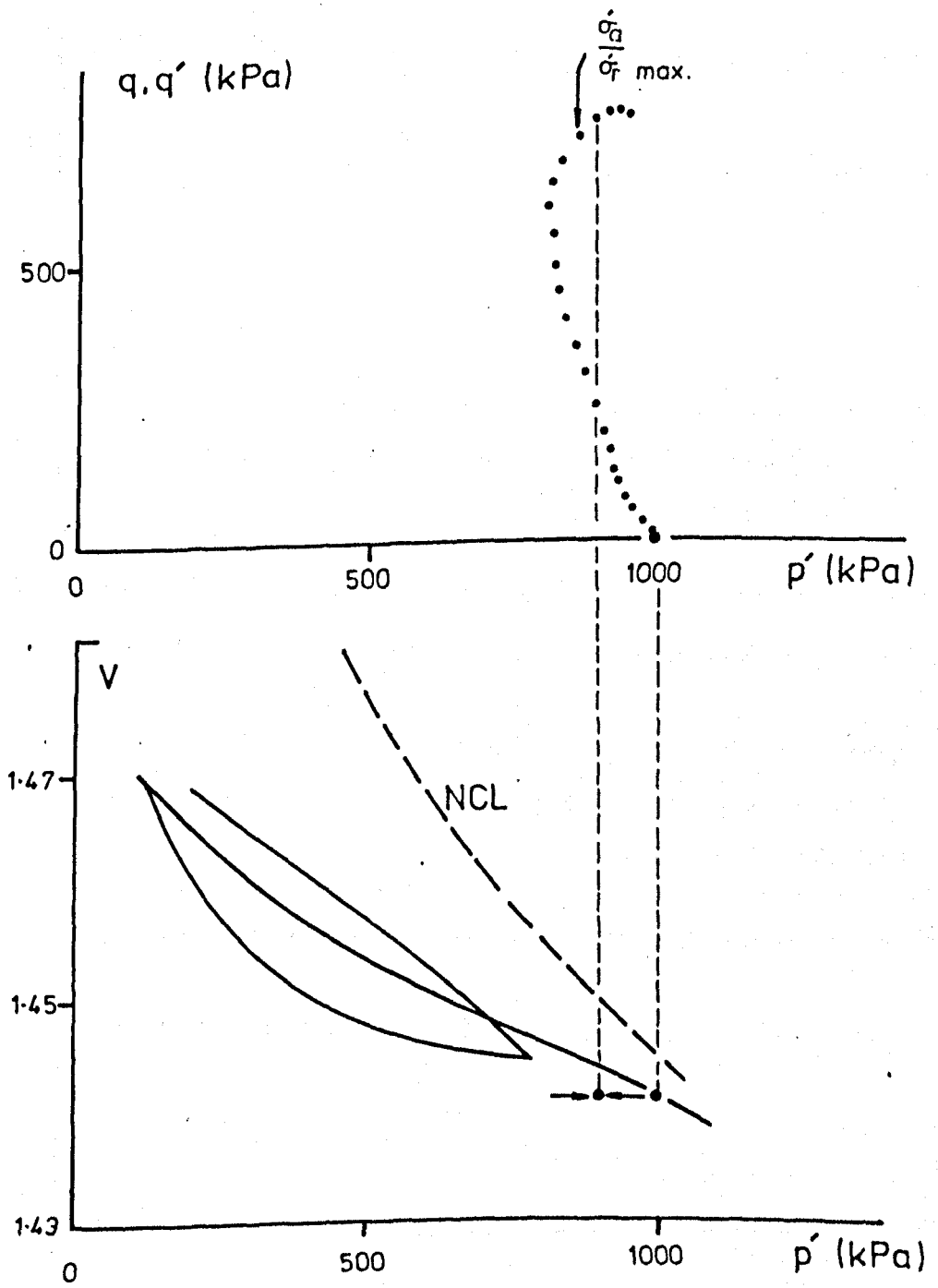

Figure 7.54 q , q′ : p′ and V : p′ : UA1(iii).

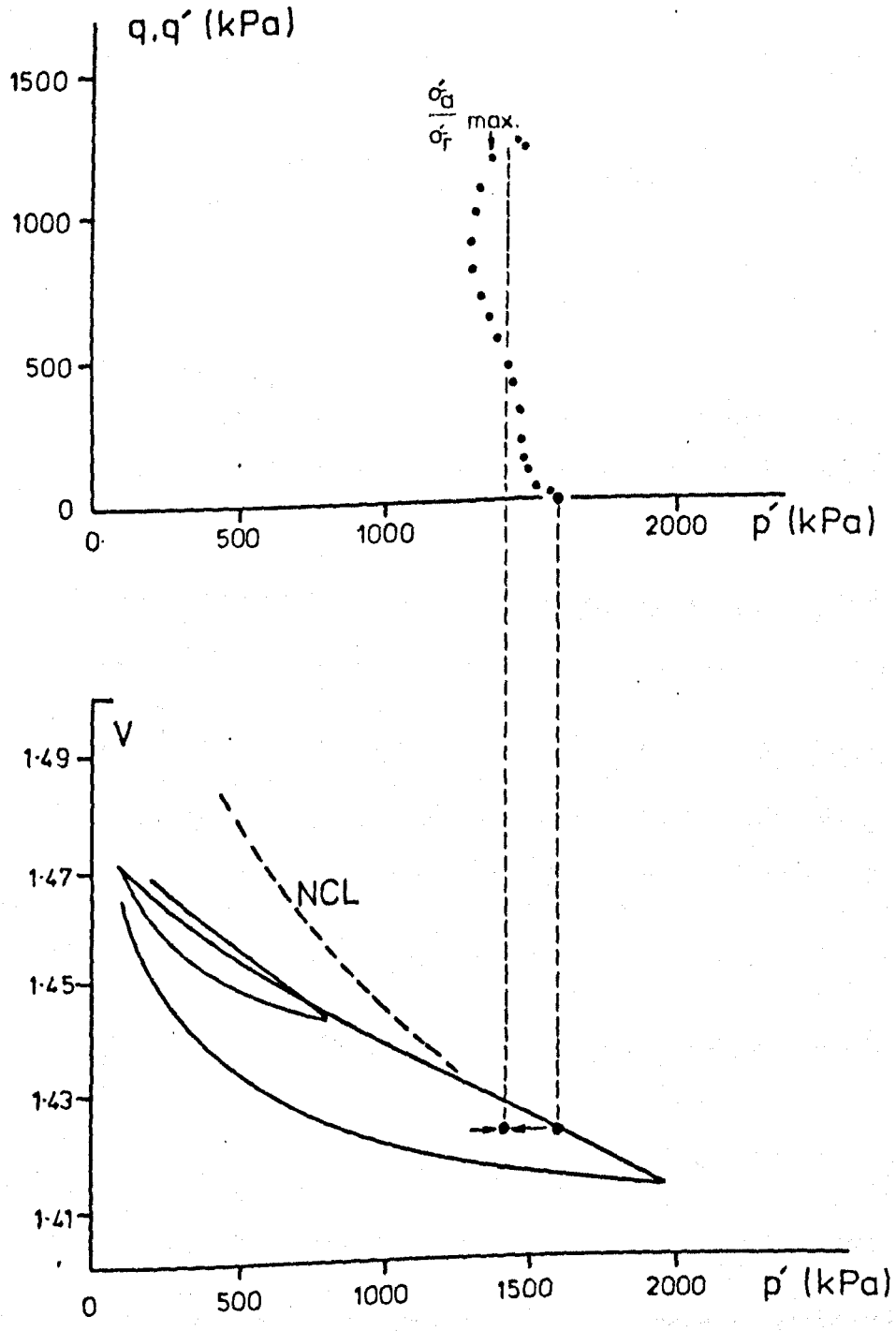

Figure 7.55 q , q′ : p′ and V : p′ : UA1(v).

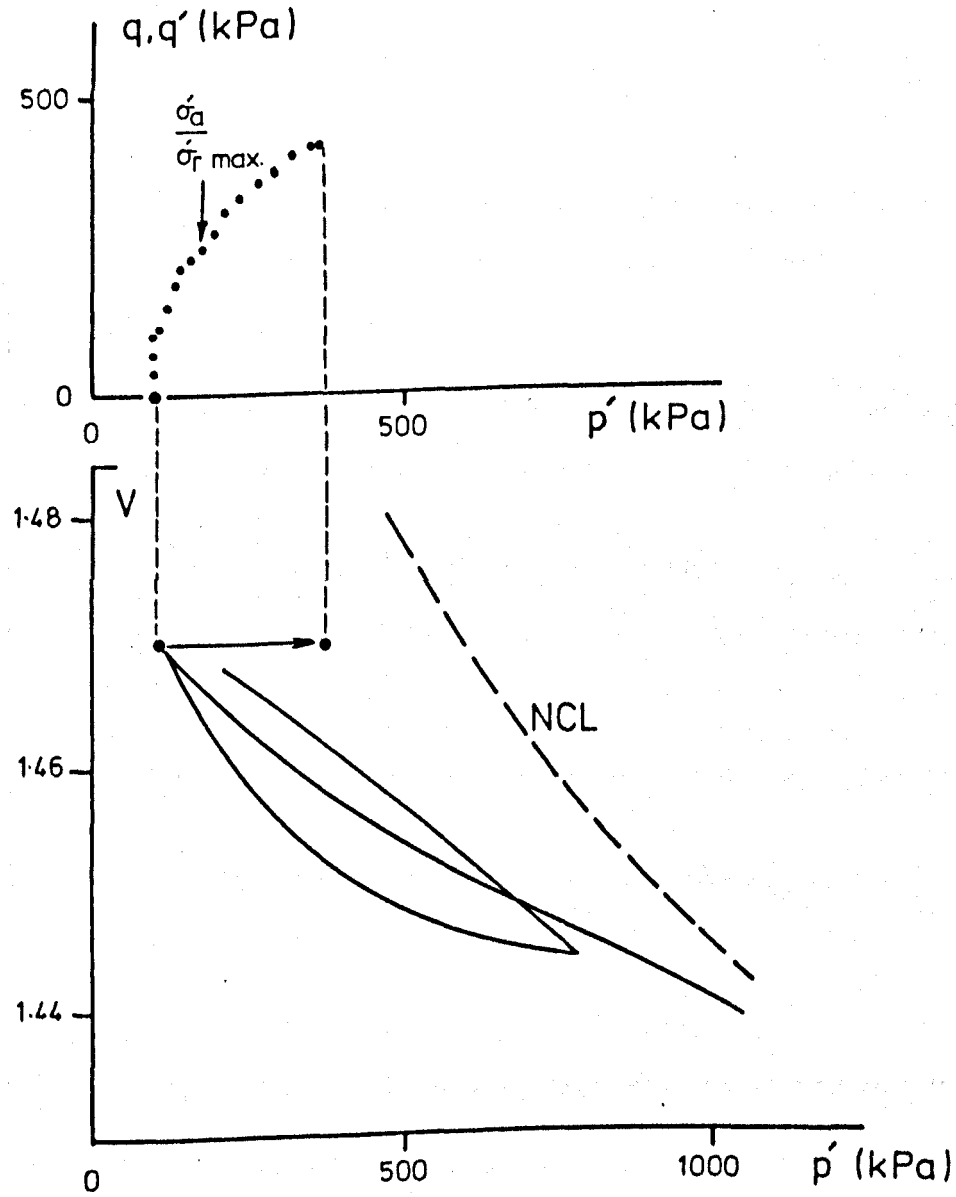

Figure 7.56 q , q′ : p′ and V : p′ : UA2(i).

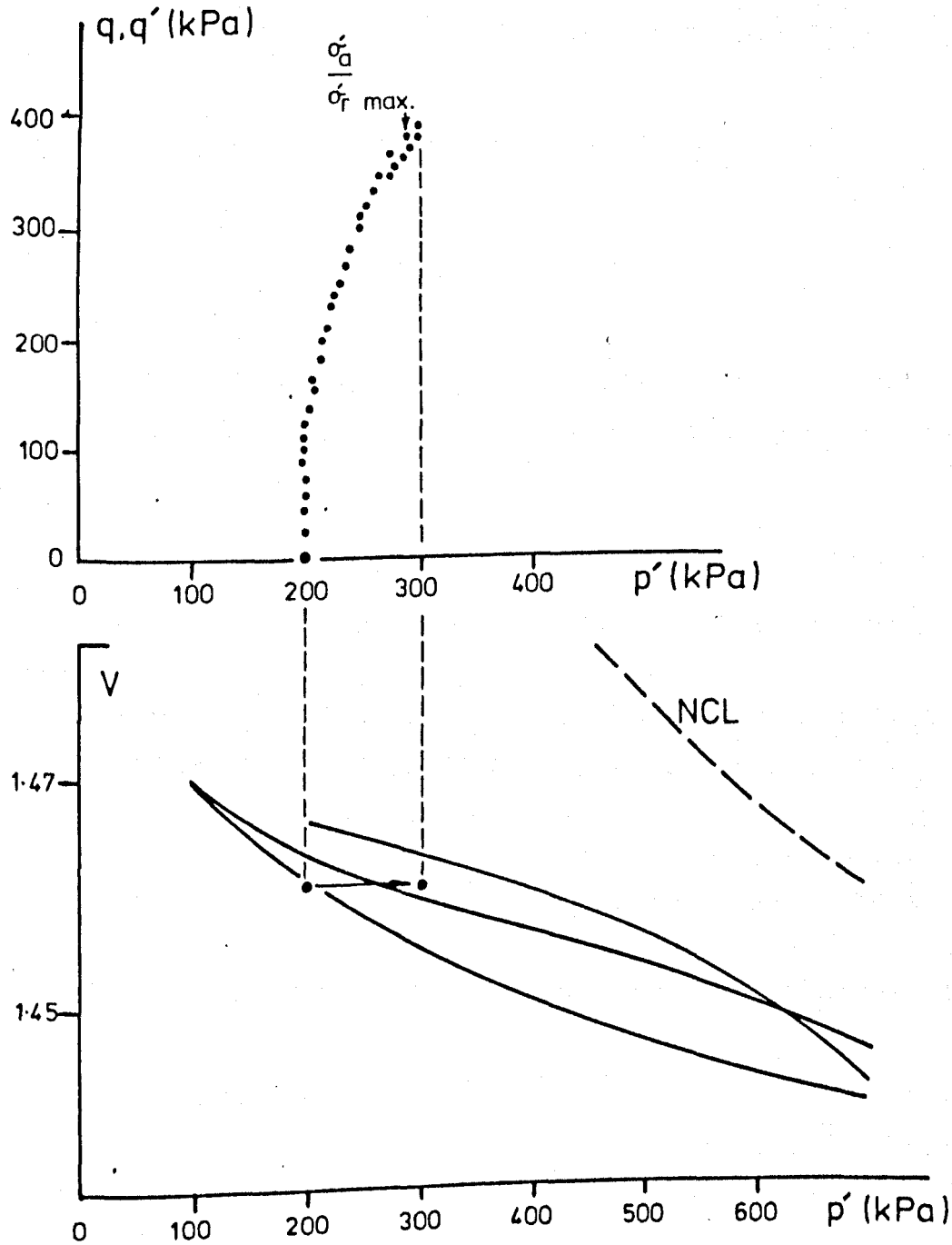

Figure 7.57 q , q′ : p′ and V : p′ : UA2(ii).

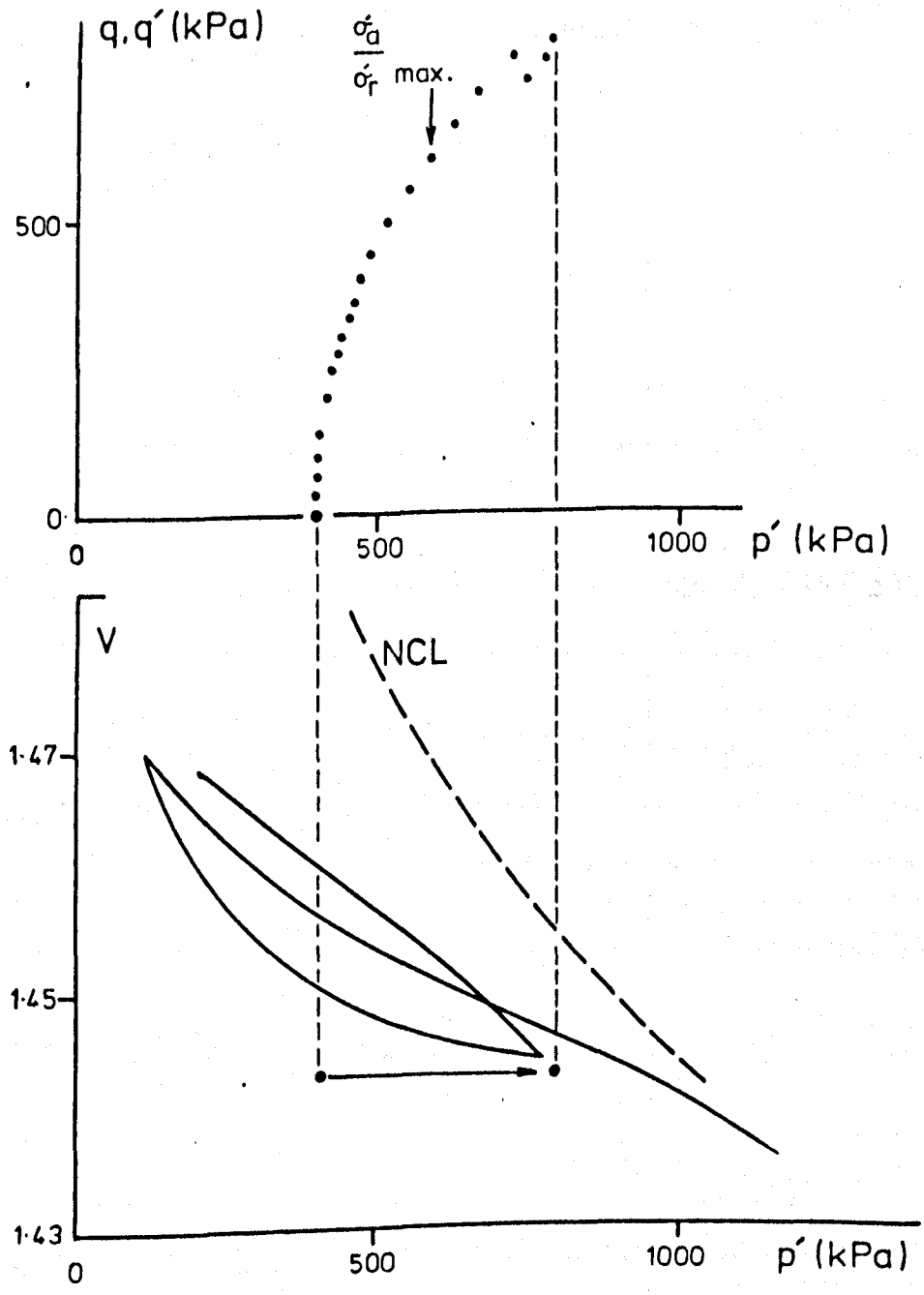

Figure 7.58 q , q′ : p′ and V : p′ : UA2(iii).

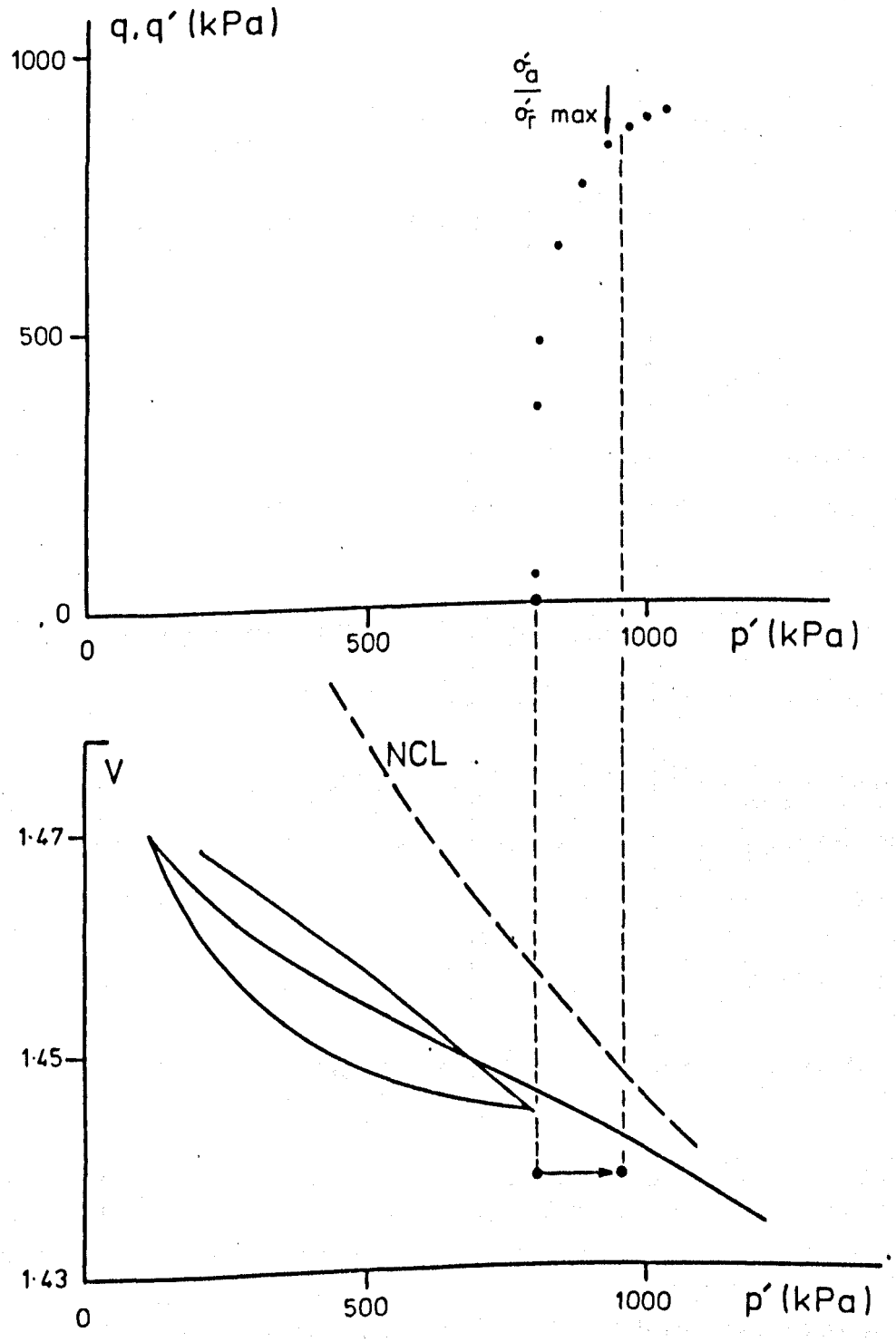

Figure 7.59 q , q′ : p′ and V : p′ : UB(i).

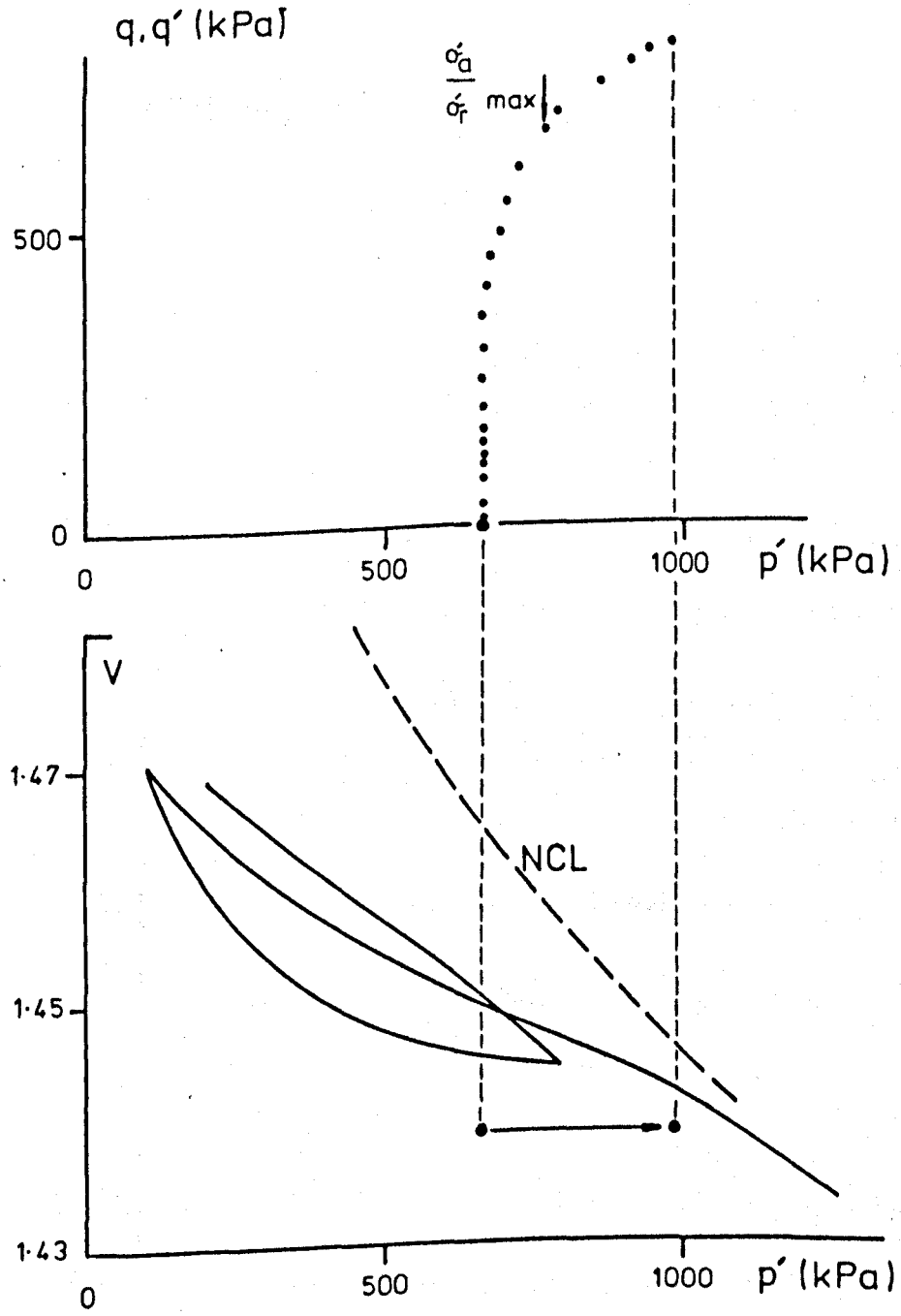

Figure 7.60 q , q′ : p′ and V : p′ : UB(ii)a.

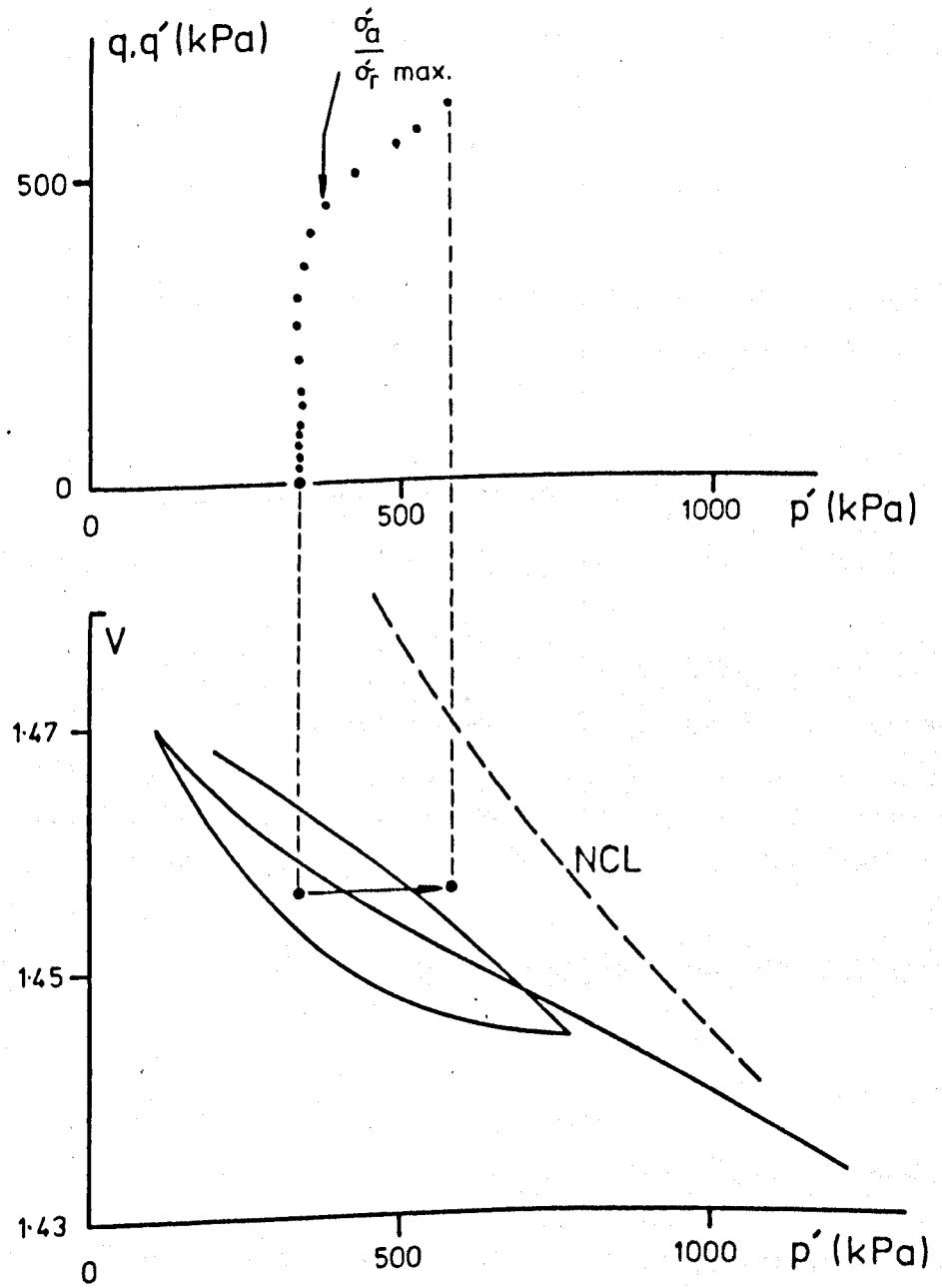

Figure 7.61 q , q′ : p′ and V : p′ : UB(ii)b.

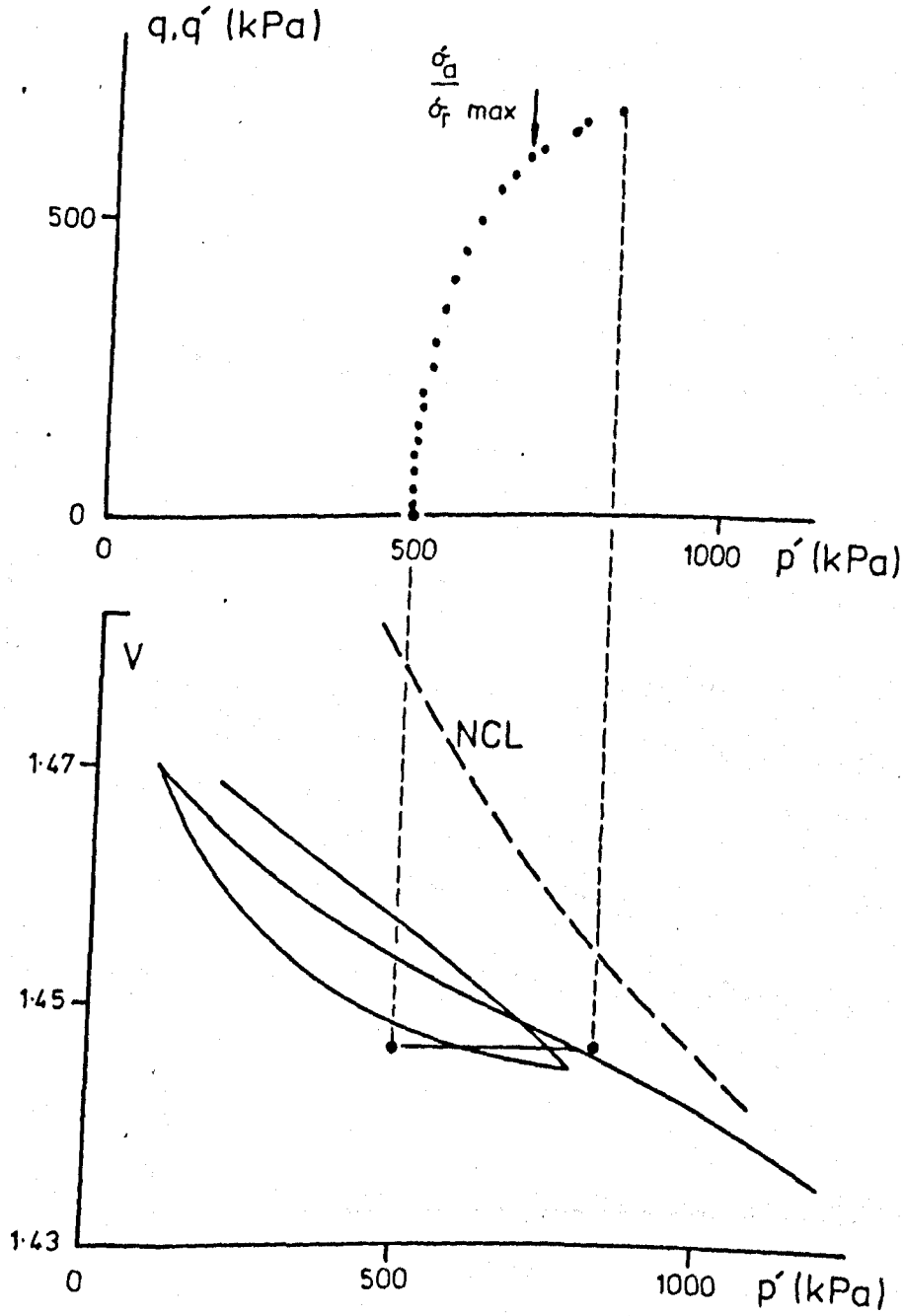

Figure 7.62 q , q′ : p′ and V : p′ : UB(iii).

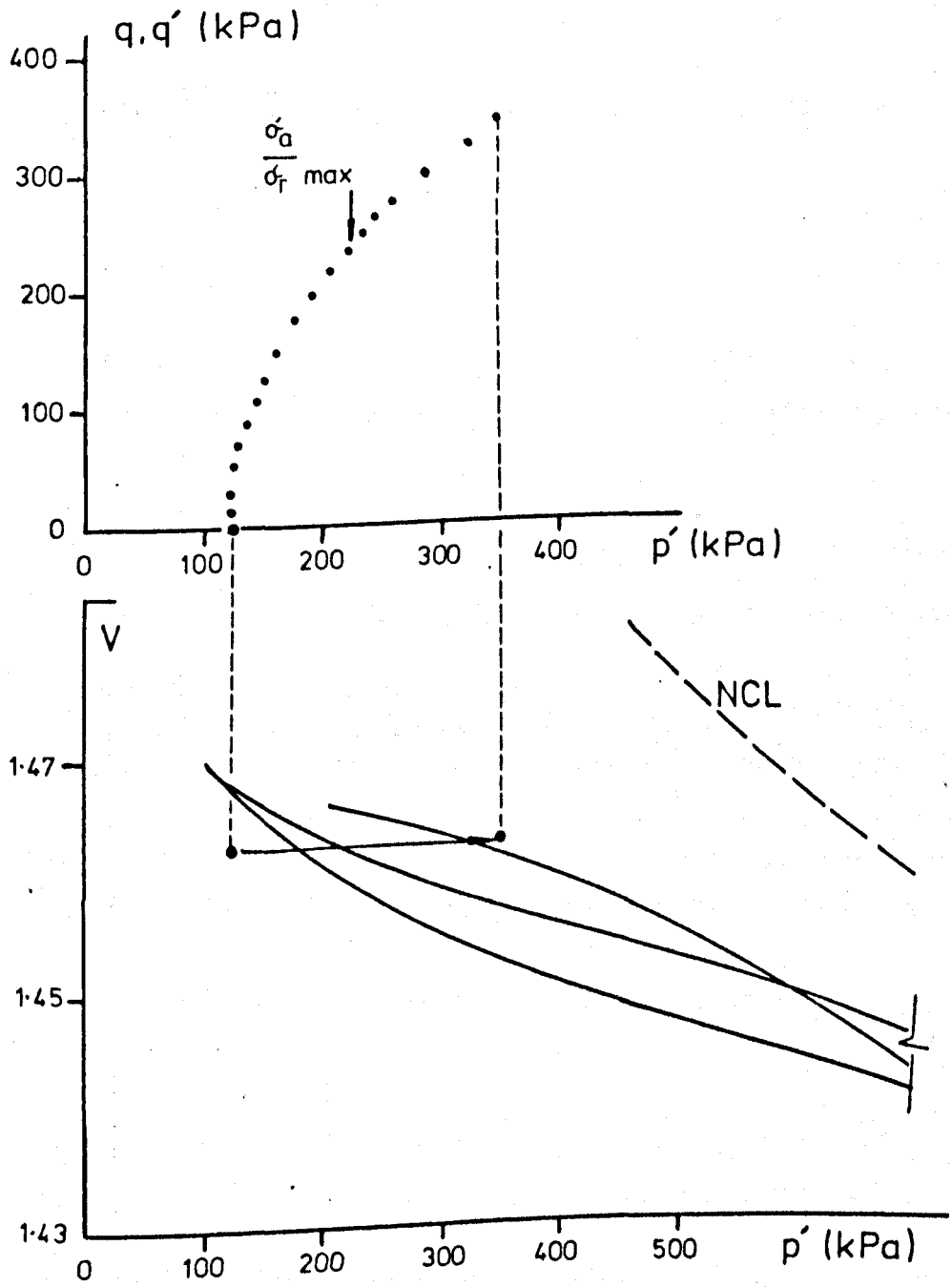

Figure 7.63 q , q′ : p′ and V : p′ : UB(v).

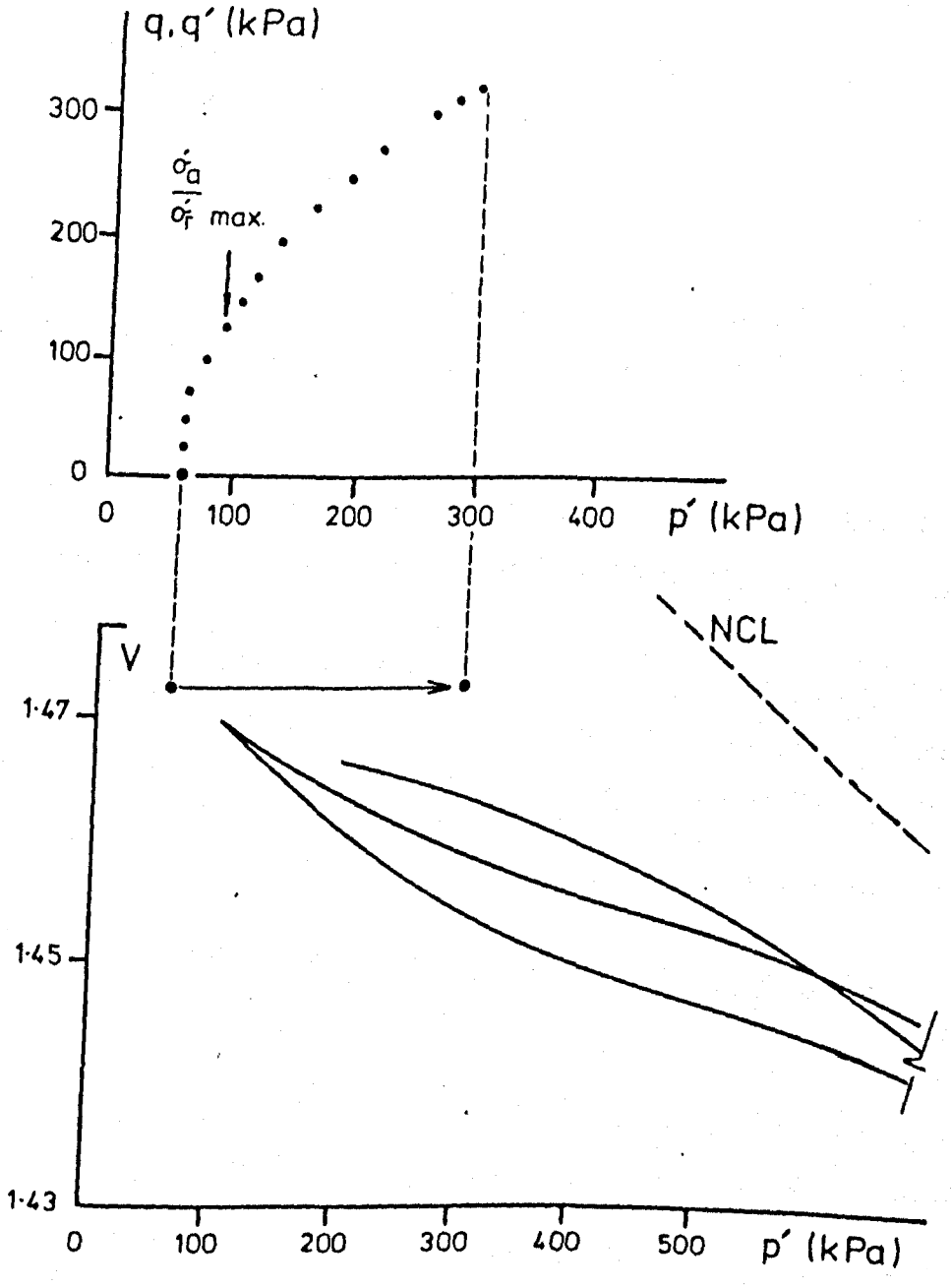

Figure 7.64 q , q′ : p′ and V : p′ : UB(vi).

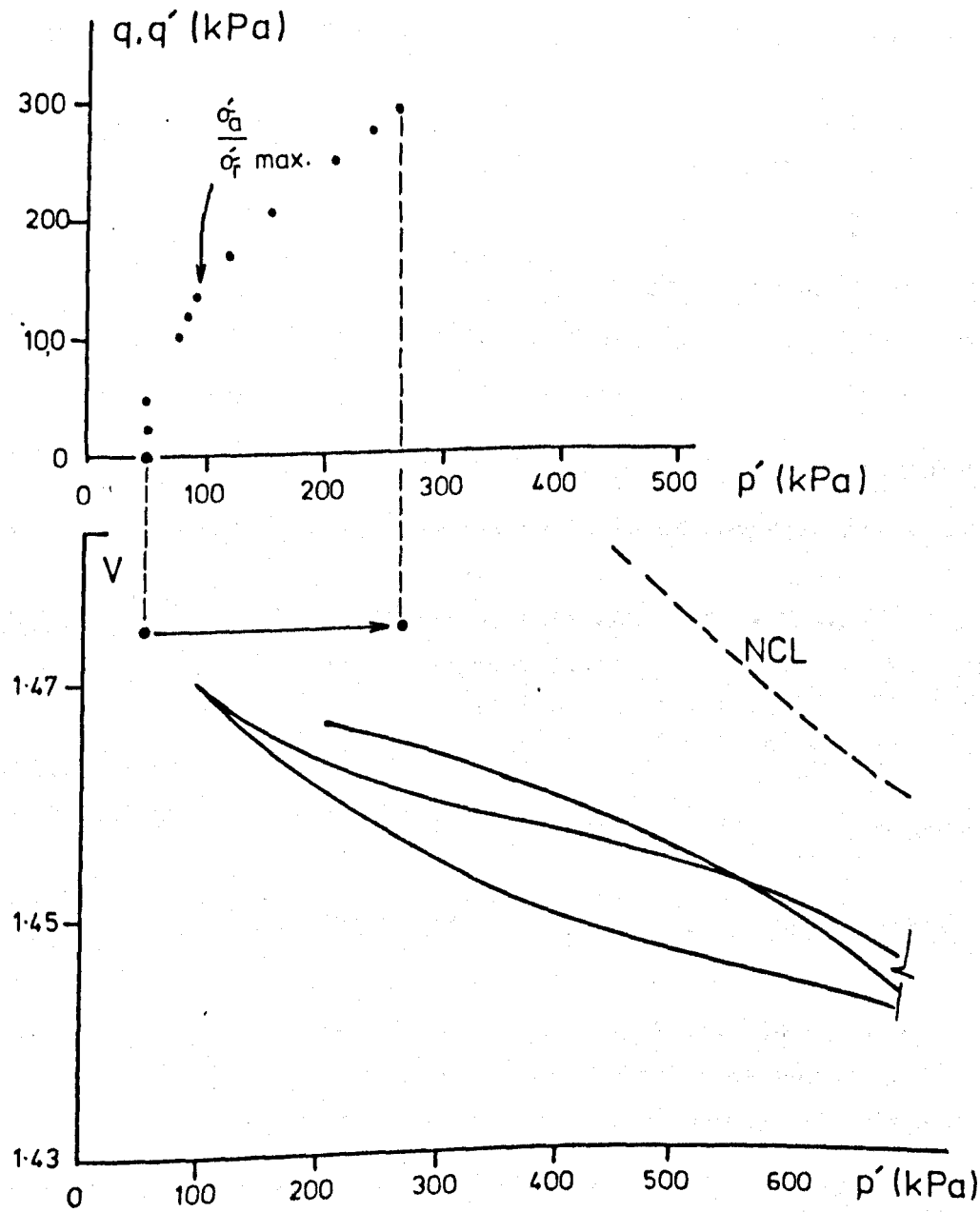

Figure 7.65 q , q′ : p′ and V : p′ : UB(vii).

CHAPTER 8. ANALYSIS AND DISCUSSION.

8.1 Engineering classification of the tills.

8.1.1 Plasticity.

The results of the Atterberg limit tests on the 14 till samples taken from the various sites in the Vale of St. Albans show a range of values for liquid limit (40 - 58) and plastic limit (15 - 22). Natural water contents determined for these soils varied between 15% - 20% , corresponding to liquidity index values between -0·143 and 0·069. The contrast in liquidity index between these tills and the other sediments associated with them in the Vale is very noticeable. With the exception of soil type M(g) - a grey brown silty sand found within the till at Moor Mill, these other clays have LI values varying from 0·150 to 0·700. The very low natural water contents of the Vale of St. Albans tills is a characteristic feature of lodgement tills elsewhere reported by others. For example, data reported by Fookes et al (1975) for the 'Upper Till' and 'Lower Till' at the site of the Hartlepool 'A' Power Station (4.5.1) gave LI values for these lodgement tills of 0·115 and -0·105 respectively. Eyles and Sladen (1981) also report plasticity and natural water content data for lodgement tills at various sites in Northumberland; here LI values calculated from their results show a range between 0·043 and -0·176. Again, data from Marsland (1977) for (lodgement) till from Redcar give an average LI value for this soil of -0·02. The rather more granular lodgement tills (Glasgow Grey Till, Kilmarnock Grey Till, Glasgow Red Till) reported by McGown et al (1975) for West Central Scotland show LI values as low as -0·21.

A plot of plasticity index against liquid limit on the plasticity chart, Fig. 7.1, indicates that although the 'T' line (Boulton and Paul, 1976) is not a line unique to tills, nevertheless the tills from the Vale of St. Albans demonstrate a close proximity to it. These authors have shown that this line, lying as it does above both the Casagrande 'A' line and the Skempton trend line for marine clays, is common to many different types of till. They have suggested that it owes its position relative to Skempton's line to the difference in

grading between till and sedimentary clay. They argue that the effect of an increasing coarse fraction will be to reduce both LL and PI (due to a larger percentage reduction in the LL than the PI) on a line towards the origin by an amount proportional to the percentage of coarse material present. By this argument, therefore, granular tills will occupy a lower position on the 'T' line than will the more clayey tills. A comparison of Fig. 4.1 with Fig. 7.1 does indeed show this to be the case.

The position of the Vale of St. Albans tills on this chart classifies them as clays of medium to high plasticity.

8.1.2 Grading characteristics.

The grading characteristics of the 5 till samples shown in Fig. 7.2 indicate a high degree of uniformity of particle size for these soils. These grading curves show that the tills contain more than 70% material finer than 0·063mm. Approximately 20% of the material is sand and the remaining 10% is gravel sized. Within this coarse fraction there is consistent evidence to suggest a gap in the grading in the medium to coarse sand and fine gravel range. Dreimanis and Vagners (1971) have stated that every lithological component of till will have a bimodal particle size distribution, irrespective of distance transported by the ice. One of these modes is to be found in the clast-size group and another in the till matrix. (Several such modes will exist when the crushed and comminuted parent rock type consists of minerals whose physical properties differ). McGown (1971) has suggested that the split point or mid-gap so produced by plotting grading data for a bimodal till on semi-logarithmic paper may be used as the separation point of two size fractions for identification and testing purposes. In this case the mid-gap (in the medium sand range) separates the Vale of St. Albans tills into fine sand, silt and clay (fine fraction) and medium to coarse gravel (coarse fraction). Generally speaking, the coarse fraction comprises durable clasts of Tertiary and, more especially, Cretaceous flint together with less durable gravel-sized Chalk. The finer fraction comprises the matrix produced by the comminution of older sediments (presumably mainly Jurassic, see Table 6.1) during ice transportation from the source area.

The manner of plotting soil grading data for engineering purposes (logarithmic particle size : summation percentage) is not a sympathetic one if a detailed analysis of particle size is required. Clearer

indications of bi- or multimodality in the grading characteristics of tills could be accomplished by using the more sensitive Modified Wentworth (1922) 'phi' scale and class terms. Cheshire (1981, 1983) has clearly demonstrated the benefits of such a treatment for Anglian tills in Hertfordshire and Essex.

Utilising the criteria later proposed by McGown and Derbyshire (1977), the Vale of St. Albans tills may be classed as 'matrix dominant', that is, these soils have greater than 30% fines (< 0·060mm). These authors have also recognised the need for a further textural description of the dominant fraction and suggest the terms 'granular matrix till' and 'cohesive matrix till' depending on whether the matrix is, or is not, predominantly granular in nature. Examination of the grading curves at the 0·002mm size indicates a clay-sized fraction of between 35% - 45% for these soils. On this basis, these tills would be classed as cohesive matrix types. These results are consistent with those reported by Marsland (1977) for the chalky Boulder Clay at the site of the Building Research Station, near Watford. Here, this author reports the grading characteristics of a chalky till recovered from a borehole down to 8·8m possessing between 36% and 41% clay content. It is also interesting to note that the grading curves shown for these soils demonstrate similar gap grading characteristics to those shown in Fig. 7.2.

Making use of the latest guidelines on the basis of grading and plasticity, these fine grained soils are classified CMS, CHS sandy CLAY of medium (and high) plasticity according to the British Scheme for the Classification of Soils for Engineering Purposes (BSCS), BS5930 (1981).

8.1.3 Activity of the tills.

The activity of the tills varies from 0·571 (till HH(a)) to 0·726 (till F(b)). This range of values classes the soils as 'inactive' (Skempton, 1953). These results agree generally with those of Skempton who, whilst noting the variability of activity in 'boulder clays', states that those in E. Anglia, being derived from the Jurassic and Cretaceous clays of the southern and eastern Midlands, would be more active than those of northern England and Scotland, consisting largely as they do of finely ground rock minerals with little if any true clay minerals incorporated in the matrix. There are exceptions, however, to this rule; for whilst it is the case that the lodgement tills in Northumberland have an activity range between 0·64 and 0·68, and those from Redcar are as low as 0·547, the activity value for the Lower Till

at Hartlepool is 0·94.

The activity of a soil will directly reflect the principle types rather than the total percentage of minerals present in its clay-sized fraction. Thus, a soil containing ground quartz will have a low activity whilst the presence of sodium montmorillonite (with an activity of 7·2 ; Samuels, 1950) within the clay fraction will noticeably increase activity. Therefore, whilst the Vale of St. Albans tills do possess appreciable clay-sized fractions, they do also contain ground quartz in large quantities, Table 7.5. And whilst it will be seen from Table 7.2 that the till with the highest activity (F(b) : 0·726) also contains the largest percentage of quartz, it is nevertheless also a naturally decalcified till possessing very little, if any, calcite (activity 0·18 ; Von Moos,1938, reported in Skempton, op cit). The relatively low activities of these tills therefore, despite the presence of both illite (activity 0·90 ; Northey,1950) and calcium montmorillonite in modest quantities, is due to the predominant effect of quartz and calcite in the groundmass. This is quite clearly shown in till HH(b) for here, although both illite and calcium montmorillonite are present in the largest quantities (where together they constitute 15·3% of the soil), so are quartz and calcite (where together they constitute 41·2% of the soil); hence its relative inactivity.

8.1.4 The distribution and effect of chalk in the tills.

The proximity of the Vale of St. Albans to the north-east/south-west trending outcrop of Cretaceous limestone (the Chalk) shown in Fig. 2.3, in combination with the inferred direction of ice movement into the Vale (e.g. West and Donner, 1956; Gibbard, 1974, 1977) from the north-west across the Chiltern escarpment and from the north and north-east along the length of this outcrop, has resulted in the incorporation of chalk in significant quantities in the tills in the study area.

An examination of its quantity and distribution in tills HH(a), HH(b), in the range 16mm down to 0·063mm, Table 7.4 , confirms this fact. The results of the sieving tests carried out on these soils before and after the removal of chalk from them (6.2.4) indicate that down to 0·5mm , 18·98% and 23·1% of the total mass of HH(a), HH(b) respectively are made up of chalk. Total acid solubles at this size are 19·6% and 30·5% respectively. A distinction is made here between chalk and acid soluble content for, during the process of separating the chalk

particles from the other lithologies, it became clear that two different forms of chalk were present in both tills. The distinction between the two only became obvious when the particles were examined with the aid of a binocular microscope. Clasts of 'primary' chalk were observed as smooth, white rounded and spherical particles with open, porous textures. However, irregularly shaped nodular lumps of creamy white carbonate concretions with closed, less porous textures were also present in smaller quantities. This latter type of 'chalk' is thought to be a secondary feature and could represent a dissolution product of the primary chalk material. It is present in considerably greater quantities in till HH(b) (where it constitutes 32.03% of the total acid solubles down to 0·5mm) than in till HH(a) (where it constitutes only 3·26%).

In the fractions below 0·5mm it becomes very difficult to visually separate the chalk and therefore only total acid soluble contents have been determined in the range 0·5mm - 0·063mm. Although representing relatively small proportions of both these soils in the medium to fine sand and silt fractions, (2·36% , HH(a) ; 3·27% , HH(b)), there are noticeable increases in acid soluble content at the 0·063mm size in both tills.

These acid soluble data for both tills are plotted in combination with the total lithology grading curves employing the Modified Wentworth (phi) convention in Figs. 7.3, 7.4. The bimodal nature of the non-carbonate lithologies and, to a lesser extent, the acid solubles (particularly HH(a)) in these tills is clearly shown. (There is some evidence suggesting an additional mode at -1·5 phi (2·80mm) in HH(b)).

The results of the sedimentation tests to determine the distribution of carbonates in the range 0·063mm down to 0·002mm in these same tills and, additionally, in tills F(b), W(b), W(d), Table 7.3, are consistent with these findings. With the exception of F(b), the tills demonstrate a tendency to increased carbonate concentrations with reducing particle size. Hence, at the 0·006mm (fine silt) size, carbonates represent between 3·08% (W(b)) and 9·28% (W(d)) of this fraction. The effect of removing carbonate on the < 0·002mm (clay) fraction is also evident. Excluding F(b), clay fractions increase from 6·46% (W(b)) to 12·57% (W(d)). That this should be so has already been discussed in 6.2.4. The apparently inconsistent pattern of results shown by F(b) in the Table is due, it is suggested, to the fact that

this till is a naturally decalcified soil and therefore would contain very little carbonate (if any) in these finer fractions. This is substantiated by the very small (negative) difference in the clay content for this soil determined after acid treatment.[1]

The presence of chalk in the coarse fractions together with finely dispersed carbonate in the matrix of these tills might be expected to influence behaviour in some way and therefore to affect measured properties. The influence of carbonate on the less than 0·425mm particle sizes may be examined by inspection of the LL, PL results in Table 7.1 for tills HH(a), HH(b), (see 6.2.1). The effect of removing the carbonate has resulted in 35%, 25·6% increases in LL and 27·8%, 16·7% increases in PL for HH(a), HH(b) respectively, corresponding to 40·9% , 50% increases in PI. Interestingly, the PI of these carbonate free soils (31,33) approaches the 36 for till F(b). That the PI should increase in this way is perhaps not surprising in view of the fact that Chalk itself contains very little colloidally active fines and typically possesses a LL as low as 25 (Clayton, 1983).

The activity (8.1.3) would also be affected by the presence of carbonate in this fraction. An increase in the percentage (carbonate free) clay content of the soil will cause a reduction in activity, Table 7.2. Again, although these soils show reductions in activity varying from 18·3% (W(b)) to 23·9% (W(d)) [2] there is no significant change in activity for till F(b). If, in addition, the carbonate-free PI value is used in the calculation of activity as for HH(a), HH(b) in this Table, then the activity will increase. Whilst it is not being suggested that the values of 0·654, 0·689 so obtained here for HH(a), HH(b) would represent more realistically the activity of the source materials for the tills , it is interesting nevertheless that the average activity for the mudrocks of the Jurassic of the British Isles calculated from the data presented by Cripps and Taylor (1981) is 0·694.

---

1. Arguably, the soil cannot have less clay (i.e. more carbonate) after treatment with acid; it is more likely that this is a reflection of the expected level of experimental error here.

2. It is significant that these tills are those with the least W(b), and the most W(d), carbonate in < 0·002mm fraction, Table 7.3.

8.2 One-dimensional and isotropic compression.

The relationship between pressure and specific volume in one-dimensional compression for both the reconstituted and undisturbed tills shown in Figs. 7.7 to 7.11 demonstrate the stiffness of the two types of the same material in a comparative way. The compression index C_c (3.3) may be used to quantify the stiffness of a normally consolidated soil in $\log_{10} \sigma'_v$: V space; alternatively, the critical state constant λ (ibid) may be used if the compression data are in the form $\log_e p'$: V .

Without direct measurement of the radial stress σ'_h during one-dimensional compression and unloading, assumptions regarding the variation of K_o with overconsolidation ratio have to be made which will enable values for vertical effective stress σ'_v to be expressed as average effective pressure p'.

Brooker and Ireland (1965) report the results of a series of tests on five natural soils with PI values ranging from 10 to 78, (Chicago Clay, Goose Lake Flour, Weald Clay, London Clay, Bearpaw Shale) using an instrumented oedometer from which direct measurements of radial stress could be made during compression and unloading. These authors have concluded from their experimental results that K_o is related to both ϕ' and PI as well as stress history and present interesting data relating K_o to PI over a range of overconsolidation ratios for these soils, Fig. 8.1 . Using their published findings it has been possible, via the plasticity data for the tills (Table 7.1), to infer values for K_o at each loading and unloading stage for the oedometer tests OR(1) to OR(5) and OU(1)V to OU(5)V .

The validity of deriving K_o for one-dimensionally unloaded soils from their plasticity data has been tested using the results of Nadarajah's (1973) work. Fig. 8.2 shows how the findings of this author (who measured K_o for Spestone Kaolin, PI = 32, using an instrumented oedometer) agree very well with those values for K_o predicted at various overconsolidation ratios using Brooker and Ireland's data.

Also plotted in this Figure is the graph K_p versus Ro based on data for the same kaolin, from Schofield and Wroth (1968). The maximum possible value of K_o is the coefficient of passive earth pressure K_p , therefore the value for K_o should increase with overconsolidation ratio and eventually become an asymptote to a curve representing the coefficient of passive earth pressure. This tendency is clearly

demonstrated, even over the limited range of overconsolidation ratios ($Ro \leqslant 12$) examined in this Figure.

Oedometer testing of a reconstituted (at natural water content) sample of London Clay[1] (LL = 81, PL = 31) was also carried out at this time so as to provide additional data which could be evaluated in the manner described and compared with those published by others for this same soil type. Interpretation of the resultant data using derived K_o values based on PI = 50 yielded $\lambda = 0{\cdot}152$, $\kappa = 0{\cdot}073$; these values compare reasonably well with those published for London Clay (PI = 52 , $\lambda = 0{\cdot}161$, $\kappa = 0{\cdot}062$) by Schofield and Wroth (op cit, page 157).

The till compression data are therefore shown plotted in the alternative form $\log_e p' : V$, Figs. 8.3a to 8.12a , thus enabling the soil constants λ , $\bar{\kappa}$ (see below) for each soil type to be determined. Values of K_o for the undisturbed soils have been determined from the calculated values of p'_c from the appropriate $\log_{10} \sigma'_v : V$ graphs (see Figs. 7.7 to 7.11).

A summary of these data is shown in Table 8.1 . In this Table a value for $\bar{\kappa}$ represents the average gradient of a swelling line over its entire range of (final) unloading. Values for $C_c/2{\cdot}303$ (equation 3.16) are also shown and these should be compared with those λ values derived from the plasticity data.

Whilst it will be seen from this Table that the values for λ_R for reconstituted tills HH(a), HH(b), W(b), W(d) are all within the range 0·066 – 0·083 , and those for λ_U (undisturbed) lie between 0·049 and 0·060 , those for the naturally decalcified till F(b) are quite different : $\lambda_R = 0{\cdot}116$, $\lambda_U = 0{\cdot}120$.

The relative stiffness of the reconstituted and undisturbed tills in compression may be expressed as the ratio λ_R / λ_U . Again, whilst λ_R / λ_U has values between 1·20 and 1·50 for tills HH(a), HH(b), W(b), W(d) , the value for F(b) is 0·97 . This suggests that whilst those tills which contain dispersed chalk in quantity within their matrix undergo smaller compressions when undisturbed, the till with very little carbonate does not. A similar effect on unloading is, however, not evident. An examination of the comparable (unloading) ratios $\bar{\kappa}_R / \bar{\kappa}_U$ for these tills shows a range of values 1·14 to 1·42 . That for F(b) is 1·23 . Therefore, whilst the reconstituted

1. The writer is grateful to Messrs. Ground Engineering Ltd. for supplying this soil.

carbonate-rich tills undergo larger positive volumetric changes than do the undisturbed tills when unloaded, so does the carbonate-free till. It could be hypothesised therefore that, although the presence or absence of carbonate in the matrix (possibly in the form of calcite, see Table 7.5) is significant during compression, its effect on the unloading characteristics of these soils is not significant. In this respect, the presence of other (clay) minerals might be more important, notably perhaps montmorillonite. It is interesting to note (Table 7.5) that this clay mineral is present in similar quantities in all of the tills, including F(b), as indeed are illite and kaolinite.

The isotropic and oedometer compression characteristics ($\log_{10} \sigma'_v$, σ'_r : V) for the reconstituted and undisturbed tills HH(a), HH(b), which are shown comparatively in Figs. 8.13 to 8.16 demonstrate a reasonably consistent volumetric response of these soils (and particularly so the reconstituted ones), when subjected to the two different test conditions. Relative positioning of the compression curves on the specific volume axis at the lowest (vertical, isotropic) consolidation pressure will depend on the different values for initial water content of the soil (Fig.8.13 ; TR(1) , OR(1)) and, where these water contents are more nearly equal (Fig.8.15 ; TR(2) , OR(2)), then less difference is evident in terms of response to subsequent compression and unloading.

The soil constants λ , $\bar{\kappa}$, for the reconstituted and undisturbed tills HH(a) , HH(b) , have been evaluated during isotropic compression and these data are summarised in Table 8.2 . The isotropic normal compression characteristics shown here may be compared with those determined for tills HH(a) , HH(b) , from the oedometer tests in Table 8.1 . Whilst the agreement between λ_R for the reconstituted tills in tests OR(1) , TR(1) and OR(2) , TR(2) is very good indeed ($\lambda_{isotropic}/\lambda_{oedometer}$: 0·97 , 1·08 respectively), there is a larger discrepancy in λ_U for the undisturbed tills in tests OU(1)V, TU(1) and OU(2)V , TU(2) ($\lambda_{isotropic}/\lambda_{oedometer}$: 0·80 , 0·76 respectively). That this should be so is due to the lower maximum effective pressure (2000 kPa) to which the undisturbed soils were subjected in the isotropic compression tests. The true normal compression characteristics of these naturally overconsolidated soils would be more clearly defined in the higher pressure range 1600 kPa - 3200 kPa (oedometer) than in the range 1600 kPa - 2000 kPa (triaxial). In both cases, however, it has been assumed that normal compressions

have been achieved at the maximum test pressures. Clearly, on examination of the evidence this is less likely to have been the case in tests TU(1) and TU(2).

The response of soil to laterally constrained and isotropic compression and unloading can be expressed in dimensionless form as the ratio λ/κ. (Here κ represents the local gradient of a swelling or, alternatively, recompression line between adjacent average effective pressure points.) The effect of increasing and reducing overconsolidation ratios on the value of λ/κ has been investigated for reconstituted and undisturbed tills HH(a), HH(b), F(b), W(b), W(d) in oedometer compression and for reconstituted and undisturbed tills HH(a), HH(b), in isotropic compression. Graphs of λ/κ : Ro for these tests are shown in Figs. 8.3b to 8.12b (oedometer) and Figs. 8.17 to 8.20 (triaxial). In these graphs a state of normal compression exists when $\lambda/\kappa = 1$; when $\lambda/\kappa > 1$, the soil has a state either on a reloading or a swelling line and is no longer normally consolidated. During initial loading of a reconstituted soil (for example till HH(a), test OR(1) in Figs. 8.3a and b) soil response is along the compression line C1 (Fig. 8.3a). Although the soil is showing the effects of being lightly overconsolidated at values for $\log_e p' \lesssim 5{\cdot}0$ (due to the method of sample preparation), it is assumed that the soil is normally compressed here, and therefore the normal compression path C1 in Fig. 8.3a becomes the point C1 in Fig. 8.3b with λ/κ, Ro = 1. When the soil is unloaded at 800 kPa ($\log_e p' = 6{\cdot}68$) along path S1 to produce a sample with Ro = 2, the ratio λ/κ increases in a way which will reflect the relatively stiff response of the soil at this small overconsolidation ratio. With increasing overconsolidation ratio, λ/κ reduces and eventually reaches a sensibly constant value (approximately 1·5 at Ro = 32 for this soil). The effect of an intermediate recompression C2, and final unloading S2 cycle can also be observed in this Figure.

During initial loading of an undisturbed soil (for example till HH(a), Fig. 8.4a, B (i) compression to 6400 kPa) the soil is being compressed along a reloading line at reducing values of Ro. Eventually the soil becomes normally compressed with λ/κ, Ro = 1. This loading sequence is represented by path C(i) in Fig. 8.4b. Estimates of overconsolidation ratio along this path are made on the basis of established values for the maximum effective preconsolidation pressure p'_c (see 7.3). Having achieved normal compression, overconsolidation

ratios on unloading can be precisely determined and related to corresponding values for λ / κ (path S(i) in Fig. 8.4b .). One of the benefits of this type of graph is that it enables comparisons of response to loading/unloading to be made both between the reconstituted and undisturbed forms of the same till and also between the various till types. Whilst considerably more experimental work on a variety of different soil types would be required before meaningful conclusions could be drawn, it is nevertheless an interesting prospect to suppose that all soils might possess their own unique 'compression signature'. This supposition has been tested in two ways :

(i) the compression data for the undisturbed North Sea tills A , D , (4.5.3) have been interpreted in this manner and a compression graph of this type has been compiled for each till. These are shown in Figs. 8.21 , 8.22 . A very clear definition of the initial loading path C1 in both cases is evident here. The same general characteristics are observed for both soils during unloading and reloading. On final unloading (path S2), and at large overconsolidation ratios, λ / κ reaches a sensibly constant value of approximately 2 .

(ii) the writer has compression (oedometer) tested other soils (Kaolin, London Clay, Black Cotton, Bentonite) with PI in the range 14 - 125 and compression graphs for these are shown in Fig. 8.23 . With the possible exception of the reconstituted London Clay (PI = 50) there is evidence from these graphs to suggest a relationship between the maximum value λ / κ and the plasticity index of the soil. The soils with the largest PI (Bentonite, Black Cotton) show the largest λ / κ ratio , particularly during reloading (C2) and this tendency becomes more pronounced when PI $\gtrsim$ 35 , Fig. 8.24 . In this Figure are included the range of λ / κ maximum values for the tills in the Vale of St. Albans ; their presence here is in an area away from the tentative PI : λ/κ trend indicated, and this could again be reflecting the colloidally inactive nature of the fines in these soils, containing as they do a large amount of chalk in their matrix.

8.3 Permeability and consolidation.

The oedometer derived c_v values given in Tables 7.7 to 7.16 show a range from 0·07 - 3·12mm^2 min^{-1} (0·13 - 5·94 m^2 yr^{-1}) for the reconstituted tills in tests OR(1) - OR(5) and 0·13 - 6·18 mm^2 min^{-1} (0·25 - 11·76 m^2 yr^{-1}) for the undisturbed tills in tests OU(1)V - OU(5)V . A comparison of reconstituted (R) with the undisturbed (U)

c_v values in these tests is given in Figs. 8.25 to 8.29 . In these Figures are shown the calculated values for c_vR , c_vU at the same overconsolidation ratios. The plotted paths of changing c_v values during the loading/unloading stages of these tests show quite clearly (excepting parts of the c_v paths for till W(d), Fig. 8.29) that consolidation rates for the undisturbed tills exceed those for the reconstituted tills over a large range of overconsolidation ratios. This effect is most clearly marked ($c_vR \simeq \frac{1}{4}c_vU$) in the oxidised and decalcified till F(b) , Fig. 8.27 . That consolidation rates in the natural soils should be larger is not an unexpected finding in view of the fact that those aspects of the soils' natural fabric which will enhance consolidation are destroyed during the process of reconstituting the soil.

The very large increases in c_v demonstrated by both reconstituted and undisturbed tills in moving from Ro = 1 to Ro = 2 is a characteristic reflecting the increased stiffness of these soils during this unloading stage, a phenomenon which has been discussed in 8.2 . The reducing values for c_v with increasing Ro is also a characteristic of these soils and is one which is evident for the North Sea tills (Fig. 4.9 , 4.5.4).

The comparable data from the isotropic consolidation tests TR(1) , TU(1) and TR(2) , TU(2) on reconstituted and undisturbed tills HH(a) , HH(b) , reported in Tables 7.33 to 7.36 are also included in Figs. 8.25 , 8.26 . Whilst those data for till HH(a) generally show a rather large difference in isotropic consolidation rates between the reconstituted and undisturbed till, eg. $c_vU/c_vR \simeq 10$ (at Ro = 2) reducing to $c_vU/c_vR \simeq 2$ (at Ro = 1, 4), those for till HH(b) exhibit a more consistent relationship with the oedometer data. It can also be seen that isotropic c_v values are consistently lower than the oedometer values for the same soil calculated at the same overconsolidation ratio. That this is so may well only be reflecting the different basis on which the coefficient of consolidation is calculated in the two types of test, (see 7.3 and 7.6(i)).

The calculated oedometer permeabilities for the reconstituted tills shown in Tables 7.7 to 7.11 indicate values ranging between $1{\cdot}29 \times 10^{-11} ms^{-1}$ (OR(1), till HH(a); OR(2), HH(b)) and $7{\cdot}29 \times 10^{-13} ms^{-1}$ (OR(3), till F(b)) for these soils, whilst the range for the undisturbed tills shown in Tables 7.12 to 7.31 is $1{\cdot}06 \times 10^{-9} ms^{-1}$ (OU(5) H(n), till W(d)) to $2{\cdot}72 \times 10^{-13} ms^{-1}$ (OU(5) H(r), till W(d)).

The reducing permeabilities corresponding to increasing consolidation pressures and increasing permeabilities resulting from reducing consolidation pressures which are evident from these data, may be appreciated by plotting permeability against the corresponding equilibrium specific volume, Figs. 8.30 to 8.34. In these Figures, the permeabilities for each of the undisturbed soils (both vertical drainage and horizontal drainage, parallel and normal to clast fabric vector) during compression and unloading are shown, together with the permeability for the reconstituted soil. By matching the specific volume of each undisturbed soil to that of the reconstituted soil arbitrarily at σ'_v = 3200 kPa , permeability can be viewed as a comparative variable over the entire range of consolidating pressures.

The loading/unloading permeability paths so produced by the reconstituted soil in each case defines an envelope (shaded in these Figures) against which the corresponding paths for the undisturbed soil may be compared. It is clear from these graphs that the undisturbed soils initially possess permeabilities which are at least an order of magnitude greater than the reconstituted ones, and only approach the intrinsic permeability of the reconstituted matrix at the highest consolidation pressures achieved. Even at these pressures, the permeability of undisturbed till F(b), Fig. 8.32, never reaches its intrinsic permeability envelope; this corroborates the earlier observations regarding this till's particularly high c_v values, Fig. 8.27 . No significant differences can be observed between the vertical and horizontal permeabilities of the undisturbed soil; also, the presence of a clast fabric does not appear to be exercising a control on permeability. This is, perhaps, not surprising - the permeability of the clay matrix dominant tills will be governed predominantly by the geometric arrangement of the matrix rather than by that of the coarser clast fractions (on which the fabric analyses were carried out). It is also interesting to note that, with the exception of till F(b), the permeability paths for the undisturbed soils during unloading are generally contained within the permeability envelope of the reconstituted soil.

The relationship between permeability, coefficient of consolidation and the modulus of volume decrease derived from the oedometer tests for the reconstituted and undisturbed tills in tests OR(1) - OR(5) and OU(1)V - OU(5)V is shown in Figs. 8.35 to 8.41 . Whilst the data plotted in the form $k : c_v : m_v$ of Figs. 8.35 to 8.37 for tills

HH(a), HH(b), F(b) clearly demonstrate the expected variations of these interrelated parameters with the changing stress regime, (and which have been discussed in this section and in 8.2), Figs. 8.38 to 8.41 (reconstituted and undisturbed tills W(b), W(d)) have the additional advantage of showing the variation of c_v , m_v as separated components of the $k : c_v : m_v$ diagonal. It is evident from these graphs that the reductions and increases in permeability observed during the reloading stages of these tills from Ro = 4 to Ro = 1 , (eg. C2 of Figs. 8.11, 8.12) and also during the initial unloading stages from Ro = 1 to Ro = 4 (initial portion of S2) result primarily from significant changes in the modulus m_v . With increasing overconsolidation ratio (up to Ro = 32 along S2), however, increases in permeability are not so marked due to a noticeable reduction in c_v as well as a reduction in soil stiffness.

The permeabilities observed for the Vale of St. Albans tills, whilst extending outside of his limits, are not inconsistent with the range of values reported by Lloyd (1983) for matrix dominant tills (see Fig. 4.8).

8.4 The strength of the tills.

8.4.1 Undrained shear strength from the vane tests.

The results of the motorised shear vane testing of reconstituted tills HH(a), HH(b), F(b) reported in Table 7.32 are shown plotted in the form LI : $\log_{10}$ undrained shear strength (cu) in Fig. 8.42 . Included in this Figure are the results of the in situ shear vane tests on (undisturbed) tills HH(a), HH(b), W(b), W(d) . These latter results are expressed in the form peak (p) and remoulded (r) strengths.

The range of measured shear strengths for the reconstituted tills is between 0·20 kPa (HH(a), w = 0·523) and 55·7 kPa (HH(b), w = 0·210). At the liquid limit (LI = 1), the shear strength for these soils is approximately 1·5 kPa; by extrapolation to the plastic limit (LI = 0), shear strengths of approximately 75 kPa are indicated. These results generally confirm the findings of others (Skempton and Northey, 1952; Youssef et al, 1965) regarding the unique relationship between the undrained shear strength and liquidity index of a soil irrespective of the actual values for LL , PL. Wroth and Wood (1978), quoting the results of Youssef et al (op cit) , advocate a mean value of 1·7 kPa for the undrained shear strength of a soil when at the liquid limit.

From the evidence of Skempton and Northey (op cit) these authors also assume that the shear strength at the plastic limit is 100 times that at the liquid limit. It will be seen that this assumption, when applied to these reconstituted tills, will considerably overestimate their measured strength at the plastic limit. Taking into account the variation of the shear strength at the plastic limit, and assuming

$$\frac{c_u \text{ PL}}{c_u \text{ LL}} \simeq 50 \quad \text{for these soils (from Fig. 8.42)}$$

then, assuming a linear relationship between LI , log c_u :

$$c_u = 75 \exp\ (-3{\cdot}91 \text{ LI}) \text{ kPa} .$$

Although the in situ vane testing was carried out on natural soil containing material greater than the 0·425 mm maximum particle size of the reconstituted soils, it is interesting that the remoulded shear strengths measured for these soils in situ produce a cluster of data points in the region $c_u \simeq 100$ kPa at LI values between 0 , -0·2 , and through which the extrapolated trend line for the laboratory data passes. Whilst the peak undrained shear strength for a reconstituted (<0·425 mm) soil is not synonymous with the remoulded strength of its undisturbed counterpart, the expression shown above would more reliably predict these remoulded strengths than it would the very high peak strengths of the undisturbed till, (maximum 493 kPa).

That these remoulded values are so much lower than the measured peak undrained shear strengths is also significant. Table 5.2 shows that the ratio of peak to remoulded strengths for these soils varies between 3·72 and 5·78. The average is 4·46 . If, in the usual way, the ratio c_u p/c_u r is assumed to be a measure of the soil's sensitivity , then not only are these results at variance with the commonly accepted view that tills possess little or no sensitivity, (for example, Sladen and Wrigley, 1983), it would also explain why there is a poor correlation between their undisturbed undrained shear strength and liquidity index.

Estimates of undisturbed undrained shear strength can only satisfactorily be made on the basis of laboratory tests on good

quality undisturbed soil. It has already been shown (3.4) that, assuming the soil fails on the critical state line, estimates of undrained shear strength c_u may be obtained from :

$$c_u = \tfrac{1}{2} M \exp\left[(\Gamma - V) / \lambda \right] \quad \text{(equation 3.27)}$$

where M, Γ, λ are soil constants previously defined. In this equation V represents the in situ specific volume of the soil ; assuming full saturation and using measured values for undisturbed till HH(a) ,

$$V = 1 + 0{\cdot}156\ (2{\cdot}71)$$

(2·71 is the measured particle specific gravity)
(0·156 represents the average water content of 12 triaxial samples)

$$\therefore\ V = 1{\cdot}423.$$

Inserting measured values for the critical state parameters for this undisturbed soil, viz.

λ = 0·048 ... Table 8.1 (oedometer rather than isotropic, see discussion in 8.2)

Γ = 1·763 } ... (see 8.4.3)

M = 0·89 }

gives

$$c_u = \tfrac{1}{2} \times 0{\cdot}89 \exp\left[(1{\cdot}763 - 1{\cdot}423) / 0{\cdot}048 \right] \text{kPa}$$

$$= \underline{530 \text{ kPa}}$$

This value, derived from consolidated undrained triaxial tests, should be compared with those obtained from the in situ vane tests on the same till in Table 5.2 . Here, the measured values for $c_u p$ (till HH(a)) are 484 kPa (horizontal vane test) and 459 kPa (vertical vane test). Although estimates of undrained shear strength based on the expression above are sensitive to very small variations in the value for λ , nevertheless it is argued that they are more realistic than those based on a consideration of the reconstituted soils' properties.

8.4.2 Peak (Mohr - Coulomb) states from the triaxial tests.

The graphs of total axial stress and pore water pressure against axial strain for reconstituted and undisturbed till HH(a), which are shown in Figs. 7.18 to 7.41 , have been used to construct Mohr's circles for effective stress for this till, Fig. 8.43 . In the calculations for these circles the maximum values for additional axial stress, identified from each of the stress : strain curves, have been used. The Mohr -Coulomb envelopes which are shown for the reconstituted and undisturbed materials therefore correspond to the peak shearing resistance of the soil in each case. The intercepts of these envelopes on the shear stress axis give measured values for the effective cohesion $c'R = 25$ kPa , $c'U = 75$ kPa , for the reconstituted and undisturbed tills respectively. The measured inclination of these envelopes gives $\phi'R = 20^\circ$, $\phi'U = 20^\circ$. There are, of course, difficulties in establishing the true nature of the Mohr - Coulomb parameters c' , ϕ', in this way based as they are on the dual assumptions that a failure envelope is both linear and also tangential to all the Mohr circles drawn which, in this case, belong to soils tested over a very large range of overconsolidation ratios.

Nevertheless, these effective stress parameters may be compared with those for other tills reported by others and which are shown in Fig. 4.12 . The results from the drained shear box tests on reconstituted and undisturbed till HH(a), and undisturbed till F(b), have been plotted in the form shear stress at failure (τ_p) to corresponding effective vertical stress σ'_v in Fig. 8.44 . These data are also shown on Fig. 8.43 . An examination of Fig. 8.44 shows very little difference in the peak drained (D) shear strengths for these three materials. The Mohr - Coulomb failure envelope shown gives $\phi'_D = 25^\circ$, $c'_D = 0$. Whilst recognising the considerable differences in the two testing methods (CU triaxial, CD shear box), it is noticeable that the effective cohesion component of shear strength evident for till HH(a) in undrained triaxial compression is conspicuously absent in drained direct shear.

8.4.3 Ultimate or critical states.

The p' : q' : V stress paths for reconstituted and undisturbed till HH(a) during undrained triaxial compression which are shown individually in Figs. 7.42 to 7.65 are shown plotted collectively in

Fig. 8.45 (reconstituted) and 8.46 (undisturbed). Included in these diagrams are the isotropic overconsolidation ratios for the soils or, where an undisturbed soil has been isotropically consolidated at an effective stress level below the estimated p'_c, its assumed overconsolidation ratio (based on test OU(1)V) is quoted (in parenthesis).

The pattern of behaviour demonstrated by the effective stress paths for the reconstituted till is consistent with that expected from the undrained compression of isotropically consolidated and overconsolidated samples (3.4). It can be seen from Figs. 7.42 to 7.44 and Fig. 8.45 that, whilst the three normally consolidated samples (RA1(i), (ii), (iii)) have generated positive excess pore pressures which reduce p' at constant volume away from the normal compression line, the isotropically overconsolidated samples (RA2(ii), (iii), RB(v), R2 - O2, R2 - O3) have generated negative excess pore pressures which increase p' at constant volume in a direction towards the normal compression line. The small positive excess pore pressures generated by the lightly overconsolidated samples RB(ii) (Ro = 1·5) and RB(iii) (Ro = 2) are also consistent with these expectations.

The relationship between the isotropic compression line for this soil (from TR(1)) and the locus of end states for these samples defines a line in p' : V space (lower diagram, Fig. 8.45) and in $\log_e p'$: V space (Fig. 8.47) which may be identified as the critical state line for this material. This line, also shown in q' : p' space (upper diagram, Fig. 8.45) gives a value MR = 0·80 for the critical state frictional constant. The other critical state parameters for this reconstituted soil obtained from Fig. 8.47 are V_o = 1·899 (compare N_o = 1·87 from Table 8.1) and Γ = 1·876 .

The position of the isotropic normal compression line for the undisturbed till is more difficult to locate (see discussion in 8.2). Its approximate position, based on λ_{oed} = 0·048 (Table 8.1), V_o = 1·780 (from V = 1·413 at p' = 2000 kPa , TU(1), Table 7.35) may be established from the equivalent pressure relationship (3.5) :

$$p'_e = \exp\left[(V_o - V)/\lambda\right] \qquad \text{(equation 3.33)}$$

The relationship between this assumed normal compression line and the isotropic compression line from TU(1) is shown in Fig. 8.46.

Along with the uncertainty of clearly defining the normal compression characteristics for the undisturbed soil will also come uncertainty regarding precise overconsolidation ratios for those samples which are isotropically consolidated and overconsolidated at effective pressures below p_c. On the other hand, an undisturbed soil which is initially isotropically normally consolidated and then overconsolidated will produce a sample with a known overconsolidation ratio. Despite these uncertainties, it is clear that the general pattern of behaviour observed in the reconstituted till is also demonstrated by the undisturbed soil, Figs. 7.52 to 7.65 and Fig. 8.46 . It is interesting to note that whilst points representing end states for this soil (lower diagram, Fig. 8.46) lie to the right of the isotropic compression line, they are all to the left of the assumed normal compression line in the Figure. This is entirely consistent with the assumption that the isotropic compression line shown represents a reloading path for this natural sediment.

A critical state line for this soil has been inferred in Fig. 8.46; it is clear from its inferred position that the most heavily overconsolidated soils have failed furthest away from it. These data are also shown in the form $\log_e p' : V$ in Fig. 8.48 . The critical state parameters obtained from this Figure are $V_o = 1{\cdot}78$ (compare with $N_o = 1{\cdot}72$, Table 8.1) and $\Gamma = 1{\cdot}763$; from Fig. 8·46, $MU = 0{\cdot}89$.

Predictions of ultimate failure q'_u at the critical state for the normally consolidated and overconsolidated samples and for peak states of effective stress q' for the overconsolidated samples (that is, when these samples will first reach the Hvorslev surface assuming only elastic deformations occur) can be made on the basis of equations 3.26 and 3.36 respectively,

$$q'_u = M \exp\left[(\Gamma - V)/\lambda\right]$$

and

$$q' = (M - h) \exp\left(\frac{\Gamma - V}{\lambda}\right) + hp'$$

Tables 8.3 , 8.4 and 8.5 contain summaries of these predictions for the normally consolidated and overconsolidated samples of reconstituted and undisturbed till and these have been compared with the actual values for q'_u , q', obtained from the various tests.

An examination of these Tables will show that whilst there is a reasonable agreement between the predicted and actual values for q'_u at Ro = 1 for both the reconstituted and undisturbed till (Table 8.3 shows a range q'_u actual/q'_u predicted from 1·01 to 1·28), predictions for the overconsolidated samples do not demonstrate the same agreement. Tables 8.4 , 8.5 show that predicted peak overconsolidated strengths are consistently underestimated. (q'actual/ q'predicted ranges from 1·22 to 2·15 for the undisturbed till and from 1·0 to 1·90 for the reconstituted till). The amount of underestimation also generally becomes larger with increasing overconsolidation ratio. This is not surprising; it has already been noted that the most overconsolidated samples have deformed elastically only over a small initial range of compression. Estimates of q' based on the assumption of linear elastic deformations in these soils are therefore here not entirely appropriate. Tables 8.4, 8.5 also show the results of testing the prediction for q' at the stress level $q' = (\sigma'_a / \sigma'_r)$ maximum, identified from Figs. 7.18 to 7.41 . As might be expected, the predictions here give a better agreement with the actual values; Figs. 7.42 to 7.65 clearly show that (σ'_a / σ'_r) maximum is attained before the test paths for the most heavily overconsolidated samples reach the Hvorslev surface. These Tables also indicate that predictions of stresses q'_u at the ultimate state are overestimated for all the overconsolidated reconstituted samples and also for the most heavily overconsolidated undisturbed samples.

8.5 Normalised critical state parameters : the Hvorslev and Roscoe state boundary surfaces.

It will be noted that whilst the stress paths for the normally consolidated reconstituted and undisturbed till in $q' : p'$ space are generally of similar shape in each case, they are of different size. Differences in size due to differences in initial isotropic stress p'_e and hence initial specific volume can be accounted for by scaling all stresses with regard to p'_e in the manner described in 3.5 .

Stress paths normalised with respect to p'_e for the reconstituted till are shown in Fig. 8.49 . (Also shown in this Figure are the approximate axial strain contours for each of the tests.) It will be observed from these normalised data that the undrained stress paths for tests RA(i), (ii), (iii) clearly define a Roscoe surface for these normally consolidated samples extending from p'/p'_e = 1·0 to

meet the critical state line at $q'/p'_e \simeq 0{\cdot}6$. The test path for the most lightly overconsolidated sample, RB(ii) (Ro = 1·5), originates at a point almost directly beneath the critical state line at p'/p'_e = 0·65 and rises linearly (up to a point $\varepsilon_a \simeq 0{\cdot}03$) towards it. The test paths for the most heavily overconsolidated samples, however, are linear only up to points on these paths corresponding to $\varepsilon_a \simeq 0{\cdot}01$ (tests RB(iv)/RA2(iii) , RA2(ii) , Ro = 4) and $\varepsilon_a \simeq 0{\cdot}005$ (tests RB(v) , Ro = 8; R2 - 02, Ro = 16 ; R2 - 03, Ro = 32). Beyond these points the paths curve round and eventually move in the direction of the critical state line along a Hvorslev surface which can also be clearly identified for this material. From the geometry of the inferred position of the Hvorslev surface, h = 0·5 , g = 0·24 (see 3.5).

Stress paths normalised with respect to p'_e are also shown for the undisturbed till in Fig. 8.50 . (Again, approximate axial strain contours are indicated on this Figure.) Whilst the same general pattern of behaviour observed for the reconstituted samples in Fig. 8.49 is demonstrated by the test paths here for those samples with known overconsolidation ratios (and including the normally consolidated ones), it is evident that test numbers UA1(i) , UA2(i) , UA2(ii) and UB(ii)b (for which precise overconsolidation ratios are not known) have test paths which are not entirely consistent with this pattern. The test paths for these samples 'cross over' those for the other overconsolidated samples and there are indications that a separate Hvorslev surface for these samples exists a little way above the one shown. This supposition, and its consequences, will be discussed more fully later on. However, an inferred position for a Hvorslev surface is shown in this Figure. From the geometry of its position h = 0·575 , g = 0·36 .

An alternative method for normalising these data based on a constant p' section has also been described in 3.5 . In this method a reference section of the state boundary surface at p' = 1 kPa is selected so that, on this section, $V = V_o$ for the normal consolidation line and $V = \Gamma$ for the critical state line. Values for specific volume V_λ on the reference section are then found from equation 3.38 :

$$V_\lambda = V + \lambda \ln p' .$$

Figs. 8.51 , 8.52 show the relationship between V_λ and q'/p' for

the reconstituted and undisturbed till. The graphs contained in these Figures demonstrate clearly how the normally consolidated samples define a Roscoe state boundary surface for these materials extending from $V_\lambda = V_o$ at $q'/p' = 0$ on the normal compression line to $V_\lambda = \Gamma$ at $q'/p' = M$ at the critical state. With increasing overconsolidation ratios the normalised stress paths (initial $V_\lambda < V_o$) extend into the region where $q'/p' > M$, a behaviour consistent with the observation that the most heavily overconsolidated of these soils exhibit marked peaks in their $\sigma'_a / \sigma'_r : \varepsilon_a$ curves, in contrast to those of the normally consolidated samples. (For example, compare Fig. 7.20 , RA1(iii), Ro = 1 with Fig. 7.27, R2 - 03, Ro = 32.) The position of the contour representing (σ'_a / σ'_r) maximum is shown in these Figures and, although being somewhat arbitrary choices, the positions of the contours representing $\times \frac{1}{2}$, $\times \frac{3}{4}$, $\times 1$ (σ'_a / σ'_r) maximum are also shown. With reference to these contours it can be seen that the test paths for the overconsolidated samples approach the Hvorslev surface shortly after (σ'_a / σ'_r) maximum has been reached and then proceed down this state boundary surface towards the critical state line.

Fig. 8.52 is interesting for it shows that whilst the undisturbed samples with known overconsolidation ratios are identified with the Hvorslev surface indicated, the overconsolidated samples UB(ii)b , UA2(ii) , UA2(i) and, perhaps, UA1(iii) , which do not have known overconsolidation ratios, have test paths which extend beyond this surface. It is also interesting to note that the positions of the points $\times \frac{1}{2}$, $\times \frac{3}{4}$, $\times 1$ (σ'_a / σ'_r) maximum on these particular paths have produced a marked shift of the stress ratio contours upwards. That these samples are behaving in a different manner is quite clear : they demonstrate higher peak strengths and require larger deviator stresses to achieve the same stress ratios than do the other undisturbed samples.

The $q'/p' : V$ data for the reconstituted and undisturbed materials can be compared directly by matching the reference sections at a convenient point, for example, $V_\lambda = V_o$ for the reconstituted soil, Fig. 8.53 . In this Figure, comparisons can be made between the reconstituted and undisturbed soil for Ro = 1 , 8 , 16 , 20 and 32 . State boundary surfaces for both materials are also shown.

8.6 Aspects of behaviour inside and on the state boundary surface.

8.6.1 Pore pressure response.

Parry (1958) examined the rate and relative sign of the excess pore pressures generated during the undrained compression of remoulded London Clay and used these findings to infer the directions in which both normally consolidated and overconsolidated samples were moving at failure (failure here is defined as maximum deviator stress). By plotting the ratio :

$$\left\{ \left(\frac{\Delta u}{p'} \right) / \Delta \varepsilon_s \right\}_f \quad \text{..... (rate of pore pressure change at failure)}$$

against p'_u / p' for his tests, he was able to demonstrate that this rate of change was largest for those samples failing (at p') furthest away from the critical state line (where the equivalent pressure = p'_u) . In addition, the sign of the pore pressure change was such as to move the specimen towards the critical state line. A more detailed interpretation of these results and their significance has been presented by Schofield and Wroth (1968) and Atkinson and Bransby (1978) .

A similar approach has been adopted for the pore pressure data from the CU tests in this study. Here, however, the rate of pore pressure change throughout each test :

$$\left\{ \left(\frac{\delta u}{\delta p'} \right) / \delta \varepsilon_s \right\}$$

has been evaluated and plotted against p'_u / p'. Here, $\delta p'$ is the increment in effective pressure over the corresponding shear strain increment $\delta \varepsilon_s$ in which the pore pressure increment δu is recorded. In this way, the pore pressure paths for the normally consolidated and overconsolidated samples can be examined over the entire range of axial compression.

These results are presented in Figs. 8.54 , 8.55 . Values for the overconsolidation ratio are shown (circled) against each pore pressure path; the estimated overconsolidation ratios are shown uncircled. (The extent of Parry's data for London Clay is also shown in Fig. 8.54.)

Both reconstituted and undisturbed normally consolidated samples show reducing rates of positive excess pore pressure change over a narrow

band either side of $p'_u/p' = 1{\cdot}0$. Normally consolidated samples approach the critical state line from within the top left hand quadrant of the graph. If pore pressures remain positive then end points will plot above the point $\left\{ \left(\frac{\delta u}{\delta p'}\right) \Big/ \delta\varepsilon_s \right\} = 0$ and at or near the point $p'_u/p = 1$ at the critical state. This is generally the case, except that at the large axial strains experienced by these samples pore pressures were showing slight reductions, differences were negative, hence end points cluster above <u>and</u> below the line of zero pore pressure change.

With increasing overconsolidation ratios, the positions of the pore pressure paths shift further into the top right hand quadrant to increasing positive values for the ratio p'_u/p'. This is consistent with the observation that overconsolidated samples initially approach the critical state line with reducing pore water pressures and therefore increasing effective stresses. Within each set of paths (reconstituted, undisturbed), increasing overconsolidation ratios are also associated with increasingly larger negative values for the ratio $\left\{ \left(\frac{\delta u}{\delta p'}\right) \Big/ \delta\varepsilon_s \right\}$; however, the undisturbed samples show larger negative rates of change, for example in test R2 - 03 (Ro = 32) this ratio = -10 , yet in test UB(vii) (Ro = 20) this ratio = -14·5 . Comparing behaviour at similar overconsolidation ratios also suggests that these maxima occur further away from the critical state line in the undisturbed soil. Compare, for example, the value for $p'_u/p' = 4{\cdot}2$ for the undisturbed sample UB(vi) (Ro = 16) with $p'_u/p' = 1{\cdot}9$ for the reconstituted sample R2 - 02 (Ro = 16) at the points on their paths corresponding to the maximum rate of pore pressure reduction.

The positions on each of these paths where the pore pressures first become negative (relative to the initial pore pressure) are also indicated (by open circles). These show that (relative) negative pore pressures only occurred in the reconstituted samples with Ro $\geqslant$ 4 (although tests RB(ii), Ro = 1·5 ; RB(iii), Ro = 2 , were unfortunately terminated before ultimate failure, there seemed to be no likelihood of negative pore pressures occurring in these samples); however, a (relative) negative pore pressure was shown by the undisturbed sample UB(ii)a at an overconsolidation ratio of only 1·5. An extrapolation of the trend line so indicated by joining these points will intersect the p'_u/p' axes in both cases at small positive

values (dry side of critical) generally within the region where the pore pressure paths for the lightly overconsolidated samples first traverse them.

Finally, the superimposition of the stress ratio contours at the arbitrary intervals x $\frac{1}{2}$, x $\frac{3}{4}$, x 1 (σ'_a / σ'_r) maximum for both materials shows a similar contour pattern for the reconstituted and undisturbed soil. These contours trace continuous surfaces across the mapped region over a large range of overconsolidation ratios. The contour (σ'_a / σ'_r) maximum appears particularly significant in this respect : it apparently defines a surface beyond which the samples do not move, and along which the overconsolidated soils approach the critical state. The direction of movement of these paths parallel to this stress ratio contour in opposite directions either side of the vertical through $p'_u / p' = 1$ is , of course , a manifestation of the same effect observed by Parry (op cit).

The response of the pore water pressure to undrained compression may also be expressed in terms of the two empirical parameters A , B , (see 3.6) according to equation 3.39 . Usually the pore pressure parameter at failure A_f , is determined corresponding to the observed pore pressure response at maximum deviator stress. Bishop and Henkel (1976) quote values for A_f varying from +1·3 for normally consolidated undisturbed marine clay to -0·62 for undisturbed Weald clay; remoulded Weald clay with an overconsolidation ratio = 8 has A_f = -0·22 , for example.

Values for A_f have been calculated from the pore pressure data for the reconstituted and undisturbed till and these are shown plotted against overconsolidation ratio in Fig. 8.56 . From this Figure it can be seen that A_f varies from +0·710 at Ro = 1 to A_f = -0·385 at Ro = 32 (but note A_f = -0·449 at Ro = 16), for the reconstituted soil, whilst over the range of overconsolidation ratios Ro = 1 to 20 for the undisturbed soil A_f varies from +0·423 to -0·406 .

Wroth has proposed an alternative parameter $A_{c.s.}$ (see 3.6) which is evaluated on the basis that the soil fails at the critical state :

$$A_{c.s.} = \frac{1}{M} \left[\left(\frac{R}{r} \right)^{-\Lambda} + \frac{M}{3} - 1 \right] , \quad \text{(equation 3.48)}$$

Values for $A_{c.s.}$ calculated for the reconstituted and undisturbed till are shown in Figs. 8.57 , 8.58 respectively; these are shown plotted against the corresponding overconsolidation ratio. Also

included in these Figures are the values for A_f from Fig. 8.56 . It can be seen that the closest correspondence between A_f , $A_{c.s.}$ exists for the normally consolidated and lightly overconsolidated samples. However, with increasing overconsolidation ratio (Ro $\geqslant$ 8), the disparity between A_f , $A_{c.s.}$ increases. It has already been shown that the most heavily overconsolidated soils have failed furthest away from the critical state line, and that predictions of ultimate failure at the critical state for these samples are therefore overestimated. It is not surprising, therefore, that the pore pressure response based on the assumption that these soils are at the critical state is also overestimated.

8.6.2 Undrained elastic modulus.

In the undrained triaxial compression test estimates of the undrained modulus of elasticity E_u can be made by an evaluation of the soil's stress : strain characteristics, (4.5.6). The value for E_u is of course dependent on the stress level at which the calculation is made and therefore, along with quoted values for E_u , there should also be a note regarding this.

The stress : strain data from the CU triaxial tests for the reconstituted and undisturbed till HH(a) have been examined in this light and values for E_u at three stress levels have been calculated: E_i ; $E(\sigma'_a/\sigma'_r)$ maximum ; $E(\sigma_a - \sigma_r)$ maximum. These three moduli correspond to the initial tangent modulus, the modulus at the point corresponding to the maximum principal effective stress ratio and the modulus at the point of maximum deviator stress. These results are shown in Tables 8.6 , 8.7 .

From these Tables it can be seen that values for E_u for the reconstituted till vary from 116·67 MNm^{-2} for E_i at Ro = 1 to 1·50 MNm^{-2} for $E(\sigma_a - \sigma_r)$ maximum at Ro = 32 . From these data the expected reduction in the value for E_u from E_i to $E(\sigma_a - \sigma_r)$ maximum at the same overconsolidation ratio is also observed. In the undisturbed till E_u varies from 133·33 MNm^{-2} for E_i at Ro = 1 to 2·20 MNm^{-2} for $E(\sigma_a - \sigma_r)$ maximum at Ro = 20 .

The large variations observed in these moduli only become meaningful when values for E_u are normalised with respect to the initial isotropic radial stress σ'_r at which each sample was brought to equilibrium before shearing, (see for example Fig. 4.17). Therefore,

the E_u / σ'_r normalised moduli are also shown in these Tables. Whilst there is still some evidence of variation and inconsistency in the normalised values for E_i in both reconstituted and undisturbed soils, (for example note the variation E_u / σ'_r = 75 , 208·8 at Ro = 1 for RA1(iii) , RA1(ii) respectively, Table 8.6 and E_u / σ'_r = 44·12 , 170 at Ro = 1 for UA1(ii) , UA1(iii) , Table 8.7) , there is nevertheless now a clearer basis for comparisons to be made within and between these two materials.

The striking feature characterising these normalised data is the consistency of E_u / σ'_r at similar overconsolidation ratios. Note the values E_u / σ'_r = 9·23 , 8·12 , 6·13 for Ro = 1 at $E(\sigma'_a / \sigma'_r)$ maximum and E_u / σ'_r = 4·49 , 4·48 , 4·89 at the same overconsolidation ratio for $E(\sigma_a - \sigma_r)$ maximum , (Table 8.6, reconstituted). The same consistent pattern is also evident with the undisturbed till.

With increasing Ro the relative stiffness of each soil also increases. For the reconstituted till the (minimum to maximum) range of increase is 75 (Ro = 1) to 281·2 (Ro = 32) ; 6·13 to 74·97 ; 4·48 to 29·97 at E_i , $E(\sigma'_a / \sigma'_r)$ maximum , $E(\sigma_a - \sigma_r)$ maximum respectively. The corresponding ranges of increase for the undisturbed soil are 44·12 to 814·8 (Ro = 16) ; 13·39 to 203·4 (Ro = 20) ; 6·44 to 44·88 (Ro = 20) .

Graphs of E_u / σ'_r : Ro for the reconstituted and undisturbed till are shown in Figs. 8.59 , 8.60 . It is clear from these graphs that the undisturbed soil has a greater stiffness at the two stress levels shown, (E_i has not been included in these Figures). This difference in stiffness (expressed as $E_u(U) / E_u(R)$), although different at each of the two stress levels, is preserved over the entire range of overconsolidation ratios. Therefore, at Ro = 1 , $E_u(U) / E_u(R) \simeq 2{\cdot}5$ (σ'_a / σ'_r) maximum , and $\simeq 1{\cdot}68$ ($\sigma_a - \sigma_r$) maximum. At Ro = 4 , $E_u(U) / E_u(R) \simeq 3{\cdot}33$, 1·50 ; at Ro = 20 $\simeq 3{\cdot}33$, 1·80 .

The very large range of measured undrained moduli for the undisturbed till in this series of CU triaxial compression tests (2·20 to 170 MNm^{-2}) endorses the observations of others regarding the very large differences in the modulus of tills measured in this way (see Fig. 4.16) but it is suggested that normalisation of the data in the manner shown will enable direct and meaningful comparisons of E_u to be made from material to material.

The effect of isotropically consolidating undisturbed samples below

p'_c and then allowing them to come to equilibrium at reduced effective stress (that is producing overconsolidated asmples with unknown overconsolidation ratios) can again be observed in Fig. 8.60 for the two samples (circled) UA2(i) and UA2(ii) . It is clear that the values for E_u at (σ'_a / σ'_r) maximum for these two samples are somewhat in excess of the expectation from the trend indicated by the graph. A compilation of the graphs of principal stress ratio to axial strain for all the reconstituted and undisturbed samples at similar overconsolidation ratios (Figs. 8.61 to 8.67), whilst demonstrating the consistent behaviour of the normally consolidated and overconsolidated samples, confirms the apparently anomalous behaviour of these two particular samples. Fig. 8.66 , for example , shows (σ'_a / σ'_r) maximum $\simeq$ 4 for UA2(i) (nominal Ro = 8), well in excess of (σ'_a / σ'_r) maximum $\simeq$ 2·75 for UB(v) , Ro = 8 and 2·25 for RB(v) at the same overconsolidation ratio. Again, Fig. 8.65 shows (σ'_a / σ'_r) maximum $\simeq$ 3·5 for UA2(ii) (nominal Ro = 4) contrasting with values ranging from $\simeq$ 2·1 for RA2(iii) to $\simeq$ 2·55 for UA2(iii) at the same overconsolidation ratio. Examination of Fig. 8.63 (UB (ii)b) and Fig. 8.64 (UA1(i)) also shows a similar effect for these other undisturbed samples with ill-defined overconsolidation ratios , although enhanced stiffness (from Fig. 8.59) does not appear to characterise these in the same way.

8.7 Carbonate cementation.

Whilst this could not have been envisaged at the beginning of the programme of work described herein, it has subsequently become clear, following a detailed examination of the results of the laboratory work, that certain aspects of the engineering behaviour of these chalky tills can be explained by hypothesising the existence of a cementing agent, almost certainly carbonate, within their matrix.

The occurrence and characteristics of naturally cemented glacial soils of the Quaternary have been recognised and reported by others, notably in N. America and Europe, but the literature does not contain any reference to the occurrence of naturally cemented tills in the UK. Flach et al (1969) describe the processes of pedocementation which they attribute to the effects of silica, sesquioxides and carbonates in solution in a variety of Pleistocene soils in the USA. Rosauer and Frechen (1960) have recognised various forms of carbonate concretions and cement in the Würm and Riss (= Devensian, Bowen , 1978) loess in

Kärlich, near Koblenz. These authors have used the evidence from the stratigraphical distribution of these carbonates and their petrological properties (occurring as they do in forms from finely dispersed powder to lumpy concretions) as the basis for a climatic differentiation of the Würm loess in Europe.

Townsend (1965) notes the possible cementing effect of carbonate in the New Liskeard varved glacial clays of Ontario and speculates that increased concentrations of CO_2 (which is known to exist in greater concentrations in the water at the bottom of a glacier than would be found at the same temperature but under atmospheric conditions, see Tamm, 1924) might be the cause of the cementation. Sangrey (1972a), concurring with these findings, also notes that all of the naturally cemented soft silt and clay deposits studied by him in Canada and the northern United States are of glacial (but not necessarily glacigenic) origin. Whilst not discussing the effects of carbonate cementation in particular, he does remark on the increased strength and resistance to compression resulting from cementation and notes that remoulded strengths will be very much lower than peak strengths in these soils.

In a later paper, Sangrey (1972b) describes the results of his findings on the mechanical behaviour of the naturally cemented, extremely sensitive brackish marine Leda-type clay deposits. From his results he is able to identify the point at which the cement breaks down and makes the observation that the influence of the cement on strength and compressibility is greatest at low effective stresses. Interestingly, in this paper Sangrey states "However, no-one has yet been able to define a specific cementing compound for a particular soil even though the evidence for some sort of cementation is strong."

There are several pieces of evidence which are available to suggest the presence of a carbonate cement in the tills of the Vale of St. Albans and these will now be examined.

8.7.1 The mineralogical evidence.

The results of the XRD and EDAX tests shown in Tables 7.5 , 7.6 demonstrate that the tills have total calcite contents varying from 4·3% , W(b) to 14·9% , HH(b) . Till HH(a) had 10% calcite. Conspicuously, the naturally decalcified till F(b) contained no detectable calcite. The acid soluble content present in the clay fractions of these soils (shown in Table 7.5), determined independently

from sedimentation testing of the carbonate-free minus 63 microns fraction (6.2.4) , indicates that the carbonates in this fraction are wholly calcitic. Furthermore, if it is assumed that the 6·5% calcium in till F(b) detected by EDAX (Table 7.6) is wholy accounted for by the 12% contribution of calcium montmorillonite to the clay fraction of this soil determined by XRD, then it can be shown that the 24·9% difference (EDAX) in calcium in tills W(b) , W(d) may be accounted for exactly by the 8·3% difference (XRD) in calcite calculated for these same soils.

The results of a combined EDAX - image analyser element analysis on the chalk and matrix in samples of tills HH(a) , HH(b) shown in Figs. 7.5 and 7.6 are quite conclusive : whilst the chalk in both samples comprises calcium and a little silica, the matrix contains a suite of elements associated with the clay minerals identified. However, the clay matrix in both tills also contains a surprisingly large amount of calcium, almost as much as the chalk itself, and far more than can be accounted for solely by the presence of the calcic clay minerals.

8.7.2 The evidence from the grading analyses.

In the reporting of their observations on carbonate pedocementation, Flach et al (op cit) remark "In early stages of carbonate accumulation and in materials with little or no gravel, these (carbonate) concentrations are in the form of nodules scattered throughout.... The nodules range in size from about 1mm to more than 1cm." Elsewhere, Rosauer and Frechen (op cit) have also recognised a variety of carbonate concretions including open and closed cylinders and 'single-spherical' and 'complex-spherical' nodules.

It will be remembered that visual observations made during the grading tests on tills HH(a) , HH(b) , (8.1.4) also indicated the presence of irregularly-shaped carbonate concretions, and particularly in the upper till, HH(b) . Here, they varied in size from 0·5mm up to 8mm , Table 7.4 . That carbonates have accumulated in considerable quantity to form the hard impervious 'plugged' petrocalcic horizon in the Westmill Upper Gravel directly beneath this till's probable correlative at Westmill Quarry has already been noted (see 2.4.5).

Furthermore, the removal of the relatively small amounts of carbonate in the matrix of tills HH(a) , HH(b) , W(b) , W(d). has been shown to

increase the true clay content of these tills by varying amounts up to 12·5% (the increase in till HH(a) was 8·86%). Again, the notable exception was till F(b), the naturally decalcified soil; the removal of carbonate made no significant difference to this till's coarse and fine grading characteristics. The conclusion here, therefore, is that the presence of carbonate in the 2mm down fraction has inhibited complete disaggregation of the clay colloids during sedimentation, even after the usual pretreatment techniques have been employed.

8.7.3 The evidence from the oedometer tests.

Whilst not being as satisfactory as, for example, triaxial compression testing in this respect, the results from the oedometer tests can be examined and reviewed for evidence for cementation.

According to Sangrey (1972 b), quoting Terzaghi and Peck (1967), "A typical e against log p (= $\log_{10}\sigma'_v$) curve for a sensitive soil... is quite flat at low stresses then breaks abruptly as the soil structure collapses. The characteristic of this curve ... is an apparent preconsolidation stress ... which is larger than any past stress history of the soil." This observation does, however, require qualifying in two respects: it will also depend on the degree of overconsolidation of the sediment, and on the relative strength of the cementing agent. The post-glacial Leda and Mattagami Mines-type clays investigated by Sangrey have not been ice-loaded and are therefore not heavily overconsolidated, unlike the lodgement tills in the Vale of St. Albans. Furthermore, the effect of a relatively strong cement within an otherwise soft to firm (lacustrine or estuarine) sediment is likely to significantly affect its compressibility; on the other hand, it will be more difficult to detect the presence of cement in the matrix of an already very stiff soil.

Whilst a 'breakdown in soil structure' has not been observed in the same way for these tills, nevertheless the results of the oedometer compression tests do provide conclusive evidence suggesting that the presence of a carbonate cement in these tills is affecting their compressibility. The results of tests OR(3) and OU(3)V show quite clearly that the compression characteristics of the decalcified till F(b) are comparable in both its reconstituted and undisturbed forms, (λ_R/λ_U = 0·97 , Table 8.1). This was not the case with the other soils tested; here the undisturbed tills were far less compressible

than their reconstituted counterparts (for example $\lambda R/\lambda U = 1{\cdot}5$ for HH(a). Although the process of reconstituting a soil will not remove any carbonate present it will, however, completely destroy any cementing effect it might have. This 'destroying' effect has clearly been demonstrated in reconstituted tills HH(a) , HH(b) , W(b), W(d) .

It has been shown that there is sufficient chalk present in the coarser fractions of these tills (Table 7.4)to supply the carbonate required for this process, but the rate at which cementation takes place will depend on the rate at which the supersaturated solutions permeate through the soil body. Whilst the oedometer tests show that the intrinsic permeability of the reconstituted till matrix is very low, it is also evident from the oedometer tests on the undisturbed material that in their naturally overconsolidated state they will be considerably more permeable. The in situ soil will have enhanced permeability due to its coarser grading (Fig. 7.2) , the presence and continuity of any sand pockets or lenses (5.2.1) and, particularly, the spacing and continuity of any discontinuities present (4.4.2). An earlier observation regarding carbonate deposition on the surfaces of the discontinuities examined within till HH(a) at Holwell Hyde Quarry (5.2.3) would tend to confirm this.

8.7.4 The evidence from the strength tests.

Despite the limitations implicit in the use of the shear vane to determine in situ undrained shear strength (see 5.3.4), the consistent evidence provided by these tests in tills HH(a) , HH(b) , W(b) , W(d) (Table 5.2) does suggest that a degree of 'sensitivity' is apparent in these soils, sufficient to classify them as 'medium' to 'sensitive' (Smith, 1982). That such significantly large differences exist between the measured peak and remoulded strengths for these tills could certainly indicate that a cementation bond of the type being proposed has been broken down on first time shearing. These results are not conclusive, however, for unfortunately no comparative shear vane testing could be carried out in the decalcified till F(b) at Foxholes Quarry prior to its infilling during 1981.

Neither is the evidence from the drained shear box tests conclusive. The results shown in Fig. 8.44 do not indicate the presence of such a cementitous bond in the undisturbed till HH(a) , nor do they

indicate its absence in the undisturbed till F(b). However, it should also be noted that the behaviour of these two 'undisturbed' tills in these tests did not conform to the pattern expected from these naturally overconsolidated soils, (Figs. 7.14 , 7.15), unlike that which had been demonstrated for the reconstituted and overconsolidated till HH(a) in the same test (Fig. 7.13). Arguments and reasons can be put forward explaining these aberrant results: uppermost amongst these must be considered the possibility that the method of transferring the sample from its former to fit snugly into the split box of the shear apparatus could, despite due care in this process, have disturbed the soil.

However, unlike the direct shear tests, the results from the triaxial tests discussed in 8.4 do demonstrate the existence of tensile bonding in the undisturbed soil over and above that which can be attributed solely to the process of overconsolidation. Although the brittle type of behaviour in compression reported by Townsend et al (1969) for naturally cemented post-glacial clays has not been observed in these tills, there are nevertheless enhanced effects in terms of both strength and stiffness which characterise those soils which have been isotropically consolidated and overconsolidated below $\sigma'_r \simeq 800$ kPa.

The difference in response during compression between this latter category (referred to as Type I) of undisturbed soil and those soils which have been isotropically consolidated to $\sigma'_r \gtrsim 1000$ kPa and then overconsolidated (Type II) can be appreciated by examining the graphs σ'_a / σ'_r : ε_a . The representation of the stress: strain data in this form is a particularly sensitive indicator of this phenomenon. The evidence suggests that Type I till attains peak shear stress ratios up to 40% larger than those for Type II at the same apparent Ro , Figs. 8.65 , 8.66 , and are comparable in magnitude with those for the more heavily overconsolidated soils (eg. Ro = 16 , 20 , Fig. 8.67).

Other means of contrasting these differences have been explored and presented : for example, V_λ normalisation of p', q' data (Fig. 8.52) and insertion of the contours representing the arbitrary intervals of $\times \frac{1}{2}$, $\times \frac{3}{4}$, $\times 1$ (σ'_a / σ'_r) maximum on the resultant stress paths. Here, it has been shown that a consistent, but different, contour arrangement exists across a range of overconsolidation ratios in the two types of materials. In Type I till equivalent stress ratio points are supported by higher deviator stresses - an effect which shifts

their stress paths upwards towards a higher common Hvorslev surface, above that for the Type II material. With reducing overconsolidation ratio this effect, as might be expected, becomes less marked.

Finally, evidence has been produced showing that Type I soil also has enhanced stiffness in terms of the undrained modulus E_u . Figs. 8.65 , 8.66 clearly show that equivalent values for (σ'_a / σ'_r) are mobilised at a faster rate and that the point (σ'_a / σ'_r) maximum occurs at a smaller strain value than in the Type II category till at the equivalent Ro . Again, this particular feature is consistent with the presence of a carbonate cement in these materials.

In view of the fact that the effects on measured strength and modulus herein described were not apparent in those samples isotropically consolidated at the higher pressures, then it can only be supposed that the cementitous bond had been broken down during this process of drained spherical compression. There are insufficient data available from the present series of tests, however, to indicate the precise stress level of this occurrence, and this could only be established satisfactorily by a series of further isotropic compression tests involving smaller incremental loading stages.

Soil Properties / Till Type	HH(a)		HH(b)		F(b)		W(b)		W(d)	
	R	U	R	U	R	U	R	U	R	U
$(C_c/2{\cdot}303)$	0·069	0·046	0·063	0·046	0·107	0·120	0·081	0·060	0·071	0·052
λ	0·072	0·048	0·066	0·050	0·116	0·120	0·083	0·060	0·070	0·052
$\bar{\kappa}$	0·032	0·025*	0·029	0·022	0·052	0·042	0·047	0·033	0·032	0·028
λ_R/λ_U	1·50		1·20		0·97		1·38		1·35	
$\bar{\kappa}_R/\bar{\kappa}_U$	1·28		1·32		1·23		1·42		1·14	
N_o for $p' = 1$kPa	1·87	1·72*	1·87	1·74	2·39	2·44	2·11	1·90	1·95	1·80

* Average of two tests. R , U , reconstituted , undisturbed .

Table 8.1 Soil constants derived from the oedometer tests.

Properties	HH(a)		HH(b)	
	R	U	R	U
λ	0·070	0·036	0·071	0·038
$\bar{\kappa}$	0·029	0·018	0·025	0·020
λ_R / λ_U	1·94		1·87	
$\bar{\kappa}_R / \bar{\kappa}_U$	1·61		1·25	
V_o for $p' = 1$ kPa	1·899	1·690	1·915	1·670

R , U reconstituted , undisturbed.

Table 8.2 Soil constants for HH(a) , HH(b) from the isotropic compression tests.

Test number (Ro = 1)	(1) q'_u predicted (kPa)	(2) q'_u actual (kPa)	(3) 2/1
RA1(i)	241•5	309•2	1•28
RA1(ii)	456•0	514•8	1•12
RA1(iii)	931•6	976•2	1•05
UA1(iii)	768•1	777•4	1•01
UA1(v)	1099•0	1144•4	1•04

Table 8.3 Critical state predictions, q'_u, reconstituted and undisturbed till HH(a), Ro = 1.

Test number	1 q' predicted (kPa)	2 q' actual (kPa)	3 q' $(\sigma'_a/\sigma'_r)_{max}$ (kPa)	4 2/1	5 3/1
RB(ii) Ro=1·5	221·9	221·6	-	1·0	-
q'_u	235·7	221·6		0·94	
RB(iii) Ro=2	181·1	190·3	-	1·05	-
q'_u	216·3	190·3		0·88	
{RB(iv) {RA2(iii) Ro=4	414·3	541·0	526·0	1·31	1·27
q'_u	571·5	461·4		0·81	
RA2(ii). Ro=4	209·0	341·4	302·3	1·63	1·45
q'_u	290·8	301·3		1·04	
RB(v) Ro=8	257·9	361·1	304·9	1·40	1·18
q'_u	421·0	272·7		0·65	
R2-02 Ro=16	167·6	318·4	228·3	1·90	1·36
q'_u	313·7	262·8		0·84	
R2-03 Ro=32	109·0	194·4	124·5	1·78	1·14
q'_u	223·9	190·9		0·85	

Table 8.4 Critical state predictions, q'_u, q', overconsolidated reconstituted till HH(a).

Test number	1 q' predicted (kPa)	2 q' actual (kPa)	3 q' $(\sigma'_a/\sigma'_r)_{max}$ (kPa)	4 2/1	5 3/1
UA1(ii) Ro=1·2	708·0	861·7	762·1	1·22	1·08
q'_u	700·8	860·0		1·23	
UB(i) Ro=1·25	731·8	898·7	826·5	1·23	1·13
q'_u	768·1	898·7		1·17	
UB(ii)a Ro=1·5	652·6	818·3	668·6	1·25	1·02
q'_u	760·1	818·3		1·08	
UA1(i) Ro=2	402·6	624·4	536·4	1·55	1·33
q'_u	487·7	619·8		1·27	
UB(iii) Ro=2	520·0	687·2	595·8	1·32	1·15
q'_u	657·0	687·2		1·05	
UB(ii)b Ro=2·4	380·3	611·7	464·7	1·61	1·22
q'_u	533·4	608·0		1·14	
UA2(ii) Ro=4	285·8	387·9	368·7	1·36	1·29
q'_u	482·7	318·7		0·66	
UA2(iii) Ro=4	480·1	817·4	612·4	1·70	1·28
q'_u	706·7	817·4		1·16	
UA2(i) Ro=8	198·5	427·2	256·1	2·15	1·29
q'_u	398·5	427·2		1·07	
UB(v) Ro=8	236·8	359·0	249·7	1·52	1·05
q'_u	465·9	359·0		0·77	
UB(vi) Ro=16	169·8	325·5	152·2	1·92	0·90
q'_u	378·2	325·5		0·86	
UB(vii) Ro=20	155·8	294·2	133·2	1·89	0·86
q'_u	359·1	294·2		0·82	

Table 8.5 Critical state predictions, q'_u, q', overconsolidated undisturbed till HH(a).

Test	Ro	E_i (MNm^{-2})	$\frac{E_u}{\sigma'_r}$	$E(\sigma'_a/\sigma'_r)max$ (MNm^{-2})	$\frac{E_u}{\sigma'_r}$	$E(\sigma_a-\sigma_r)max$ (MNm^{-2})	$\frac{E_u}{\sigma'_r}$
RA1(i)	1	47•1	117•7	3•69	9•23	1•80	4•49
RA1(ii)	1	116•67	208•3	6•50	8•12	3•58	4•48
RA1(iii)	1	120•0	75•0	9•81	6•13	7•82	4•89
RB(ii)	1•5	53•33	199•7	15•27	5•74	-	-
RB(iii)	2	16•67	299•9	5•94	5•0	-	-
RB(iv)/ RA2(iii)	4	40•0	100•0	5•84	14•61	4•62	11•54
RA2(ii)	4	60•0	300•0	4•69	11•72	2•33	11•67
RB(v)	8	35•0	175•0	6•49	32•44	3•50	17•51
R2 - 02	16	23•53	235•3	7•11	71•05	2•27	22•71
R2 - 03	32	14•06	281•2	3•75	74•97	1•50	29•97

Table 8.6 Undrained modulus , reconstituted till HH(a) .

Test	Ro	E_i (MNm^{-2})	$\frac{E_u}{\sigma'_r}$	$E(\sigma'_a/\sigma'_r)max$ (MNm^{-2})	$\frac{E_u}{\sigma'_r}$	$E(\sigma'_a-\sigma'_r)max$ (MNm^{-2})	$\frac{E_u}{\sigma'_r}$
UA1(ii)	1	35•29	44•12	15•60	19•50	5•15	6•44
UA1(iii)	1	170•0	170•0	17•58	17•58	8•92	8•92
UA1(v)	1	133•33	83•33	21•42	13•39	11•55	7•22
UB(i)	1•25	41•67	52•08	17•11	21•39	8•08	10•10
UB(ii)a	1•5	97•17	145•68	21•78	32•65	5•0	7•49
UA1(i)	2	60•0	150•0	9•0	22•5	3•16	7•89
UB(iii)	2	75•0	150•0	12•52	25•03	5•51	11•02
UB(ii)b	2•4	27•1	81•22	13•23	39•73	4•50	13•52
UA2(ii)	4	91•67	458•0	16•03	80•16	9•60	48•01
UA2(iii)	4	36•36	90•91	21•26	53•16	7•24	18•10
UB(v)	8	16•25	130•0	7•57	60•53	2•60	20•80
UB(vi)	16	50•93	814•8	10•28	164•5	2•20	35•23
UB(vii)	20	21•74	434•8	10•17	203•4	2•24	44•88

Table 8.7 Undrained modulus , undisturbed till HH(a).

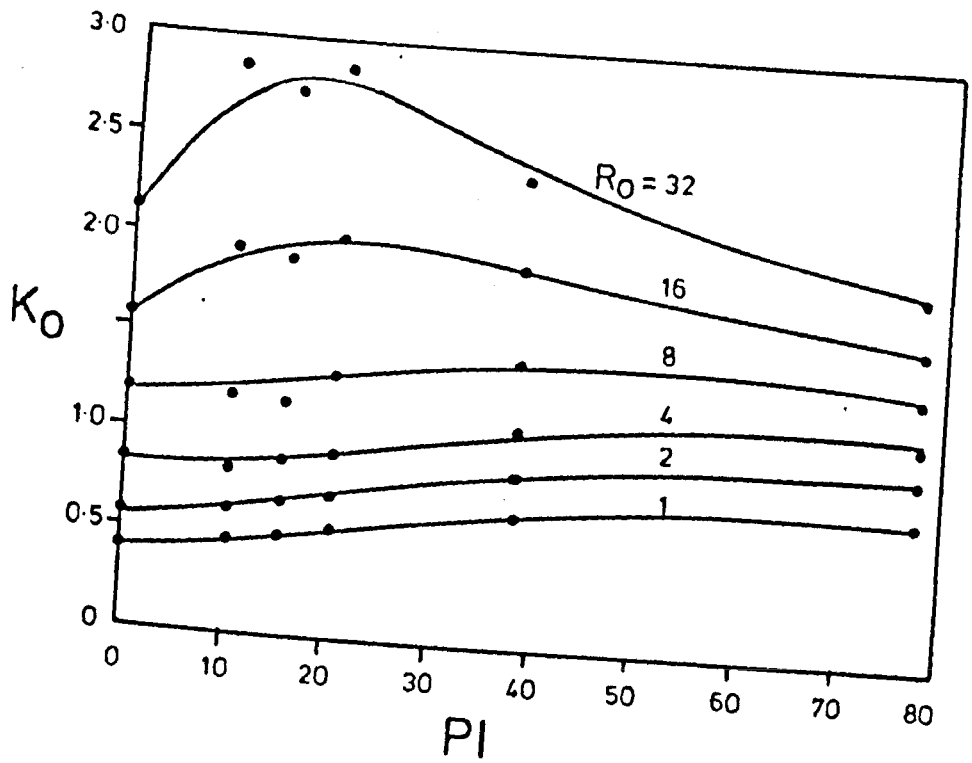

Figure 8.1 K_o as a function of overconsolidation ratio and plasticity index. (From Brooker and Ireland, 1965).

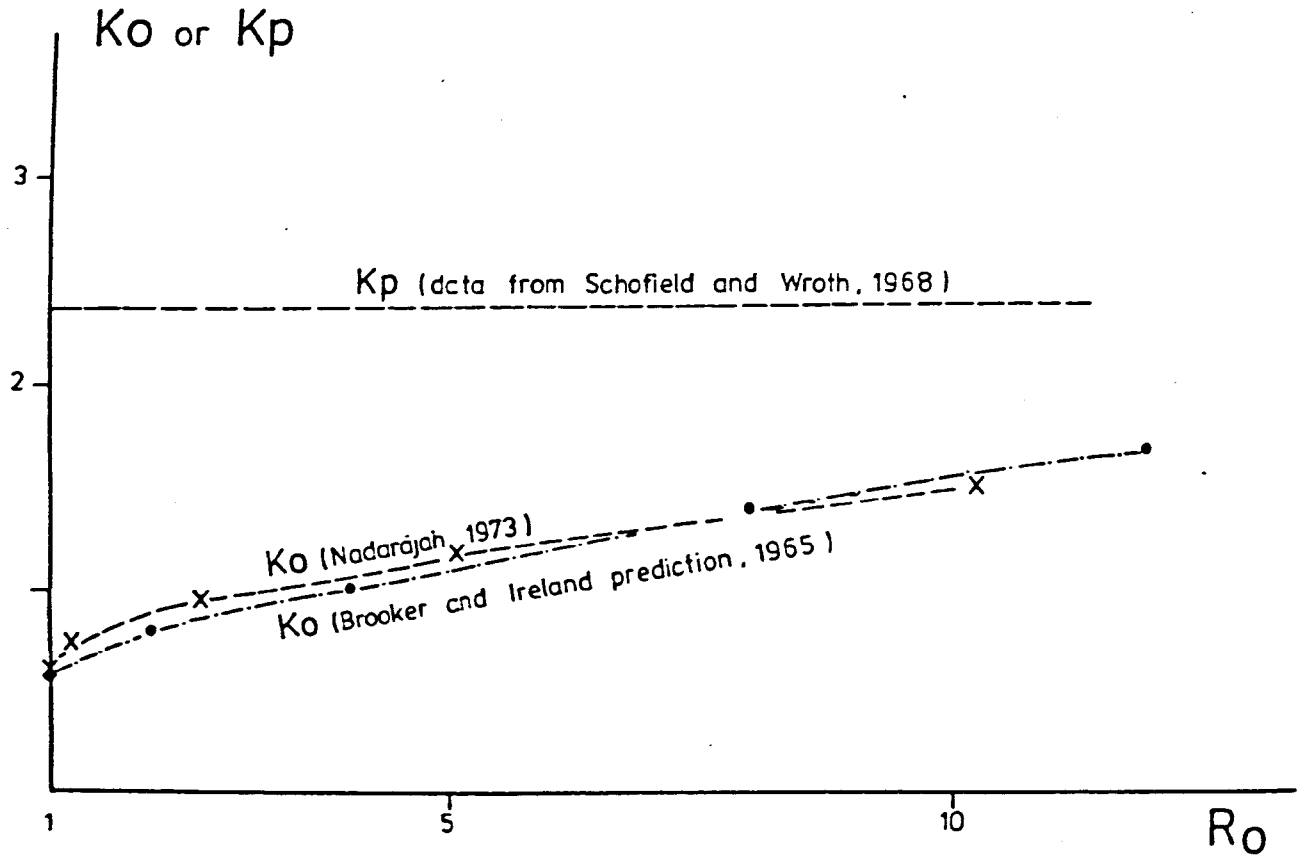

Figure 8.2 Variation of K_o with overconsolidation ratio for one-dimensionally unloaded kaolin.

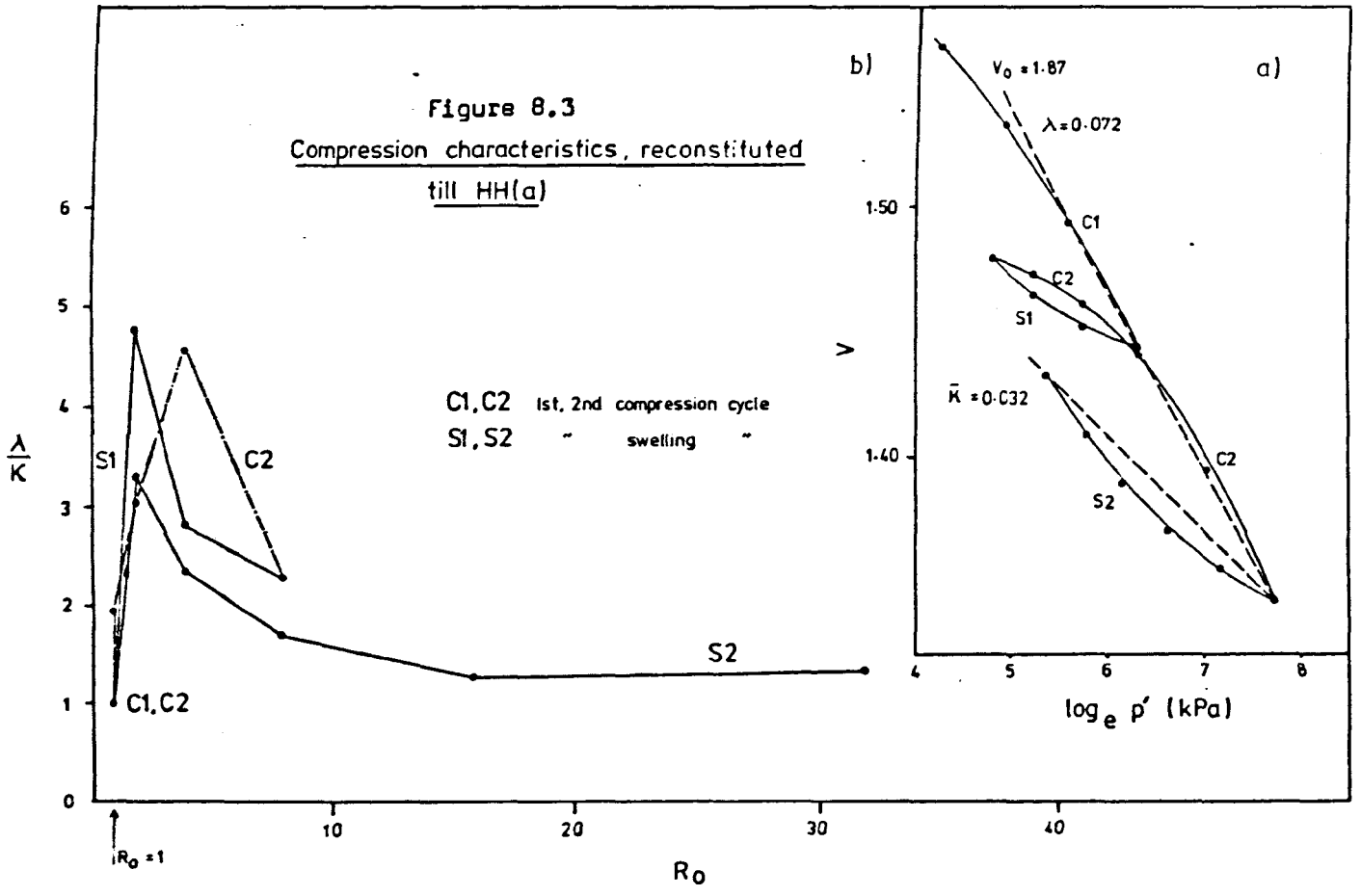

Figure 8.3

Compression characteristics, reconstituted till HH(a)

C1,C2 1st, 2nd compression cycle

S1,S2 " swelling "

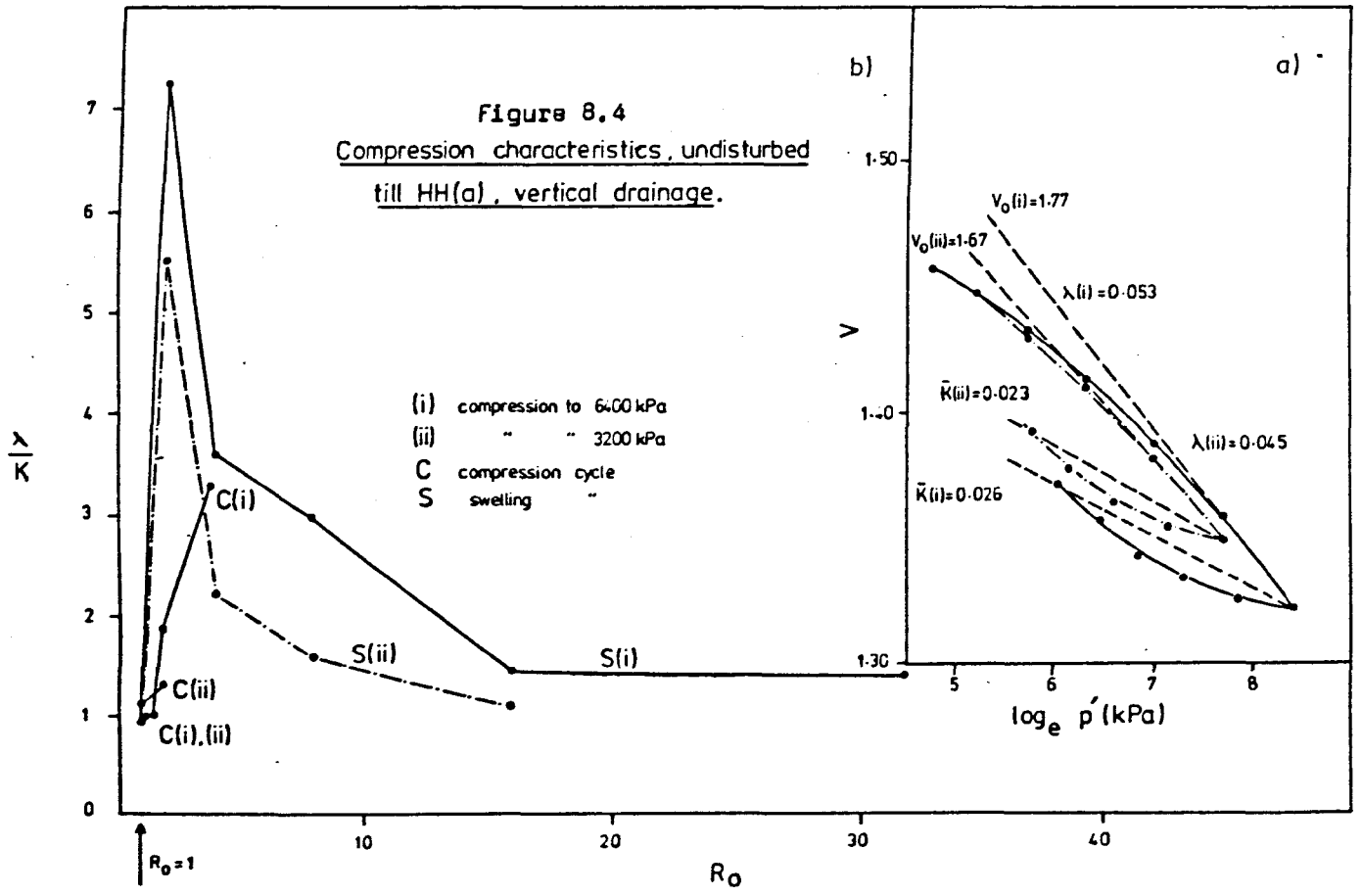

Figure 8.4
Compression characteristics, undisturbed till HH(a), vertical drainage.

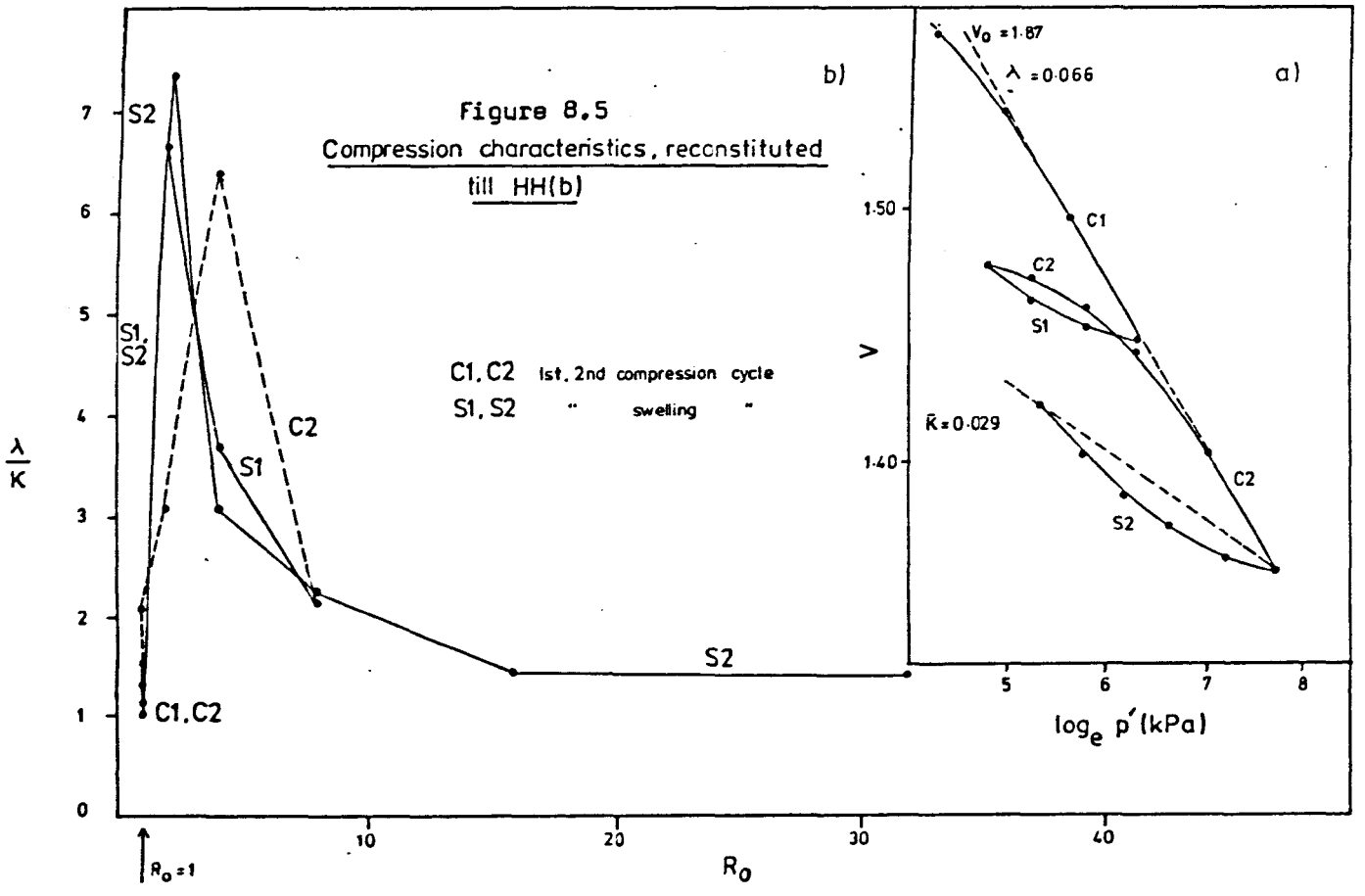

Figure 8.5
Compression characteristics, reconstituted till HH(b)

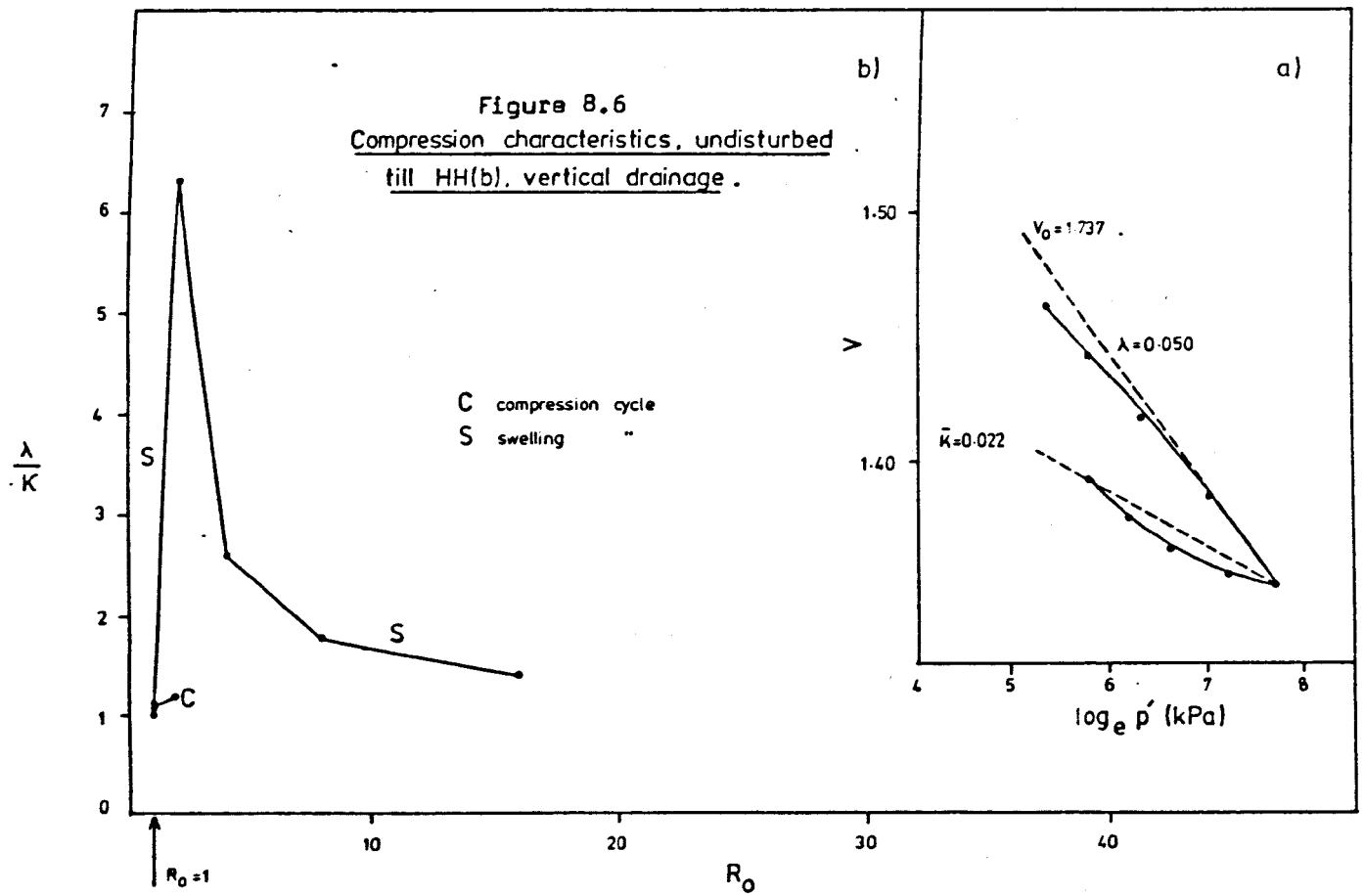

Figure 8.6
Compression characteristics, undisturbed till HH(b), vertical drainage.

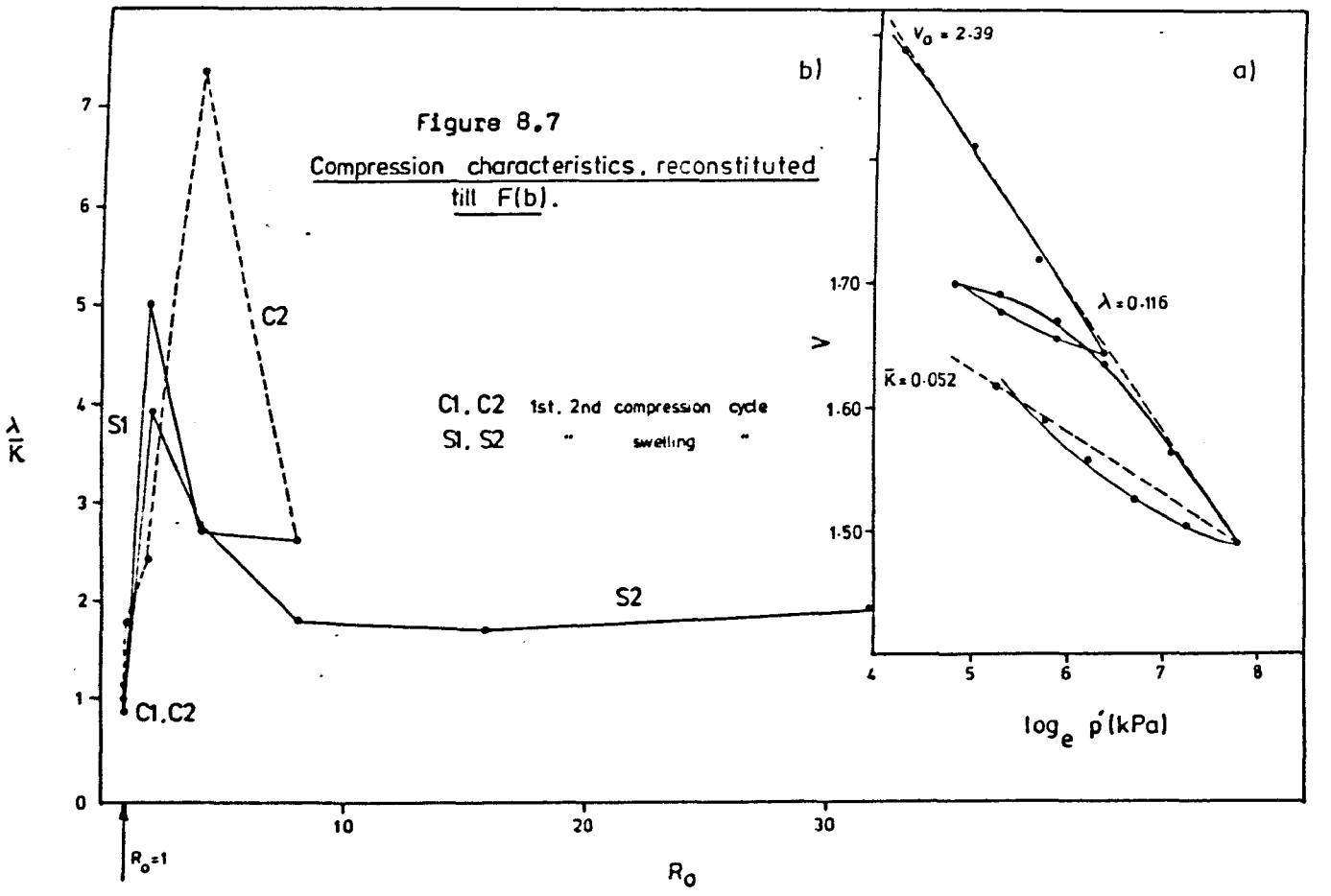

Figure 8.7

Compression characteristics, reconstituted till F(b).

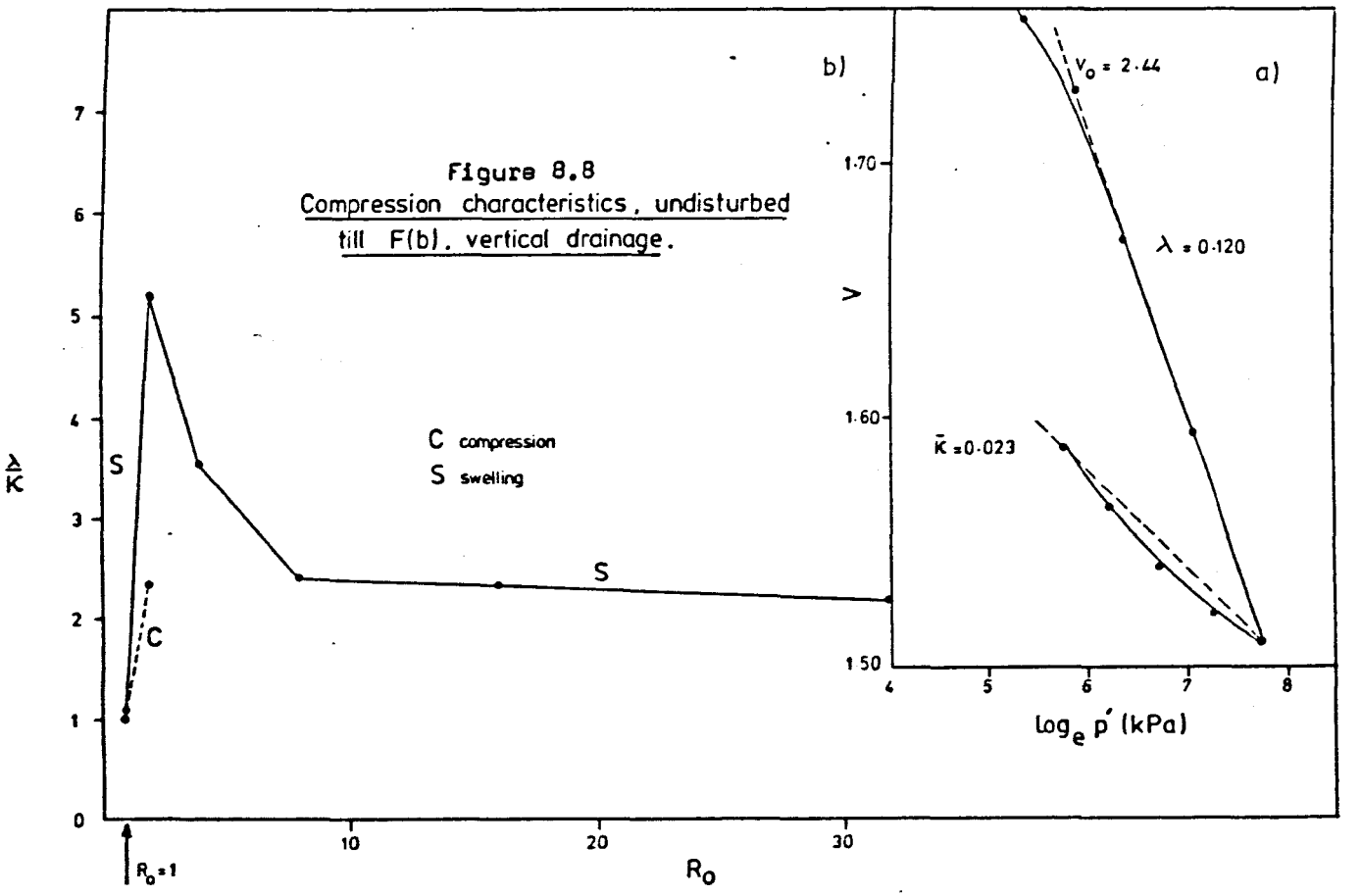

Figure 8.8
Compression characteristics, undisturbed till F(b), vertical drainage.

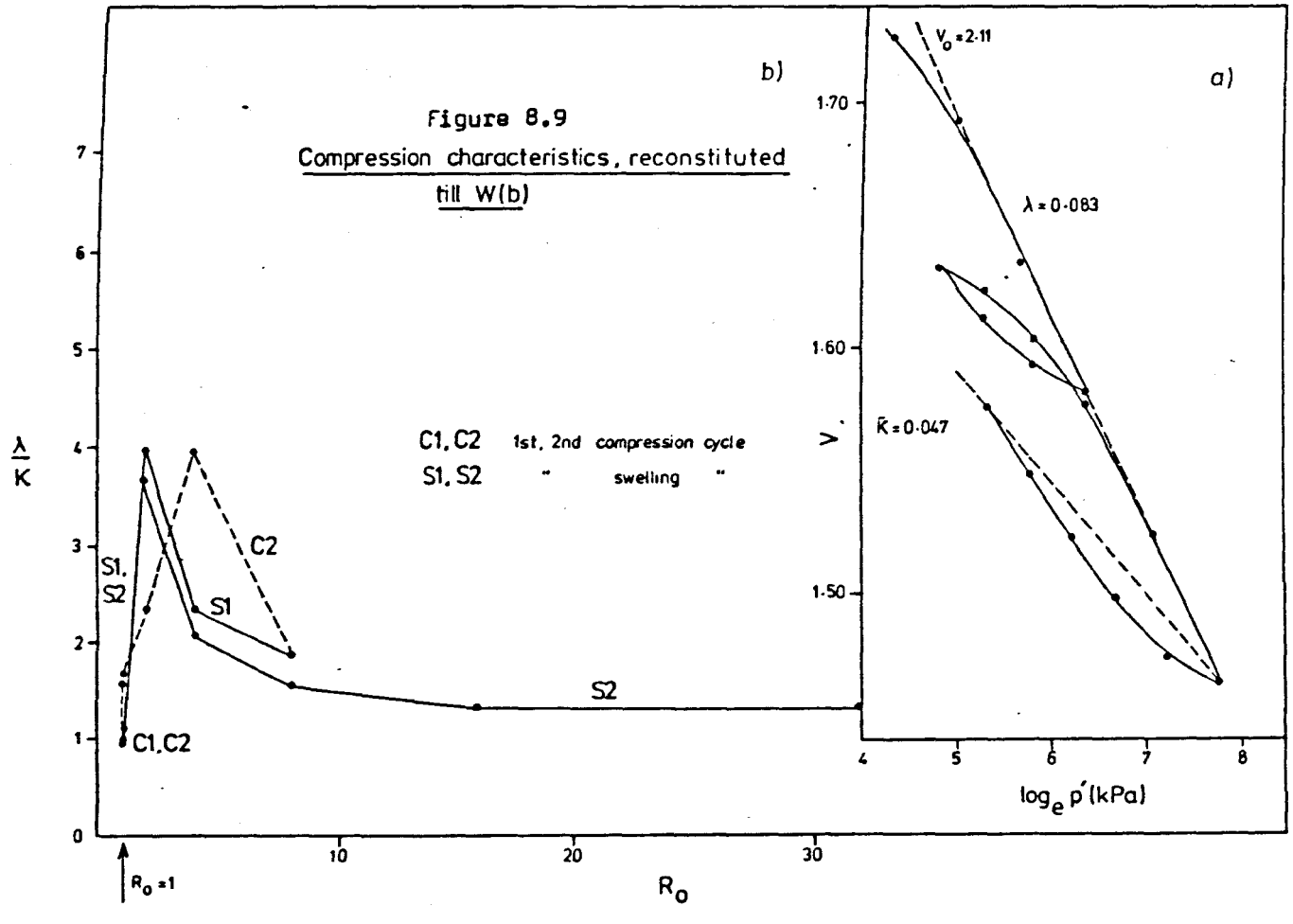

Figure 8.9
Compression characteristics, reconstituted till W(b)

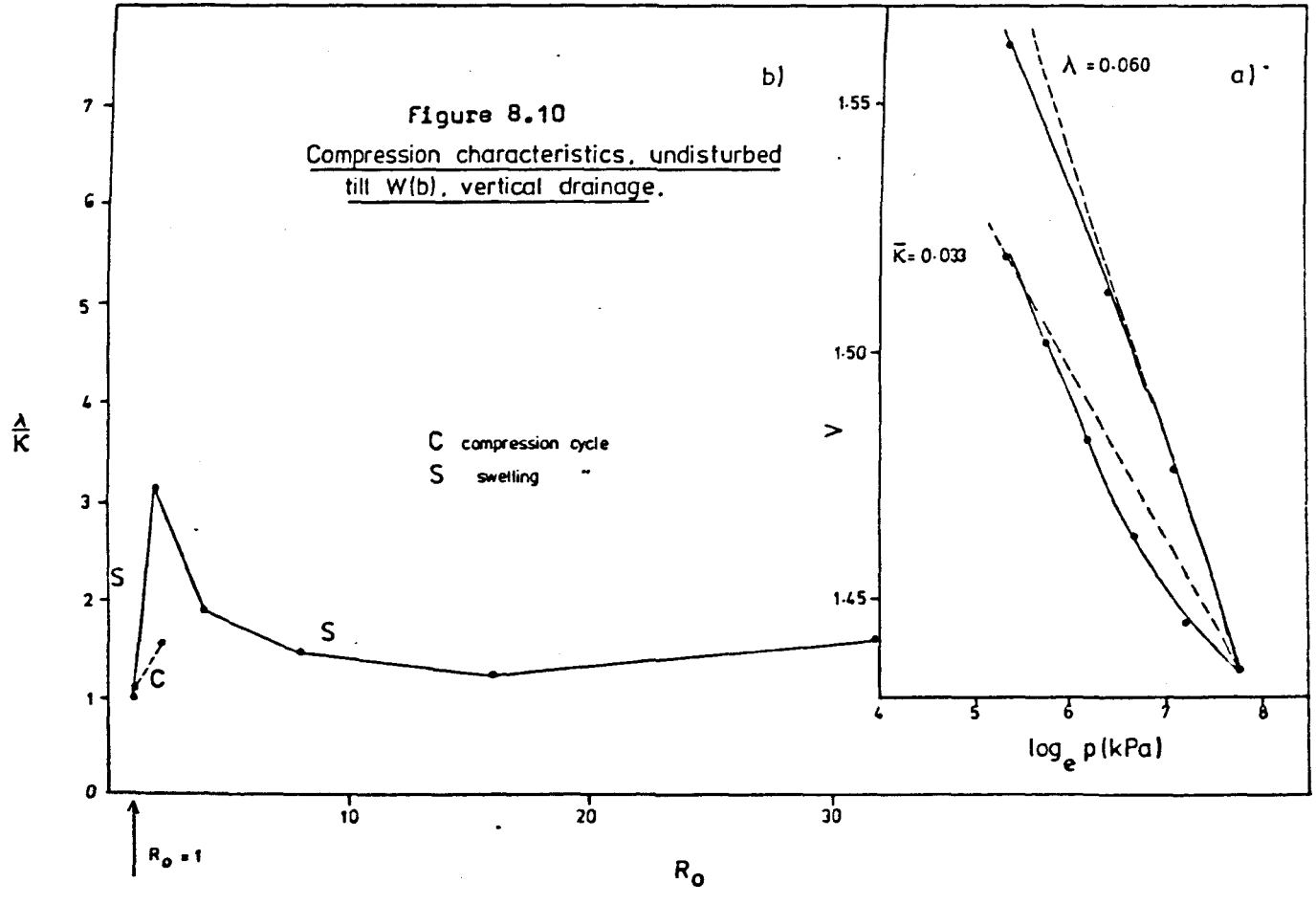

Figure 8.10

Compression characteristics, undisturbed till W(b), vertical drainage.

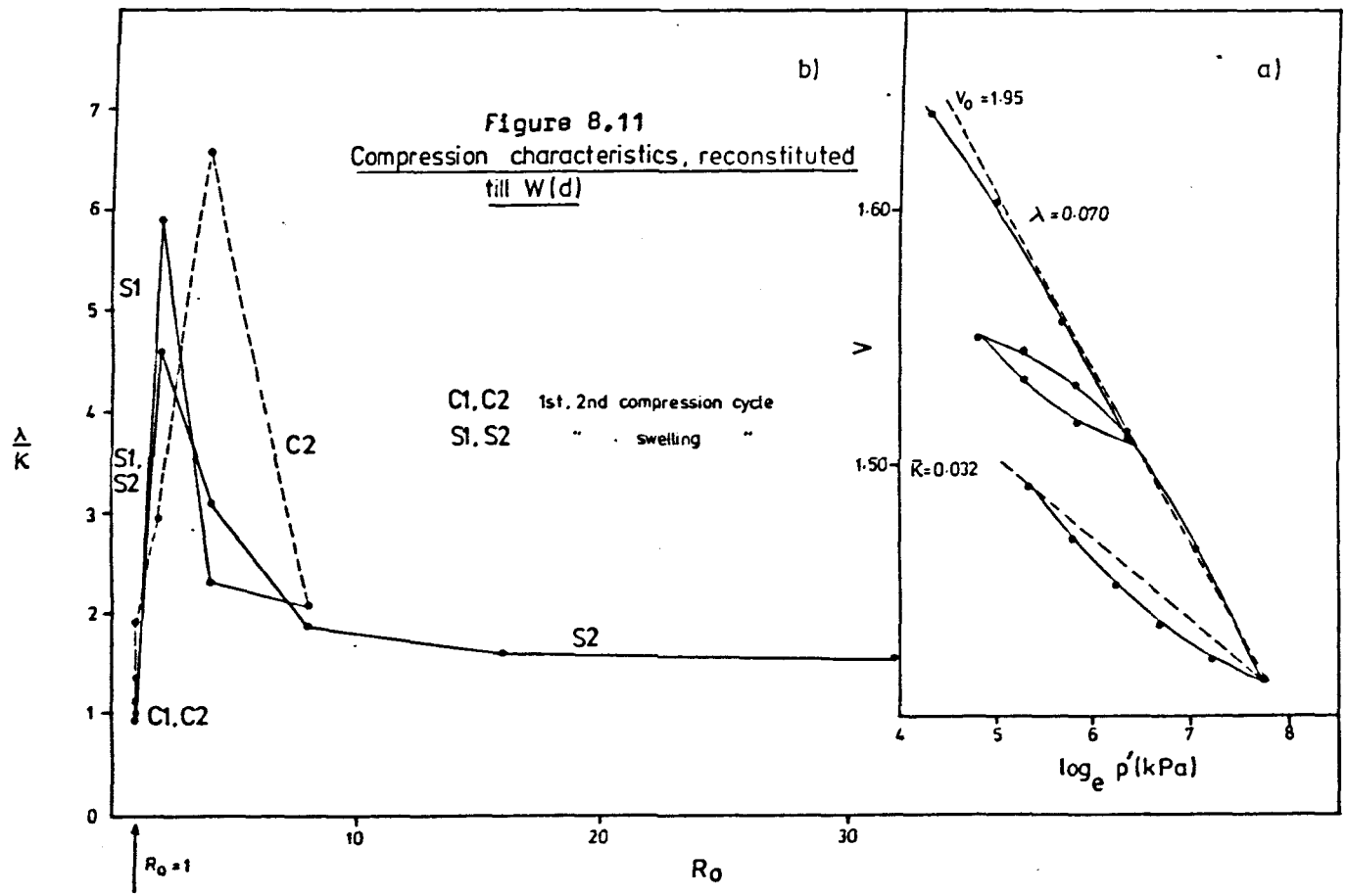

Figure 8.11
Compression characteristics, reconstituted till W(d)

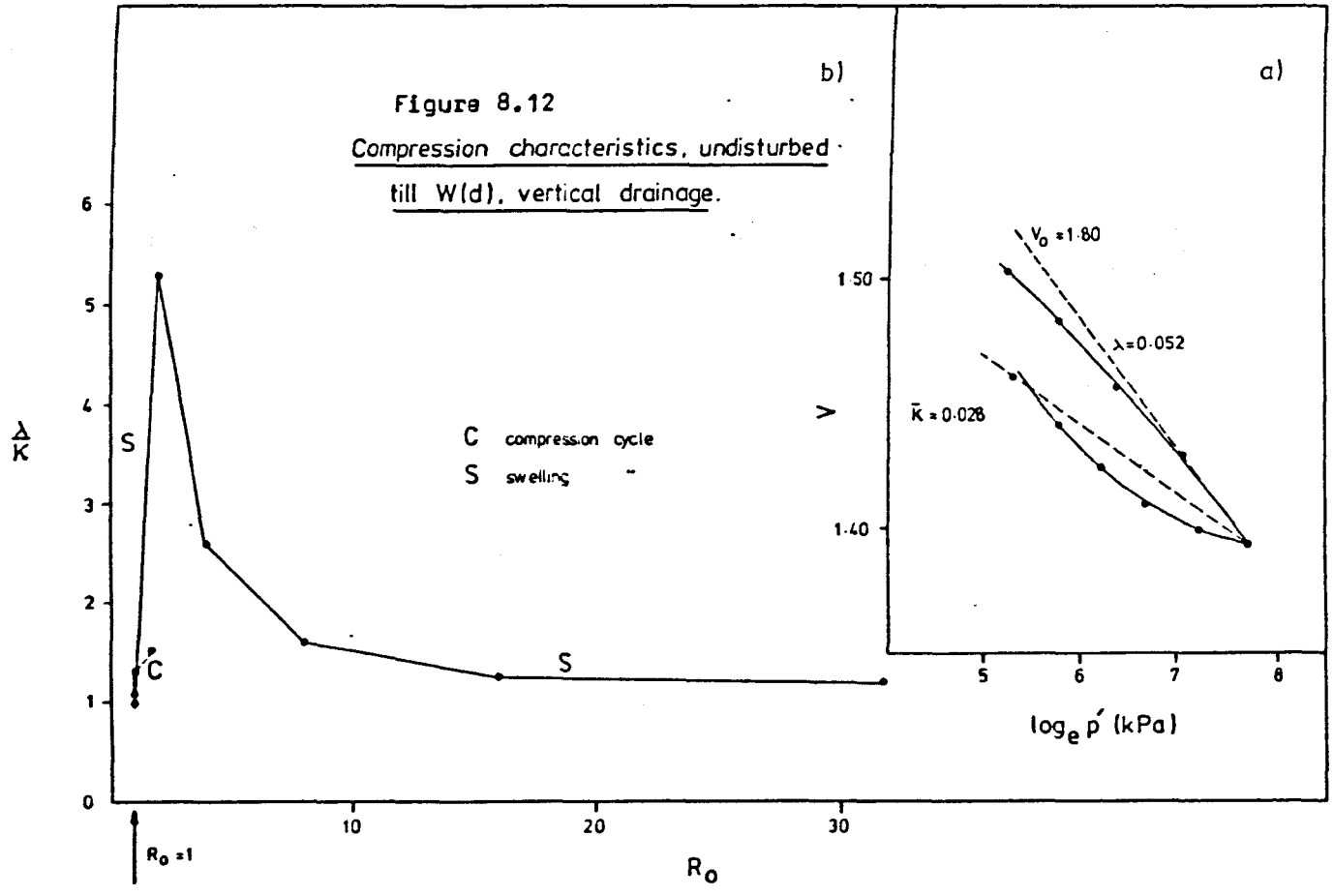

Figure 8.12

Compression characteristics, undisturbed till W(d), vertical drainage.

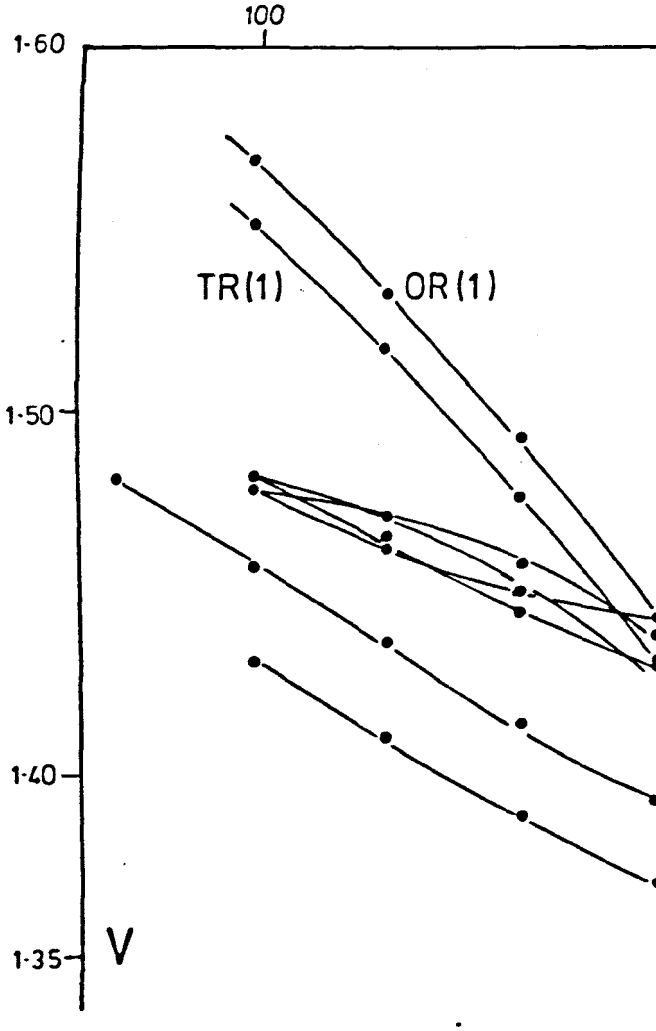
100
1·60
1·50
1·40
1·35
V
TR(1)
OR(1)

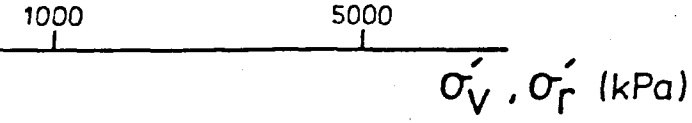

Figure 8.13 Isotropic and oedometer compression characteristics, reconstituted till HH(a).

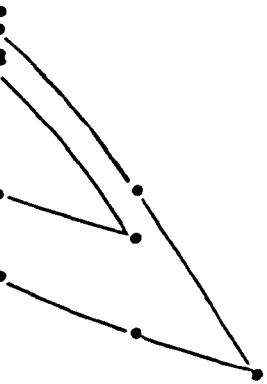

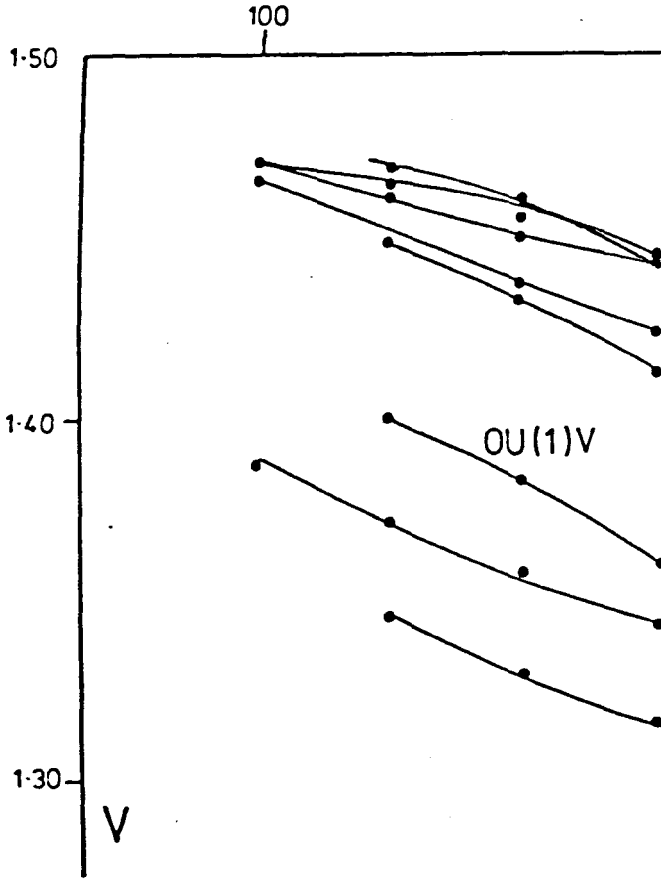
100
1·50
1·40
1·30
V
OU(1)V

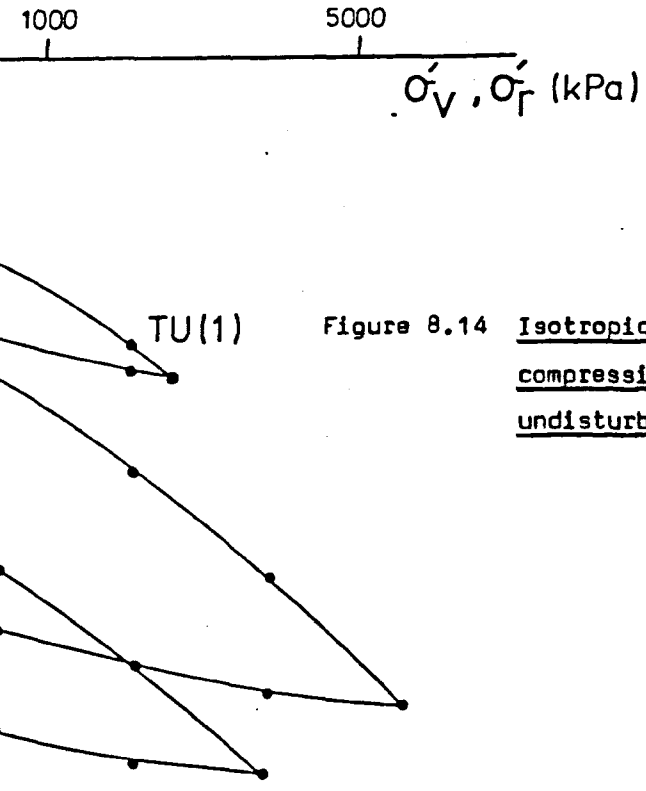

Figure 8.14 Isotropic and oedometer compression characteristics, undisturbed till HH(a).

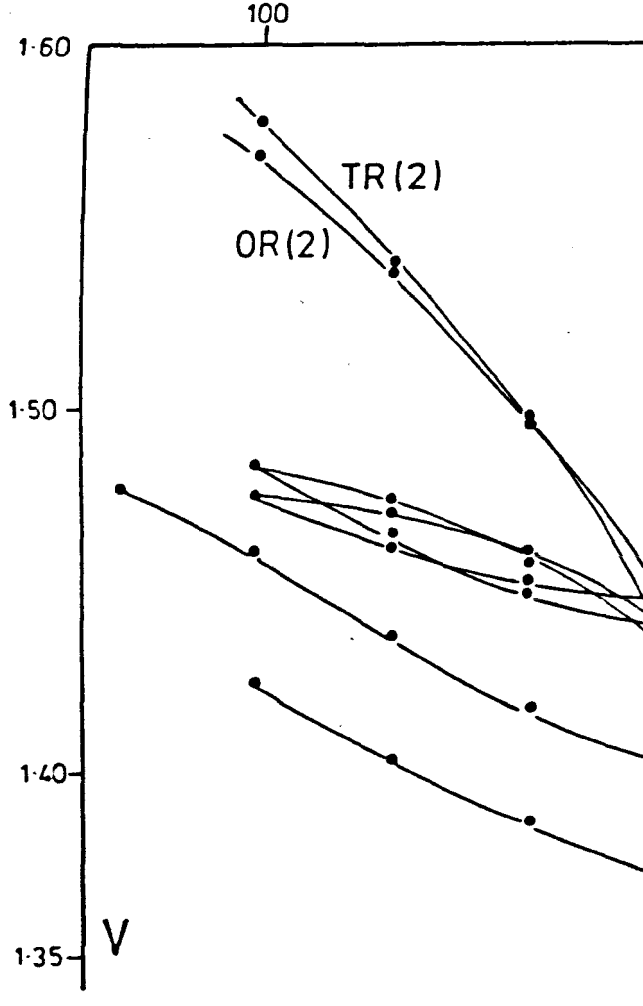
100
1·60
1·50
1·40
1·35
V
TR(2)
OR(2)

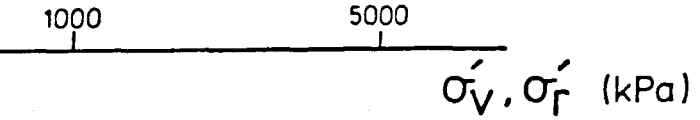

Figure 8.15 Isotropic and oedometer compression characteristics , reconstituted till HH(b).

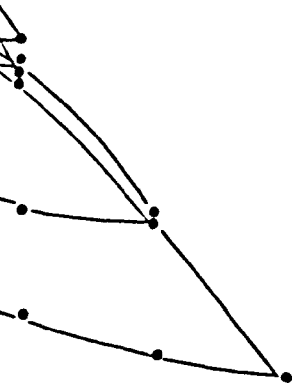

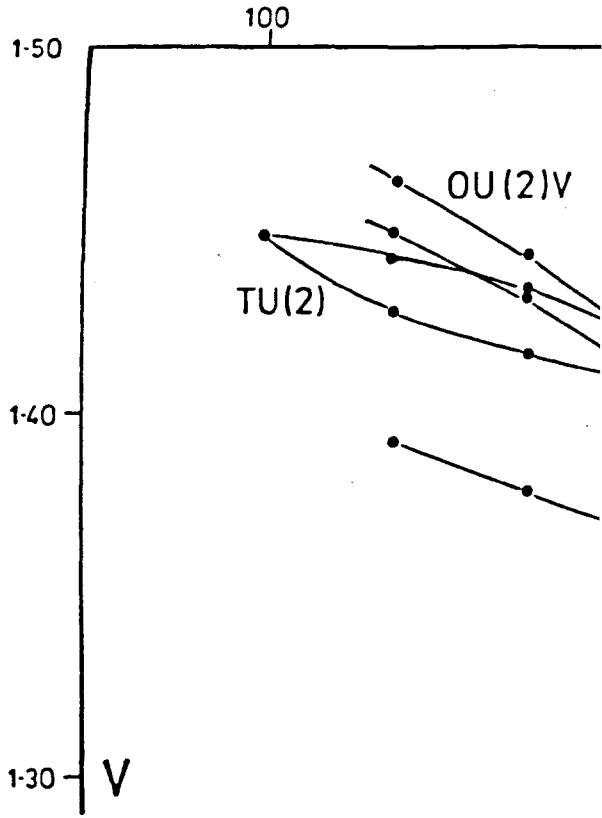
100
1·50
1·40
1·30
V
OU(2)V
TU(2)

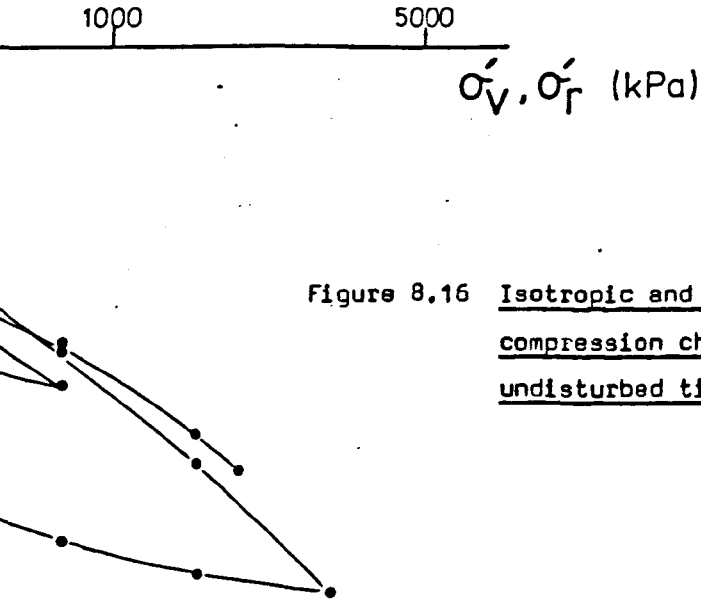

Figure 8.16 Isotropic and oedometer compression characteristics, undisturbed till HH(b).

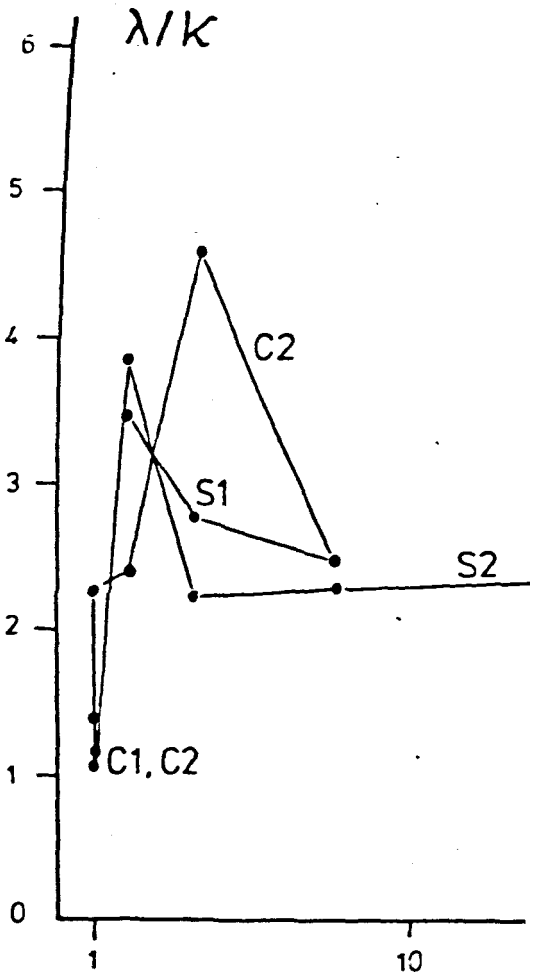
λ/K
6
5
4
3
2
1
0
C2
S1
S2
C1, C2
1
10

Figure 8.17 λ/κ : Ro , test TR(1) , till HH(a).

C1, C2 1st, 2nd compression cycle

S1, S2 " swelling "

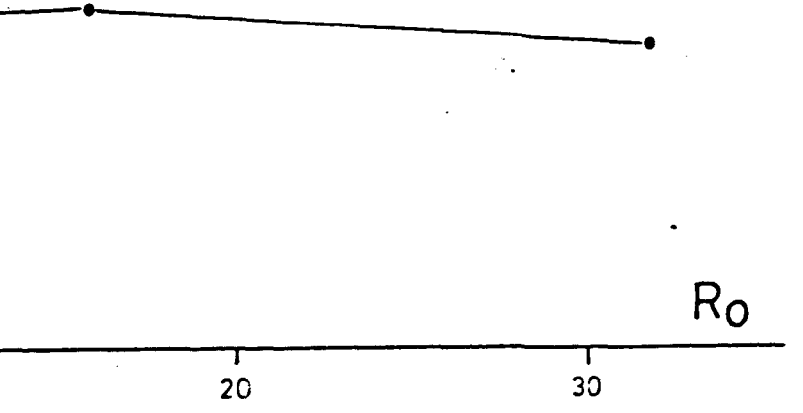

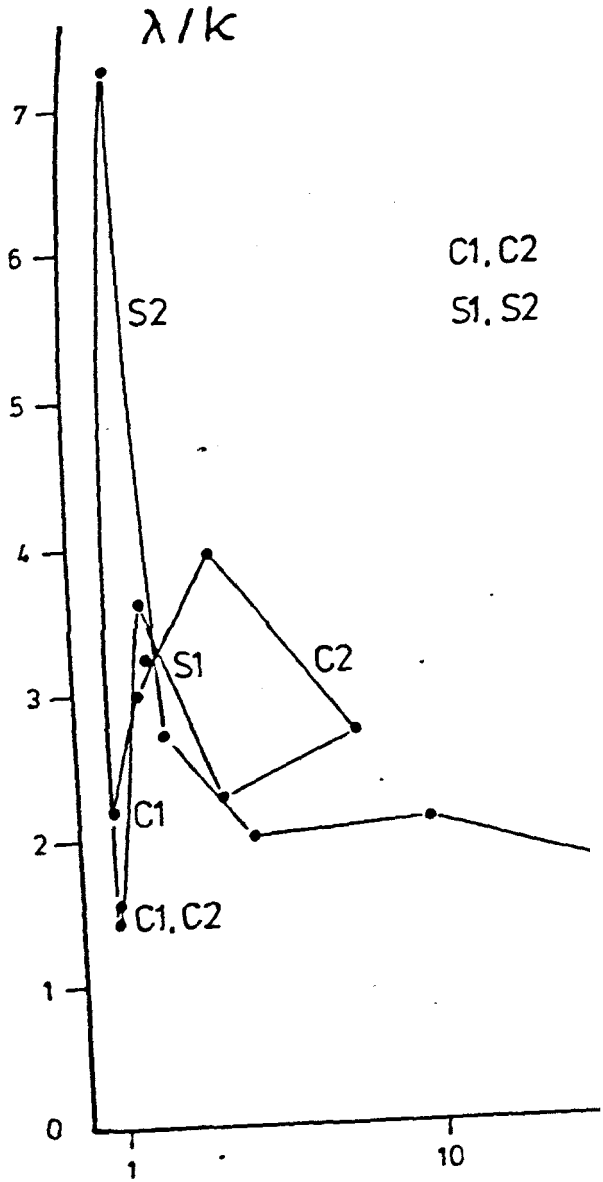
λ/k
7
6
5
4
3
2
1
0
1
10
C1, C2
S1, S2
S2
S1
C2
C1
C1, C2

Ist, 2nd compression cycle

" swelling "

Figure 8.18 λ/K: Ro, test TU(1), till HH(a).

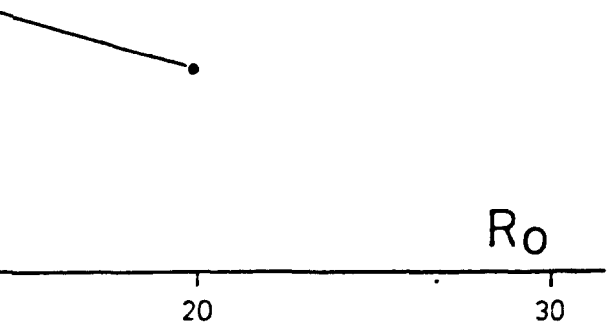

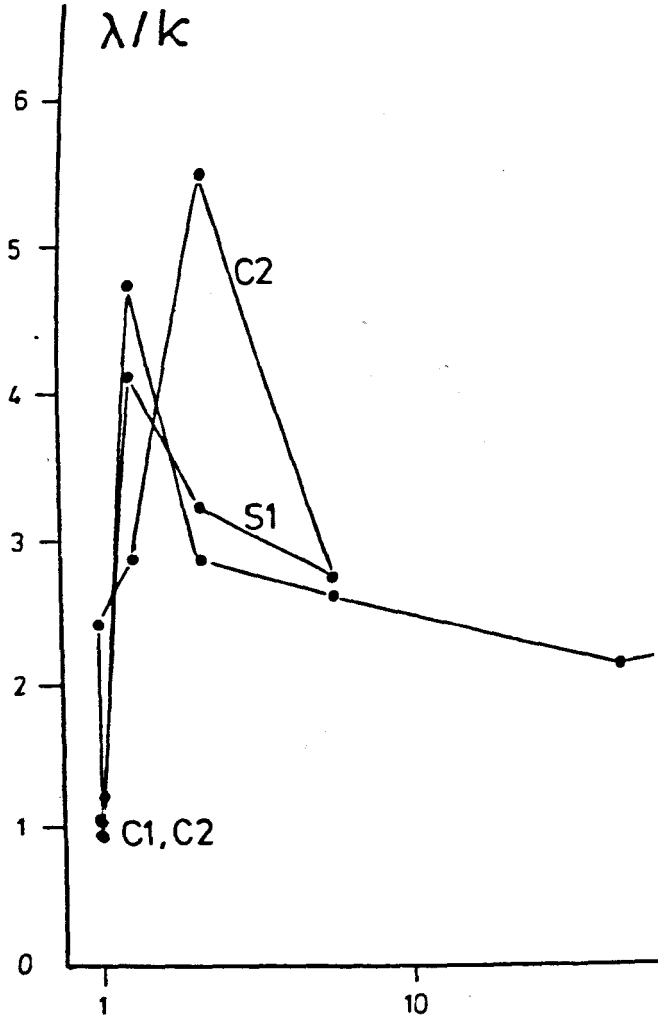
λ/k
6
5
4
3
2
1
0
C2
S1
C1, C2
1
10

Figure 8.19 λ/κ : Ro , test TR(2) , till HH(b).

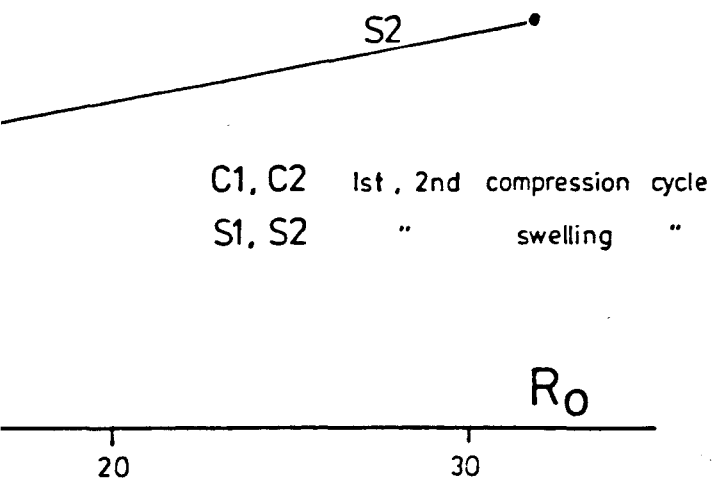

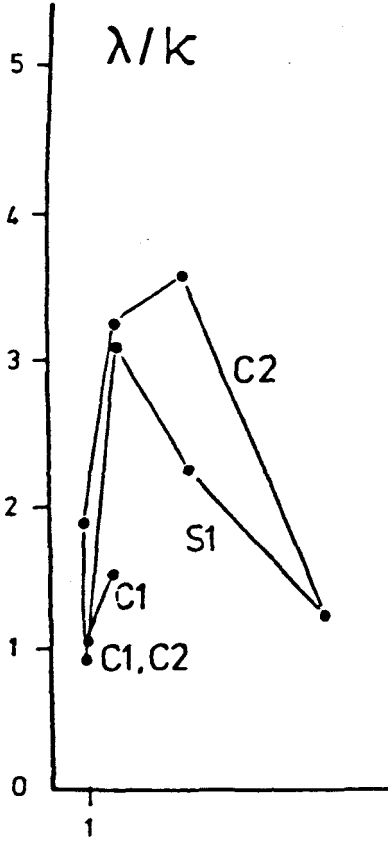
λ/K
5
4
3
2
1
0
1
C2
S1
C1
C1,C2

Figure 8.20 λ/K : Ro , test TU(2) , till HH(b).

C1, C2 1st, 2nd compression cycle

S1 " swelling "

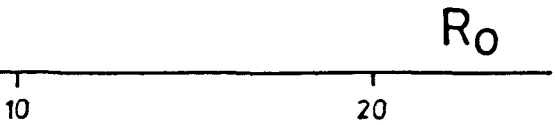

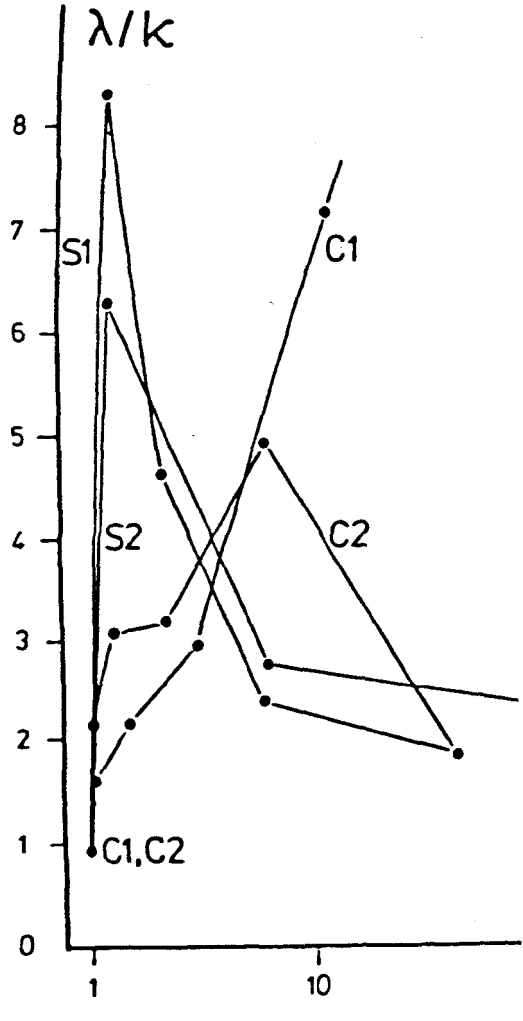
λ/k
8
7
6
5
4
3
2
1
0
S1
S2
C1
C2
C1,C2
1
10

Figure 8.21 λ / κ : Ro , N.Sea till , boring D.

C1, C2 Ist, 2nd compression cycle
S1, S2 " swelling "

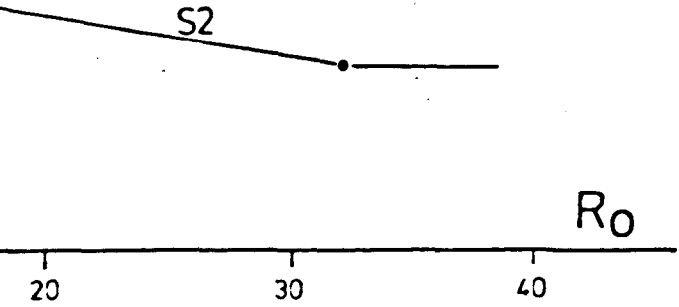

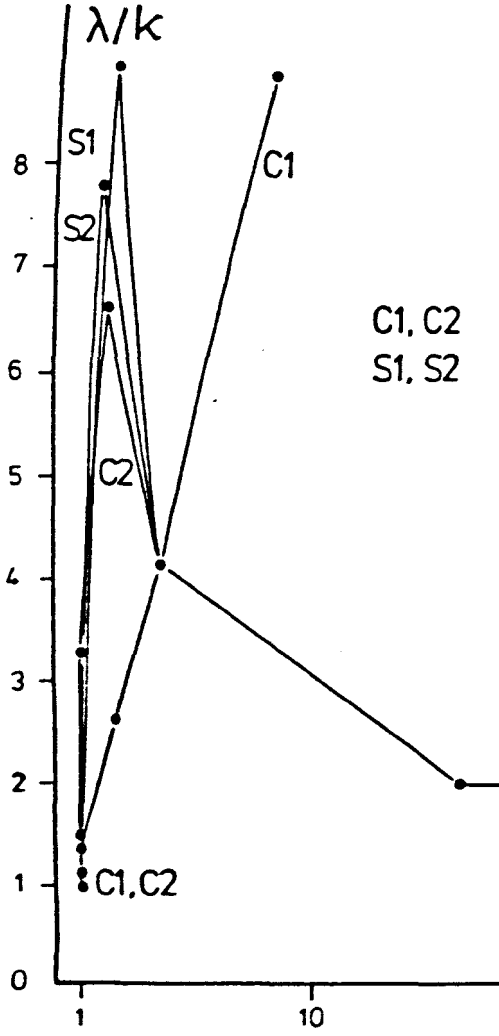
λ/k
S1
S2
C1
C2
C1, C2
S1, S2
C1,C2
0
1
2
3
4
5
6
7
8
1
10

Ist, 2nd compression cycle
" swelling "

Figure 8.22 λ/κ : Ro , N.Sea till , boring A.

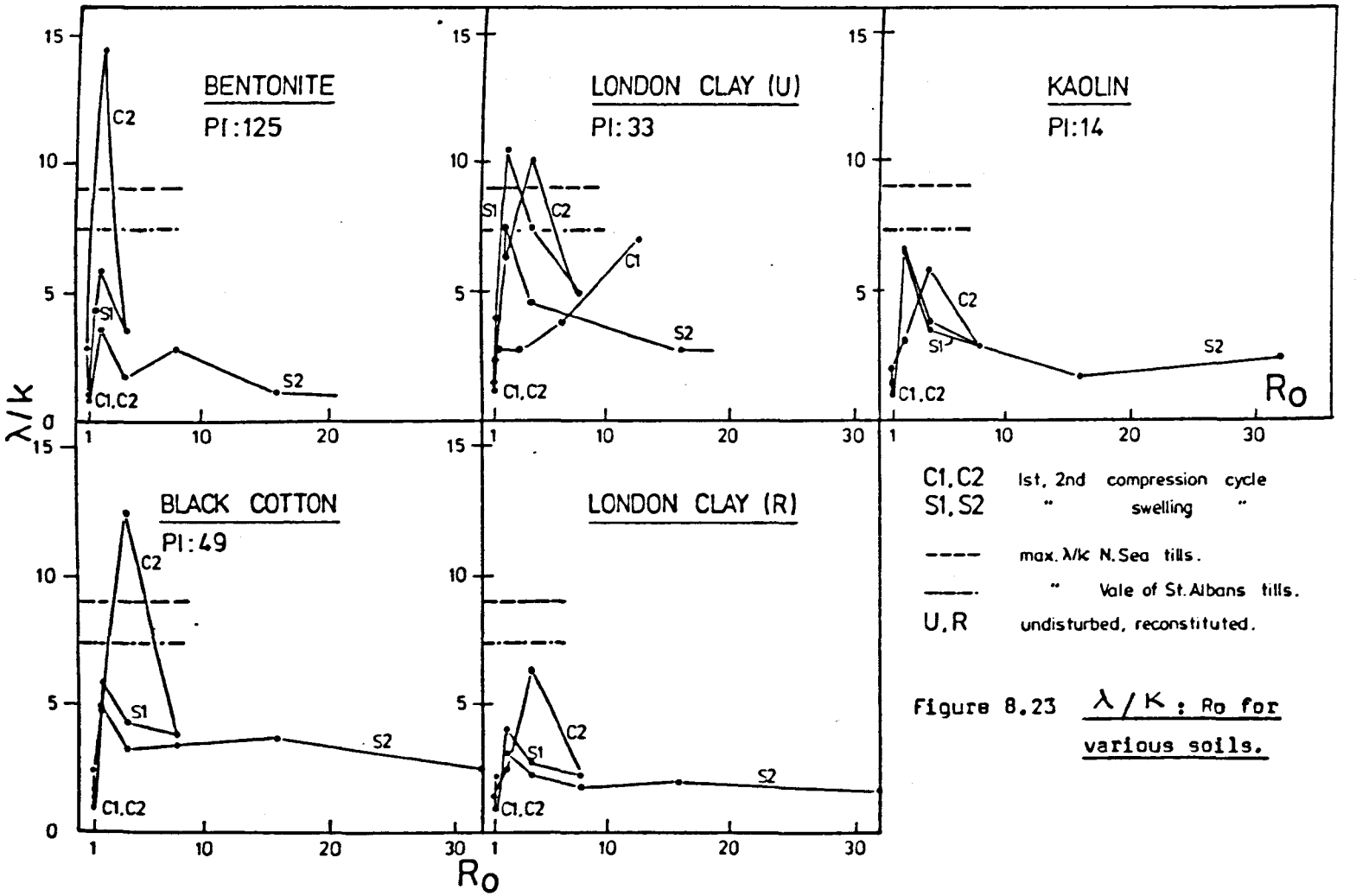

Figure 8.23 λ/K : Ro for various soils.

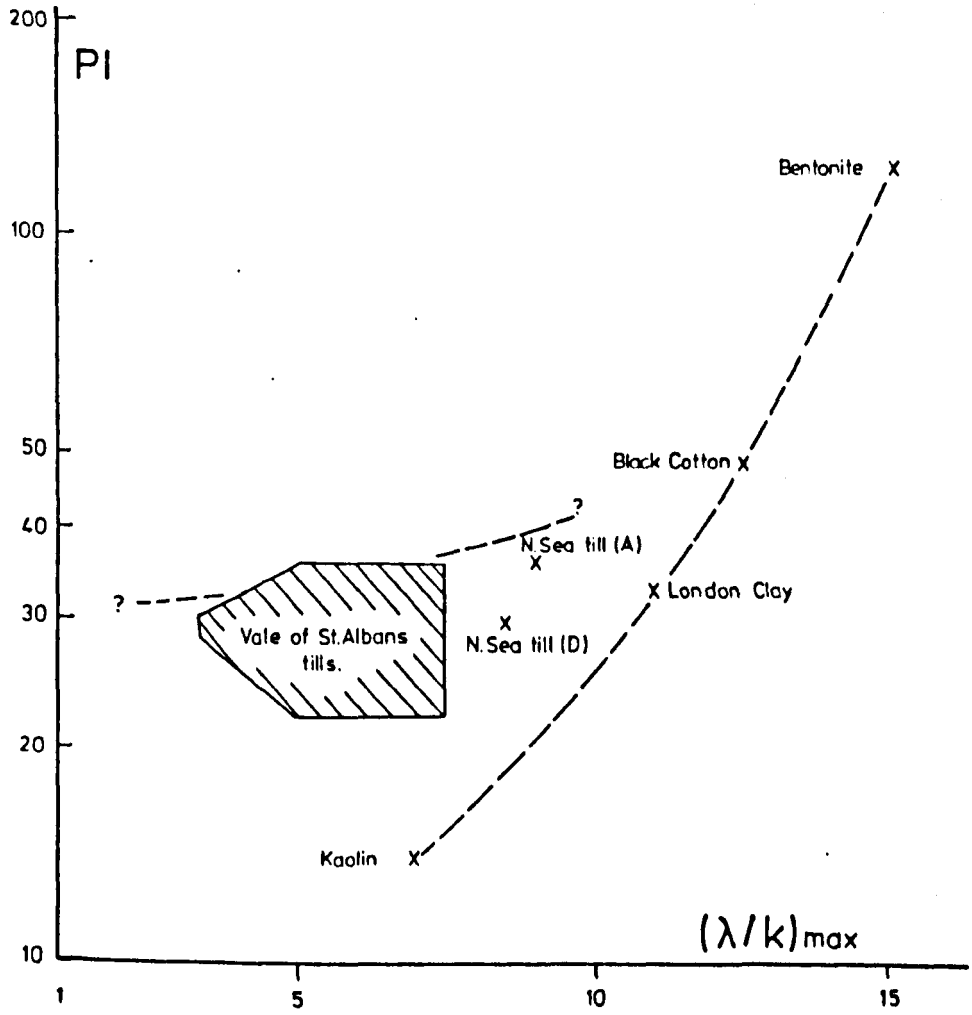

Figure 8.24 (λ / K) max : Ro for Vale of St. Albans tills and other soils.

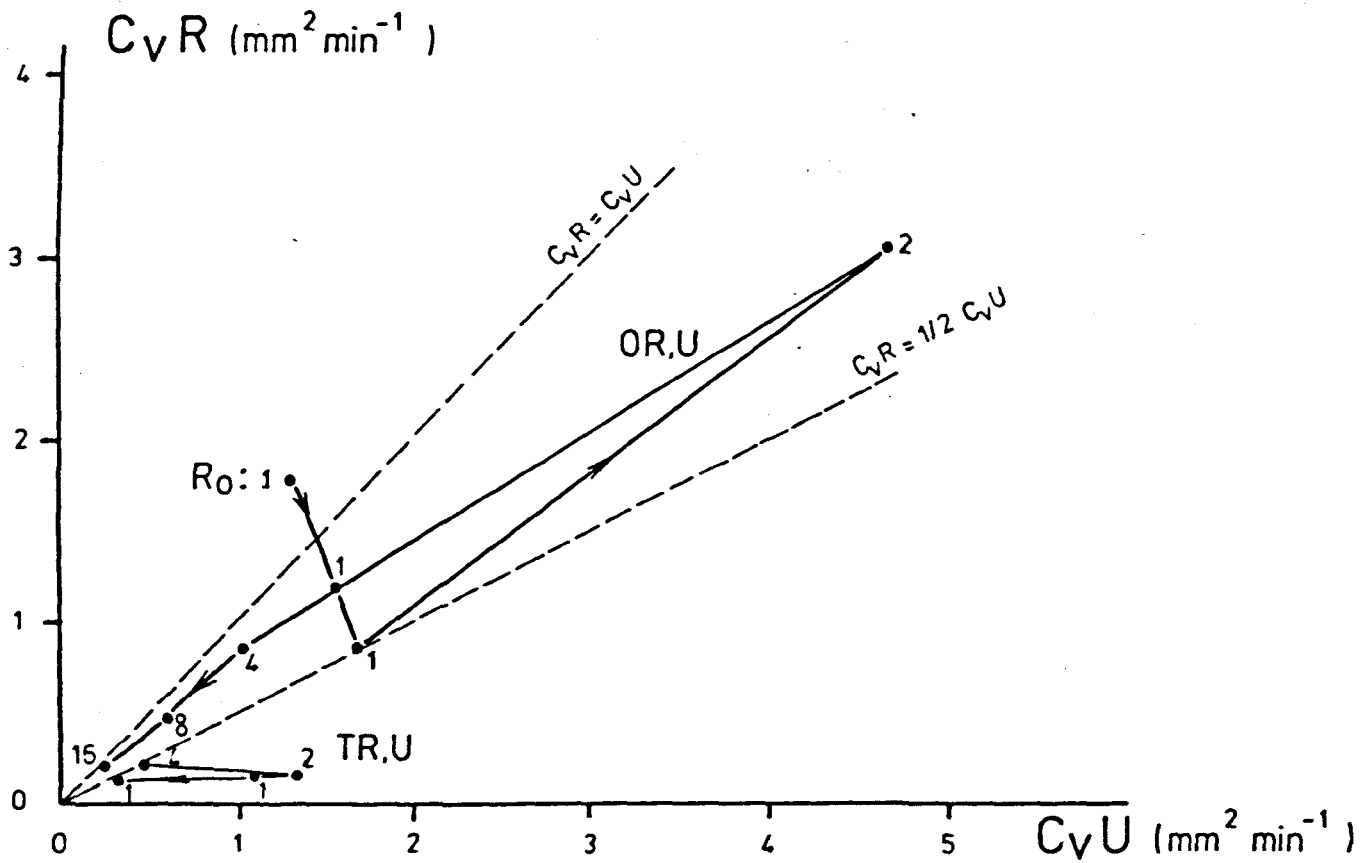

Figure 8.25 c_vR : c_vU : till HH(a) (Tests OR(1) , OU(1)V ; TR(1) , TU(1)).

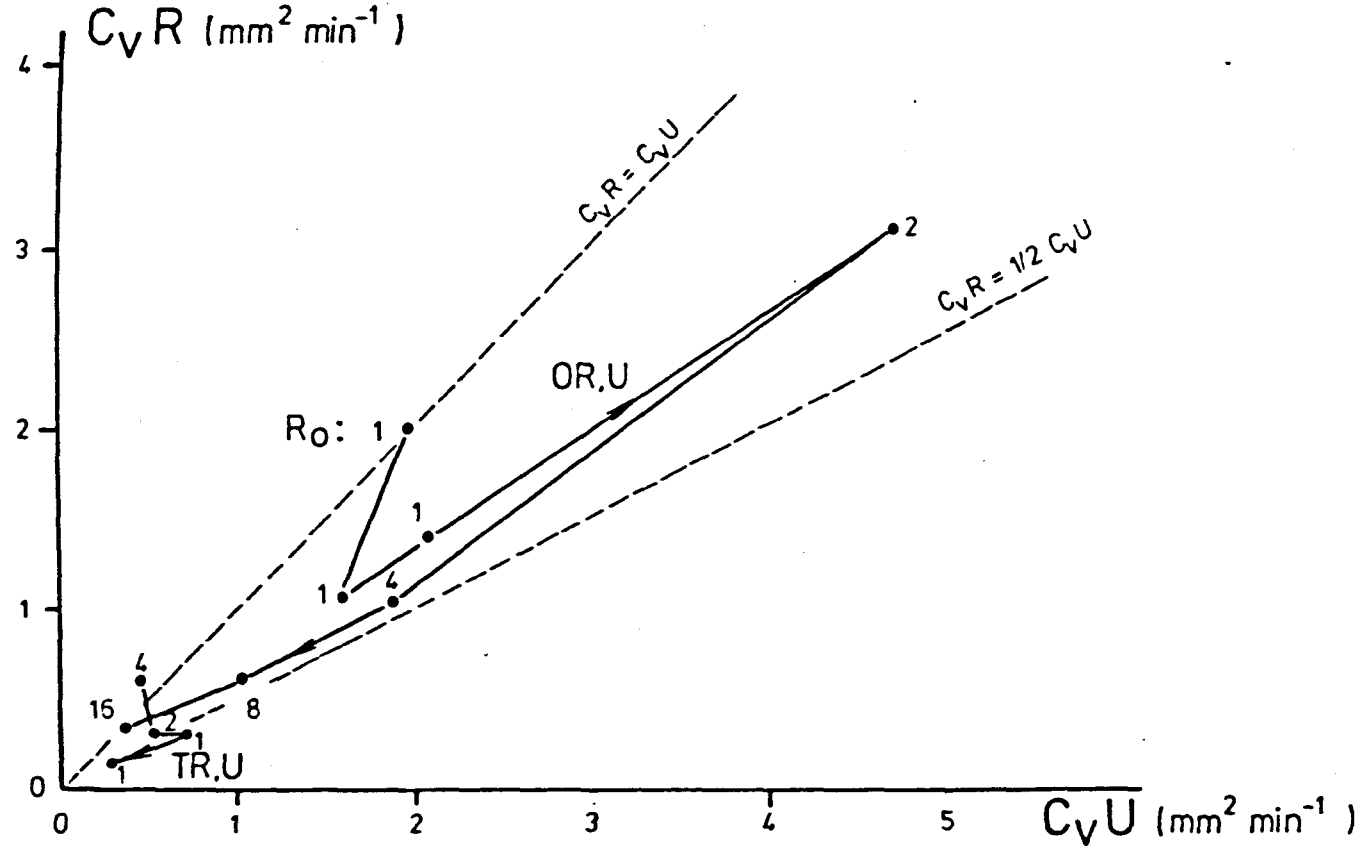

Figure 8.26 $c_v R$: $c_v U$: till HH(b) (Tests OR(2) , OU(2)V ; TR(2) , TU(2).

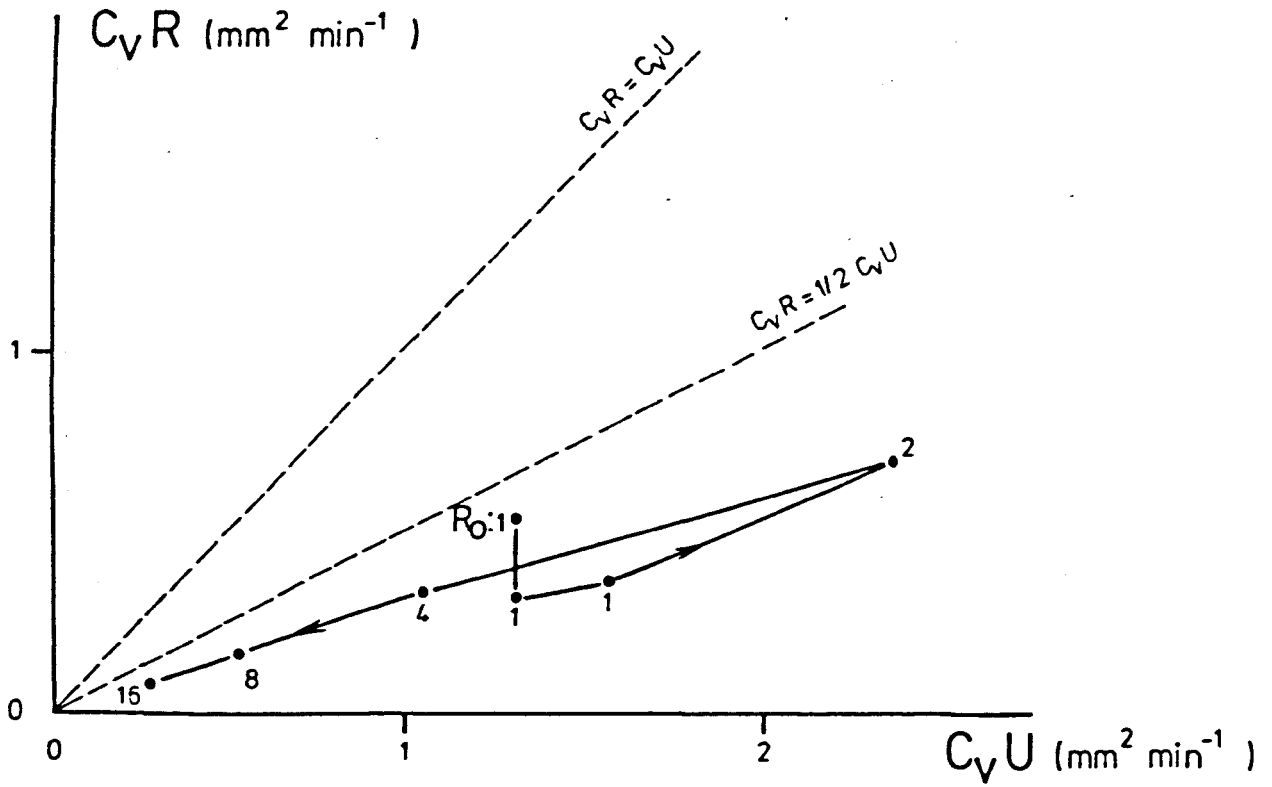

Figure 8.27 c_vR : c_vU : till F(b) (Tests OR(3) , OU(3)V).

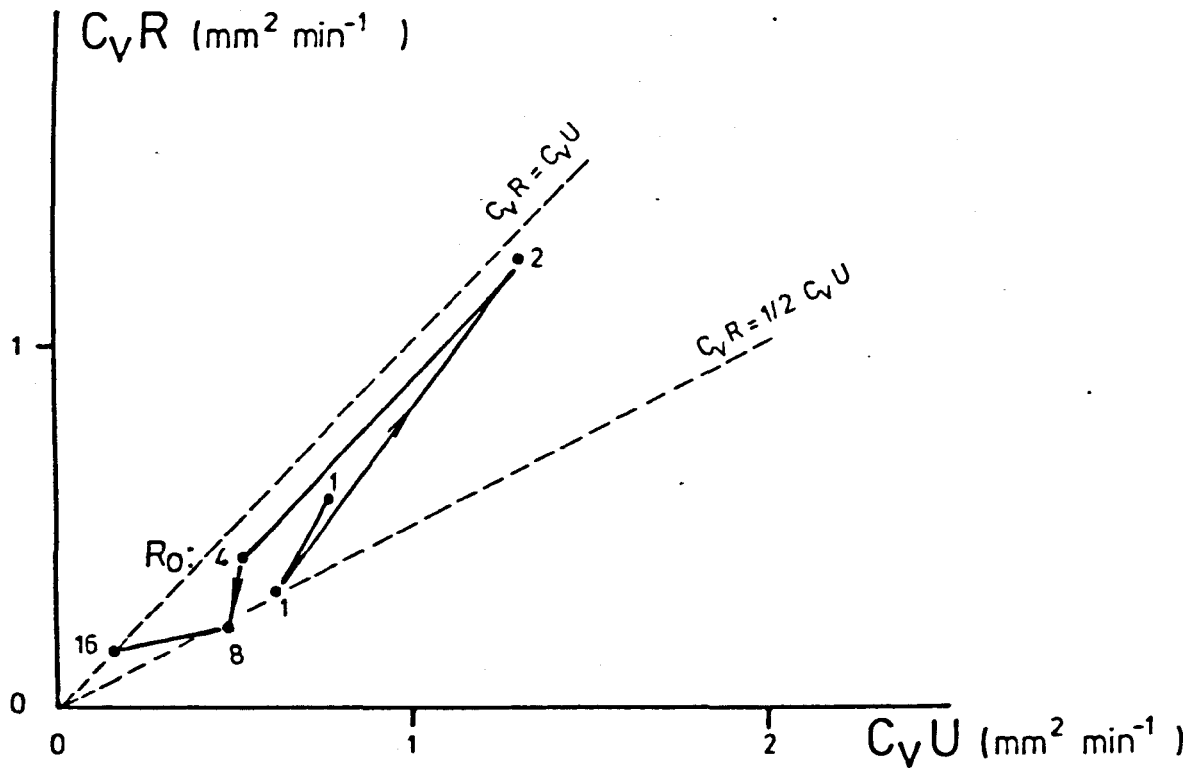

Figure 8.28 c_vR : c_vU : till W(b) (Tests OR(4) , OU(4)V).

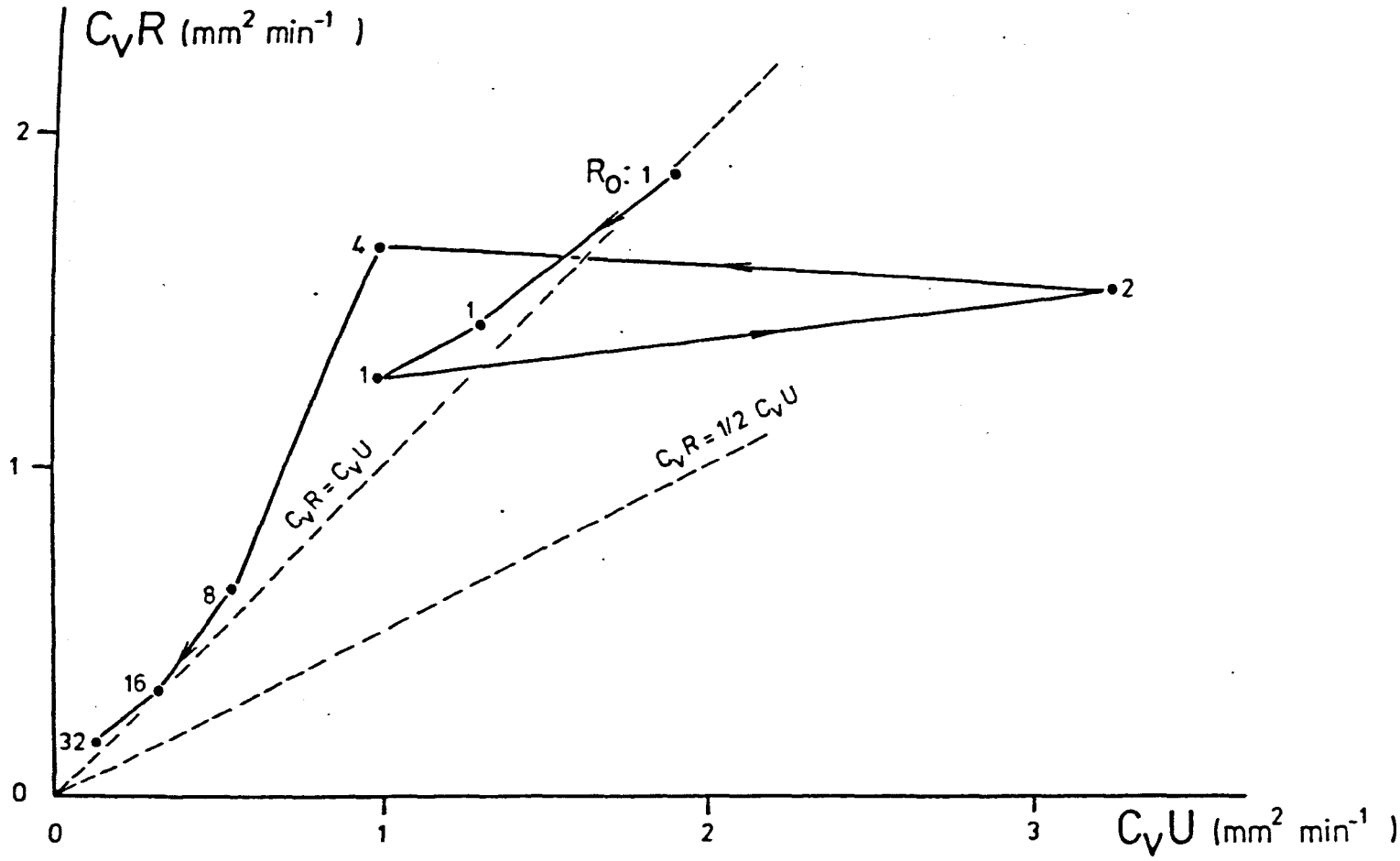

Figure 8.29 c_vR : c_vU : till W(d) (Tests DR(5) , DU(5)V).

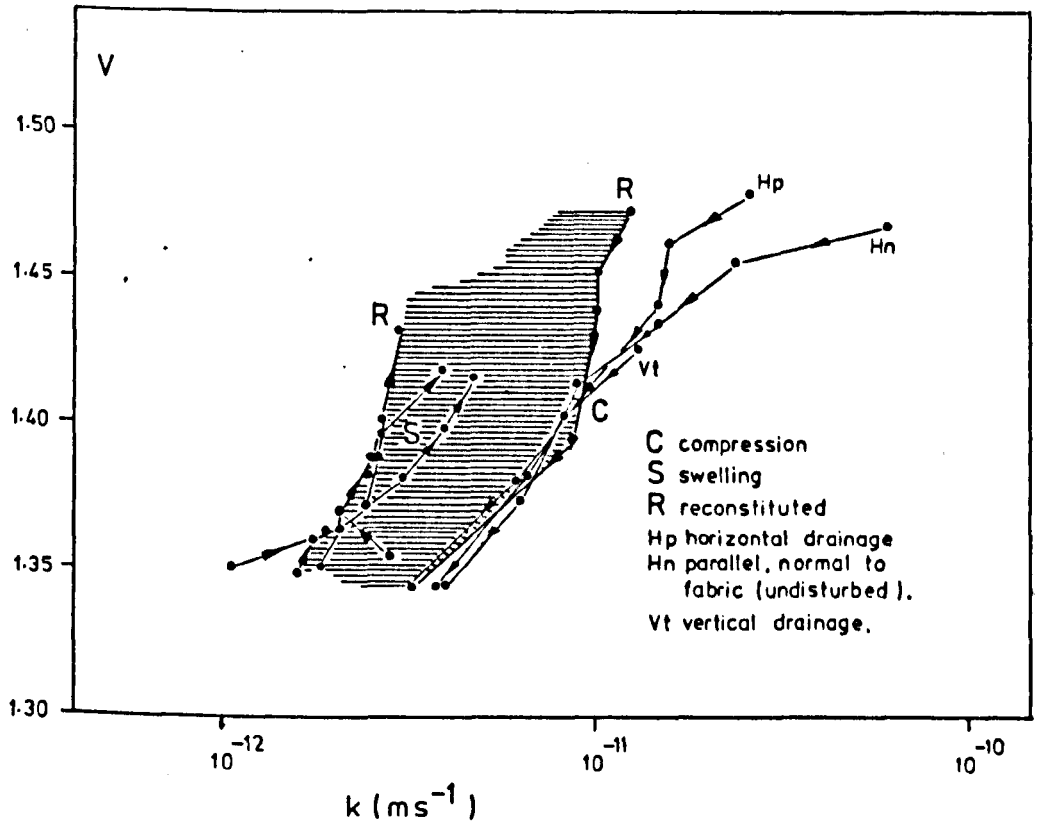

Figure 8.30 Oedometer determined permeability, till HH(a).

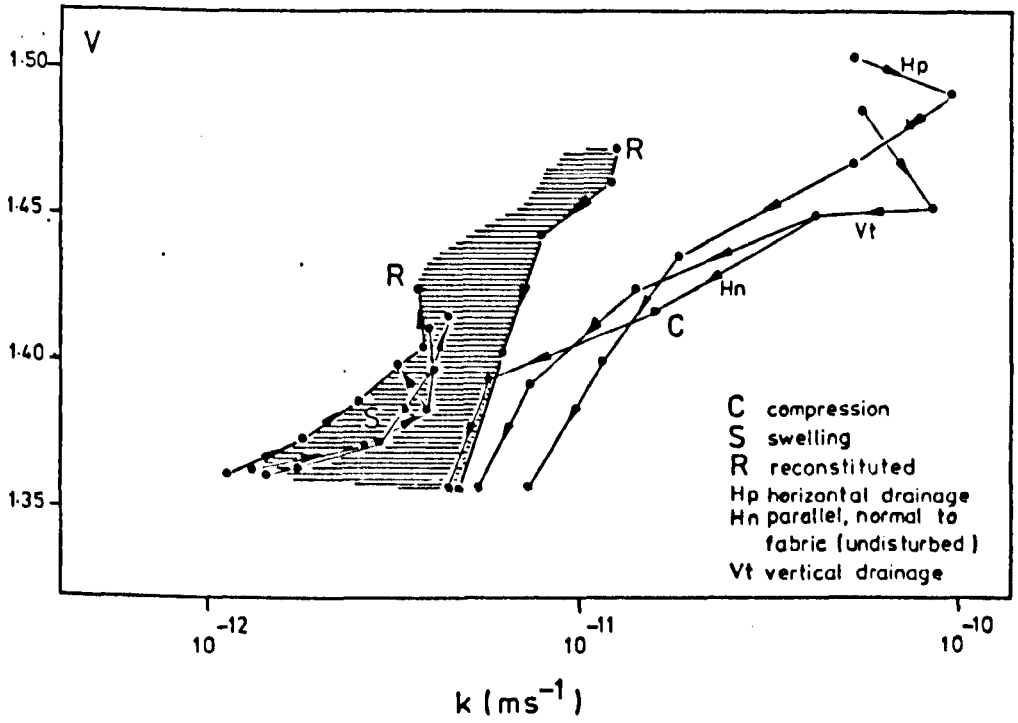

Figure 8.31 Oedometer determined permeability, till HH(b).

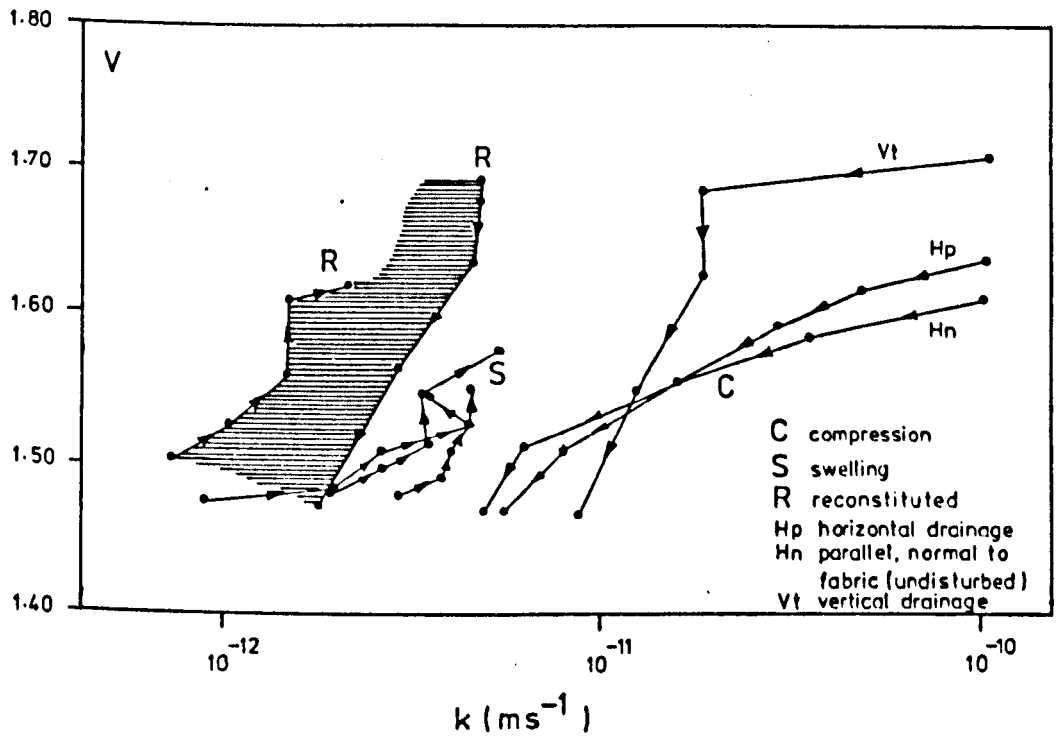

Figure 8.32 Oedometer determined permeability, till F(b).

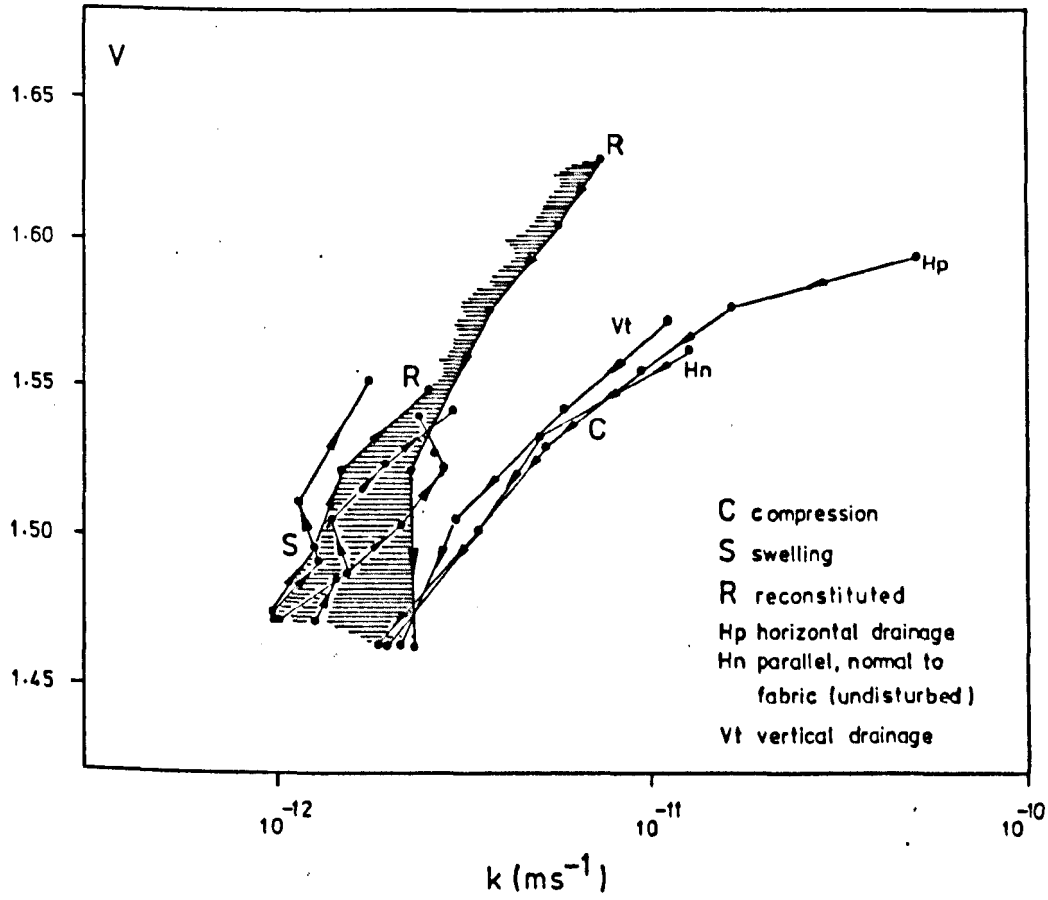

Figure 8.33 Oedometer determined permeability, till W(b)

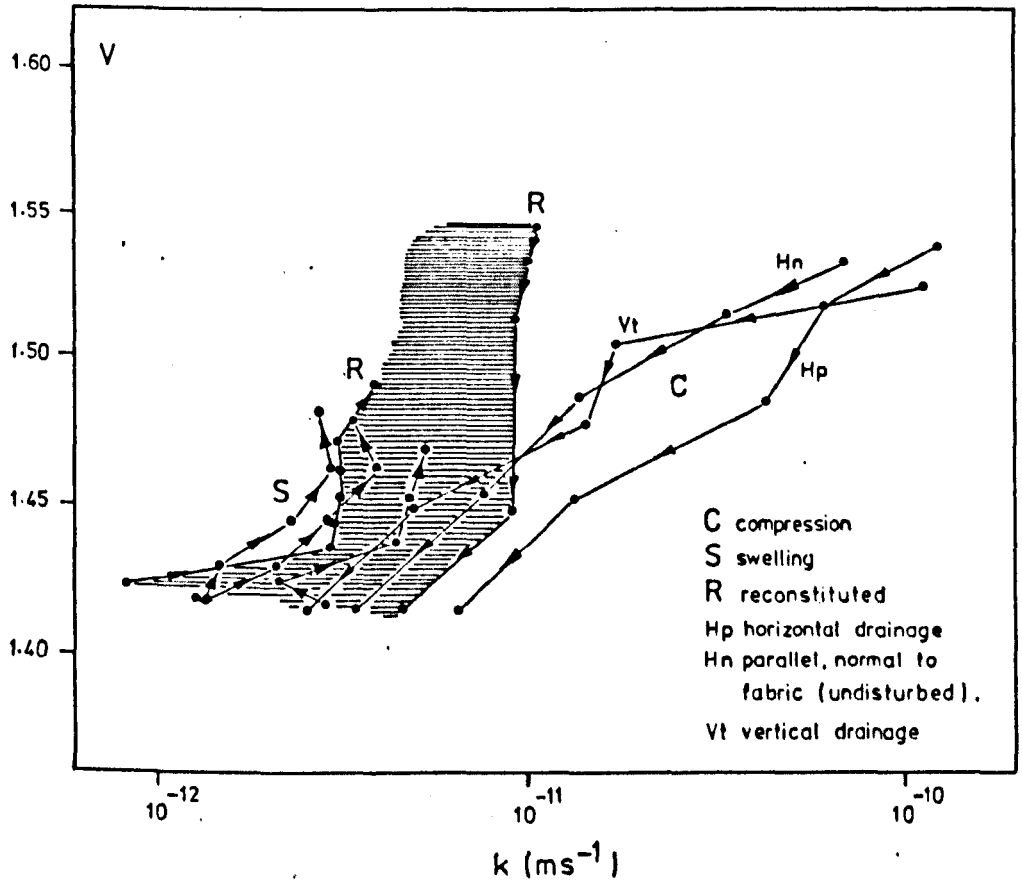

Figure 8.34 Oedometer determined permeability, till W(d).

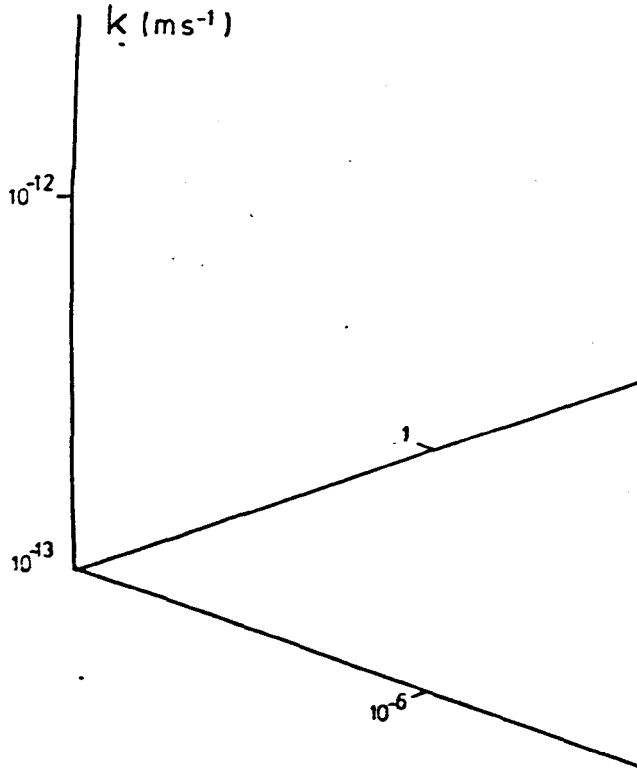
k (ms-1)
10-12
10-13
1
10-6

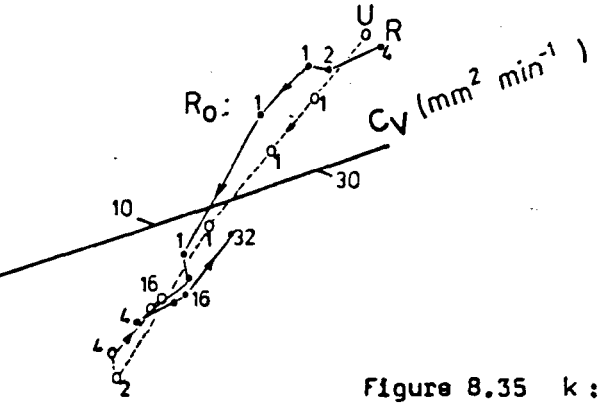

Figure 8.35 k : c_v : m_v relationship, till HH(a).
(Reconstituted, undisturbed)

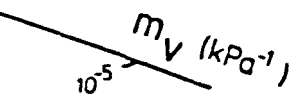

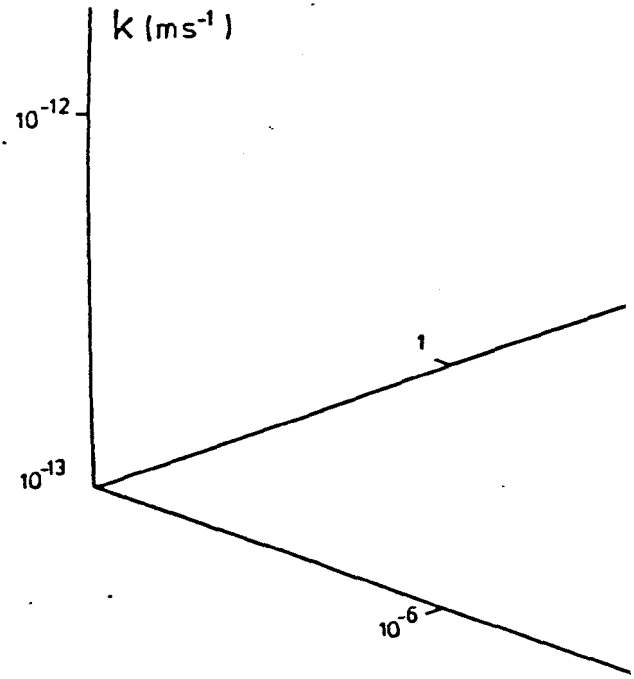
k (ms-1)
10-12
10-13
1
10-6

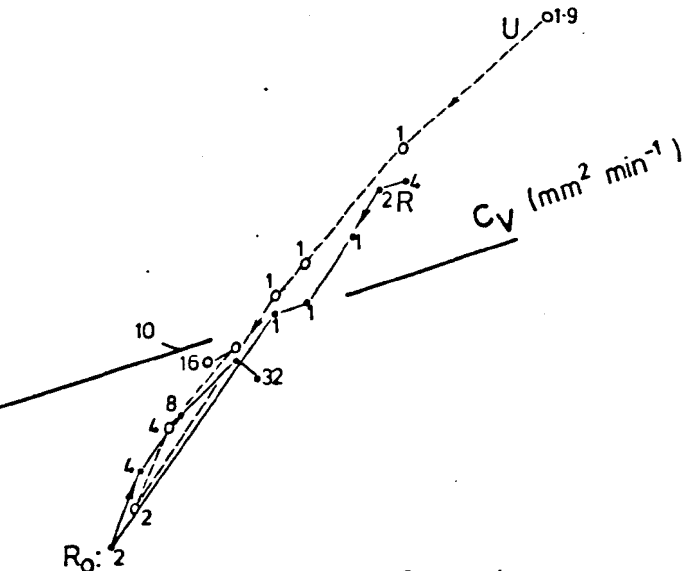

Figure 8.36 k : c_v : m_v relationship, till HH(b).

(Reconstituted, undisturbed)

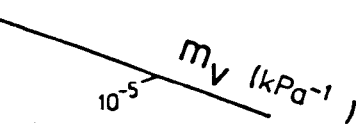

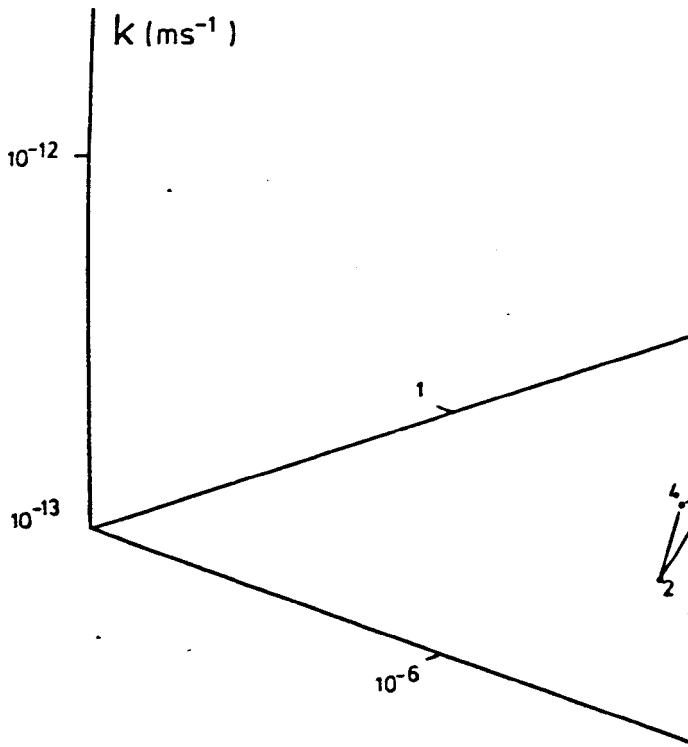
k (ms^{-1})
10^{-12}
10^{-13}
10^{-6}
1
2
4

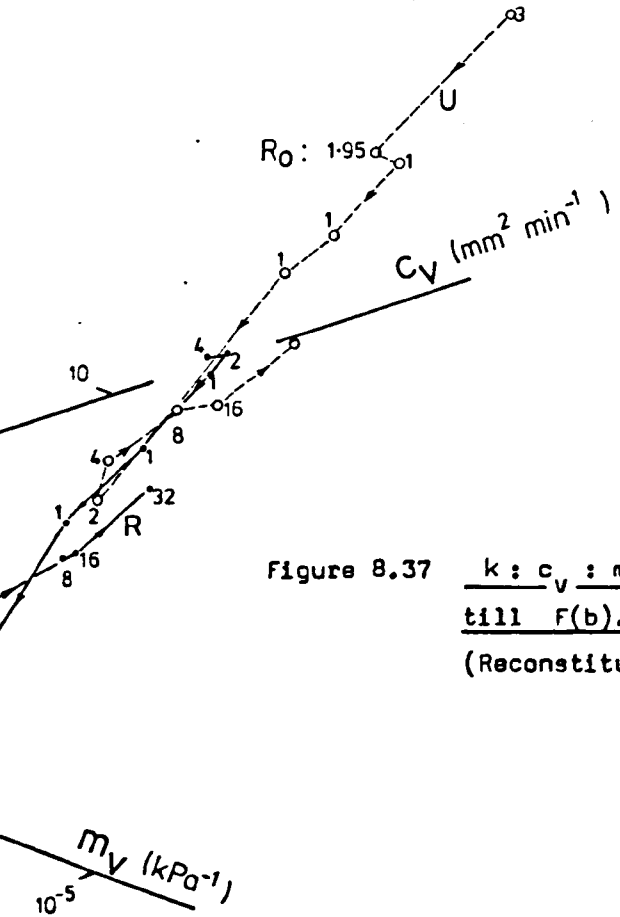

Figure 8.37 k : c_v : m_v relationship, till F(b).

(Reconstituted, undisturbed)

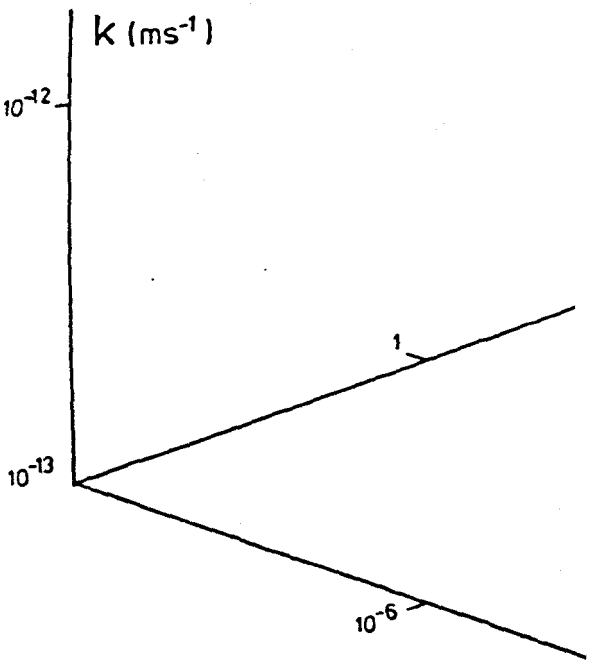
k (ms^{-1})
10^{-12}
10^{-13}
1
10^{-6}

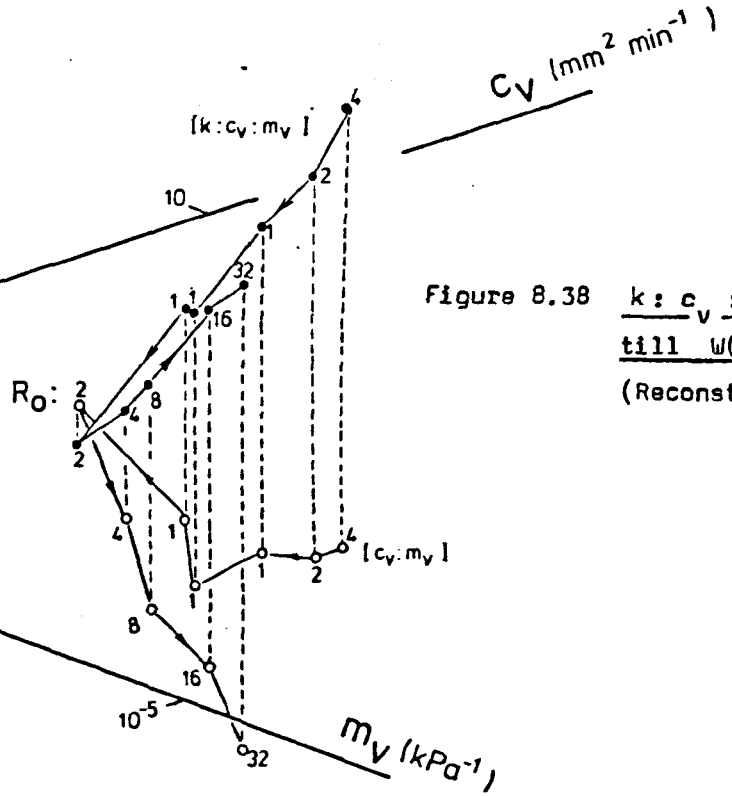

Figure 8.38 k : c_v : m_v relationship, till W(b).

(Reconstituted)

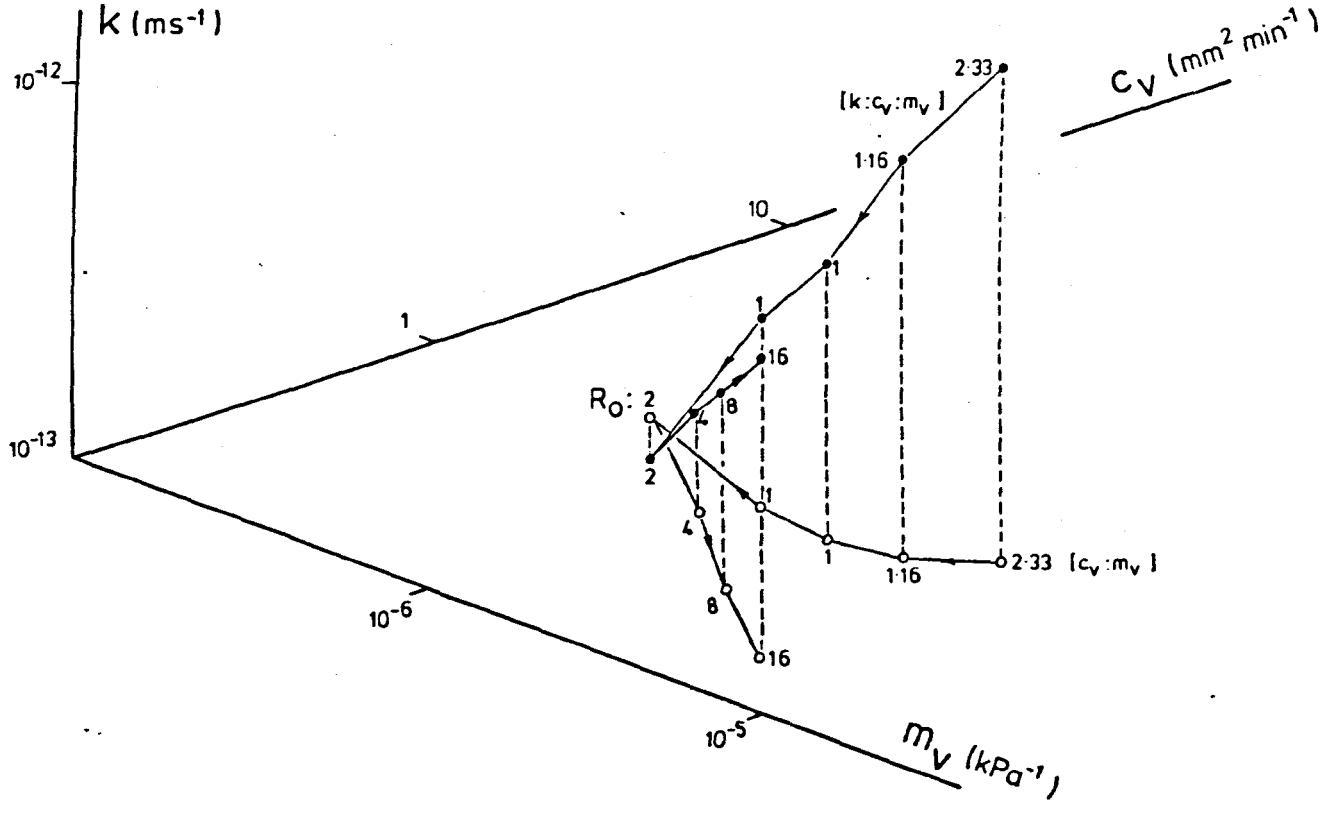

Figure 8.39 k : c_v : m_v relationship, till W(b). (Undisturbed)

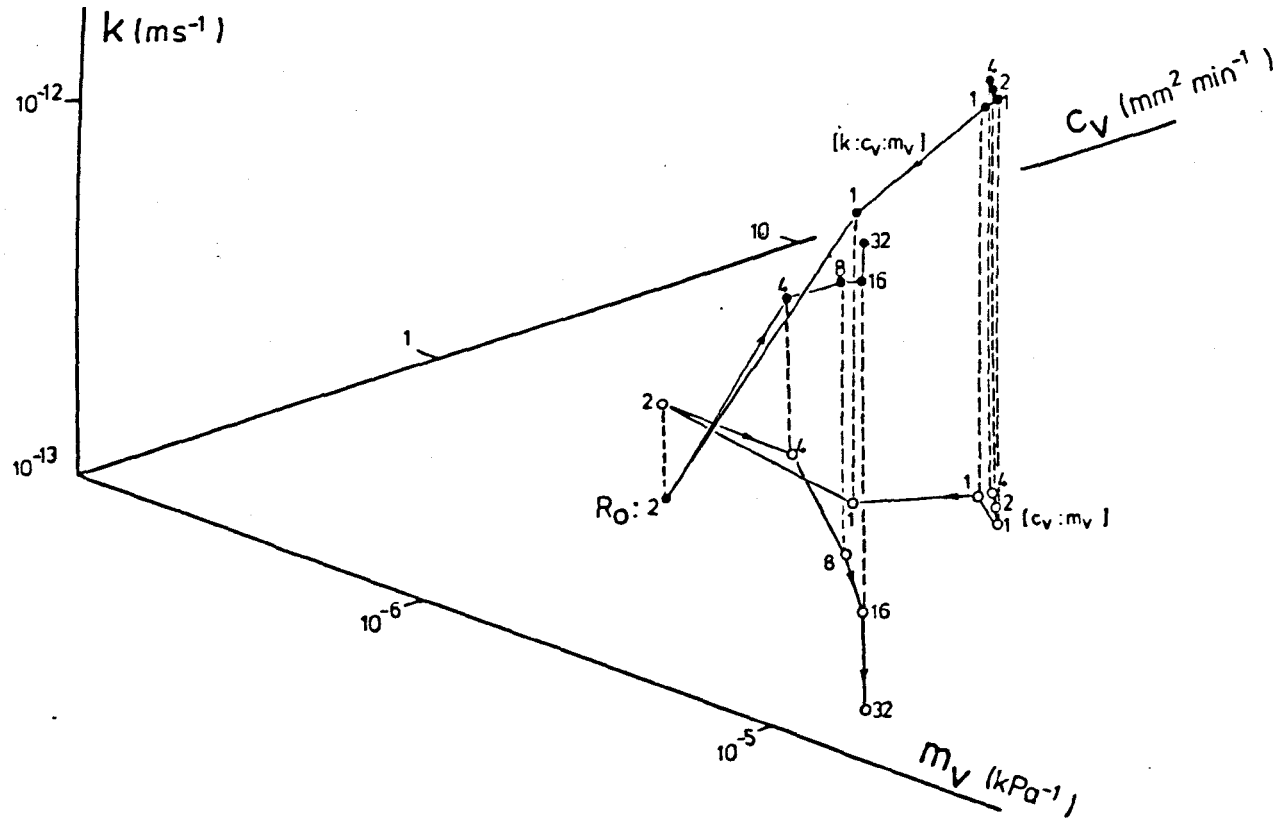

Figure 8.40 k : c_v : m_v relationship, till W(d). (Reconstituted)

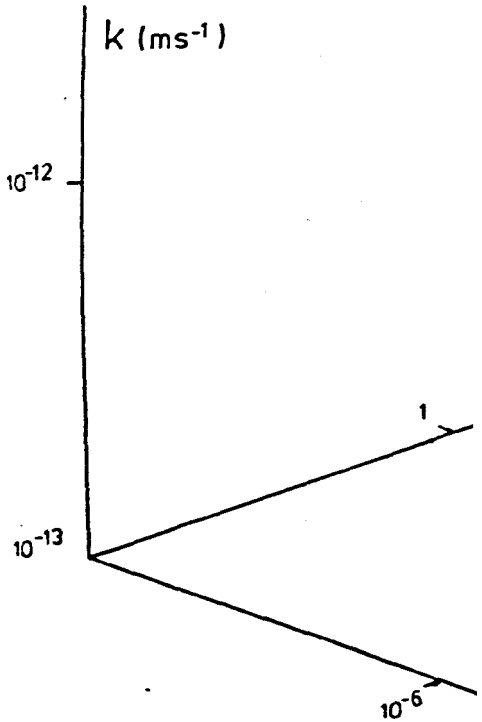

Figure 8.41 k : c_v :

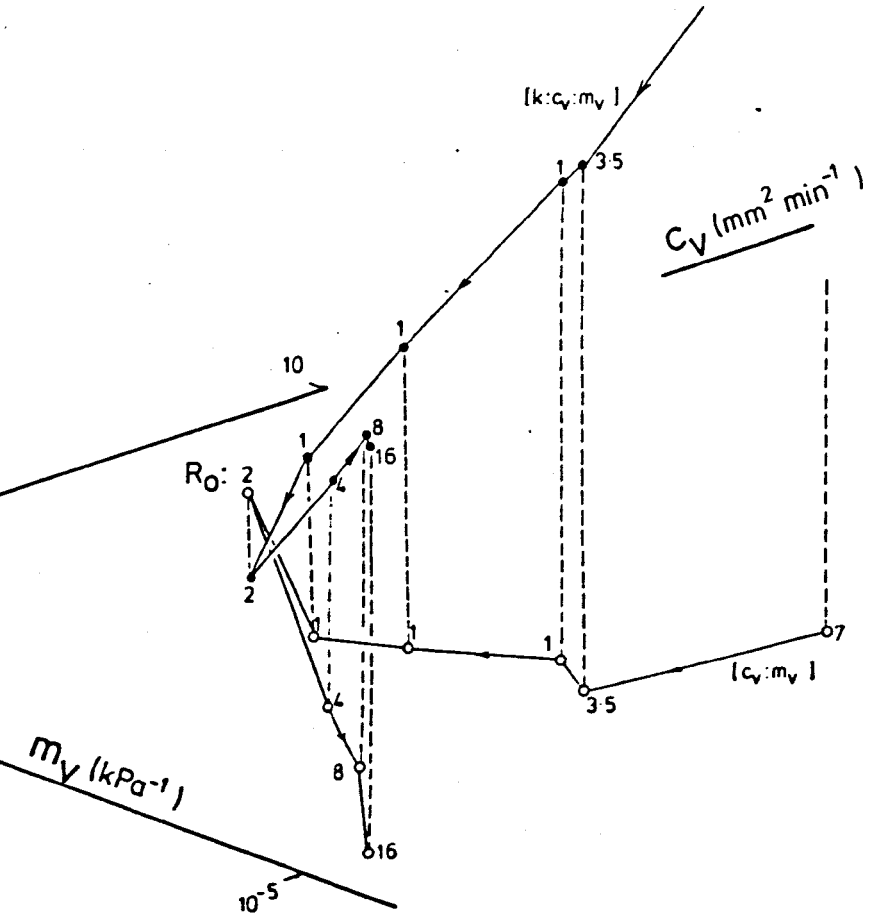

m_v relationship, till W(d). (Undisturbed)

Figure 8.42

Relationship between shear strength and liquidity index.

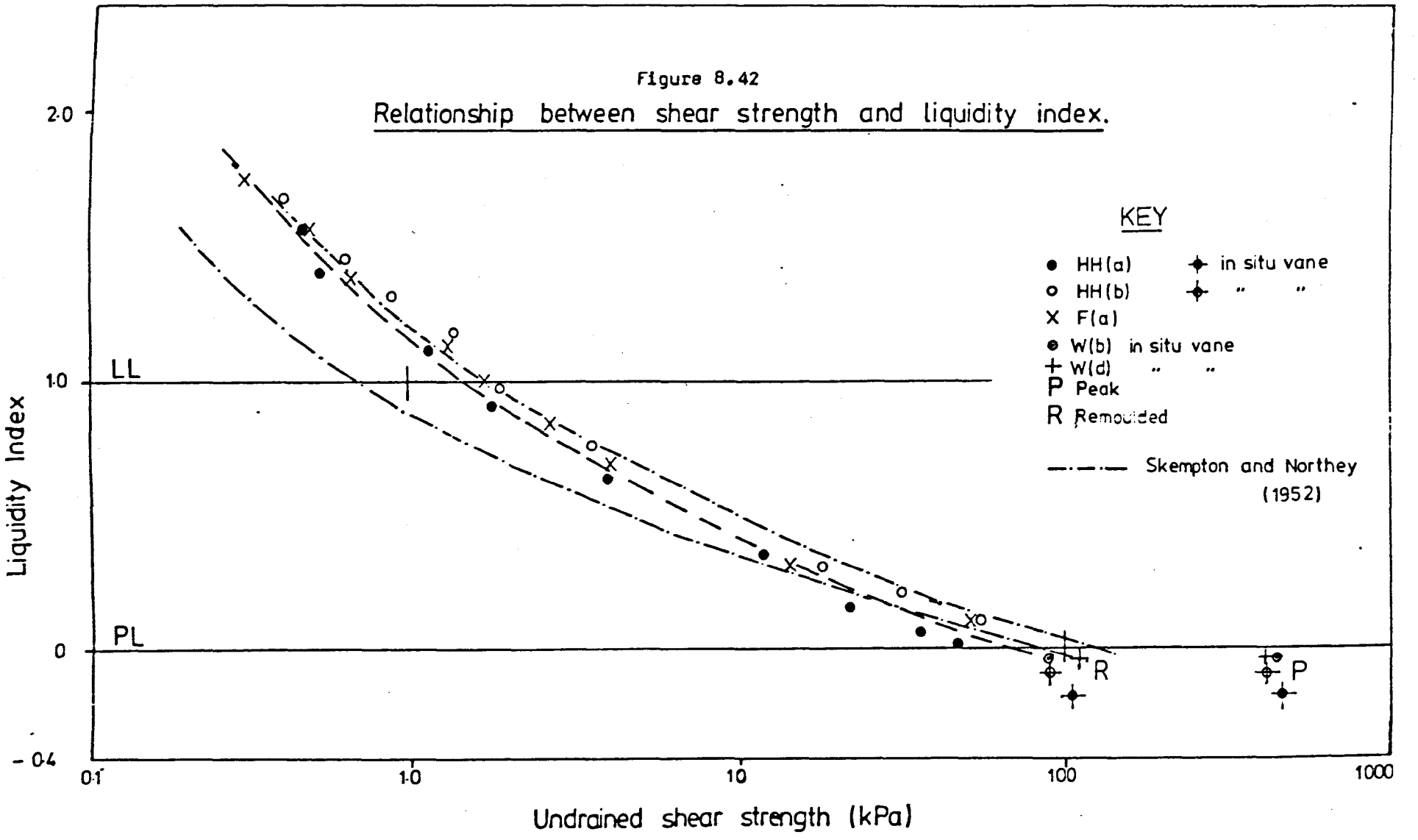

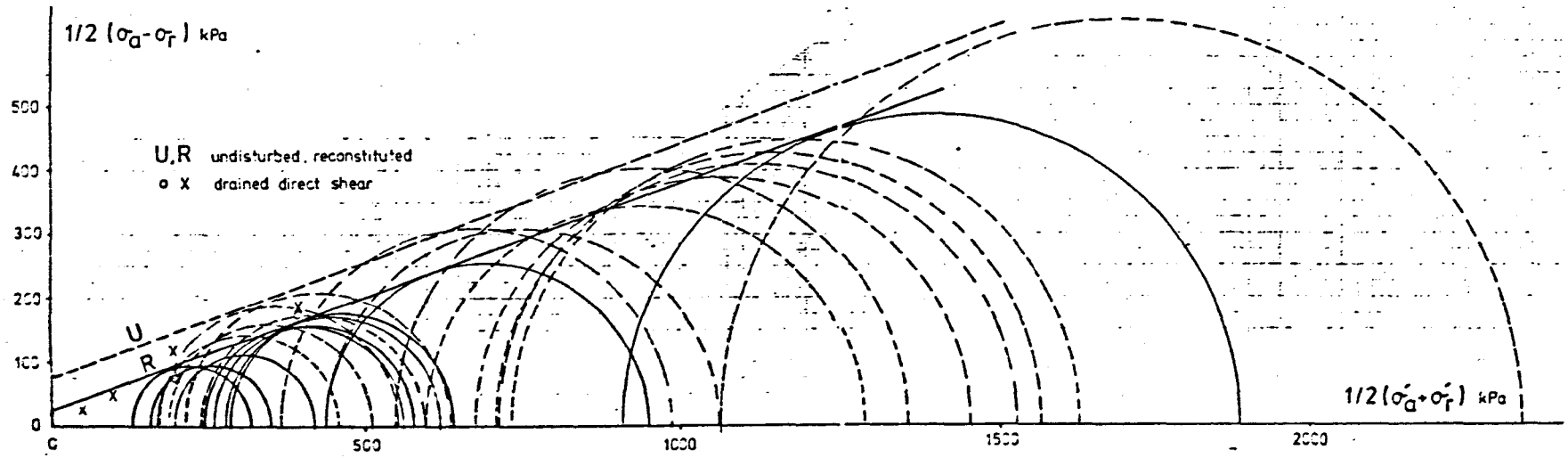

Figure 8.43 Mohr - Coulomb peak effective stress circles, undisturbed and reconstituted till HH(a).

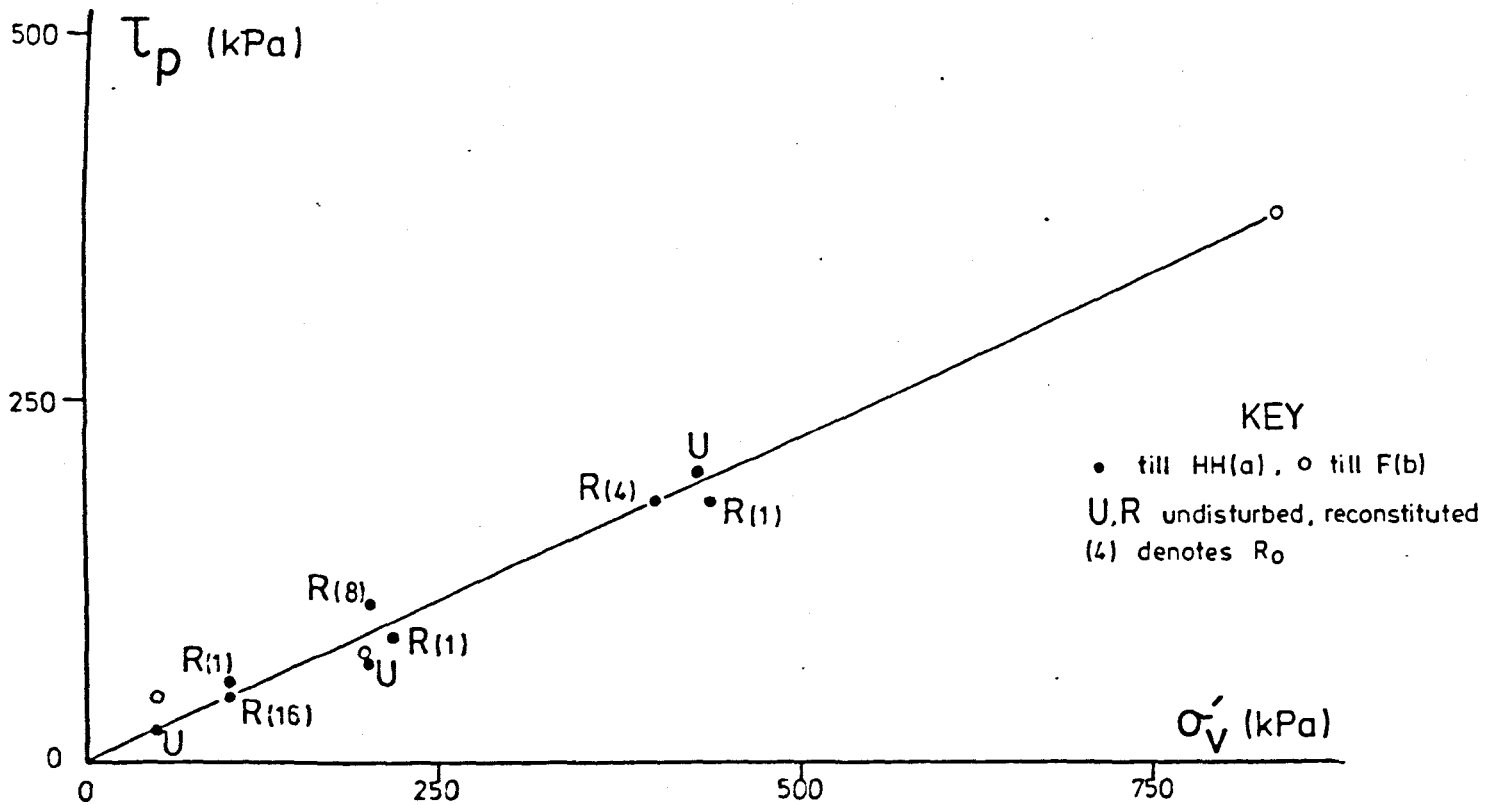

Figure 8.44 Peak drained shear strength, direct shear tests.

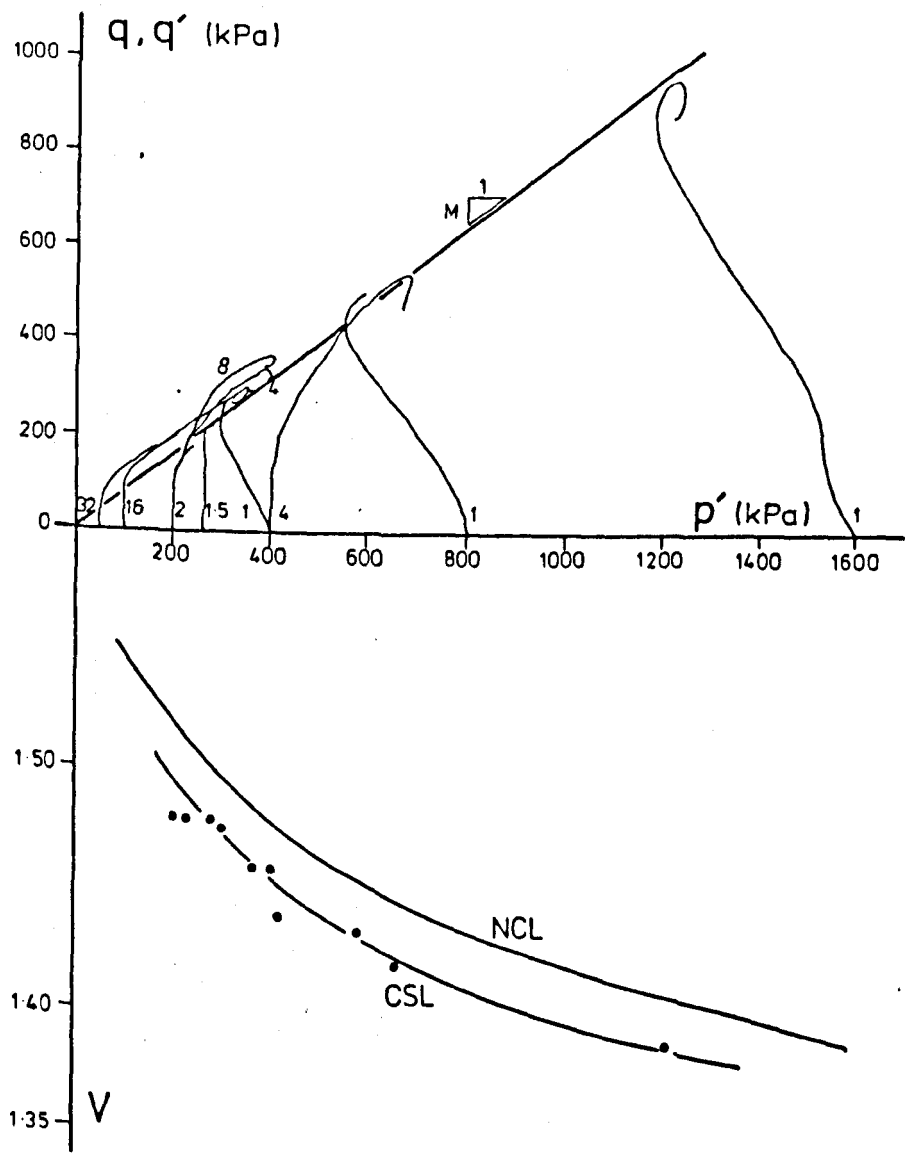

Figure 8.45 q , q′ : p′ and V : p′, reconstituted till HH(s).

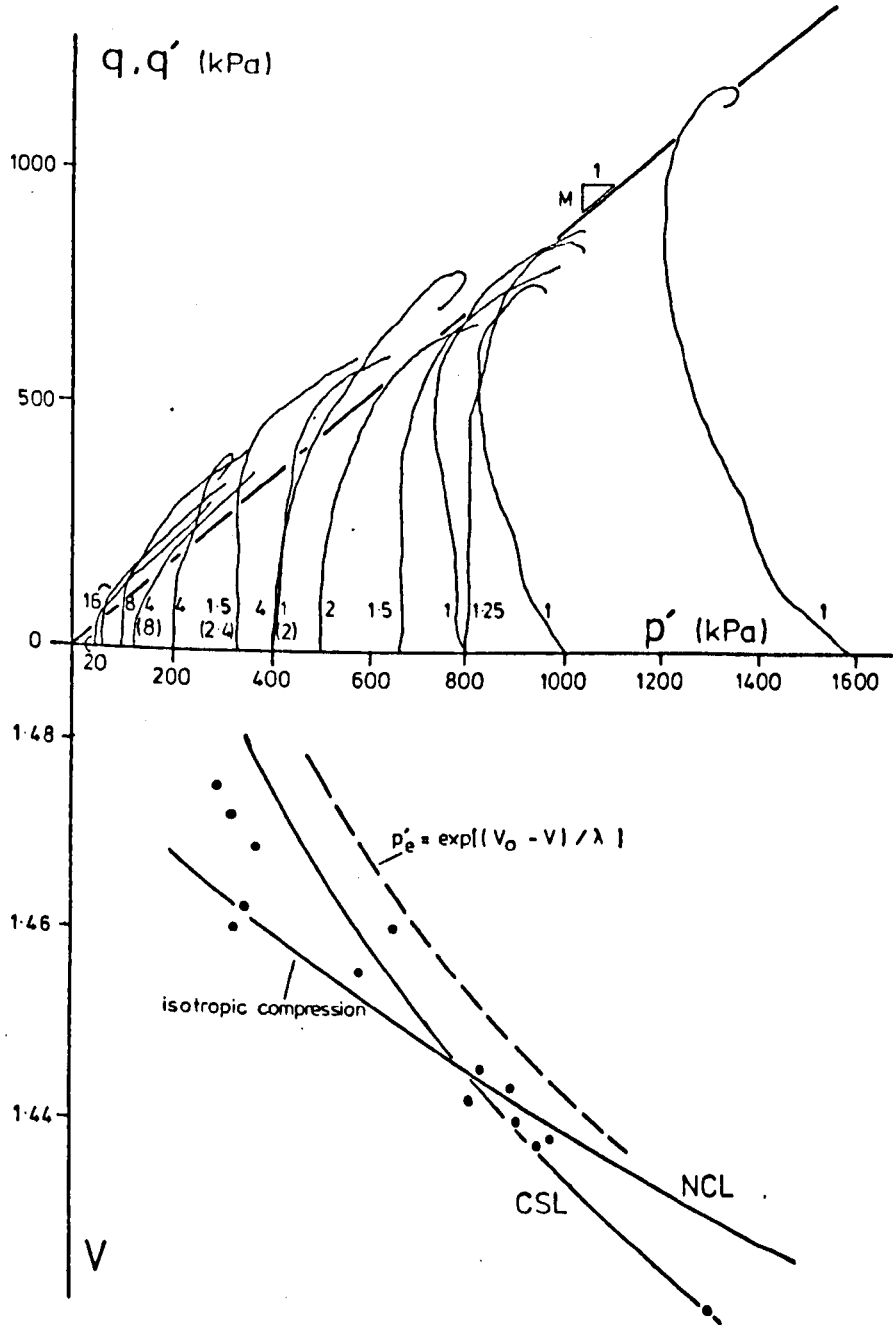

Figure 8.46 q , q′ : p′ and V : p′, undisturbed till HH(a).

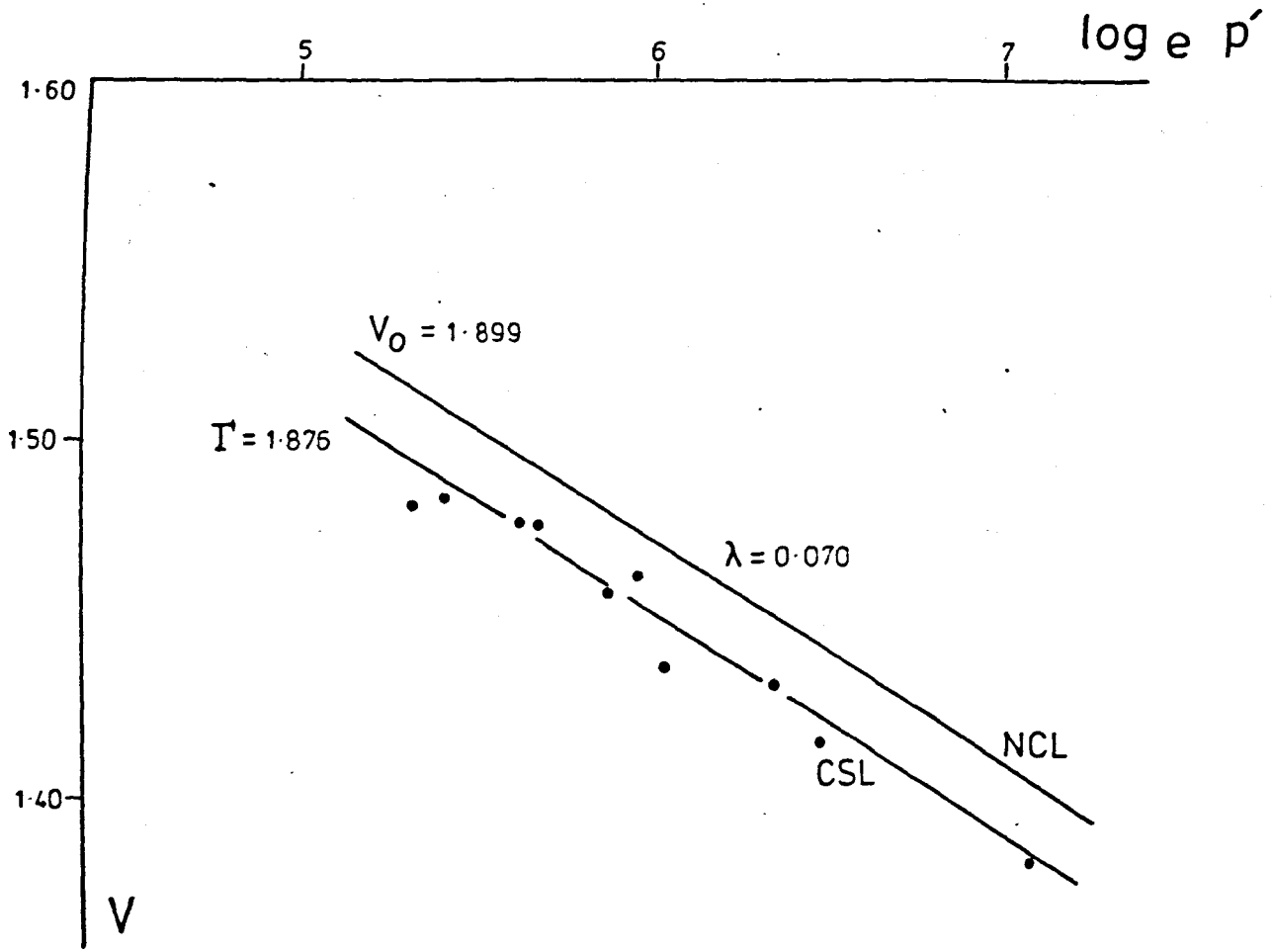

Figure 8.47 $\log_e p'$: V , reconstituted till HH(a).

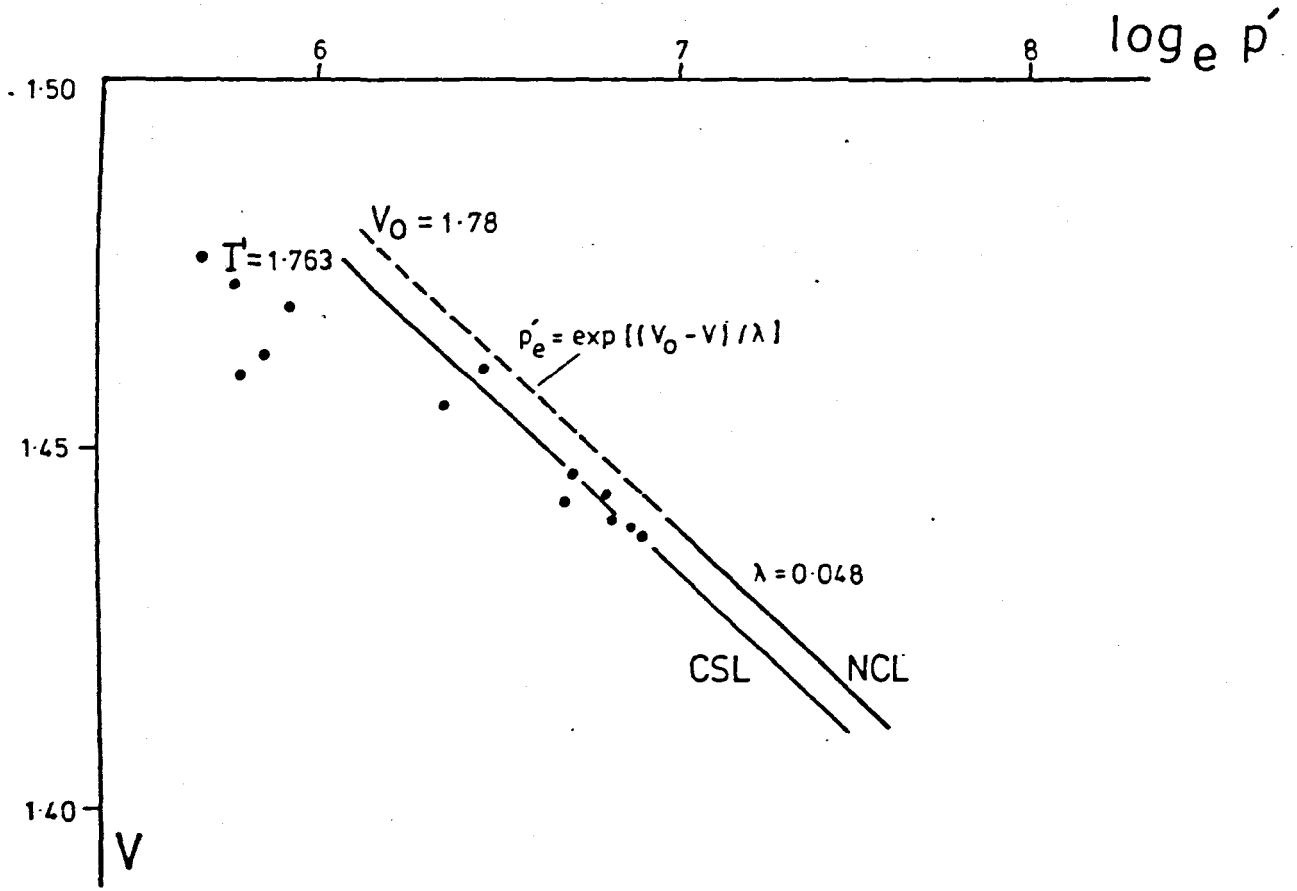

Figure 8.48 log$_e$ p′ : V , undisturbed till HH(a).

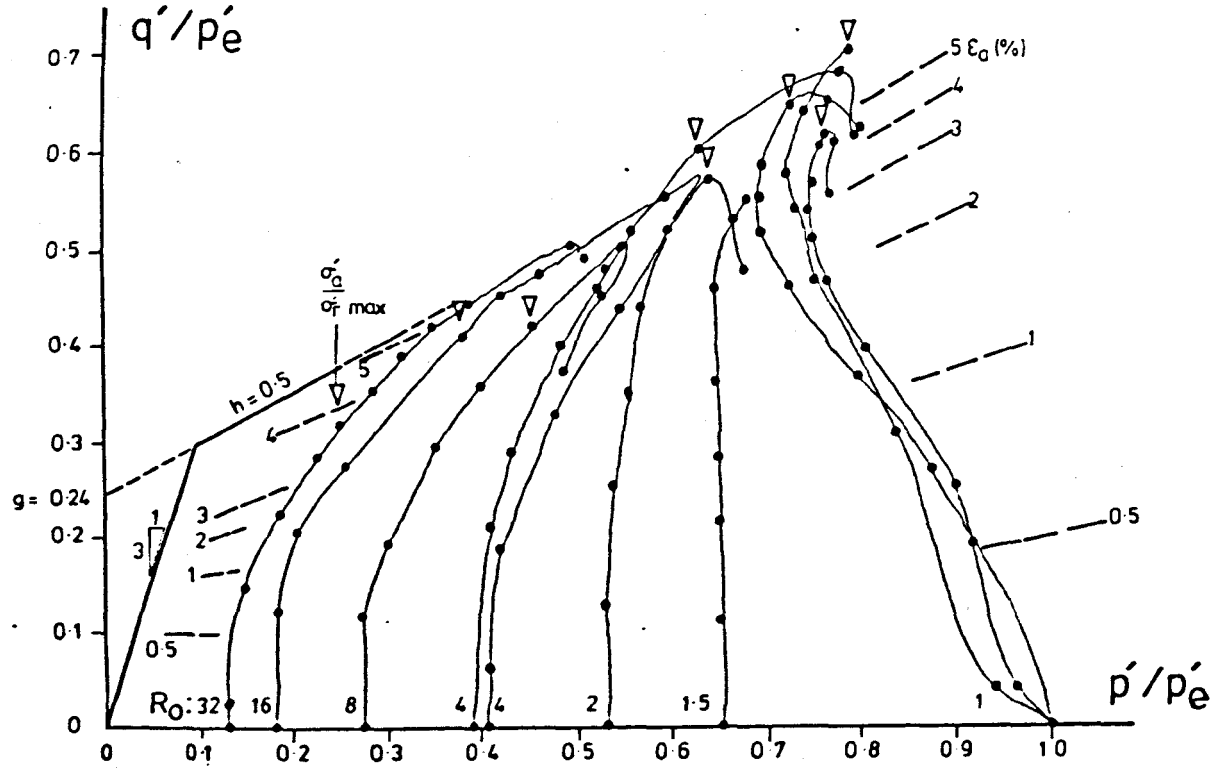

Figure 8.49 Normalised stress paths, reconstituted till HH(a).

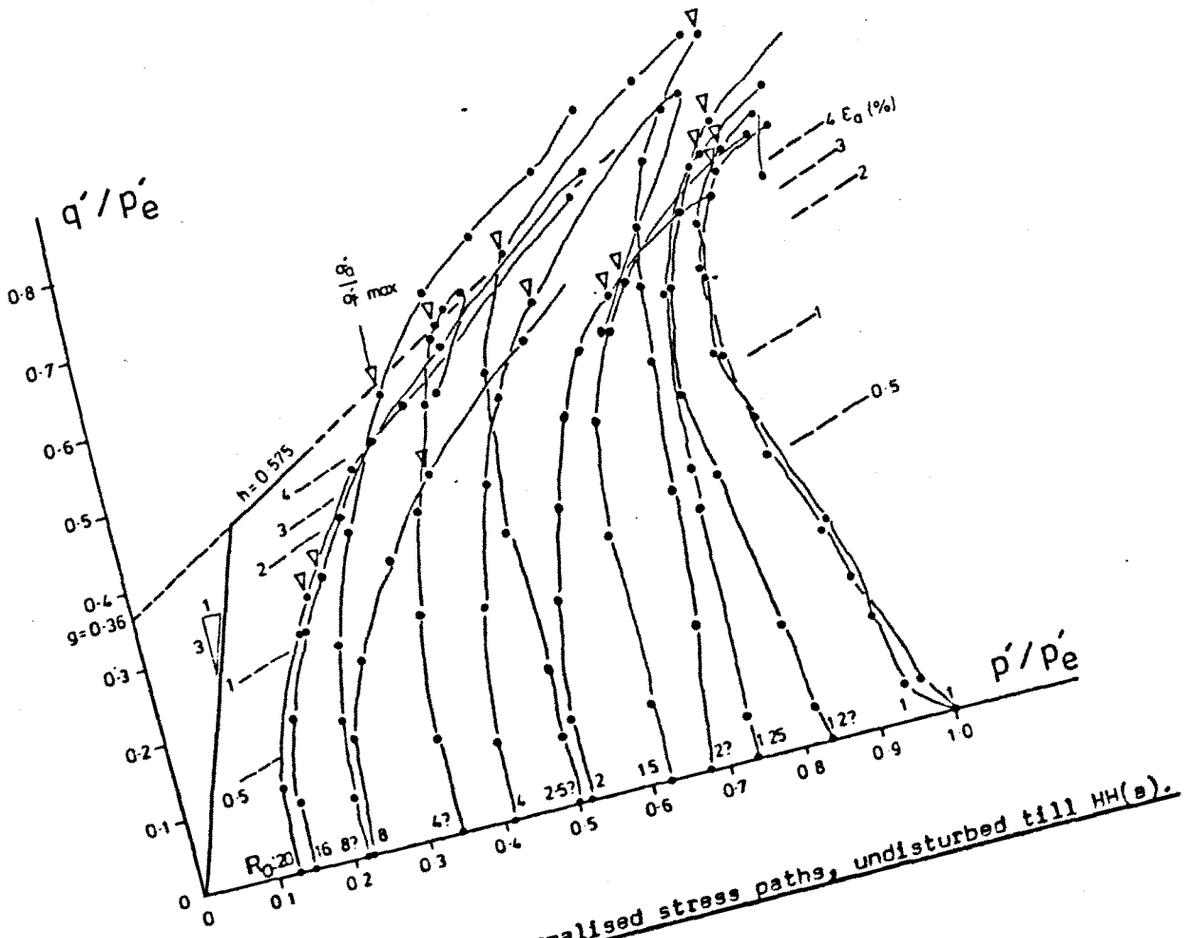

Figure 8.50 Normalised stress paths, undisturbed till HH(a).

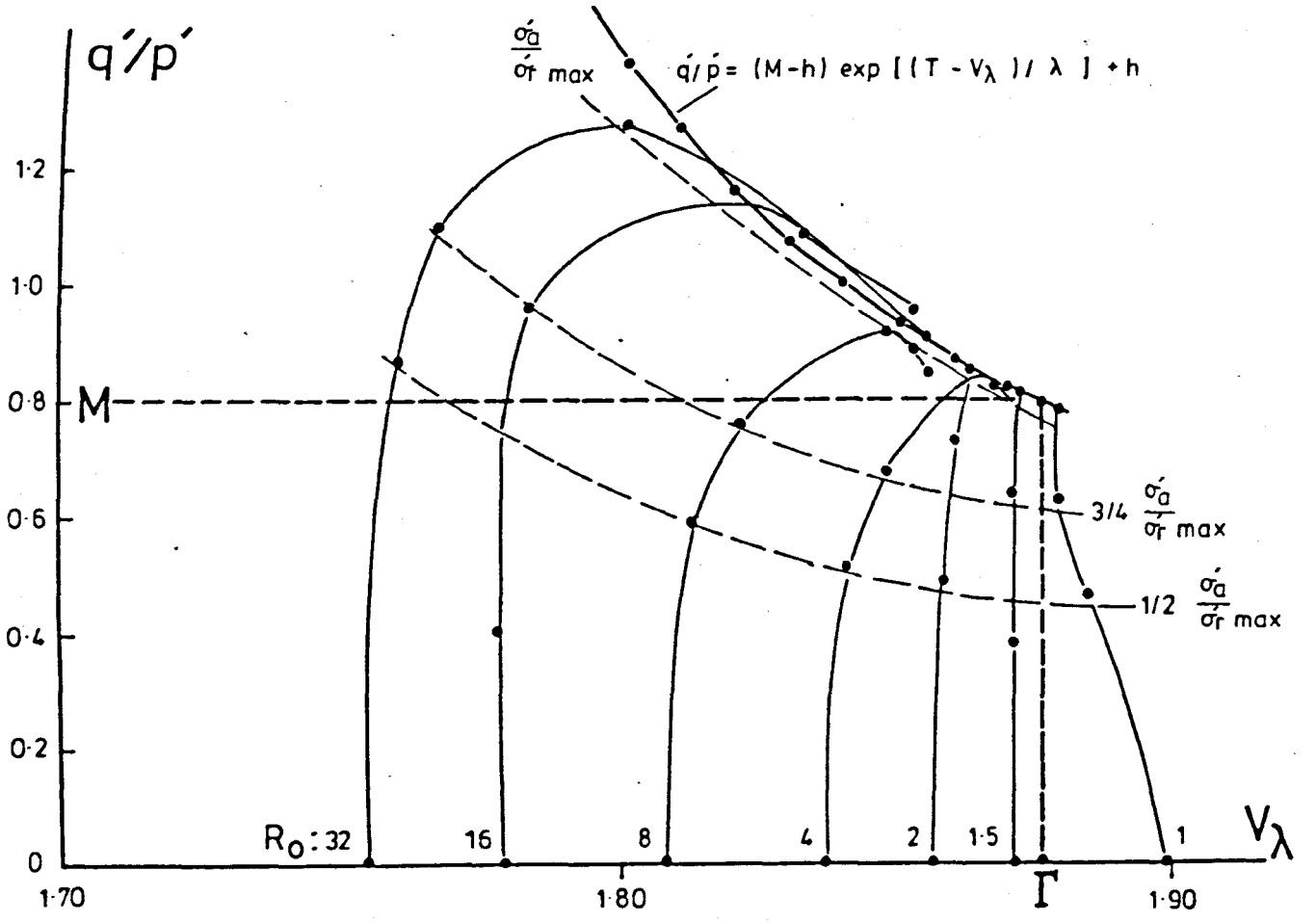

Figure 8.51 The reference section in q'/p' : $V\lambda$ space : reconstituted till HH(a).

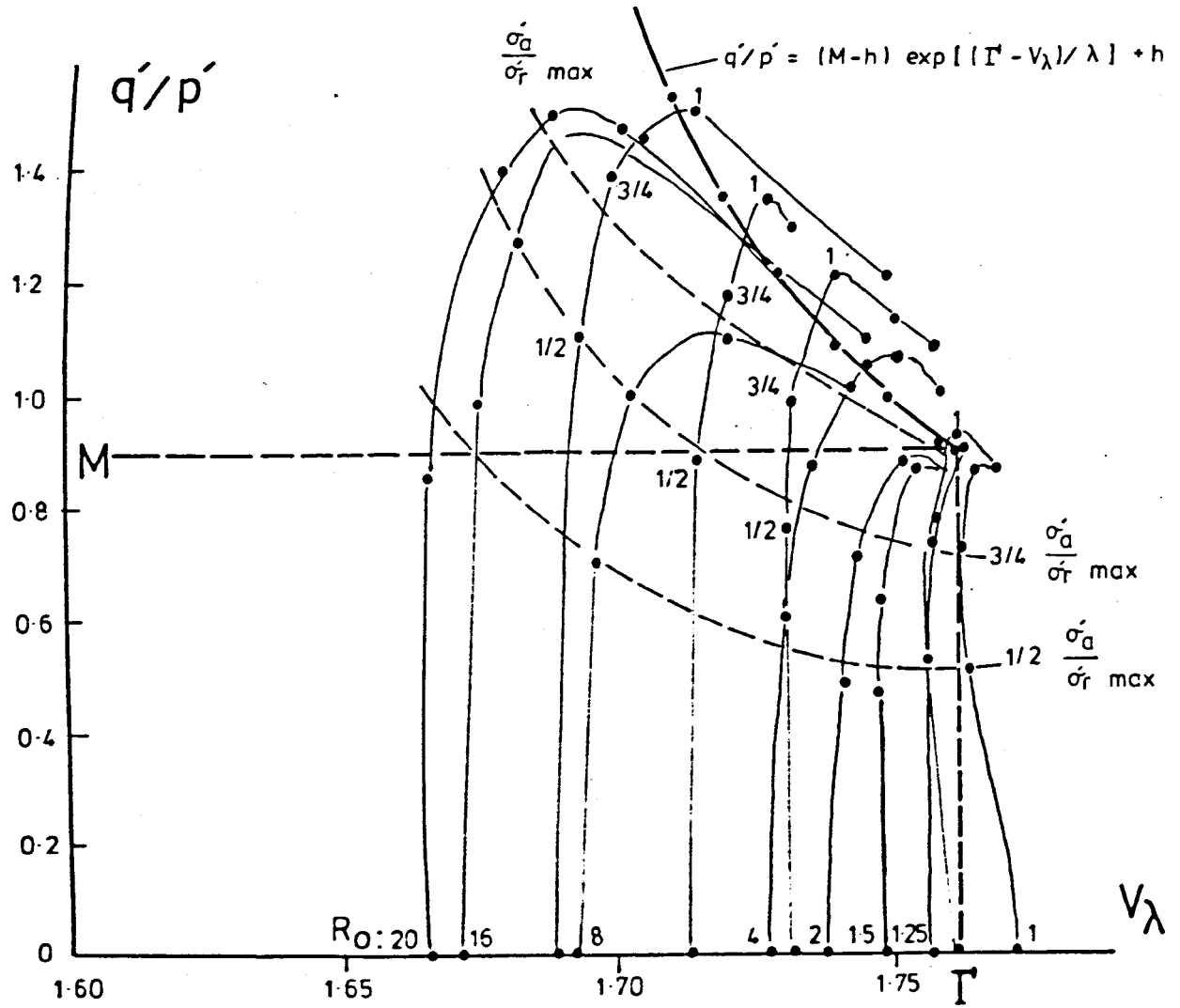

Figure 8.52 The reference section in q'/p' : $V\lambda$ space : undisturbed till HH(a).

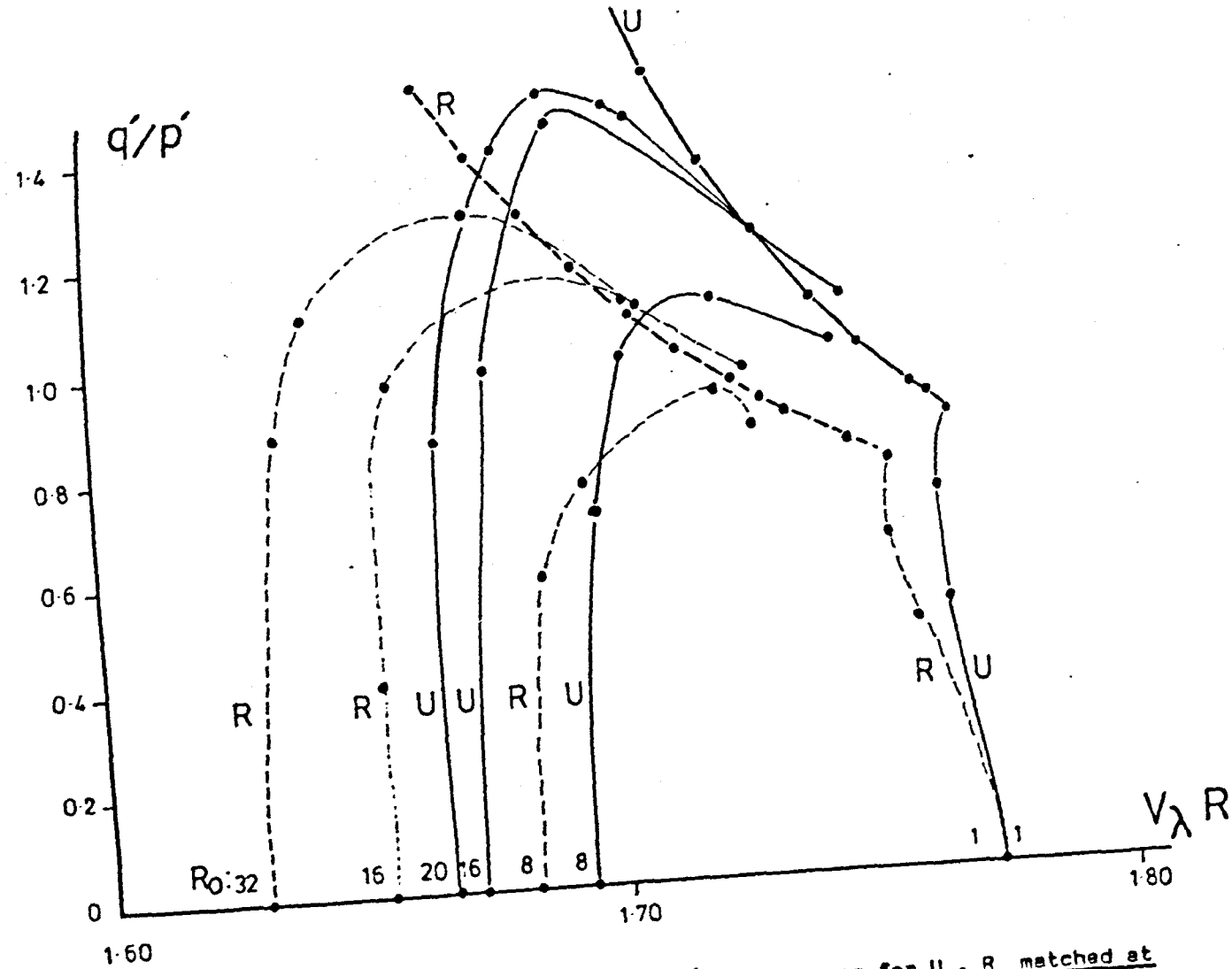

Figure 8.53 Reference sections in q'/p' : $V\lambda$ space for U , R matched at $V\lambda = V_o$ for the reconstituted soil.

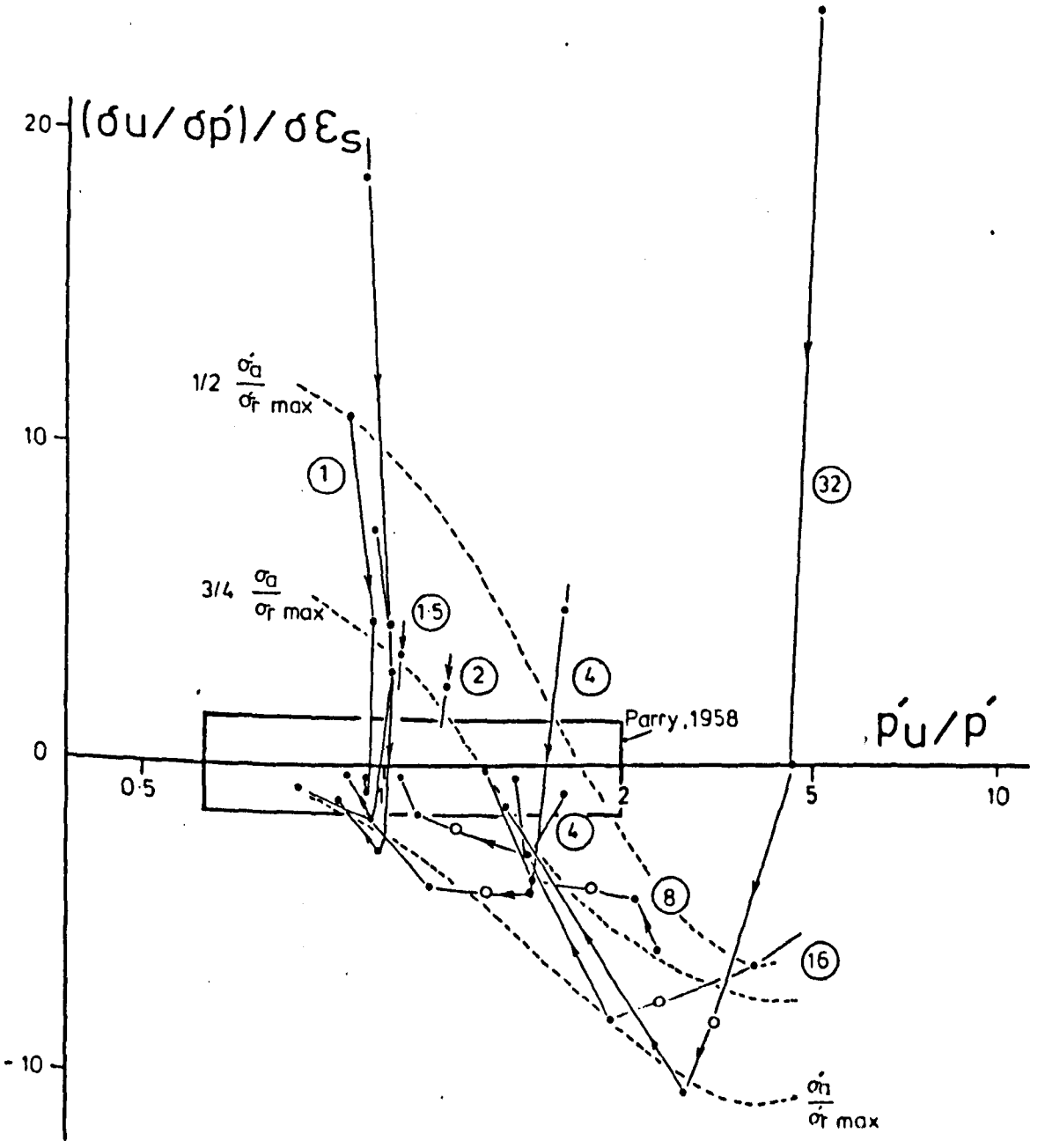

Figure 8.54 Rates of pore pressure change, reconstituted till HH(a).

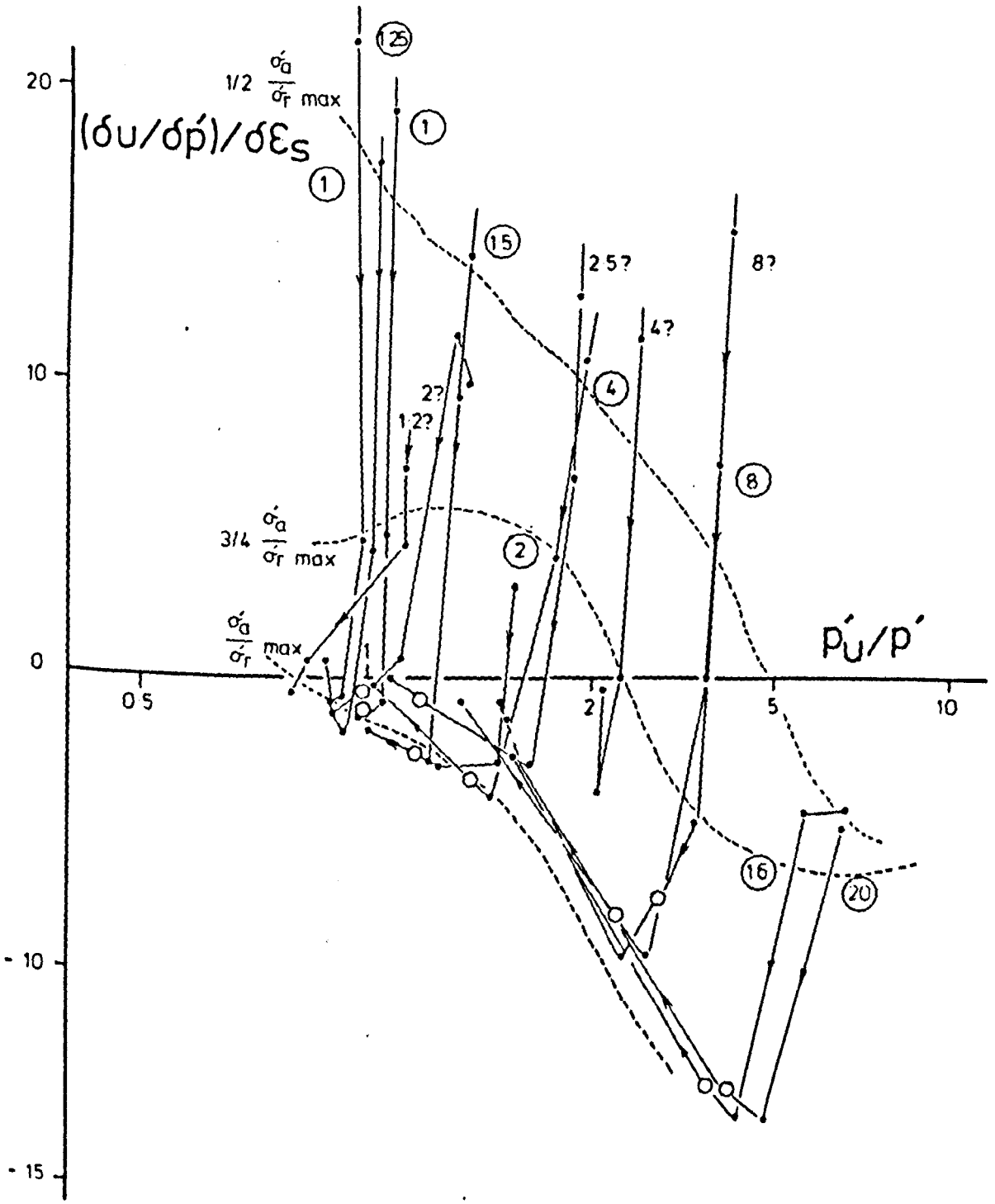

Figure 8.55 Rates of pore pressure change, undisturbed till HH(a).

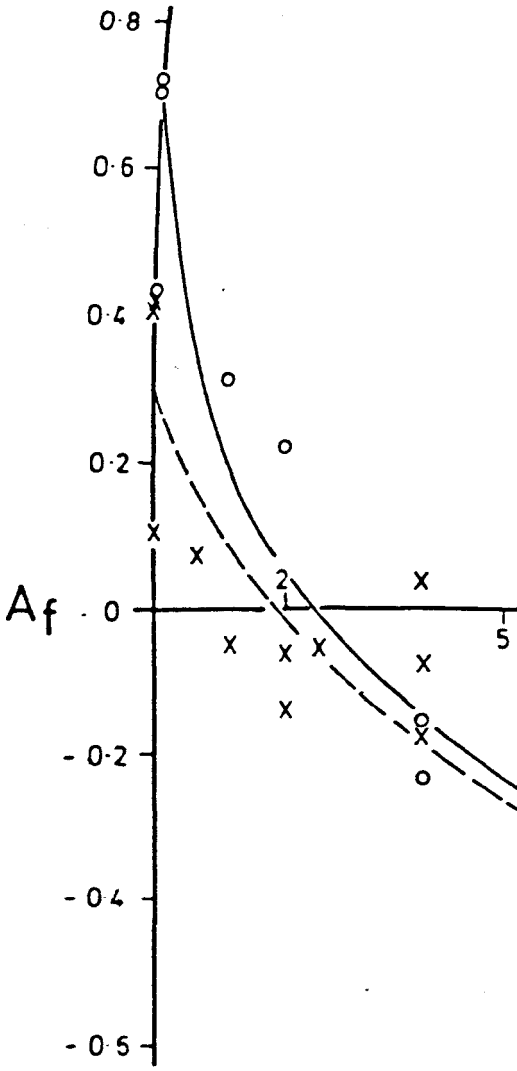
0·8
0·6
0·4
0·2
A_f
0
- 0·2
- 0·4
- 0·5
2
5

Figure 8.56 Pore pressure parameter A_f versus overconsolidation ratio.

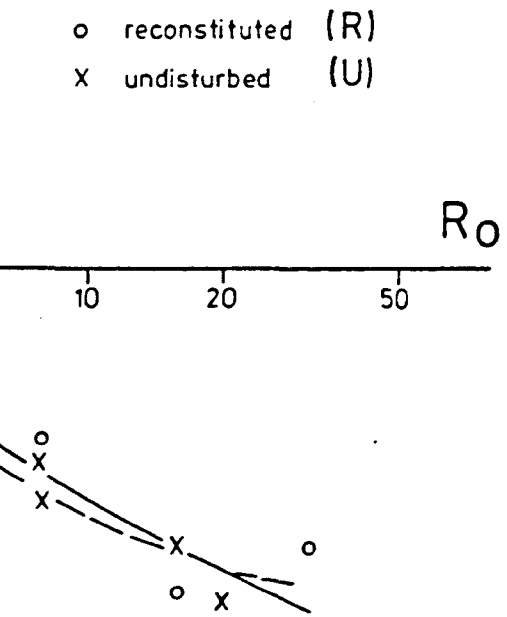

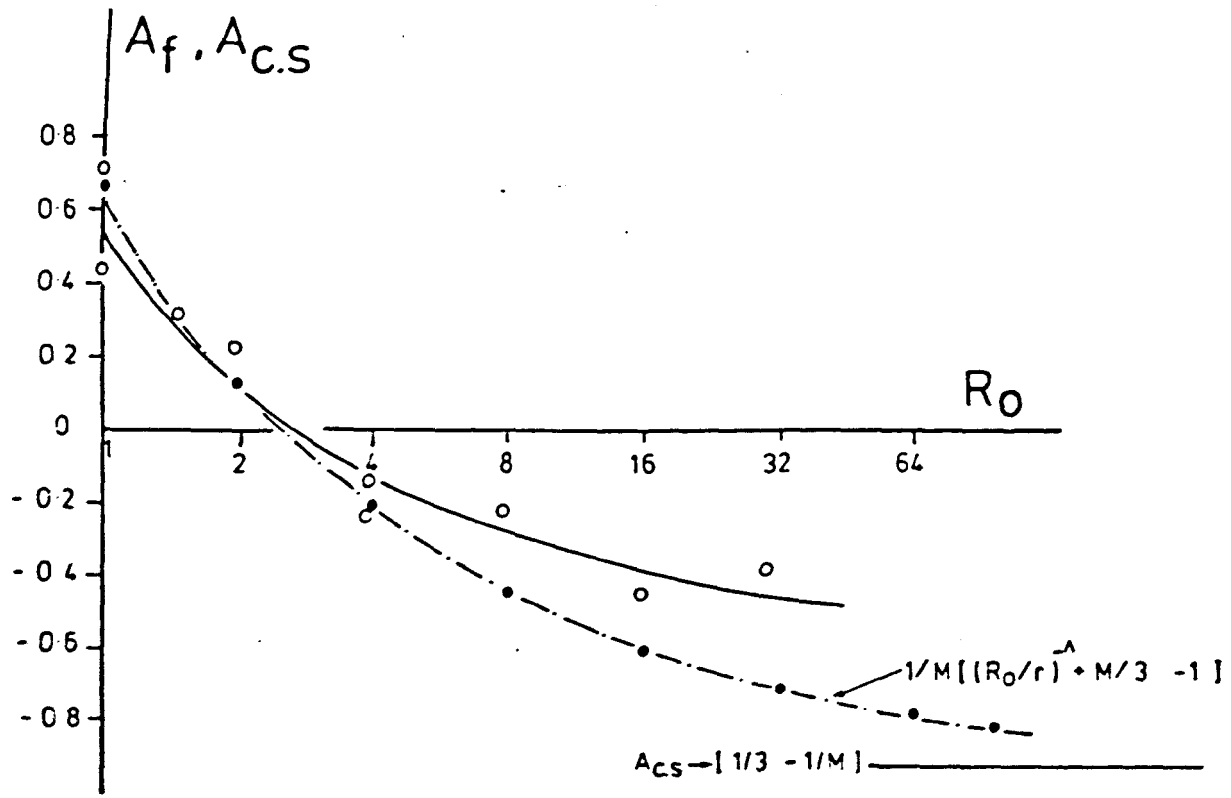

Figure 8.57 Pore pressure parameters $A_{c.s.}$, A_f versus overconsolidation ratio, reconstituted till HH(a).

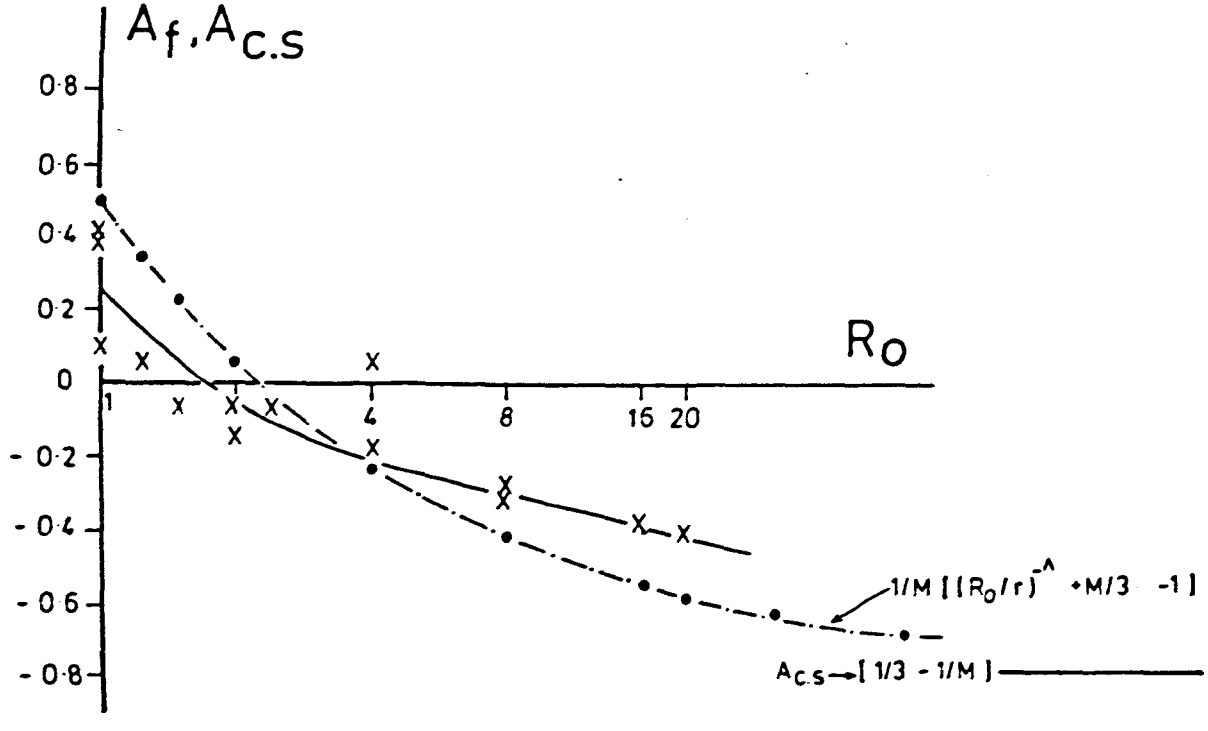

Figure 8.58 Pore pressure parameters $A_{c.s.}$ ——, A_f —— versus overconsolidation ratio, undisturbed till HH(a).

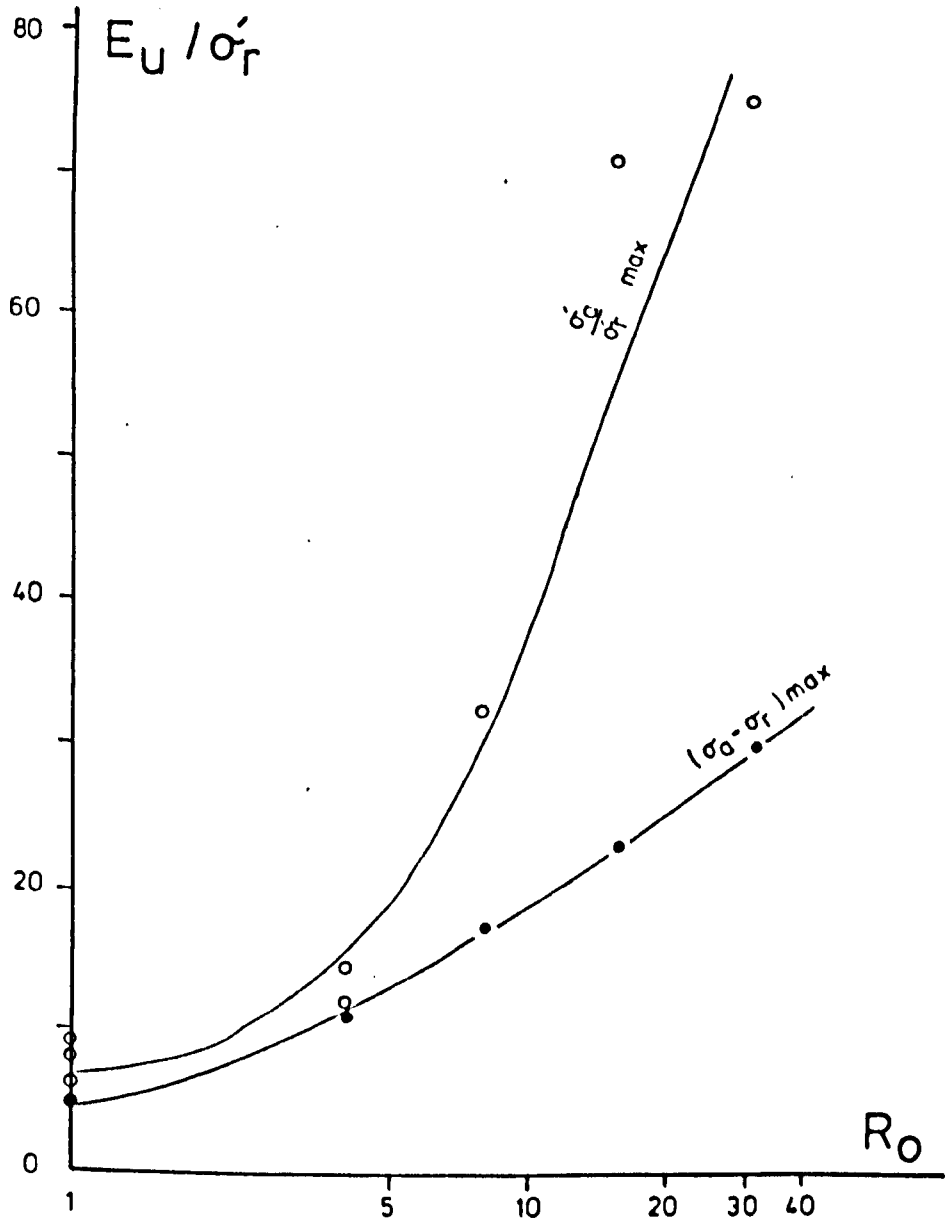

Figure 8.59 E_u / σ'_r : Ro , reconstituted till HH(a).

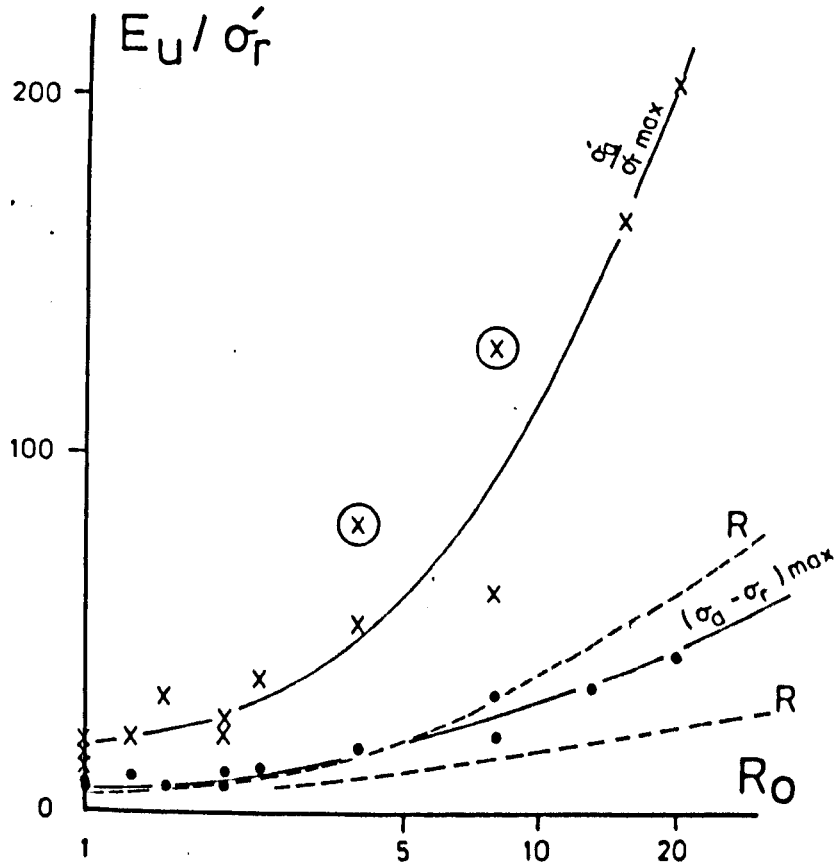

Figure 8.60 E_u / σ'_r : Ro , undisturbed till HH(a).

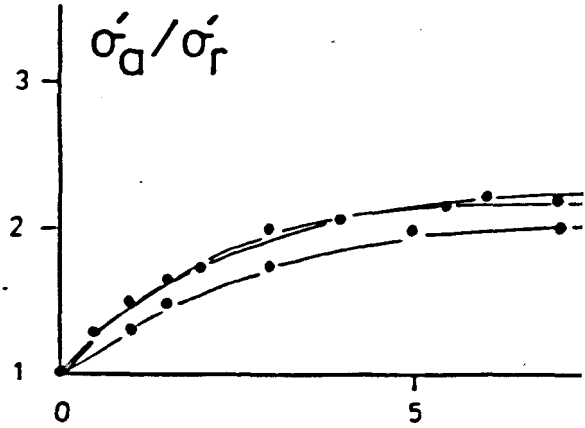

Figure 8.61 σ'_a / σ'_r

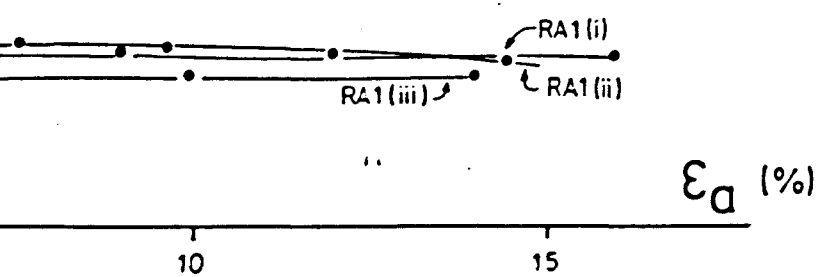

: ε_a (%) : normally consolidated, reconstituted.

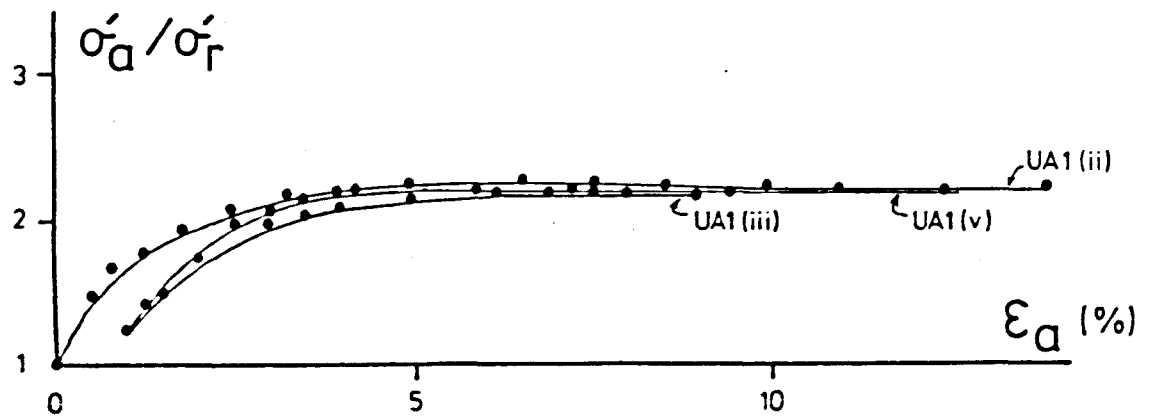

Figure 9.62 σ'_a / σ'_r : ε_a (%) : normally consolidated, undisturbed.

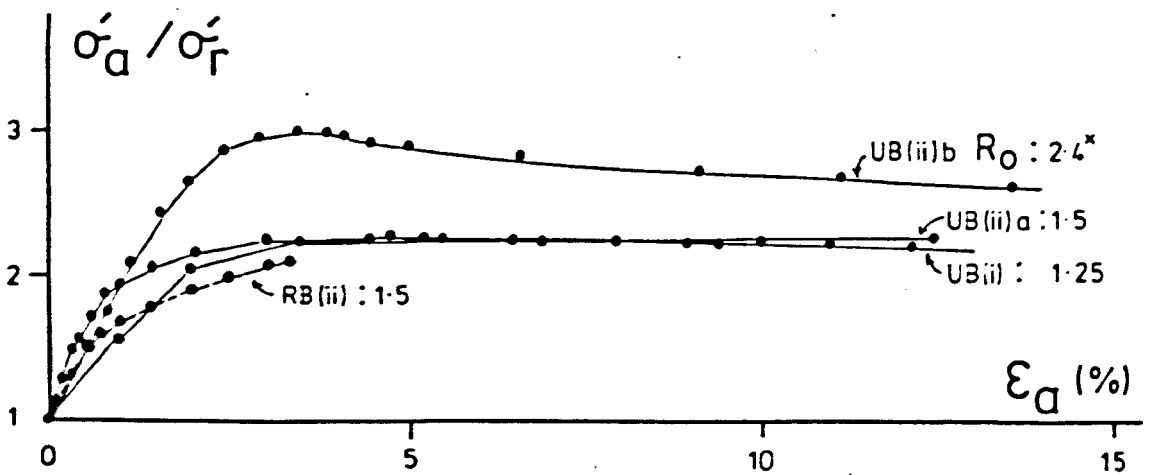

Figure 8.63 σ'_a / σ'_r : ε_a (%) : lightly overconsolidated (reconstituted and undisturbed).

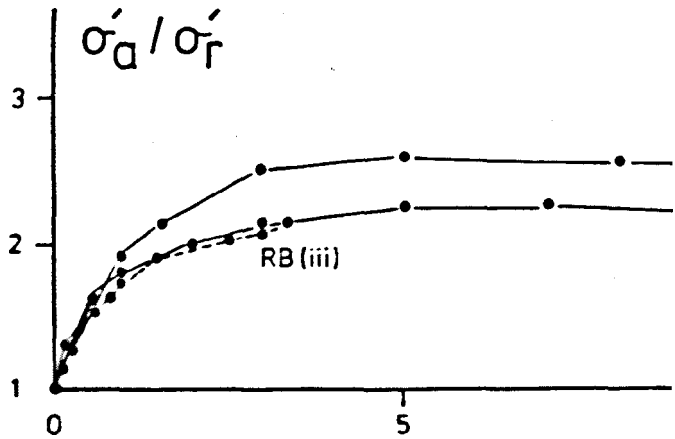

Figure 8.64 σ'_a / σ'_r :

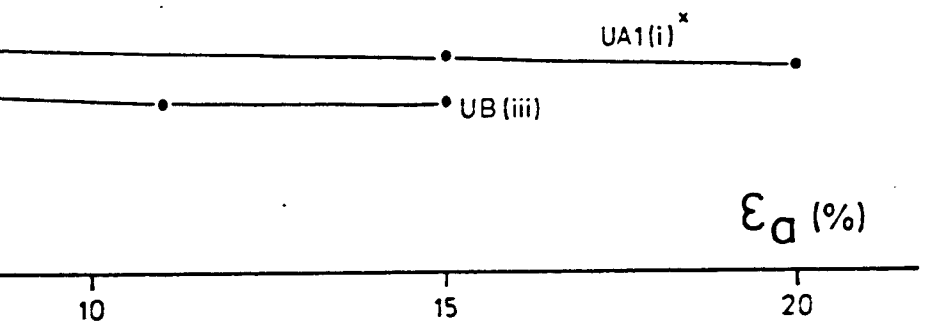

ε_a (%) : Ro = 2 .

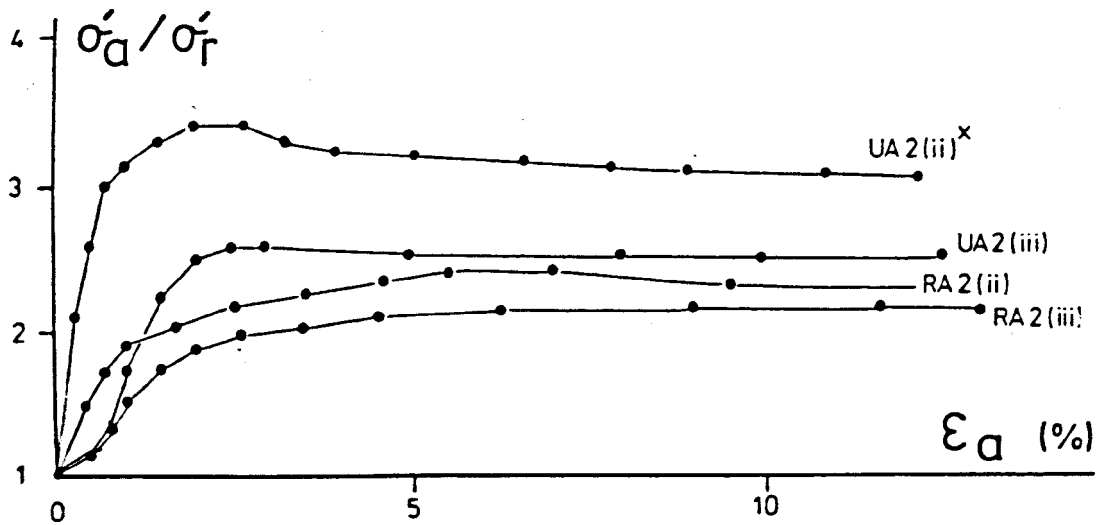

Figure 8.65 σ'_a / σ'_r : ε_a (%) : Ro = 4 .

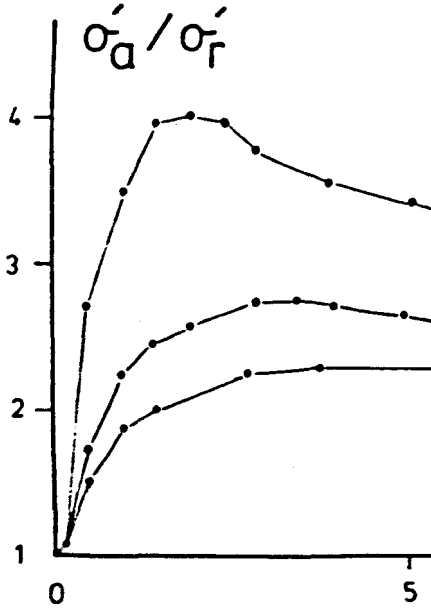

Figure 8.66

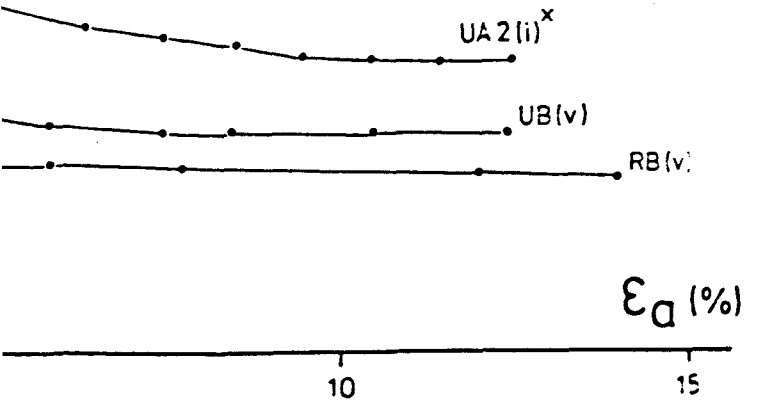

σ'_a / σ'_r : ε_a (%) : Ro = 8 .

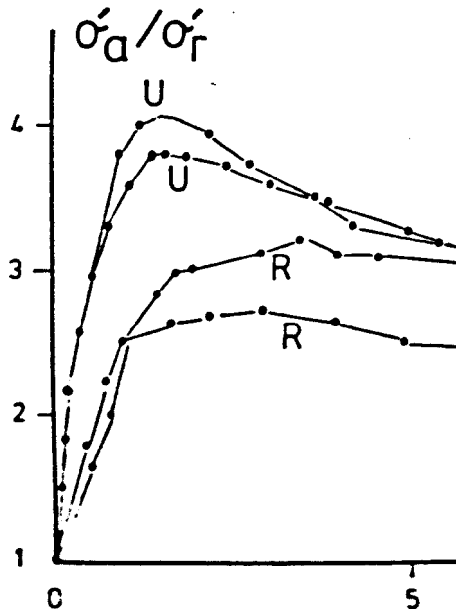

Figure 8.67

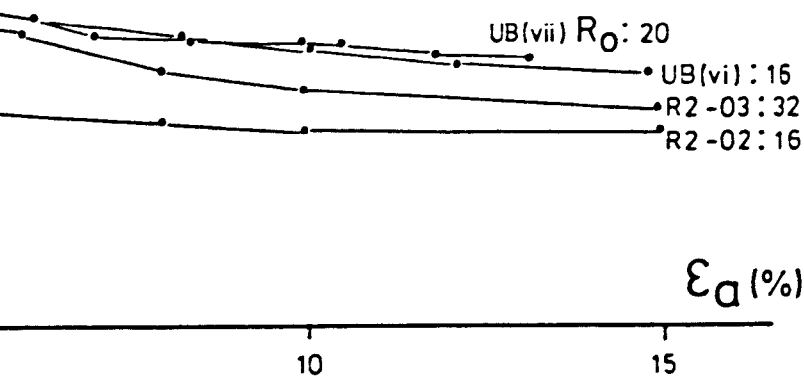

σ'_a / σ'_r : ε_a (%) : Ro = 16 - 32 .

CHAPTER 9. SUMMARY AND CONCLUSIONS.

9.1 The geological origin of the tills.

The broad stratigraphic relationships of the tills in the Vale with the other glacial and proglacial sediments, which are found associated with them, are now reasonably well established. Whilst there is general agreement that a proglacial Thames drained the Vale of St. Albans in a north-easterly direction, there is not universal agreement on when its diversion out of the Vale occurred. The most recent view is that Ware Till ice, of much greater extent than previously thought, moved down the Vale generally from the north-east and dammed the flow of this major river; in so doing, it caused the formation of an extensive lake in which accumulated the varved silts and clays represented by those now seen at Moor Mill. Two, possibly three, subsequent glacial episodes are represented in the Vale. The glacigenic sediments characterising these events conform with the established criteria for a basal lodgement origin (with the possible exception of Westmill Middle Till).

The evidence presented by others suggests movement into the Vale from the north-west (Ware Till) and the north-east (Eastend Green Till). The larger amounts of chalk found in this younger till have been attributed (Gibbard, 1977) to the parallelism of ice direction with the strike of the Chalk outcrop to the north and north-east of the study area.

The nature of both the macro- and microfauna found within the two tills HH(a) , HH(b) , at Holwell Hyde indicates that the source material for these sediments is of Jurassic and Cretaceous age. Whilst there are representatives in the microfauna of till HH(a) from the Lias to the Kimmeridge, no evidence of a Kimmeridgian fauna has been found in till HH(b); however, Cretaceous foraminifera and ostracods are present. The Kimmeridge outcrop thins west of Newmarket in E. Anglia (Geological Survey G.B. 'Ten Mile' Geological Map, Sheet 2, 1957) and is absent altogether over a distance of 50 km (with the exception of a small outcrop around Ampthill) to the north of the Vale. It eventually reappears west of Leighton Buzzard. A provenance for

till HH(a) from west of north-west is possible, therefore; the absence of Kimmeridge clay immediately to the north of the Vale makes this area a less likely provenance. Furthermore, the results of the field fabric study on this till do not exclude this as a possibilty. The presence of a Lias fauna in these tills will extend the distances over which ice sheets carrying these materials must have travelled. The nearest outcrops of the Lower Jurassic are found at Bedford (50 km NNW of the Vale) and Northampton (70 km NW). No Lias is found in E. Anglia; a provenance from the east and east north east therefore seems unlikely, even for till HH(b). However, the possibility that 'pulsing', ice sheet confluence and a degree of 'mixing' may be responsible for the sequence of till deposits seen at Holwell Hyde should not be excluded.

Despite being an ice marginal area during the Anglian, (for example see Bowen, 1978), there can be no doubt that Anglian ice topped the Tertiary ridge of the South Hertfordshire Plateau, as is evidenced by the presence of chalky tills found at Northaw Great Wood, approximately 6 km SE of Hatfield (Thomasson, 1961; Moffat and Catt, 1982; Avery et al, 1982) and also at Potters Bar at 113m O.D. (personal communication, Cheshire, 1984). Assuming, therefore, that the Anglian ice margin occupied a position no further north than approximately 10 km south of Welwyn Garden City, and by using the Devensian ice sheet analogue for the modelling of ice surface topography proposed by Boulton et al, (1978), it can be readily demonstrated that ice thickness during the Anglian at this locality would have been in the order of 200 m. Making an allowance for till HH(a) having been stripped of all soil overburden prior to its sampling, an effective preconsolidation pressure, due to ice loading of approximately 2000 kPa, is indicated for this till.

9.2 The post-depositional history of the tills.

Subsequent to their emplacement by ice during the Anglian, the history of the tills in the Vale of St. Albans is one which will have been governed by fluctuations in the Pleistocene climate. Those tills which occupy the lowest stratigraphical horizons in the Vale (for example the lowermost till at Holwell Hyde at approximately 62 m O.D. ; Ware Till at Westmill, approximately the same elevation) will have experienced at least one, and possibly two, further episodes of (vertical) ice loading and unloading. Within these dynamic glacial

environments there will also have been a component of horizontal drag (Boulton, 1975) induced by the advancing and retreating ice, an effect which could have been very significant where ice from one advance moved directly over till from a previous one (as at Holwell Hyde) or, alternatively, over a relatively thin sequence of interglacial sediments separating them (as at Hatfield Quarry).

The considerable effects of periglaciation which will have been experienced by these tills, situated as they were on the proximal fringes of subsequent Anglian, Wolstonian and Devensian ice sheets, also must not be overlooked. West (1968), reported in Sparks and West (1972, page 115), shows the effects of prolonged periglaciation (ice wedges, stone polygons and stripes) in the superficial deposits along the south coast of England at least 100 km distance from the inferred margin of the Anglian ice sheet and in excess of 500 km from that of the Devensian, (Fig. 2.1). These authors (op cit, page 114) also state "Chalk and chalky drift are among the most frost-susceptible materials exposed at the surface in Britain."

In addition, the effects of permafrost in areas adjacent to large ice masses can extend to considerable depths. Washburn (1973), quoting Grave (1968) reports permafrost 1400 m thick in the Upper Markha River in Siberia; thicknesses up to 610 m at Prudhoe Bay, Alaska (Stovely in Lachenbruch, 1970) have also been reported. Stearnes (1966) also shows values in excess of 600 m in Nordvik, USSR . Assuming, therefore, that considerable thicknesses of post-Anglian sediments have not been removed by erosion from above those tills presently exposed at the highest altitudinal elevation in the Vale, then the altitudinally lowest tills will have been positioned only 15 - 20 m below the ground surface at that time. That they were periodically frozen is, therefore, without doubt.

The effects of diurnal and seasonal freeze-thaw in the topmost layers of these sediments will also have been evident. Periglacial solifluction of water laden soils on relatively shallow slopes during the Devensian, for example, was probably far more extensive in England than is generally realised, (Jones and Derbyshire, 1983).

Post-glacial (= Holocene) changes experienced in the tills during the last 10,000 years are also likely to have been significant. The oxidation and partial decalcification shown in the Ware Till, for example, is most probably a product of this time. Eyles and Sladen (1981) describe an 8 m deep weathering (i.e. decalcification) profile

which has developed in a till of assumed Devensian age in Northumberland. Based on their own extensive observations of this soil, the authors concur with the general opinion of Madgett and Catt (1978) that decalcification of till is likely to be initiated by the bacterial oxidation of finely disseminated pyrite present in the original sediment with sulphuric acid as a by-product. The rate at which this effect ensues will also be accelerated by the imposition of a climatic control based on a large summer soil moisture deficit which will allow seasonal soil cracking to promote oxidation, (Johnson, 1969).

The tills which have been described from the Vale of St. Albans, in common with other tills of similar age, therefore represent the end products of a long and complex post-depositional history which has been brought about primarily by the fluctuating climatic regime of the Pleistocene. The various processes which have been noted: the effects of repeated ice loading and unloading, along with the resultant consolidation and swelling; the severe effects of a deeply penetrating permafrost and freeze-thaw on soil structure; the unknown effects of inter- and post-glacial soil desiccation, must all have necessarily greatly affected and changed the physical nature of these soils.

Even the post-glacial period of relative climatic stability characterising the last 10,000 years has resulted in landsurface and subsurface weathering and oxidation processes which have probably significantly altered the chemical composition of these tills. Whilst it is not known with certainty either the age or the precise mechanism of formation of the carbonate cement present in at least one of these tills, and the evidence for which has been presented and discussed in 8.7 , it is nevertheless another manifestation of the varied and complex legacy imposed on these soils by their environment.

9.3 An overview of the engineering properties of the tills.

The results of the field and laboratory investigations on the tills have identified certain key points which are summarised below:

1. The natural water contents, Atterberg limits and activity of the soils are consistent with those expected for lodgement tills. The removal of the colloidally inactive carbonate component produces a soil with an activity comparable to those of certain Jurassic mudrocks, the demonstrable source materials for the tills.

2. The particle size characteristics of the five graded tills show

surprisingly little variation. A more sensitive treatment of particle size data using the Modified Wentworth (phi) method could be helpful in identifying the degree of modality in the grading and could also be used as the basis for distinguishing between different tills.

The percentage clay content determined from sedimentation testing shows these to be clay matrix dominant tills.

The distribution of chalk in considerable quantity in the coarse and fine fraction is a particularly distinguishing feature of these tills. The presence of 'nodular' chalk, observed by others in certain carbonate cemented soils, together with the other evidence, reinforces the view that a carbonate, possibly calcitic, cement is present in the undisturbed tills.

3. An examination of the mechanical properties of the screened and reconstituted tills is, it is suggested, a very useful way of observing the fundamental behaviour of the basic engineering material and against which the effects of sampling, soil fabric, previous stress history, cementation, etc... can be quantified. Comparative one-dimensional testing of overconsolidated reconstituted and undisturbed till has shown the following :

(i) The compression indices of the chalky reconstituted soils are up to 1·5 times those of the undisturbed soils in their normally compressed states. The compression index of the naturally decalcified reconstituted soil, however, has the same value as this till in its undisturbed state.

(ii) Preconsolidation pressures for the undisturbed soils indicated by the method of Casagrande (1936) which are of the order of 800 kPa, underpredict p_c' based on estimates ($\simeq$ 2000 kPa) of probable ice thicknesses in the Vale using the alternative criteria of till altitude and ice sheet surface topography. In view of the long and complex post-depositional history of the tills, this discrepancy is perhaps not surprising and indeed ought to be expected.

(iii) The permeability of the undisturbed soil is greater than that of the reconstituted soil at the same overconsolidation ratio; the difference increases with increasing Ro.

(iv) The vertical and horizontal drainage oedometer tests on undisturbed till indicate that there is no significant difference in calculated values for k_v , k_h .

(v) An horizontal permeability which is dependent on drainage through the undisturbed till relative to the established clast fabric has not been demonstrated. It has been indicated that the permeability of these clayey tills is more likely to be governed by the nature of their matrix, rather than by any preferred geometrical arrangement of the contained clasts.

(vi) A method based on the findings of Brooker and Ireland whereby the ratio σ'_h / σ'_v is inferred from plasticity data during one-dimensional unloading of the reconstituted and undisturbed tills has been examined. The interpretation of the results of oedometer tests on kaolin and reconstituted London Clay in this manner has confirmed the validity of the approach, thus enabling the soil constants λ, κ, N_o, to be evaluated for the tills in this type of test.

(vii) An alternative way of graphically demonstrating the variations in soil stiffness during compression, unloading and recompression is suggested. Graphs of λ / κ : Ro are shown for the reconstituted and undisturbed tills and, whilst the amount of data are limited, a relationship between increasing (λ / κ) maximum with increasing PI is shown for these and other soils which have also been tested.

4. The isotropic compression testing of reconstituted tills HH(a), HH(b), has shown a very close agreement between λ isotropic and λ oedometer for these materials. The same tests on the undisturbed tills, whilst showing a reasonable consistency with oedometer κ, N_o (= V_o isotropic), did not show the same measure of agreement in this (λU) respect due, it is thought, to not having satisfactorily isotropically normally consolidated these heavily overconsolidated sediments even at the highest isotropic stresses which were possible.

5. Values for c_u LL $\simeq$ 1·5 kPa, c_u PL $\simeq$ 75 kPa, are indicated for the reconstituted (< 0·425mm) tills. Estimates of undrained shear strength for undisturbed till HH(a), assuming a relationship of the form :

$$c_u = 75 \exp (-3{\cdot}91 \text{ LI}) \text{ kPa}$$

for the reconstituted soil give, not unnaturally, lower strengths than those obtained from in situ shear vane tests in this till. However, it is suggested that an expression of the form shown above is more likely

to satisfactorily predict the remoulded strength of the natural soil. A far better agreement between measured and predicted peak undrained in situ shear strength is obtained by using measured values for the soil constants M, Γ', from consolidated undrained triaxial tests on the undisturbed soil in conjunction with λU (oedometer) and an appropriate volumetric parameter.

6. The range of measured values for $c_u p/c_u r$ (3·72 – 5·78) indicates a medium to sensitive nature for these soils, a feature not usually characteristic of tills. This degree of 'sensitivity' is thought to result from the breakdown of a cementitious (carbonate) bond during shearing.

7. Mohr – Coulomb peak strength parameters obtained from the CU triaxial tests on reconstituted (R) and undisturbed (U) till HH(a) are $c'R = 25$ kPa, $c'U = 75$ kPa; $\phi'R = \phi'U = 20°$.

8. Critical state ultimate strength parameters obtained from the CU triaxial tests are $MR = 0·8$, $MU = 0·89$; $\Gamma'R = 1·876$, $\Gamma'U = 1·763$.

9. Stress paths normalised with respect to p'_e demonstrate the existence of both Roscoe and Hvorslev state boundary surfaces for the normally consolidated and overconsolidated samples respectively. A no tension cut-off ($q' = 3p'$) limits the behaviour of the most heavily overconsolidated samples. The geometry of the Hvorslev surfaces indicate $hR = 0·5$, $hU = 0·575$; $gR = 0·24$, $gU = 0·36$.

10. Good agreement exists between predicted and measured values of ultimate stress q'_u at $Ro = 1$ for both the reconstituted and undisturbed till; however, predictions of peak stress q' for the overconsolidated samples consistently underestimate the measured values.

11. The nature of the $V\lambda : q'/p'$ normalised stress paths for the undisturbed till suggests a different behaviour pattern for those samples which were initially isotropically consolidated to $\sigma'_r \lesssim$ 800 kPa. These (Type I) samples are both stronger and stiffer than Type II (initial $\sigma'_r \gtrsim$ 1000 kPa) and demonstrate larger values for (σ'_a/σ'_r) maximum at the same Ro.

12. An examination of the measured rates of pore pressure changes occurring during the undrained compression of till HH(a) indicate that samples are moving towards the critical state line at rates corresponding to their distance from it at failure. Testing which is carried out slowly enough will permit the plotting of complete pore

pressure paths, and on which may be superimposed contours of the principal effective stress ratio (σ'_a / σ'_r) maximum (or any arbitrary proportion of it).

13. Values for the pore pressure parameter A_f calculated from the tests show a pattern consistent with expectations, (ie. reducing A_f with increasing Ro). The equivalent critical state parameter $A_{c.s.}$ overestimates the size of the (negative) pore pressure response at the largest overconsolidation ratios in both reconstituted and undisturbed tills.

14. The undisturbed till has a higher undrained modulus E_u than the reconstituted till at the same stress level. Apparently large variations in measured E_u for all the samples can be accounted for by normalising E_u with respect to the effective isotropic stress at which the sample is initially brought to equilibrium. The normalised parameter E_u / σ'_r increases with overconsolidation ratio for these soils, but is largest in the undisturbed till.

15. Evidence is presented from the results of the mineralogical, grading, oedometer and strength tests carried out on the tills that suggests a carbonate cement is present in these chalky soils. Its precise nature and form have not been examined in detail although its effects can be observed by comparing the engineering properties of these soils with those of a naturally decalcified horizon of the Ware Till.

9.4 An overview of the field and laboratory methods used in the sampling and testing of the tills.

1. It has been shown that, with care, it is possible to take good quality undisturbed samples in these tills for 38mm triaxial and oedometer testing purposes. By extruding all triaxial samples from their sampling tubes whilst still on site and rejecting those which had obviously been disturbed in the process of sampling, an important monitoring procedure was introduced at an early stage of the testing. Subsequent care in the transportation, storage and testing of these undisturbed samples has produced, it is felt, meaningful and realistic data which hopefully reflect the behaviour of the undisturbed soil. The sampling procedures which have been described are particularly suited to clay rich tills of the type found in the Vale of St. Albans; alternative sampling techniques will almost certainly be required in

the more granular, clast dominant types of till.

2. Although being very time consuming, it is nevertheless considered important to remove the larger pieces of chalk when preparing the soil in the laboratory for Atterberg limit testing. Their inclusion by crushing and grinding into the $<$ 0·425mm fraction will produce a soil with a disproportionately high percentage of colloidally inactive material which will be reflected in the low values for LL , PL obtained.

3. The procedures described in BS 1377 : 1975 for the mechanical grading and fine sediment analysis of tills are not entirely adequate. These are difficult materials to grade as they require a lengthy pretreatment process to deflocculate and disperse the clay prior to washing and sieving the coarse fractions.

4. The method of applying a back pressure through the pore fluid of the undisturbed till, whilst reasonably satisfactory, requires further investigation. For example, consideration could be given to achieving full back saturation by the application of small increments of pressure through a non-return valve positioned along the drainage line. In this way the smallest possible difference between the chamber pressure and the pore fluid could be maintained without the fear of reverse drainage occurring. This technique would also guarantee that the minimum permissable back pressure required to ensure full saturation could be confidently used; these minimum pressures may, however, be surprisingly large.

5. Higher pressure soil triaxial equipment than is presently available is needed if the isotropic normal compression characteristics of heavily overconsolidated tills are to be investigated. Considerable modifications were required to existing equipment (including the manufacturing of a new high pressure Nylatron triaxial chamber) before the undisturbed tills could be consolidated over a range of (effective) pressures up to 2000 kPa. High pressure air regulating valves, Budenberg gauges and pore pressure transducers are also necessary. This is considered an important aspect of any future work in this area.

6. Rates of application of axial stress in consolidated undrained triaxial tests are too fast. If a good definition of the initial portion of a stress path is required, then the testing rate should be very slow, and particularly with heavily overconsolidated samples which attain maximum (σ'_a / σ'_r) at very small values of axial strain.

Corrigendum.

In list of references pp. 386 - 405, page 391 should read 392, and vice-versa.

REFERENCES.

AARIO, R. (1971). Consolidation of Finnish sediments by loading ice sheets. Bulletin of the Geological Society of Finland 43 : 55 - 65.

ALPAN, I. (1967). The empirical evaluation of the coefficients K_0 and K_{OR} . Soils and Foundations 7 (1) : 31 - 40.

ANDERSON, W.F. (1974). The use of multistage triaxial tests to find the undrained strength parameters of stony boulder clay. Proceedings of the Institution of Civil Engineers 57 (2) (Technical Note 89) : 367 - 372.

ANDERSON, W.F. (1983). Foundation engineering in glaciated terrain. In : Glacial geology, ed. by N. Eyles. (Oxford : Pergamon).

ANDERSON, W.F. and McKINLAY, D.G. (1975). Tests to find the modulus of deformation of till. In : SYMPOSIUM ON THE ENGINEERING BEHAVIOUR OF GLACIAL MATERIALS. Proceedings.(Revised and reprinted edition : Geo Abstacts, Norwich, 1978). pp. 165 - 178.

ANDREWS, J.T. (1971). Techniques of till fabric analysis. Technical Bulletin of the British Geomorphological Research Group 6 .

ANDREWS, J.T. and SHIMIZU, K. (1966). Three-dimensional vector technique for analysing till fabrics : discussion and FORTRAN program. Geographical Bulletin 8 : 151 - 165.

ANDREWS, J.T. and SMITHSON, B.B. (1966). Till fabrics of cross-valley moraines of Baffin Island. Bulletin of the Geological Society of America 77 : 271 - 290.

ANDREWS, J.T. and KING, C.A.M. (1968). Comparative till fabrics and till fabric variability in a till sheet and a drumlin : a small scale study. Proceedings of the Yorkshire Geological Society 36 : 435 - 461.

ATKINSON, J.H. (1981). Foundations and slopes. (London : McGraw - Hill).

ATKINSON, J.H. (1984a). Rate of loading in drained and undrained stress path and triaxial tests. Research Report GE/84/1 , Geotechnical Engineering Research Centre, The City University.

ATKINSON, J.H. (1984b). Basic properties of soils. In : Ground engineers reference book, ed. by F.G. Bell . (To be published).

ATKINSON, J.H. and BRANSBY, P.L. (1978). The mechanics of soils. (London : McGraw - Hill).

AVERY, B.W., CATT, J.A. and CHESHIRE, D.A. (1982). Northaw Great Wood. In : The diversion of the Thames, ed. by J. Rose. Field guide of the Quaternary Research Association : 96 - 101.

BANHAM, P.H. (1971). Pleistocene beds at Corton, Suffolk. Geological Magazine 108 : 281 - 285.

BARDEN, L. (1965). Consolidation of compacted and unsaturated clay. Geotechnique 15 (3): 267 - 286.

BARDEN, L. and McDERMOTT, J.W. (1965). The use of free ends in the triaxial testing of soils. Journal of the Soil Mechanics and Foundations Division, ASCE 91 (SM6).

BELL, D. (1888). On some boulders near Arden, Lochlomond. Transactions of the Geological Society of Glasgow 8 (2) : 254 - 261.

BENEDICT, J.B. (1968). Microfabric of patterned ground. Arctic and Alpine Research 1 (1) : 45 - 48.

BERNELL, L. (1957). Properties of moraines. In : INTERNATIONAL CONFERENCE ON SOIL MECHANICS AND FOUNDATION ENGINEERING, 4th, Proceedings. Vol. 2 , pp. 286 - 290.

BISHOP, A.W. (1954). The use of pore-pressure coefficients in practice. Geotechnique 4 : 148 - 152.

BISHOP, A.W. (1967). Progressive failure with special reference to the mechanism causing it. In : GEOTECHNICAL CONFERENCE, OSLO, Proceedings. pp. 142 - 150.

BISHOP, A.W. and GREEN, G.E. (1965). The influence of end restraint on the compression strength of a cohesionless soil. Geotechnique 15 (3): 243 - 266.

BISHOP, A.W., GREEN, G.E., GARGA, V.K., ANDERSON, A. and BROWN, J.D. (1971). A new ring shear apparatus and its application to the measurement of residual strength. Geotechnique 21 : 273 - 328.

BISHOP, A.W. and HENKEL, D.J. (1976). The measurement of soil properties in the triaxial test. 2nd Edition. (London : Arnold).

BOULTON, G.S. (1970). The deposition of subglacial and meltout tills at the margins of certain Svalbord glaciers. Journal of Glaciology 9 : 213 - 245.

BOULTON, G.S. (1972). Modern Arctic glaciers as depositional models for former ice sheets. Journal of the Geological Society of London 128 : 361 - 393.

BOULTON, G.S. (1976a). A genetic classification of tills and criteria for distinguishing tills of different origin. Geografia 12 : 65 - 80.

BOULTON, G.S. (1976b). The development of geotechnical properties in glacial tills. In : Glacial till , ed. by R.F. Legget. The Royal Society of Canada Special Publications, No. 12.

BOULTON, G.S. and DENT, D.L. (1974). The nature and rates of post - depositional changes in recently deposited till from south-east Iceland. Geografiska Annaler 56 : 121 - 134.

BOULTON, G.S., DENT, D.L. and MORRIS, E.M. (1974). Subglacial shearing and crushing and the role of water pressures in tills from south-east Iceland. Geografiska Annaler 56 : 135 - 145.

BOULTON, G.S. and PAUL, M.A. (1976). The influence of genetic processes on some geotechnical properties of glacial tills. Quarterly Journal of Engineering Geology 9 (3) : 159 - 194.

BOULTON, G.S., JONES, A.S., CLAYTON, K.M. and KENNING, M.J. (1978). A British ice sheet model and patterns of glacial erosion and deposition in Britain. In : British Quaternary Studies, ed. by F.W. Shotton. (Oxford : Clarendon Press).

BOWEN, D.Q. (1981). Quaternary Geology. A stratigraphic framework for multidisciplinary work. (Oxford : Pergamon Press).

BRITISH STANDARDS INSTITUTION (1975). Methods of test for soils for civil engineering purposes. BS1377. HMSO. London.

BRITISH STANDARDS INSTITUTION (1981). Code of Practice for Site Investigation. BS5930. HMSO. London.

BROOKER, E.W. and IRELAND, H.O. (1965). Earth pressures at rest related to stress history. Canadian Geotechnical Journal 2 (1) : 1 - 15.

BUTLER, F.G. (1974). Heavily overconsolidated clays. Review Paper to Session III. In : CONFERENCE ON THE SETTLEMENT OF STRUCTURES, Cambridge, April 1974. Proceedings. pp. 531 -578.

CASAGRANDE, A. (1936). The determination of the pre-consolidation load and its practical significance. In : INTERNATIONAL CONFERENCE ON SOIL MECHANICS AND FOUNDATION ENGINEERING, 1st , Proceedings. Vol. 3 .

CASAGRANDE, A. (1958). Notes on the design of the liquid limit device. Geotechnique 8 (2) : 84 - 91.

CATT, J.A. (1980). Soils and Quaternary geology in Britain. Journal of Soil Science 30 : 607 - 642.

CATT, J.A. (1981). The Quaternary history of the Hertfordshire area. Transactions of the Hertfordshire Natural History Society 28 (4) : 27 - 53.

CHANDLER, R.J. (1973). A study of structural discontinuities in stiff clays using a polarising microscope. In : INTERNATIONAL SYMPOSIUM ON SOIL STRUCTURE, Gothenburg, 1973 . Proceedings. pp. 78 - 85.

CHESHIRE, D.A. (1981). A contribution towards a glacial stratigraphy of the Lower Lee Valley, and implications for the Anglian Thames. Quaternary Studies 1 : 27 - 69.

CHESHIRE, D.A. (1983). Till lithology in Hertfordshire and West Essex. In : Diversion of the Thames, ed. by J. Rose. Field guide of the Quaternary Research Association : 50 - 59.

CHRISTIAN, C.S. and STEWART, G.A. (1957). Survey of Katherine - Darwin area. CSIRO Land Resource Series 1 . Melbourne.

CHRISTIAN, C.S. and STEWART, G.A. (1968). Methodology of integrated surveys. Natural Resource Research, UNESCO 6 : 233 - 280.

CLAYTON, C.R.I. (1983). The influence of diagenesis on some index properties of Chalk in England. Geotechnique 33 (3) : 225 - 241.

CLAYTON, K.M. and BROWN, J.C. (1958). The glacial deposits around Hertford. Proceedings of the Geologists Association 69 : 103 - 119.

COCKSEDGE, J.E. (1983). Road construction in glaciated terrain. In : Glacial geology, ed. by N. Eyles. (Oxford : Pergamon Press).

COWAN, W.R. (1968). Ribbed moraine : till fabric analysis and origin. Canadian Journal of Earth Sciences 5 : 1145 - 1160.

COX, F.C. (1981). The 'Gipping Till' revisited. In : The Quaternary in Britain, ed. by J. Neale and J. Flenley. (Oxford : Pergamon Press).

CRATCHLEY, C.R. and DENNESS, B. (1972). Engineering geology in urban planning with an example from the new city of Milton Keynes. In : International Geological Congress , 24th , Montreal , 1972. Proceedings. 13 : 13 - 22.

CRAWFORD, C.B. and BURN, K.N. (1962). Settlement studies on the Mt. Sinai Hospital, Toronto. Engineering Journal, Dec.: 31 - 37.

CRIPPS, J.C. and TAYLOR, R.K.T. (1981). The engineering properties of mudrocks. Quarterly Journal of Engineering Geology 14 : 325 - 346.

CURRAY, J.R. (1956). The anlysis of two-dimensional orientation data. Journal of Geology 64 : 117 - 131.

De JONG, J. and HARRIS, M.C. (1971). Settlement of two multistorey buildings in Edmonton. Canadian Geotechnical Journal 8 : 217 - 235.

DENNESS, B. (1974). Engineering aspects of the chalky boulder clay at the new town of Milton Keynes in Buckinghamshire. Quarterly Journal of Engineering Geology 7 (3) : 297 - 309.

DERBYSHIRE, E. (1975). Distribution of glacial soils in Great Britain. In : SYMPOSIUM ON THE ENGINEERING BEHAVIOUR OF GLACIAL MATERIALS, Proceedings. (Revised and reprinted edition : Geo Abstracts, Norwich, 1978). pp. 6 - 17.

DERBYSHIRE, E., McGOWN, A. and RADWAN, A.M. (1976). 'Total' fabric of some till landforms. Earth Surface Processes 1 : 25 -36.

DERBYSHIRE, E. and JONES, P.F. (1980). Systematic fissuring of a matrix-dominated lodgement till at Church Wilne, Derbyshire, England. Geological Magazine 117 (3) : 243 - 254.

DESNOYERS, J. (1829). Ann. Sci. Nat. 16 : 171 - 214, 402 - 491.

DOEGLAS, D.J. (1968). Grain size indices, classification and environment. Sedimentology 10 : 81 - 82.

DREIMANIS, A. (1980). Tills : their origin and properties. In : Glacial till, ed. by R.F. Legget. The Royal Society of Canada Special Publications, No. 12.

DREIMANIS, A. and VAGNERS, U.J. (1965). Till-bedrock lithologic relationship. In : CONGRESS OF THE INTERNATIONAL UNION FOR QUATERNARY RESEARCH (INQUA) , 7th , 1965 , Boulder, USA, Abstracts, General Sessions. pp. 110 - 111.

DREIMANIS, A. and VAGNERS, U.J. (1971). Bimodal distribution of rock and mineral fragments in basal till. In : Till : a symposium, ed. by R.P. Goldthwait (University of Ohio Press).

DUNCAN, J.M. and DUNLOP, P. (1968). Significance of cap and base restraint. Journal of the Soil Mechanics and Foundations Division, ASCE 94 (SMI) : 271 - 290.

GEIKIE, A. (1863). On the phenomena of the glacial drift of Scotland. Transactions of the Geological Society of Glasgow 1 (2) : 190.

GENS, A. (1982). Stress-strain and strength characteristics of a low plasticity clay. Ph.D. thesis : University of London.

GIBBARD, P.L. (1974). Pleistocene stratigraphy and vegetational history of Hertfordshire. Ph.D. thesis : University of Cambridge.

GIBBARD, P.L. (1977). Pleistocene history of the Vale of St. Albans. Philosophical Transactions of the Royal Society of London 280 (B975) : 445 - 483.

GIBBARD, P.L. (1983). The Middle Thames Region : Slade Oak Lane. In : Diversion of the Thames , ed. by J. Rose. Field guide of the Quaternary Research Association : 85 - 91.

GIBBARD, P.L. and CHESHIRE, D.A. (1983). Hatfield Polytechnic (Roe Hyde Pit). In : Diversion of the Thames, ed. by J. Rose. Field guide of the Quaternary Research Association : 110 - 119.

GLEN, J.W., DONNER, J.J. and WEST, R.G. (1957). On the mechanism by which stones become orientated. American Journal of Science 255 : 194 - 205.

GOODWIN, H. (1978). Quaternary history of the British flora. In : British Quaternary Studies, ed. by F.W. Shotton. (Oxford : Clarendon Press).

GOLDTHWAITE, L. (1948). Glacial till in New Hampshire. Report of the New Hampshire State Planning and Development Commission , 1948 .

GRAVE, N.A. (1968). Merzlye tolshchi zemli. Priroda 1 : 46 - 53.

GREGORY, J.W. (1894). The evolution of the Thames. Nat. Science 5 .

GREEN, C.P. and McGREGOR, D.F.M. (1978). Pleistocene gravel trains of the River Thames. Proceedings of the Geologists Association 89 (2) : 143 - 156.

GRIFFITH, J.C. and ONDRICK, C.W. (1968). Sampling a geological population. Kansas State Geological Survey, Computer Contribution. Vol. 30 .

GRISAK, G.E., CHERRY, J.A., VONHOF, J.A. and BLUMELE, J.P. (1976). Hydrogeologic and hydrochemical properties of fractured till in the Interior Plains Region. In : Glacial till , ed. by R.F, Legget. The Royal Society of Canada Special Publications , No. 12 .

EL - GHAMRAWY, M.K. (1978). A sandy clay till - some properties measured during consolidation and shear. Ph.D. thesis : University of London.

ELSON, J.A. (1961). The geology of tills. In : CANADIAN SOIL MECHANICS CONFERENCE , 14th , Ottawa , 1961. Proceedings. National Research Council Technical Memorandum No. 69. pp. 5 - 17.

EYLES, N. (1983). Glacial geology : a landsystems approach. In : Glacial geology , ed. by N. Eyles. (Oxford : Pergamon Press).

EYLES, N. and SLADEN, J.A. (1981). Stratigraphy and geotechnical properties of weathered lodgement till in Northumberland, England. Quarterly Journal of Engineering Geology 14 (2) : 129 - 141.

EYLES, N., DEARMAN, W.R. and DOUGLAS, T.D. (1983). The distribution of glacial landsystems in Britain and North America. In : Glacial geology , ed. by N. Eyles. (Oxford : Pergamon Press).

FLACH, K.W., NETTLETON, W.D., GILE, L.H. and CADY, J.G. (1969). Pedocementation : induration by silica, carbonates and sesquioxides in the Quaternary. Soil Science 107 (6) : 442 - 453.

FOOKES, P.G. (1965). Orientation of fissures in stiff overconsolidated clay of the Siwalik System. Geotechnique 15 : 195 - 206.

FOOKES, P.G. and WILSON, D.D. (1966). The geometry of discontinuities and slope failures in Siwalik clay. Geotechnique 16 (4) : 305 - 320.

FOOKES, P.G. and BEST, R. (1969). Consolidation characteristics of some Pleistocene periglacial metastable soils of East Kent. Quarterly Journal of Engineering Geology 2 : 103 - 128.

FOOKES, P.G. and DENNESS, B. (1969). Observational studies on fissure patterns in Cretaceous sediments of South-East England. Geotechnique 19 (4) : 453 - 477.

FOOKES, P.G., GORDON, D.L. and HIGGINBOTTOM, I.E. (1975). Glacial landforms, their deposits and engineering characteristics. In : SYMPOSIUM ON THE ENGINEERING BEHAVIOUR OF GLACIAL MATERIALS. Proceedings. (Revised and reprinted edition : Geo Abstracts, Norwich, 1978). pp. 18 - 51.

GEER,M. and YANCEY,H.F.(1938). Expression and interpretation of the size composition of coal. Transactions of the American Institution of Mining Engineers 130 : 250 - 269.

GROMME, C.S. and HAY, R.L. (1971). Geomagnetic polarity epochs : age and duration of the Olduvai normal polarity event. Earth planet. Sci. Lett. 10 : 179 - 185.

HAQ, B.U., BERGGREN, W.A. and COUVERING, J.A. van (1977). Corrected age of the Pliocene boundary. Nature 269 : 483 - 488.

HARA, N. and MIDGLEY, H.G. (1980). The determination of crystallinity of tobermorite in autoclaved products. Cement and Concrete Research 10 : 213 - 221.

HARE, F.K. (1947). The geomorphology of a part of the Middle Thames. Proceedings of the Geologists Association 58 : 294 - 339.

HARRIS, S.A. (1969). The meaning of till fabrics. Canadian Geographer 8 : 317 - 337.

HEAD, K.H. (1980). Manual of soil laboratory testing, Vol. 1. (London : Pentech Press).

HENKEL, D.J. (1956). The effect of overconsolidation on the behaviour of clays during shear. Geotechnique 6 : 139 - 150.

HEY, R.W. (1965). Highly quartzose gravels in the London Basin. Proceedings of the Geologists Association 13 : 403 - 420.

HIGHT, D.W. and GENS, A. (1979). Discussion In : EUROPEAN CONFERENCE ON SOIL MECHANICS AND FOUNDATION ENGINEERING ON DESIGN PARAMETERS FOR STIFF CLAYS, 7th , Brighton. Proceedings. Vol.4 , pp. 128 - 129.

HILL, A.R. (1968). An experimental test of the field technique of till macrofabric analysis. Transactions of the Institute of British Geographers 45 : 93 - 106.

HIND, H.Y. (1859). A preliminary and general report on the Assiniboine and Saskatchewan exploring expedition. Canada, Legislative Assembly Journal 19, Appendix 36 In : Elson, J.A., Early Discoverers XXIII. Till-stone orientation : Henry Youle Hind (1823 - 1908), Journal of Glaciology 6 : 303 - 306.

HOLMES, C.D. (1941). Till fabric. Bulletin of the Geological Society of America 52 : 1299 - 1354.

HUGHES, T.McK. (1868). On the two plains of Hertfordshire and their gravels. Quarterly Journal of the Geological Society of London 24 : 283.

IDEL, K.H., MUHS, H. and VON SOOS, P. (1969). Proposals for quality classes in soil sampling and the importance of boring methods and sampling equipment. In : INTERNATIONAL CONFERENCE ON SOIL MECHANICS AND FOUNDATION ENGINEERING, 7th , Mexico , 1969. Proceedings. Speciality session No. 1.

INGOLD, T.S. (1975). Variation of effective residual angle of shearing with plasticity index. In : SYMPOSIUM ON THE ENGINEERING BEHAVIOUR OF GLACIAL MATERIALS. Proceedings. (Revised and reprinted edition : Geo Abstracts, Norwich, 1978). pp. 221 - 227.

JACOBSEN, M. (1970). Strength and deformation properties of preconsolidated moraine clay. Dansk Geoteknisk Institut, Bulletin No. 27. pp. 21 - 45.

JAKY, J. (1944). The coefficient of earth pressure at rest. Magyar Mernok es Epitesz Egylet Kozlonye, Oct. 1944 : 355 - 358.

JOHNSON, P.A. (1969). Soils and land use on Chalky Boulder Clay. East Midland Geographer 4 : 447 - 453.

JONES, P.F. and DERBYSHIRE, E. (1983). Late Pleistocene periglacial degradation of lowland Britain : implications for civil engineering. Quarterly Journal of Engineering Geology 16 (3) : 197 - 210.

KARLSTROM, T.N.V. (1952). Improved equipment and techniques for orientation studies of large particles in sediments. Journal of Geology 60 : 489 - 493.

KAZI, A.N. and KNILL, J.L. (1969). The sedimentation and geotechnical properties of the Cromer Till between Happisburgh and Cromer, Norfolk. Quarterly Journal of Engineering Geology 2 : 63 - 86.

KAZI, A.N. and KNILL, J.L. (1973). Fissuring in glacial lake clays and tills on the Norfolk coast, United Kingdom. Engineering Geology 7 : 35 - 48.

KENNEY, T.C. (1967). The influence of mineral composition on the residual strength of natural soils. In : GEOTECHNICAL CONFERENCE, OSLO. Proceedings. pp. 123 - 131.

KIRBY, R.P. (1969). Till fabric analyses from the Lothians, Central Scotland. Geografiska Annaler 51A : 48 - 60.

KLOHN, E.J. (1965). The elastic properties of a dense glacial till deposit. Canadian Geotechnical Journal 11 : 396 - 408.

KOO, Y.C. (1981). Recording and interpreting soil macrofabric data. Discussion. Geotechnique 31 (4) : 577 - 580.

KORINA, N.A. and FAUSTOVA, M.A. (1964). Microfabric of modern and old moraines. In : Soil micromorphology, ed. by A. Jongerius. (Amsterdam : Elsevier).

KRUMBEIN, W.C. (1933). Textural and lithological variations in glacial till. Journal of Geology 41 : 382 - 408.

KRUMBEIN, W.C. (1939). Preferred orientation of pebbles in sedimentary deposits. Journal of Geology 47 : 673 - 706.

KUPSCH, W.O. (1955). Drumlins with jointed boulders near Dollard, Saskatchewan. Bulletin of the Geological Society of America 66 : 327 - 338.

LACHENBRUCH, A.H. (1970). Some estimates of the thermal effects of a heated pipeline in permafrost. U.S. Geological Survey Circular 632.

LEGGET, R.F. (1942). An engineering study of glacial drift for an earth dam, near Fergus, Ontario. Economic Geology 37 (7) : 531 - 556.

LINNELL, K.A. and SHEA, H.F. (1960). Strength and deformation characteristics of various glacial tills in New England. In : RESEARCH CONFERENCE ON SHEAR STRENGTH OF COHESIVE SOILS, University of Colorado, June 1960. Proceedings. American Society of Civil Engineers. pp. 275 - 314.

LLOYD, J.W. (1983). Hydrogeology in glaciated terrains. In : Glacial geology , ed. by N. Eyles. (Oxford : Pergamon Press).

LO, K.Y. (1961). Stress-strain relationship and pore water pressure characteristics of a normally consolidated clay. Norges Geoteknisk Institut, Publication No. 45.

LO, K.Y. (1962). Shear strength properties of a sample of volcanic material of the valley of Mexico. Geotechnique 12 : 303 - 316.

LO, K.Y. (1970). The operational strength of fissured clays. Geotechnique 20 (1) : 57 - 74.

LOISELLE, A.A. and HURTUBISE, J.E. (1980). Properties and behaviour of till as construction material. In : Glacial till, ed. by R.F. Legget. The Royal Society of Canada Special Publications, No. 12.

LOWE, J. and JOHNSON, T.C. (1960). Use of back pressure to increase degree of saturation of triaxial test specimens. In : RESEARCH CONFERENCE ON SHEAR STRENGTH OF COHESIVE SOILS, University of Colorado, June 1960. Proceedings. American Society of Civil Engineers. pp. 819 - 836.

LUPINI, J.F. SKINNER, A.E. and VAUGHAN, P.A. (1981). The drained residual strength of cohesive soils. Geotechnique 31 : 181 - 213.

LUTENEGGER, A.J., KEMMIS, T.J. and HALLBERG, G.R. (1983). Origin and properties of glacial till and diamictons. In : Geological environment and soil properties, ed. by R.N. Young. Special Publication of the American Society of Civil Engineers, Geotechnical Engineering Division.

LYELL, C. (1839). Nouveaux elements de geologie. (Paris).

MADGETT, P.A. and CATT, J.A. (1978). Petrography, stratigraphy and weathering of late Pleistocene tills in East Yorkshire, Lincolnshire and North Norfolk. Proceedings of the Yorkshire Geological Society 42 : 55 - 108.

MARSLAND, A. (1971). The shear strength of stiff fissured clays. In : ROSCOE MEMORIAL SYMPOSIUM, CAMBRIDGE 1971. Proceedings. pp. 59 - 68. (Also Building Research Station Current Paper CP 21/71).

MARSLAND, A. (1975). In situ and laboratory tests on glacial clays at Redcar. In : SYMPOSIUM ON THE ENGINEERING BEHAVIOUR OF GLACIAL MATERIALS. Proceedings. (Revised and reprinted edition : Geo Abstracts, Norwich, 1978). pp. 149 - 164. (Also Building Research Station Current Paper CP 65/76).

MARSLAND, A. (1977). The evaluation of the engineering design parameters for glacial clays. Quarterly Journal of Engineering Geology 10 (1) : 1 - 26. (Also Building Research Station Current Paper CP 19/77).

MARSLAND, A. (1980). The interpretation of in situ tests in glacial clays. In : INTERNATIONAL CONFERENCE ON OFFSHORE SITE INVESTIGATION, London , March 1979 . Proceedings. pp. 218 - 228.

MARSLAND, A. and BUTLER, M.E. (1967). Strength measurements on stiff fissured Barton Clay from Fawley, Hampshire. In : GEOTECHNICAL CONFERENCE, Oslo. Proceedings. pp. 139 - 145.

MARSLAND, A., PRINCE, A. and LOVE, M.A. (1982). The role of soil fabric studies in the evaluation of the engineering parameters of offshore deposits. In : INTERNATIONAL CONFERENCE ON THE BEHAVIOUR OF OFFSHORE STRUCTURES, Houston , June 1972. Proceedings.

MAYNE, P.W. and KULHAWY, F.H. (1982). K_o - OCR relationships in soil. Proceedings of the American Society of Civil Engineers 108 (GT6) : 851 - 872.

McGOWN, A. (1971). The classification for engineering purposes of tills from moraines and associated landforms. Quarterly Journal of Engineering Geology 4 : 115 - 130.

McGOWN, A. and DERBYSHIRE, E. (1974). Technical developments in the study of particulate matter in glacial tills. Journal of Geology 82 : 225 - 236.

McGOWN, A., SALI, A. and RADWAN, A.M. (1974). Fissure patterns and slope failures in boulder clay at Hurlford, Ayrshire. Quarterly Journal of Engineering Geology 7 : 1 - 26.

McGOWN, A., ANDERSON, W.F. and RADWAN, A.M. (1975). Geotechnical properties of the tills in West Central Scotland. In : SYMPOSIUM ON THE ENGINEERING BEHAVIOUR OF GLACIAL MATERIALS. Proceedings. (Revised and reprinted edition : Geo Abstracts, Norwich, 1978). pp. 81 - 91.

McGOWN, A. and DERBYSHIRE, E. (1977). Genetic influences on properties of tills. Quarterly Journal of Engineering Geology 10 : 389 - 410.

McGOWN, A., MARSLAND, A., RADWAN, A.M. and GABR, A.W.A. (1980). Recording and interpreting soil macrofabric data. Geotechnique 30 (4): 417 - 447.

McKINLAY, D.G., TOMLINSON, M.J. and ANDERSON, W.F. (1974). Observations on the undrained strength of a glacial till. Geotechnique 24 (4) : 503 - 516.

McKINLAY, D.G., McGOWN, A., RADWAN, A.M. and HOSSAIN, D. (1975). Representative sampling and testing in fissured lodgement tills. In : SYMPOSIUM ON THE ENGINEERING BEHAVIOUR OF GLACIAL MATERIALS. Proceedings.(Revised and reprinted edition : Geo Abstracts, Norwich, 1978). pp. 129 - 140.

MENZIES, B.K. and MERRIFIELD, C.M. (1980). Measurements of shear stress distribution on the edges of a shear vane blade. Geotechnique 30 : 3 pp. 314 - 318.

MEYERHOF, G.G. (1976). Bearing capacity and settlement of pile foundations. Proceedings of the American Society of Civil Engineers 102 : 197 - 228.

MIDGLEY, H.G. (1976). Quantitative determination of phases in high alumina cement clinkers by X - ray diffraction. Cement and Concrete Research 6 : 217 - 224.

MILLER, H. (1884). On boulder-glaciation. Proceedings of the Royal Physical Society of Edinburgh 8 : 156 - 189.

MILLIGAN, V. (1976). Geotechnical aspects of glacial tills. In : Glacial till , ed. by R.F, Legget. The Royal Society of Canada Special Publications , No. 12.

MITCHELL, G.F., PENNY, L.F., SHOTTON, F.W. and WEST, R.G. (1973). A correlation of Quaternary deposits in the British Isles. Geological Society of London Special Report 4 .

MITCHELL, J.K. (1956). The fabric of natural clay and its relation to engineering properties. Proceedings of the Highways Research Board 35: 693 - 713.

MOFFAT, A.J. and CATT, J.A. (1982). The nature of the pebbly clay drift at Epping Green, south-east Hertfordshire. Transactions of the Hertfordshire Natural History Society 28 (6) : 16 - 24.

MOOS, A. von. (1938). Geotechnische Eigenschaften und Untersuchungs methoden der Lockergesteine. Erdbaukurs der E.T.H. No. 4 (Zurich).

Munsell Soil Colour Charts : 1975 edition.

NADARAJAH, V. (1973). Stress-strain properties of lightly overconsolidated clays. Ph.D. thesis : University of Cambridge.

NORTHEY, R.D. (1950). An experimental study of the structural sensitivity of clays. Ph.D. thesis : University of London.

OLMSTEAD, T.L. (1969). Geological aspects and engineering properties of glacial till in the Puget Lowland, Washington. In : SYMPOSIUM ON ENGINEERING GEOLOGY AND SOILS ENGINEERING , Boise, Idaho. Proceedings. pp. 223 - 233.

OSTRY, R.C. and DEANE, R.E. (1963). Microfabric analyses of till. Bulletin of the Geological Society of America 74 : 165 - 168.

PARRY, R.H.G. (1958). Discussion. Geotechnique 8 : 183 - 186.

PARRY, R.H.G. (1960). Triaxial compression and extension tests on remoulded saturated clay. Geotechnique 10 : 166 - 180.

PENNY, L.F., COOPE, G.R. and CATT, J.A. (1969). Age and insect fauna of the Dimlington silts, East Yorkshire. Nature 224 : 65 - 67.

PETERSON, D.N. (1970). Glaciological studies on the Casement Glacier, south-east Alaska. Report of the Ohio State University Institute of Polar Studies, 36.

POWELL, J.J.M., MARSLAND, A. and AL-KHAFAGI, A.N. (1983). Pressuremeter testing of glacial clay tills. In : INTERNATIONAL SYMPOSIUM ON IN SITU TESTING OF SOILS AND ROCK , Paris. Proceedings. Vol. 2 , pp. 373 - 378.

PREST, V.K. (1961). Geology of the soils of Canada. In : Soils in Canada. The Royal Society of Canada Special Publications , No. 3.

PRESTWICH, J. (1890). On the relation of the Westleton Beds or pebbly sands of Suffolk to those of Norfolk and their extension inland; with some observations on the period of final elevation and denudation of the Weald and of the Thames Valley etc. Quarterly Journal of the Geological Society of London 46 : 120 - 154.

QUIGLEY, R.M. and THOMPSON, C.D. (1966). The fabric of anisotropically consolidated sensitive marine clay. Canadian Geotechnical Journal 3 : 61 - 73.

REBOUL, H. (1833). Geologie de la Periode Quaternaire. (Paris).

RADHAKRISHNA, H.S. and KLYM, T.W. (1974). Geotechnical properties of a very dense till. Canadian Geotechnical Journal 11 : 396 - 408.

RAYLEIGH, Lord (STRUTT, J.W.) (1894). The theory of sound, 2nd Edition, Volume 1 . (New York : Dover Publications).

REICHE, P. (1938). An analysis of cross-lamination : the Coconino sandstone. Journal of Geology 46 : 905 - 932.

REID, C. (1882). The geology of the country around Cromer. Memoir of the Geological Survey of England and Wales.

RICHTER, K. (1932). Die Bewegungsrichtung des Inlandeis reconstruiert aus den Kritzen und Längsachsen der Geschiebe, Zeitschrift Geschiebeforschung 8 : 62 - 66.

RICHTER, K. (1933). Gefüge und Zusammensetzung des norddeutschen Jungmoränengebietes. Abh. geol - paleont. Inst. Greifswald 11 : 1 - 63.

RICHTER, K. (1936). Gefügestudien im Engebrae, Fondalsbrae und ihren Vorlandsedimenten. Zeitschrift Gletscherkunde 24 : 22 - 30.

ROSAUER, E. and FRECHEN, J. (1960). Carbonate concretions in the Karlicher loess profile, Rheinland. Proceedings of the Iowa Academy of Science 67 : 346 - 356.

ROSCOE, K.H., SCHOFIELD, A.N. and WROTH, C.P. (1958). On the yielding of soils. Geotechnique 8 : 22 - 53.

ROSE, J. (1974). Small scale spatial variability of some sedimentary properties of lodgement and slumped till. Proceedings of the Geologists Association 85 : 223 - 237.

ROWE, P.W. (1971). Representative sampling in location quality and size. In : Sampling of soil and rock, ASTM STP 483 , American Society for Testing and Materials. pp. 77 - 108.

ROWE, P.W. (1972). The relevance of soil fabric to site investigation practice. Geotechnique 22 : 195 - 300.

SAADA, A.S. and TOWNSEND, F.C. (1981). State of the art: laboratory strength testing of soils. In : Laboratory shear strength of soil, ed. by R.N. Yong and F.C. Townsend. American Society for Testing and Materials Special Technical Publication 740.

SALTER, A.E. (1905). On the superficial deposits of Central and parts of Southern England. Proceedings of the Geologists Association 19 : 1 - 56.

SAMUELS, S.G. (1950). The effect of base exchange on the engineering properties of soils. Building Research Station Note No. C176.

SANGREY, D.A. (1972a). The causes of natural cementation in sensitive soils. Canadian Geotechnical Journal 9 : 117 - 119.

SANGREY, D.A. (1972b). Naturally cemented sensitive soils. Geotechnique 22 (1) : 139 - 152.

SCHMERTMANN, J.H. (1953). Estimating the true consolidation behaviour of clay from laboratory test results. Proceedings of the American Society of Civil Engineers 79 : Separate No. 311.

SCHMIDT, B. (1966). Earth pressures at rest related to stress history. Discussion. Canadian Geotechnical Journal 3 (4) : 239 - 242.

SCHOFIELD, A.N. and WROTH, C.P. (1968). Critical state soil mechanics. (London : McGraw-Hill).

SCOTT, J.S. (1980). Geology of Canadian tills. In : Glacial till, ed. by R.F. Legget. The Royal Society of Canada Special Publications, No. 12.

SCOTT, J.S. and St. ONGE, D.A. (1969). Guide to the description of till. Geological Survey of Canada. Paper 68 - 6.

SHACKLETON, N.J. and OPDYKE, N.D. (1973). Oxygen isotope and palaeomagnetic stratigraphy of Equatorial Pacific core V28 - 238 : oxygen isotope temperatures and ice volumes on a 10^5 year and 10^6 year scale. Quaternary Research 3 : 39 - 55.

SHEPPS, V.C. (1958). 'Size factors', a means of analysis of data from textural studies of till. Journal of Sedimentary Petrology 28 : 482 - 485.

SHERLOCK, R.L. and NOBLE, A.H. (1912). On the glacial origin of the Clay-with-flints of Buckinghamshire and on a former course of the Thames. Quarterly Journal of the Geological Society of London 68 : 199 - 212.

SHERLOCK, R.L. and POCOCK, R.W. (1924). The geology of the country around Hertford. Memoir of the Geological Survey of the U.K.

SHOTTON, F.W. (1975). Introduction to the Quaternary. In : Ice Ages: Ancient and Modern , ed. by A.E. Wright and F. Moseley. (Liverpool : Seel House Press).

SHOTTON, F.W. (1976). Amplification of the Wolstonian Stage of the British Pleistocene. Geological Magazine 113 : 241 - 250.

SINGH, P.N., TATIOUSSIAN, S.V. and FLAGG, C.G. (1983). A study of the geotechnical properties of Milwaukee area soils. In : Geological environment and soil properties, ed. by R.N. Yong. Special Publication of the American Society of Civil Engineers, Geotechnical Engineering Division.

SITTER, L.U. de. (1964). Structural Geology. (New York : McGraw-Hill).

SKEMPTON, A.W. (1953). The colloidal activity of clays. In : INTERNATIONAL CONFERENCE ON SOIL MECHANICS AND FOUNDATION ENGINEERING, 3rd , Switzerland. Proceedings. Vol. 1 , pp. 57 - 61 .

SKEMPTON, A.W. (1954). The pore pressure coefficients A and B . Geotechnique 4 : 143 - 147.

SKEMPTON, A.W. (1964). Long-term stability of clay slopes. Geotechnique 14 : 77 - 101.

SKEMPTON, A.W. and NORTHEY, R.D. (1952). The sensitivity of clays. Geotechnique 3 : 30 - 53.

SKEMPTON, A.W. and BROWN, J.D. (1961). A landslide in boulder clay at Selset, Yorkshire. Geotechnique 11 : 280 - 293.

SKEMPTON, A.W., SCHUSTER, R.L. and PETLEY, D.J. (1969). Joints and fissures in the London Clay at Wraysbury and Edgware. Geotechnique 19 (2) : 205 - 217.

SLADEN, J.A. and WRIGLEY, W. (1983). Geotechnical properties of lodgement till - a review. In : Glacial geology , ed. by N. Eyles. (Oxford : Pergamon Press).

SMITH, G.N. (1982). Elements of soil mechanics for civil and mining engineers. 5th Edition. (London : Granada).

SODERMAN, L.G., KIM, Y.D. and MILLIGAN, V. (1968). Field and laboratory studies of modulus of elasticity of a clay till. In : SYMPOSIUM ON SOIL PROPERTIES FROM IN SITU MEASUREMENTS. Highways Research Board, National Research Council (Canada), Publication No. 243, pp. 1 - 11.

SOLIMAN, N. (1983). Effect of geologic history on the design parameters of heavily overconsolidated till. In : Geological environments and soil properties , ed. by R.N.Yong. Special Publication of the American Society of Civil Engineers, Geotechnical Engineering Division.

SOLOMON, J.D. (1932). The glacial succession on the North Norfolk coast. Proceedings of the Geologists Association 43 : 241 - 271.

SOMERVILLE, S. (1983). Site investigation procedures and engineering testing of glacial sediments. In : Glacial geology , ed. by N. Eyles. (Oxford : Pergamon Press).

SPARKS, B.W., WEST, R.G., WILLIAMS, R.B.G. and RANSOM, M. (1969). Hoxnian interglacial deposits near Hatfield, Herts. Proceedings of the Geologists Association 80 : 243 - 267.

SPARKS, B.W. and WEST, R.G. (1972). The Ice Age in Britain. (London : Methuen).

STEARNS, S.R. (1966). Permafrost (perennially frozen ground) : U.S. Army Cold Regions Research and Engineering Laboratory , Cold Regions Science and Engineering 1 (A2).

STROUD, M.A. and BUTLER, F.G. (1975). The standard penetration test and the engineering properties of glacial materials. In : SYMPOSIUM ON THE ENGINEERING BEHAVIOUR OF GLACIAL MATERIALS. Proceedings.(Revised and reprinted edition : Geo Abstracts, Norwich, 1978). pp. 117 - 128.

TAMM, O. (1924). Experimental studies on chemical processes in the formation of glacial clays. Sveriges Geologiska Undersokning, Series C, No. 333.

TARBET, M.A. (1973). Geotechnical properties and sedimentation characteristics of tills in south-east Northumberland. Ph.D. thesis: University of Newcastle-Upon-Tyne.

TAYLOR, D.W. (1941). Seventh progress report on shear research to U.S. Engineers. MIT publication, Massachusetts Institute of Technology, Cambridge, Mass.

TERZHAGI, K. (1936). The shearing resistance of saturated soils. In: INTERNATIONAL CONFERENCE ON SOIL MECHANICS, 1st, Harvard, 1936. Proceedings. pp. 54 - 56.

TERZHAGI, K. and PECK, R.B. (1967). Soil mechanics in engineering practice. 2nd. Edition. (New York : Wiley).

THOMASSON, A.J. (1961). Some aspects of the drift deposits and geomorphology of south-east Hertfordshire. Proceedings of the Geologists Association 72 : 415 - 436.

THORBURN, S. and REID, W.W. (1973). Stability of slopes in lodgement till within the Glasgow district. Civil Engineering and Public Works Review, April : 321 - 325.

TOWNSEND, D.L. (1965). Discussion. Canadian Geotechnical Journal 2 (2) : 190 - 193.

TOWNSEND, D.L., SANGREY, D.A. and WALKER, L.K. (1969). The brittle behaviour of naturally cemented soils. In : INTERNATIONAL CONFERENCE ON SOIL MECHANICS AND FOUNDATION ENGINEERING, 7th, Mexico. Proceedings. Vol. 2, pp. 411 - 417.

UPHAM, W. (1891). Criteria of englacial and subglacial drift. American Geologist 8 : 376 - 385.

VAUGHAN, P.R. and WALBANCKE, H.J. (1975). The stability of cut and fill slopes in boulder clay. In : SYMPOSIUM ON THE ENGINEERING BEHAVIOUR OF GLACIAL MATERIALS. Proceedings. (Revised and reprinted edition : Geo Abstracts, Norwich, 1978). pp. 185 - 195.

WARD, W.H., MARSLAND, A. and SAMUELS, S.G. (1965). Properties of the London Clay at the Ashford Common Shaft : in situ and drained strength tests. Geotechnique 15 (4) : 321 - 344.

WASHBURN, A.L. (1973). Periglacial processes and environments. (London : Arnold).

WELTMAN, A.J. and HEALY, P.R. (1978). Piling in 'boulder clay' and other glacial tills. DOE and CIRIA Piling Development Group Report PG5 . (Also PSA Civil Engineering Technical Guide 23).

WEST, R.G. (1956). The Quaternary deposits at Hoxne, Suffolk. Philosophical Transactions of the Royal Society of London. Series B. 239 : 265 - 356.

WEST, R.G. (1963). Problems of the British Quaternary. (Special Lecture, 1962). Proceedings of the Geologists Association 74 : 147 - 186.

WEST, R.G. (1968). Pleistocene geology and biology. (London : Longmans).

WEST, R.G. and DONNER, J.J. (1956). The glaciation of East Anglia and the East Midlands : a differentiation based on stone-orientation measurements of tills. Quarterly Journal of the Geological Society of London 112 : 69 - 91.

WEST, R.G. and WILSON, D.G. (1966). Cromer Forest Series. Nature 209 : 497 - 498.

WHALLEY, W.B. (1975). Abnormally steep slopes on moraines constructed by valley glaciers. In : SYMPOSIUM ON THE ENGINEERING BEHAVIOUR OF GLACIAL MATERIALS. Proceedings. (Revised and reprinted edition : Geo Abstracts, Norwich, 1978). pp. 60 - 74.

WHITAKER, W. (1889). The geology of London and of part of the Thames Valley (Vol. 1). Memoir of the Geological Survey of England and Wales.

WOODWARD, H.B. (1897). The Chalky Boulder Clay and glacial phenomena of the Western-Midland counties of England. Geological Magazine 4 : 485 - 497.

WOOLDRIDGE, S.W. (1938). The glaciation of the London Basin and the evolution of the Lower Thames drainage system. Quarterly Journal of the Geological Society of London 64 : 627 - 664.

WOOLDRIDGE, S.W. (1960). The Pleistocene succession in the London Basin. Proceedings of the Geologists Association 71 : 113 - 129.

WOOLDRIDGE, S.W. and HENDERSON, H.C.K. (1955). Some aspects of the physiography of the eastern part of the London Basin. Transactions of the Institute of British Geographers 21 : 19 - 31.

WOOLDRIDGE, S.W. and LINTON, D.L. (1955). Structure, surface and drainage in south-east England. (London : Philip).

WROTH, C.P. (1979). Correlations of some engineering properties of soils. INTERNATIONAL CONFERENCE ON BEHAVIOUR OF OFFSHORE STRUCTURES, 2nd . Proceedings. Vol. 1 , pp. 121 - 132.

WROTH, C.P. (1981). Critical State Soil Mechanics. Unpublished course notes, University of Oxford Engineering Sciences Department, September 1981.

WROTH, C.P. and WOOD, D.M. (1978). The correlation of index properties with some basic engineering properties of soils. Canadian Geotechnical Journal 15 (2) : 137 - 154.

YOUSSEF, M.S., EL RAMLI, A.H. and EL DEMERY, M. (1965). Relationships between shear strength, consolidation, liquid limit and plastic limit for remoulded clays. In : INTERNATIONAL CONFERENCE ON SOIL MECHANICS AND FOUNDATION ENGINEERING, 6th , Montreal. Proceedings. Vol. 1 , pp. 126 - 129.

Addenda.

EISENSTEIN, Z. and MORRISON, N.A. (1973). Prediction of foundation deformation in Edmonton using an in situ pressure probe. Canadian Geotechnical Journal 10 : 193 - 210.

TURNER, C. (1970). The Middle Pleistocene deposits at Marks Tey, Essex. Philosophical Transactions of the Royal Society of London. B257 : 373 - 440.

TURNER, C. (1975). The correlation and duration of Middle Pleistocene interglacial periods in Northwest Europe. In : After the Australopithecines, ed. by K.W. Butzer and G. Issac. (The Hague : Mouton).

APPENDIX I.

Till fabric instrument : engineering drawings.

Parts List Schedule

Machine: Till Fabric Instrument.

Drg No.	Description	Matl	No off	Supplier
H 273	General Arrangement.			
H 270 /1	Compass Plate	Aluminium	1	
/2	Trowel Holder	Aluminium	1	
/3	Cover	Perspex	1.	
/4	Cover Screw	Brass	1.	
/5	Cover Screw Nut	Brass	1.	
/6	Trowel Plate	Aluminium	1	
/7	Trowel Plate Screws	Brass	2	
/8	Thumb Screw.	Brass	1	
H 271 /1	No. 1. Trowel.	Stainless St	1.	
/2	No. 2. Trowel.	Stainless St	1.	
/3	Screwdriver	Brass/S S	1.	
/4	Washer	Brass	6	
/5	Fork.	Aluminium	1	
/6	Angle Bracket Screw.	Brass	2	
/7	Angle Bracket	Aluminium	1	
/8	Needle Holder	Stainless St	4	
/9	Needle.	Stainless St	4	
/10	Chisel.	Stainless St	1	
H 272 / 1	Needle Holder Bracket	Aluminium	1	
/2	Needle Holder Ferrule	Brass	1	
/3	Needle Ferrule	Brass	1.	
/4	Needle Holder Bracket Screw.	Brass	1	
/5	Sight Glass.	Br/Mirror Gl	1	
/6	Thumb Screw	Brass	1	
S 1.	Suunto Compass Code: KB - 14/360		1	Suunto Instrument Finland.
S 2.	Suunto Clinometer Code: PM - 5/360 PC		1	
S 3.	13 x 35 long Spirit Level.		2	
S 4.	3 ϕ Ball Bearing.		1	
S 5.	Carl Zeiss Measuring Magnifier.		1	Carl Zeiss Jena

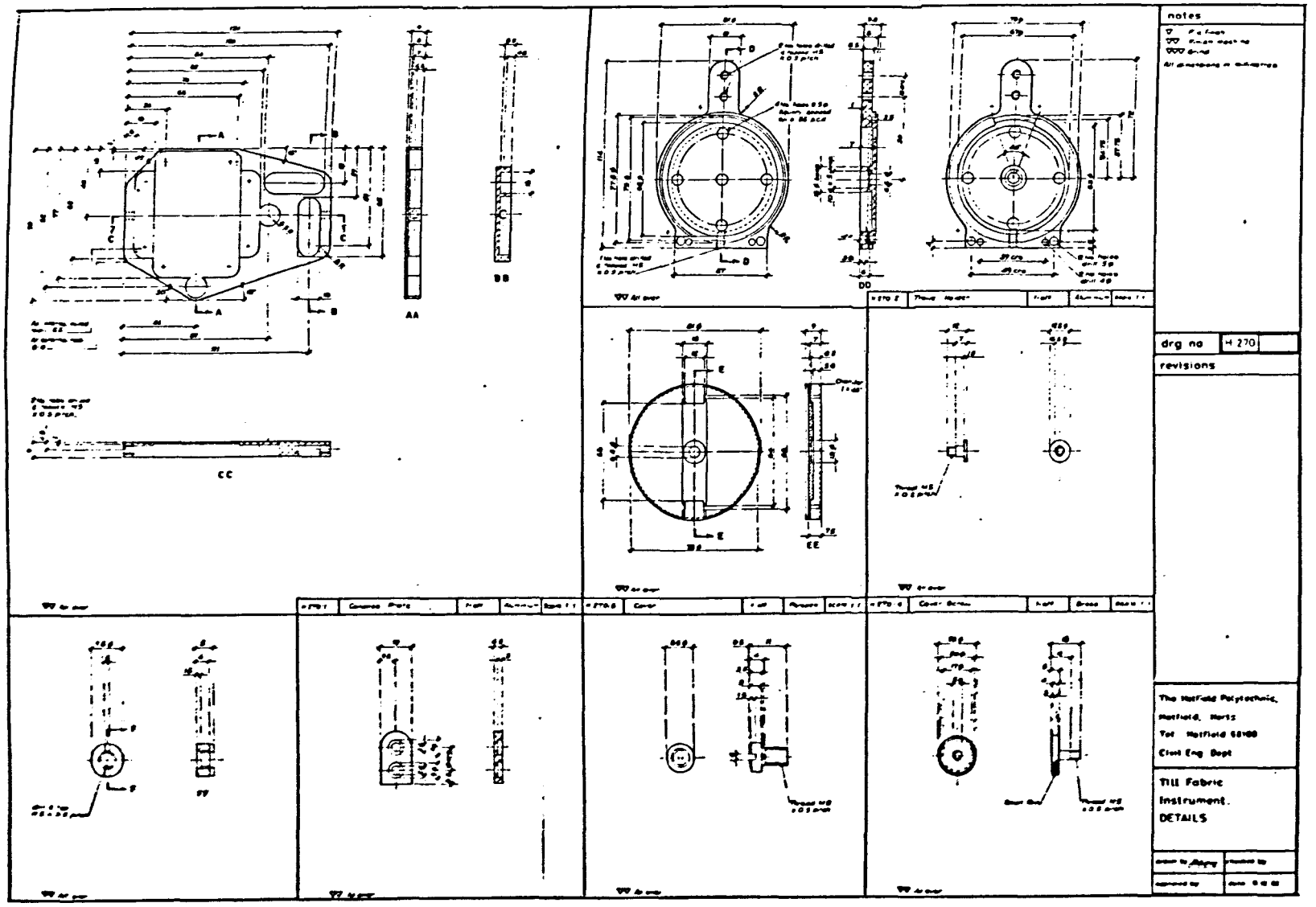
notes
drg no
H 270
revisions
The Hatfield Polytechnic,
Hatfield, Herts
Tel Hatfield 68100
Civil Eng Dept
Till Fabric
Instrument.
DETAILS
AA
BB
CC
DD
EE

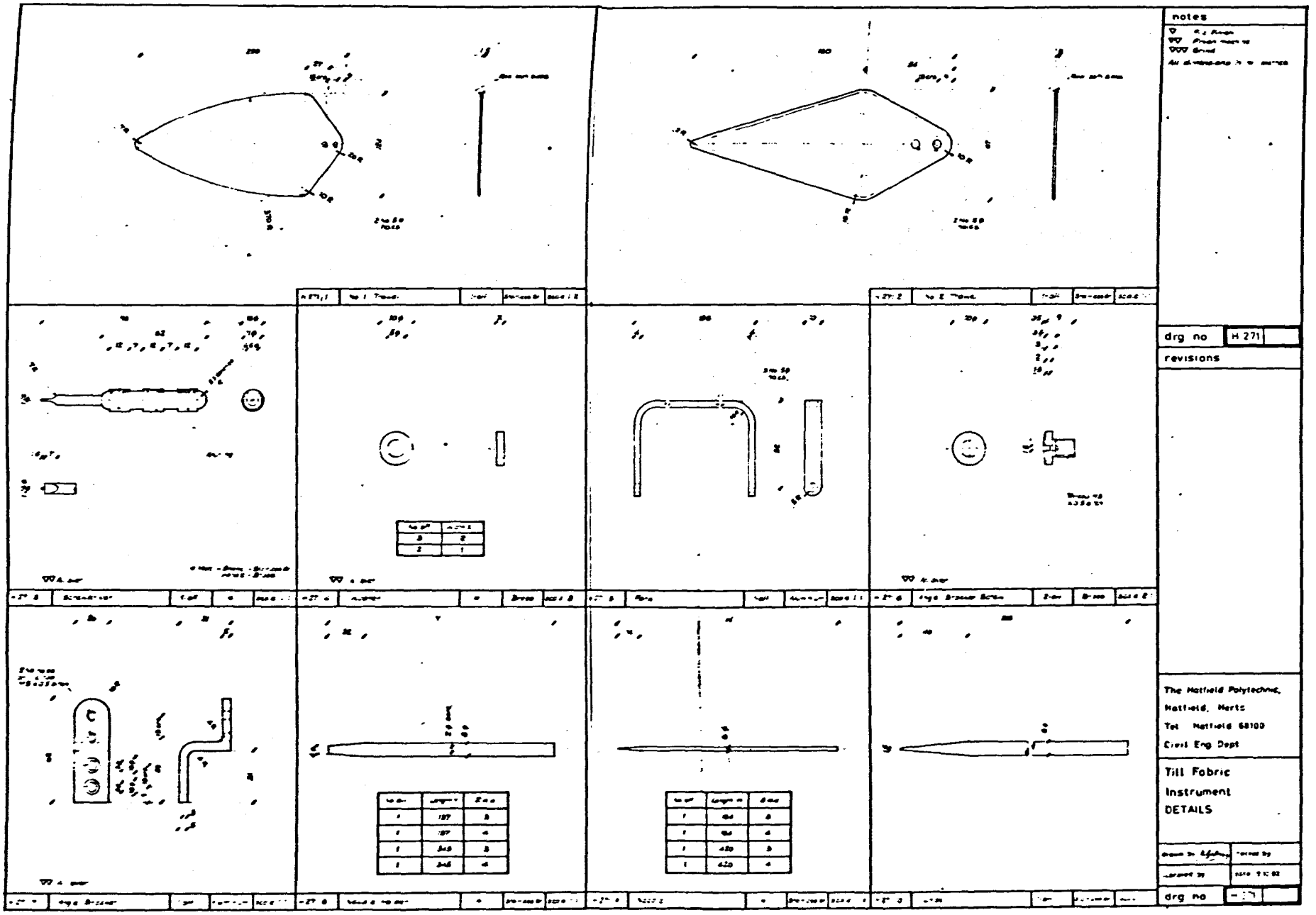
notes
drg no
H 271
revisions
The Hatfield Polytechnic,
Hatfield, Herts
Tel Hatfield 68100
Civil Eng Dept
Till Fabric
Instrument
DETAILS
drg no

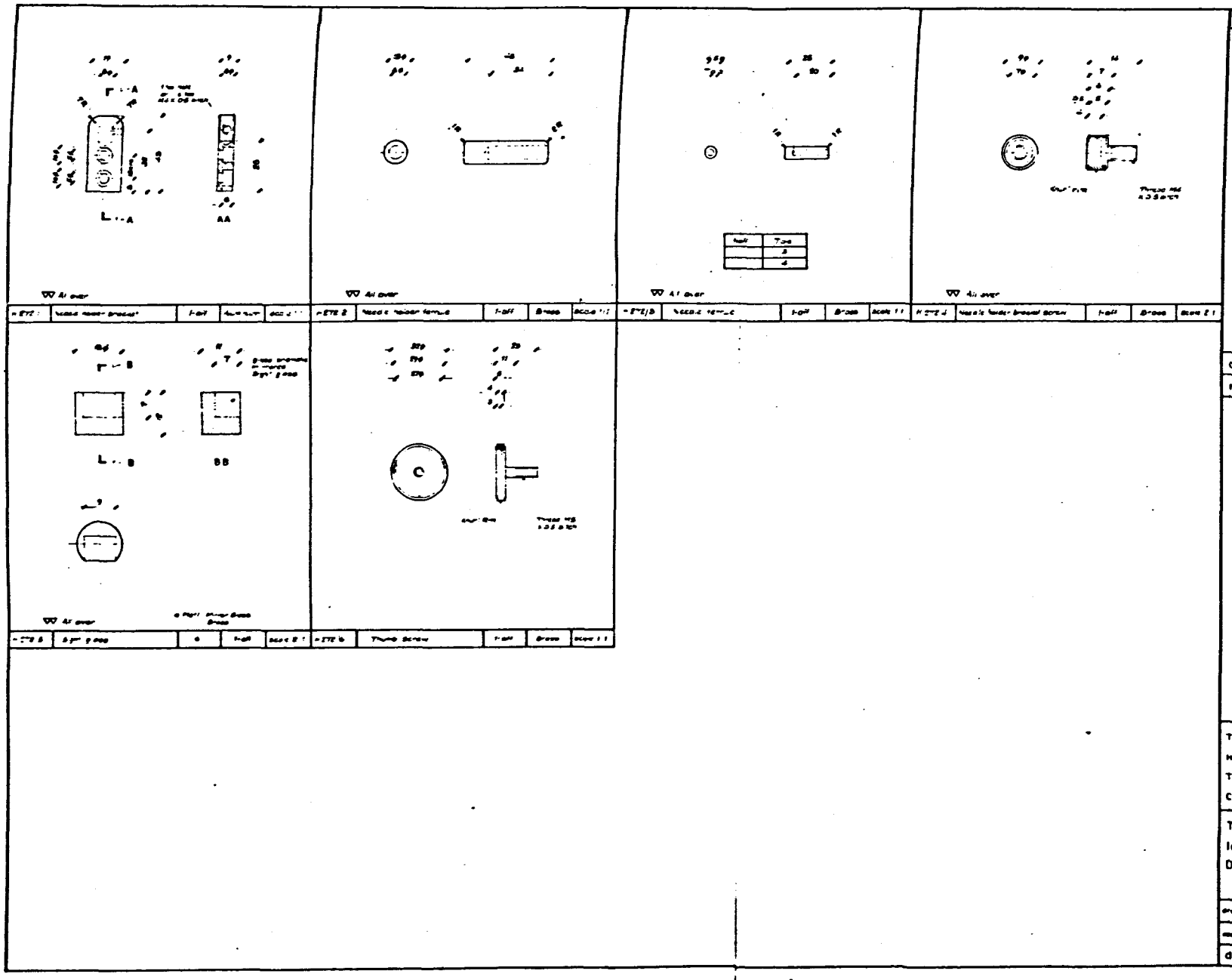
notes
drg no H 272
revisions
The Hatfield Polytechnic,
Hatfield, Herts
Tel Hatfield 68100
Civil Eng Dept.
Till Fabric
Instrument
DETAILS
drg no H 272

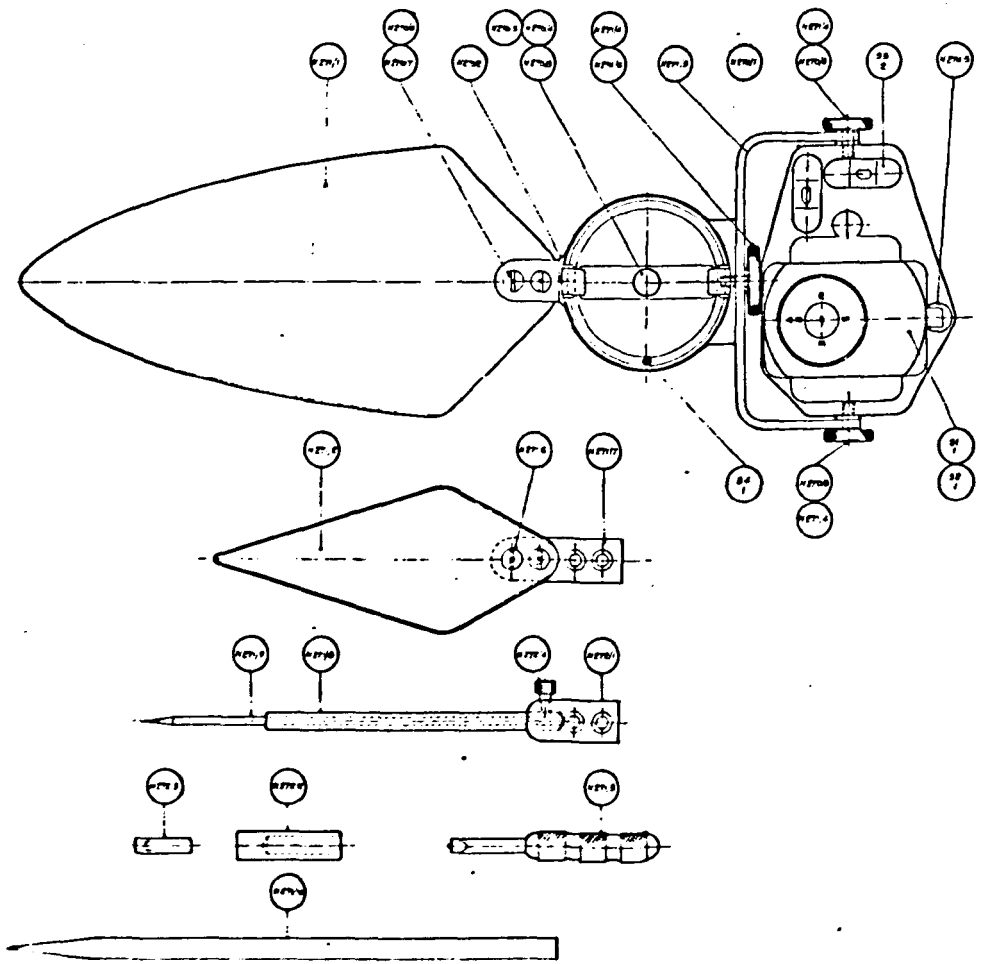

notes

drg no H 273

revisions

The Hatfield Polytechnic,
Hatfield, Herts
Tel Hatfield 68100
Buildings & Estates Dept

Till Fabric
Instrument
GENERAL
ARRANGEMENT